

N7472579


NOTES ON SPACE TECHNOLOGY

Compiled by the
Flight Research Division

Langley Aeronautical Laboratory
Langley Field, Va.

February - May 1958

(NASA-TM-X-69992) NOTES ON SPACE
TECHNOLOGY (NASA) -636 p

N74-72579
THRU
N74-72596
Unclas

00/99 32270

REPRODUCED BY
NATIONAL TECHNICAL
INFORMATION SERVICE
U.S. DEPARTMENT OF COMMERCE
SPRINGFIELD, VA. 22161

GENERAL DISCLAIMER

This document may be affected by one or more of the following statements

- **This document has been reproduced from the best copy furnished by the sponsoring agency. It is being released in the interest of making available as much information as possible.**
- **This document may contain data which exceeds the sheet parameters. It was furnished in this condition by the sponsoring agency and is the best copy available.**
- **This document may contain tone-on-tone or color graphs, charts and/or pictures which have been reproduced in black and white.**
- **This document is paginated as submitted by the original source.**
- **Portions of this document are not fully legible due to the historical nature of some of the material. However, it is the best reproduction available from the original submission.**

PREFACE

These notes are part of a space technology course given at the Flight Research Division of the NACA Langley Aeronautical Laboratory during the early part of 1958. The course was conducted as a self-education program within the Flight Research Division and the various Sections of the notes were prepared for the most part by members of the Division; however, four of the seventeen Sections were prepared by personnel from the Pilotless Aircraft Research Division and the Compressibility Research Division who were very helpful in making the program more complete.

The notes have been compiled on a brief time schedule and it will be apparent to the reader that the present version is incomplete and to some extent may lack uniformity in length, type of presentation, and technical detail in the various Sections. Nevertheless, there has been a demand for the notes from those who have seen them, and it is thought that they might serve a useful purpose if they were made available on a wider basis. It is believed that for the sake of expediency this goal is best achieved by making the material available now in its present unedited form instead of following the usual NACA editing procedures.

The notes are arranged under five broad headings. The first four Sections are concerned with Space Mechanics; the next four with Trajectories and Guidance; the next two with Propulsion; the next three with Heating and Materials; and the final four with Space Environment and Related Problems.

Since these notes have not been technically edited, they are not suitable for reference in NACA reports.

Henry A. Pearson
Course Coordinator
Maneuver Loads Branch
Flight Research Division

INDEX

- | | | |
|--------|---|--------------------------------------|
| ✓ I | Elementary Orbital Mechanics | W. B. Huston and J. P. Mayer |
| ✓ II | Satellite Time and Position With
Respect To A Rotating Earth Surface | T. H. Stopinski |
| ✓ III | The Motion of A Space Vehicle Within
The Earth Moon System: The Restricted
Three Body Problem | J. P. Mayer |
| ✓ IV | Orbital Transfer | A. P. Mayo |
| ✓ V | Re-entry With Two Degrees of Freedom | A. P. Mayo |
| ✓ VI | Six Degree of Freedom Equations of Motion
and Trajectory Equations of a Rigid Fin
Stabilized Missile with Variable Mass | J. J. Donegan |
| ✓ VII | Inertial Space Navigation | D. C. Cheatham |
| ✓ VIII | Guidance and Control of Space Vehicles | C. W. Mathews |
| ✓ IX | Elements of Rocket Propulsion | H. A. Hamer |
| ✓ X | Characteristics of Modern Rockets
and Propellants | J. G. Thibodaux, Jr. and H. A. Hamer |
| ✓ XI | Aerodynamic Heating and Heat
Transmission | W. B. Huston |
| ✓ XII | Heat Protection | W. S. Aiken, Jr. |
| ✓ XIII | Properties of High Temperature
Materials | E. M. Fields |
| ✓ XIV | The Solar System | C. R. Huss |
| ✓ | Appendix on the Earth's Atmosphere | W. J. O'Sullivan and J. L. Mitchell |
| ✓ XV | Communication and Tracking | P. A. Gainer and R. L. Schott |
| ✓ XVI | Some Dynamical Aspects of the Special
and General Theories of Relativity | D. Adamson |
| ✓ XVII | Environmental Requirements | W. A. McGowan |

SECTION I

ELEMENTARY ORBITAL MECHANICS

1.1 Motion in a Plane.

When a particle moves in a plane (or space) its acceleration satisfies the equation $F = ma$, but the quantities F and a have not only magnitude but also direction. In order to deal with magnitudes, we can take components along a set of coordinate axes, say the rectangular XY axes, thus if the component of F along a line is F_x , and the component of a along that line is a_x , then,

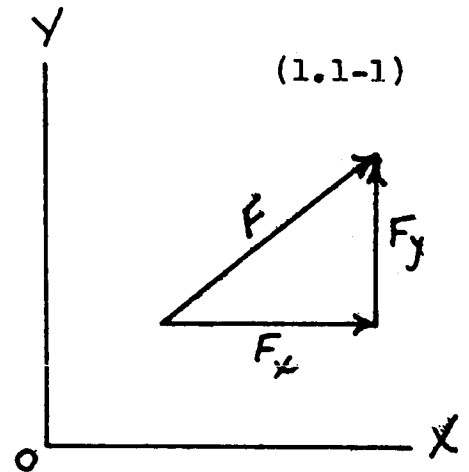
$$F_x = ma_x$$

and so on.

If the particle moves in a plane, and its coordinates are (x,y) , the components of acceleration along the coordinate axes are

$$a_x = \frac{d^2x}{dt^2}, \quad a_y = \frac{d^2y}{dt^2}$$

If F_x, F_y are the components of the force, the motion of the particle is determined by the equations



$$m \frac{d^2x}{dt^2} = F_x \quad (1.1-2)$$

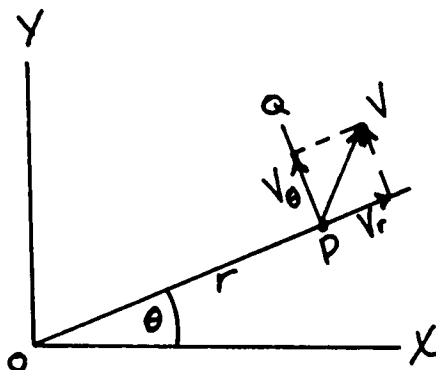
$$m \frac{d^2y}{dt^2} = F_y \quad (1.1-3)$$

In many cases it is more convenient to use polar coordinates. A particle at P is related to the origin by the coordinates (r, θ) . Its velocity V is resolved into components v_r along the line OP, and v_θ along the line PQ normal to OP.

These components have the values:

$$v_r = \frac{dr}{dt} \quad (1.1-4)$$

$$v_\theta = r \frac{d\theta}{dt} \quad (1.1-5)$$



The acceleration also has components a_r along OP and a_θ along PQ. Projection along the appropriate axes and a little manipulation will show that

$$a_r = \frac{d^2r}{dt^2} - r \left(\frac{d\theta}{dt} \right)^2 \quad (1.1-6)$$

$$a_\theta = \frac{1}{r} \frac{d}{dt} \left(r^2 \frac{d\theta}{dt} \right) \quad (1.1-7)$$

If the force F acting on the particle has the component F_r along OP and F_θ perpendicular to OP, the motion of the particle can be obtained by solving the equations

$$ma_r = F_r \quad (1.1-8)$$

$$ma_\theta = F_\theta \quad (1.1-9)$$

These equations are the starting point for studying the orbit of an earth satellite.

1.2 Gravitational Forces.

Two bodies of masses m and M are attracted by a force proportional to the product of the masses, and inversely proportional to the distance between them, or $\frac{G m M}{r^2}$. The inverse square concept, associated with the name of Newton (1687) which was also independently proposed by Hooke (of Hooke's Law fame) has been called "the greatest discovery in nature that ever was since the World's Creation". If the origin is taken as the center of mass M , the point P as the center of mass m , then the positive direction of r is outward, while the force is directed back along r and thus

$$F_r = - \frac{G m M}{r^2} \quad (1.2-1)$$

Hence, the differential equations of motion from (1.1-8) and (1.1-9) are

$$m \left[\frac{d^2 r}{dt^2} - r \left(\frac{d\theta}{dt} \right)^2 \right] = - \frac{G m M}{r^2} \quad (1.2-2)$$

$$\frac{m}{r} \frac{d}{dt} \left(r^2 \frac{d\theta}{dt} \right) = 0 \quad (1.2-3)$$

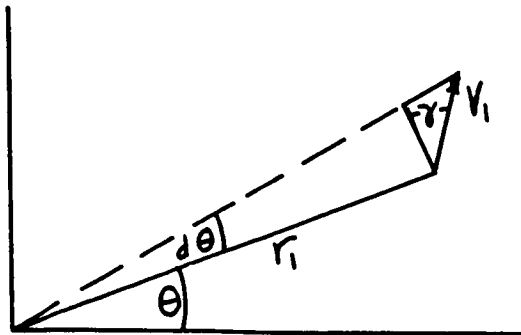
We are thus assuming that there are no drag or accelerating forces at right angles to the radius vector and affecting the rotational motion, that is, $F_{\theta} = 0$.

Equation (1.2-3) can be integrated immediately,

$$r^2 \frac{d\theta}{dt} = K \quad (1.2-4)$$

This result, which is known as Kepler's Second Law is independent of the form or nature of the attracting force (in this case, gravity). The constant K has a physical meaning which can be seen from an examination of the initial conditions. At $t = 0$ let the radius be r_1 , the velocity V_1 in a direction γ relative to the normal to r . Since $r d\theta = V \cos \gamma dt$ the value of K will be

$$r^2 \frac{d\theta}{dt} = r_1 V_1 \cos \gamma = K \quad (1.2-5)$$



The element of area dA swept out by r in moving through an angle $d\theta$ is

$$dA = \frac{1}{2} (r)(r d\theta)$$

Hence
$$K = 2 \frac{dA}{dt} \quad (1.2-6)$$

from which follows Kepler's Second Law (derived originally from observation of planetary motion and published in 1618), "each planet revolves so that the line joining it to the sun sweeps over equal areas in equal intervals of time". (It should be noted that Kepler's Constant is usually given in the literature as $\frac{dA}{dt}$ or $\frac{K}{2}$.)

We now have the set of simultaneous equations

$$\frac{d^2 r}{dt^2} - r \left(\frac{d\theta}{dt} \right)^2 = - \frac{GM}{r^2} \quad (1.2-7)$$

$$r^2 \frac{d\theta}{dt} = K \quad (1.2-8)$$

To find the path or the variation of r with θ we must eliminate time between (1.2-7) and (1.2-8). It is convenient to change the variable from r to $u = 1/r$, whence

$$\frac{dr}{d\theta} = -r^2 \frac{du}{d\theta}$$

Then

$$\frac{d\theta}{dt} = K u^2$$

$$\frac{dr}{dt} = \frac{dr}{d\theta} \frac{d\theta}{dt} = \frac{K}{r^2} \frac{dr}{d\theta} = -K \frac{du}{d\theta}$$

$$\frac{d^2 r}{dt^2} = -K \frac{d^2 u}{d\theta^2} \frac{d\theta}{dt} = -K^2 u^2 \frac{d^2 u}{d\theta^2}$$

With these substitutions equation (1.2-7) becomes

$$\frac{d^2 u}{d \theta^2} + u = \frac{GM}{K^2} \quad (1.2-9)$$

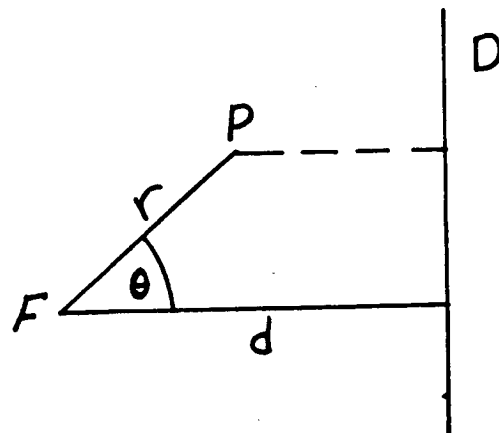
The solution of equation (1.2-9) can be determined by inspection as

$$u = \frac{GM}{K^2} + A \cos \theta \quad (1.2-10)$$

where A is a constant the significance of which remains to be determined, and thus the path of our mass m about the center is

$$\frac{1}{r} = \frac{GM}{K^2} + A \cos \theta \quad (1.2-11)$$

To determine the significance of A we need to remember that there is a set of curves called conic sections defined by the situation shown in the figure on this page. Given a point F called the Focus at a fixed distance d from a straight line D called the Directrix. Then if a point P at distance r from F is made to move in such a way that for any value of θ the ratio of distance of P from F to the distance of P from D is constant or



$$\frac{r}{PD} = \text{constant}$$

then the curve defined by the point P is called a CONIC SECTION. The constant in the above ratio is a characteristic constant of the curve called its eccentricity ϵ which determines the nature of the curve. Since the distance PD is $d - r \cos \theta$, the eccentricity is

$$\epsilon = \frac{r}{d - r \cos \theta} \quad (1.2-12)$$

or

$$\frac{1}{r} = \frac{1}{\epsilon d} + \frac{1}{d} \cos \theta \quad (1.2-13)$$

But this is just the relation (1.2-11) that came out of our equations for the motion of a body under an inverse square law of attraction.

What do these curves look like.

$$\epsilon = 0 \quad \text{circle}$$

$$0 < \epsilon < 1 \quad \text{ellipse}$$

$$\epsilon = 1 \quad \text{parabola}$$

$$\epsilon > 1 \quad \text{hyperbola}$$

These curves are illustrated in figures 1-1 and 1-2, plotted from equation (1.2-13) rewritten as

$$r = \frac{\epsilon d}{1 + \epsilon \cos \theta} \quad (1.2-14)$$

and as

$$\frac{r(\theta)}{r(0)} = \frac{1 + \epsilon}{1 + \epsilon \cos \theta}$$

$\theta \leftarrow$

For an ellipse there is a characteristic dimension which is more useful than d . It is the length of the major axis, the longest distance from one side to the other through the focus, from perigee to apogee. Usually we use the semi-major axis a , which is related to d by the formula

$$a = \frac{\epsilon d}{1 - \epsilon^2} \quad (1.2-15)$$

Using this relation the orbit equation is

$$r = \frac{a(1 - \epsilon^2)}{1 + \epsilon \cos \theta} \quad (1.2-16)$$

The physical significance of the constants in equation (1.2-11) has thus been shown by comparison with equations (1.2-13). The constant $A = 1/d$ while the gravitational constant G , the primary mass M , and Kepler's constant K together determine the value ϵd , that is

$$\frac{GM}{K^2} = \frac{1}{\epsilon d}$$

or

$$\epsilon = \frac{K^2}{GMd} \quad (1.2-17)$$

The mass m moves in a path about M which is a conic section. Which conic section and why are questions which must be deferred pending a study of just what it is that fixes the values of ϵ and d . For this purpose we need to reconsider the motion in terms of the potential and kinetic energy of the mass m .

1.3 Total Energy.

We write our principal conclusion thus far by the equation for the motion of m about M .

$$\frac{1}{r} = \frac{GM}{K^2} + \frac{1}{d} \cos \theta \quad (1.3-1)$$

In order to establish the factors which determine the eccentricity and the size of the orbit it is necessary to examine the total energy.

The kinetic energy is

$$K_E = \frac{1}{2} m V^2 \quad (1.3-2)$$

The potential energy is defined for conservative forces by

$$dP_E = -dW \quad (1.3-3)$$

where W is the work defined by

$$W = \int^r F dr \quad (1.3-4)$$

The potential energy is

$$P_E = -\int^r F dr = \int \frac{GMm}{r^2} dr = -\frac{GMm}{r} \quad (1.3-5)$$

The total energy is then

$$U = \frac{1}{2} m V^2 - \frac{GMm}{r} \quad (1.3-6)$$

One explanation for the negative sign is that the potential energy at infinity is taken to be zero, and since potential energy must increase as the distance from the attracting center increases then at all distances less than infinity the potential energy must be negative.

If we can calculate the value of U for one point in the orbit, we know it for every point. At perigee, where r is a minimum and $\theta = 0$, by equation (1.3-1),

$$\frac{1}{r_p} = \frac{GM}{K^2} + \frac{1}{d} \quad (1.3-7)$$

At this point all of the velocity is rotational, there is no radial component and

$$V = r_p \frac{d\theta}{dt}$$

But by Kepler's Law, for this, (or any) point in the orbit

$$r^2 \frac{d\theta}{dt} = K \quad , \quad \text{or with equation (1.3-7)}$$

$$V_p = \frac{K}{r_p} = \frac{GM}{K} + \frac{K}{d} \quad (1.3-8)$$

Inserting the values from equations (1.3-7) and (1.3-8) in (1.3-6) gives for the Total Energy

$$\begin{aligned} U &= \frac{1}{2} m \left(\frac{GM}{K} + \frac{K}{d} \right)^2 - m \left[\left(\frac{GM}{K} \right)^2 - \frac{GM}{d} \right] \\ &= -\frac{m}{2} \left(\frac{GM}{K} \right)^2 \left[1 - \left(\frac{K^2}{GMd} \right)^2 \right] \end{aligned}$$

or, from equation (1.2-17)

$$U = -\frac{m}{2} \left(\frac{GM}{K} \right)^2 (1 - \epsilon^2) \quad (1.3-9)$$

or

$$\epsilon = \sqrt{1 + \frac{2U}{m} \left(\frac{K}{GM} \right)^2} \quad (1.3-10)$$

Thus the orbit is elliptic, parabolic or hyperbolic, as the total energy is negative, zero, or positive. This in turn depends upon the relative magnitudes of the kinetic and potential energy. Hyperbolic orbits require the most kinetic energy (or speed). For the most part we shall be interested in elliptic orbits, (negative total energy). Such an orbit is specified by a value of eccentricity, ϵ , equation (1.3-10) and by the semi-major axis a . From equations (1.2-15) and (1.2-17)

$$a = \frac{K^2}{GM(1 - \epsilon^2)} \quad (1.3-11)$$

From equations (1.3-9) and (1.3-11) the total energy for an elliptical orbit is

$$U = \frac{-GMm}{2a} \quad (1.3-12)$$

Thus it is seen that the total energy in an elliptical orbit is inversely proportional only to the semi-major axis of the orbit.

The velocity at any point in the orbit can be obtained by substituting equation (1.3-12) into equation (1.3-6).

$$U = \frac{-GMm}{2a} = \frac{1}{2} m V^2 - \frac{GMm}{r}$$

$$V^2 = GM \left[\frac{2}{r} - \frac{1}{a} \right] \quad (1.3-13)$$

1.4 Establishment of an Orbit.

Thus far we have written equations for orbits in terms of gravitational constants, G , the mass of the principal body M , a constant K , the total energy U , all of which are hard to grasp physically. In this Section we shall convert the equations to a form containing constants which are more familiar to us.

For example, a body of mass m has a weight mg_0 at the surface of the earth because of the attractive force of gravity. Thus we can relate this weight to the force as

$$mg_0 = \frac{GMm}{R^2} \quad (1.4-1)$$

and we could substitute for the term GM its equivalent

$$GM = R^2 g_0 \quad (1.4-2)$$

Similarly the constant K is fixed, for a rocket by conditions at the instant of burnout, i.e. its distance r_1 from the origin, its Velocity V_1 and the angle γ its path makes with the normal to r_1 . At this instant, from equation (1.2-5)

$$K = r_1 V_1 \cos \gamma \quad (1.4-3)$$

The total energy is

$$\begin{aligned} U &= \frac{1}{2} m V^2 - \frac{GMm}{r} \\ &= \frac{1}{2} m V_1^2 - \frac{R^2 g_0 m}{r_1} \end{aligned} \quad (1.4-4)$$

Hence

$$\frac{2U}{m} = -Rg_0 \left[\frac{2}{r_1/R} - \frac{V_1^2}{Rg_0} \right] \quad (1.4-5)$$

Inserting these values in the expressions for ϵ (eq. 1.3-10) and a (eq. 1.3-11) we find that

$$\epsilon = \sqrt{1 - \left(\frac{r_1}{R}\right)^2 \left(\frac{V_1}{Rg_0}\right)^2 \left(\frac{2}{r_1/R} - \frac{V_1^2}{Rg_0}\right) \cos^2 \gamma} \quad (1.4-6)$$

It is worth looking at this term Rg_0 . It has the dimensions of velocity squared. Suppose we wanted to establish a circular orbit of the radius of the earth $r_1 = R$ with zero eccentricity. The eccentricity can be zero only if the term on the right under the radical is unity. If $r_1 = R$, $\gamma = 0$, $\cos \gamma = 1$, then this can be true only if $V_1^2 = Rg_0$. Hence Rg_0 is the square of a velocity V_0 equal to the velocity for a circular orbit of radius R . We shall write it this way, i.e.,

$$V_0 = \sqrt{Rg_0} \quad (1.4-7)$$

and with this substitution,

$$\epsilon = \sqrt{1 - \left(\frac{r_1}{R} \frac{V_1}{V_0}\right)^2 \left[\frac{2}{r_1/R} - \left(\frac{V_1}{V_0}\right)^2\right] \cos^2 \gamma} \quad (1.4-8)$$

Similarly

$$a = \frac{K^2/GM}{1-\epsilon^2} \quad (1.3-11)$$

leads to

$$a = \frac{R}{\frac{2}{r_1/R} - \left(\frac{V_1}{V_s}\right)^2} \quad (1.4-9)$$

or

$$\frac{a}{r_1} = \frac{1}{2 - (V_1/V_s)^2} \quad (1.4-10)$$

These last equations (1.4-8), (1.4-9) and (1.4-10) determine uniquely the size and shape of an orbit in terms of the three parameters (r_1, V_1, γ_1) which characterize a body at the instant it becomes a free body, i.e. for a rocket - the instant of burnout.

1.5 Orientation of Orbits.

In addition to knowing the size and shape of an orbit it is necessary to know the orientation of the orbit in space, that is the location of the major axis relative to the point of burnout. If the vehicle is launched as a free body with the initial elevation angle (γ_1) equal to zero, burnout is the perigee or apogee, depending on the speed. If γ_1 is not zero then the position of the major axis in space is rotated with respect to the position for zero angle of elevation.

In calculating orbits with an initial launch elevation angle we shall use the basic orbit equation (equation 1.2-16) with the origin of θ at the perigee and calculate the

initial orientation angle of launch (θ_1) using the usual initial conditions at burnout (V_1, r_1, γ_1).

The orbit equation is

$$r = \frac{a(1 - \epsilon^2)}{1 + \epsilon \cos \theta} \quad (1.2-16)$$

This can be expressed as

$$r = \frac{p}{1 + \epsilon \cos \theta} \quad (1.5-1)$$

At launch

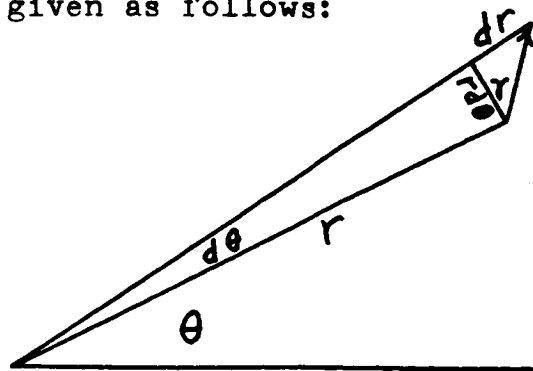
$$r_1 = \frac{p}{1 + \epsilon \cos \theta_1} \quad (1.5-2)$$

so that

$$\cos \theta_1 = \frac{(p/r_1) - 1}{\epsilon} \quad (1.5-3)$$

The eccentricity ϵ could be calculated from equation (1.4-8); however, it will be found more convenient to use a slightly different form.

The angle (γ) between the instantaneous direction of the velocity (V) and the normal to the radius (r) can be given as follows:



$$\tan \gamma = \frac{dr}{r d\theta}$$

Differentiating equation (1.5-1) we obtain

$$\frac{dr}{d\theta} = \frac{-p}{(1 + \epsilon \cos \theta)^2} (-\epsilon \sin \theta) \quad (1.5-5)$$

But from equation (1.5-1)

$$(1 + \epsilon \cos \theta)^2 = \left(\frac{p}{r}\right)^2 \quad (1.5-6)$$

and thus

$$\frac{dr}{d\theta} = \epsilon \frac{r^2}{p} \sin \theta \quad (1.5-7)$$

Therefore,

$$\tan \gamma = \epsilon \frac{r}{p} \sin \theta$$

$$\text{or } \tan \gamma = \frac{\epsilon \sin \theta}{1 + \epsilon \cos \theta} \quad (1.5-8)$$

and

$$\epsilon = \frac{p}{r} \frac{\tan \gamma}{\sin \theta} \quad (1.5-9)$$

Substituting ϵ from equation (1.5-9) into equation (1.5-3) we obtain for the initial conditions:

$$\cos \theta_1 = \frac{(p/r_1 - 1)}{p/r_1} \frac{\sin \theta_1}{\tan \gamma_1} \quad (1.5-10)$$

$$\text{or } \tan \theta_1 = \tan \gamma_1 \left[\frac{p/r_1}{p/r_1 - 1} \right] \quad (1.5-11)$$

In order to obtain the parameter p/r_1 in terms of the launch conditions, we note from equation (1.3-11) that

$$p = a(1 - \epsilon^2) = \frac{K^2}{GM} \quad (1.5-12)$$

and from equations (1.4-2)

$$p = a(1 - \epsilon^2) = \frac{K^2}{g \cdot R^2} \quad (1.5-13)$$

But from equation (1.4-3)

$$K^2 = r_1^2 V_1^2 \cos^2 \gamma_1 \quad (1.5-14)$$

Therefore

$$p = \frac{r_1^2 V_1^2 \cos^2 \gamma_1}{g \cdot R^2} \quad (1.5-15)$$

and in terms of circular satellite velocity V_s at radius r_1

$$\frac{p}{r_1} = (V_1 / V_s)^2 \cos^2 \gamma_1 \quad (1.5-16)$$

Thus all the elements for calculating orbits have been found. These equations are listed below, and repeated in Table 1-1a in the order usually found most convenient for computing orbits. In addition, formulas frequently used in orbit calculations are given in Table 1-1b.

$$r = \frac{p}{1 - \epsilon \cos \theta} \quad (1.5-1)$$

Step 1.

$$\frac{p}{r_1} = (V_1/V_s)^2 \cos^2 \gamma_1 \quad (1.5-16)$$

Step 2.

$$\tan \theta_1 = \tan \gamma_1 \left[\frac{p/r_1}{p/r_1 - 1} \right] \quad (1.5-11) \quad (1.5-17)$$

Step 3.

$$\epsilon = \frac{1}{\cos \theta_1} \left[\frac{p}{r_1} - 1 \right] \quad (1.5-3)$$

or

$$\epsilon = \frac{p}{r_1} \frac{\tan \gamma_1}{\sin \theta_1} \quad (1.5-9)$$

Since the angle (γ) at any point in the orbit is often required (i.e. for re-entry angles) equation (1.5-8) is also repeated:

$$\tan \gamma = \frac{\epsilon \sin \theta}{1 + \epsilon \cos \theta} \quad (1.5-8)$$

The semi-major axis is given in terms of p as

$$a = \frac{p}{1 - \epsilon^2} \quad (1.5-18)$$

The semi-minor axis is

$$b = \sqrt{ap} \quad (1.5-19)$$

The foregoing equations (1.5-17) are well suited for the calculation of the elements of orbits including orientation when the initial velocity V_1 , initial elevation angle γ_1 , and initial radius r_1 are known. A consistent set of numerical constants for use in orbit computations is given in Table 1-2.

These equations are written in terms of the circular satellite velocity (V_S). In some cases it might be preferable to use the escape velocity V_E or the circular satellite velocity at the surface of the earth V_0 as a reference velocity. Therefore, the equations for these velocities are given:

$$V_S = \sqrt{g_0 \frac{R^2}{r_1}} \quad (1.5-20)$$

$$V_E = \sqrt{2g_0 \frac{R^2}{r_1}} \quad (1.5-21)$$

$$V_0 = \sqrt{g_0 R} \quad (1.5-22)$$

The orbit equation is illustrated in figure 1-3 and the boundary conditions for the orientation angle θ_1 are shown in figure 1-4.

In figure 1-3 the origin is at the right focus and the angle θ is measured in the counter clockwise direction from

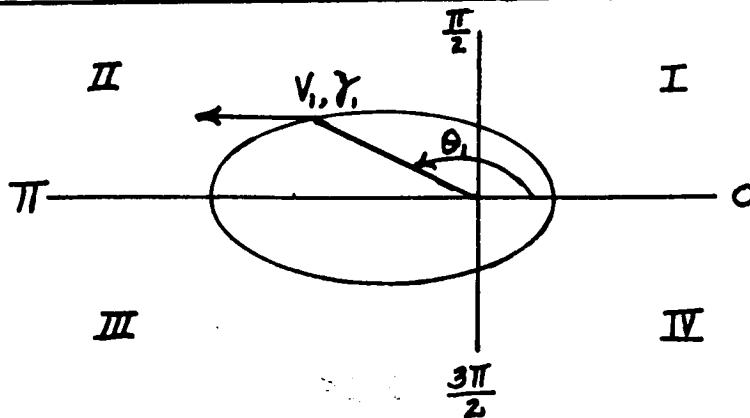
perigee. The vehicle is assumed to be launched as a free body at $\theta = \theta_1$. The initial elevation angle γ_1 is positive when the initial velocity vector V_1 is inclined outward from the perpendicular to the initial radius r_1 .

Boundaries separating various values of the orientation angle θ_1 are shown in figure 1-4. The curve shown represents the values of (V_1/V_s) and γ_1 where θ_1 equals 90° or 270° as defined by

$$\frac{V_1}{V_s} \cos \gamma_1 = 1 \tag{1.5-23}$$

This curve and the axis where $\gamma_1 = 0$ divide the area into the four quadrants as shown in figure 1-4 and as indicated below:

Conditions	Quadrant
$\gamma +, 1.0 < \frac{V_1}{V_s} \cos \gamma_1 < \sqrt{2} \cos \gamma_1$	I
$\gamma +, 0 < \frac{V_1}{V_s} \cos \gamma_1 < 1.0$	II
$\gamma -, 0 < \frac{V_1}{V_s} \cos \gamma_1 < 1.0$	III
$\gamma -, 1.0 < \frac{V_1}{V_s} \cos \gamma_1 < \sqrt{2} \cos \gamma_1$	IV



The eccentricity ϵ is always positive when using these definitions.

The effect of initial velocity (V_1) on orbits is shown in figure 1-5 for zero initial elevation angle and in figure 1-6 for $\gamma_1 = 10^\circ$. It should be noted in figure 1-4 that when the initial elevation angle is zero that $\theta_1 = 0^\circ$ for $(V_1/V_s) > 1$ and that $\theta_1 = 180^\circ$ for $(V_1/V_s) < 1$ so that the eccentricity for $\gamma_1 = 0$ is

$$\epsilon = \left| \frac{r}{r_1} - 1 \right|; \gamma_1 = 0 \quad (1.5-24)$$

or

$$\epsilon = \left| \left(\frac{V_1}{V_s} \right)^2 - 1 \right|; \gamma_1 = 0 \quad (1.5-25)$$

In figure 1-6 it can be seen that when the initial elevation angle is not zero the orientation angle θ_1 is not zero but is a function of (V_1/V_s) . The eccentricities ϵ are larger than those in figure 1-5 but the major axes (a) do not change from those given in figure 1-5 since the length of the major axis depends on V_1 and r_1 but not γ_1 .

The effect of initial launch angle γ_1 on orbits for a constant initial launch velocity V_1 is shown in figure 1-7. It is seen that the effect of changing the initial launch

elevation angle γ_1 is to change the orientation of the orbit in space and to increase the eccentricity ϵ . For example given it is seen that a 10° elevation angle causes a rotation of the major axis of about 32° .

In plotting orbits with different orientation angles the second and succeeding orbits must be rotated through an angle $\Delta\theta$:

$$\Delta\theta = \theta_{1i} - \theta_{1j} \quad (1.5-26)$$

in order to make the launch points coincide with the launch point for the first orbit; or the orientation can be accounted for by defining the orbit as

$$r = \frac{P}{1 + \epsilon \cos(\theta' + \theta_i)} \quad (1.5-27)$$

where θ' is measured counterclockwise from the initial radius r_1 .

1.6 Time-Speed relationship in an Orbit.

In addition to the shape and the orientation of orbits it is also important to know the lapse time between points in the orbit and the speed at each point in the orbit.

The speed can be obtained using the relationship of equation (1.4-3):

$$rV \cos \gamma = K \quad (1.4-3)$$

$$\text{or } r V \cos \gamma = r_1 V_1 \cos \gamma_1 \quad (1.6-1)$$

or from equation (1.3-13):

$$V^2 = g_0 R^2 \left[\frac{2}{r} - \frac{1}{a} \right] \quad (1.6-2)$$

$$\text{or } V^2 = g_0 R^2 \left[\frac{2}{r} - \frac{(1-\epsilon^2)}{p} \right] \quad (1.6-3)$$

$$\text{or } (V_1 / V_s)^2 = \frac{2r_1}{r} - \frac{r_1}{p} (1-\epsilon^2) \quad (1.6-4)$$

The time relationship is not as obvious and will be derived in SECTION II. The equation derived is:

$$t(\theta) = C \frac{1}{(1-\epsilon^2)} \left[\frac{-\epsilon \sin \theta}{1+\epsilon \cos \theta} + \frac{2}{\sqrt{1-\epsilon^2}} \tan^{-1} \left(\frac{\sqrt{1-\epsilon^2}}{1+\epsilon} \tan \frac{\theta}{2} \right) \right] \quad (1.6-5)$$

For parabolic and hyperbolic orbits, ($\epsilon > 1$) the equation becomes

$$t(\theta) = C \frac{1}{(1-\epsilon^2)} \left[\frac{-\epsilon \sin \theta}{1+\epsilon \cos \theta} + \frac{1}{\sqrt{\epsilon^2-1}} \ln \left(\frac{\epsilon + \cos \theta + \sqrt{\epsilon^2-1} \sin \theta}{1+\epsilon \cos \theta} \right) \right] \quad (1.6-5a)$$

where C can be given in the following forms:

$$C = \frac{p}{R} \sqrt{\frac{p}{g_0}} \quad (1.6-6a)$$

$$C = \frac{r_1}{V_s} \left(\frac{V_1}{V_s} \right)^3 \cos^3 \gamma_1 \quad (1.6-6b)$$

$$C = \sqrt{\frac{R}{g_0}} \sqrt{\left(\frac{a}{R}\right)^3} \sqrt{(1-\epsilon^2)^3} \quad (1.6-6c)$$

The time in equation (1.6-5) is measured from the origin of θ which is the perigee.

If the time from launch or from some other point is desired, equation (1.6-5) can be used to get the difference in the time between any two points. The time from launch becomes:

$$\Delta t_1 = t(\theta) - t(\theta_1) \quad (1.6-7)$$

From equation (1.6-5) the period of the orbit can be determined to be

$$T = 2\pi \sqrt{\frac{R}{g_0}} \sqrt{\left(\frac{a}{R}\right)^3} \quad (1.6-8)$$

or

$$T = \frac{2\pi}{(1-\epsilon^2)^{3/2}} \frac{p}{R} \left(\frac{p}{g_0}\right)^{1/2} \quad (1.6-9)$$

1.7 Realizable Orbits.

Thus far our principal results are embodied in the equations which show the relationship between the three parameters, r_1, v_1, γ_1 , which define the position and path of a rocket at the instant of burnout, and the orbit which results as characterized by its semi-major axis a , its eccentricity ϵ , and its orientation angle θ_1 . It would be nice to be able to make plots showing the relationship of these factors, but 4 parameters are hard to plot.

Since the elevation angle γ does not enter into the expression for a , we can plot this as a function of r_1 and V_1 as in figure 1-8. The distances have been expressed in earth radii R , the speed in terms of V_0 , the speed for a circular orbit of radius R . The plot shows how as we go farther and farther out, to establish an orbit, we need to provide less and less speed to establish it. In fact, if we provide too much, we will lose it altogether to a parabolic or hyperbolic orbit, if at any time

$$V_1 \geq \sqrt{\frac{2g_0 R^2}{r_1}} = \sqrt{\frac{2Rg_0}{r_1/R}} = V_E \quad (1.7-1)$$

a speed which is called the escape velocity. At $r_1 = R$,

$$\begin{aligned} V_E &= 36,695 \text{ ft/sec} \\ &= 25,019 \text{ mph} \end{aligned}$$

For many purposes, it is convenient to normalize the velocity not with V_0 , but with a speed V_s , which varies with altitude and is the speed for a circular orbit of radius r_1 ; thus the satellite velocity is

$$V_s = \sqrt{\frac{g_0 R^2}{r_1}} = \sqrt{\frac{Rg_0}{r_1/R}} = \frac{V_0}{\sqrt{r_1/R}} \quad (1.7-2)$$

On this basis, figure 1-8 changes its form slightly, and becomes figure 1-9.

In order to illustrate the relationship between eccentricity ϵ and launching conditions it is simplest

first to use V_s , rather than V_0 . On this basis, equation (1.4-8) becomes

$$\epsilon = \sqrt{1 - \left(\frac{V_1}{V_s}\right)^2 \left[2 - \left(\frac{V_1}{V_s}\right)^2\right]} \cos^2 \gamma \quad (1.7-3)$$

It is simpler in this case to use $(V_1/V_s)^2$ as the independent variable, since for $\gamma = 0$,

$$\epsilon = \left| 1 - \left(\frac{V_1}{V_s}\right)^2 \right| \quad 0 \leq \left(\frac{V_1}{V_s}\right)^2 \leq 2$$

which is simple and symmetrical to plot as shown in figure 1-10. There is only one speed $V_1 = V_s$ which at the altitude r_1 will produce a circular orbit, and this only if $\gamma = 0$. Any other speed or any departure from $\gamma = 0$ will produce a finite value of eccentricity. Thus circular orbits are exceedingly difficult to establish as the programming requirements on both thrust and direction control are very stiff. If we want to show the same information as is given in figure 1-10 in terms of V_1/V_0 , r_1 and γ the plot is somewhat more complicated, as shown in figure 1-11, which is a nomogram for the solution of equation (1.4-8).

The variation of V_s and V_E with the distance from the center of the earth is shown in figure 1-12.

The real question, of course, in establishing an orbit, is one of whether it will clear the earth. We can launch a rocket at some distance r_1 , and give it a speed V_1 at

some angle γ , but unless the perigee distance, the point of minimum radius, is greater than the radius of the earth, we will not clear it, and will not even get one pass. This ignores the atmosphere, of course, and in the practical case, unless the perigee distance is at least 50 miles above the surface, the orbit is of little use.

Now the orbit, in terms of a and ϵ may be written as

$$r = \frac{a(1 - \epsilon^2)}{1 + \epsilon \cos \theta} \quad (1.2-16)$$

Hence perigee distance ($\theta = 0$) is $a(1 - \epsilon)$. This distance does not seem to be expressible as a simple function of (r_1, v_1, γ) , but we can easily write a condition for the limiting elevation angle γ_L which must not be exceeded if

$$a(1 - \epsilon) \geq R \quad (1.7-4)$$

Combination of equations (1.4-6) and (1.4-8) with (1.7-4) yields the condition that

$$\cos \gamma_L = \frac{\sqrt{2 - \left[\frac{2}{r_1/R} - \left(\frac{v_1}{v_0} \right)^2 \right]}}{\left(\frac{r_1}{R} \right) \left(\frac{v_1}{v_0} \right)} = \frac{1}{r_1/R} \sqrt{\frac{2(r_1/R - 1)}{\left(\frac{v_1}{v_0} \right)^2} + 1} \quad (1.7-5)$$

relations which are plotted in figures 1-13 and 1-14, for various values of r_1/R from 1 to 60. Note that for $r_1 = R$, γ must be zero, while if we wish to establish an elliptic orbit at some other values of r_1 and V_1 , then the elevation angle must be less than the value of γ_L shown for each value of r_1 . Another limiting condition applies here; V_1 cannot exceed the escape velocity if an orbit is to be established.

1.8 Minimum Altitude Orbits.

The practical use of figures 1-13 and 1-14 is limited by the existence of the atmosphere. The requirement for an orbit which does not approach the earth closer than some specified distance

$$h_{min} = r_{min} - R$$

is shown in figure 1-15 where the ratio

$$\frac{r_{min}}{r_1} = \frac{R + h_{min}}{R + h_1}$$

is plotted as a function of V_1/V_s for various values of γ .

For example, let us assume we have a satellite vehicle which we wish to launch into a circular orbit at 150 miles above the earth, and the maximum expected error in launch

angle ($\Delta \gamma$) is 3 degrees. Let us further assume that we do not want the vehicle to descend below 90 miles. In this case

$$\frac{r_{\min}}{r_1} = \frac{4050}{4110} = 0.9854$$

From figure 1-15 we can see that we need an initial velocity of about $V_1/V_s = 1.05$ or 5 percent above circular satellite velocity to assure that the vehicle does not go below 90 miles.

A small section of figure 1-15 has been replotted in figure 1-16 for values of V_1/V_s in the neighborhood of $V_1/V_s = 1.0$. Also shown in figure 1-16, are the eccentricities and orientation angles associated with the orbits.

In order to obtain a more direct measure of the minimum altitude figure 1-17 is presented to be used in conjunction with figures 1-15 and 1-16. Shown plotted in figure 1-17 is the ratio r_{\min}/r_1 plotted against the minimum altitude h_{\min} for constant values of the launch altitude. For example, if the vehicle were launched at 150 miles altitude at a speed ratio of $V_1/V_s = 1.05$ and $\gamma_1 = 3$ degrees the value of r_{\min}/r_1 from figure 1-15 is $r_{\min}/r_1 = 0.985$. From figure 1-17 we see that the minimum (perigee) altitude will be about 90 miles.

TABLE 1-1a

CONVENIENT FORM FOR CALCULATING CHARACTERISTICS OF ORBITS

FOR THE INITIAL CONDITIONS r_1, v_1, γ_1

$$r = \frac{p}{1 + \epsilon \cos \theta} ; \quad v_s = \sqrt{\frac{g_0 R^2}{r}}$$

$$1. \quad \frac{p}{r_1} = \left(\frac{v_1}{v_s} \right)^2 \cos^2 \gamma_1$$

$$2. \quad \tan \theta_1 = \tan \gamma_1 \left[\frac{p/r_1}{p/r_1 - 1} \right]$$

$$3. \quad \epsilon = \frac{1}{\cos \theta_1} \left[\frac{p}{r_1} - 1 \right]$$

$$4. \quad \tan \gamma = \frac{\epsilon \sin \theta}{1 + \epsilon \cos \theta}$$

$$5. \quad a = \frac{p}{1 - \epsilon^2} ; \quad b = \sqrt{ap}$$

$$6. \quad v^2 = g_0 R^2 \left[\frac{2}{r} - \frac{1}{a} \right]$$

$$7. \quad T = 2\pi \sqrt{\frac{R}{g_0}} \sqrt{\left(\frac{a}{R} \right)^3}$$

TABLE 1-16

FORMULAS FREQUENTLY USED IN ORBIT CALCULATIONS

Total Energy

$$U = \frac{1}{2} mV^2 - \frac{GMm}{r} = -\frac{GMm}{2a}$$

Physical Constants

$$GM = g \cdot R^2 = \mu$$

$$h = r_1 V_1 \cos \gamma_1$$

Characteristic Velocities

Circular Satellite Velocity at Surface of Earth

$$V_0 = \sqrt{g \cdot R}$$

Circular Satellite Velocity

$$V_s = \sqrt{g \cdot \frac{R^2}{r_1^2}}$$

Escape Velocity

$$V_E = \sqrt{2g \cdot \frac{R^2}{r_1^2}}$$

Time Relationships

Time to Reach θ (from perigee)

$$t(\theta) = \frac{C}{1-\epsilon^2} \left[\frac{-\epsilon \sin \theta}{1+\epsilon \cos \theta} + \frac{2}{\sqrt{1-\epsilon^2}} \tan^{-1} \left(\frac{\sqrt{1-\epsilon^2} \tan \frac{\theta}{2}}{1+\epsilon} \right) \right]$$

where

$$C = \frac{p}{R} \sqrt{\frac{p}{g}} = \frac{r_1}{V_s} \left(\frac{V_1}{V_s} \right)^3 \cos^3 \gamma$$

$$= \sqrt{\frac{R}{g}} \left(\frac{a}{R} \right)^3 \sqrt{(1-\epsilon^2)^3}$$

Period

$$T = 2\pi \sqrt{\frac{R}{g}} \sqrt{\left(\frac{a}{R} \right)^3}$$

$$= \frac{2\pi}{(1-\epsilon^2)^{3/2}} \frac{p}{R} \sqrt{\frac{p}{g}}$$

TABLE 1 - 1b CONCLUDED

ELLIPTICAL ORBIT CHARACTERISTICS

<p>Orbit Equation</p> $r = \frac{a(1-\epsilon^2)}{1+\epsilon \cos \theta} = \frac{p}{1+\epsilon \cos \theta}$	<p>Semi-major Axis</p> $a = \frac{R}{2R/r - (V_1/V_0)^2} = \frac{r}{2 - (V_1/V_0)^2} = \frac{p}{1-\epsilon^2}$
<p>Eccentricity</p> $\epsilon = \sqrt{1 + \frac{2U}{m} \left(\frac{K}{GM}\right)^2}$	<p>Semi-minor Axis</p> $b = \sqrt{ap} = a\sqrt{1-\epsilon^2}$
<p>$\epsilon = \sqrt{1 - \left(\frac{r}{R}\right)^2 \left(\frac{V_1^2}{g_0 R}\right) \left[\frac{2}{r/R} - \frac{V_1^2}{g_0 R}\right] \cos^2 \gamma}$</p>	<p>Semi-latus Rectum</p> $p = a(1-\epsilon^2) = \frac{K^2}{GM}$
<p>$\epsilon = \sqrt{1 - \left(\frac{r}{R}\right)^2 \left(\frac{V_1}{V_0}\right)^2 \left[\frac{2}{r/R} - \left(\frac{V_1}{V_0}\right)^2\right] \cos^2 \gamma}$</p>	$= \frac{r_1^2 V_1^2 \cos^2 \gamma_1}{g_0 R^2} = r_1 \left(\frac{V_1}{V_0}\right)^2 \cos^2 \gamma_1$
<p>$\epsilon = \sqrt{1 - \left(\frac{V_1}{V_0}\right)^2 \left[2 - \left(\frac{V_1}{V_0}\right)^2\right] \cos^2 \gamma}$</p>	$= r_p (1-\epsilon) = r_p (1+\epsilon)$
<p>$\epsilon = \left \left(\frac{V_1}{V_0}\right)^2 - 1 \right ; \gamma = 0$</p>	<p>Orbital Velocity</p> $V^2 = g_0 R^2 \left[\frac{2}{r} - \frac{1}{a} \right]$
<p>$\epsilon = \frac{1}{\cos \theta_1} \left[\frac{p}{r_1} - 1 \right]$</p>	
<p>$\epsilon = \frac{\sin \gamma_1}{\sin(\theta_1 - \gamma_1)} = \frac{p}{r_1} \frac{\tan \gamma_1}{\sin \theta_1}$</p>	

Table 1-2

Consistent Set of Numerical Constants for Use in
Orbit Computations

Various reference sources give values of the numerical constants (μ , G , R , and g_0) used in orbit computations, which differ. It would be desirable to adopt a consistent set, that is, a set which satisfies the relation

$$\mu = GM = R^2 g_0$$

The following set is a consistent set.

$G = 3.44 \times 10^{-8} \text{ ft}^4/\text{lb sec}^4$	universal gravitation constant
$= 6.66 \times 10^{-8} \frac{\text{dynes cm}^2}{\text{gm}^2}$	
$\mu = 1.4077 \times 10^{16} \text{ ft}^3/\text{sec}^2$	
$3.986 \times 10^{20} \text{ cm}^3/\text{sec}^2$	
$W = 6.59 \times 10^{21} \text{ short tons}$	weight of earth
$M = 4.092 \times 10^{23} \text{ slugs}$	mass of earth
$g_0 = 32.2 \text{ ft}/\text{sec}^2$	
$R = 3960 \text{ miles}$	radius of earth

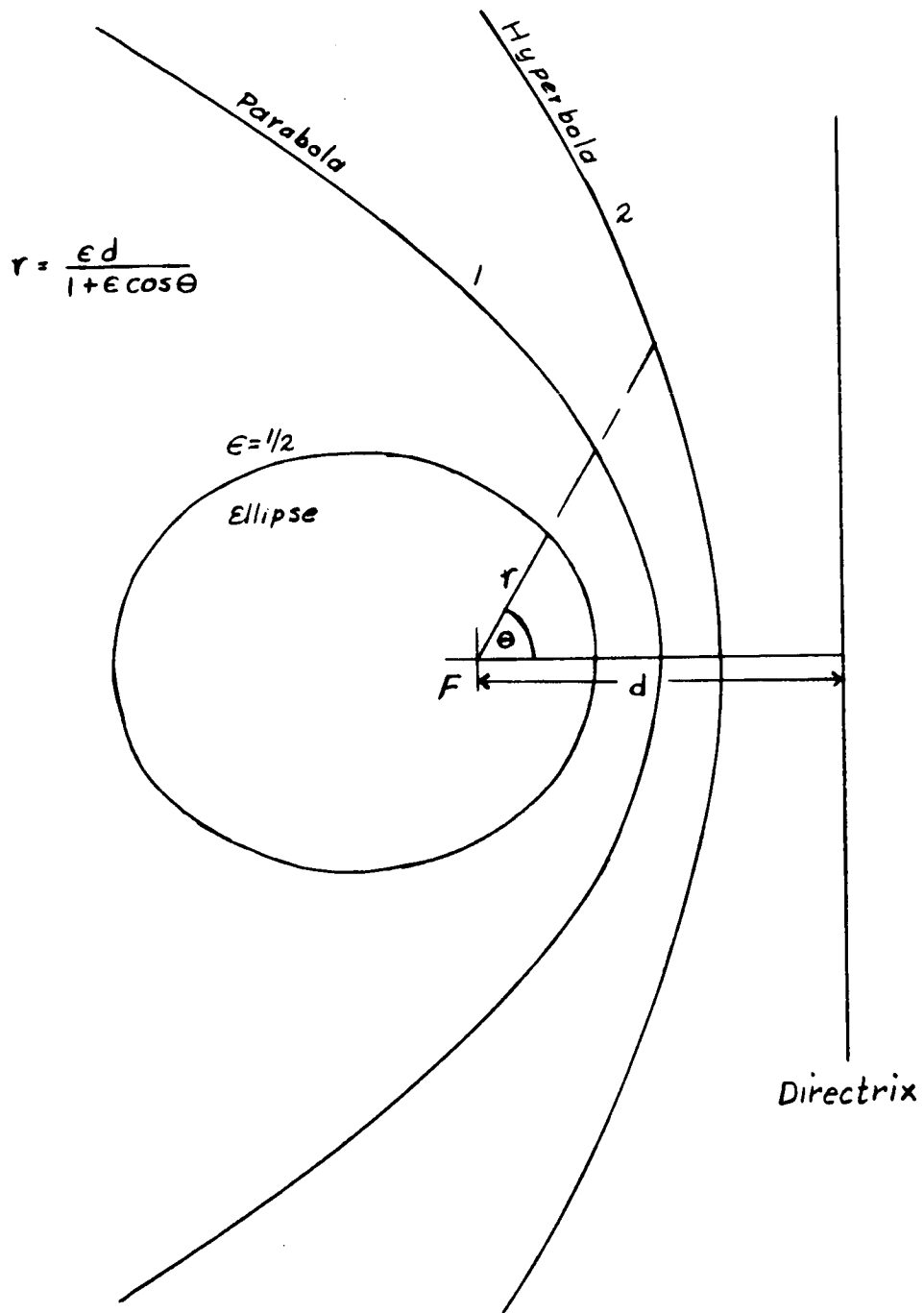


Fig 1-1.- Conic sections, ellipse, parabola, hyperbola

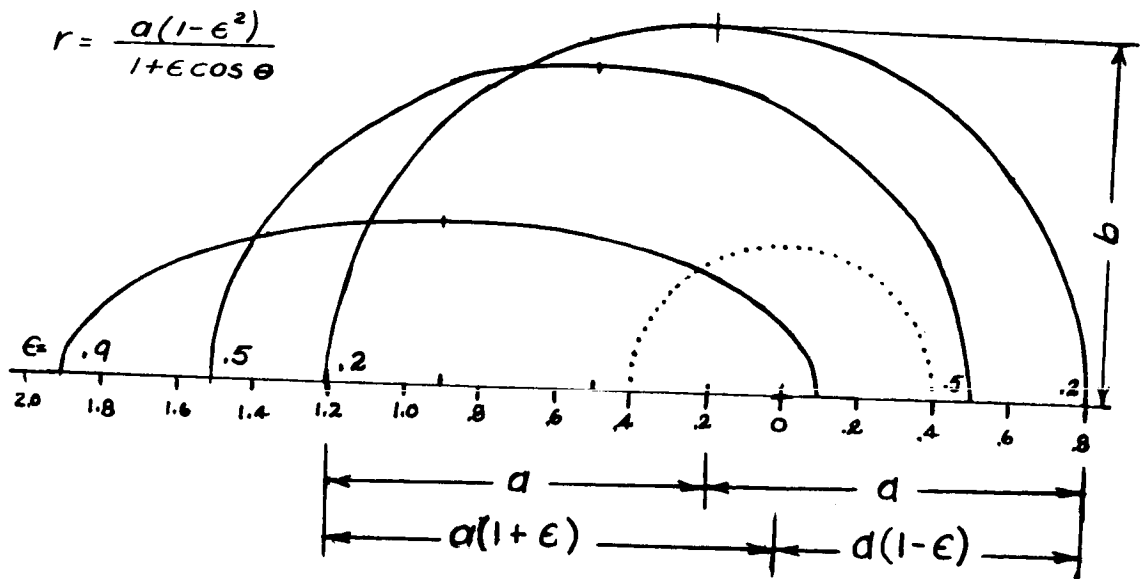
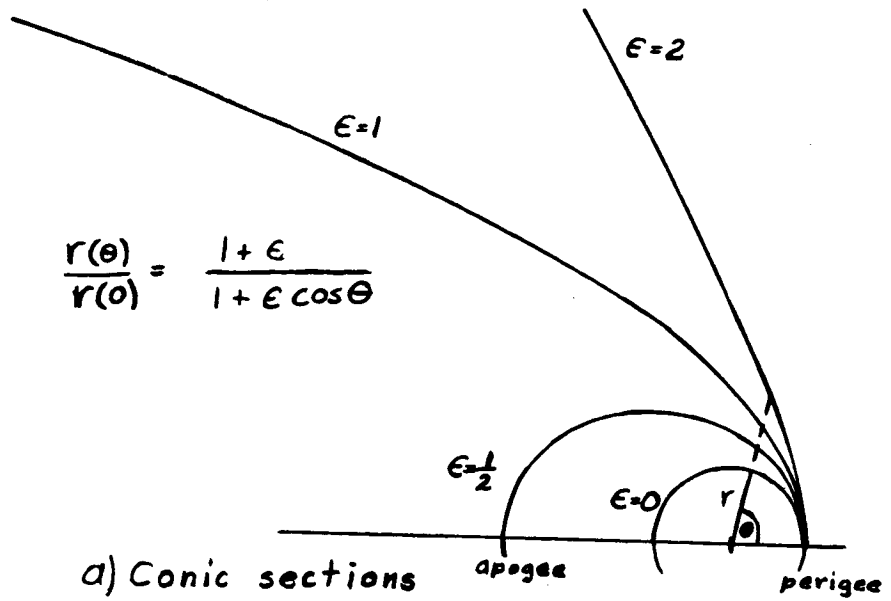
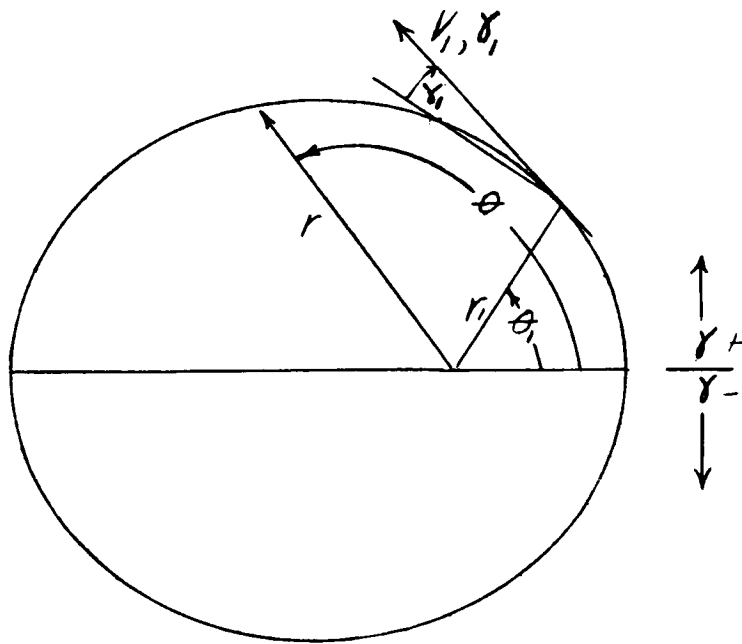


Fig 1-2.- Characteristics and dimensions of various conic sections and ellipses.



$$r = \frac{p}{1 + e \cos \theta}$$

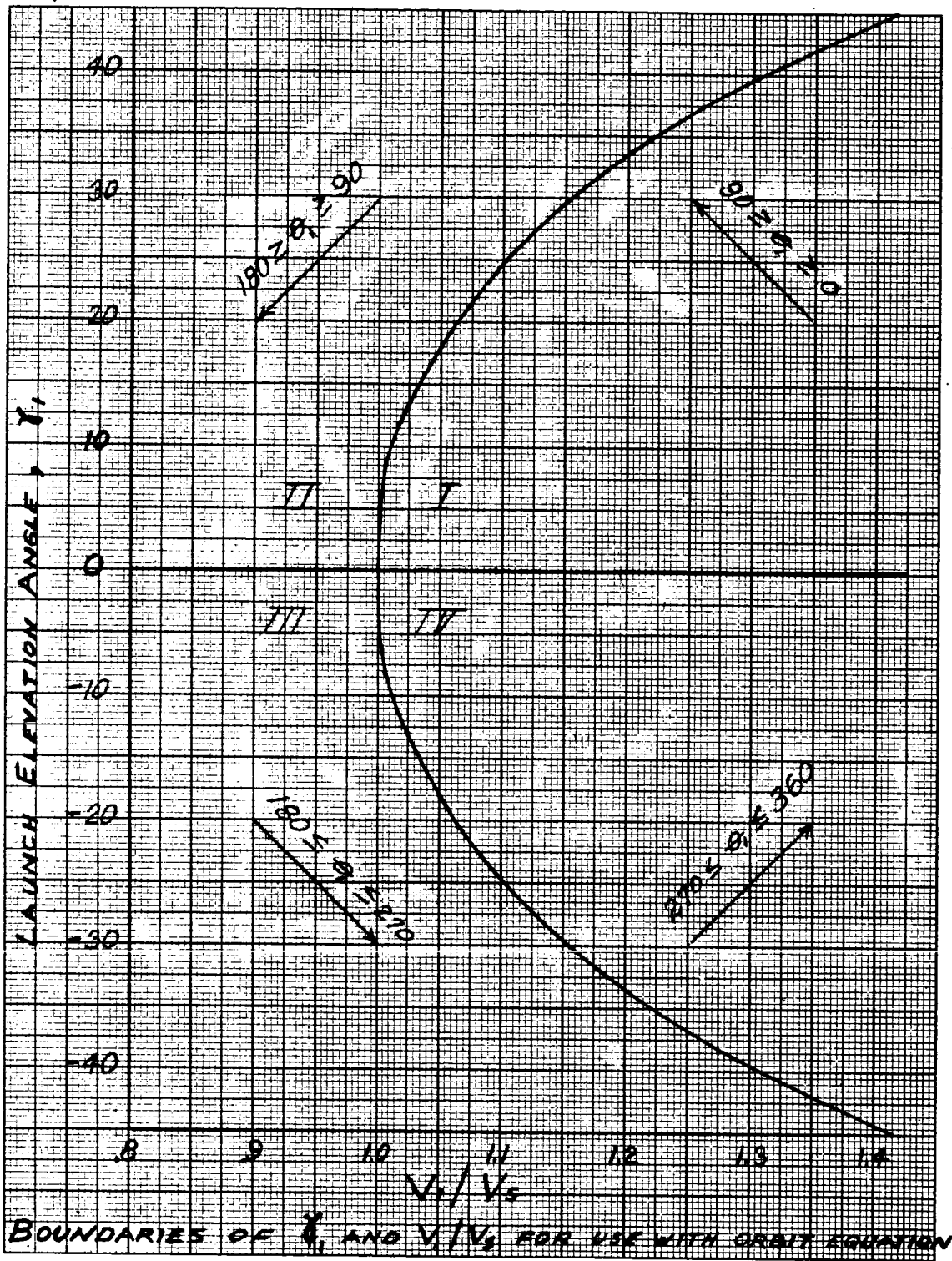
$$p = r_1 \left(\frac{v_1}{v_s} \right)^2 \cos^2 \gamma_1$$

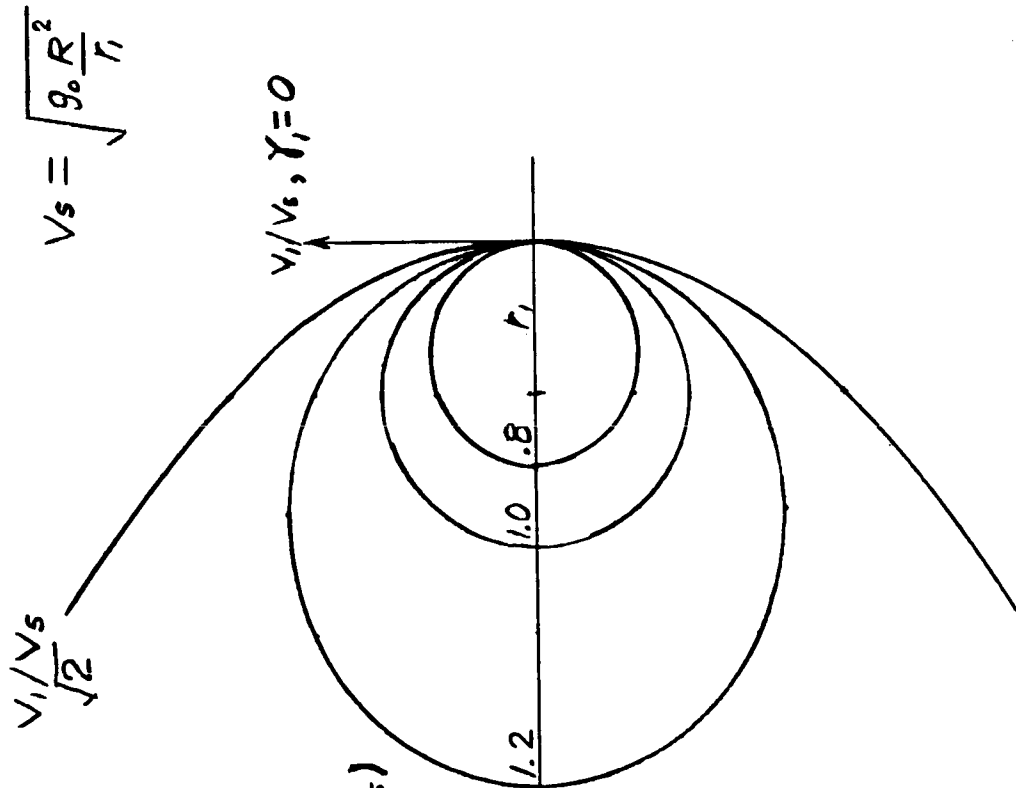
$$\tan \theta_1 = \tan \gamma_1 \left[\frac{p/r_1}{p/r_1 - 1} \right]$$

$$e = \frac{1}{\cos \theta_1} \left[\frac{p}{r_1} - 1 \right]$$

$$\text{when } \gamma_1 = 0, e = \left| \left(\frac{v_1}{v_s} \right)^2 - 1 \right|$$

Fig. 1-3.- Illustration of orbit equation

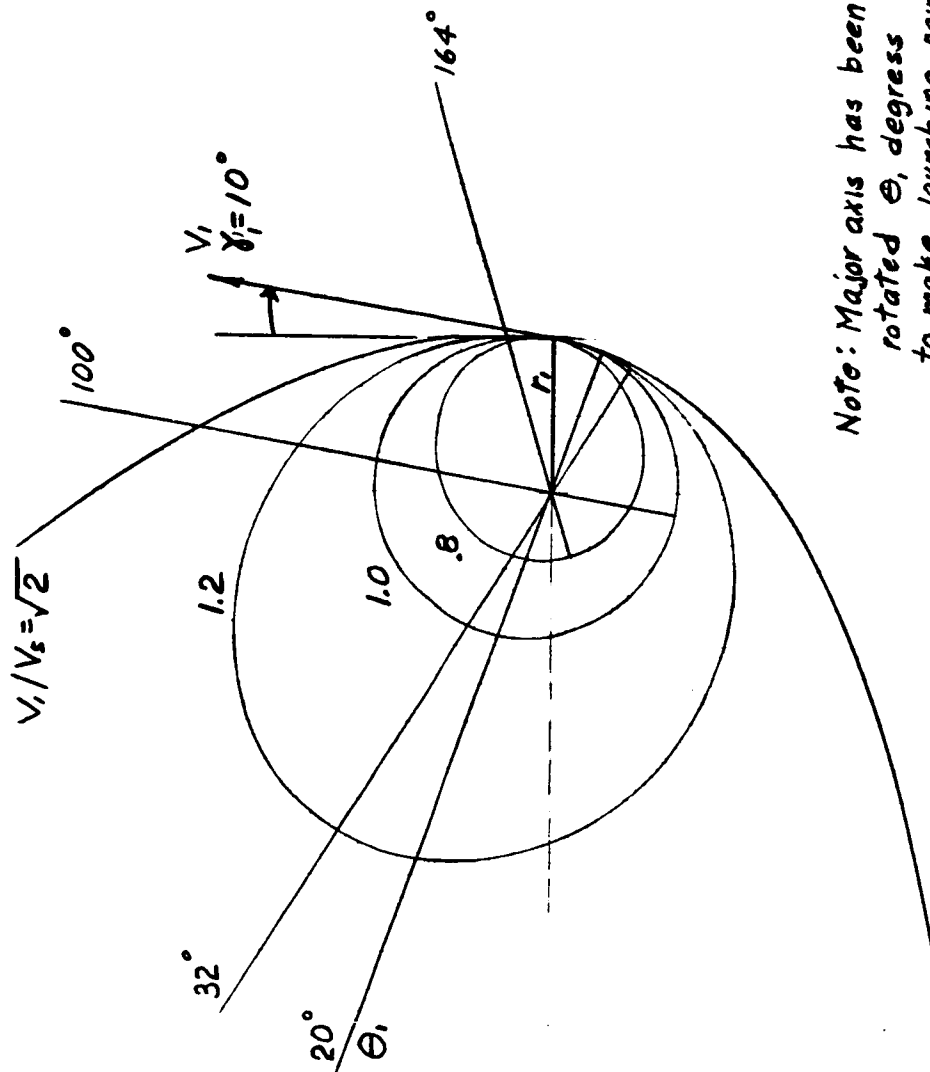




V_1/V_s	ϵ	θ_1	q/r_1
.8	.36	180	.74
1.0	0	0	1.00
1.2	.44	0	1.79
$\frac{1}{\sqrt{2}}$	1	0	-

NOTE: IF $\gamma_1 \neq 0$, $\theta_1 = f(V_1/V_s)$
 THUS ORIENTATION WILL
 VARY AND ϵ WILL BE
 LARGER; q/r_1 WILL NOT
 CHANGE FROM
 VALUES GIVEN

Fig. 1-5- Effect of launch speed on orbits, $\gamma_1 = 0$



Note: Major axis has been rotated θ_1 degrees to make launching points coincident at 0 degrees.

V_1/V_2	ϵ	θ_1	a/r
.8	.39	164	.74
1.0	.17	100	1
1.2	.47	32	1.79
$\sqrt{2}$	1.0	20	-

Fig. 1-6.- Effect of launch speed on orbits, $\gamma_1 = 10^\circ$

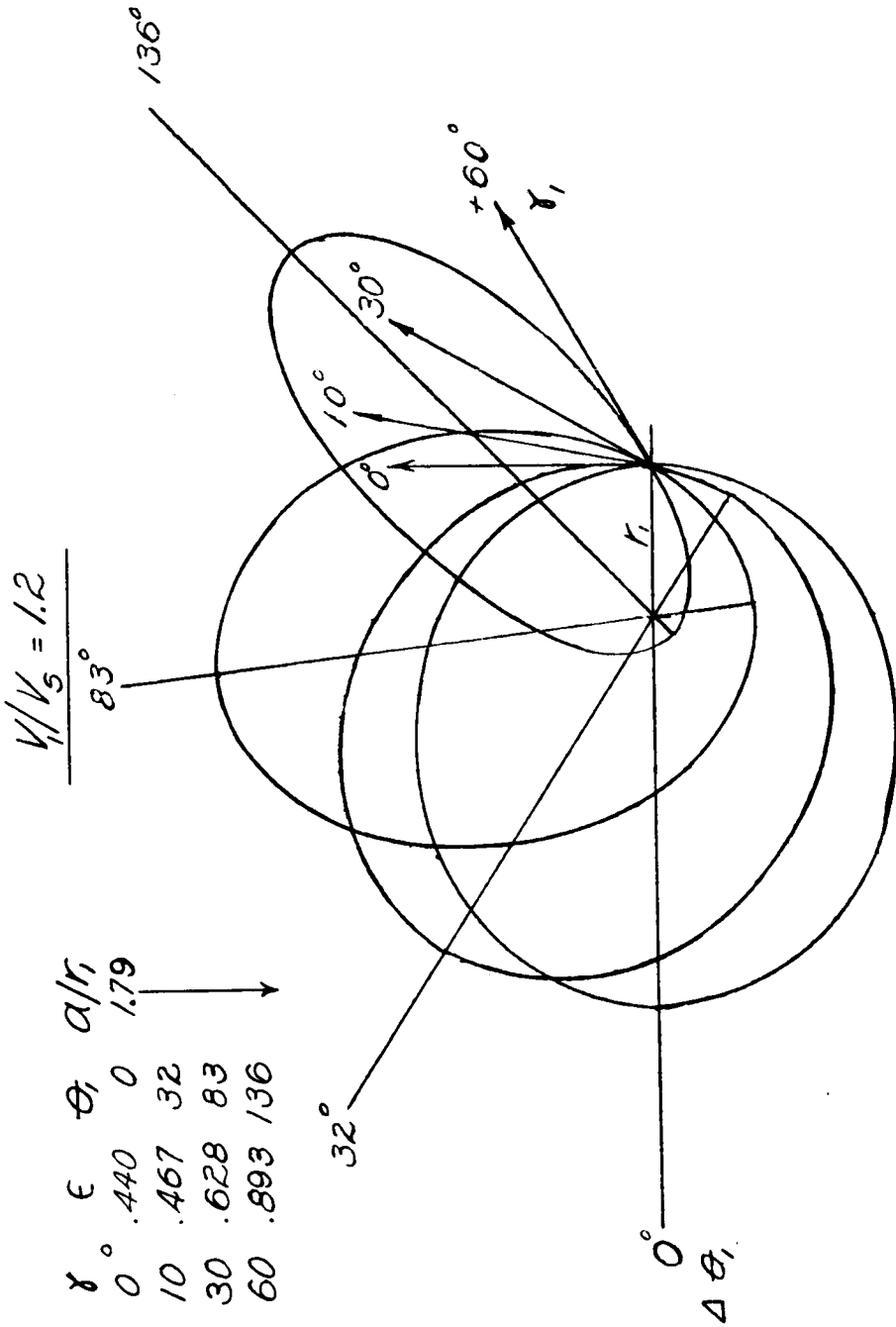


Fig.1-7.- Effect of launch elevation angle on orientation and shape of orbits

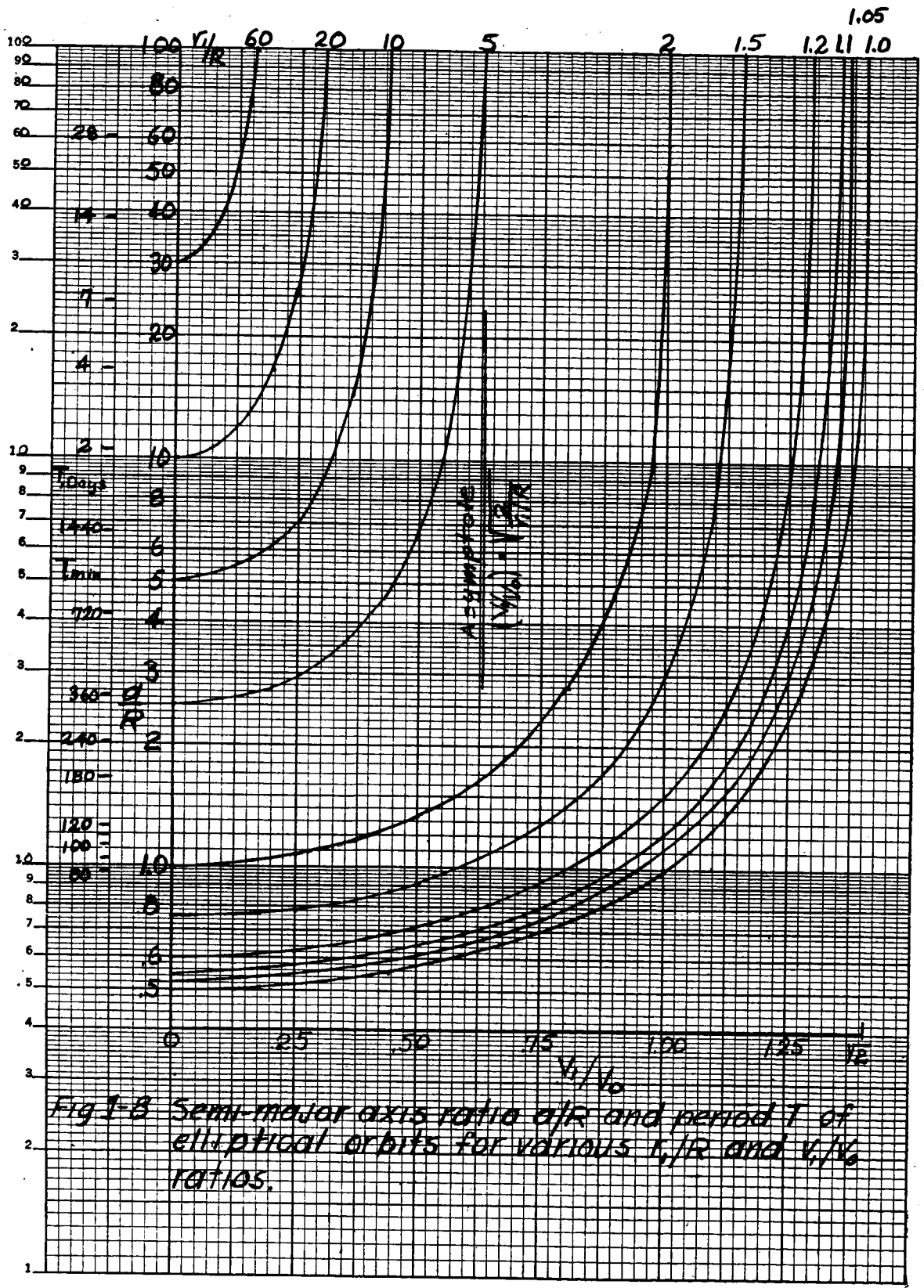


Fig 1-B Semi-major axis ratio a/R and period T of elliptical orbits for various r/R and v/v_0 ratios.

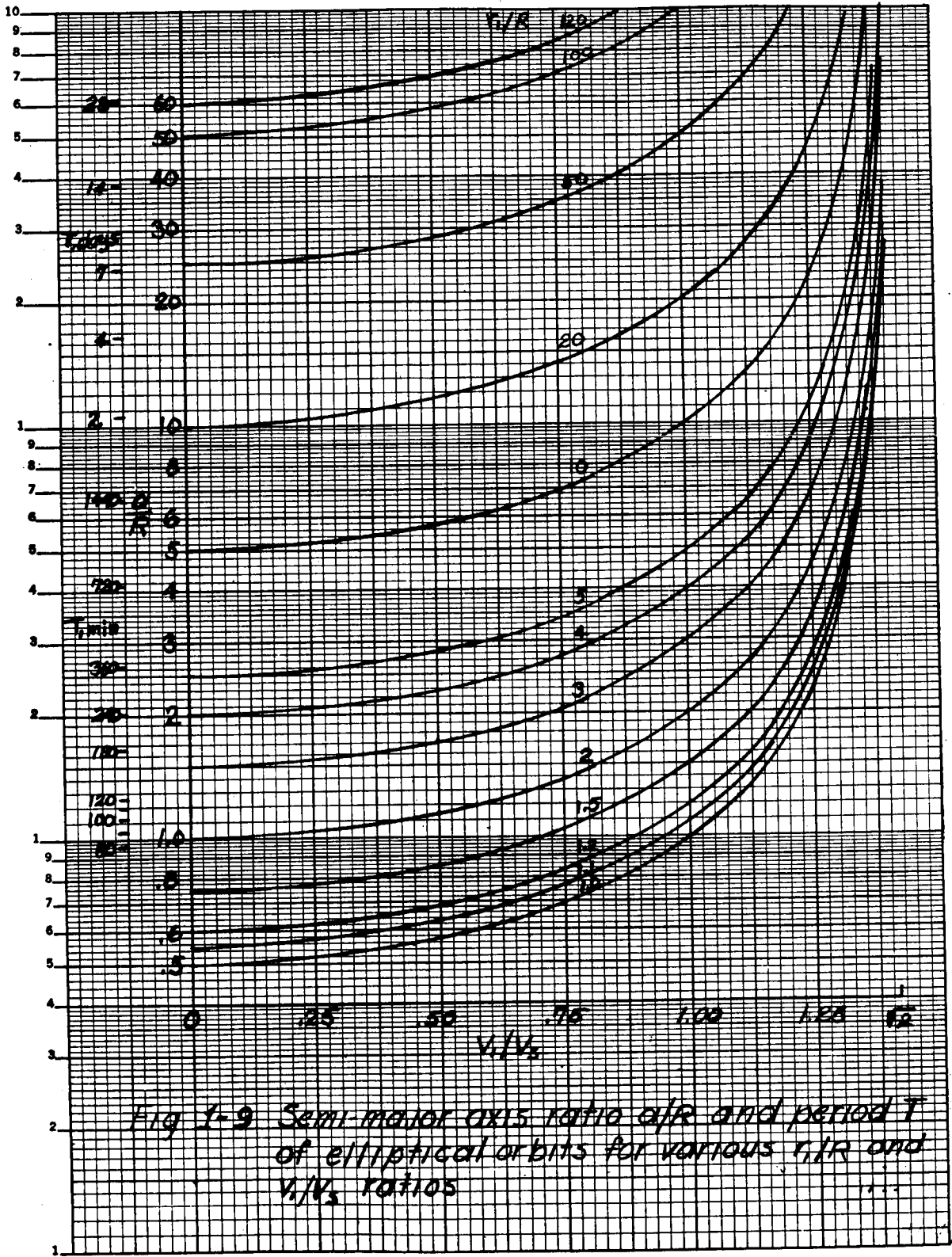


Fig 1-9 Semi-major axis ratio a/R and period T of elliptical orbits for various r/R and v/v_c ratios

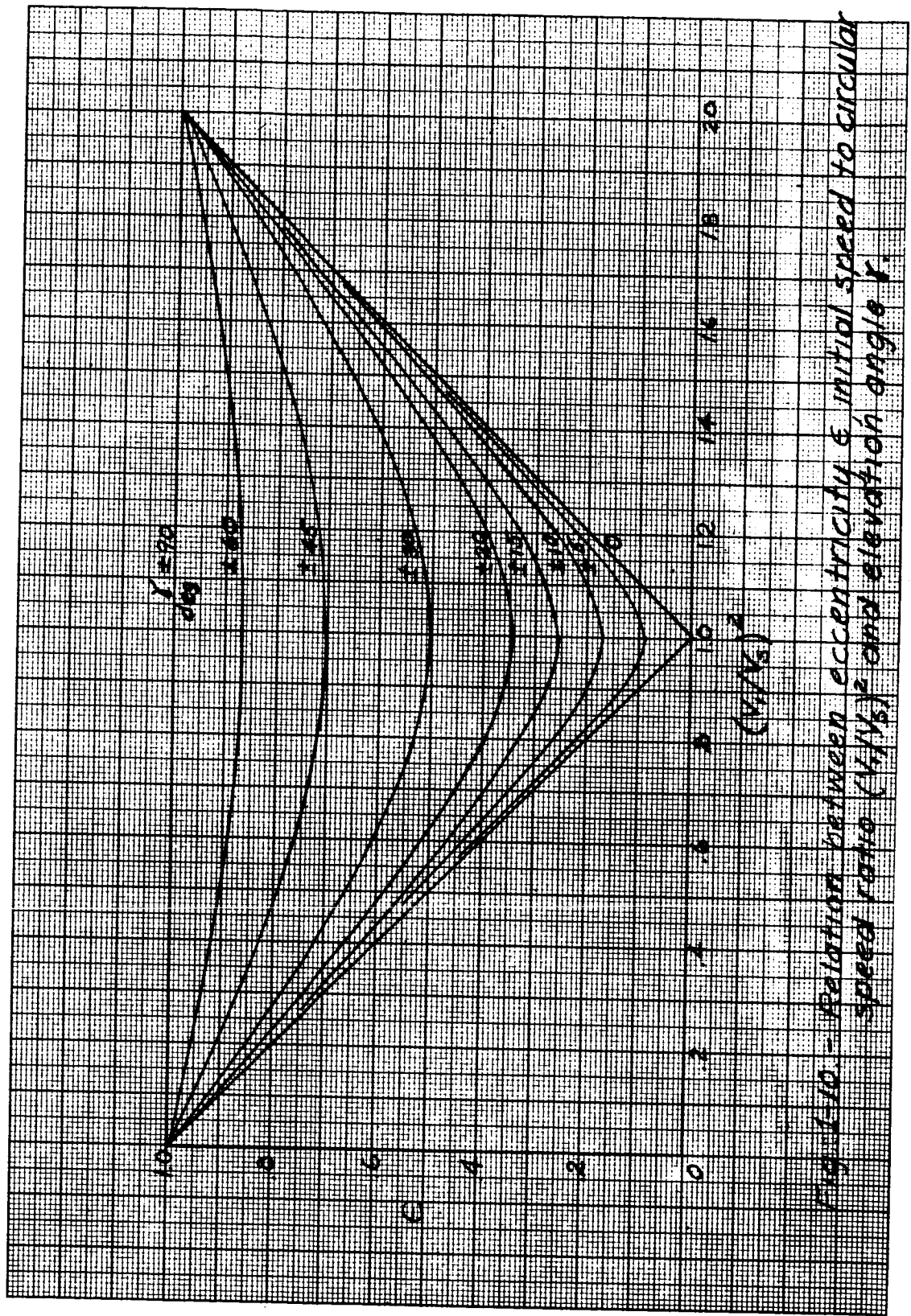


Fig. 6-10 - Relation between eccentricity & initial speed to circular speed ratio $(v/v_c)^2$ and elevation angle γ .

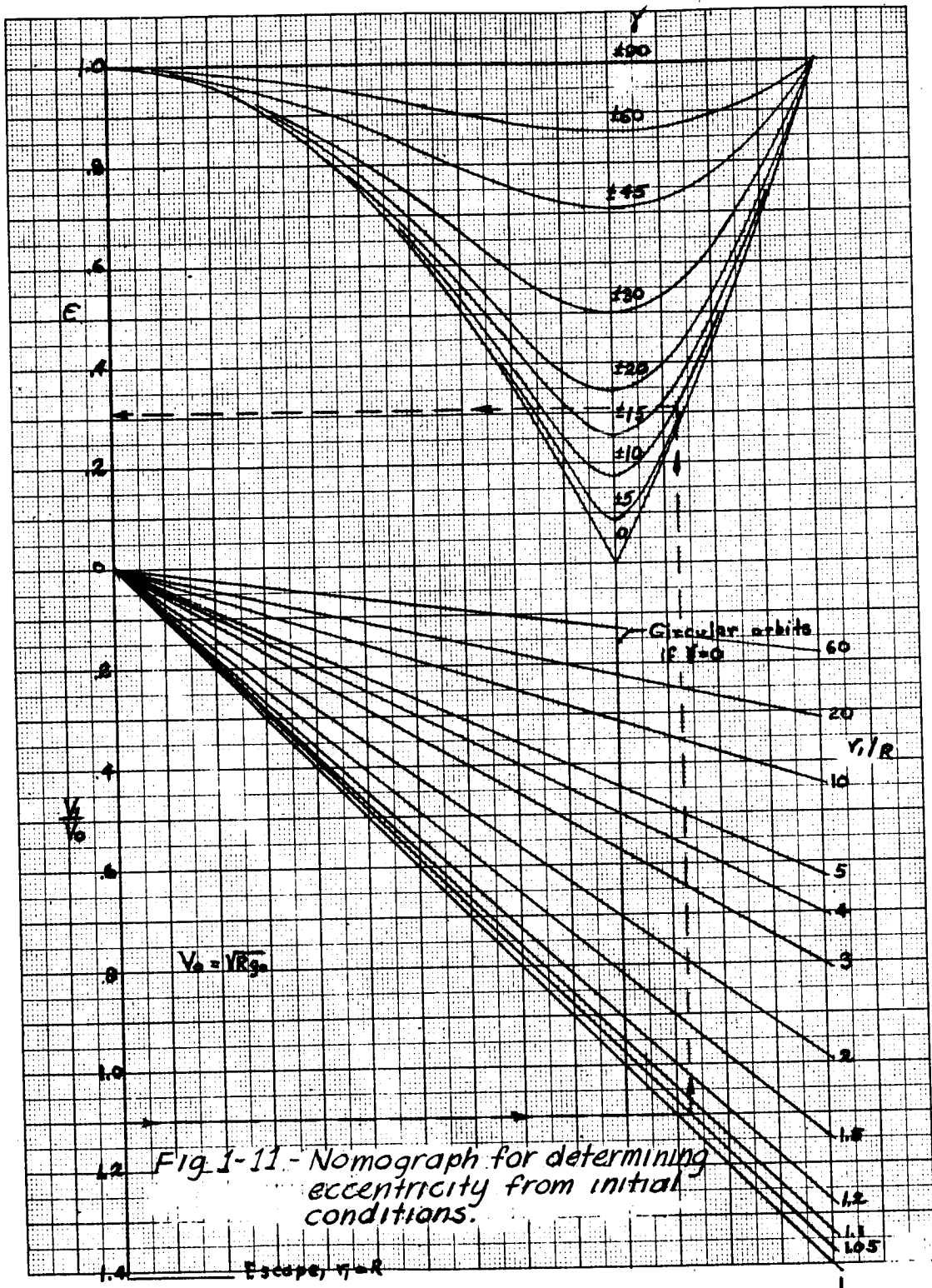
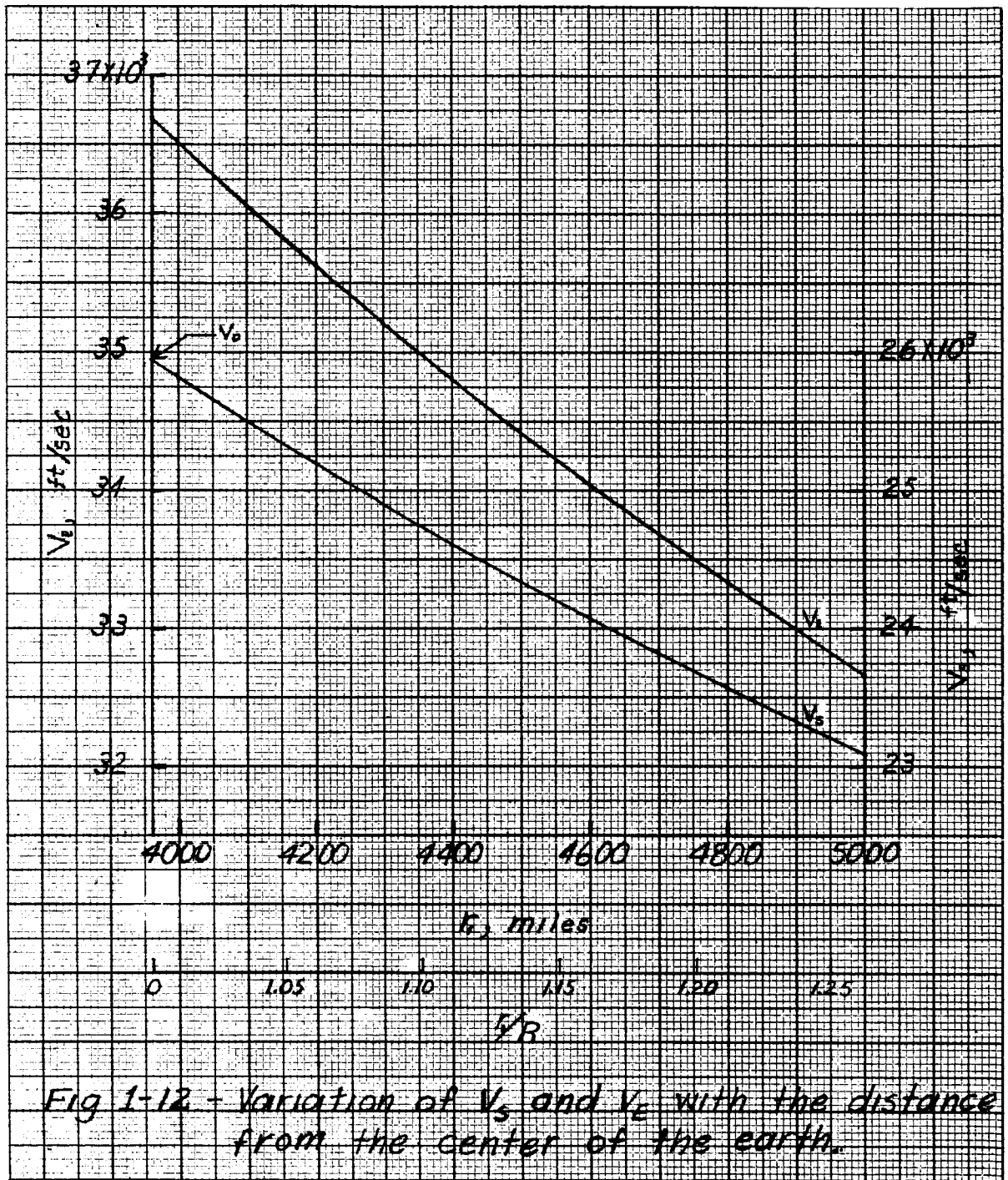


Fig 1-11 - Nomograph for determining eccentricity from initial conditions.

2 b.



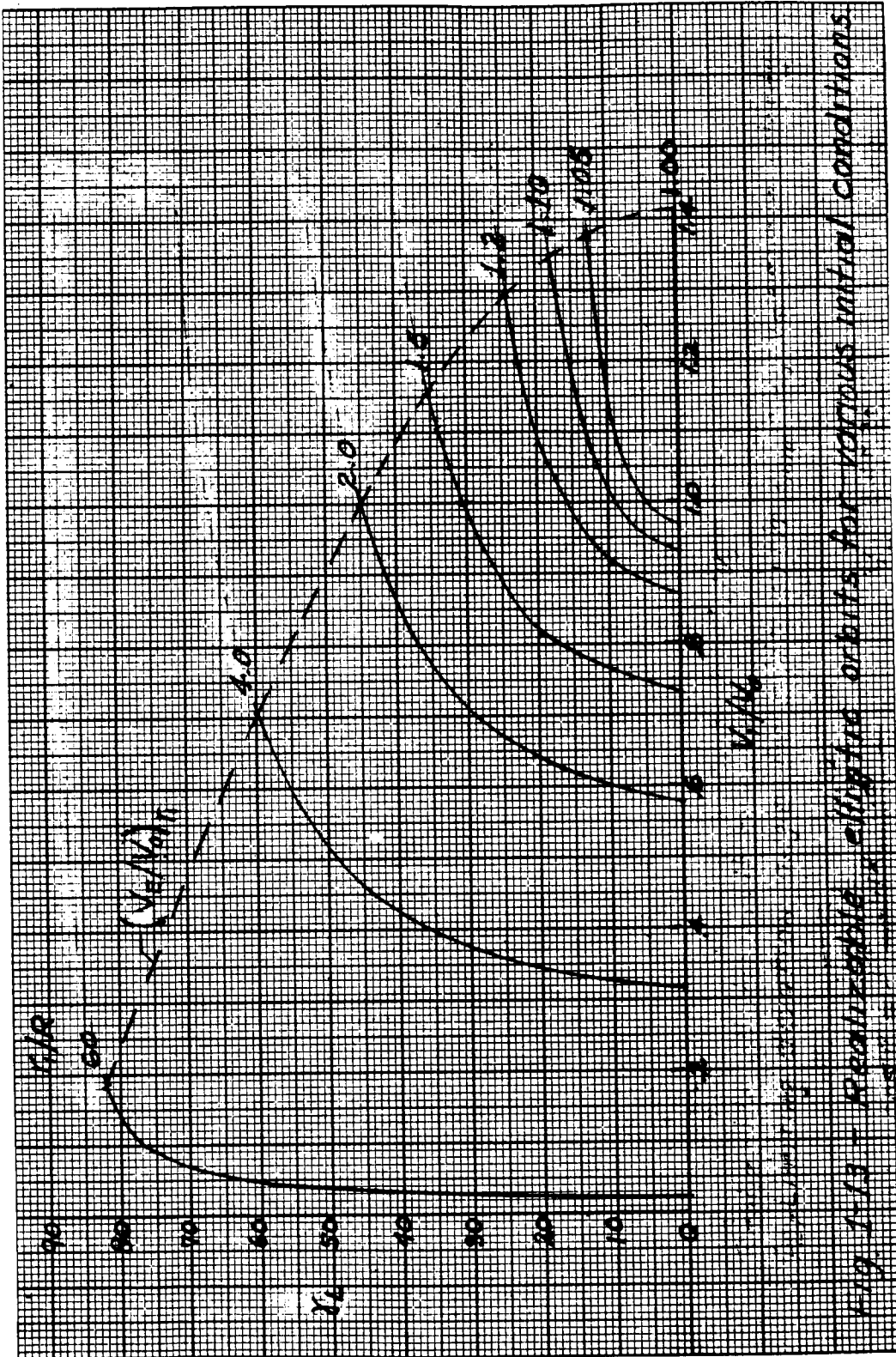


Fig. 1-13 - Realizable elliptic orbits for various initial conditions.

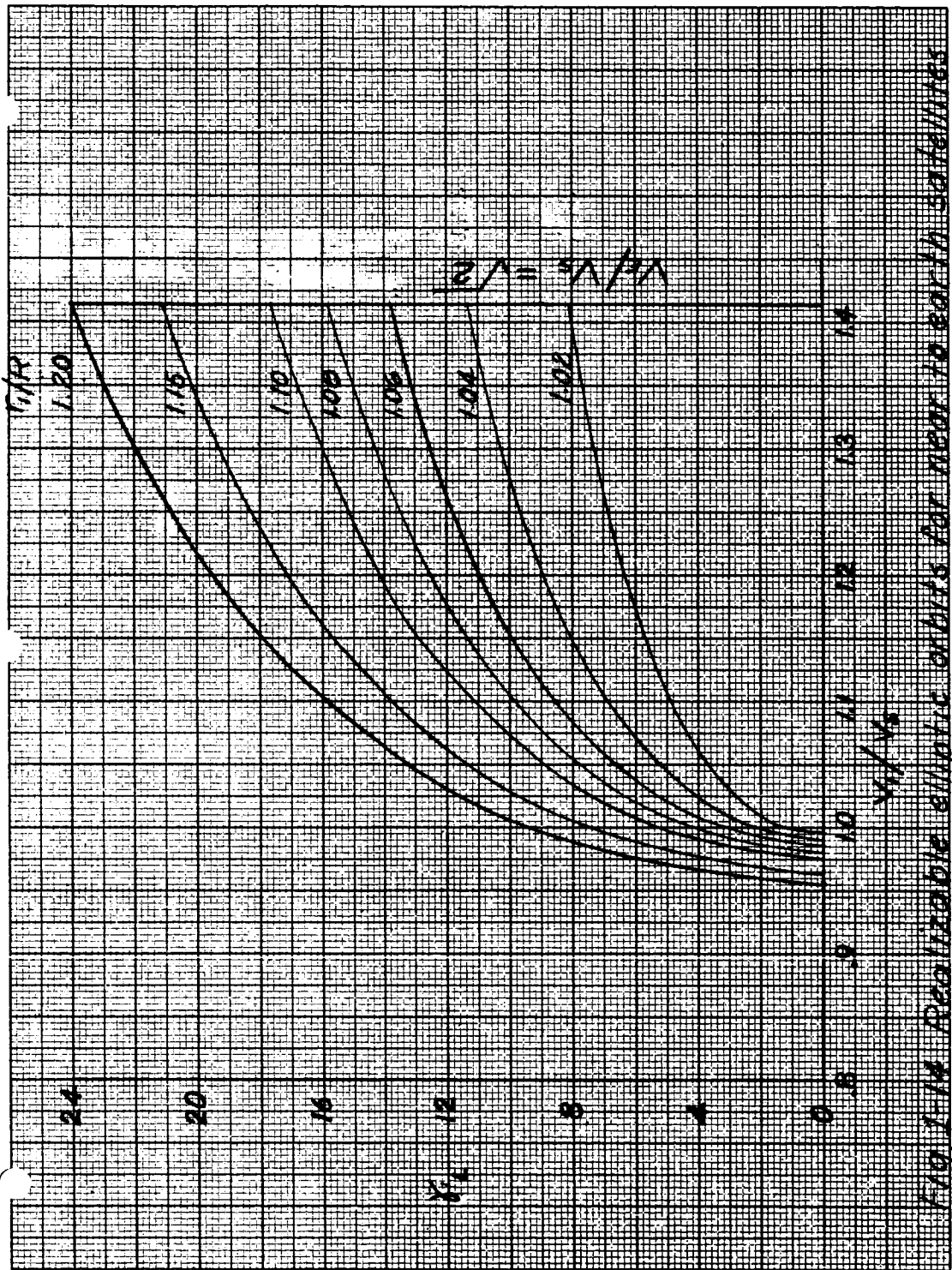


Fig. 1.14 Realizable elliptic orbits for near to earth satellites at various initial conditions.

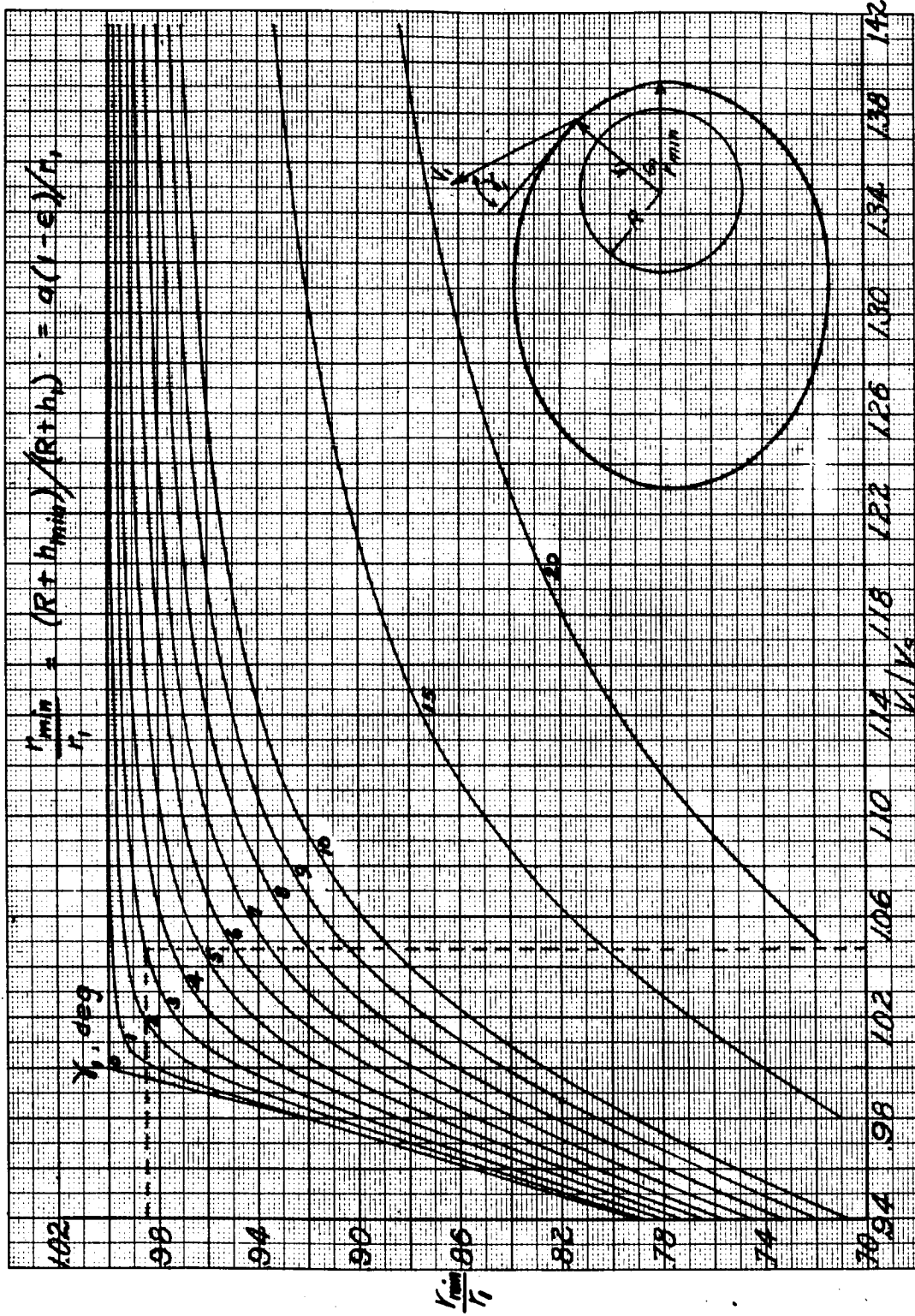


Fig. 1-15- Limiting conditions for launch

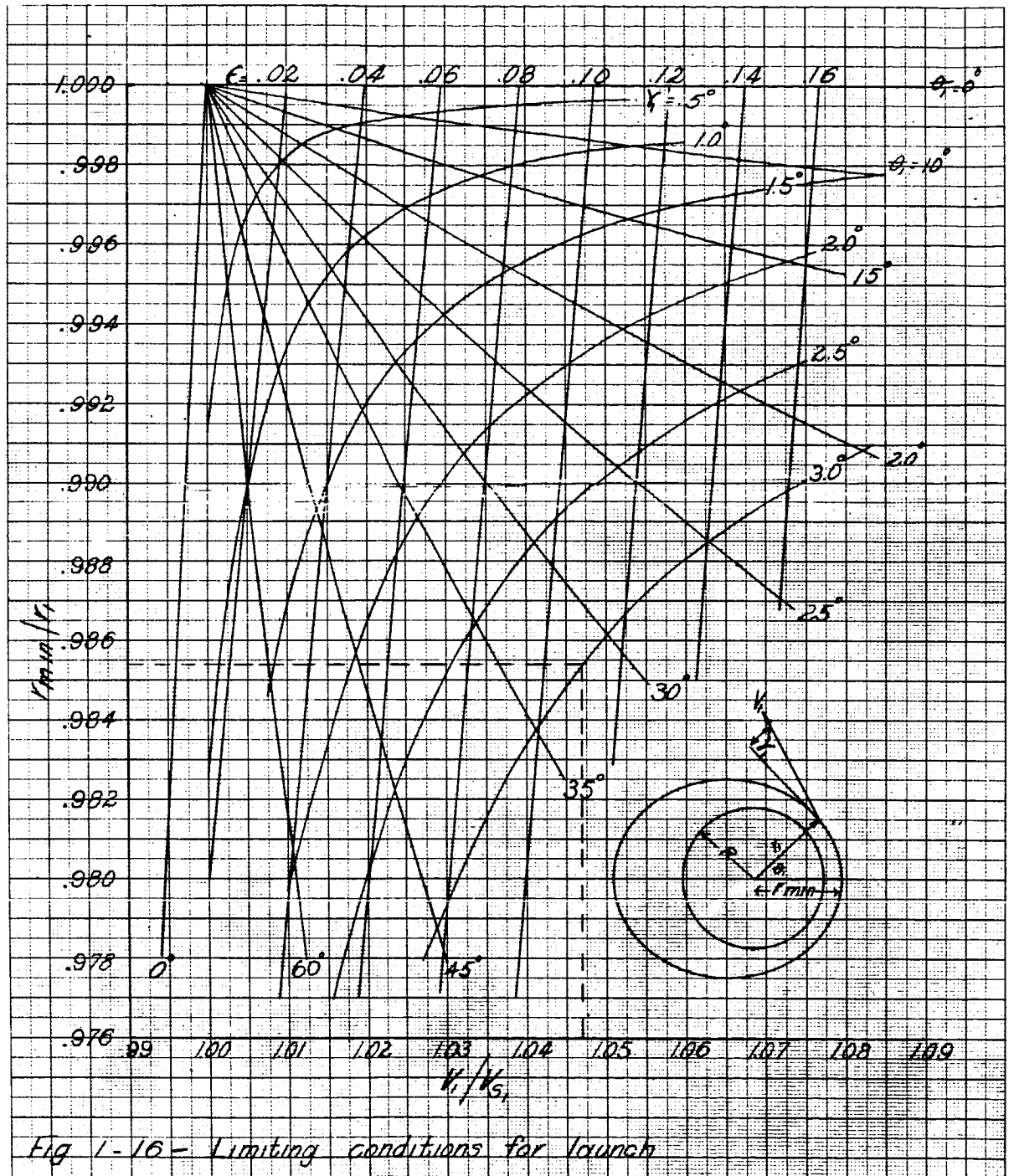


Fig 1-16 - Limiting conditions for launch

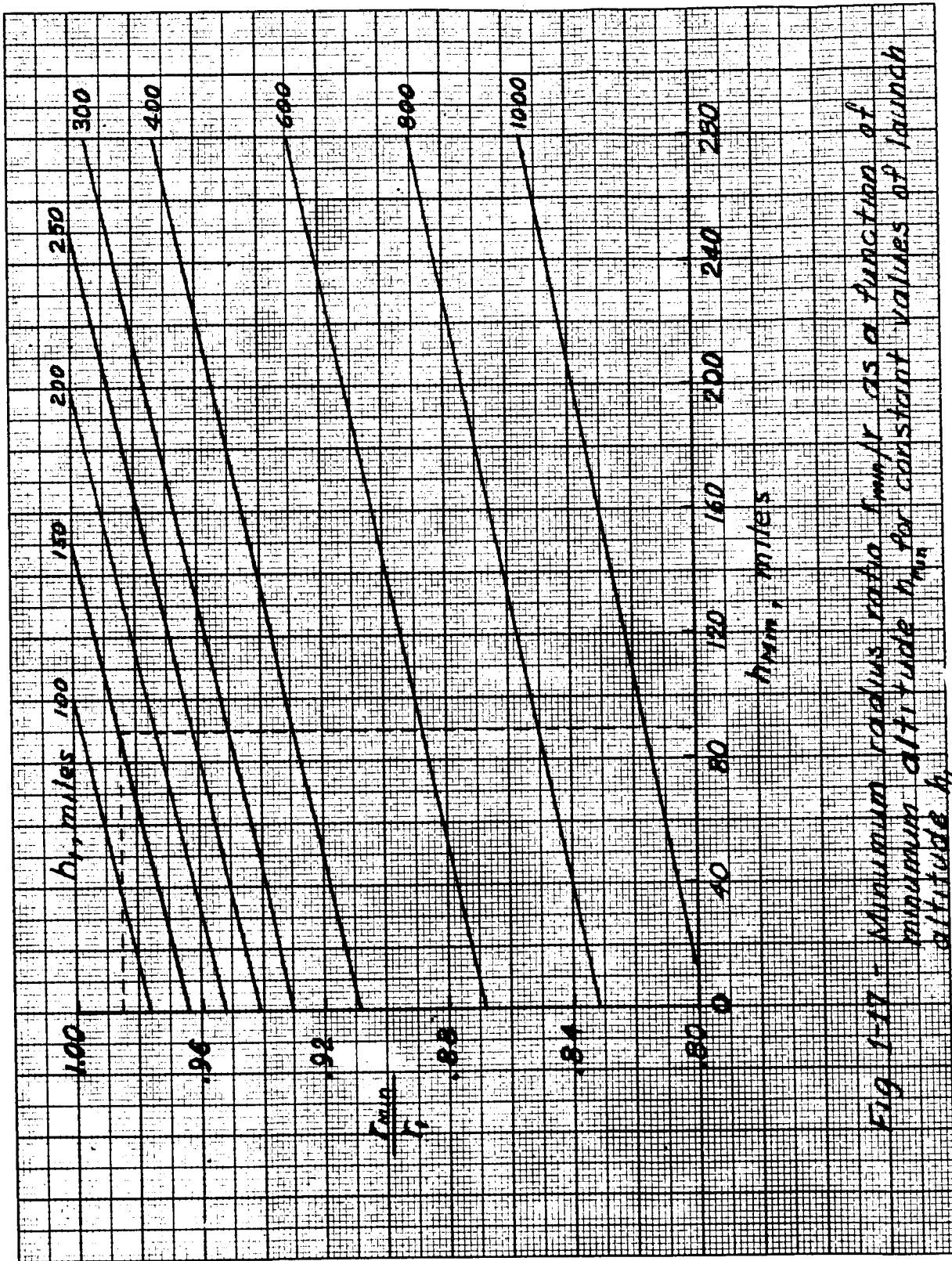


Fig. 1-17 - Minimum radius ratio $\frac{r_{min}}{r}$ as a function of minimum altitude h_{min} for constant values of launch altitude h .

SECTION II

SATELLITE TIME AND POSITION WITH RESPECT
TO A ROTATING EARTH SURFACE

2. Introduction.

It is interesting and often necessary to know the satellite time of passage and its position over a rotating earth surface. The object of this Section is to use the orbit equations presented in the preceding Sections and develop time and position relationships that are a function of the angle in the orbit plane. A brief discussion of some general features of satellite orbits will also be presented.

2.1 Time Relationship

According to the laws of planetary motion, the three initial or launch conditions V_1 , r_1 , and γ_1 , determine the future path of the satellite neglecting drag or accelerating forces acting parallel to its path. From the preceding Sections we know that the satellite will move in an elliptic path

$$r = \frac{a(1 - \epsilon^2)}{1 + \epsilon \cos \theta} \quad (2.1-1)$$

or

$$r = \frac{p}{1 + \epsilon \cos \theta} \quad (2.1-2)$$

We also know that its motion will obey the second of Kepler's Laws that the radius vector sweeps out equal

areas in equal increments of time or

$$r^2 \frac{d\theta}{dt} = K \quad (2.1-3)$$

The value of K is simply twice the area of any triangle described by the radius vector r in a time dt and sweeping through an angle $d\theta$.

Transposing and integrating (2.1-3) we obtain

$$Kt = \int_0^\theta r^2 d\theta \quad (2.1-4a)$$

or

$$t = \frac{1}{K} \int_0^\theta r^2 d\theta \quad (2.1-4b)$$

Substituting equation (2.1-2) into equation (2.1-4b) we see that

$$t = \frac{p^2}{K} \int_0^\theta \frac{d\theta}{(1 + \epsilon \cos \theta)^2} \quad (2.1-5)$$

Integrating and putting in the limits we get the expression for time from the perigee as

$$t(\theta) = \frac{p^2}{K} \frac{1}{(1-\epsilon^2)} \left[\frac{-\epsilon \sin \theta}{1 + \epsilon \cos \theta} + \frac{2}{\sqrt{1-\epsilon^2}} \tan^{-1} \left(\frac{\sqrt{1-\epsilon^2} \tan \theta/2}{1 + \epsilon} \right) \right] \quad (2.1-6)$$

From our previous notes we know that

$$p = a(1 - \epsilon^2) = K^2 / g_0 R^2 \quad (2.1-7)$$

So that equation (2.1-6) can be written as

$$t(\theta) = \frac{K^3}{g_0^2 R^4 (1 - \epsilon^2)} \left[\frac{-\epsilon \sin \theta + 2 \tan^{-1} \left(\frac{\sqrt{1 - \epsilon^2} \tan \theta / 2}{1 + \epsilon} \right)}{1 + \epsilon \cos \theta \sqrt{1 - \epsilon^2}} \right] \quad (2.1-8)$$

If we let

$$C = \frac{K^3}{g_0^2 R^4} \quad (2.1-9)$$

Now from our previous Sections we have the following expressions

$$K = r_1 V_1 \cos \gamma_1 \quad (1.4-3)$$

$$p = r_1 \left(\frac{V_1}{V_s} \right)^2 \cos \gamma_1 \quad (1.5-16)$$

$$g_0 R^2 = V_s^2 r_1 \quad (1.5-19)$$

Thus the value of C can be written in the following forms

$$C = \frac{p}{R} \left(\frac{p}{g_0} \right)^{\frac{1}{2}} \quad (2.1-10a)$$

$$C = \frac{r_1}{V_s} \left(\frac{V_1}{V_s} \right)^3 \cos^3 \gamma_1 \quad (2.1-10b)$$

$$C = \left(\frac{R}{g_0} \right)^{\frac{1}{2}} \left(\frac{a}{R} \right)^{\frac{3}{2}} (1 - \epsilon^2)^{\frac{3}{2}} \quad (2.1-10c)$$

The period is simply the value of $t(\theta)$ for $\theta = 2\pi$
so that from equations (2.1-8) and (2.1-10)

$$T = \frac{2\pi}{(1 - \epsilon^2)^{3/2}} \left[\frac{p^{3/2}}{g_0^{1/2} R} \right] \quad (2.1-11a)$$

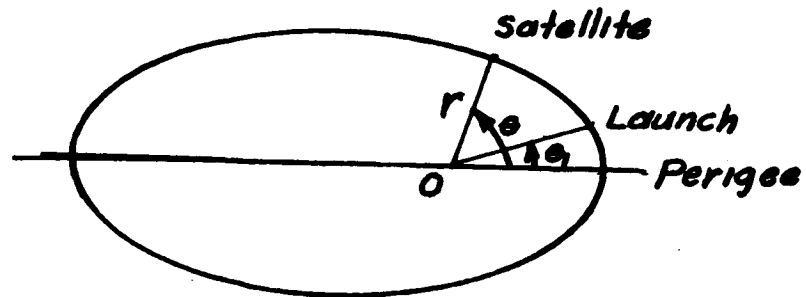
$$T = \frac{2\pi}{(1 - \epsilon^2)^{3/2}} \frac{p}{R} \left(\frac{p}{g_0} \right)^{1/2} \quad (2.1-11b)$$

$$T = 2\pi \sqrt{\frac{R}{g_0}} \sqrt{\left(\frac{a}{R} \right)^3} \quad (2.1-11c)$$

where the semi-major axis

$$a = \frac{p}{1 - \epsilon^2}$$

The previous section on "Orientation of Orbits" shows that perigee point and the launching point are a function of θ_1 as sketched on page 2-5.



The angle between the perigee and the launching point is related to the launching angle γ_1 by

$$\tan \theta_1 = \tan \gamma_1 \left[\frac{p/r_1}{p/r_1 - 1} \right]$$

The time from the perigee to the launching point is simply the value of t from equation (2.1-8) for $\theta = \theta_1$.

Predicting Satellite Position

One of the objectives of the IGY satellite program is to determine the shape of the earth and its gravitational potential. We know that the earth is not a sphere, but

an oblate shape. Consequently an artificial earth satellite is attracted to the earth by a net force that does not vary exactly as the inverse square of the distance from the earth's center and the force is not directed exactly toward the center of the planet. However, for locating manned satellites that may be in orbit for only a few hours or for obtaining useful first approximations of the orbit elements of unmanned satellites the assumption that the earth is a uniform sphere should give results that are reasonably accurate.

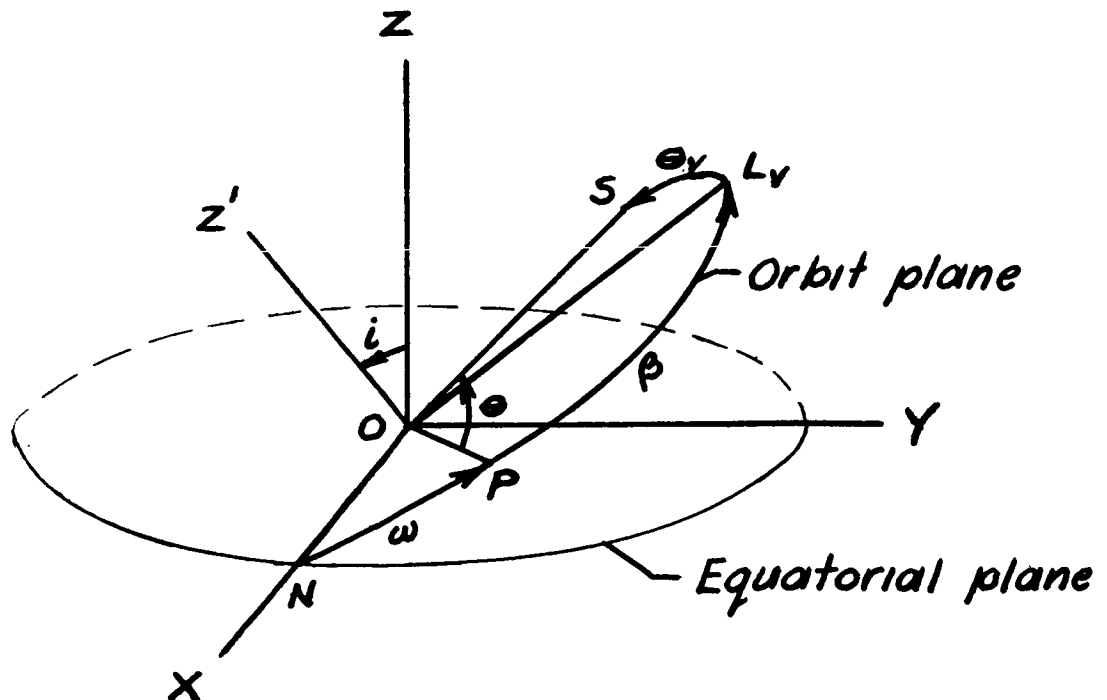
Two methods for obtaining the satellite position can be used both of which produce identical relations provided the same reference positions are used. One method utilizes relationships existing in spherical triangles in locating the orbital plane on the earth surface while a second method uses an equatorial system of co-ordinates used by astrophysical laboratories and other investigators (see reference 1, 2 and 3 for example). Since the second method requires familiarization of vector products which will be discussed in a later section on trajectories, the position relations using spherical triangles will be developed in this section.

2.2 Reference Conditions

Before we establish the reference condition which will enable us to orient ourselves on the projected path of the

satellite, let's familiarize ourselves with how the satellite might move around the earth and let's review some relationships that exist in any spherical triangle.

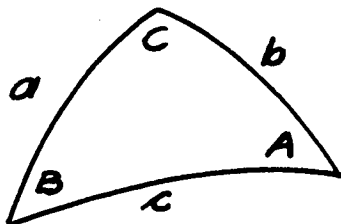
If the earth is taken as a sphere the plane of the satellite orbit remains fixed in direction and the notation shown in figure 2.1 is chosen to take advantage of this fact. The inclination angle i of the orbit plane or the maximum latitude reached and the point N at which the satellite crosses the equator from South to North specify the orientation of the orbital plane in space. The following additional notations are presented for orientation in the equatorial and orbital planes.



where

- O - is the center of the earth
- XOY - is the plane of the earth's equator
- OX - is directed towards the point where the satellite crosses the equator going North
- OZ - points to the North pole
- N - point at which the satellite crosses the equator from South to North and is called the ascending node
- P - perigee location
- ω - angle NOP measured in the orbit plane from where the satellite crosses the equator to the perigee
- L_v - vertex or maximum latitude reached by the satellite (the point where the orbit cuts the plane OYZ)
- β - angle in orbit plane between perigee and the apex or maximum latitude reached by the satellite ($\omega + \beta = 90^\circ$)
- S - any subsequent position of the satellite
- θ_v = angle in orbital plane from the apex to the subsequent position S of the satellite
- θ - angle in orbital plane measured from the perigee ($\theta = \beta + \theta_v$) (usually called the true anomaly angle)
- i - inclination angle of the orbit plane

To derive the relation between the latitude, longitude, and the angle θ_V we use the following spherical triangle relations



Where A, B, and C are three angles and a, b, and c are the arc lengths of the opposite sides. From the sine law we know that

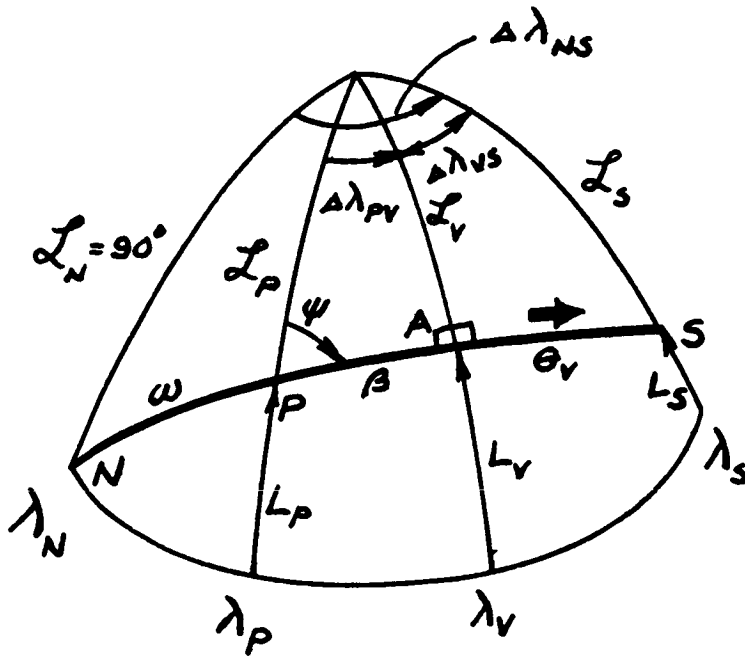
$$\frac{\sin A}{\sin a} = \frac{\sin B}{\sin b} = \frac{\sin C}{\sin c}$$

and from the cosine laws

$$\cos a = \cos b \cos c + \sin b \sin c \cos A$$

$$\cos C = -\cos A \cos B + \sin A \sin B \cos c$$

If we know two sides and one angle or two angles and one side we can solve for the unknown side or angle. The following additional notations are presented for defining the various additional elements



where the elements not defined previously are

A - apex or vertex angle = 90°

ψ - angle measured from the North to satellite position at perigee

$\Delta\lambda_{PV}$ - difference in longitude from perigee to vertex $\Delta\lambda_{PV} = \lambda_P - \lambda_V$

$\Delta\lambda_{VS}$ - difference in longitude from vertex to satellite $\Delta\lambda_{VS} = \lambda_V - \lambda_S$

$\Delta\lambda_{NS}$ - difference in longitude from nodal point N and the satellite $\Delta\lambda_{NS} = \lambda_N - \lambda_S$

L - latitude measured North or South of the equator

\mathcal{L} - colatitude = $(90 - L)$

λ - longitude measured East or West of the prime meridian at Greenwich

Subscripts refer to particular position in orbit plane.

From the sine law

$$\frac{\sin A}{\sin (90 - L_p)} = \frac{\sin \psi}{\sin (90 - L_v)} = \frac{\sin \psi}{\sin (90 - i)}$$

Since the apex or vertex angle $A = 90^\circ$

$$\text{and } \sin (90 - L) = \cos L$$

then

$$\boxed{\sin \psi = \frac{\cos i}{\cos L_p}} \quad (2.2-1)$$

From the cosine law for two sides and one angle

$$\begin{aligned} \cos (90 - L_p) &= \cos (90 - i) \cos \beta \\ &+ \sin (90 - i) \sin \beta \cos 90^\circ \end{aligned}$$

$$\text{or } \sin L_p = \sin i \cos \beta$$

$$\text{and } \boxed{\cos \beta = \frac{\sin L_p}{\sin i}} \quad (2.2-2)$$

From the cosine law for two angles and one side

$$\cos \Delta \lambda_{pv} = -\cos 90^\circ \cos \psi + \sin 90^\circ \sin \psi \cos \beta$$

$$\boxed{\cos \Delta \lambda_{pv} = \sin \psi \cos \beta}$$

(2.2-3)

2.3 Position from Nodal Point

For any other latitude and longitude location from the ascending node position N on the equator the following quantities for a non-rotating earth are derived:

Latitude*

From the cosine law

$$\cos(90 - L_s) = \cos(90 - l) \cos \theta_v$$

or

$$\sin L_s = \sin l \cos \theta_v$$

$$\cos \theta_v = \frac{\sin L_s}{\sin l}$$

(2.3-1)

now from our previous notations we know that

$$\omega + \beta = 90^\circ$$

and

$$\theta_v = \theta - \beta$$

- * 1. Latitude on the earth surface is directly related to declination which is reckoned in degrees North and South of the celestial equator.

then

$$\theta_v = (\omega + \theta) - 90$$

$$\theta_v = -[90 - (\omega + \theta)]$$

so

$$\cos \theta_v = \sin(\omega + \theta) \quad (2.3-2)$$

and

$$\sin \theta_v = -\cos(\omega + \theta) \quad (2.3-3)$$

Substituting (2.3-2) into (2.3-1) we get the latitude of the satellite.

$$\boxed{\sin L_s = \sin i \sin(\omega + \theta)} \quad (2.3-4)$$

Longitude**

From the sine law

$$\frac{1}{\sin(90 - L_s)} = \frac{\sin \Delta \lambda_{vs}}{\sin \theta_v}$$

we get that

$$\sin \Delta \lambda_{vs} = \frac{\sin \theta_v}{\cos L_s} \quad (2.3-5)$$

- ** 2. Longitude on the earth surface is related to the right ascension, the hour angle and sidereal time in the equatorial system of coordinates.

since

$$\Delta \lambda_{NS} = 90^\circ + \Delta \lambda_{VS}$$

or

$$\Delta \lambda_{VS} = -[90^\circ - \Delta \lambda_{NS}]$$

then

$$\sin \Delta \lambda_{VS} = -\cos \Delta \lambda_{NS} \quad (2.3-6)$$

substituting (2.3-6) and (2.3-3) into (2.3-5) we get

$$\cos \Delta \lambda_{NS} = \frac{\cos(\omega + \theta)}{\cos L_s} \quad (2.3-7)$$

Equation (2.3-7) can be put into a more convenient form by writing it as

$$\frac{\sin \Delta \lambda_{NS}}{\tan \Delta \lambda_{NS}} = \cos(\omega + \theta) \frac{\tan L_s}{\sin L_s} \quad (2.3-7a)$$

It can very easily be shown by dotting a unit vector along the normal to the orbital plane into a unit vector along a line drawn from the center of the earth to the satellite position that

$$\sin \Delta \lambda_{NS} = \frac{\tan L_s}{\tan i} \quad (2.3-8)$$

Substituting (2.3-8) and (2.3-4) into (2.3-7a) we get

$$\frac{\tan L_s}{\tan \Delta \lambda_{NS} \tan i} = \cos(\omega + \theta) \frac{\tan L_s}{\sin i \sin(\omega + \theta)}$$

or

$$\tan \Delta \lambda_{NS} = \frac{\sin i}{\tan i} \tan(\omega + \theta)$$

So the longitude of the satellite for a non-rotating earth is given by

$$\Delta \lambda_{NS} = \tan^{-1} [\cos i \tan(\omega + \theta)] \quad (2.3-9)$$

Since only the longitude position of the satellite is affected by the earth's rotation the final expression for the longitude position from the nodal point is

$$\Delta \lambda_{NS} = \tan^{-1} [\cos i \tan(\omega + \theta)] \pm \omega_e t(\theta) \quad (2.3-10)$$

where

- ω_e - rotational velocity of the earth
equal to $15^\circ/\text{hour}$ or $0.25^\circ/\text{min}$
- $t(\theta)$ - time from perigee given by equation
(2.1-8)

The sign of the $\omega_e t(\theta)$ term is negative for satellites launched East or with the earth's rotation and positive for launchings to the West. Since equations (2.3-4) and (2.3-10) relate the latitude and longitude as a function

of the angle θ in the orbit plane and time is a function of θ from equation (2.1-8) then equations (2.3-4) and (2.3-10) are obviously also a function of time. Once the longitude position of the nodal point N is established with reference to Greenwich then a plot of $L_s(t)$ as the ordinate and $\lambda(t)$ as the abscissa is useful in locating the satellite on a Mercator projection. Each successive orbit is displaced in longitude by

$$\Delta\lambda = \pm\omega_e T$$

where the period 'T' is calculated from equation (2.1-11).

A few words about the earth's rotational velocity before some typical results are presented. We know that the earth's rotational velocity at the equator is

$$v_{\text{equator}} = \frac{2\pi R}{24} = 1037.6 \text{ mi/hr}$$

The rotational velocity at any latitude L above or below the equator for a given angle ψ measured from the North is

$$v_L = 1037.6 \cos L \sin \psi$$

Then for a given latitude you gain the most benefit from the earth's rotation by launching due East ($\psi = 90^\circ$)

2.4 Typical results

Typical results are presented to illustrate the application of the above developed procedure. The example presented is for the following specified requirements:

1. The satellite height, h_1 above the launching point is to be 150 miles. The launching velocity, V_1 should be great enough to tolerate an initial flight path angle γ_1 of $\pm 3^\circ$ and a minimum radius over the launching radius r_{\min}/r_1 ratio of 0.986.
2. The launching angle should be such that the satellite comes directly over the launch position at Cape Canaveral, Florida on the second orbit around the earth.

The orbit characteristics for the above requirements using equations (1.5-17) from the previous Section are tabulated below

Orbit

Launching radius $r_1 = 4113$ miles

Launching velocity ratio, $\frac{V_1}{V_s} = 1.05$

Initial flight path angle, $\gamma_1 = 0$

Angle between perigee and launching point, $\theta_1 = 0$

Semi-latus rectum, $p = 4,535$ miles

Eccentricity, $\epsilon = 0.1025$

Perigee distance, $r_p = 4,113$ miles ($h_p = 150$ miles)

Apogee distance, $r_a = 5,053$ miles ($h_a = 1,090$ miles)

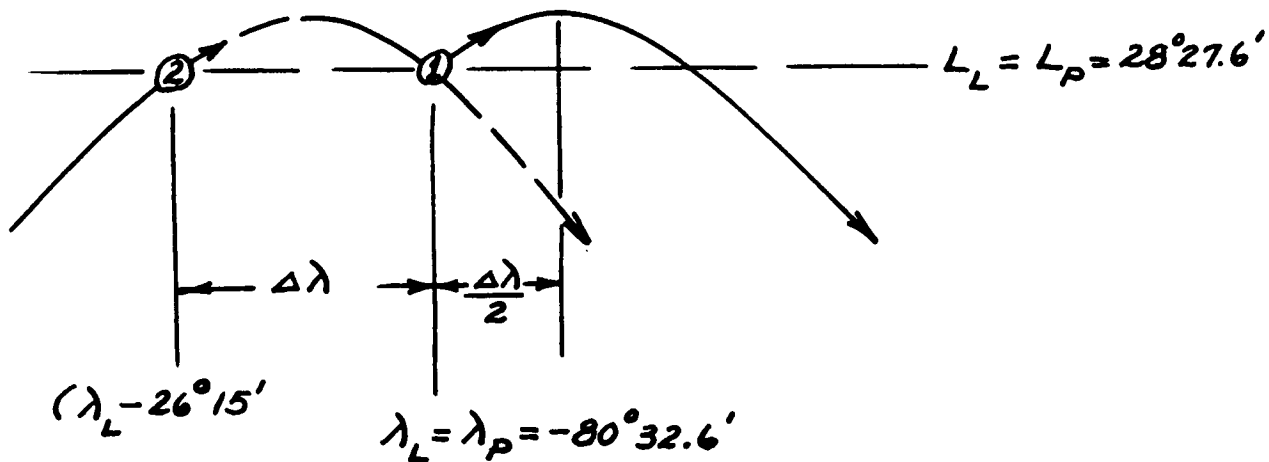
Period $T = 105$ minutes

Radius in elliptic orbit, $r = \frac{4534.6}{1 + 0.1025 \cos \theta}$ miles

Because γ_1 and θ_1 were zero the perigee point occurred over the launching point and consequently the launching height was also the height at the perigee.

We now solve for the difference in longitude between the perigee and the vertex point knowing that due to the earth's rotation

$$\begin{aligned} \Delta\lambda &= -\omega_e T \\ &= -0.25 \times 105 \\ \Delta\lambda &= -26^\circ 15' \end{aligned}$$



then $\Delta \lambda_{PV} = 13^\circ 7.5'$

Knowing L_P and $\Delta \lambda_{PV}$ we solve equations (2.2-1), (2.2-2) and (2.2-3) for ψ and obtain

$$\psi = 83^\circ 39'$$

From the same three equations then the inclination of the orbit plane or the maximum latitude reached is

$$i = L_V = 29^\circ 6'$$

and the angle in the orbit plane between the perigee and the vertex is

$$\beta = 11^\circ 31.5'$$

Since $\omega + \beta = 90^\circ$,

then $\omega = 78^\circ 28.5'$

Knowing the inclination angle i and the angle ω in the orbit plane from where the satellite crosses the equator to the perigee the declination or the latitude of the satellite from equation (2.3-4) was simply

$$L_S(t) = \sin^{-1} [0.40634 \sin(78^\circ 28.5' + \theta)]$$

and the incremental longitude from equation (2.3-10) is

$$\Delta \lambda_{NS}(t) = \tan^{-1} [0.87377 \tan(78^\circ 28.5' + \theta)] - 0.25 t(\theta)$$

when

$$t = 0$$

$$\Delta \lambda_{NS}(0) = \Delta \lambda_{NP} = 90 - \Delta \lambda_{PV}$$

or

$$\Delta \lambda_{NS}(0) = 76^\circ 52.5'$$

then

$$\begin{aligned} \lambda_N(0) &= \lambda_P - \Delta \lambda_{NP} \\ &= -80^\circ 32.6' - 76^\circ 52.5' \end{aligned}$$

$$\lambda_N(0) = -157^\circ 25.1' \text{ West of Greenwich}$$

so the final expression for the longitude or the right ascension of the satellite as measured from Greenwich was

$$\lambda_s(t) = \lambda_N + \Delta \lambda_{NS}(t)$$

or

$$\begin{aligned} \lambda_s(t) &= -157^\circ 25.1' + \tan^{-1} [0.87377 \tan(78^\circ 28.5' + \theta)] \\ &\quad - 0.25 t(\theta) \end{aligned}$$

where the time from perigee from equation (2.1-8) was

$$t(\theta) = 16.6177 \left[\frac{0.1025 \sin \theta}{1 + 0.1025 \cos \theta} + 2.0106 \tan^{-1}(0.9022 \tan \theta/2) \right]$$

The Mercator projection of the initial orbit for the above example is plotted in figure 2.2. The surface of the earth covered did not include Europe or Asia. The only land areas crossed other than parts of the United States and Mexico included parts of Africa and Australia.

A plot of the distance of the satellite from the center of the earth r as a function of the latitude L is shown in figure 2.3. The height on the southern passage being greater than the northern passage for the same latitude. Changes in launch angle γ_1 and ψ have been examined and the results indicate that changes in γ_1 influence the eccentricity e and the longitude λ , while changes in ψ effect the latitude L . Neither γ_1 or ψ effect the period T .

2.5 Perturbation of a Satellite.

Without disturbing forces the orbital elements would not vary with time and the satellite would travel in a elliptical orbit described by the elements. In reality the continued action of the disturbing forces causes the elements or characteristics of the orbit to change with time. These forces arise because as mentioned previously the net force that attracts the satellite to the earth does not vary exactly as the inverse square of the distance from the earth's center and is not directed exactly toward the earth's center. The other main disturbing force to the basic elliptic orbit results from the atmosphere. It should be of interest, therefore, to mention what some of the disturbing force effects are on the elements appearing in our derived expressions for time and position.

Because of gravity's more powerful effect at the

earth's bulging equator the satellite's orbit precesses or pivots, like a child's top slowing down. The resultant effect does not decrease the inclination angle of the orbital plane but if one revolution about a non-rotating earth carries the satellite over the equator at N (figure 2.1) the next circuit will cross at some point west of point N. The rate of regression of the line of nodes according to reference 4 is a function of the cosine of inclination angle and is, therefore, the greatest for an equatorial orbit. For example, for a mean satellite radius of 4,500 miles the rate of regression is calculated to be -6.54 deg/day for an equatorial orbit and -4.61 deg/day for an orbit inclined 45° from the equator.

Another effect of the earth's oblateness is to rotate the orbital plane about the earth's axis in the direction opposite to the motion of the satellite. This rotation in degrees/day for a given height is, according to reference 1, a function of the cosine of the inclination angle i and is, therefore, the greatest for an equatorial orbit. Rate of rotation of Sputnik II orbital plane which was inclined 65° to the NE was between 2.69 and 2.88 deg/day.

It is also found that the major axis of the ellipse rotates in the orbital plane by so many degrees per day for a given height. This rotation is in the same direction as the satellite motion if the inclination angle is less than

63.4° and in the opposite direction if i is greater than 63.4 . For example, for a 200 nautical mile orbital altitude the major axis rotates about 16 deg/day in the same direction as the satellite for a near-equatorial orbit and at about 4 deg/day in the opposite direction for a polar orbit. Both of the above mentioned disturbances cause the perigee point P to move along the orbit so that ω the angle from where the satellite crosses the equator to the perigee point is not constant. Consequently the satellite has different periods than would be predicted by theory. Also the height of the satellite as it crosses any latitude going North say, may be different on successive days.

The main effect of the atmosphere is to reduce the length of the major axis making the orbit more nearly circular. This is because most of the retardation due to drag occurs near perigee; consequently there is a loss of altitude at the subsequent apogee. The reduction in the length of the major axis shortens the orbital period by so many seconds per day and it is possible to estimate the air density and the life-time of a satellite from the rate of decrease of the period.

References

1. King-Hele, D. G. and Gilmore, D. M. C.: "The Effect of the Earth's Oblateness on the Orbit of a Near Satellite." RAE Tech Note GW 475, October 1957.
2. Ashbrook, J., Schilling, G. F. and Sterve, T. E.: "Glossary of Astronautical Terms for the Description of Satellite Orbits." Smithsonian Institution Astrophysical Observatory Special Report 4, Nov. 30, 1957.
3. Kooy, J. M. J.: "On the Application of the Method of Variation of Elliptic Orbit Elements in Case of a Satellite Vehicle." *Astronautics Acts* 3 (3) p 179-214. 1957
4. Spitzer, Lyman, Jr.: "Perturbations of a Satellite Orbit." *British Interplanetary Society Journal* v. 9, May 1950, p 131-136.

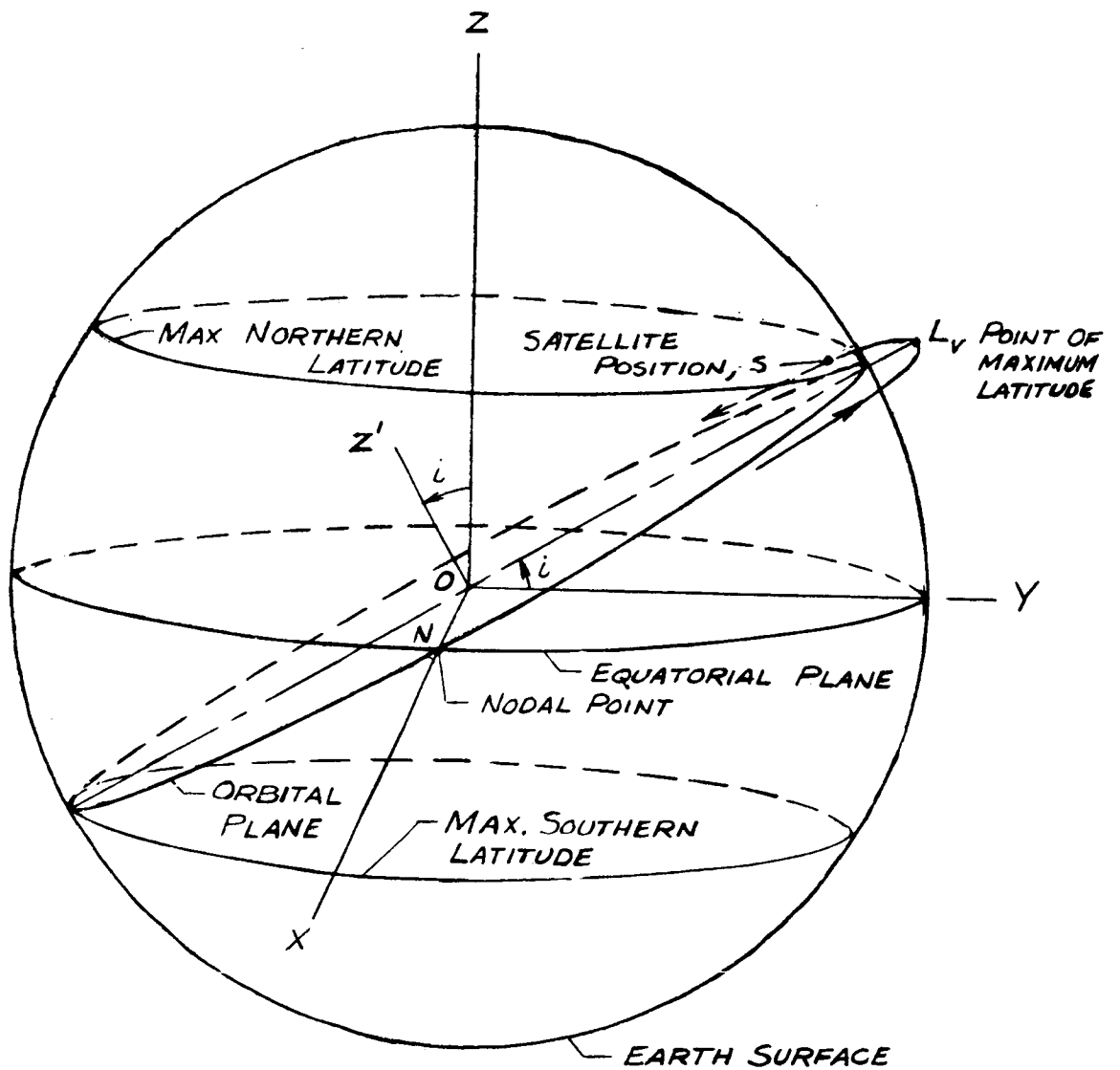


Fig. 2-1.- NOTATION FOR SATELLITE OVER SPHERICAL EARTH.

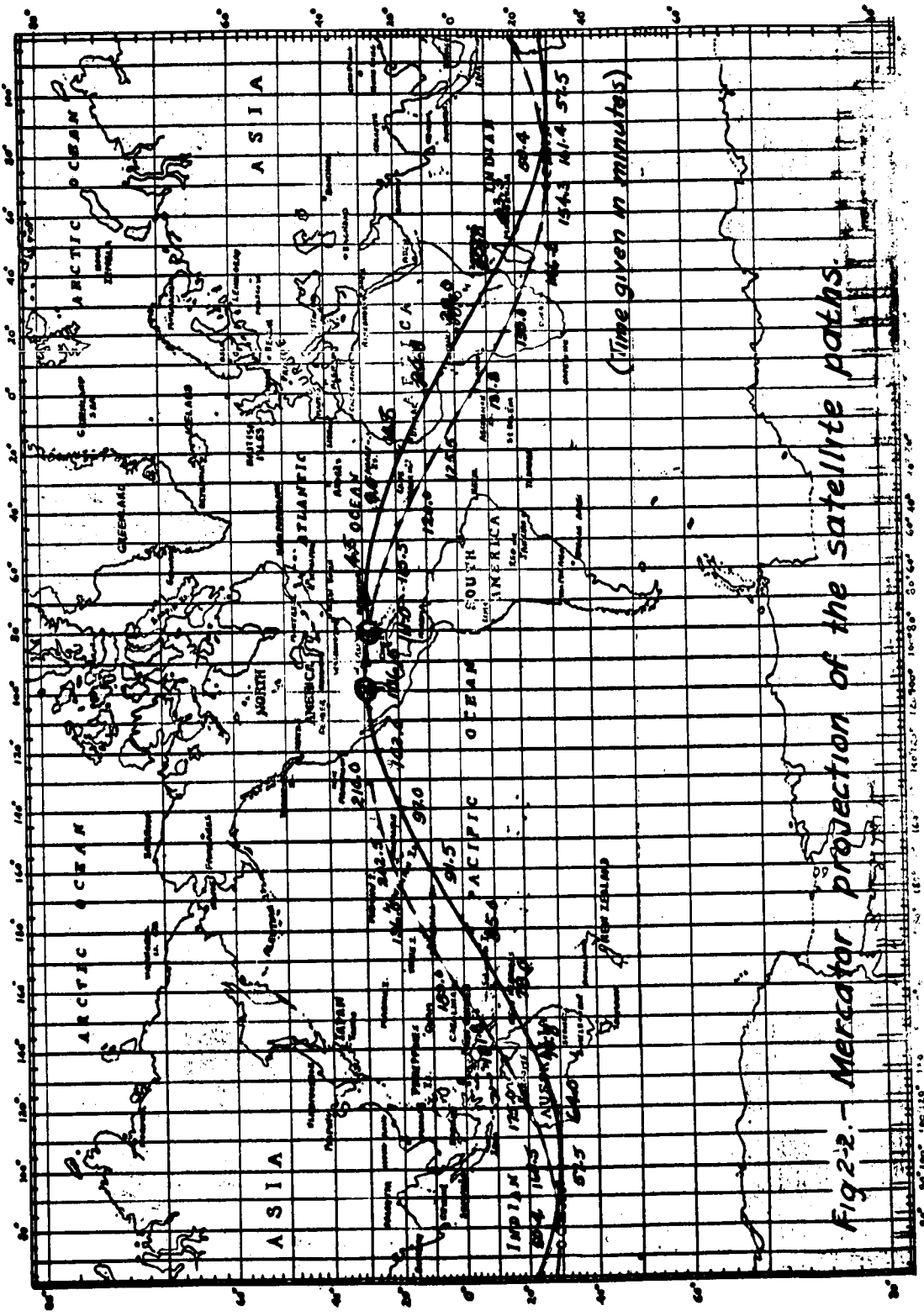


Fig 2-2. - Mercator projection of the satellite paths.

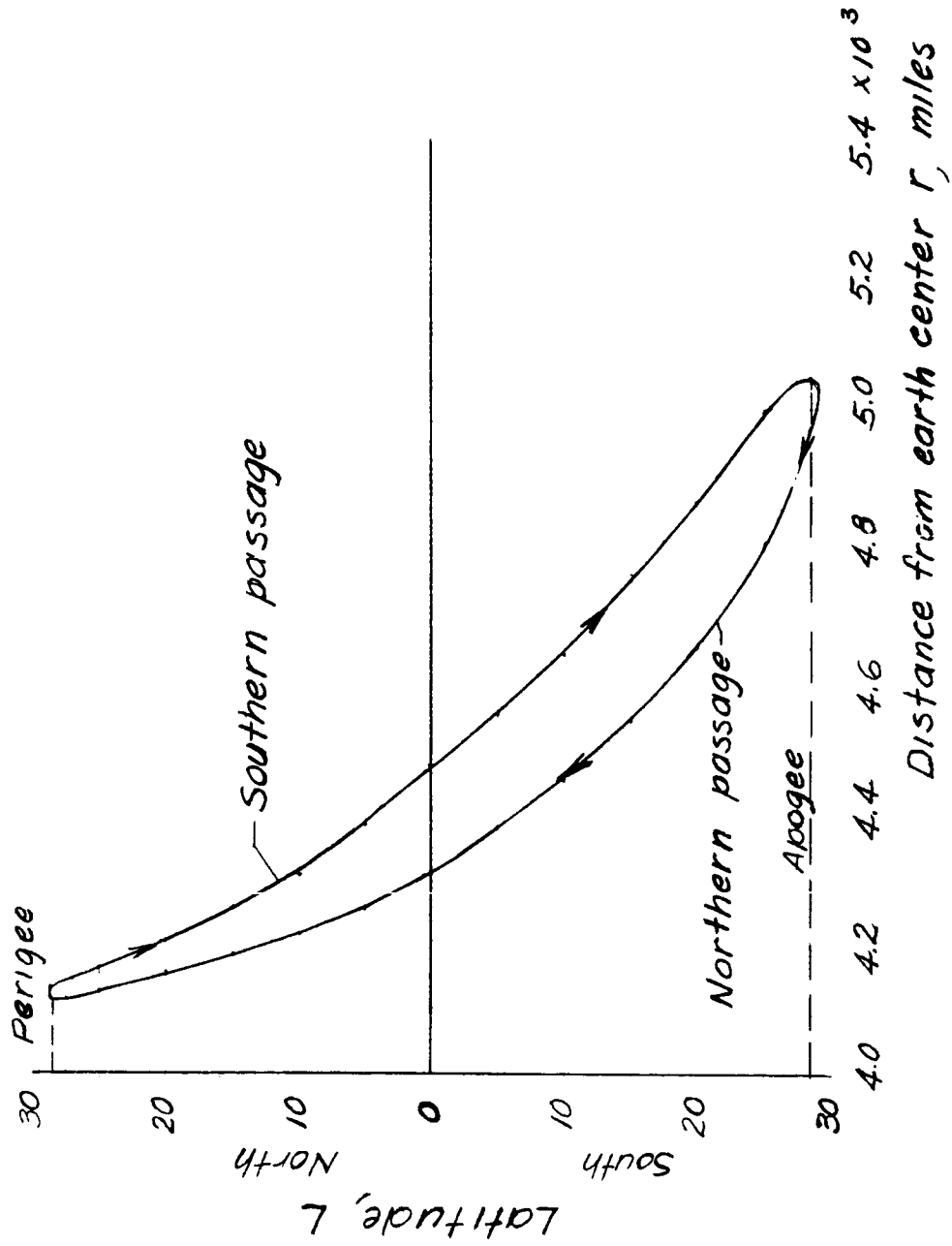


Fig. 2-3.- Satellite distance from earth center for various latitudes

SECTION III

THE MOTION OF A SPACE VEHICLE WITHIN THE EARTH-MOON SYSTEM

INDEX

	Page
3.0 Introduction	3-1
3.1 Equations of Motion (Inertial Reference Axes)	3-2
3.2 Equations of Motion (Rotating Axes)	3-4
3.3 Jacobi's Integral	3-9
3.4 Surfaces of Zero Relative Velocity	3-11
3.5 Points of Coalescence	3-14
3.6 Velocities Near the Surface of the Earth Corresponding to C_2 , C_4 , C_6 , and C_8	3-18
3.7 Conversion of Relative Velocity to Velocity in the Earth Inertial System	3-20
3.8 Effects of Neglected Factors	3-23
3.9 Trajectories Near Minimum Velocities	3-25
3.10 Use of Two-Body Ellipses to Approximate Lunar Orbits	3-28
3.11 Locus of Points of Equal Attraction Between the Earth and the Moon	3-31
3.12 Sphere of Influence	3-34
3.13 Approximate Method of Calculating Trajectories of Lunar Vehicles	3-39
3.14 Characteristics of Approach Trajectories	3-51
3.15 Trajectories to Strike the Moon	3-53
3.16 Circum-Lunar Trajectories	3-59
3.17 Allunar Trajectories	3-62
3.18 Periodic Trajectories	3-63
3.19 Establishing an Artificial Satellite of the Moon	3-65
3.20 Use of the Moon for Accelerating Space Vehicles	3-69
3.21 Propulsion Requirements for Lunar Vehicles	3-72
References	3-73

SECTION III

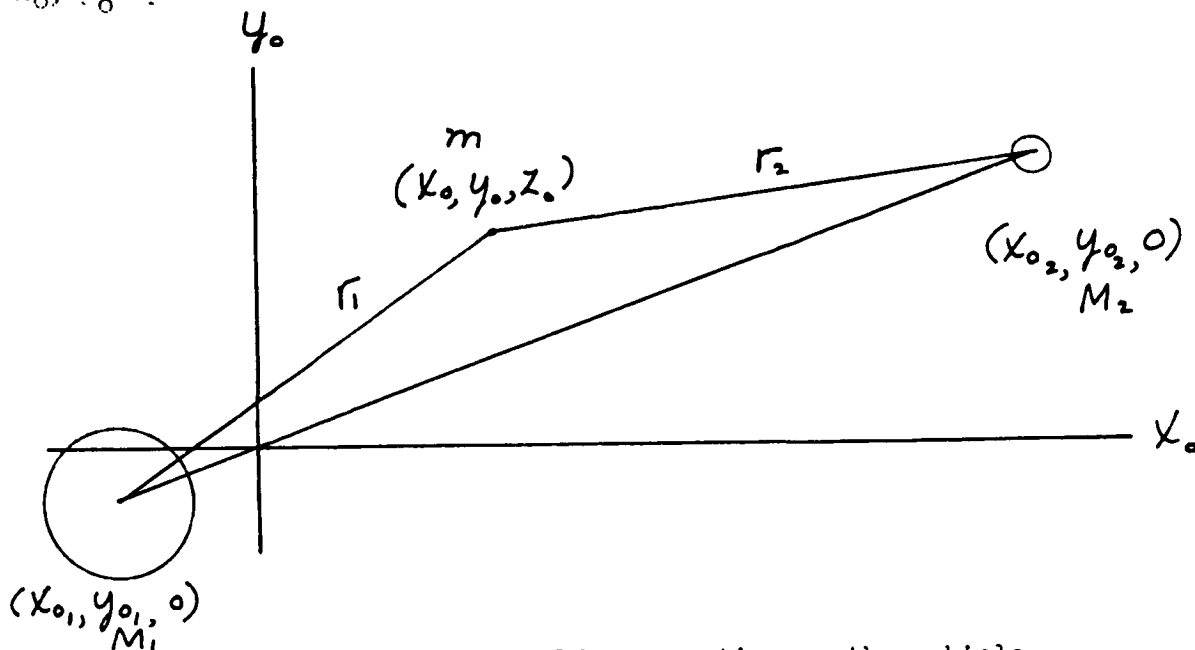
THE MOTION OF A SPACE VEHICLE WITHIN THE EARTH-MOON SYSTEM

3.0 The Restricted Three-Body Problem

So far we have been dealing with the motion of a vehicle under the attraction of one large body (the Earth). If, however, the vehicle is to operate at large distances from the Earth (in the vicinity of the Moon, for example) then the orbit equations which have been developed are no longer valid and we must take into account the forces due to the second large body (the Moon). If the mass of the space vehicle was comparable to the masses of the Moon and Earth, we would have to consider the classical Three-Body Problem. In this section we will deal with the restricted Three-Body Problem in which the mass of one of the bodies (the space vehicle) is infinitesimal in comparison with the other two bodies (the Earth and the Moon). The Three-Body Problem is one of the classical problems of celestial mechanics and the names of Lagrange (1772), Jacobi (1843), Hill (1878), and Poincare are closely associated with the problem. In this section the development of the equations of motion follows that of Moulton (1902) in reference 3-1. The basic development in reference 3-1, however, follows that of Hill (1878) in reference 3-2. The trajectories shown and many of the results given in this section were taken from results of studies by the RAND Corporation (Buchheim reference 3-3) and by the Russians (Yegorov, reference 3-4). (It should be noted that both references 3-3 and 3-4 made wide use of the book An Introduction to Celestial Mechanics by F. R. Moulton; reference 3-1.)

3.1 Equations of Motion (Inertial Reference Axes)

The system of axes used is the inertial axes system shown in Figure 3-1 and 3-2 where the origin is taken at the center of mass of the Earth-Moon system, and the plane of rotation of the moon about the Earth is in the x_0, y_0 plane.



There are two radial gravitational forces acting on the vehicle

$$F_{r_1} = ma_1 = - \frac{Gm M_1}{r_1^2}$$

3.1-1

$$F_{r_2} = ma_2 = - \frac{Gm M_2}{r_2^2}$$

where

$$r_1^2 = (x_0 - x_{01})^2 + (y_0 - y_{01})^2 + z_0^2$$

3.1-2

$$r_2^2 = (x_0 - x_{02})^2 + (y_0 - y_{02})^2 + z_0^2$$

The forces due to the earth in the x_0 , y_0 , and z_0 directions are:

$$F_{x_1} = F_{r_1} \frac{(x_0 - x_{01})}{r_1}$$

$$F_{y_1} = F_{r_1} \frac{(y_0 - y_{01})}{r_1}$$

3.1-3

$$F_{z_1} = F_{r_1} \frac{z_0}{r_1}$$

Summing the forces due to the earth and the moon in the x_0 , y_0 , and z_0 directions we have:

$$m \ddot{x}_0 = - Gm M_1 \frac{(x_0 - x_{01})}{r_1^3} - Gm M_2 \frac{(x_0 - x_{02})}{r_2^3}$$

$$m \ddot{y}_0 = - Gm M_1 \frac{(y_0 - y_{01})}{r_1^3} - Gm M_2 \frac{(y_0 - y_{02})}{r_2^3}$$

3.1-4

$$m \ddot{z}_0 = - Gm M_1 \frac{z_0}{r_1^3} - Gm M_2 \frac{z_0}{r_2^3}$$

or

$$\ddot{x}_0 = - G M_1 \frac{(x_0 - x_{01})}{r_1^3} - G M_2 \frac{(x_0 - x_{02})}{r_2^3}$$

$$\ddot{y}_0 = - G M_1 \frac{(y_0 - y_{01})}{r_1^3} - G M_2 \frac{(y_0 - y_{02})}{r_2^3}$$

3.1-5

$$\ddot{z}_0 = - G M_1 \frac{z_0}{r_1^3} - G M_2 \frac{z_0}{r_2^3}$$

3.2 Equations of Motion (Rotating Axes).

Now, let us assume that the earth and the moon revolve in circles about their common center of mass. (At least for the time it would take a vehicle to complete an orbit to the moon.) Actually, the eccentricity is 0.0549 - not quite circular.

Let the motion be referred to a new system of axes rotating with the uniform angular velocity ω , - the mean angular velocity of the earth-moon system. (See Figure 3-2.) The coordinates in the new system are defined by the following transformations:

$$\begin{Bmatrix} x_0 \\ y_0 \\ z_0 \end{Bmatrix} = \begin{bmatrix} \cos \omega t & -\sin \omega t & 0 \\ \sin \omega t & \cos \omega t & 0 \\ 0 & 0 & 1 \end{bmatrix} \begin{Bmatrix} x \\ y \\ z \end{Bmatrix} \quad 3.2-1$$

$$\begin{Bmatrix} \dot{x}_0 \\ \dot{y}_0 \\ \dot{z}_0 \end{Bmatrix} = \begin{bmatrix} \cos \omega t & -\sin \omega t & 0 \\ \sin \omega t & \cos \omega t & 0 \\ 0 & 0 & 1 \end{bmatrix} \begin{Bmatrix} \dot{x} - \omega y \\ \dot{y} + \omega x \\ \dot{z} \end{Bmatrix} \quad 3.2-2$$

$$\begin{Bmatrix} \ddot{x}_0 \\ \ddot{y}_0 \\ \ddot{z}_0 \end{Bmatrix} = \begin{bmatrix} \cos \omega t & -\sin \omega t & 0 \\ \sin \omega t & \cos \omega t & 0 \\ 0 & 0 & 1 \end{bmatrix} \begin{Bmatrix} \ddot{x} - 2\omega \dot{y} - \omega^2 x \\ \ddot{y} + 2\omega \dot{x} - \omega^2 y \\ \ddot{z} \end{Bmatrix} \quad 3.2-3$$

Other useful transformations are given in table 3-1.

Substituting the values from equations (3.2-1), (3.2-2), and (3.2-3) into equations (3.1-5) we get:

$$\ddot{x} - 2\omega\dot{y} - \omega^2 x) \cos \omega t - (\ddot{y} + 2\omega\dot{x} - \omega^2 y) \sin \omega t =$$

$$\left[G M_1 \frac{(y - y_1)}{r_1^3} + G M_2 \frac{(y - y_2)}{r_2^3} \right] \sin \omega t - \left[G M_1 \frac{(x - x_1)}{r_1^3} + G M_2 \frac{(x - x_2)}{r_2^3} \right] \cos \omega t$$

$$\ddot{y} + 2\omega\dot{x} - \omega^2 y) \cos \omega t + (\ddot{x} - 2\omega\dot{y} - \omega^2 x) \sin \omega t =$$

$$- \left[G M_1 \frac{(x - x_1)}{r_1^3} + G M_2 \frac{(x - x_2)}{r_2^3} \right] \sin \omega t - \left[G M_1 \frac{(y - y_1)}{r_1^3} + G M_2 \frac{(y - y_2)}{r_2^3} \right] \cos \omega t$$

3-5

3-5

$$\ddot{z} = - G M_1 \frac{z}{r_1^3} - G M_2 \frac{z}{r_2^3}$$

3.2-4

The first two equations can be written as

$$A \cos \omega t - B \sin \omega t = C \sin \omega t - D \cos \omega t$$

$$B \cos \omega t + A \sin \omega t = - D \sin \omega t - C \cos \omega t$$

Multiplying by $\cos \omega t$ and $\sin \omega t$ respectively and adding we obtain:

$$A = - D$$

Multiplying by $-\sin \omega t$ and $\cos \omega t$ respectively and adding we obtain:

$$B = - C$$

Substituting the values for A, B, C, and D we have:

$$\begin{aligned} \ddot{x} - 2\omega\dot{y} - \omega^2x &= -G M_1 \frac{(x - x_1)}{r_1^3} - G M_2 \frac{(x - x_2)}{r_2^3} \\ \ddot{y} + 2\omega\dot{x} - \omega^2y &= -G M_1 \frac{(y - y_1)}{r_1^3} - G M_2 \frac{(y - y_2)}{r_2^3} \end{aligned} \quad 3.2-5$$

and

$$\ddot{z} = -G M_1 \frac{z}{r_1^3} - G M_2 \frac{z}{r_2^3}$$

If the position of the x rotating axis is taken through the earth-moon axis then $y_1 = 0$ and $y_2 = 0$ so that

$$\begin{aligned} \ddot{x} - 2\omega\dot{y} &= \omega^2x - G M_1 \frac{(x - x_1)}{r_1^3} - G M_2 \frac{(x - x_2)}{r_2^3} \\ \ddot{y} + 2\omega\dot{x} &= \omega^2y - G M_1 \frac{y}{r_1^3} - G M_2 \frac{y}{r_2^3} \end{aligned} \quad 3.2-6$$

$$\ddot{z} = -G M_1 \frac{z}{r_1^3} - G M_2 \frac{z}{r_2^3}$$

Note that

$$r_1^2 = (x_0 - x_{01})^2 + (y_0 - y_{01})^2 + z_0^2$$

Then from the transformation equations (3.2-1), (3.2-2), and (3.2-3):

$$r_1^2 = (x - x_1)^2 + (y - y_1)^2 + z^2$$

which is independent of t .

Thus these equations have the important property that they do not involve explicitly the independent variable t because the coordinates of the finite bodies have become constants because of the manner in which the axes are rotated.

The general problem of determining the motion of a small vehicle is of the sixth order; if it moves in the plane of the motion of the finite bodies, it becomes fourth order.

The terms $2\omega\dot{y}$ and $2\omega\dot{x}$ are the so-called Coriolis accelerations and ω^2x and ω^2y are centrifugal terms.

In the practical case it is convenient to use a units system that does not require either very large or very small numbers. Therefore, the units will be changed to:

Unit of time	-	1 day
unit of distance	-	1 lunar unit,
		distance from earth to moon

In this system: (Ref. 3-3)

$$\omega = 0.22997084 \text{ rad/day}$$

$$D = 1 \text{ lunar unit}$$

$$GM = 0.052886587 (\text{lunar unit})^3 (\text{day})^{-2}$$

$$R = 0.01655926 \text{ lunar units}$$

$$X_1 = -0.012128563 \text{ lunar units} = -\mu$$

$$X_2 = 0.98787144 \text{ lunar units} = 1 - \mu$$

$$M = \text{Mass of earth plus mass of moon}$$

$$M_1 = \text{Mass of earth}$$

$$M_2 = \text{Mass of moon}$$

Letting $\mu = \frac{M_2}{M} = \frac{1}{82.45}$ $(1 - \mu) = \frac{M_1}{M}$

Equations (3.2-6) then become :

$$\ddot{x} - 2\omega\dot{y} = \omega^2 x - G M (1 - \mu) \frac{(x - x_1)}{r_1^3} - G M \mu \frac{(x - x_2)}{r_2^3}$$

$$\ddot{y} + 2\omega\dot{x} = \omega^2 y - G M (1 - \mu) \frac{y}{r_1^3} - G M \mu \frac{y}{r_2^3} \quad 3.2-7$$

$$\ddot{z} = - G M (1 - \mu) \frac{z}{r_1^3} - G M \mu \frac{z}{r_2^3}$$

where

$$r_1^2 = (x - x_1)^2 + y^2 + z^2$$

$$r_2^2 = (x - x_2)^2 + y^2 + z^2$$

These are the equations with which trajectories of moon rockets can be computed.

3.3 Jacobi's Integral

The only known solution of the above equation is the Jacobi integral.

If

$$W = \frac{1}{2} \omega^2 (x^2 + y^2) + G M \frac{(1 - \mu)}{r_1} + G M \frac{\mu}{r_2} \quad 3.3-1$$

then the equations of motion (3.2-6) can be written as

$$\ddot{x} - 2\omega\dot{y} = \frac{\partial W}{\partial x}$$

$$\ddot{y} + 2\omega\dot{x} = \frac{\partial W}{\partial y} \quad 3.3-2$$

$$\ddot{z} = \frac{\partial W}{\partial z}$$

For example

$$\begin{aligned} \frac{\partial W}{\partial x} &= \frac{1}{2} \omega^2 (2x) - G M \frac{(1 - \mu)}{r_1^2} \frac{2}{2r_1} (x - x_1) - G M \frac{\mu}{r_2^2} \frac{2}{2r_2} (x - x_2) \\ &= \omega^2 x - G M (1 - \mu) \frac{(x - x_1)}{r_1^3} - G M \mu \frac{(x - x_2)}{r_2^3} \end{aligned}$$

Multiplying equations (3.3-2) by $2\dot{x}$, $2\dot{y}$, and $2\dot{z}$ respectively we have:

$$2\dot{x}\ddot{x} - 4\omega\dot{x}\dot{y} = 2\dot{x} \frac{\partial W}{\partial x}$$

$$2\dot{y}\ddot{y} + 4\omega\dot{x}\dot{y} = 2\dot{y} \frac{\partial W}{\partial y} \quad 3.3-3$$

$$2\dot{z}\ddot{z} = 2\dot{z} \frac{\partial W}{\partial z}$$

adding these equations we obtain:

$$2\ddot{x}\dot{x} + 2\ddot{y}\dot{y} + 2\ddot{z}\dot{z} = 2\dot{x} \frac{\partial W}{\partial x} + 2\dot{y} \frac{\partial W}{\partial y} + 2\dot{z} \frac{\partial W}{\partial z} \quad 3.3-4$$

This equation can be integrated. For example

$$\int \ddot{x} \dot{x} dt = \int \dot{x} d\dot{x} = \frac{(\dot{x})^2}{2}$$

and

$$\dot{x} \frac{\partial W}{\partial x} dt = \frac{\partial W}{\partial x} dx$$

$$dW = \frac{\partial W}{\partial x} dx + \frac{\partial W}{\partial y} dy + \frac{\partial W}{\partial z} dz$$

$$(\dot{x})^2 + (\dot{y})^2 + (\dot{z})^2 - 2 \int \left(\frac{\partial W}{\partial x} dx + \frac{\partial W}{\partial y} dy + \frac{\partial W}{\partial z} dz \right) + C = 0 \quad 3.3-5$$

or

$$v^2 = 2W - C \quad 3.3-6$$

Substituting the value of W from equation (3.3-1) into equation (3.3-6)

we have:

$$v^2 = \omega^2(x^2 + y^2) + 2GM \frac{(1-\mu)}{r_1} + 2GM \frac{\mu}{r_2} - C \quad 3.3-7$$

This is the only known integral for the equations of motion. In general, solutions of the equations of motion (equation (3.2-7)) must be obtained by step by step integration.

3.4 Surfaces of Zero Relative Velocity

Jacobi's Integral (equation (3.3-7)) will give us a great deal of information about the motion in an earth-moon system. When the constant of integration has been determined by the initial conditions, equation (3.3-7) determines the velocity in the rotating plane at all points in space. It is evident that V^2 must be positive for real motion in the earth-moon system. Thus the boundaries for possible motion are given for $V = 0$ as:

$$\omega^2(x^2 + y^2) + 2 G M \frac{(1 - \mu)}{r_1} + 2 G M \frac{\mu}{r_2} = C$$

$$r_1^2 = (x - x_1)^2 + y^2 + z^2 \quad 3.4-1$$

$$r_2^2 = (x - x_2)^2 + y^2 + z^2$$

Curves of zero relative velocity in the XY plane are shown in Figure 3-3. (These curves are for illustration only and are not to scale. Curves of zero relative velocity in the yz and yz planes are shown in Figures 3-4 and 3-5.) The surfaces of zero relative velocity, for large values of C, may be roughly described as consisting of a closed fold about spherical in form about each of the large bodies, and of curtains hanging from an asymptotic cylinder symmetrically with respect to the XY plane. For smaller values of C the folds of the two bodies expand until they reach each other, and then open up forming one surface surrounding both earth and moon. For still smaller values of C the folds and curtains meet and open up. The motion is real within the folds or outside of the curtains.

In Figure 3-3 the values of C are numbered such that $C_1 > C_2 > C_3 \dots$. For initial conditions of $C = C_1$ the body can move either in a closed region about the earth or in a closed region about the moon -- it cannot travel from the earth to the moon. Earth Satellites and ballistic missiles will be in this class.

(It can also be shown that if the Sun and Earth are considered the finite bodies and the moon the infinitesimal body, the constant C , determined by the motion of the moon, is so large that fold around the earth is closed with the moon within it. Therefore, the moon cannot recede indefinitely from the earth within the assumptions of the method.)

For $C = C_3$, the body can move within the closed contour around the earth and moon so that travel to the moon is now possible. $C = C_2$ represents the limiting case separating regions in which it is not possible.

For $C = C_5$, the body can escape the earth-moon system since the region is open behind the moon. $C = C_4$ is the limiting case at which escape becomes possible.

In addition to these contours, within which motion is possible, there are, for the same C values, outer boundaries beyond which motion is possible. For example, a body (infinitesimal) from outer space cannot approach any closer than these boundaries (curtains).

At $C = C_4$ the inner and outer branches of the surfaces coalesce and for $C < C_4$ a vehicle can enter the earth-moon system.

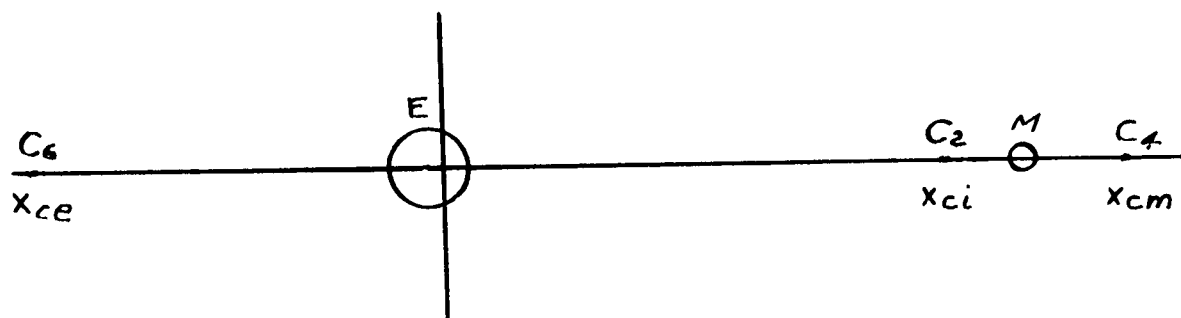
As C decreases from C_4 the opening behind the moon widens. When $C = C_6$ the contour also begins to open behind the earth and when $C = C_7$ only the interiors of the kidney-shaped regions can not have real motion.

As C decreases further the area precluding motion decreases until finally at $C = C_8$ the regions become a point. These points make equilateral triangles with the earth and the moon. When $C < C_8$ no region in the x - y plane is excluded.

The surfaces of zero relative velocity may also be described as the envelopes of all possible orbits for given initial conditions. In Figure 3-6 the zero relative velocity contours corresponding to C_2 , C_4 , C_6 , and C_8 are shown drawn to scale for the earth-moon system. In Figure 3-7 are shown the contours corresponding to a value of C similar to C_1 of Figure 3-3, and in Figure 3-8 the contour about the earth is shown for a value of C corresponding to that of an earth satellite. For the earth-moon system the contours are almost circles in the x - y plane for values of C numerically greater than C_2 , (i.e. C_1) since the mass of the moon is only 1/81.45 that of the earth.

3.5 Points of Coalescence

From Figure 3-3 and 3-6 it can be seen that there are three points on the x axis called points of coalescence at which double solutions are obtained and the regions of possible motion are enlarged. These points correspond to C_2 , C_4 , and C_6 and are indicated below:



Equation (3.3-7) in the xy plane is

$$F(x, y) = \omega^2(x^2 + y^2) + 2GM \frac{(1-\mu)}{r_1} + 2GM \frac{\mu}{r_2} - C = 0 \quad 3.5-1$$

The conditions for double points are:

$$\frac{\partial F}{\partial x} = 2\omega^2 x - 2GM(1-\mu) \frac{(x-x_1)}{r_1^3} - 2GM\mu \frac{(x-x_2)}{r_2^3} = 0$$

$$\frac{\partial F}{\partial y} = 2\omega^2 y - 2GM(1-\mu) \frac{y}{r_1^3} - 2GM\mu \frac{y}{r_2^3} = 0$$

3.5-2

The double points on the x axis and the straight line solutions to the problem are given by the conditions:

$$\omega^2 x - \frac{GM(1-\mu)(x-x_1)}{[(x-x_1)^2]^{3/2}} - \frac{GM\mu(x-x_2)}{[(x-x_2)^2]^{3/2}} = 0$$

3.5-3

This equation is also the first equation of (3.2-7) with

$$\ddot{x} = \ddot{y} = 0$$

Moulton (ref 3-1) has solved for the roots of this equation and they are:

$$r_{2ci} = \left(\frac{\mu}{3}\right)^{1/3} - \frac{1}{3} \left(\frac{\mu}{3}\right)^{2/3} - \frac{1}{9} \left(\frac{\mu}{3}\right)^{3/3} + \dots$$

$$r_{2cm} = \left(\frac{\mu}{3}\right)^{1/3} + \frac{1}{3} \left(\frac{\mu}{3}\right)^{2/3} - \frac{1}{9} \left(\frac{\mu}{3}\right)^{3/3} + \dots$$

3.5-4

$$r_{2ce} = 2 - \frac{7}{12} \mu - 23 \frac{(7)^2}{(12)^4} \mu^3 + \dots$$

It can also be shown that the double points not on the x axis are

$r_1 = 1, r_2 = 1$, such that the points form equilateral triangles with the finite bodies regardless of their masses. These are the points labeled C8 in Figures 3-3 and 3-6. (Note that the values of r are in lunar units.)

It can also be shown that the particular solutions on the x axis are unstable - i.e., if a small body were displaced a very little from the point of solution it would, in general, depart to a comparatively great distance. The equilateral triangle solutions, on the other hand, are stable; - a body displaced a little would oscillate about the point of solution.

It is of interest to note that the equilateral triangle solutions are known to exist in the Solar system. These are the well known Trojan Asteroids between the Sun and the planet Jupiter. There are twelve known asteroids in the Trojan Group, seven of which precede Jupiter in its revolution about the Sun and five of which follow. These asteroids have an average diameter of about 80 miles and oscillate near the equilateral triangle point.

The real roots in terms of distances along the x axis are:

$$x_{ci} = 1 - \mu - r_{2ci}$$

3.5-5

$$x_{cm} = 1 - \mu + r_{2cm}$$

$$x_{ce} = 1 - \mu - r_{2ce}$$

Since $\mu = \frac{M_2}{M} = \frac{1}{82.45}$:

$$x_{ci} = 0.83702 \text{ lunar units}$$

$$r_{1ci} = 0.84915 \text{ lunar units}$$

$$x_{cm} = 1.15560 \text{ lunar units}$$

$$r_{1cm} = 1.16773 \text{ lunar units}$$

$$x_{ce} = -1.00505 \text{ lunar units}$$

$$r_{1ce} = -0.99292 \text{ lunar units}$$

Substituting these values in Jacobi's integral (equation 3.3-7)

we can now solve for C_2 , C_4 , and C_6 . These values are:

$$C_2 = 0.16861 \text{ (lunar units/day)}^2$$

$$C_4 = 0.16776$$

$$C_6 = 0.15930$$

or

$$\sqrt{C_2} \approx 6000 \text{ ft/sec}$$

$$\sqrt{C_4} \approx 5986 \text{ ft/sec}$$

$$\sqrt{C_6} \approx 5832 \text{ ft/sec}$$

It might be interesting to compare the value of x_{ci} , the point between the earth and the moon at which a small body would remain relatively at rest, with the distance of the point of equal attraction between the earth and the moon based on the static equations.

Equating the two forces of attraction we have:

$$\frac{GM_1m}{r_1^2} = \frac{GM_2m}{r_2^2}$$

$$\left(\frac{r_1}{r_2}\right)^2 = \frac{M_1}{M_2} = 81.5$$

$$r_1 + r_2 = D$$

$$\frac{r_1}{D} = \frac{\sqrt{M_1/M_2}}{1 + \sqrt{M_1/M_2}}$$

$$\frac{r_1}{D} = 0.9$$

whereas $r_{1ci} = 0.849$. The difference, of course, is caused by the inclusion of the centrifugal force term $\omega^2 x$ in the case of the body rotating with the earth-moon system.

3.6 Velocities at the Surface of the Earth Corresponding to C_2 , C_4 , C_6 , and C_8

The significance of these values of C_2 , C_4 , and C_6 can be seen more readily if we calculate the velocity of a vehicle near the earth that corresponds to values of C equal to C_2 , C_4 , and C_6 . We shall arbitrarily choose a position 4,300 miles from the center of the earth adjacent to the moon. At this position the position of the vehicle is:

$$X_s = 0.0058575 \text{ lunar units}$$

$$Y_s = 0$$

$$Z_s = 0$$

From equation (3.3-7) then:

$$\begin{aligned} C = C_2; \quad V_{2,i} &= 2.375333 \text{ lunar units/day} \\ &= 34,703.8 \text{ ft/sec} \end{aligned}$$

$$\begin{aligned} C = C_4; \quad V_{4,m} &= 2.375513 \text{ lunar units/day} \\ &= 34,706.4 \text{ ft/sec} \end{aligned}$$

$$\begin{aligned} C = C_6; \quad V_{6,e} &= 2.377292 \text{ lunar units/day} \\ &= 34,732.4 \text{ ft/sec} \end{aligned}$$

The value of C_8 from the equilateral triangle solution is:

$$C_8 = 0.15803 \text{ (lunar units/day)}^2$$

The velocity V_8 at the surface of the earth adjacent to the moon is:

$$\begin{aligned} V_8 &= 2.377560 \text{ lunar units/day} \\ &= 34,736.3 \text{ ft/sec} \end{aligned}$$

Thus the minimum relative velocity needed to reach the moon from the reference position is 34,703.8 ft/sec and the minimum velocity needed to escape the earth-moon system is 34,706.4 ft/sec; a difference of only 2.6 ft/sec indicating the sensitivity of trajectories on initial conditions. In addition, with a velocity greater than 34,736 ft/sec the vehicle could theoretically reach any point in the earth-moon system.

Since $V_{4,m}$ is less than $V_{6,e}$ it is easier to escape from the earth-moon system by projecting toward the moon than it is by projecting away from the moon.

3.7 Conversion of Relative Velocity to Velocity

in the Earth Inertial System

It should be remembered that the velocities we have been talking about are relative velocities in a rotating axes system and are defined as

$$v^2 = (\dot{x})^2 + (\dot{y})^2 + (\dot{z})^2 \quad 3.7-1$$

whereas

$$v_e^2 = (\dot{x}_e)^2 + (\dot{y}_e)^2 + (\dot{z}_e)^2 \quad 3.7-2$$

The velocities relative to the earth are related to the velocities in the rotating axes system by the following transformation:

$$\begin{Bmatrix} \dot{x}_e \\ \dot{y}_e \\ \dot{z}_e \end{Bmatrix} \begin{bmatrix} \cos \omega t & -\sin \omega t & 0 \\ \sin \omega t & \cos \omega t & 0 \\ 0 & 0 & 0 \end{bmatrix} \begin{Bmatrix} (\dot{x} - \omega y) \\ \dot{y} + \omega(x - x_1) \\ 1 \end{Bmatrix} \quad 3.7-3$$

Therefore,

$$\begin{aligned} v_e^2 &= (\dot{x} - \omega y)^2 + [\dot{y} + \omega(x - x_1)]^2 + (\dot{z})^2 \\ &= \dot{x}^2 - 2\omega y \dot{x} + \omega^2 y^2 + \dot{y}^2 + 2\omega(x - x_1) \dot{y} + \omega^2(x - x_1)^2 + \dot{z}^2 \\ v_e^2 &= v^2 + \omega^2 [y^2 + (x - x_1)^2] + 2\omega [(x - x_1) \dot{y} - \dot{x}y] \end{aligned} \quad 3.7-4$$

Writing this in terms of the polar coordinates of earth system (r_1, r) we have in the (x_e, y_e) plane:

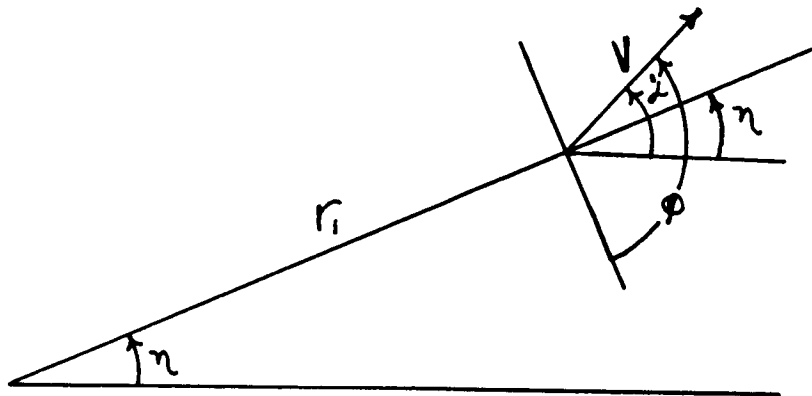
$$r_1^2 = x_e^2 + y_e^2 = (x - x_1)^2 + y^2 \quad 3.7-5$$

Then

$$V_e^2 = v^2 + r_1^2 \omega^2 + 2\omega [\dot{y}(x - x_1) - \dot{x}y] \quad 3.7-6$$

At time $t = 0$; $\omega t = 0$:

$$V_e^2 = v^2 + r_1^2 \omega^2 + 2\omega r_1 [\dot{y} \cos \eta - \dot{x} \sin \eta] \quad 3.7-7$$



In the Figure the angle ϕ between the velocity vector V and the normal to the radius r_1 from the earth is

$$\phi = 90 + \alpha' - \eta$$

and

$$\dot{x} = V \cos \alpha'$$

$$\dot{y} = V \sin \alpha'$$

Also

$$(\dot{y} \cos \eta - \dot{x} \sin \eta) = -V \cos \phi$$

Therefore

$$V_e^2 = v^2 - 2\omega r_1 \cos \phi V + r_1^2 \omega^2 \quad 3.7-8$$

The maximum value of V_e will occur, then when $\cos \phi = -1$ and the minimum value will occur when $\cos \phi = +1$ or

$$(V - \omega r_1) \leq V_e \leq (V + \omega r_1)$$

3.7-9

Now

$$\omega = 0.22997$$

$$r_1 = 0.017986$$

$$\omega r_1 = 0.004136$$

Therefore,

$$2.371197 \leq V_{e2} \leq 2.379469 \text{ lu/day}$$

$$34651 \leq V_{e2} \leq 34772 \text{ ft/sec}$$

$$2.371377 \leq V_{e4} \leq 2.379649 \text{ lu/day}$$

$$34654 \leq V_{e4} \leq 34775 \text{ ft/sec}$$

Thus the minimum velocity relative to the earth (V_e) required to send a vehicle to the moon is

$$V_e = 34651 \text{ ft/sec}$$

The minimum velocity needed to escape the earth-moon system is

$$V_e = 34654 \text{ ft/sec}$$

The escape velocity from the reference position based on the two body equations is

$$V_{E_e} = \sqrt{2g_0 \frac{R^2}{r_1}}$$

$$V_{E_e} = 2.41029198 \text{ lu/day}$$

or

$$V_{E_e} = 35,214 \text{ ft/sec}$$

Thus the two-body velocity is 560 ft/sec more than the three-body velocity.

3.8 Effects of Neglected Factors

Mean Distance from Moon

The distance to the moon used in reference 3-3 of 239,074 miles differs from the mean distance 238,857 miles determined by observation.

The distance used was derived in reference 3-3 as follows:

The period is given by

$$T = 2\pi \sqrt{\frac{a^3}{GM}} \quad 3.8-1$$

The mean angular velocity is given by

$$\bar{\omega}^2 = \left(\frac{2\pi}{T}\right)^2 = \frac{GM}{a^3} \quad 3.8-2$$

But

$$GM_e = g_0 R^2 = GM (1 - \mu)$$

Also $a = D$, the mean distance to the moon

$$D^3 = \frac{GM}{\bar{\omega}^2}$$

$$D^3 = \frac{g_0 R^2}{(1 - \mu) \bar{\omega}^2} \quad 3.8-3$$

Using appropriate values of G_0 , R , μ , and ω the distance $D = 239,074$. The difference of 217 miles is due partly to the action of the sun on the moon and partly due to **neglecting** the eccentricity of the moon's orbit.

Some factors neglected in the Three Body Problem are:

1. The gravitational field of the Sun.
2. Eccentricity of the moon's orbit.
3. Inclination of orbit of moon.

4. Oblateness of the earth.
5. Pressure of Solar radiation.

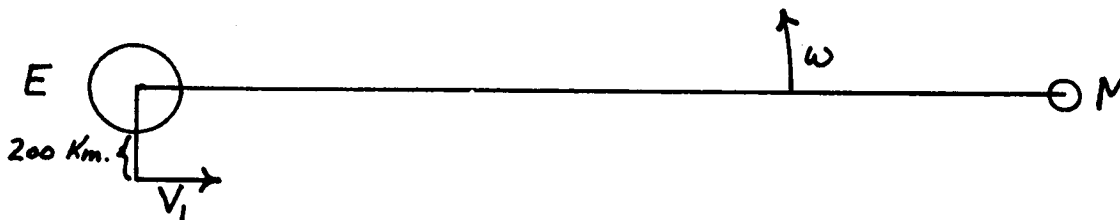
Buchheim (ref. 3-3) has investigated these effects and his results are listed below. The results are shown as a correction ΔV to the initial velocity because of the effects of these assumptions.

FACTOR	ΔV ft/sec	Percent V
1. Gravitational field of Sun	10	.03
2. Eccentricity of moon's orbit	45	.13
3. Inclination of orbit of moon	20	.06
4. Oblateness of earth	20	.06
5. Pressure of Solar radiation	.04	---

Thus you can see that the effects are small but probably should be included as corrections to any moon orbit calculations.

3.9 Trajectories Near Minimum Velocities

In Section 3.6 and 3.7 the relative velocities corresponding to the points of coalescence (C_2 , C_4 , C_6 , and C_8) were determined for a reference position 4300 miles from the center of the Earth toward the Moon. In reference 3-4 calculations of trajectories were made (three-body equations) using the minimum velocity corresponding to C_2 , but for a reference position 200 kilometers above the surface of the Earth, (reference radius 4084 miles) as indicated below:



The corresponding minimum relative velocities are indicated below:

	$r_1 = 4300 \text{ mi.}$	$r_1 = 4084 \text{ mi.}$	
	<u>ft/sec</u>	<u>ft/sec</u>	<u>km/sec</u>
V_2	34703.8	35572.2	10.84890
V_4	34706.4	35574.8	10.84968
V_6	34732.4	35600.0	10.85738
V_8	34736.3	35603.8	10.85854

For the initial calculations, the initial velocity corresponding to C_2 (V_2) was directed perpendicular to the initial geocentric (Earth)

radius and in the direction of the Moon's rotation. From equation (3.7-8) it can be seen that this orientation will give the maximum value of the initial velocity relative to the Earth (V_e). The results of these calculations are shown in Figure 3-9 from reference 3-4. (Note: This figure and many of the figures to follow are taken from reference 3-4 and distances are given in kilometers and velocities in kilometers per second.)

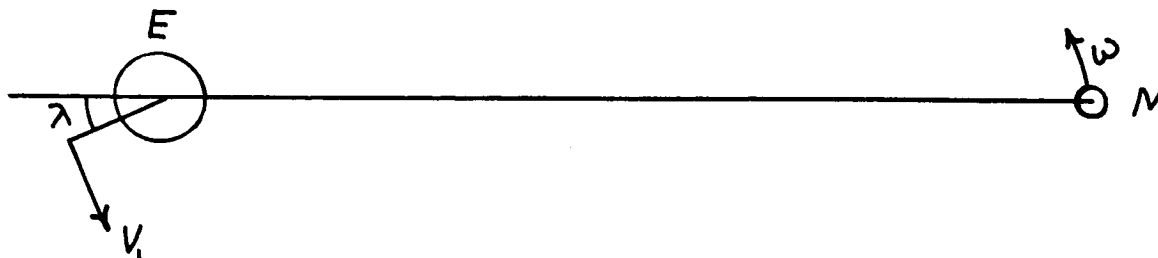
In Figure 3-9 are shown the first five orbital revolutions plotted in the $x y$ rotating axes system. Also shown are the zero relative velocity boundaries corresponding to C_2 . It can be seen that the vehicle does not reach the boundary in five orbital revolutions. The time elapsed during these five revolutions is about 29 days. The same orbits are shown in translating Earth axes (x_e, y_e) in Figure 3-10. Shown are the first and fifth orbital revolutions. It can be seen that the increase in the apogee is noticeable but small, and the orbits appear to be very close to two-body ellipses. It has been estimated that about 200 orbital revolutions would be necessary for a vehicle to reach the boundary C_2 . (This would take about 3 years.)

Calculations were also made of the first orbital revolution when the initial launch angle was changed from $\gamma = 0^\circ$ to $\gamma = 180^\circ$. Trajectories are shown in Figure 3-11 for the four cases indicated below.



From Figure 3-11 it can be noted that the initial apogee is greatest when $\gamma = 0^\circ$ or when the geocentric velocity V_e is greatest (equation (3.7-8)) since $V_{eI} > V_{eII} > V_{eIII} > V_{eIV}$.

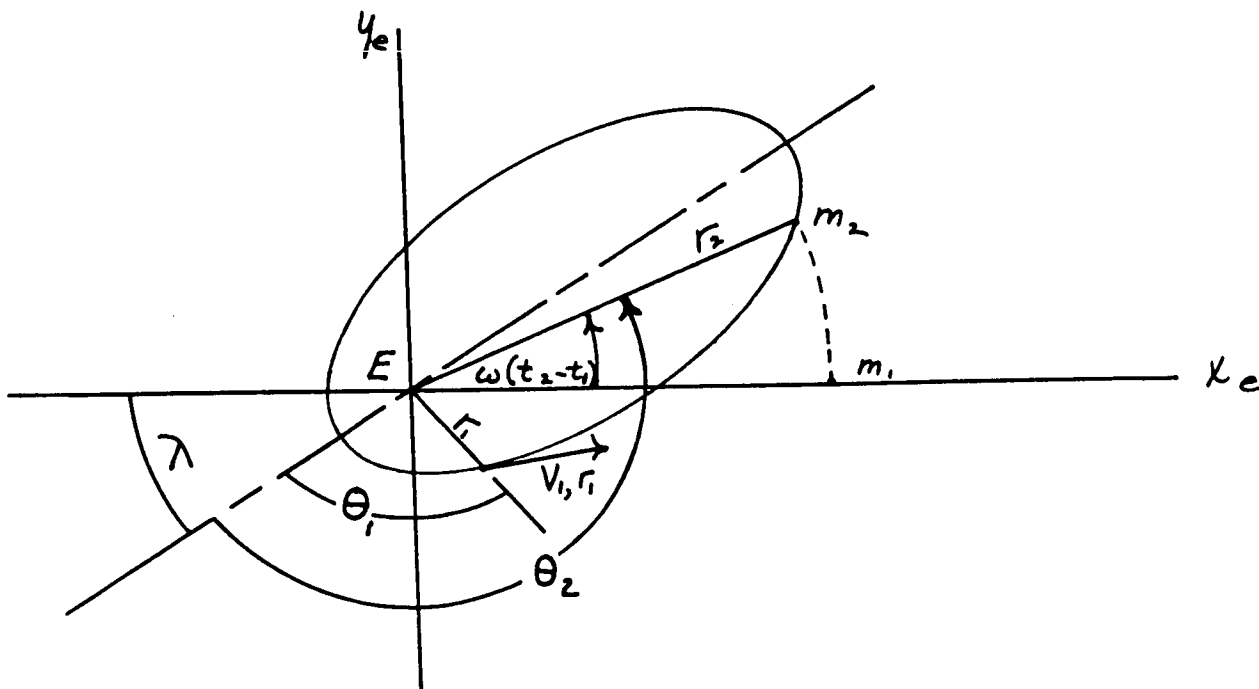
In examining Figures 3-9 and 3-11 it appears that the C_2 boundary might be approached more closely if the vehicle were launched behind the Earth, $\lambda < 90^\circ$, so that it might come closer to the Moon on the first orbital revolution:



In reference 3-4 calculations were also made using values of the initial velocity corresponding to C_4 , C_6 , and C_8 . Even when the initial velocities corresponded to the velocity for which all points in the Earth-Moon system could be reached (C_8) the trajectories did not reach even the boundary C_2 on the first orbital revolution. Therefore it is apparent that these minimum velocities are not adequate for practical considerations.

3.10 Use of Two-Body Ellipses to Approximate Lunar Orbits

Since the trajectories of Figure 3-10 are almost ellipses centered at the Earth (geocentric) the trajectory of the first orbital revolution might be approximated by neglecting the effect of the Moon.



If the initial radius, initial velocity, and initial launch elevation angle are given (r_1, V_1, γ_1) , and the initial velocity is equal to or greater than the velocity necessary to reach the Moon the eccentricity ϵ and the orientation angle θ_1 can be computed from the equations of Section I.

The angle θ_2 is given by

$$\cos \theta_2 = \frac{1}{\epsilon} \left(\frac{p}{r_2} - 1 \right) \quad 3.10-1$$

where γ_2 is the distance from the Earth to the Moon ($\gamma_2 = D$) and $p = r_p = r_1 (v_1/v_S)^2 \cos^2 \gamma_1$ (SECTION I) From the preceding sketch the angle λ between the original Earth-Moon axis and the principal axis of the orbit is:

$$\lambda = \pi + \omega [t(\theta_2) - t(\theta_1)] - \theta_2 \quad 3.10-2$$

where $t(\theta)$ is the time to reach the angle θ measured from the perigee. (See SECTION I)

The minimum condition for lunar impact is for $r_2 = r_a = D$. For this case:

$$\begin{aligned} \theta_2 &= 180^\circ \\ t(\theta_2) &= T/2 \\ \lambda &= \omega [T/2 - t(\theta_1)] \\ a &= \frac{D + r_p}{2} \\ v_p^2 &= 2 g_0 R^2 \left[\frac{1}{r_p} - \frac{1}{D + r_p} \right] \end{aligned} \quad 3.10-3$$

(where the subscripts a and p refer to apogee and perigee respectively.)

For a perigee radius of 4300 miles the initial velocity for a perigee launch would be

$$v_p = 34902 \text{ ft/sec}$$

whereas the minimum velocity to reach the Moon corresponding to C_2 is ($\varphi = 180^\circ$, see equation 3.7-8)

$$v_{e2} = 34772 \text{ ft/sec}$$

The escape velocity is

$$V_E = 35214 \text{ ft/sec}$$

Thus the velocity obtained from the two body approach is 130 ft/sec greater than the velocity corresponding to C_2 , and 312 ft/sec less than the escape velocity.

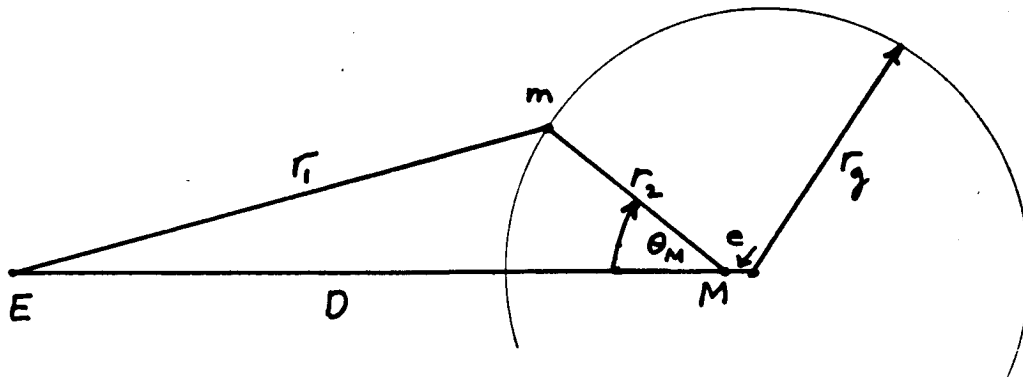
In reference 3-4 trajectories were calculated using the above equations and also using the three body equations (equation 3.2-7) for values of γ from 0 to 180° . In Figure 3-12 the results of one of these calculations are shown for $\gamma_1 = 0$ and $h = 124.3 \text{ mi (200 km)}$. The trajectory labeled I is the two body ellipse with the initial velocity equal to V_p (equation (3.10-3)). The trajectory labeled II is an impact trajectory with Moon computed using the three body equations (3.2-7). The three body trajectories are shown in both the (x, y) rotating axes system and the (x_{e_0}, y_{e_0}) inertial axes system (taken through the center of the Earth at $t = 0$). It can be seen that the trajectories are almost the same until they reach the vicinity of the Moon. It was found in reference 3-4 that equation (3.10-3) can be used for determining the minimum velocity necessary for striking the Moon with an initial velocity accuracy of approximately 0.02 meters per second. Thus the initial conditions can be calculated disregarding the influence of the Moon. Nevertheless, the actual orbits in the vicinity of the Moon will vary considerably from the simple elliptical orbit.

3.11 Locus of Points of Equal Attraction

Between the Earth and the Moon

Considerable attention has been given to the point of equal gravitational attraction between the Earth and the Moon. It has been suggested in many sources that a space vehicle need only reach this point of equal attraction to reach the Moon or "to fall into the Moon."

Let r_1 be the distance of a space vehicle from one celestial body and r_2 the distance from another celestial body.



The locus of points of equal attraction is then given by

$$\frac{r_2}{D} = \frac{-\cos \theta_M + \sqrt{M_1/M_2 - \sin^2 \theta_M}}{M_1/M_2 - 1}$$

3.11-1

where M_1 and M_2 are the mass of the two bodies (for instance, the Earth and the Moon). This locus can be shown to be equal to a sphere of radius

$$\frac{r_{gEM}}{D} = \frac{\sqrt{M_1/M_2}}{M_1/M_2 - 1} \quad 3.11-2$$

with its center located at $D + e$ where

$$\frac{e}{D} = \frac{1}{M_1/M_2 - 1} \quad 3.11-3$$

For the Earth-Sun

$$\frac{r_{gSE}}{R} = 0.00173177$$

where in this case R is the distance between the Earth and the Sun; or in terms of the distance from the Earth to the Moon:

$$\frac{r_{gSE}}{D} = 0.6743$$

For the Earth-Moon:

$$\frac{r_{gEM}}{D} = 0.1122$$

The sphere of equal gravitational attraction (sometimes called "gravisphere") between the Earth and the Sun and between the Earth and the Moon is shown in Figure 3-13. It is to be noted that the Moon is always attracted more by the Sun than by the Earth. In Figure 3-14 is shown the gravitational attraction of the Earth and of the Moon along the line joining the Earth and the Moon.

In reference 3-4 calculations were made of an orbit which would reach the point of equal gravitational attraction. The results are shown in Figure 3-15. The trajectory labeled I is the ellipse neglecting the presence of the Moon, and the curve labeled II is the result of the three-body calculations. The perturbation of the orbit caused by the Moon is very noticeable in Figure 3-15 and it can be seen that although the point of equal gravitational attraction is exceeded the vehicle would not reach the Moon. Thus the belief that the vehicle need only reach the point of equal gravitational attraction to reach the Moon is not true.

3.12 Sphere of Influence

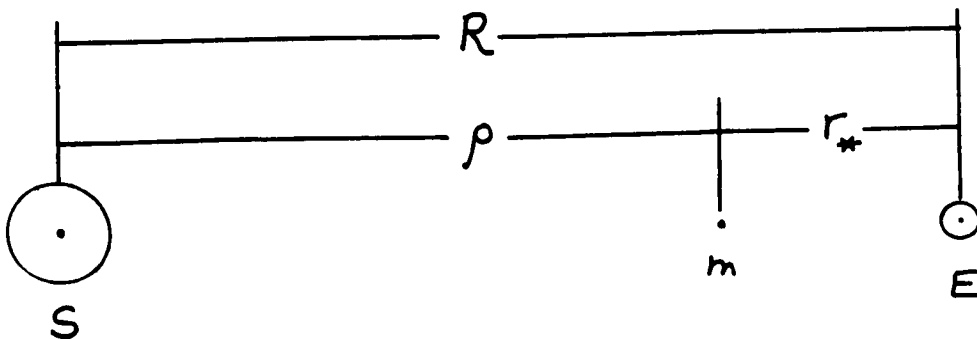
There is another space about attracting bodies called the Sphere of Influence (references 3-1 and 3-4) which is more important to trajectory studies than the "gravisphere". The Sphere of Influence is defined as follows for the Sun-Earth system:

The location in space about the Earth where the ratio of the force with which the Sun perturbs the geocentric (about Earth) motion of a vehicle (D_S) to the force of the Earth's attraction (A_E) is equal to the ratio of the force with which the Earth perturbs the heliocentric (about Sun) motion of the vehicle (D_E) to the attraction of the Sun (A_S) is called the Sphere of Influence of the Earth. This definition is more clearly stated with the equation

$$\frac{D_S}{A_E} = \frac{D_E}{A_S} \quad 3.12-1$$

where D_S and D_E represent the disturbing force of the Sun and Earth respectively and A_S and A_E represent the attraction of the Sun and Earth respectively. Within the Sphere of Influence:

$$\frac{D_S}{A_E} < \frac{D_E}{A_S} \quad 3.12-2$$



The ratio of the force with which the Sun perturbs the geocentric motion of a space vehicle to the force of attraction of the Earth is found as follows:

From the preceding the acceleration of the space vehicle due to the Earth is

$$A_{EM} = \frac{GM_E}{r_*^2} \quad 3.12-3$$

The acceleration of the space vehicle due to the Sun is

$$A_{SM} = \frac{GM_S}{\rho^2} \quad 3.12-4$$

The acceleration of the Earth due to the Sun is

$$A_{SE} = \frac{GM_S}{R^2} \quad 3.12-5$$

The ratio of the disturbing effect of the Sun to the attraction of the Earth is then

$$\frac{D_S}{A_E} = \frac{A_{SM} - A_{SE}}{A_{EM}} = \left(\frac{M_S}{M_E} \right) r_*^3 \frac{(R + \rho)}{R^2 \rho^2} \quad 3.12-6$$

In a similar manner, the ratio of the disturbing effect with which the Earth perturbs the heliocentric motion of a vehicle to the attraction of the Sun is

$$\frac{D_E}{A_S} = \left(\frac{M_E}{M_S} \right) \rho^3 \frac{(R + r_*)}{R^2 r_*^2} \quad 3.12-7$$

The Sphere of Influence is defined as the space about the Earth in which

$$\frac{D_S}{A_E} < \frac{D_E}{A_S} \quad 3.12-2$$

Equating the two sides of equation 3.12-2 the value for the boundary of the Sphere of Influence can be found to be

$$r_* = \left(\frac{R + r_*}{2R - r_*} \right)^{1/5} (R - r_*) \left(\frac{M_E}{M_S} \right)^{2/5} \quad 3.12-3$$

The disturbing effect is a maximum when r_* is positive (nearest the Sun) and a minimum when r_* is negative (farthest from the Sun).

Now since $M_S \gg M_E$, then $R \gg r_*$ and the radius of the Sphere of Influence can be given approximately by

$$r_* \approx \left(\frac{1}{2} \right)^{1/5} R \left(\frac{M_E}{M_S} \right)^{2/5}$$

$$r_* \approx 0.8705 R \left(\frac{M_E}{M_S} \right)^{2/5} \quad 3.12-4$$

For the Sun-Earth system equation (3.12-4) is an excellent approximation since $M_S/M_E = 333,434$. The Sphere of Influence given by equation (3.12-4) about the Earth is

$$r_{*SE} = 502,000 \text{ miles}$$

or about 2.1 times the distance between the Earth and the Moon. Thus the Sphere of Influence of the Earth includes the Moon.

The Sphere of Influence of the Moon found in the same manner (equation (3.12-4)) is

$$r_{*EM} = 35,800 \text{ mi} = 0.1498 D$$

This approximation for the Moon is not as exact as for the Earth since $M_E/M_M = 81.45$. Equation (3.12-4) can be used as a first estimate, however, and if more accurate values are desired this value may be substituted in equation (3.12-3) and then a more correct value found by iteration.

The location of the Sphere of Influence (on a line between the Earth and the Moon) found by iteration was 32,200 miles in front of the Moon and 39,600 miles in back of the Moon. The average of these two values is about the same as given by equation (3.12-4).

In Figure 3-16 the Sphere of Influence for the Earth and the Moon is shown. The Sphere of Influence of the Moon is also shown in Figure 3-13.

It will be of interest to compute the ratio of the disturbance of the Sun on the geocentric motion of a space vehicle to the attraction of the Earth. Within the Sphere of Influence the magnitude of the perturbing action of the Sun will be a maximum at the boundary. This value is:

$$\frac{D_S}{A_E} = 0.104$$

At a distance of the Moon's orbit this value is:

$$\frac{D_S}{A_E} = 0.011$$

and of course at distances less than the distance to the Moon from the Earth the effect of the Sun is much smaller. Thus the effect of the Sun on the motion of a space vehicle within the Earth-Moon system is small (one percent or less) and probably can be neglected in preliminary calculations for Earth-Moon vehicles.

The ratio of the perturbing effect of the Earth on the selenocentric (about Moon) motion of a space vehicle to the attraction of the Moon at the boundary of the Sphere of Influence of the Moon is

$$\frac{D_E}{A_M} = 0.702$$

Therefore the perturbing effect of the Earth is about 70 percent of the attraction of the Moon at the boundary of the Sphere of Influence.

3.13 Approximate Method of Calculating Trajectories of Lunar Vehicles

If it is assumed that within the Sphere of Influence of a body that perturbations of other bodies may be neglected then orbits can be computed using the two body equations of SECTION I. The trajectory can be divided into two parts for the Earth-Moon system:

1. Motion toward or away from the Sphere of Influence in which the effect of the Moon is neglected.
2. Motion within the Sphere of Influence in which the effect of the Earth is neglected.

The motion toward or away from the Sphere of Influence (1) is calculated by means of the two body orbit equations using the initial conditions r_1 , V_{e1} , γ_1 , and λ_1 of the geocentric coordinate system. At the point where the vehicle enters the Sphere of Influence of the Moon the coordinates and the entry velocity V_{e2} are converted to the selenocentric (Moon) coordinate system.

The approach trajectory may be an ellipse, a parabola, or a hyperbola depending on the initial velocity. In reference 3-4 it was shown that the part of the trajectory located within the Sphere of Influence of the Moon is always a hyperbola in selenocentric coordinates.

The Escape velocity of the Moon on the boundary of the Sphere of Influence is

$$V_{Em} = \sqrt{2 \frac{GM_m}{r_*}} = 1352.6 \text{ ft/sec}$$

where $GM_m = \mu_{\text{Moon}} = 1.7283 \times 10^{14} \text{ ft}^3/\text{sec}^2$

Since the entry selenocentric velocities are always greater than the Escape Velocity of the Moon it is apparent that the Moon cannot "capture" the vehicle and an artificial satellite of the Moon cannot be established without the use of retrograde rockets.

3.13.1 Method of calculating lunar orbits using approximate method.- The approximate method is illustrated in the sketch on the following page. In the following description the small rotation of the Earth about the Moon is neglected. The effects of this assumption are discussed later.

The initial conditions for the approach trajectory as indicated in sketch a and b are V_{e1} , r_{e1} , γ_{e1} , and the orientation angle λ between the major axis of the approach orbit and the initial position of the Earth-Moon axis. The point at which the approach trajectory intersects the Sphere of Influence is determined (either analytically or graphically) and at this point (point 2 in the sketch) the geocentric parameters r_{e2} , V_{e2} , and γ_{e2} are converted to the corresponding selenocentric parameters r_{m2} , V_{m2} , and γ_{m2} . These values may be found in the following manner.

Referring to sketches (a) and (b), the radial velocity of the Moon (V_ω) is

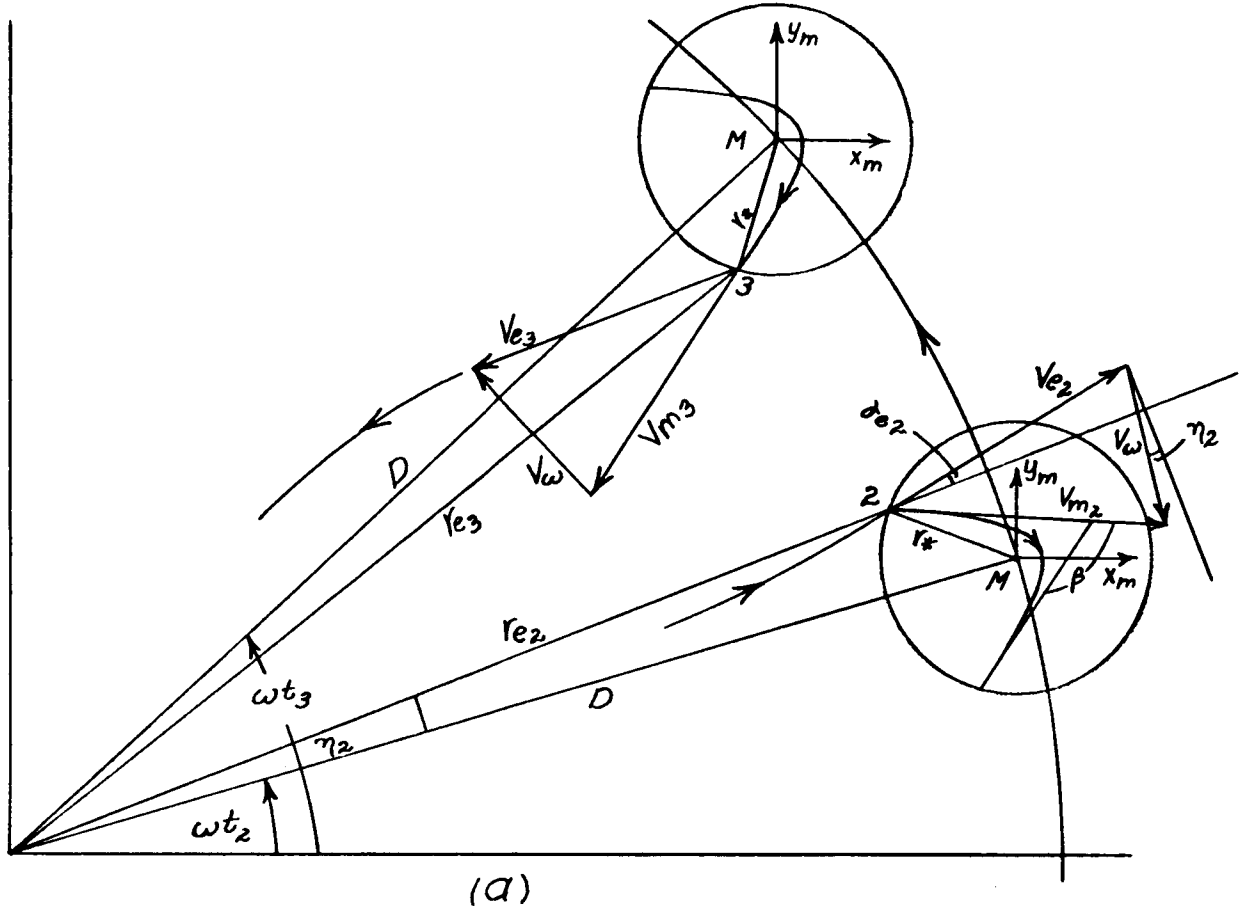
$$V_\omega = \omega D \quad 3.13-1$$

The angle η_2 between the Earth-Moon axis D and the radius r_{e2} is

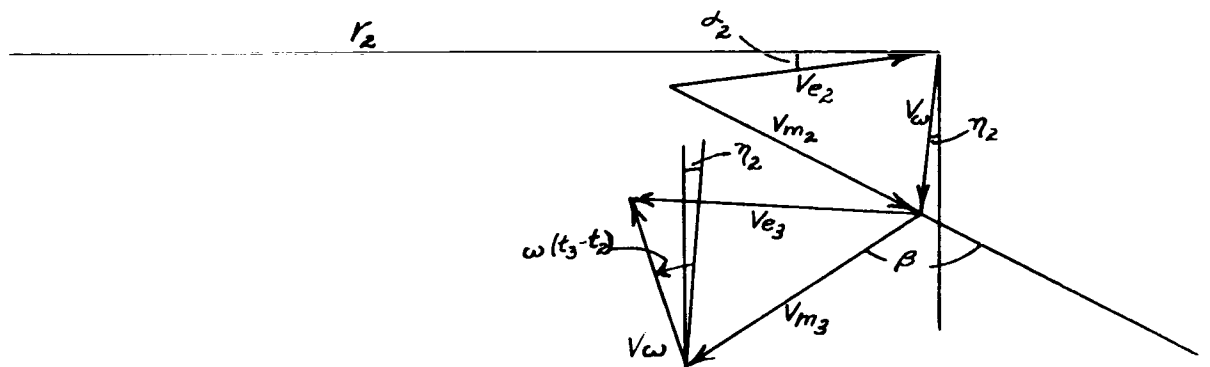
$$\eta_2 = \theta_{e2} + \lambda - \omega t_2 - \pi \quad 3.13-2$$

120<

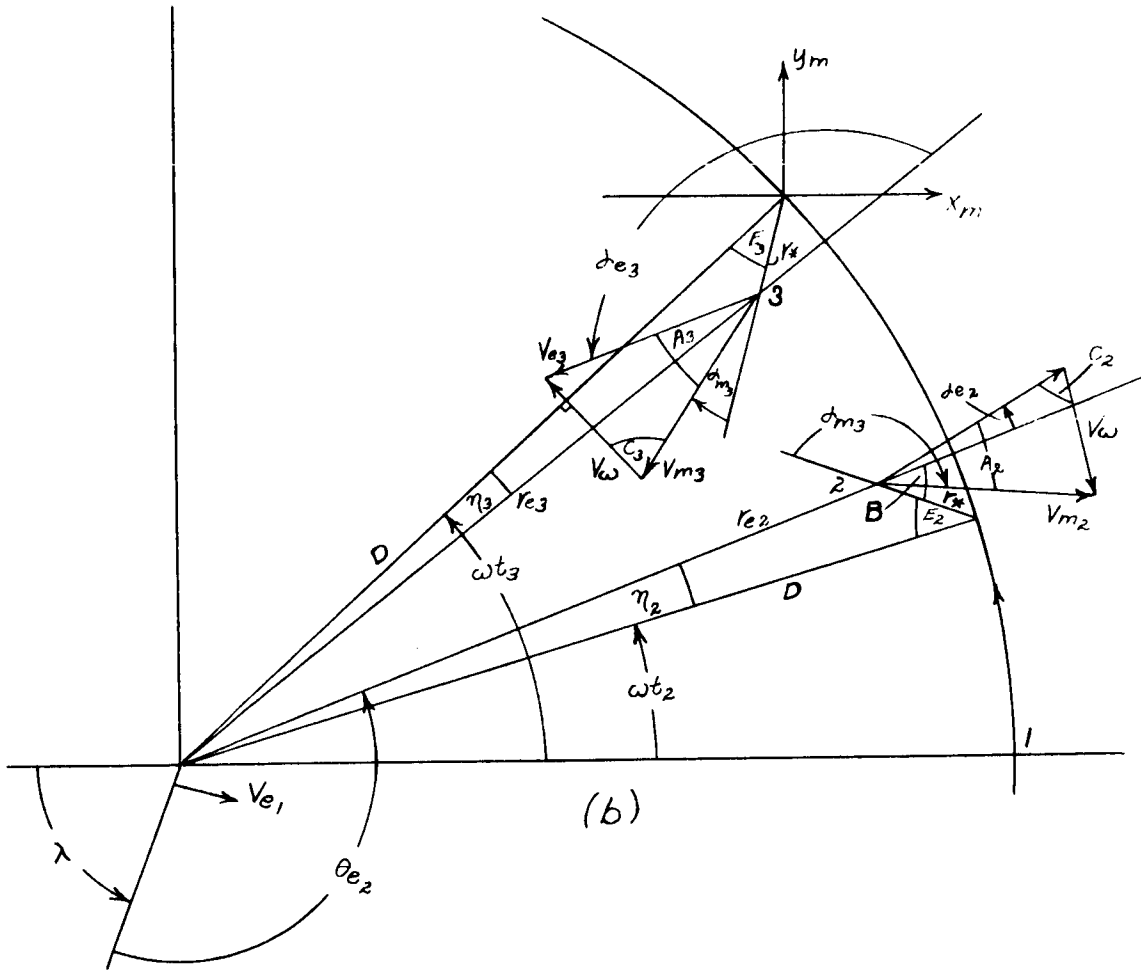
3-41

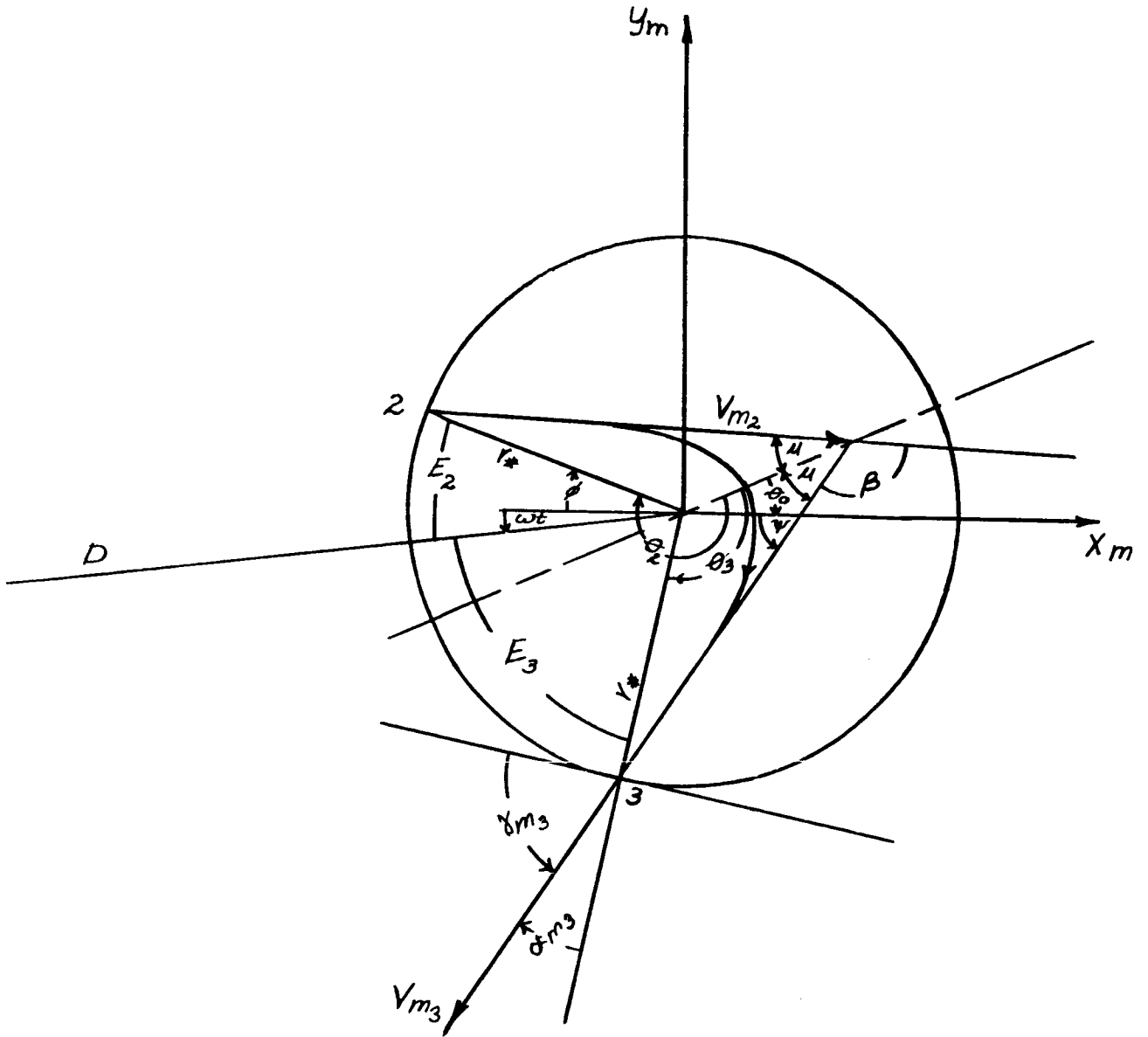


The velocity vectors may be found from the following vector diagram:



Note that the numerals 1, 2, 3 refer to times of consecutive positions of the Moon.





(c)

The angle C_2 between V_{e_2} and V_ω is

$$C_2 = \pi/2 - (\alpha_{e_2} + \eta_2) \quad 3.13-3$$

but

$$\gamma = \pi/2 - \alpha \quad 3.13-4$$

Therefore

$$C_2 = \gamma_{e_2} - \eta_2 \quad 3.13-5$$

The entry velocity in selenocentric coordinates is then

$$v_{m_2}^2 = v_{e_2}^2 + v_\omega^2 - 2 v_{e_2} v_\omega \cos C_2 \quad 3.13-6$$

The angle B between the initial selenocentric radius ($r_{m_2} = r_*$) and the geocentric radius r_{e_2} at time t_2 is given by

$$\sin B = \frac{\sin \eta_2}{r_* / D} \quad 3.13-7$$

The angle A_2 between V_{e_2} and V_{m_2} is given by

$$\sin A_2 = \frac{v_\omega}{v_{m_2}} \sin C_2 \quad 3.13-8$$

The angle α_{m_2} is then equal to

$$\alpha_{m_2} = \pi - \alpha_{e_2} - B + A_2 \quad 3.13-9$$

or

$$\gamma_{m_2} = B - A_2 - \gamma_{e_2}$$

3.13-10

and, of course, the final entry condition is

$$r_{m_2} = r_*$$

3.13-11

With these initial conditions (equations 3.13-6, 10, and 11) the orbit within the Sphere of Influence can be calculated by the methods of SECTION I.

Next we must concern ourselves with the relationships of the parameters within the Sphere of Influence. Referring to sketch (b) and (c) we note that the angle E_2 between r_* and D is given by

$$\sin E_2 = \frac{r_{e_2}}{r_*} \sin \eta_2$$

3.13-12

The angle φ between the Moon x axis and $r_{m_2} = r_*$ is

$$\varphi = E_2 - \omega t_2$$

3.13-13

The angle θ_2 in sketch (c) is the orientation angle given as θ_1 in SECTION I:

$$\theta_2 \equiv \theta_1 \text{ of SECTION I}$$

The angle θ_0 between the Moon x axis and the major axis of the selenocentric orbit is

$$\theta_0 = \theta_2 - \varphi - \pi$$

3.13-14

The angle θ_3 between the major axis and $r_{m_3} = r_*$ is

$$\theta_3 = 2\pi - \theta_2$$

3.13-15

and since $r_{m2} = r_{m3} = r_*$:

$$\gamma_{m3} = -\gamma_{m2} \quad 3.13-16$$

and

$$V_{m3} = V_{m2} \quad 3.13-17$$

The angle μ between the major axis of the selenocentric orbit and V_{m2} or V_{m3} is

$$\mu = \pi - (\alpha_{m3} + \theta_3) \quad 3.13-18$$

or since $\alpha_{m3} = \pi/2 - \gamma_{m3}$

$$\mu = \pi/2 + \gamma_{m3} - \theta_3 \quad 3.13-19$$

The angle β between the entry selenocentric velocity (V_{m2}) and the exit selenocentric velocity (V_{m3}) is

$$\beta = \pi - 2\mu \quad 3.13-20$$

or

$$\beta = 2(\theta_3 - \gamma_{m3}) \quad 3.13-21$$

The angle ψ between the Moon x axis and the exit velocity V_{m3} is

$$\psi = \theta_0 + \mu \quad 3.13-22$$

The conditions on leaving the Sphere of Influence are found as follows (see sketch (b) and (c)):

The angle E_3 between D and $r_{m3} = r_*$ is

$$E_3 = \psi - \omega t_3 + \alpha_{m3} \quad 3.13-23$$

Therefore the exit geocentric radius is

$$r_{e3}^2 = r_*^2 + D^2 - 2r_* D \cos E_3 \quad 3.13-24$$

The angle C_3 between V_{m3} and V_ω is

$$C_3 = \pi/2 - \psi + \omega t_3 \quad 3.13-25$$

Therefore exit geocentric velocity is

$$V_{e3}^2 = V_{m3}^2 + V_\omega^2 - 2 V_{m3} V_\omega \cos C_3 \quad 3.13-26$$

The angle η_3 between r_{e3} and D is given by

$$\sin \eta_3 = \frac{r_*}{r_{e3}} \sin E_3 \quad 3.13-27$$

The angle A_3 between V_{e3} and V_{m3} is given by

$$\sin A_3 = \frac{V_\omega}{V_{e3}} \sin C_3 \quad 3.13-28$$

The angle α_{e3} between the geocentric radius r_{e3} and the velocity vector V_{e3} is then

$$\alpha_{e3} = \pi - A_3 + \psi - \omega t_3 + \eta_3 \quad 3.13-29$$

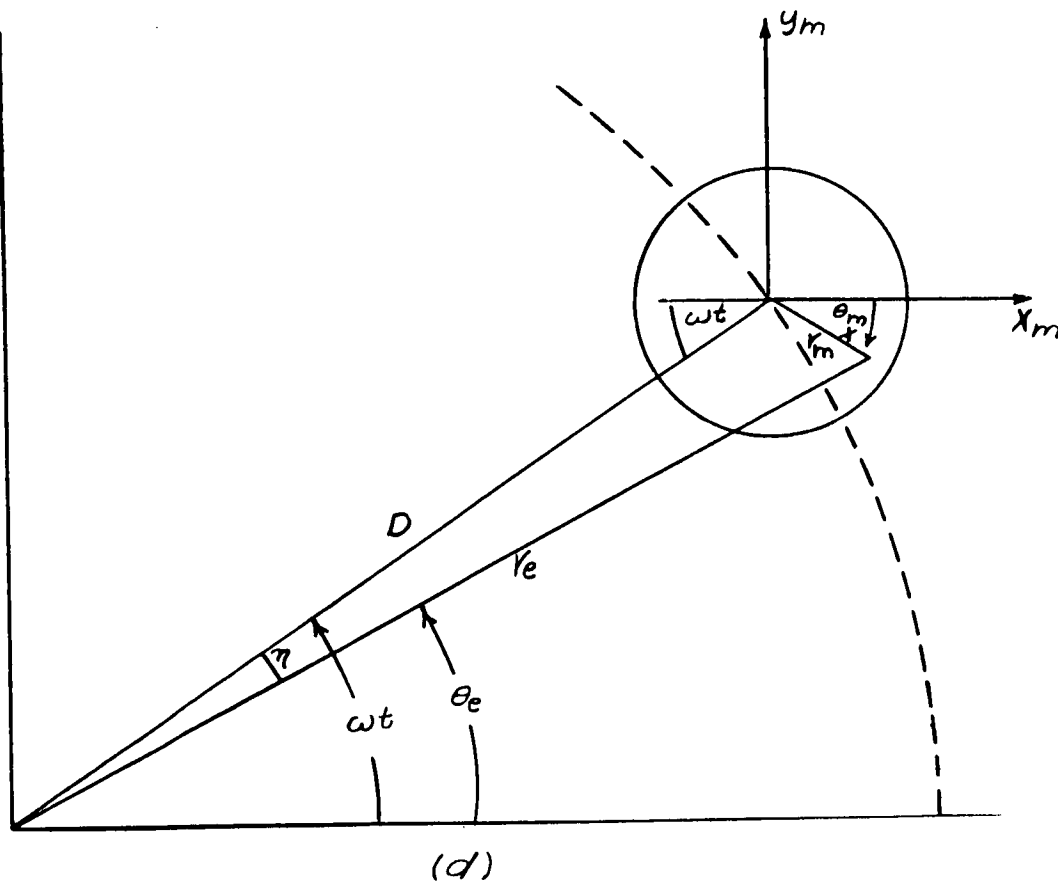
or since $\gamma = \frac{\pi}{2} - \alpha$

$$\gamma_{e3} = A_3 + C_3 - \eta_3 - \pi$$

3.13-30

Thus the exit geocentric conditions given by equations (3.13-24), (3.13-26), and (3.13-30) can be used with the methods of SECTION I to compute the orbit after leaving the Sphere of Influence.

3.13.2 Motion within the lunar Sphere of Influence in Geocentric coordinates.- The motion within the Sphere of Influence can be given in terms of the Earth coordinate system as follows:



The angle θ_{x_m} between the Moon x axis and the instantaneous radius r_m of the selenocentric orbit is

$$\theta_{x_m} = \theta_m - \theta_0 \quad 3.13-31$$

where θ_m is the angle θ (see SECTION I) for the selenocentric orbit.

The geocentric radius is then

$$r_e^2 = r_m^2 + D^2 + 2 r_m D \cos (\theta_{x_m} + \omega t) \quad 3.13-32$$

The angle η is given by

$$\sin \eta = \frac{r_m}{r_e} \sin (\theta_{x_m} + \omega t) \quad 3.13-33$$

and the angle θ_e is

$$\theta_e = \omega t - \eta \quad 3.13-34$$

3.13.3 Effect of neglecting the Earth's revolution about the Moon.-

The approximate method described in the previous section was based on the assumption that the Moon rotated about the center of the Earth instead of the center of mass of the Earth-Moon system. The major effect of this assumption is that the angle η between the Earth-Moon axis and the radius from the Earth to the vehicle will be in error by approximately 1 percent or less. (< 0.1 deg)

In calculating the approach trajectory using the two-body relationships the errors in the geocentric parameters θ_e and r_e due to the revolution of the Earth about the center of mass will be less than 2 percent. This

is a relatively large effect but can be corrected by calculating the initial approach trajectory about the revolving Earth using the equations of SECTION I in a step by step procedure.

In addition the trigonometric procedures of SECTION 3.13.1 should be used with caution since these were developed for the particular case illustrated in sketches (a), (b), and (c). In other cases certain adjustments may have to be made based on the physical characteristics of the orbit being calculated.

A trajectory calculated using the approximate method (ref. 3-4) is shown in Figure 3-17. (It should be noted in Figure 3-17 and other figures taken from reference 3-4 that the rotating y axis has been shifted to the midpoint between the Earth and the Moon and is designated as y' . Also in reference 3-4 the Moon was located at $\omega t + \pi$ as compared to the results presented in this section, and the figures taken from reference 3-4 have not been redrawn.)

3.14 Characteristics of Approach Trajectories

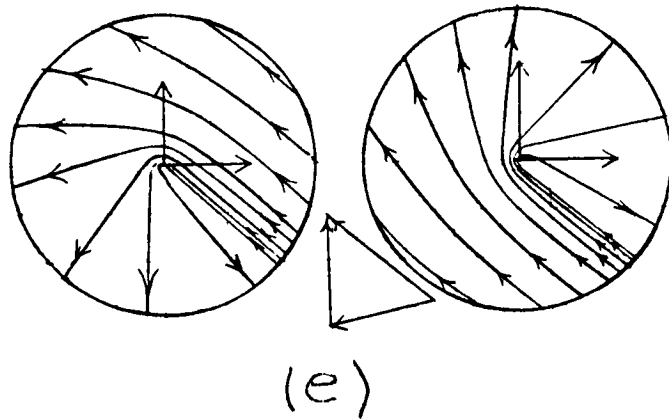
In reference 3-4 a study of the characteristics of approach trajectories at the boundary of the Sphere of Influence was made and the results are indicated in Figures 3-18 and 3-19 and in sketch (e).

In Figure 3-18 the geocentric entry angle α_{e2} , the geocentric entry velocity V_{e2} , and the initial selenocentric velocity V_{m2} are plotted against the difference between the initial geocentric velocity and the escape velocity at the launching altitude ($V_{e1} - V_{eP}$). Curves are shown for entry radii of $D \pm r_*$ and for initial launch angles of $\alpha_1 = \pm \pi/2$ ($\gamma = 0^\circ, 180^\circ$). It may be noted that for initial launching velocities greater than the escape velocity that the location of entry into the Sphere of Influence ($r_e = D \pm r_*$) does not materially alter the angle α_{e2} or the entry velocity V_{e2} . At launching speeds less than escape velocity and near the minimum velocity for reaching the Moon the effect of the location of entry is more pronounced.

Also it is indicated that the initial selenocentric velocity V_{m2} is not changed greatly by the direction of launch. ($\alpha_{e1} = \pm \pi/2$) At launch speeds near or greater than escape velocity the entry angle α_{e2} does not change rapidly and is in the range below 10 degrees.

At launch speeds greater than escape velocity an increase of 0.1 km/sec in the launching velocity V_{e1} results in an increase of about 0.4 km/sec in the entry velocity V_{e2} and the initial selenocentric velocity V_{m2} .

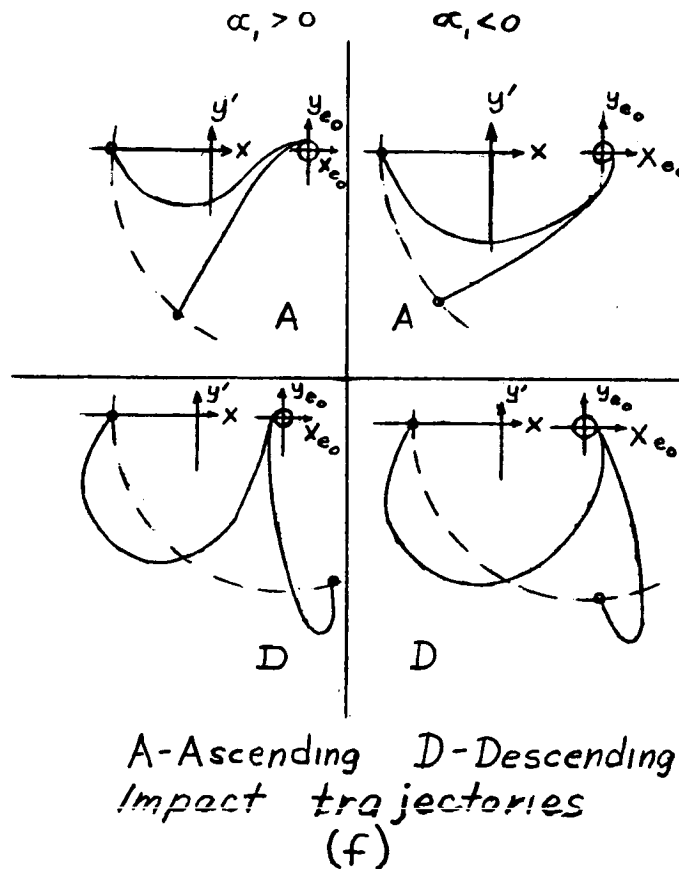
The range of possible orbits within the Sphere of Influence is indicated in the sketch (e)



The flight time required to reach the Sphere of Influence of the Moon from an altitude of 200 kilometers above the Earth is shown in Figure 3-19 as a function of the launch velocity increment ($V_{e1} - V_{eE}$). (ref. 3-4) It can be seen that the effect of the launch elevation angle (α) on the time is very small. The flight time to the Sphere of Influence varies from about 5 days near the minimum velocity to about 1 day at 0.5 kilometer/second above escape velocity.

3.15 Trajectories to Strike the Moon

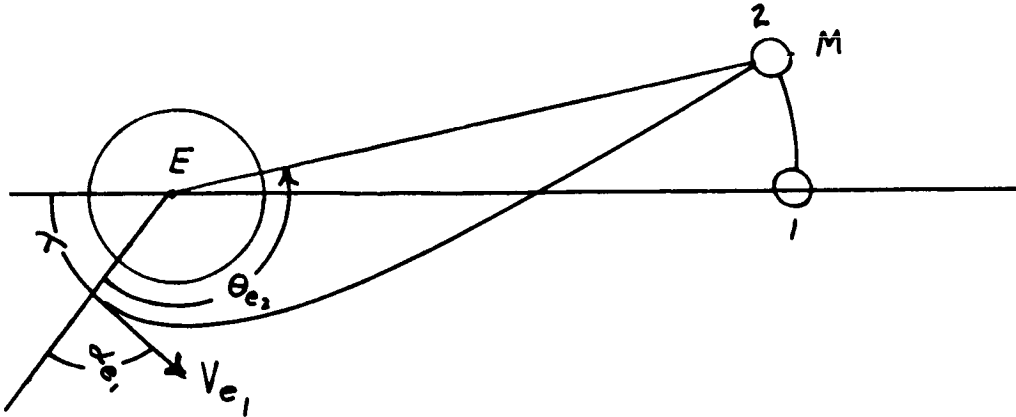
3.15.1 Types of Impact Trajectories.- In any study on lunar flight the first trajectory one thinks of is an impact trajectory. Impact trajectories can be divided into four classes (ref. 3-4) as indicated in sketch (f)



The trajectories can be classified as striking the Moon on an ascending arm A or a descending arm D; and as launched in the direction of the Moon's rotation ($\alpha > 0$) or opposite to the direction of the Moon's rotation ($\alpha < 0$).

A typical impact trajectory of class A, ($\alpha > 0$) is shown in Figure 3-20 in inertial $x_0 - y_0$ axes and in Figure 3-21 in rotating $x-y$ axes. (Ref. 3-5)

In Figure 3-22 are shown the conditions at launch for impact with the Moon calculated using the two body equations of SECTION 3.10. The orientation angle λ between the Earth-Moon axis and the initial launch radius are plotted against the launch velocity increment $V_{e1} - V_{eg}$



At a launch angle of $\alpha = 90^\circ$ ($\gamma = 0^\circ$) the variation of the launch orientation angle λ is small and $\lambda \approx .85$ radian (48.7 degrees). For a launch angle of $\alpha = -\pi/2$ which is opposite to the direction of rotation of the Moon λ varies between 1 and $-.5$ radian for the speed range shown.

The errors caused by using two-body equations for Figure 3-22 were found in reference 3-4 to amount to a distance error of 10-20 kilometers at the Moon near the minimum initial velocity and decreasing to 1 kilometer at launch speeds above escape velocity.

In Figure 3-23 (taken from reference 3-6) the launching conditions for striking the Moon are shown for three orientation angles θ_L . The orientation angle θ_L is defined by

$$\theta_L = \lambda + \theta_1 \quad 3.15-1$$

In Figure 3-22 the orbit orientation angle $\theta_1 = 0$; therefore $\lambda = \theta_L$.

In Figure 3-23 the launch velocity V_1 is plotted against the launch elevation angle γ_{e1} at values of $\theta_L = 45^\circ$, 112.5° , and 180° for a launch altitude of about 350 miles.

It can be seen from Figure 3-23 that a launch velocity greater than 34,800 ft/sec is needed to strike the Moon for a launch altitude of 350 miles. The escape velocity at this altitude is about 35,165 ft/sec. From the propulsion stand point it would be desirable to select a velocity as low as is practical, and from a guidance stand point we would like to select a set of initial conditions in a region where the necessary launch elevation angle does not vary considerably with velocity. Thus, from Figure 3-23 it is evident that the launch speed should be above the minimum speed and that, for this example, the launch elevation angle γ does not change appreciably above 35,000 ft/sec. Therefore, in reference 3-6, a speed of 35,000 ft/sec, a launch orientation angle $\theta_L = 72^\circ$, and a launch elevation angle of $\gamma_e = 14.2^\circ$ was selected for the example trajectory.

The times required to reach the Moon for the conditions of Figure 3-23 are as follows:

V_1 , ft/sec	t, days	V at Moon
34,800	4	$\approx 9,000$ ft/sec
35,000	2.5	"
35,500	1.5	"

3.15.2 Accuracy requirements for striking Moon.- The accuracy requirements for lunar vehicles will depend on the type of guidance with which the vehicle is equipped. If the vehicle is equipped with both a launch guidance system and a terminal guidance system the accuracy requirements will be different than a vehicle equipped with only a launch guidance system. In addition the accuracy requirements will depend on the type of terminal guidance such as an infrared scanner or an optical scanner. In this section we shall consider the accuracy requirements of a vehicle which has launching guidance only and follows a free body trajectory to the Moon. In this case we can consider only the errors in the initial launching velocity V_1 and launch elevation angle γ_1 .

In reference 3-6 the accuracy requirements to strike some point on the Moon were calculated for the example selected and the results are shown in Figures 3-24 and 3-25. In Figure 3-24 are shown the limiting conditions for impacting on the Moon for the given set of initial conditions. If the launch elevation angle γ were exact then the velocity could vary by about ± 45 ft/second. If the launch velocity were exact then the launch angle could vary about ± 0.3 degree. It may be seen in Figure 3-24 that the accuracy conditions are not symmetrical, however, and that the tolerances are less in one direction than another. The trajectories in the vicinity of the Moon corresponding to the limiting conditions of Figure 3-24 are shown in Figure 3-25.

In reference 3-4 approximate calculations were made of the accuracy necessary to strike some point on the Moon, and the results of these calculations are shown in Figure 3-26 for a launching altitude of

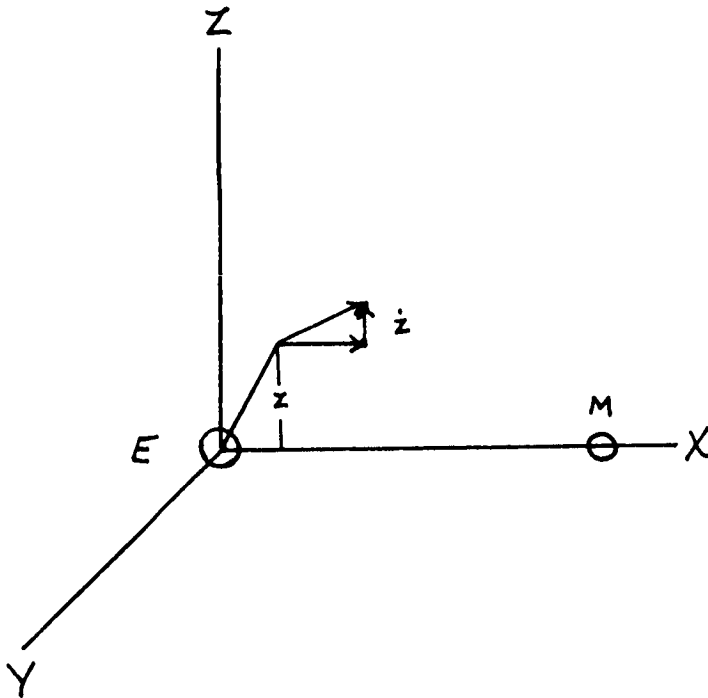
200 kilometers. The maximum errors in launch conditions are shown as a function of ^{the ratio of} the initial velocity to the escape velocity (V_1/V_E).

From this figure it is indicated that the optimum condition is near the escape velocity. At this point errors of about 180 ft/sec in velocity and about 0.3 degree in angle can be tolerated. At speeds above and below the escape velocity the allowable error in velocity decreases. Although the allowable error in launch elevation angle increases rapidly below escape velocity, the allowable error in launch velocity decreases rapidly nullifying the beneficial effect for launch angle.

In Figure 3-27 trajectories are shown (ref. 3-4) for an initial velocity close to the minimum necessary to reach the moon. In this case the allowable error in initial velocity is a minimum. For the exact initial conditions impact occurs, but for velocity errors of 2 meters per second (6.5 ft/sec) the vehicle misses the Moon.

In reference 3-4 it was found that errors in the initial radius of ± 50 km (31 miles) were negligible. The maximum permissible error in the orientation angle λ was about 1 degree which means roughly that the time of launch as a free body must be controlled within several minutes.

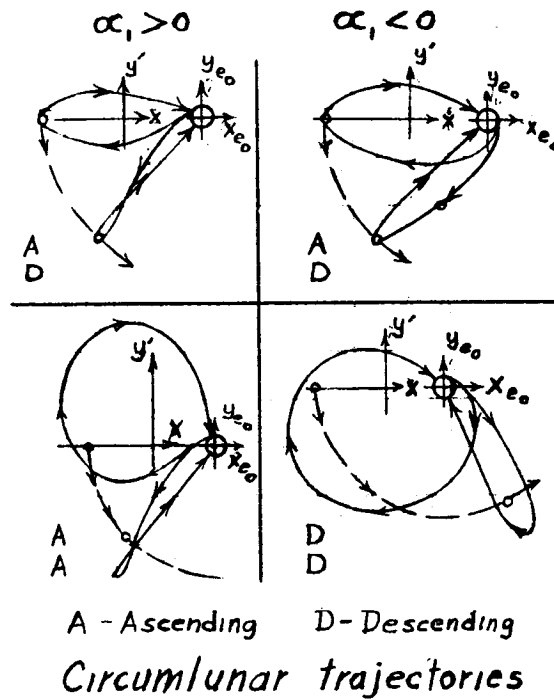
The effect of errors in the plane of the launch was investigated in reference 3-4 and it was found that an impact on the Moon would occur if the vehicle were launched within 50 km (31 miles) of the plane and with the velocity in the z direction less than 50 meters/second (164 ft/sec).



The errors indicated above are for striking the Moon on the ascending arm of the trajectory. The accuracies must be 2-5 times greater to strike the Moon on the descending arm. In addition it was found that the effect of the Sun does not appreciably change the accuracies stated above.

3.16 Circum-Lunar Trajectories

3.16.1 Trajectories with return to earth.- The next lunar trajectory of interest is the orbit which circles the Moon and then returns to the vicinity of the Earth. Trajectories of this type may be useful for study of the back side of the Moon. There are four types of circum-lunar trajectories which are indicated in the sketch below.



The trajectories can be classified as to the direction of launch: in the direction of rotation of Moon, $\alpha > 0$, or opposite to the direction of rotation, $\alpha < 0$. In addition the trajectories can be further classified as to the type of approach to and exit from the line joining the moon to

the Earth as indicated in the sketch for the rotating x-y axis system. The letter A refers to the ascending arm of the trajectory before apogee is reached and the letter D refers to the descending arm after apogee is reached. The upper letter in the sketch refers to the type of trajectory before crossing the line joining the Moon to the Earth, and the lower letter refers to the type of trajectory after crossing this line.

A typical circum-lunar trajectory from reference 3-5 is shown in Figure 3-28. This trajectory is of the type $\alpha > 0, A$. In this type of trajectory the vehicle will either return to hit the Earth or it may miss the Earth and establish an elliptic orbit about the Earth. The life time of such elliptical orbits would, of course, depend on the initial conditions. In reference 3-5 it was determined that the accuracy requirement for this type of trajectory is the least stringent of any lunar trajectory; the allowable error in initial velocity is 150 ft/sec and the allowable error in elevation angle is 10 degrees. It was found, however, that the time of the vehicle's return to Earth could vary as much as 20 days. In addition the distance of the closest approach to the Moon will vary by about 80,000 miles. Therefore, if the purpose of the vehicle were to photograph the far side of the Moon and recover an instrument package on the Earth the tolerances would be greatly reduced. In reference 3-5 it was found that for an uncertainty of 1000 miles in location of the Earth reentry point the initial velocity would have to be within 0.25 ft/sec and the initial elevation angle would have to be within 0.03 degree.

In reference 3-4 trajectories were calculated which would come within 8000 miles of the center of the Moon. The results in this case for combinations of errors in V and γ are as follows:

ΔV , ft/sec	$\Delta \gamma$, deg.	Remarks
- 3	0.6	return to Earth
+ 33	6	return to Earth
- 33	6	collide with Moon or do not circle moon

The accuracy requirements diminish rapidly with an increase in the distance that the vehicle comes from the Moon.

3.16.2 Trajectories with return to Earth with a braking ellipse.-

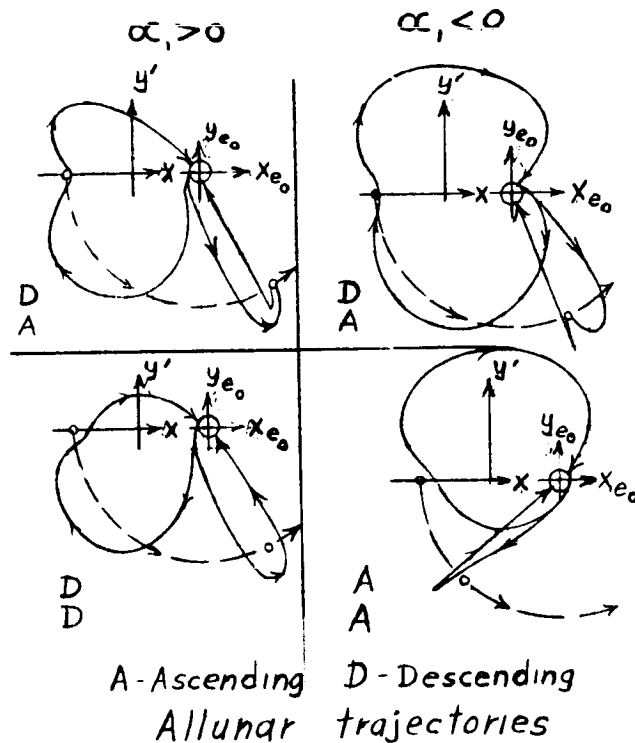
If now, we wished to have a vehicle circle the Moon and then return to Earth in a reentry orbit the accuracy requirements would be very stringent. In this case the results of reference 3-5 indicate an accuracy of 1 ft/sec in the initial velocity and 0.001 degrees in the initial launch angle to obtain an elliptic reentry orbit about the Earth with an uncertainty of 50,000 ft in perigee altitude. An example of such a trajectory is shown in Figure 3-29.

In reference 3-4 it was found that errors in initial velocity as small as 0.7 ft/sec and angle errors of 0.3 degree produced errors in altitude for reentry of 525,000 feet and 625,000 feet, respectively.

Therefore, it is evident that a reentry orbit would be very difficult to obtain without corrections in the flight path.

3.17 Allunar Trajectories

The next type of lunar trajectories is the allunar trajectory; these pass in front of the Moon but do not pass behind the Moon. The four types of allunar trajectories are indicated below (ref. 3-4).

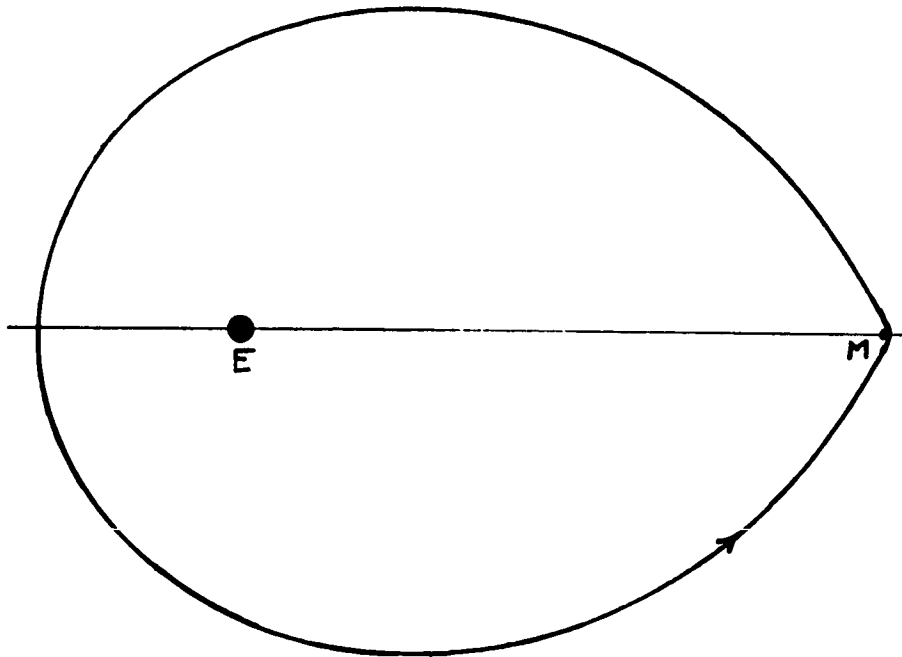


Again the trajectories are classified as the circum-lunar trajectories except in this case it is possible to approach the Moon-Earth line on a descending trajectory and exit on an ascending trajectory. This occurs when the attraction of the Moon causes the vehicle to reverse its descending trajectory as indicated in the sketch.

3.18 Periodic Trajectories

One of the interesting problems of lunar trajectories is the possibility of establishing a periodic orbit about the Earth and the Moon. Considerable work has been done on this problem, some of which is reported in reference 3-4.

3.18.1 Periodic circum-lunar trajectories.- The most interesting periodic orbit would be one which would circle both the Moon and the Earth.



There exist such orbits which appear somewhat like the sketch above. In reference 3-4 several periodic circumlunar orbits were calculated and some characteristics of these are listed in the following table:

	r_e , mi	r_m , mi	V_1 , ft/sec
1.	4,084	93	36,504
2.	26,229	513	14,441
3.	51,475	932	10,446
4.	72,325	1,243	8,995

It may be seen that the only orbit which would not strike the Moon is number 4, and for this orbit the minimum radius from the Earth is over 72,000 miles or almost 20 Earth radii. Such an orbit would probably be of little use. In addition this type of orbit is unstable and perturbations would cause it to diverge. Therefore, there seems to be little possibility of establishing a circumlunar periodic orbit about the Earth and Moon.

3.18.2 Periodic allunar trajectories.- Although there appears to be only one family of circumlunar trajectories there are an unlimited number of allunar trajectories possible. There has been considerable mathematical treatment of such trajectories which are referred to in reference 3-4. Several allunar trajectories computed in reference 3-4 are shown in Figure 3-30. The periods of the trajectories shown vary from about 0.5 to 1.5 months. Although such orbits are of interest it is doubtful that such orbits could be established for a very long period due to perturbations of the orbit.

3.19 Establishing an Artificial Satellite of the Moon

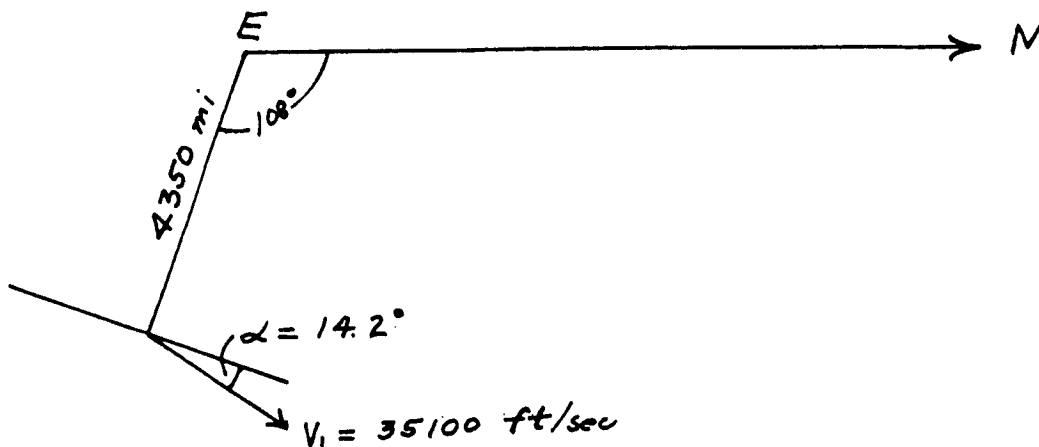
In a previous section it was indicated that the Moon could not "capture" a vehicle because the entry selenocentric velocity was greater than the escape velocity. Therefore in order to establish a satellite of the Moon it is necessary to decrease the selenocentric velocity below the escape velocity with a retrograde rocket. In order for the satellite to stay in orbit about the Moon indefinitely it would be necessary for the velocity to be reduced considerably so that the vehicle would not leave the Sphere of Influence.

The maximum velocity for the vehicle to remain in the vicinity of the Moon can be obtained from Jacobi's Integral for $C = C_2$ (see section 3.4, and Figure 3-3). In reference 3-8 a study of lunar satellite orbits was made and the maximum velocities were calculated. The maximum allowable velocity in selenocentric coordinates is shown plotted against altitude above the Moon's surface in Figure 3-31. Besides the danger of recapture by the Earth there is also the possibility of impacting on the Moon. Therefore, calculations were made in reference 3-8 of the minimum velocities corresponding to lunar impact using two body equations (see SECTION I) and these minimum velocities are also plotted in Figure 3-31. Thus for establishing a lunar satellite the selenocentric velocities must be kept approximately between the limits shown in Figure 3-31. In reference 3-8 it was found that velocities slightly in excess of the maximum could be used for retrograde orbits but that velocities slightly below this maximum would have to be used for direct (in the direction of the Moon's rotation) orbits.

A typical approach trajectory from the Earth is shown in Figure 3-32, and in Figure 3-33 circular lunar satellite orbits are shown as they would appear in x_0, y_0 inertial axes. (Reference 3-8). In Figure 3-34 a satellite orbit about the Moon is shown in rotating x, y coordinates. In Figure 3-35 an orbit is shown in which the initial selenocentric velocity was above the maximum allowable velocity and the vehicle is recaptured by the Earth. A near circular satellite orbit at a distance of 20,000 miles from the Moon is shown in Figure 3-36 (ref. 3-8).

In Figure 3-34 it is evident that the two body approach (SECTION 3.13) could not be used for many orbits of the lunar satellite since the perturbations become more noticeable after several orbital revolutions. The disturbing force of the Earth is about 70 percent of the attraction of the Moon near the Sphere of Influence. Therefore, for more than one or two revolutions about the Moon the three body equations must be used.

In reference 3-8 a typical satellite orbit about the Moon was computed and the allowable errors in launching conditions were computed. This satellite orbit is shown in Figure 3-37. The vehicle was launched as indicated below and a satellite orbit was established at 1,000 miles from the surface of the Moon.



The entry selenocentric velocity at the point where the retrograde rocket was assumed to be fired was 7707 ft/sec. For a 1,000 mile distance the velocity must be below 5,338 ft/sec. The minimum allowable velocity was 3,280 ft/sec. Therefore the value 4,309 ft/sec was selected for the satellite orbit. This requires a velocity increment of about 3,400 ft/sec from the retrograde rocket. (For other satellite orbits velocity reductions of 2000 to 6000 ft/sec are required.)

The allowable errors in initial velocity V_{e1} and launch elevation angle γ_{e1} to establish this orbit were

$$- 33 < \Delta V_{e1} < 77 \text{ ft/sec}$$

$$- .3 < \Delta \gamma_{e1} < .135 \text{ degree}$$

In addition it was found that an error in the retrograde velocity increment of a few percent would not significantly affect the allowable errors in velocity and direction given above.

For the particular satellite orbit computed in reference 3-8, the time of arrival at the Moon varies by about 4 hours for the range of errors indicated above.

The above values are representative for retrograde satellite orbits; for direct orbits the allowable errors in velocity are about one half of those indicated above, whereas the allowable errors in launch elevation angle are approximately the same as for the retrograde satellite orbit.

If we desired that the initial satellite orbit be established within 100 miles of the desired altitude of 1000 miles, then according to reference 3-5 it was found that the initial velocity from the Earth must

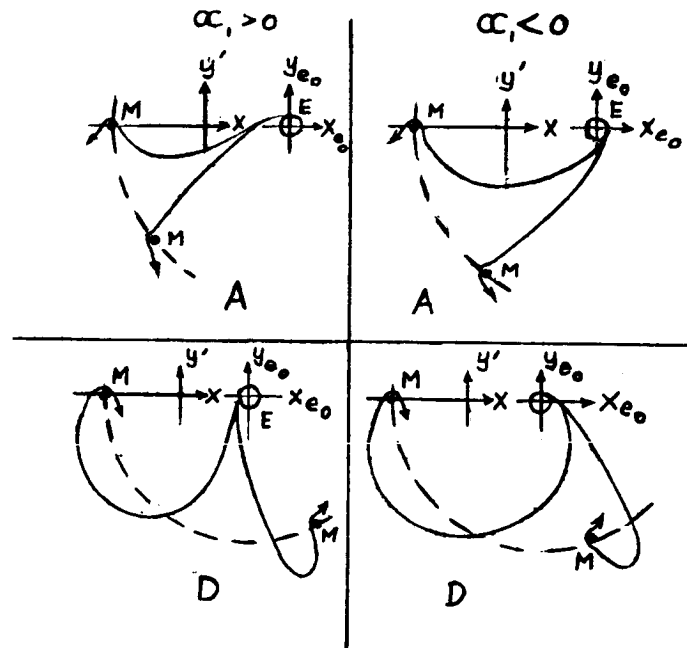
be established within 4 ft/sec and the initial launch angle must be within 0.02 degree.

In the above discussion we have tacitly assumed that the retrograde rocket can be fired at the right time and in the right direction. The direction of firing might be controlled by spin stabilizing the rocket in the correct attitude immediately after the powered portion of the approach trajectory. The timing of the retrograde rocket firing, however, might prove to be the most difficult problem. In reference 3-8 it is indicated that the use of a clock to time the firing of the retrograde rocket might be impractical because of the fairly wide range of times of arrival near the Moon. Other sources, however, have indicated that such a timing device might be satisfactory.

3.20 Use of the Moon for Accelerating Space Vehicles

There has been considerable interest in using the Moon as a means for accelerating a space vehicle for interplanetary travel. Since the Moon revolves about the Earth near the plane of other planetary orbits, at some time during each month the Moon would be in a position to accelerate a vehicle toward any planet. The use of the Moon for accelerating space vehicles was considered in reference 3-4.

There are four types of maximum acceleration trajectories as indicated below



A - Ascending D - Descending
Lunar accelerating trajectories

These four types are analogous to those for striking the Moon (see SECTION 3.15.1). In order to obtain the greatest acceleration the

vehicle should pass very close to the surface of the Moon and pass out of the Sphere of Influence of the Moon in a direction as close as possible to the direction of the Moon's velocity about the Earth.

Thus, the trajectory for maximum acceleration ($\Delta V = V_{e3} - V_{e2}$) passes around the Moon in a counter-clockwise direction for approach on an ascending arm and in a clockwise direction for descending arms as indicated in the sketch. The exit velocity V_{e3} is always greater than escape velocity and almost independent of initial velocity V_{e1} ; however, the acceleration increment ($\Delta V = V_{e3} - V_{e2}$) depends on the initial velocity V_1 and is greatest near the minimum velocity V_1 necessary to reach the Moon and decreases as the initial velocity V_1 is increased. The maximum velocity increment near the minimum velocity is

$$\Delta V = V_{e3} - V_{e2} \approx 4920 \text{ ft/sec}$$

The maximum velocity increment given above is for the turn around the Moon to be at the radius of the Moon. Because of the possibility of colliding with the Moon the trajectory must be raised from the surface of the Moon, thus reducing the gain in velocity. In reference 3-4 it is shown, for one example, that an error of 328 ft/sec would cause an error in radius at the Moon of 75 miles. An error in launch elevation angle of 1 degree would cause an error in radius of 62 miles.

In addition to using the Moon to accelerate a space vehicle it could be used to decelerate a space vehicle. The maximum deceleration would be obtained by passing out of the Sphere of Influence in a direction opposite to the Moon's rotation.

The practicality of using the Moon to accelerate a space vehicle depends on whether it costs more in weight for the additional guidance accuracy so that the vehicle could come close enough to the Moon to benefit from it or whether the extra weight could be put more efficiently into a larger power plant.

3.21 Propulsion Requirements for Lunar Vehicles

A discussion of Lunar trajectories would not be complete without an indication of the propulsion requirements for such orbits. In Figure 3-38 the velocity increments obtainable from several types of propulsion systems are shown as a function of the ratio of initial weight to payload weight. It will be noted that the range of chemical propulsion shown indicates a considerably more efficient system than that used with Vanguard type satellites. The number of rocket steps used also increases as each curve increases, starting with 2 steps at the lowest velocity increments and increasing to 5 steps at the highest velocity increments shown in Figure 3-38. The approximate velocity increments necessary to perform various lunar orbits are indicated below:

Trajectory	Total ΔV , ft/sec
1. Moon Impact	35,000
2. Circumlunar	35,000
3. Circumlunar with return to satellite orbit at Earth	47,000
4. Lunar satellite	38,000
5. Landing on Moon	41,000

The additional velocities for trajectories 3, 4, and 5 reflect the use of rockets in entering the satellite orbits or landing on Moon.

REFERENCES

- 3-1 Moulton, F. R.: An Introduction to Celestial Mechanics, The MacMillan Company, New York, 1914.
- 3-2 Hill, G. W.: Researches in the Lunar Theory, American Journal of Mathematics, Vol 1, 1878.
- 3-3 Buchheim, R. W.: Motion of a Small Body in Earth-Moon Space, The RAND Corporation, Research Memorandum RM-1726, June 1956.
- 3-4 Yegorov, V. A.: Certain Problems on the Dynamics of Flight to the Moon; Symposium of Soviet Research on Artificial Earth Satellites and Related Subjects, Washington, D. C., Oct. 1957; U. S. Joint Publications Research Service Rep. No. 187; from Uspekhi Fizicheskikh Nauk (Progress in Physical Sciences) Vol 63, No. 1-2, Sept. 1957.
- 3-5 Lieske, H. A.: Accuracy Requirements for Trajectories in the Earth-Moon System; The RAND Corporation; Rep. P-1022, Feb. 1957.
- 3-6 Clement, George H.: The Moon Rocket; The RAND Corporation, RAND Rep. p-833, May 1956.
- 3-7 Lieske, H. A.: Lunar Instrument Carrier - Trajectory Studies, The RAND Corporation, RAND RM - 1728, June 1956.
- 3-8 Buchheim, R. W.: Artificial Satellites of the Moon; The RAND Corporation; RAND Rep. P - 873, June 1956. Also: Proceedings of the VII International Astronautical Congress. Rome, Sept. 1956.
- 3-9 Klemperer, W. B., and Benedikt, E. T.: Selenoid Satellites. Astronautica Acta Vol IV, FASC 1, 1958.
- 3-10 Xenakis, George: Some Flight Control Problems of a Circumnavigating Lunar Vehicle. WADC Technical Note 58-82, March 1958.

TABLE 3-1

AXES TRANSFORMATIONS USEFUL IN THREE BODY PROBLEM

(Based on $D = 1$)

$$[A] = \begin{bmatrix} \cos \omega t & -\sin \omega t & 0 \\ \sin \omega t & \cos \omega t & 0 \\ 0 & 0 & 1 \end{bmatrix}$$

$$\begin{Bmatrix} x_0 \\ y_0 \\ z_0 \end{Bmatrix} = [A] \begin{Bmatrix} x \\ y \\ z \end{Bmatrix}$$

$$\begin{Bmatrix} x_0 - x_{01} \\ y_0 - y_{01} \\ z_0 \end{Bmatrix} = [A] \begin{Bmatrix} x - x_1 \\ y - y_1 \\ z \end{Bmatrix}$$

$$\begin{Bmatrix} \dot{x}_0 \\ \dot{y}_0 \\ \dot{z}_0 \end{Bmatrix} = [A] \begin{Bmatrix} \dot{x} - \omega y \\ \dot{y} + \omega x \\ \dot{z} \end{Bmatrix}$$

$$\begin{Bmatrix} x_e \\ y_e \\ z_e \end{Bmatrix} = [A] \begin{Bmatrix} x - x_1 \\ y \\ z \end{Bmatrix}$$

$$\begin{Bmatrix} \dot{x}_e \\ \dot{y}_e \\ \dot{z}_e \end{Bmatrix} = [A] \begin{Bmatrix} \dot{x} - \omega y \\ \dot{y} + \omega (x - x_1) \\ \dot{z} \end{Bmatrix}$$

$$\begin{Bmatrix} x_m \\ y_m \\ z_m \end{Bmatrix} = [A] \begin{Bmatrix} x - x_2 \\ y \\ z \end{Bmatrix}$$

$$\begin{Bmatrix} \dot{x}_m \\ \dot{y}_m \\ \dot{z}_m \end{Bmatrix} = [A] \begin{Bmatrix} \dot{x} - \omega y \\ \dot{y} + \omega (x - x_2) \\ \dot{z} \end{Bmatrix}$$

$$\begin{Bmatrix} x_o \\ y_o \\ z_o \end{Bmatrix} = [A] \begin{Bmatrix} x - 2\omega\dot{y} - \omega^2 x \\ y + 2\omega\dot{x} - \omega^2 y \\ z \end{Bmatrix}$$

$$\begin{Bmatrix} y \\ x - x_1 \\ z \end{Bmatrix} = [A] \begin{Bmatrix} y_e \\ x_e \\ z_e \end{Bmatrix}$$

$$\begin{Bmatrix} \dot{y} \\ \dot{x} \\ \dot{z} \end{Bmatrix} = [A] \begin{Bmatrix} \dot{y}_e - \omega x_e \\ \dot{x}_e + \omega y_e \\ \dot{z}_e \end{Bmatrix}$$

$$\begin{Bmatrix} \ddot{y} \\ \ddot{x} \\ \ddot{z} \end{Bmatrix} = [A] \begin{Bmatrix} \ddot{y}_e - 2\omega \dot{x}_e - \omega^2 y_e \\ \ddot{x}_e + 2\omega \dot{y}_e - \omega^2 x_e \\ \ddot{z}_e \end{Bmatrix}$$

$$x_{e0} = x_0 - x_1$$

$$y_{e0} = y_0$$

$$z_{e0} = z_0$$

$$\dot{x}_{e0} = \dot{x}_0$$

$$\dot{y}_{e0} = \dot{y}_0$$

$$\dot{z}_{e0} = \dot{z}_0$$

$$x_m = x_0 - x_2 \cos \omega t$$

$$y_m = y_0 - x_2 \sin \omega t$$

$$z_m = z_0$$

$$x_m = x_e - \cos \omega t$$

$$y_m = y_e - \sin \omega t$$

$$z_m = z_e$$

$$x_e = x_0 - x_1 \cos \omega t$$

$$y_e = y_0 - x_1 \sin \omega t$$

$$z_e = z_0$$

3-77

$$\dot{x}_m = \dot{x}_e + \omega \sin \omega t$$

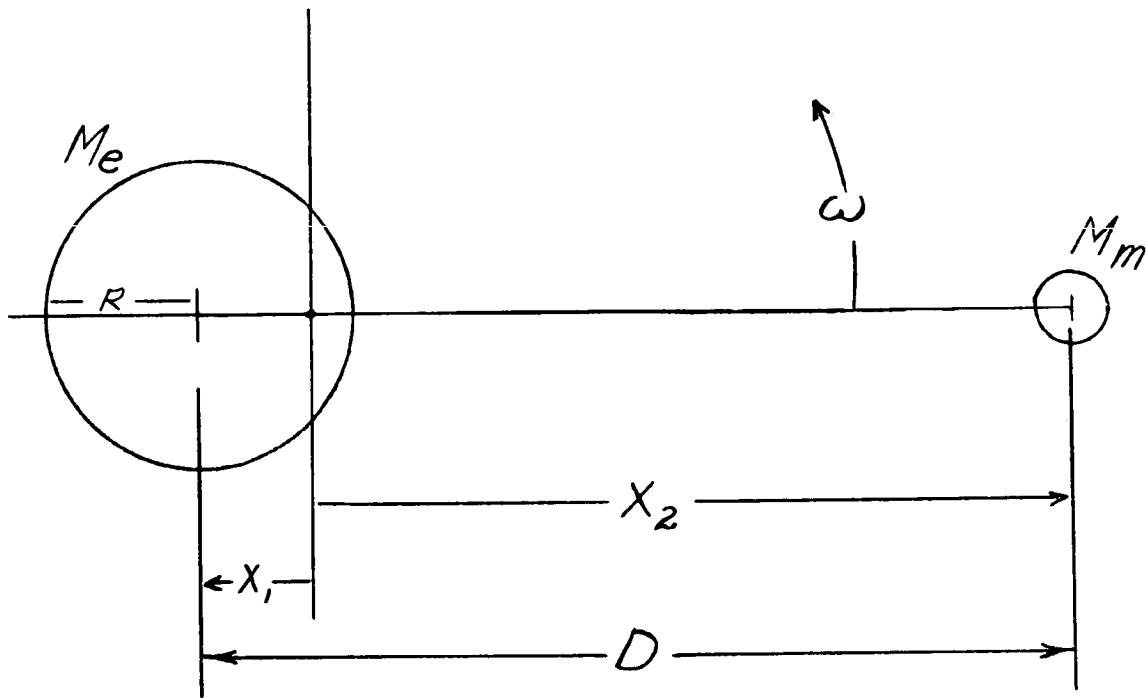
$$\dot{y}_m = \dot{y}_e - \omega \cos \omega t$$

$$\dot{z}_m = \dot{z}_e$$

$$\dot{x}_m = \dot{x}_o + \omega x_2 \sin \omega t$$

$$\dot{y}_m = \dot{y}_o - \omega x_2 \cos \omega t$$

$$\dot{z}_m = \dot{z}_o$$



$$X_1 = 2900 \text{ mi}$$

$$X_2 = 236,170 \text{ mi}$$

$$D = 239,070 \text{ mi}$$

$$M = M_e + M_m$$

$$M_e/M_m = 81.45$$

$$R = 3960 \text{ mi}$$

$$\omega = 0.22997 \text{ rad/day}$$

Fig. 3-1. Earth-Moon system

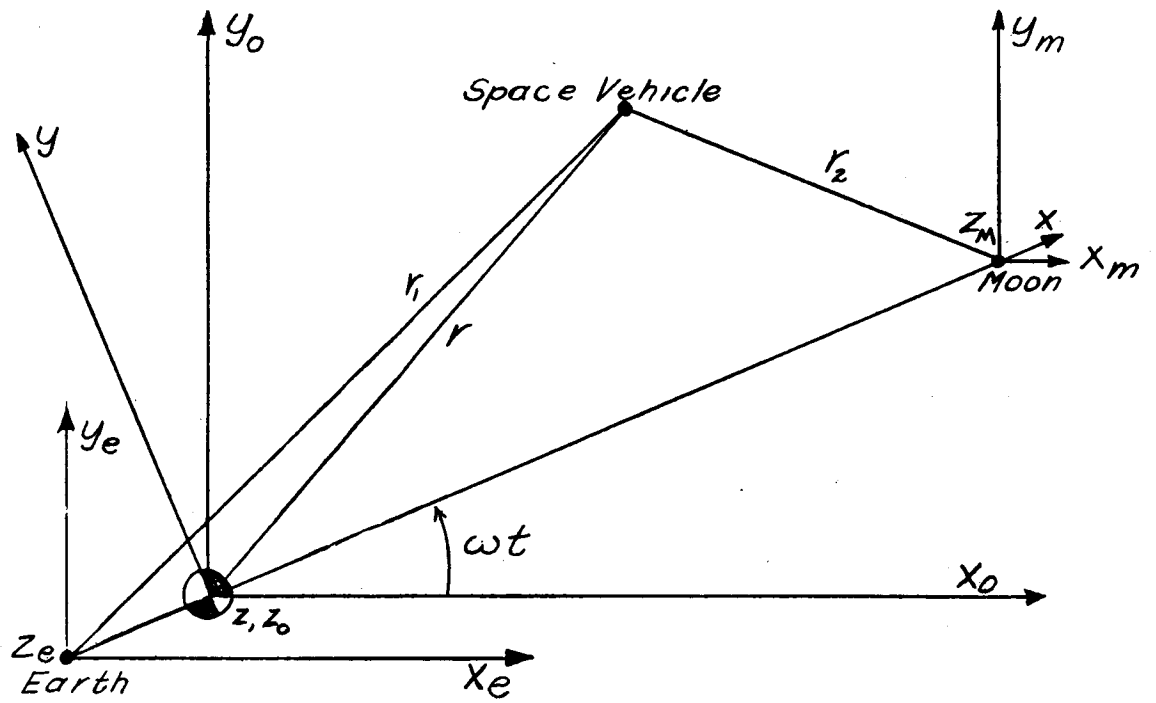


Fig.3-2 Coordinate systems

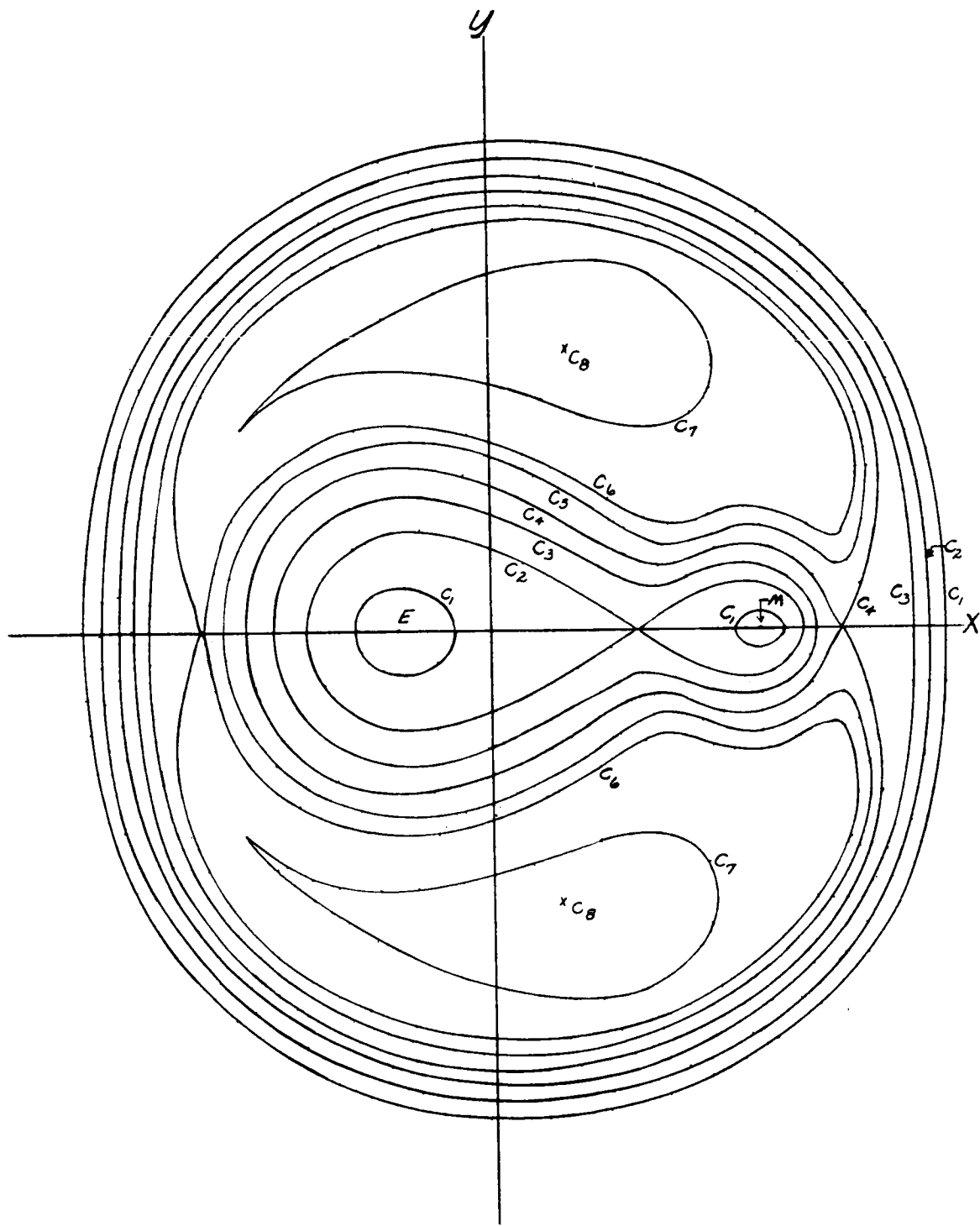


Fig.3-3 Contours of zero relative velocity in (x,y) plane.

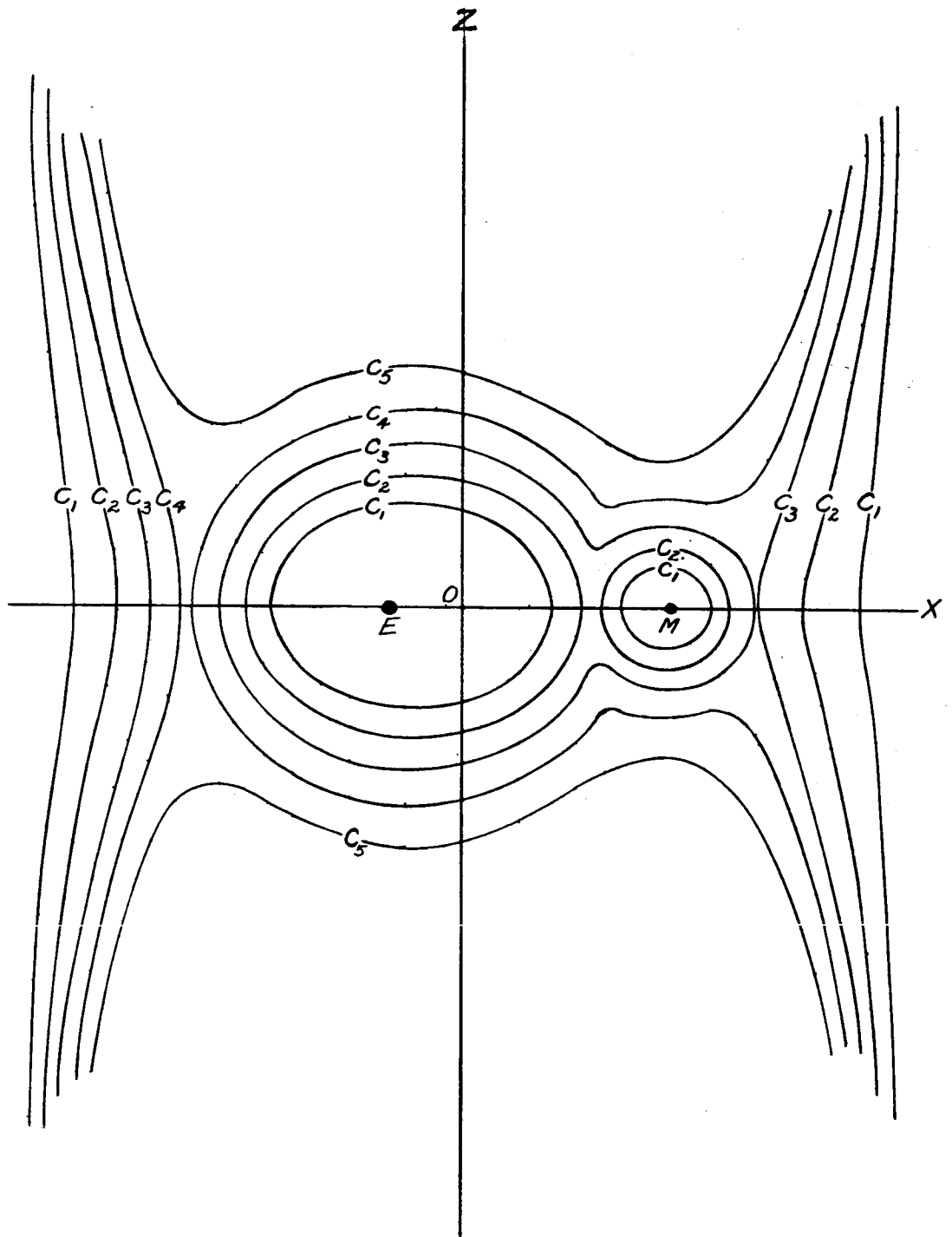


Fig. 3-4 Contours of zero relative velocity in (x, z) plane

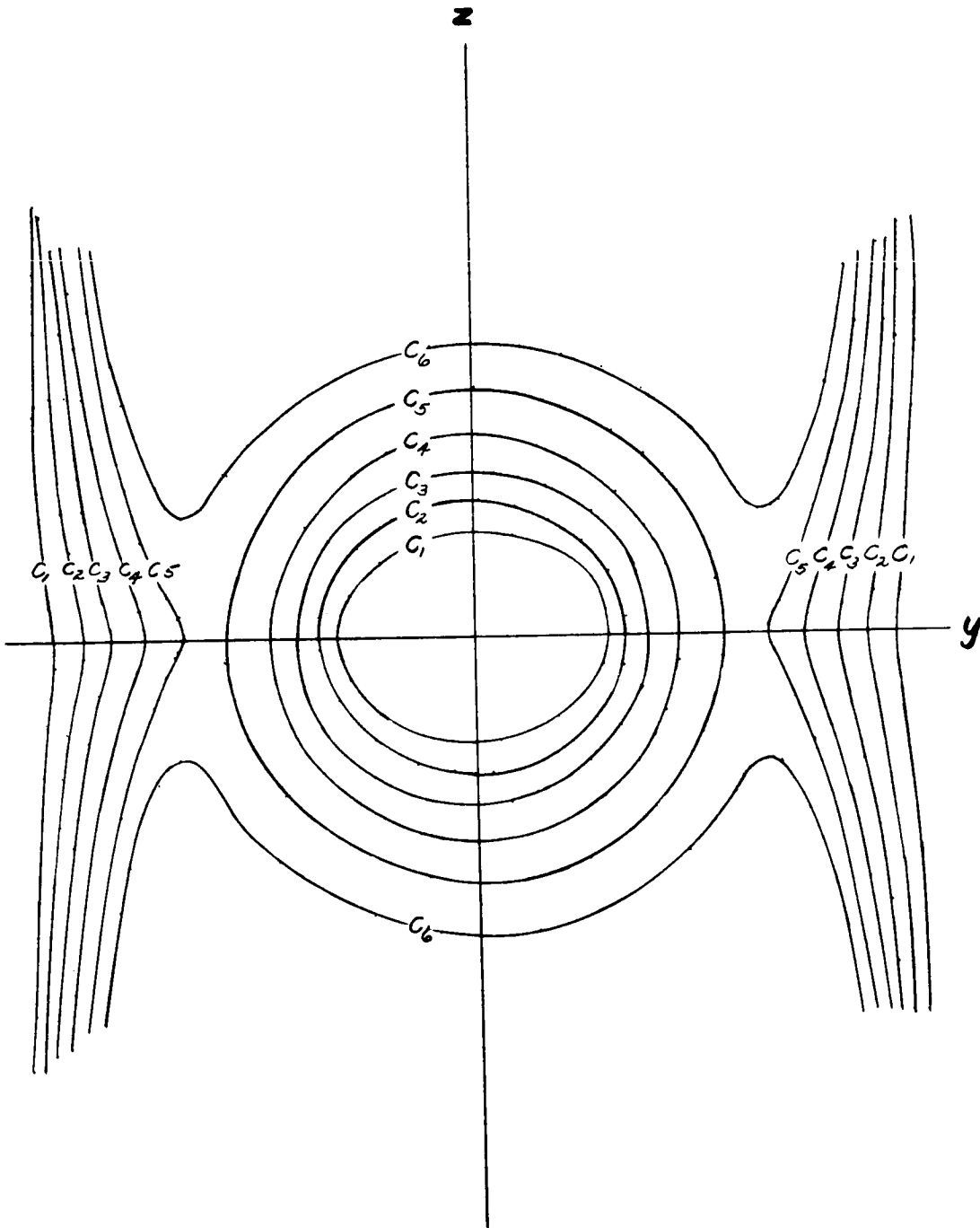


Fig. 3-5 Contours of zero relative velocity in (y, z) plane

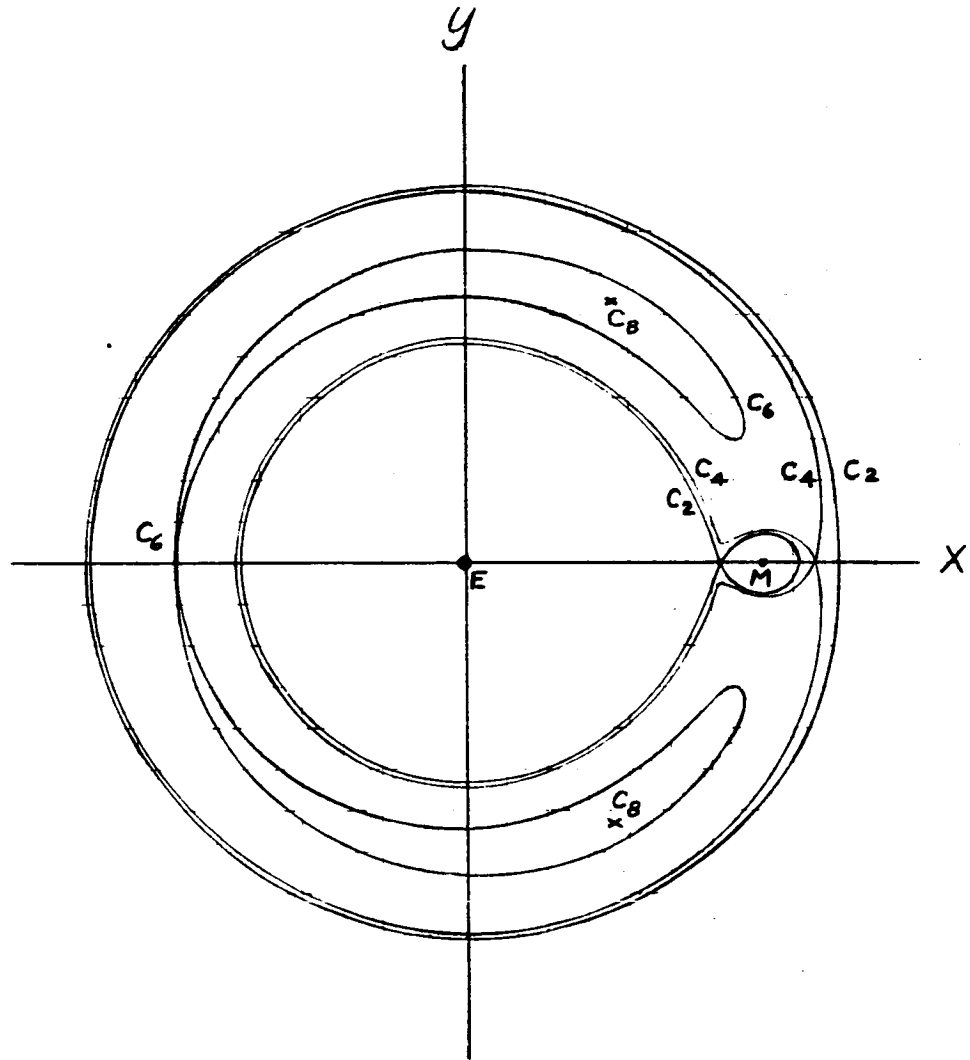


Fig. 3-6 Contours of zero relative velocity in (x,y) plane drawn to scale. (ref 3-4)

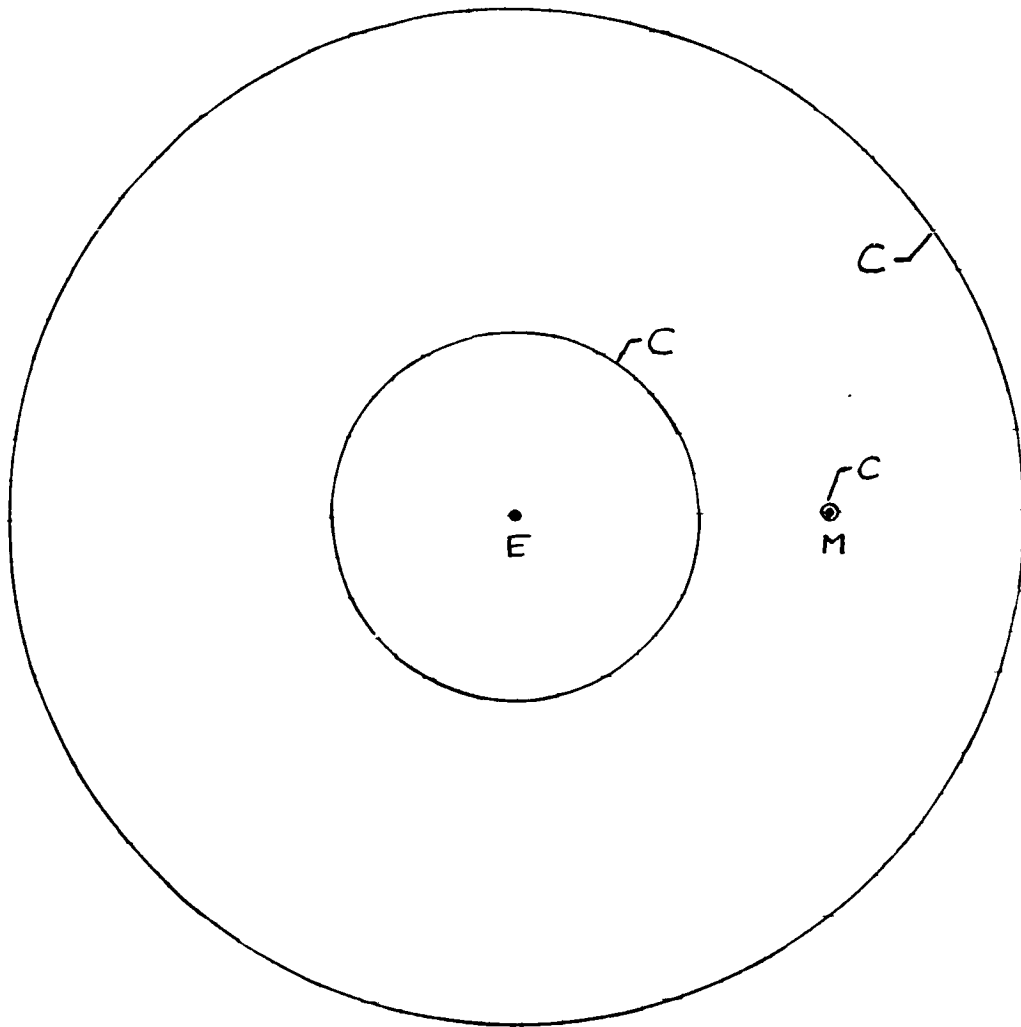


Fig. 3-7 Contours of zero relative velocity
in the x,y plane for the earth-moon
system; $C = 0.20$.

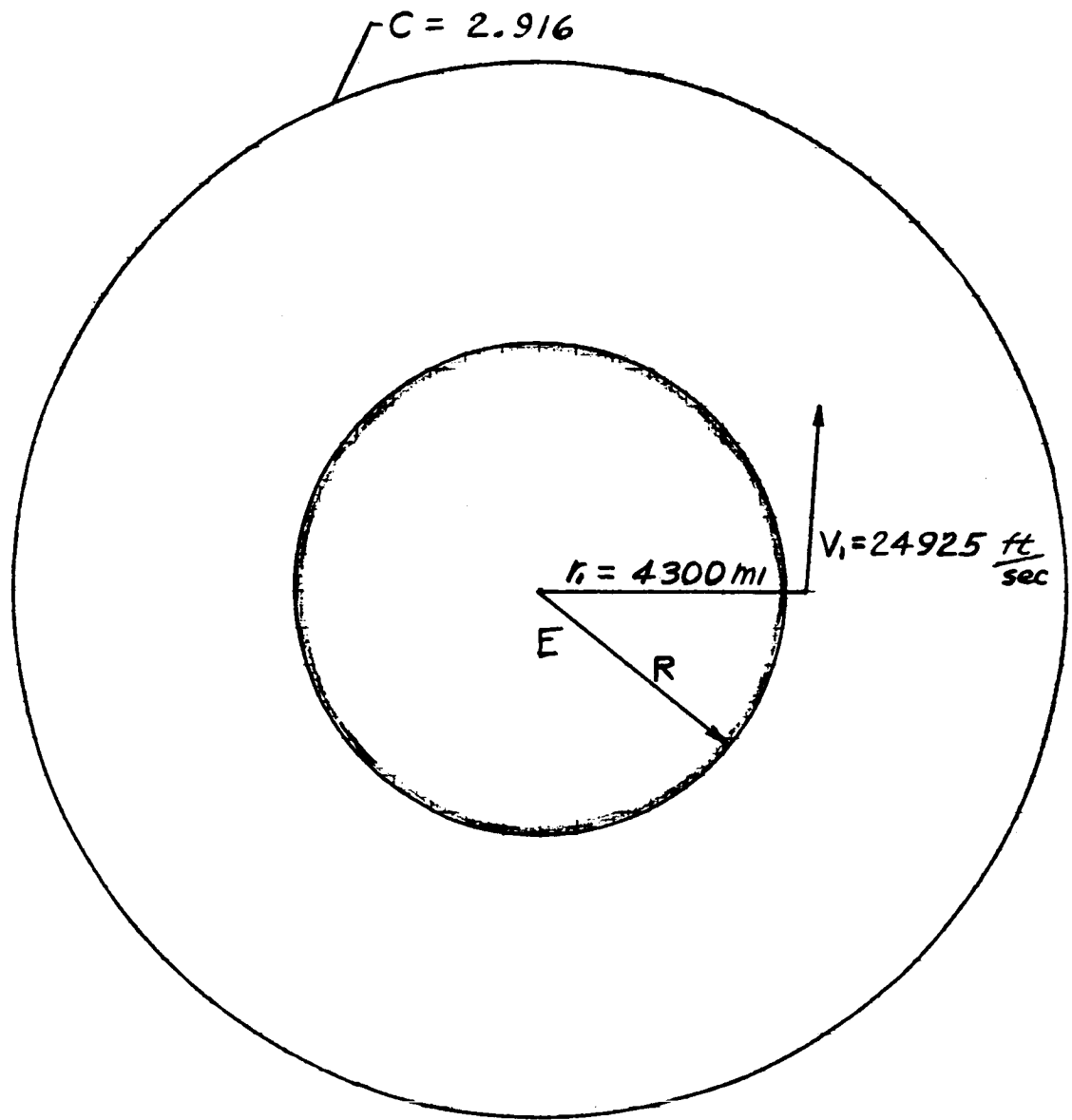


Fig. 3-8 Contour of zero relative velocity in the x, y plane for the earth-moon system;
 $C = 2.916$, $V = 24925 \text{ ft/sec}$.

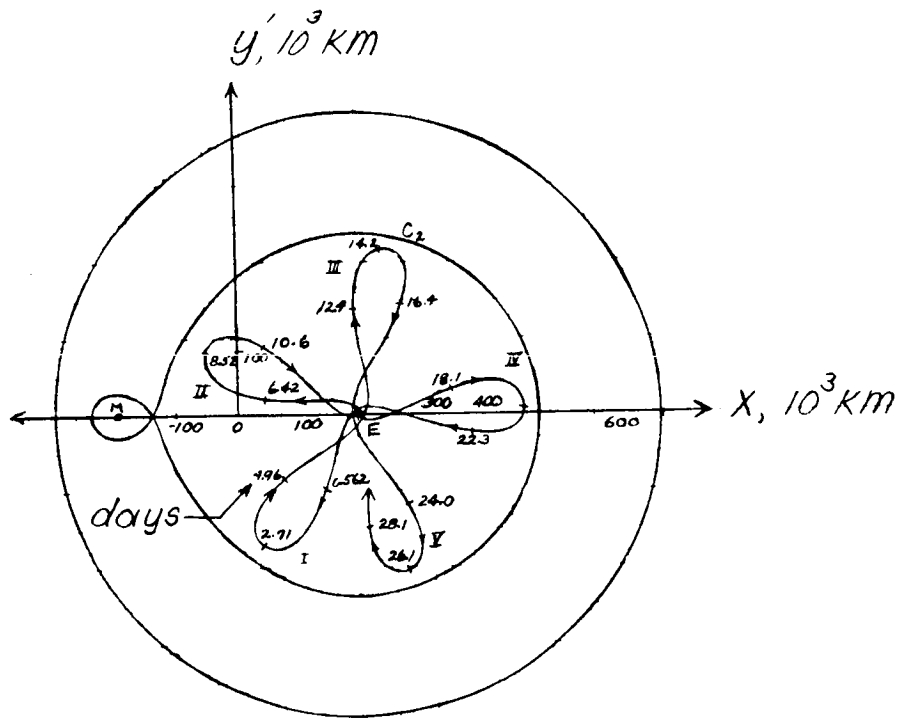


Fig. 3-9 Trajectory for minimum initial velocity (ref 3-4)

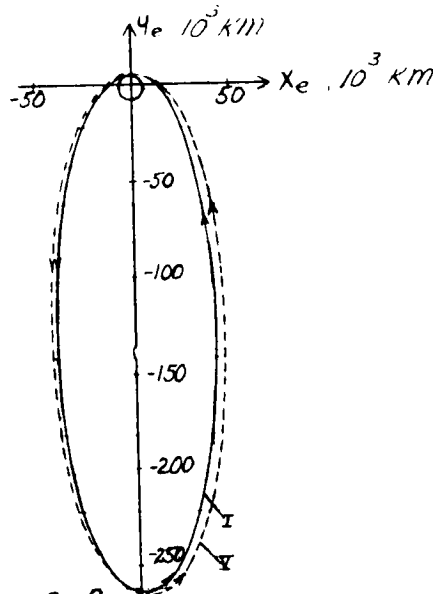


Fig 3-10 Trajectory of figure 3-9 in geocentric coordinates. (ref 3-4)

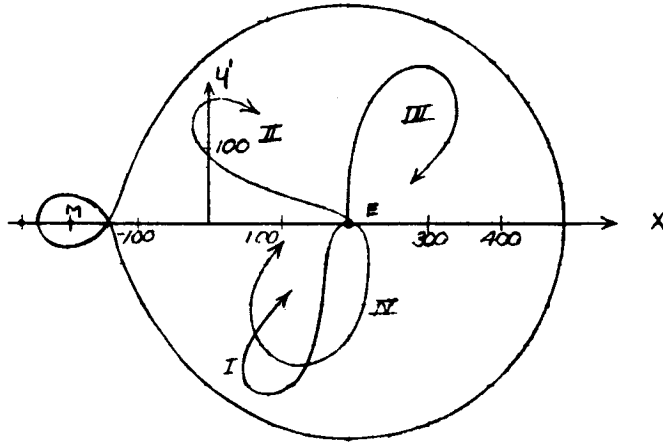


Fig. 3-11 Trajectory for minimum initial velocity
 $0 < r < 180^\circ$ (ref. 3-4)

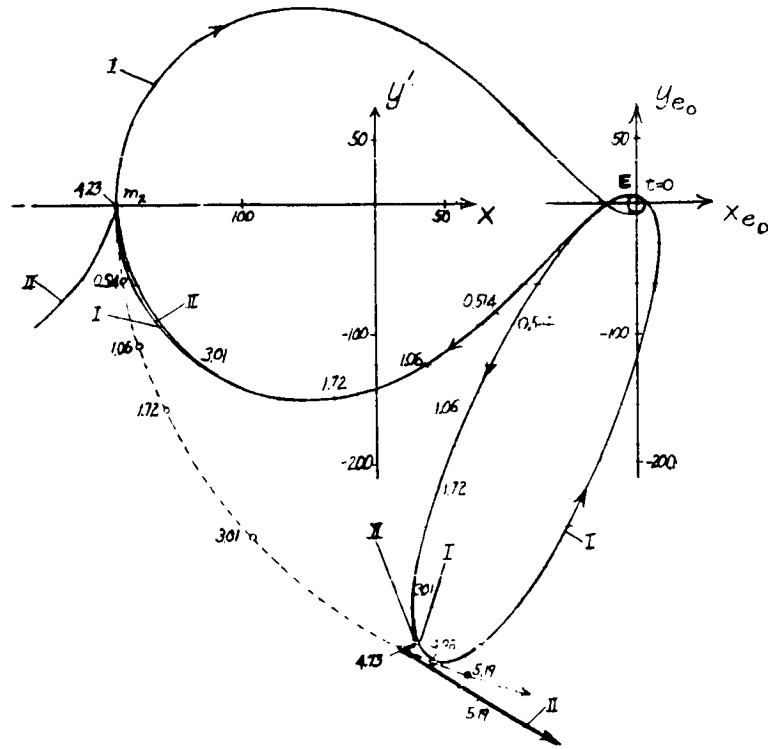


Fig 3-12 Comparison of impact trajectory calculated using two-body equations with that calculated using three-body equations (ref 3-4)

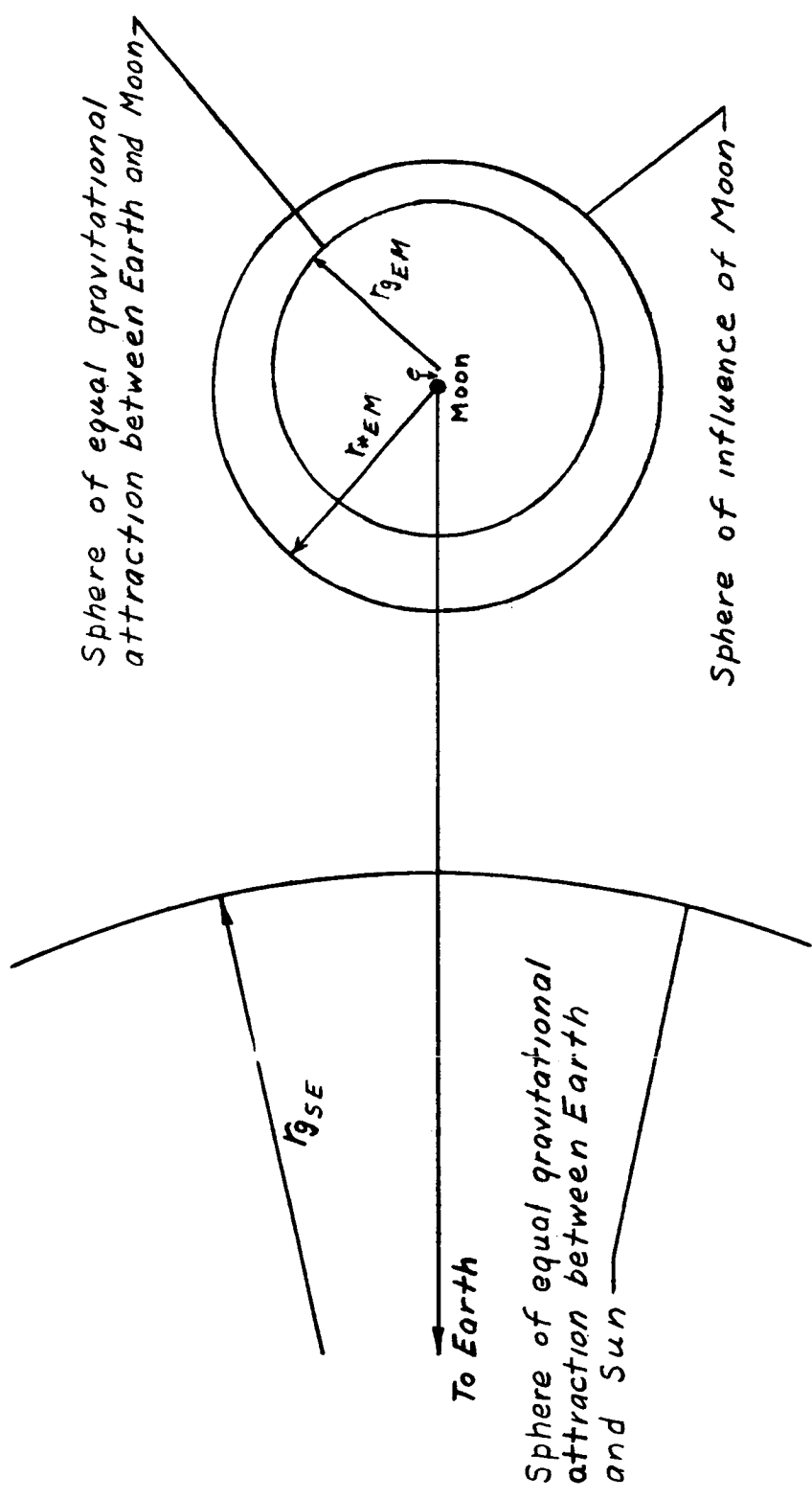


Fig.3-13- Comparison between Sphere of Influence and Sphere of equal gravitational attraction.

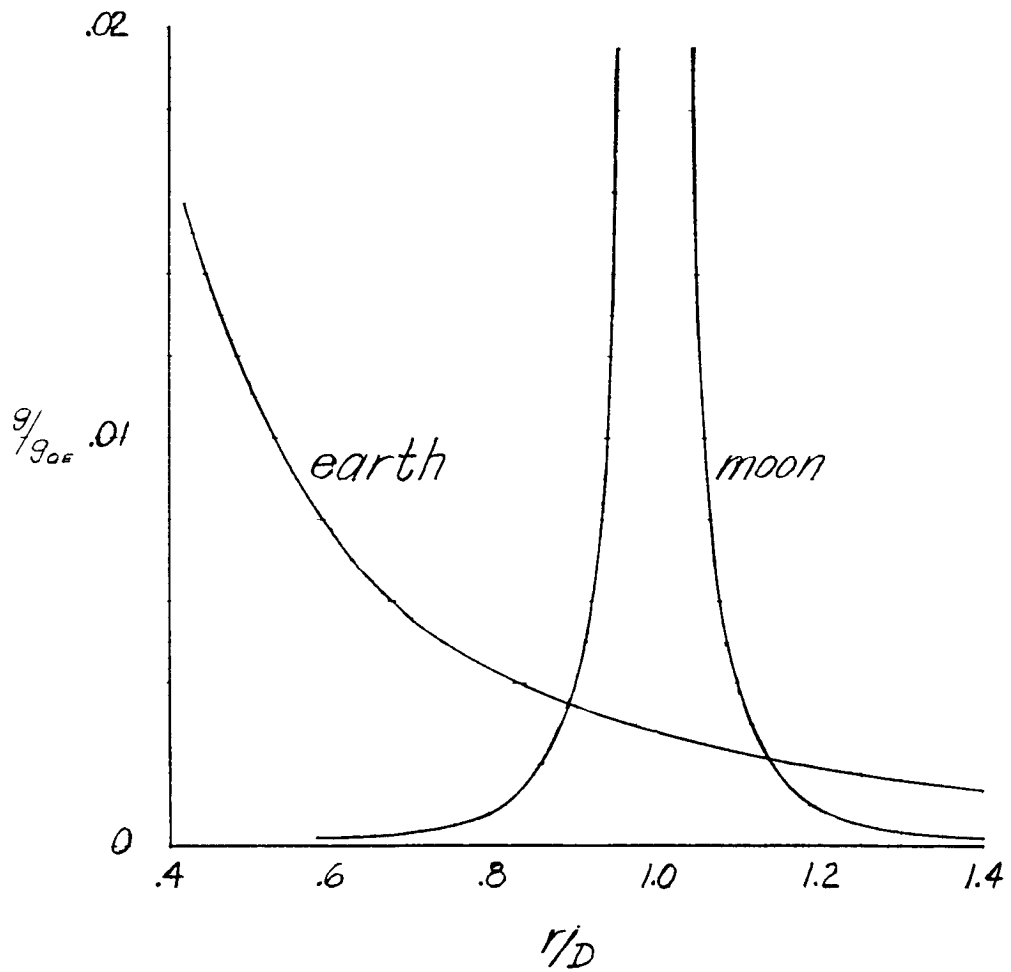


Fig 3-14 Comparison of the gravitational attraction of the Earth and the Moon in the vicinity of the moon.

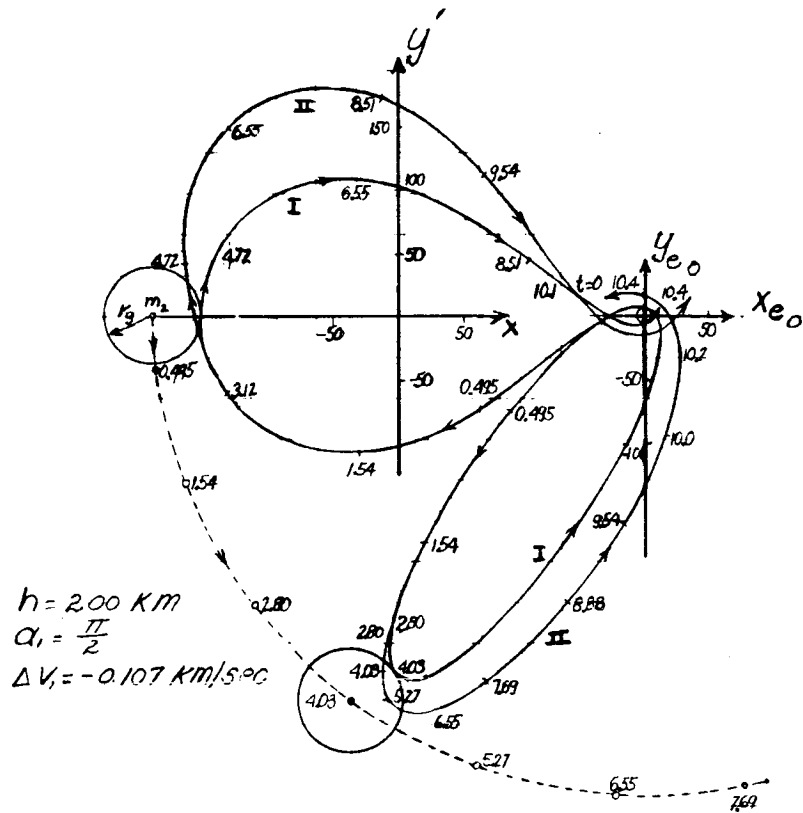


Fig. 3-15 Trajectory reaching point of equal attraction between Earth and Moon. (ref. 3-4)

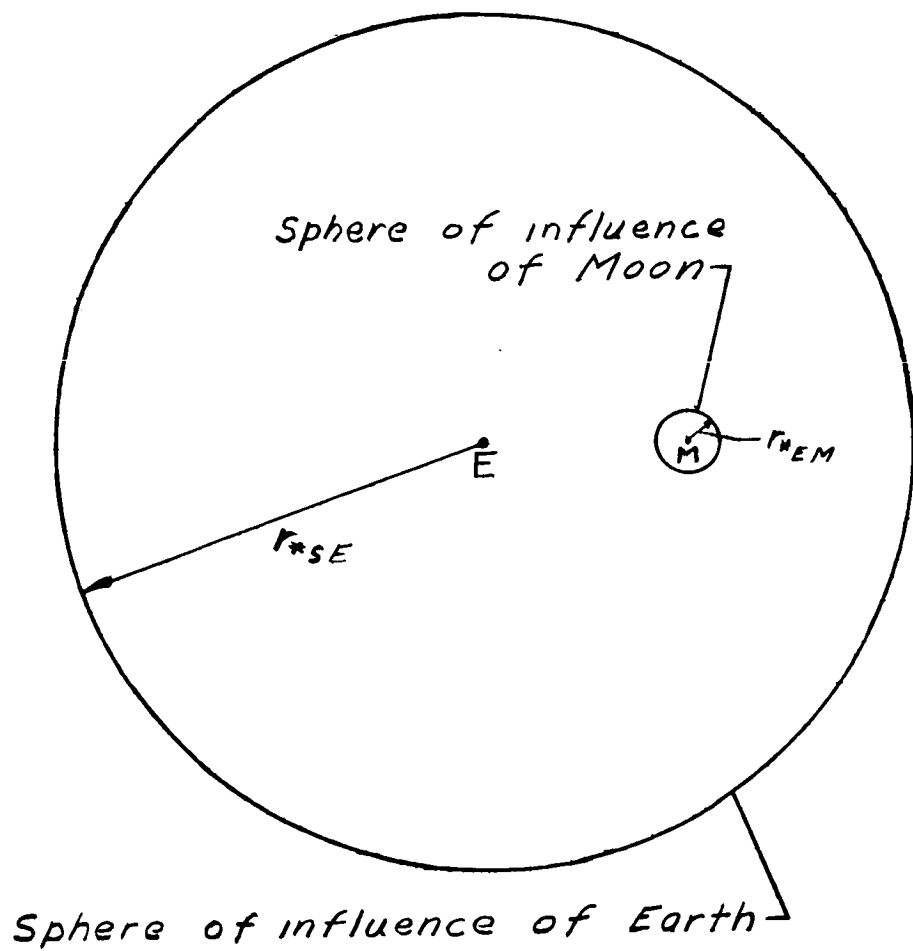
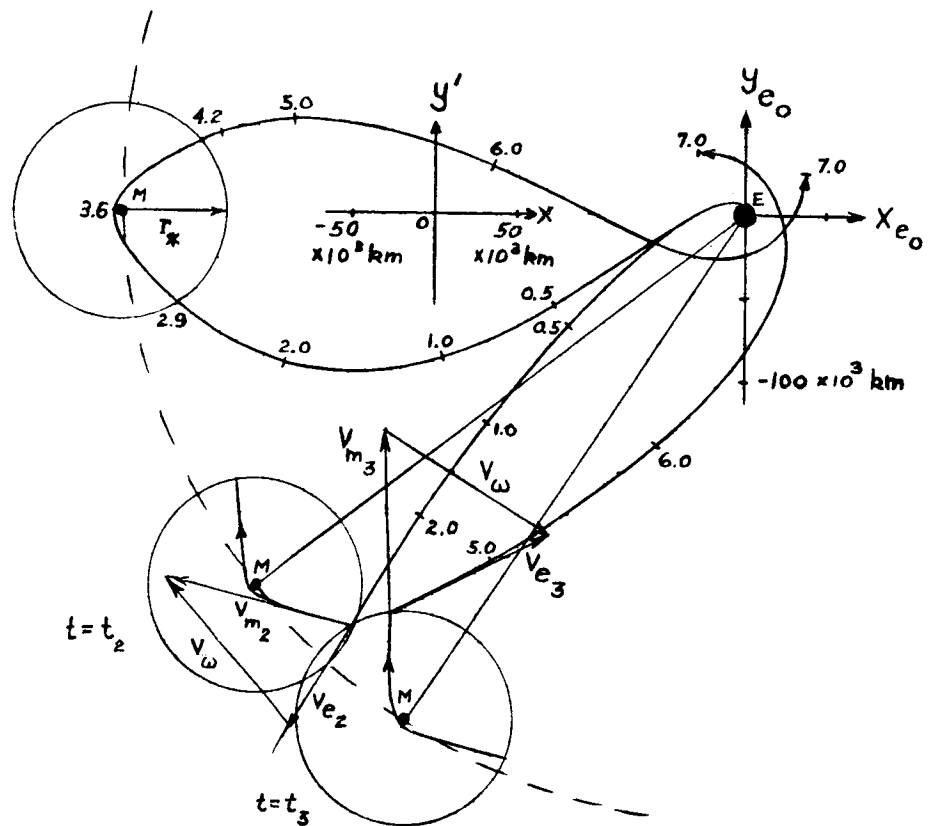
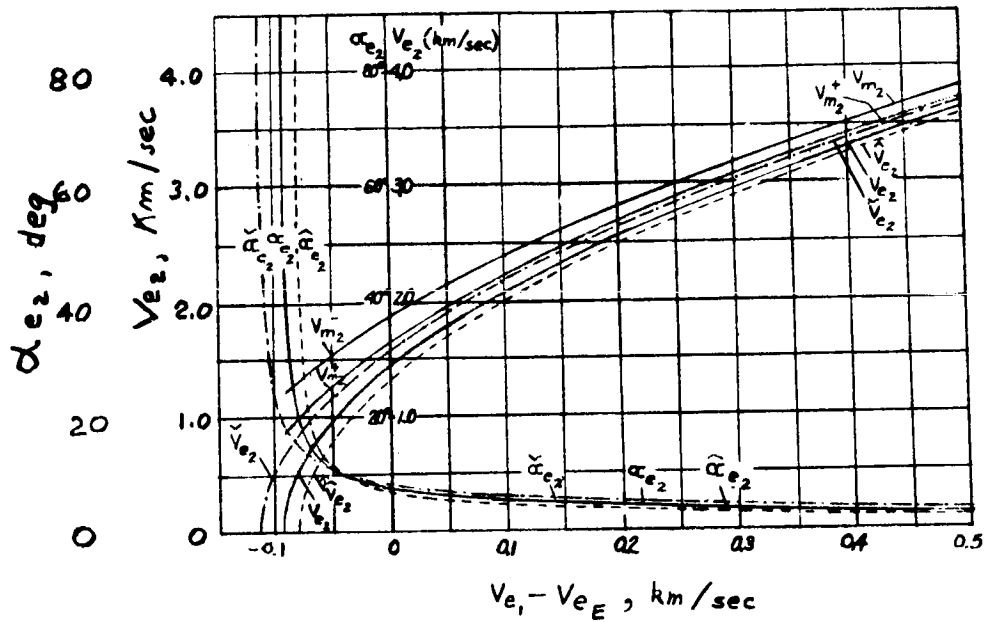


Figure 3-16.-Comparison of sphere of influence of Earth with respect to the Sun with the sphere of influence of Moon with respect to the Earth.



$H = 200 \text{ km}$
 $\alpha_1 \cong \pi/2$
 $\Delta V_1 = 0.092356 \text{ km/sec}$

Figure 3-17.- Illustration of approximate method of calculating Lunar trajectories.(ref. 3-4)



- \wedge $r_{e2} = D + r_*$
- \vee $r_{e2} = D - r_*$
- $+$ $\alpha_1 = +\pi/2$
- $-$ $\alpha_1 = -\pi/2$

Figure 3-18.- Conditions at entry into the Lunar Sphere of Influence. (ref. 3-4)

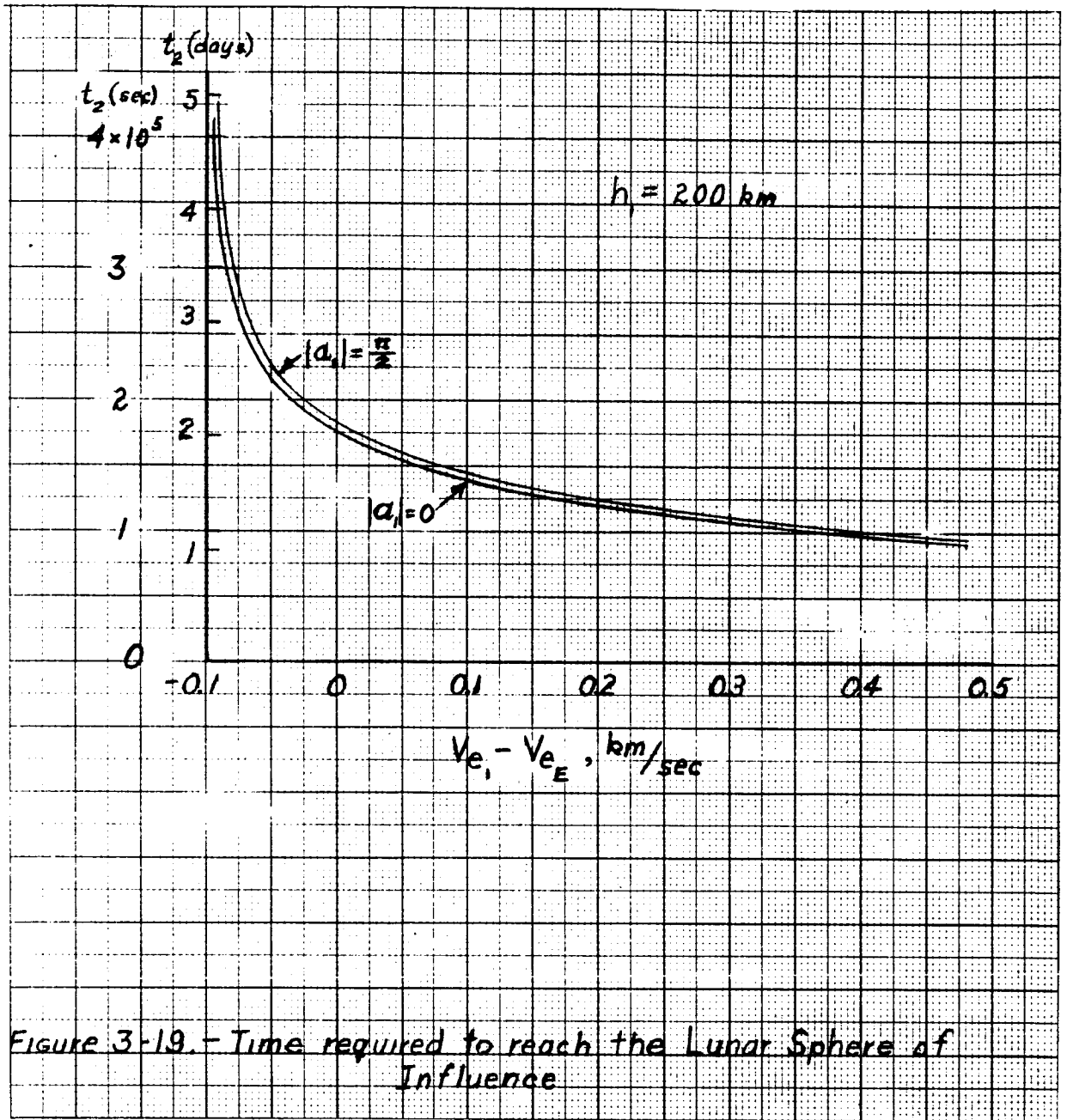


Figure 3-19. - Time required to reach the Lunar Sphere of Influence

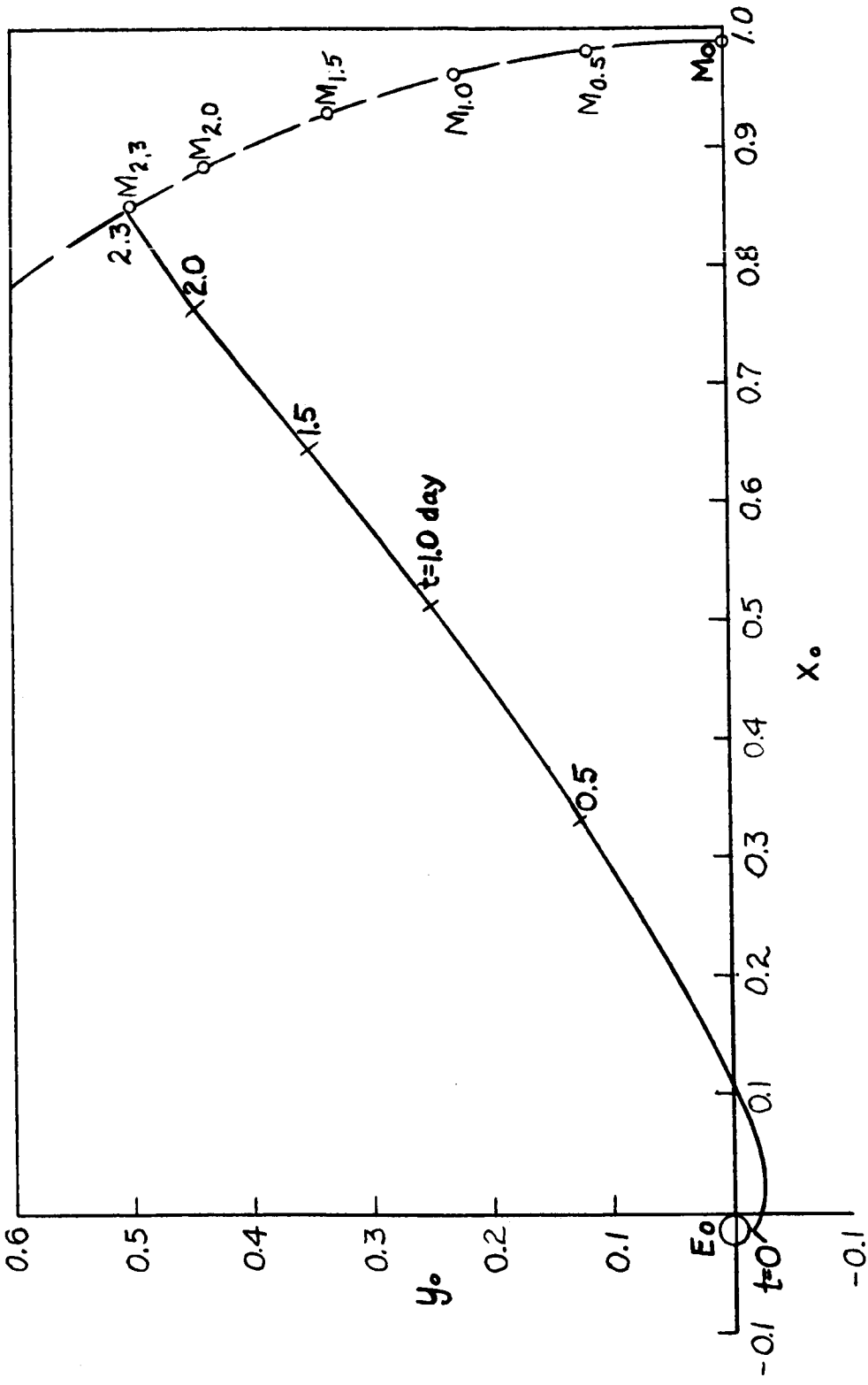


Fig.3-20. A trajectory to hit the moon, ref.3-5

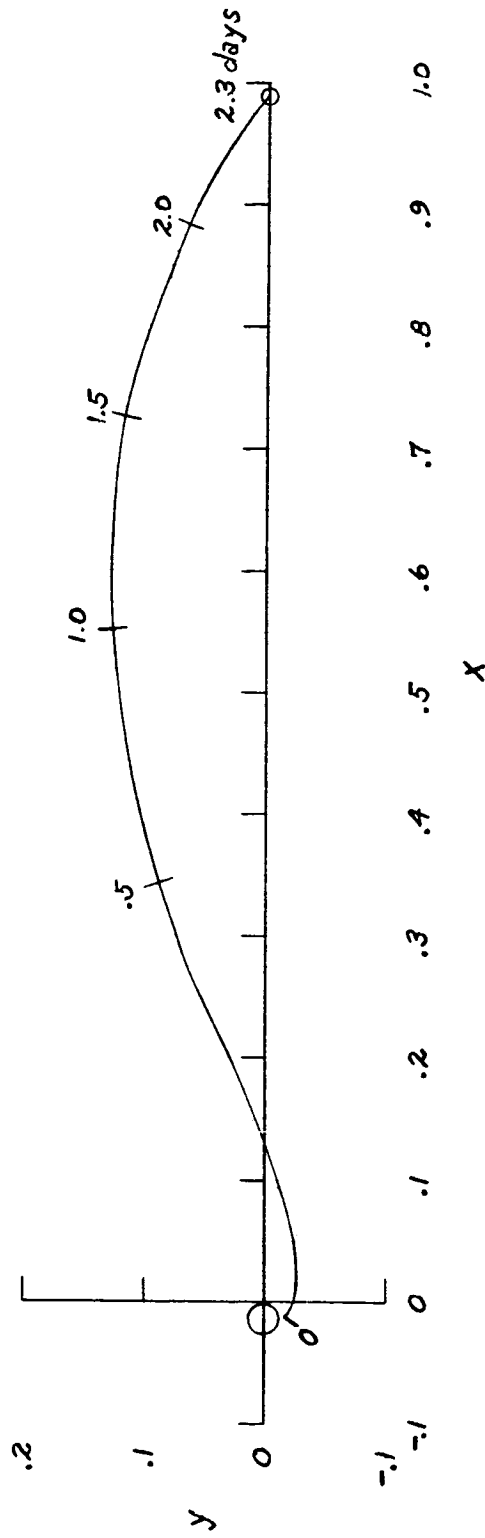


Figure 3-21.- Trajectory of figure 8 as viewed from the moon ;
 (rotating x, y coordinates); ref. 3-5

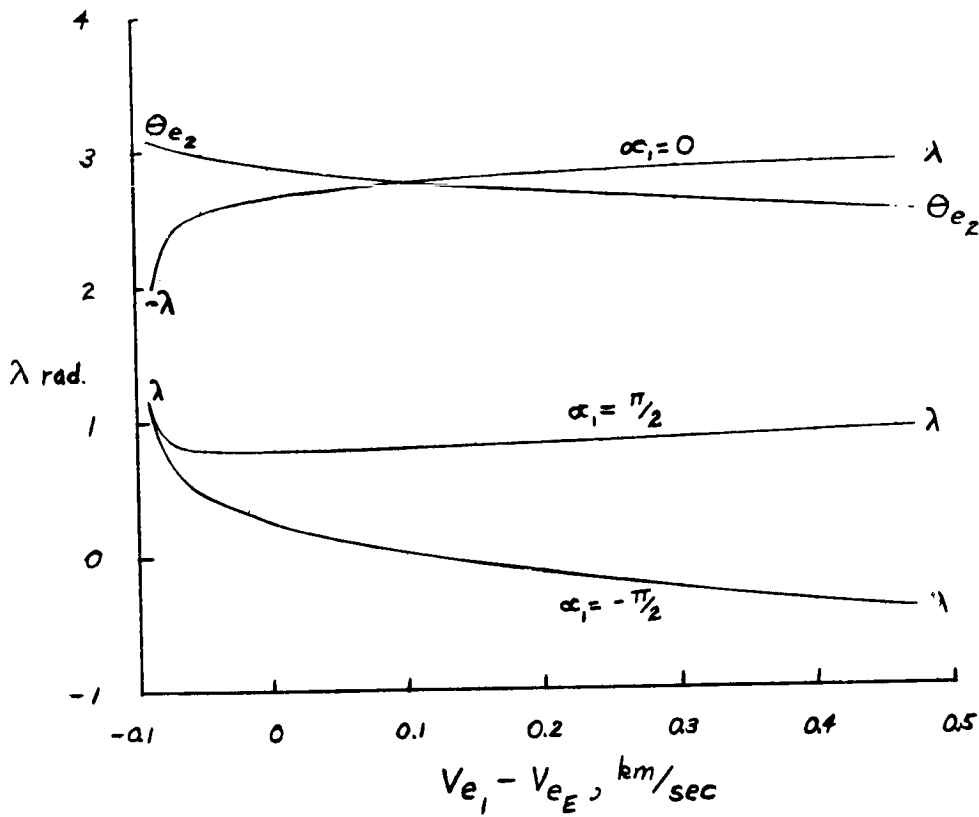


Figure 3-22.- Variation of the orientation angle, λ , with launch velocity for impact with the moon. (ref. 3-4)

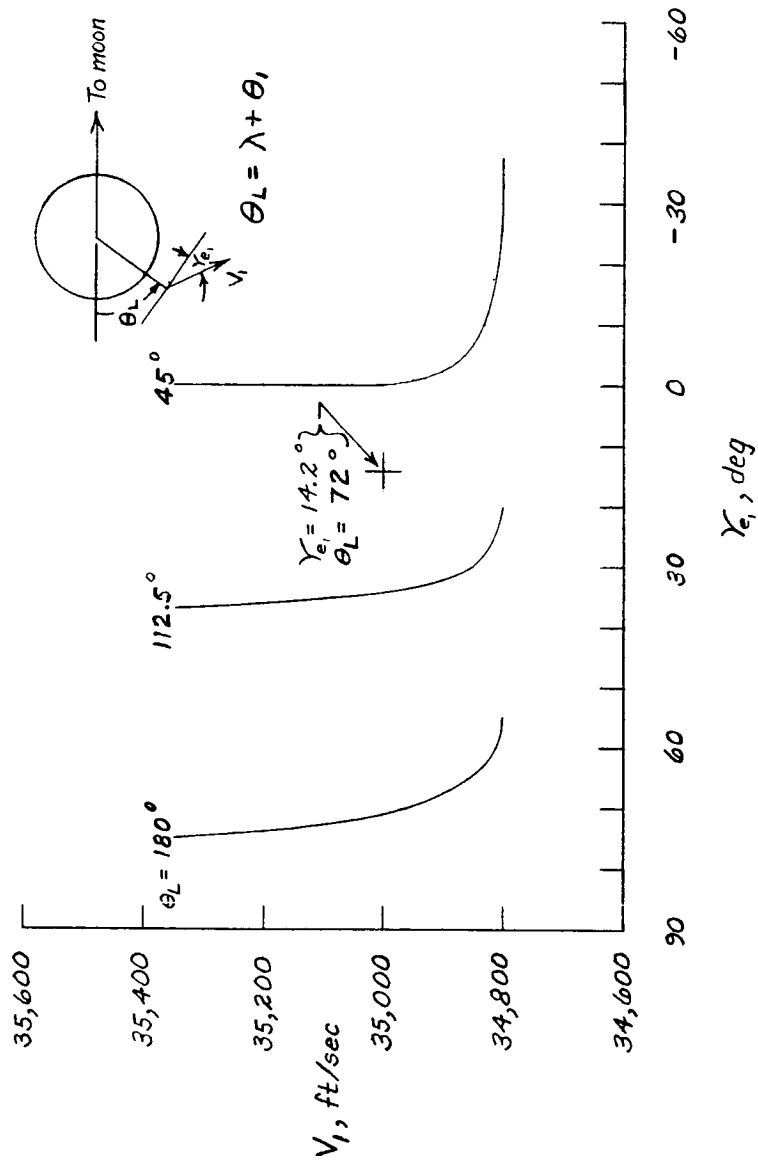


Figure 3-23.- Launch velocities and angles necessary to strike the moon ($r_e = 4,350$ mi); ref. 3-6

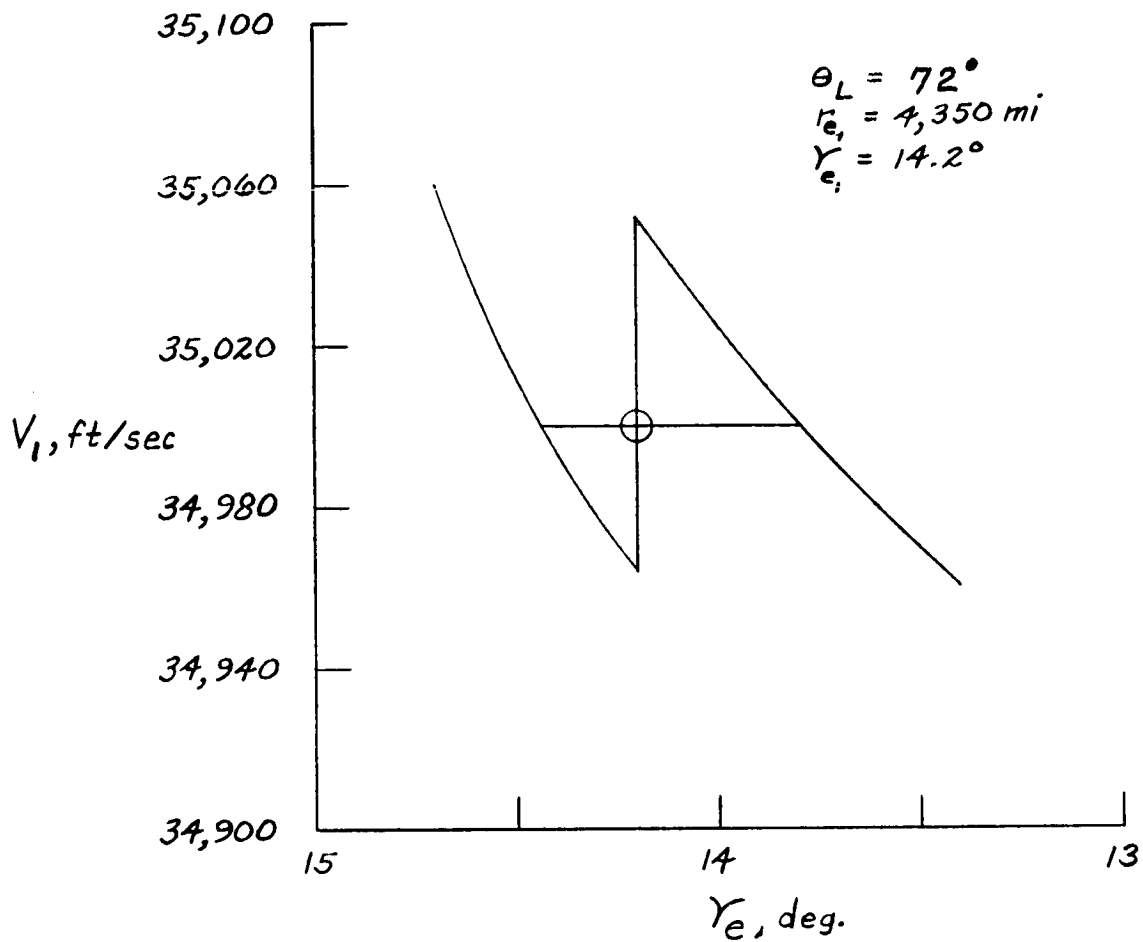


Figure 3-24.-Limiting conditions for impacting on the forward surface of the moon, ref. 3-6.

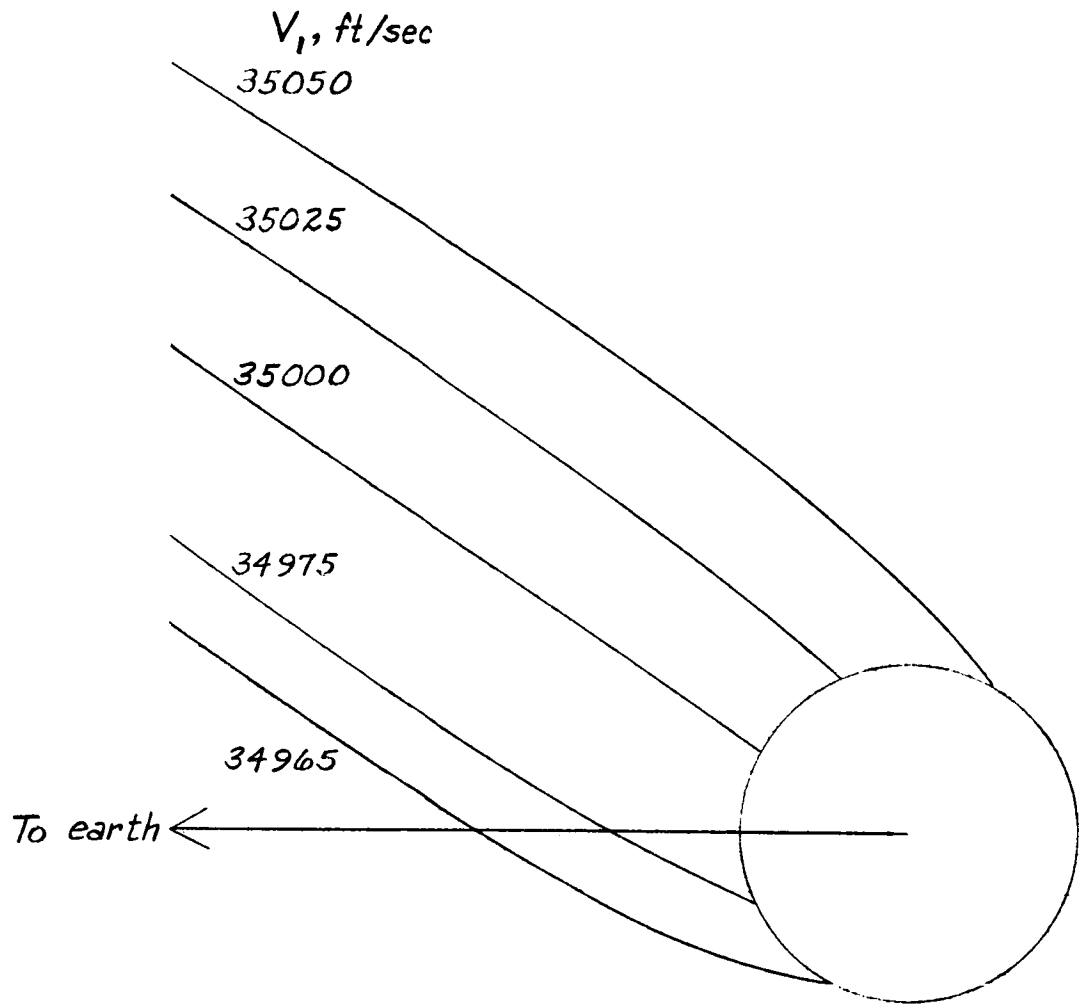


Figure 3-25.- Trajectories in the vicinity of the moon corresponding to the limiting conditions of figure 3-24, ref 3-6

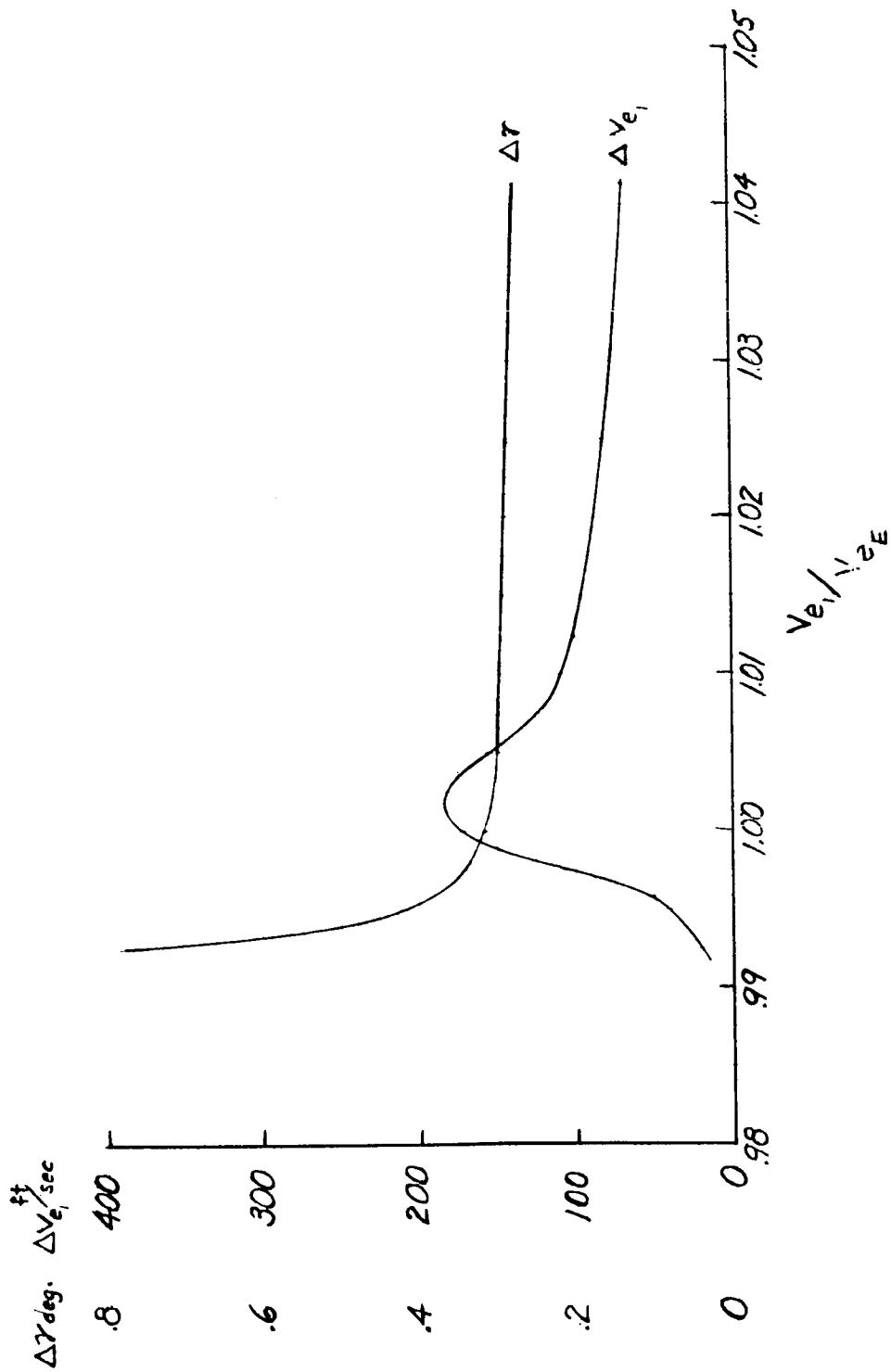
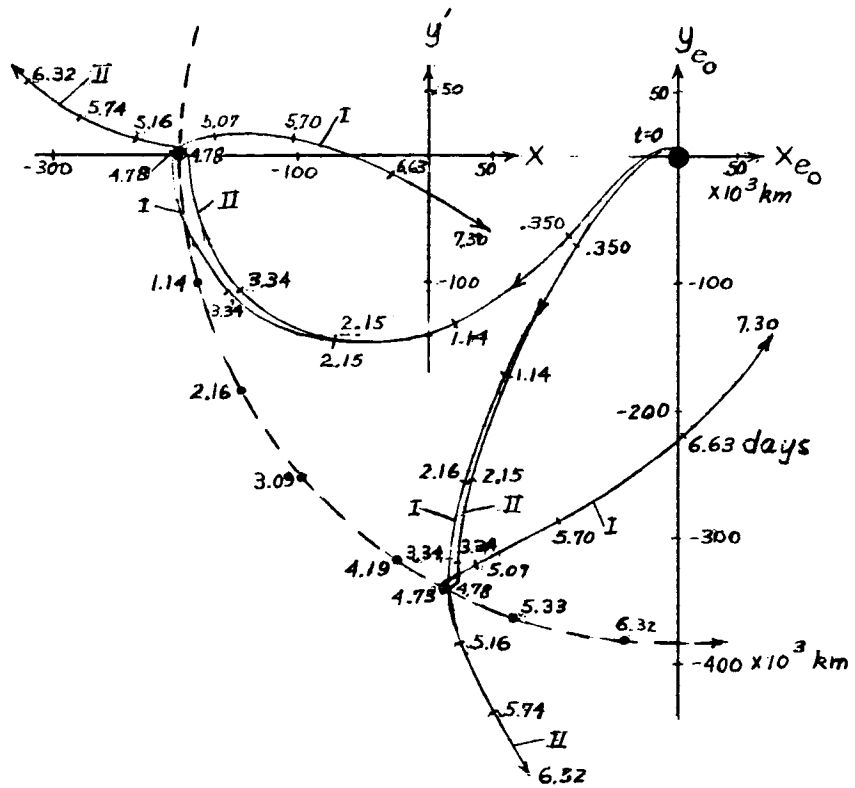


Figure 3-26.-Maximum errors in launch conditions for impact on the moon.



$h = 200 \text{ km}$
 $\alpha_0 = 75^\circ$
 $V_{e_1} - V_{e_2} = -0.0919 \text{ km/sec}$
 $\Delta V = +2 \text{ meters/sec} = \text{Case I}$
 $-2 \text{ meters/sec} = \text{Case II}$

Figure 3-27.- Trajectories with errors in initial velocity close to the minimum.

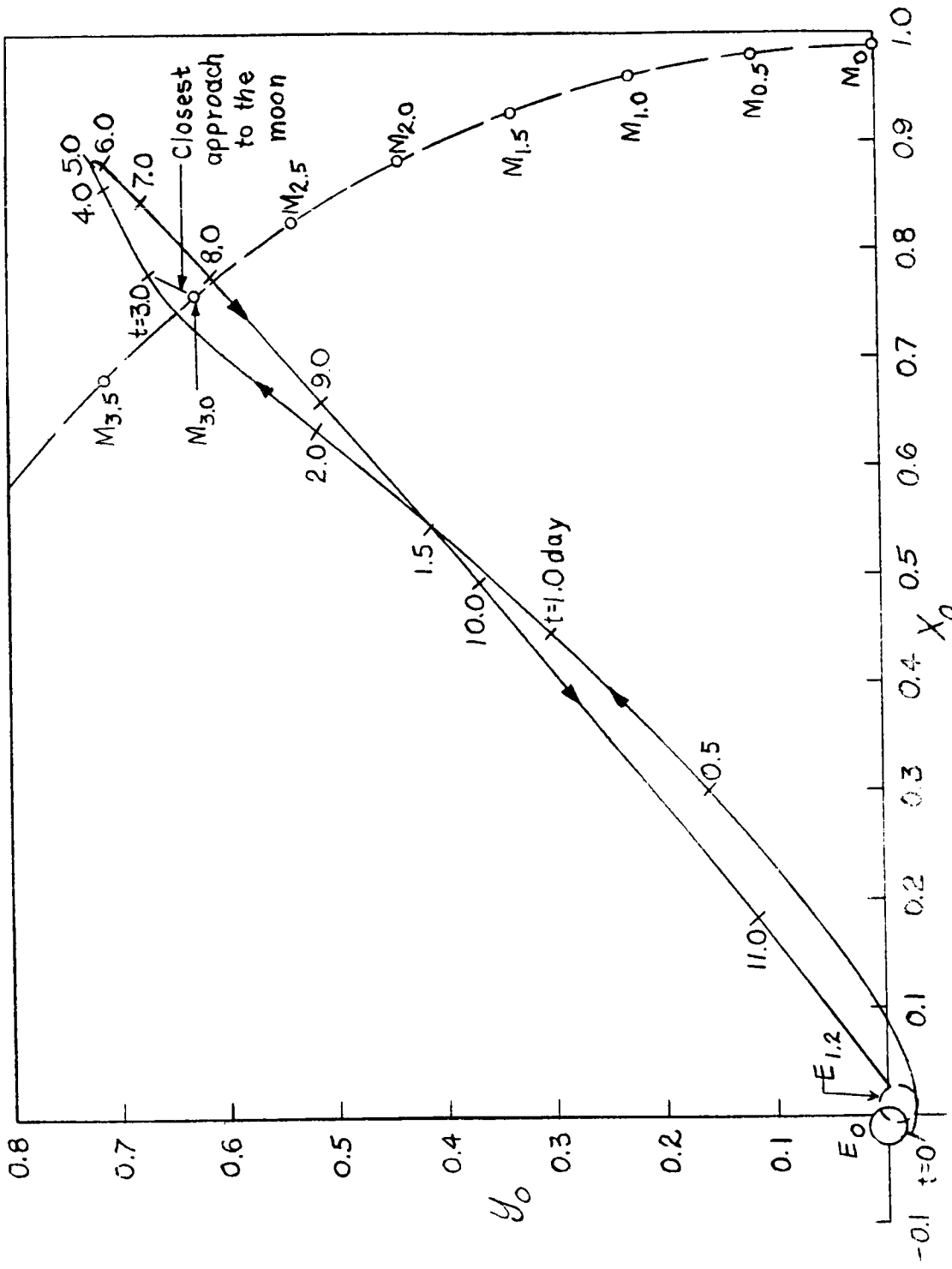


Fig 3-28. A trajectory to return to earth after passing near the moon, ref 3-5

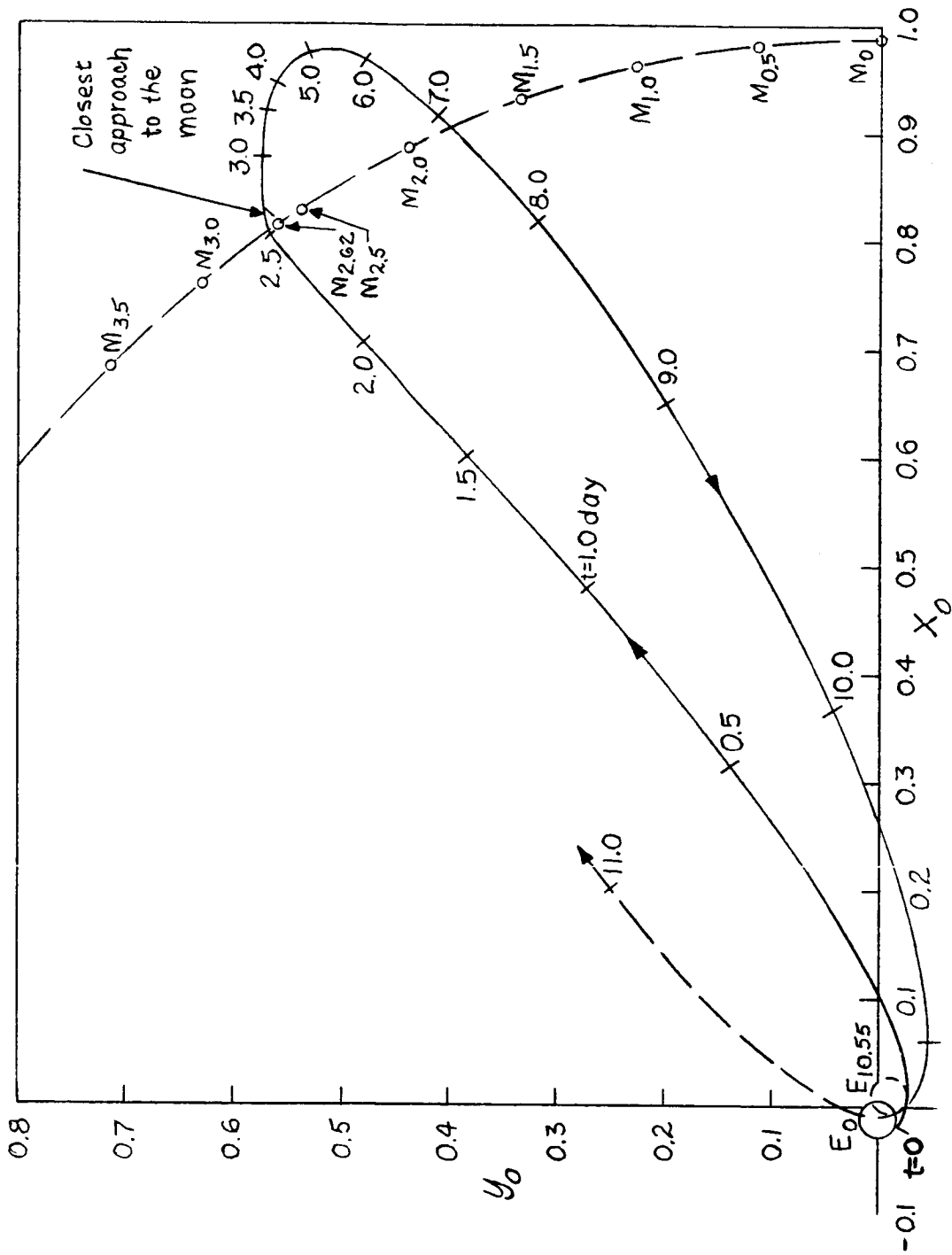


Fig. 3-29. A trajectory to orbit the earth after passing near the moon, (ref. 3-5)

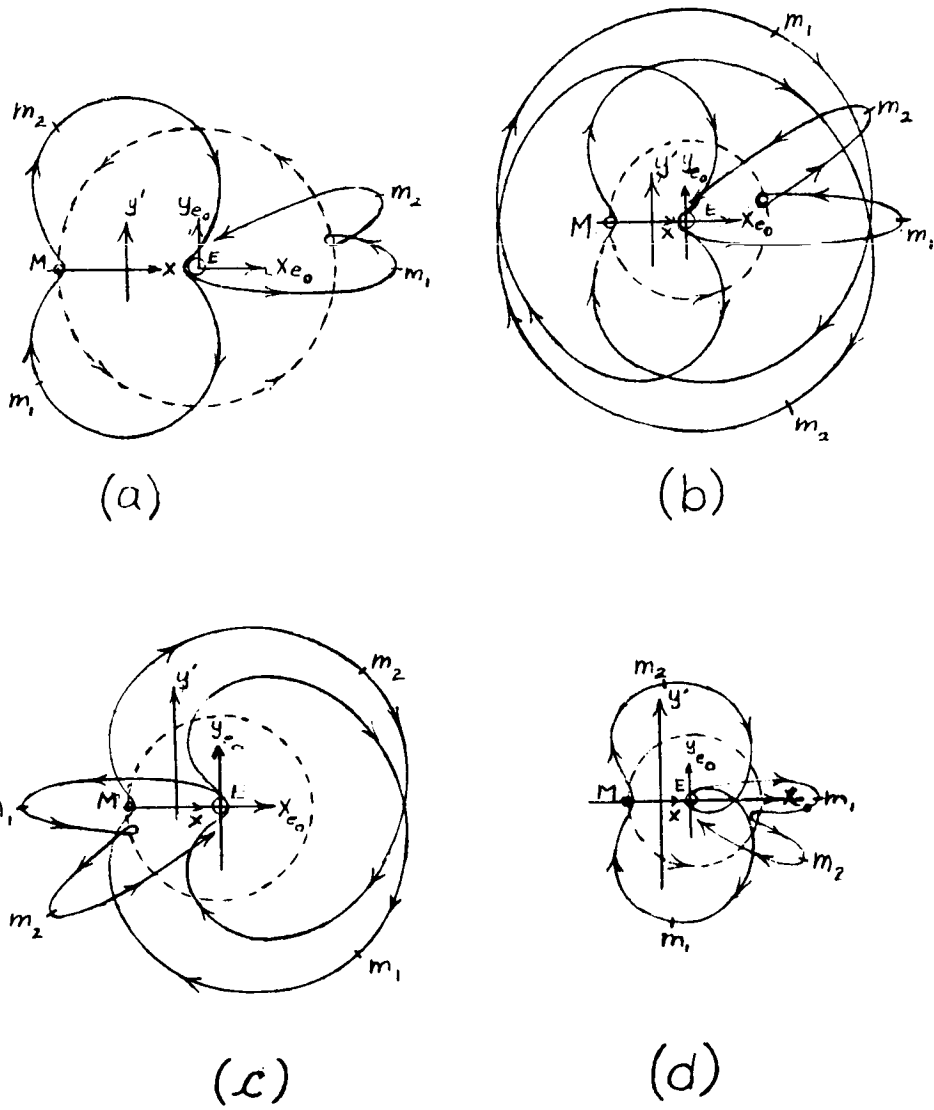


Figure 3-30 Periodic allunar trajectories.

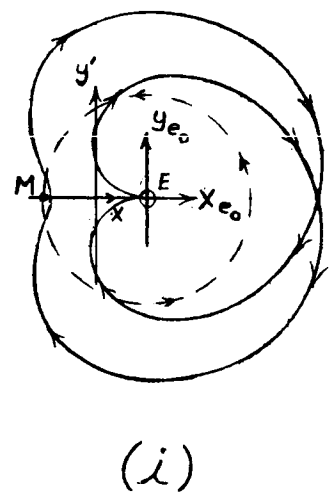
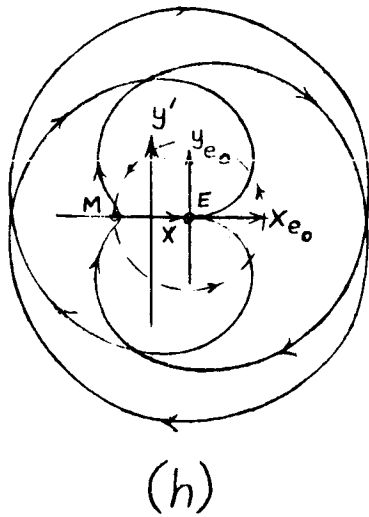
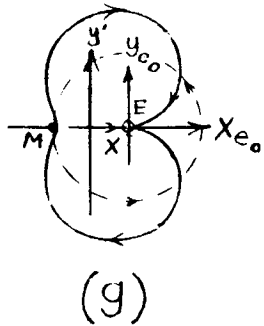
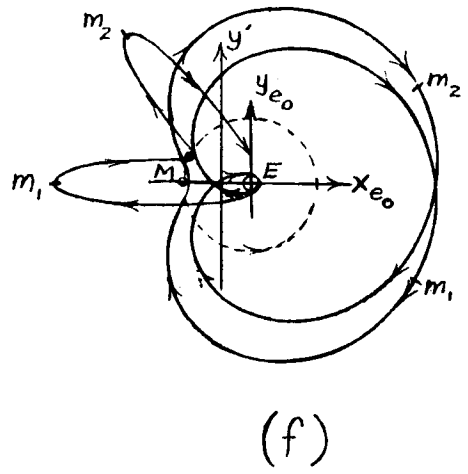
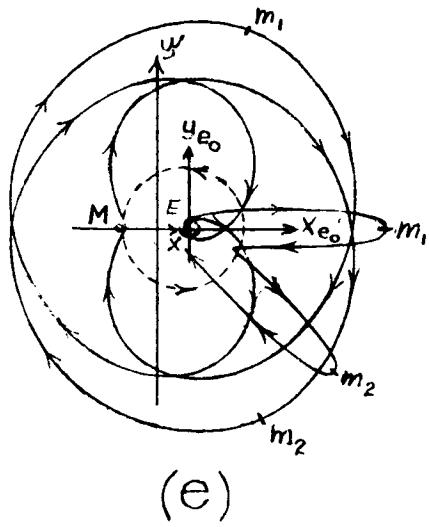


Figure 3-30.- Periodic allunar trajectories concluded.

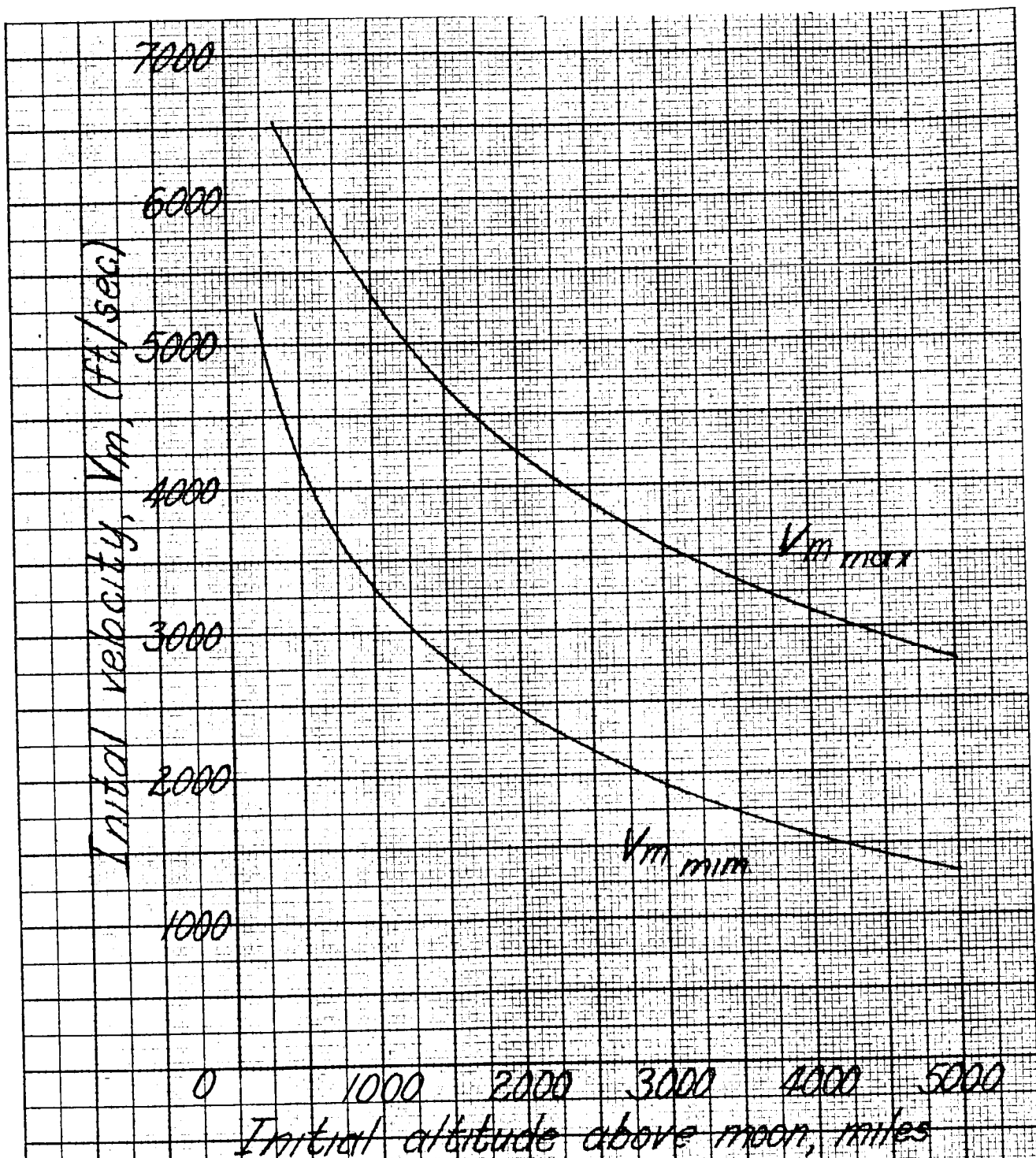


Fig. 3-31. Selenocentric velocity limitations for establishing a lunar satellite.

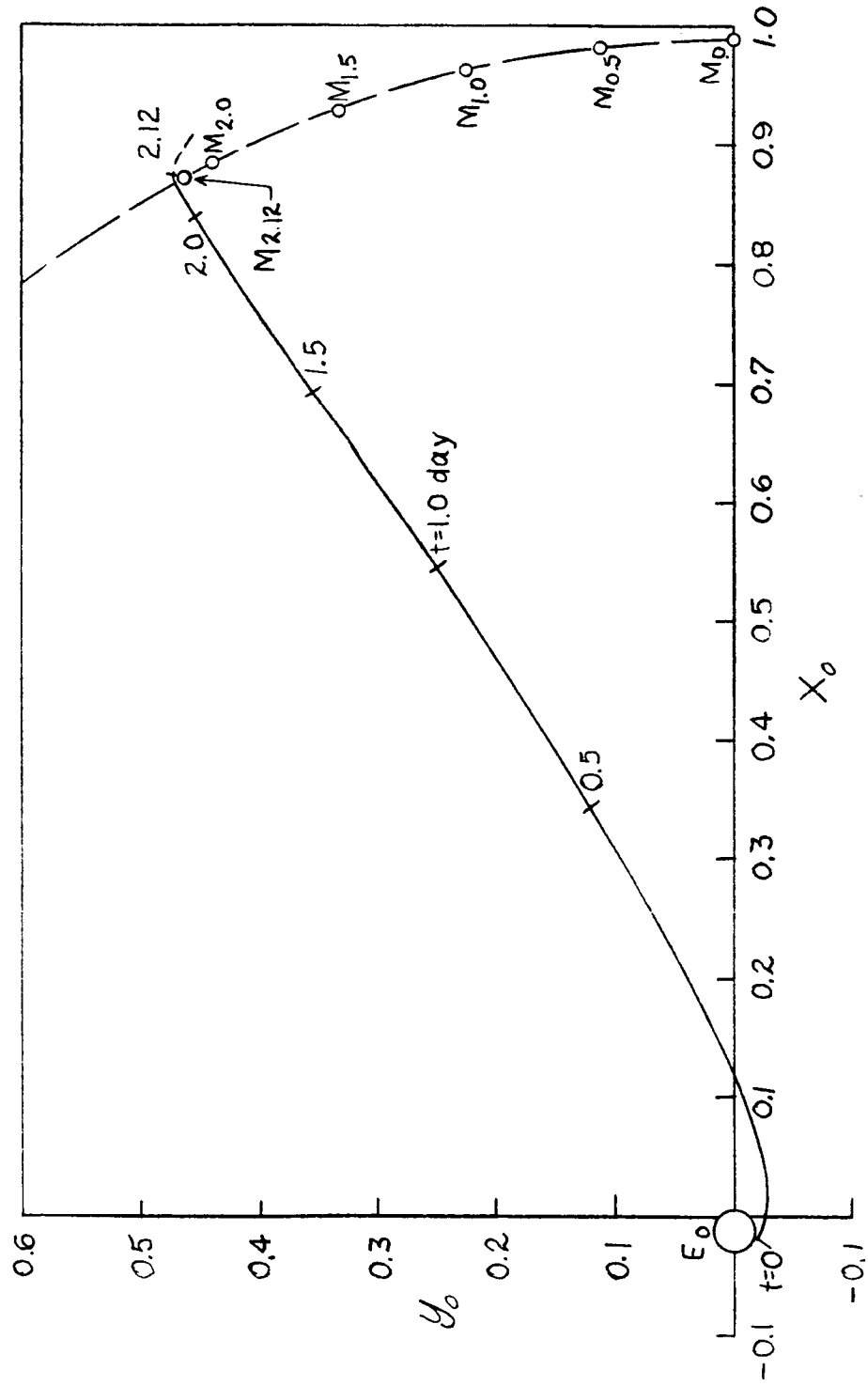


Fig. 3-32 A trajectory to establish a satellite of the moon, ref. 3-7.

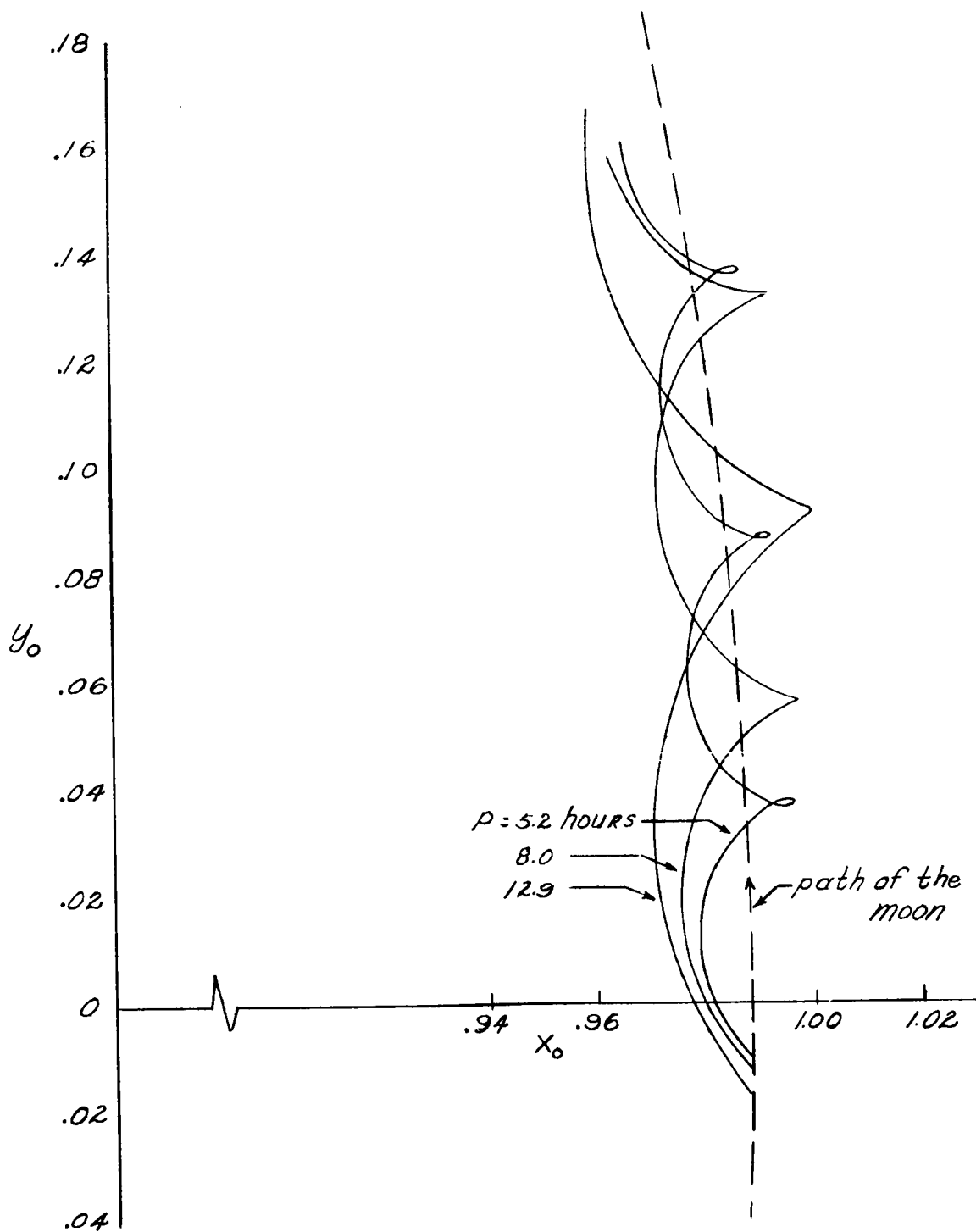


Fig 3-33 Path of lunar satellites with circular orbits as seen from inertial axes near Earth

L

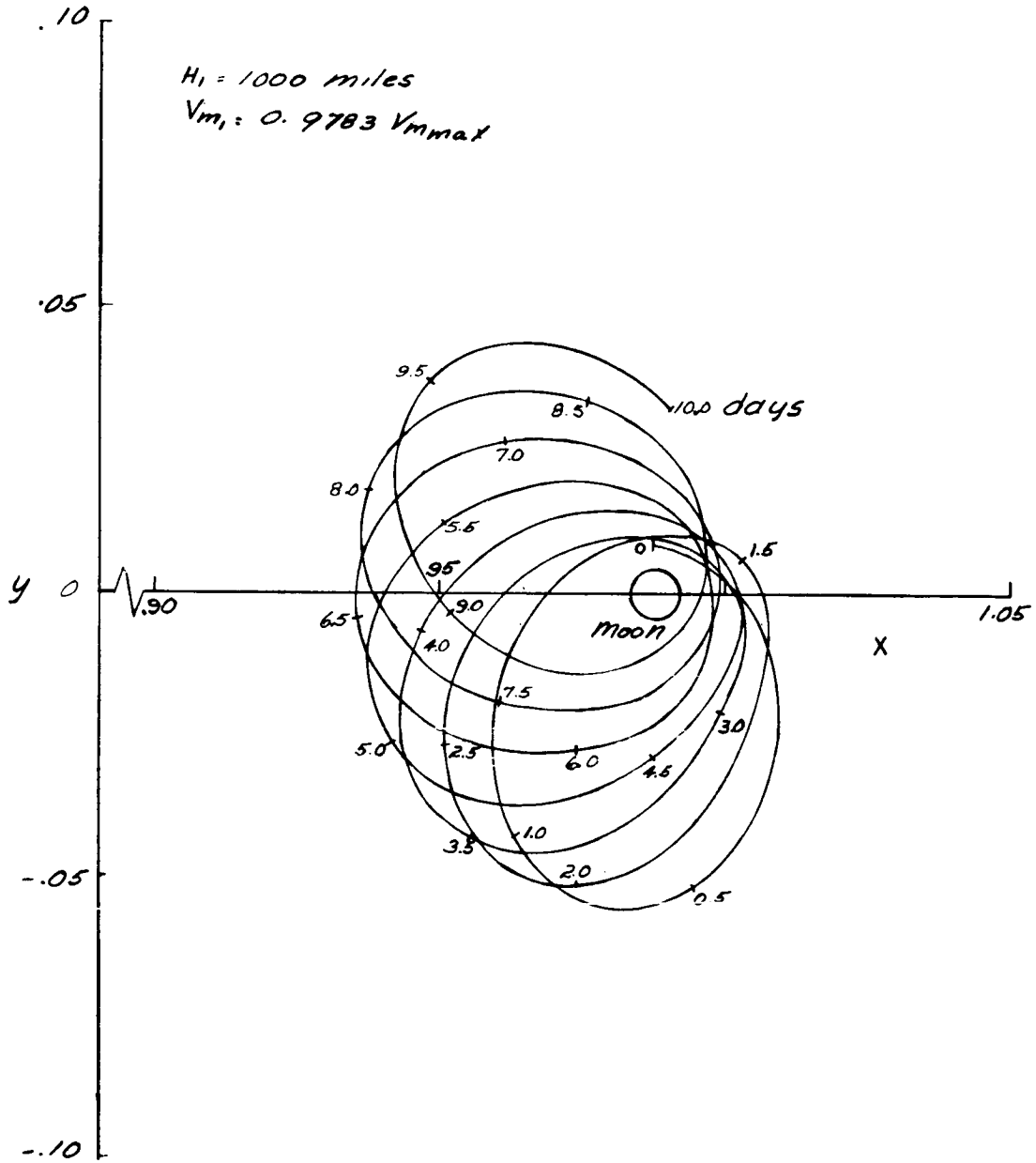


Fig. 3-34. Orbit of Lunar satellite in rotating X, Y axes system

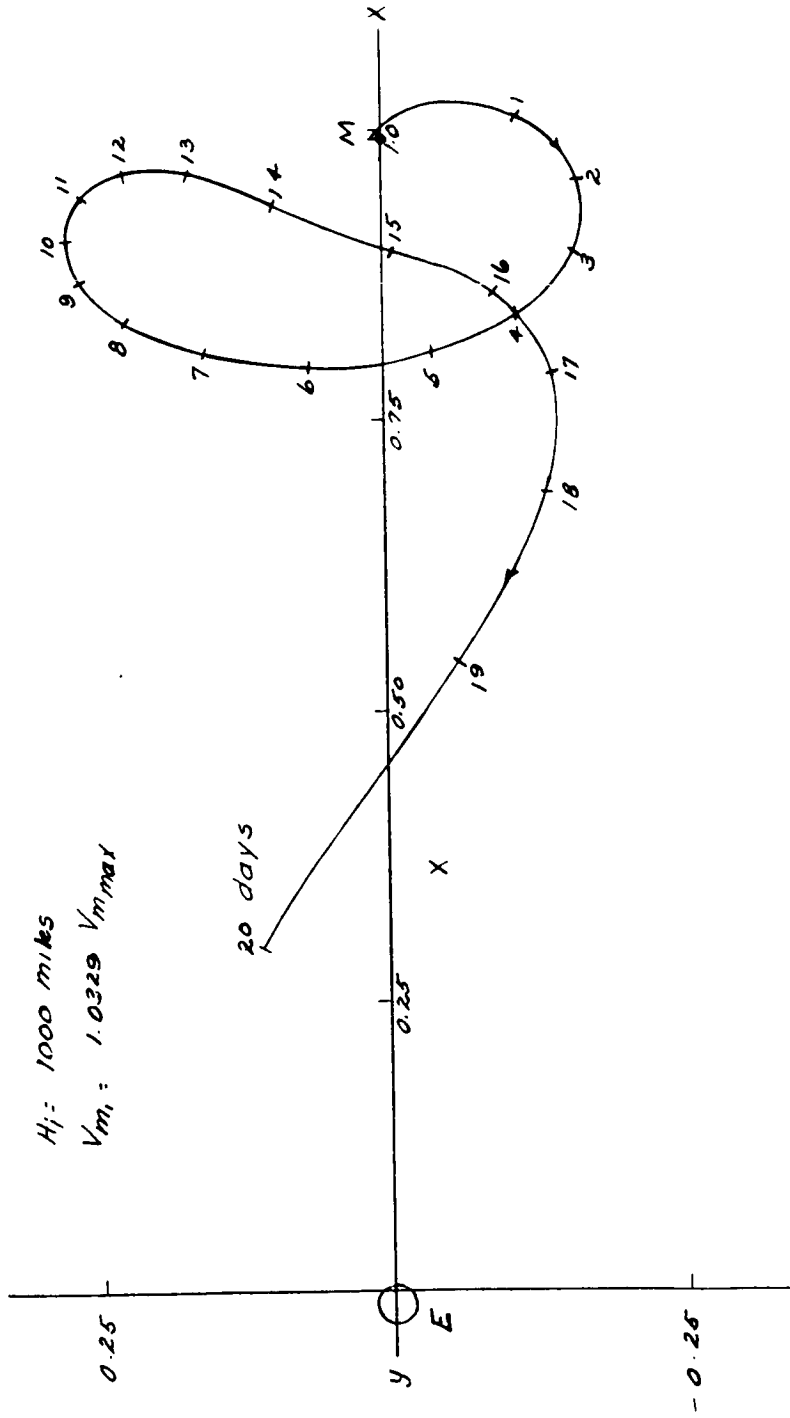


Fig 3-35 Recapture of lunar satellite by the Earth due to excessive initial velocity at moon.

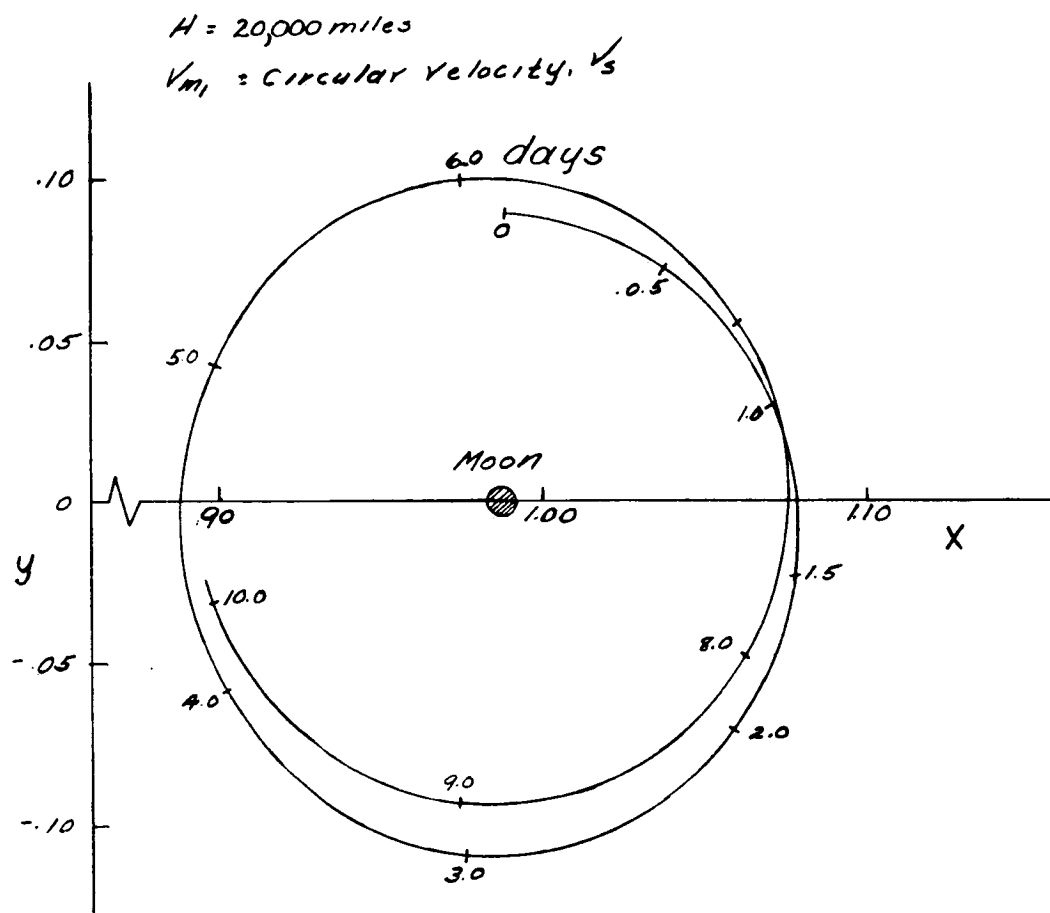


Fig 3-36 Nearly circular lunar satellite orbit.

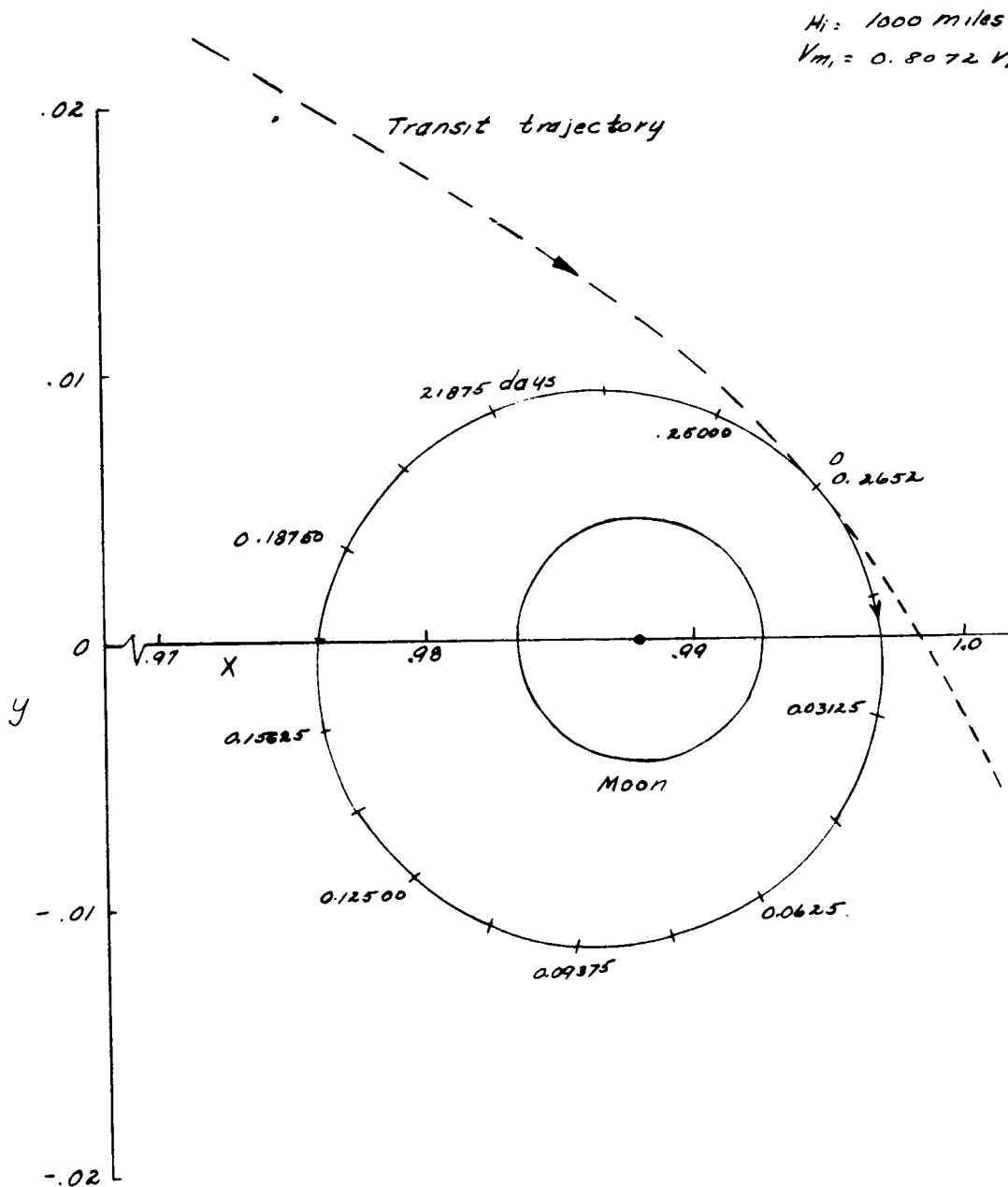


Fig 3-37 Moon satellite orbit resulting from initial conditions given in text.

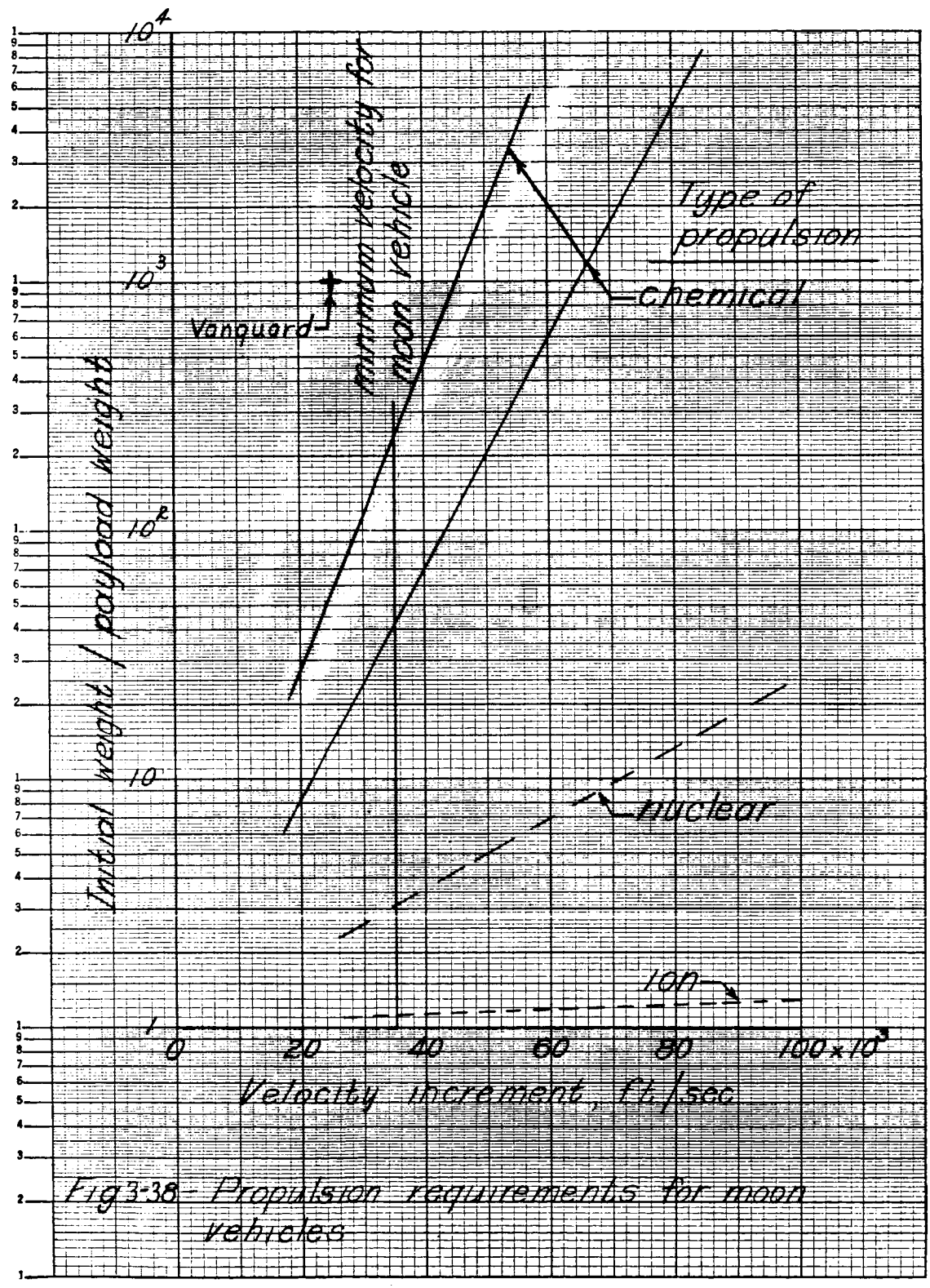


Fig 3-38 Propulsion requirements for moon vehicles

SECTION IV

ORBITAL TRANSFER

Because present interest is on the transfer from an existing orbit into a re-entry orbit, the equations to follow are directed toward the re-entry transfer problem. The first concern is given to the apogee kick transfer into the re-entry orbit and then the problem of a kick at any arbitrary point in an orbit is considered. Even though the equations are directed toward the re-entry problem they may be adapted to a variety of other non entry problems.

4.1 Apogee Kick Transfer

If it is assumed that we have a vehicle in an orbit entirely outside the main atmosphere, one of the simplest and more effective ways to cause the vehicle to enter the atmosphere is by firing a retarding rocket at the apogee. The equations which pertain to an apogee kick re-entry are derived as follows:

The following three equations were obtained from equations (1.2-17), (1.3-8), (1.4-2), and (1.4-3) of SECTION I.

$$\epsilon = \left(\frac{V_p^2 r_p^2}{g_0 R^2} \right) \frac{1}{d} \quad (4.1-1)$$

$$\frac{K}{d} = V_p - \frac{g_0 R^2}{V_p r_p} \quad (4.1-2)$$

$$V_p r_p = V_a r_a \quad (4.1-3)$$

Thus from equation (4.1-2)

$$\frac{1}{d} = \left(V_p - q_0 R^2 / V_p r_p \right) \frac{1}{K} \quad (4.1-4)$$

and combining equation (4.1-1) and (4.1-4)

$$\epsilon = \left(\frac{V_p^2 r^2}{q_0 R^2} \right) \left(\frac{V_p - q_0 R^2}{V_p r_p} \right) \left(\frac{1}{V_p r_p} \right) \quad (4.1-5)$$

which may be reduced to

$$\epsilon = \left(\frac{V_p^2 r_p}{q_0 R^2} - 1 \right) \quad (4.1-6)$$

Other combinations of equations (4.1-1), (4.1-2), and (4.1-3) yield:

$$\epsilon = \left(1 - \frac{V_a^2 r_a}{q_0 R^2} \right) \quad (4.1-7)$$

$$V_p = V_a \left(\frac{1+\epsilon}{1-\epsilon} \right); \quad r_p = r_a \left(\frac{1-\epsilon}{1+\epsilon} \right) \quad (4.1-8)$$

If the original conditions at the apogee are V_{a_0} and r_{a_0} and after the retarding rockets are fired a change in velocity (ΔV) is effectively instantaneously added, the new conditions at the apogee are now V_{a_1} and r_{a_1} where $V_{a_1} = (V_{a_0} + \Delta V)$ and $r_{a_1} = r_{a_0}$. The eccentricity, radius of the perigee and velocity at the perigee are given by

$$\epsilon = \left[1 - \frac{V_{a_1}^2 r_{a_1}}{g_0 R^2} \right] \quad (4.1-9)$$

$$r_{p_1} = r_{a_1} \left(\frac{1 - \epsilon_1}{1 + \epsilon_1} \right) \quad (4.1-10)$$

$$V_{p_1} = V_{a_1} \left(\frac{1 + \epsilon_1}{1 - \epsilon_1} \right) \quad (4.1-11)$$

Also the new semi major axis is established as

$$a_1 = \frac{r_{a_1} + r_{p_1}}{2} = \frac{1}{2} \left[r_{a_1} - r_{a_1} \left(\frac{1 - \epsilon_1}{1 + \epsilon_1} \right) \right] \quad (4.1-12)$$

$$= \frac{r_{a_1}}{1 + \epsilon_1} \quad (4.1-13)$$

The equation of the new ellipse is

$$r = \frac{r_{a_1} (1 - \epsilon)}{1 + \epsilon \cos \theta} \quad (4.1-14)$$

where ϵ_1 is defined by equation (4.1-9).

Now that the new orbit has been established, it is desired to know where the vehicle will enter the atmosphere and what will be the re-entry angle, that is, the angle between the flight path and the horizon at the point of re-entry. It is assumed that ΔV is sufficiently large to cause the re-entry. The upper limit of the atmosphere is considered at r_e which is usually taken to be somewhere about 50 - 70 miles. The re-entry will occur at the angle θ where the radius r of the ellipse is equal to r_e . From equation (4.1-14)

$$r_e = \frac{r_a(1-\epsilon_1)}{1+\epsilon_1 \cos \theta_e} \quad (4.1-15)$$

Solving for $\cos \theta_e$

$$1 + \epsilon_1 \cos \theta_e = \frac{r_a(1-\epsilon_1)}{r_e} \quad (4.1-16)$$

$$\cos \theta_e = \left[\frac{r_a(1-\epsilon_1)}{\epsilon_1 r_e} - \frac{1}{\epsilon_1} \right] \quad (4.1-17)$$

and the re-entry position θ_e is given by

$$\theta_e = \cos^{-1} \left[\frac{r_a(1-\epsilon_1)}{\epsilon_1 r_e} - \frac{1}{\epsilon_1} \right] \quad (4.1-18)$$

The re-entry angle is defined as the angle between a line perpendicular to r at θ_e and the tangent to the orbit at this point. The general equation for this angle at all values of θ was given in SECTION I as equation (1.5-8).

$$\tan \gamma = \frac{\epsilon \sin \theta}{1 + \epsilon \cos \theta} \quad (4.1-19)$$

Thus the re-entry angle γ_e at θ_e is given by

$$\gamma_e = \tan^{-1} \frac{\epsilon_1 \sin \theta_e}{1 + \epsilon_1 \cos \theta_e} \quad (4.1-20)$$

For counterclockwise vehicle motion, $\tan \gamma = +$ indicates an exit, $\tan \gamma = -$ indicates an entry. The velocity at re-entry is given from equation (1.6-2) of SECTION I as

$$V_1 = \pm \sqrt{g_0 R^2 \left(\frac{2}{r_e} - \frac{1}{a_1} \right)} \quad (4.1-21)$$

The various equations are adaptable to the following problems.

Problem Number I: It is desired to make the vehicle re-enter at a certain θ_e and r_e .

The values of θ_e and r_e are substituted in equation (4.1-17)

$$\cos \theta_e = \left[\frac{r_a (1 - \epsilon_1)}{\epsilon_1 r_e} - \frac{1}{\epsilon_1} \right] \quad (a)$$

Solving for ϵ_1 :

$$\epsilon_1 \cos \theta_e = \frac{r_a}{r_e} (1 - \epsilon_1) - 1 \quad (b)$$

$$\epsilon_1 \cos \theta_e = \frac{r_a}{r_e} - \frac{r_a}{r_e} \epsilon_1 - 1 \quad (c)$$

$$\epsilon = \frac{\frac{r_a}{r_e} - 1}{\cos \theta_e + \frac{r_a}{r_e}} = \frac{r_a - r_e}{r_e \cos \theta_e + r_a} \quad (d)$$

Thus the eccentricity required to effect the re-entry at θ_e, r_e is defined.

The velocity at the apogee, V_{a_1} , required to give this eccentricity is derived in the following equations:

From equation (4.1-9)

$$\frac{V_a^2 r_a}{g_0 R^2} = 1 - \epsilon \quad (e)$$

Solving for V_a yields:

$$V_a^2 = \frac{(1-\epsilon)g_0 R^2}{r_a} ; \quad (1-\epsilon) = 1 - \left[\frac{r_a - r_e}{r_e \cos \theta_e + r_a} \right] \quad (f)$$

$$= \frac{r_e \cos \theta_e + r_e}{r_e \cos \theta_e + r_a}$$

$$V_{a_1} = \pm \sqrt{\frac{g_0 R^2}{r_a} \left(\frac{r_e \cos \theta_e + r_e}{r_e \cos \theta_e + r_a} \right)} \quad (g)$$

This equation defines the velocity required at apogee to give re-entry at θ_e and r_e .

Thus

$$\Delta V = V_{a_0} - V_{a_1} \quad (h)$$

$$\Delta V = V_{a_0} \mp \sqrt{\frac{g_0 R^2}{r_a} \left(\frac{r_e \cos \theta_e + r_e}{r_e \cos \theta_e + r_a} \right)} \quad (i)$$

Thus the ΔV required at apogee r_a to give re-entry at θ_e, r_e is defined. The re-entry angle at γ_e is given by

$$\gamma_e = \tan^{-1} \frac{\epsilon_1 \sin \theta_e}{1 + \epsilon_1 \cos \theta_e} \quad (j)$$

The velocity at re-entry is given by equation (4.1-21). A solution of a typical problem of this type is given in figure 4-1.

Problem Number II: It is desired to make the vehicle re-enter at a certain entry angle γ_e and r_e .

Substitution of r_e into the general equation of the orbit:

$$r_e = \frac{r_a(1 - \epsilon_1)}{1 + \epsilon_1 \cos \theta_e} \quad (a)$$

Solving for ϵ_1 :

$$r_e + \epsilon_1 r_e \cos \theta_e = r_a - r_a \epsilon_1 \quad (b)$$

$$\epsilon_1 (r_e \cos \theta_e + r_a) = r_a - r_e \quad (c)$$

$$\epsilon_1 = \frac{r_a - r_e}{r_e \cos \theta_e + r_a} \quad (d)$$

Thus the eccentricity required to effect the re-entry at any θ_e , r_e is defined in (d). The interest is, however, in a particular θ_e which will give the re-entry angle γ_e .

From equation (4.1-20)

$$1 + \epsilon_1 \cos \theta_e = \frac{\epsilon_1 \sin \theta_e}{\tan \gamma_e} \quad (e)$$

$$\epsilon_1 \cos \theta_e - \epsilon_1 \frac{\sin \theta_e}{\tan \gamma_e} = -1 \quad (f)$$

$$\epsilon_1 = \frac{1}{\frac{\sin \theta_e}{\tan \gamma_e} - \cos \theta_e} \quad (g)$$

This defines the required eccentricity in terms of θ_e and γ_e .

Equating the two equations for the required eccentricity gives

$$\frac{1}{\frac{\sin \theta_e}{\tan \gamma_e} - \cos \theta_e} = \frac{r_a - r_e}{r_e \cos \theta_e + r_a} \quad (h)$$

Cross-multiplying and rearranging

$$r_a = r_a \frac{\sin \theta_e}{\tan \gamma_e} - r_e \frac{\sin \theta_e}{\tan \gamma_e} - r_a \cos \theta_e \quad (i)$$

but

$$\cos \theta = \sqrt{1 - \sin^2 \theta}$$

so that

$$r_a + \frac{r_e - r_a}{\tan \gamma_e} \sin \theta_e = -r_a \sqrt{1 - \sin^2 \theta_e} \quad (j)$$

Squaring both sides, letting

$$A = \frac{r_e - r_a}{\tan \gamma_e} \quad (k)$$

$$2 A r_a \sin \theta_e + A^2 \sin^2 \theta_e = -r_a^2 \sin^2 \theta \quad (l)$$

or

$$2 A r_a \sin \theta_e = -(A^2 + r_a^2) \sin^2 \theta_e \quad (m)$$

From which

$$\sin \theta_e = \frac{-2A r_a}{A^2 + r_a^2} \quad (n)$$

$$\theta_e = \sin^{-1} \frac{-2A r_a}{A^2 + r_a^2} \quad (o)$$

where A is defined by equation (k).

This defines the θ_e where the re-entry is to occur. Thus, the eccentricity of the re-entry ellipse is given by

$$\epsilon_1 = \frac{r_a - r_e}{r_e \cos \theta_e + r_a} \quad (p)$$

The velocity required at apogee V_{a_1} to obtain the required γ_e and r_e at re-entry is given by

$$V_{a_1}^2 = \frac{(1 - \epsilon_1) g_0 R^2}{r_a} \quad (q)$$

when equation (p) is substituted for ϵ_1 , equation (q) becomes

$$V_a = \sqrt{\frac{g_0 R^2}{r_a} \left[\frac{r_e \cos \theta_e + r_e}{r_e \cos \theta_e + r_a} \right]} \quad (r)$$

and thus the increment of velocity required at apogee to give re-entry at the prescribed γ_e and r_e is given by

$$\Delta V = V_0 \mp \sqrt{\frac{g_0 R^2}{r_a} \left[\frac{r_e \cos \theta_e + r_e}{r_e \cos \theta_e + r_a} \right]} \quad (s)$$

where θ_e is defined by equation (o). The velocity at re-entry is given by equation (4.1-21). A solution to a problem of this type is given in figure 4-2.

4.2 Use of A Kick At A Point In The Orbit Other Than Apogee

The use of the kick at a point other than apogee is directed toward the problem of re-entry at a specified angular position θ_e , altitude r_e , and re-entry angle γ_e . These arbitrary re-entry conditions cannot be obtained by a kick at apogee. The basic equations given in Section 4.1 may be adapted to this type of problem.

Problem Number III: It is required to re-enter at a certain θ_e , r_e , and γ_e .

One solution to this problem is to use the solution given in Section 4.1 to determine a re-entry orbit which will give the proper entry angle γ_e at r_e and then to rotate the major axis of the orbit to give the proper entry position θ_e . Thus a re-entry orbit is obtained which satisfies the re-entry requirements. The transfer into this re-entry orbit is made where the orbit of the vehicle intersects the re-entry orbit.

The equation of the orbit which gives the proper entry angle γ_e at r_e is given by

$$r = \frac{r_a(1 - \epsilon_e)}{1 + \epsilon_e \cos \theta} \quad (a)$$

and the equation of the orbit of the vehicle is given by

$$r = \frac{r_{a_0}(1 - \epsilon_0)}{1 + \epsilon_0 \cos \theta} \quad (b)$$

The ellipse of equation (a) which gives the proper entry angle γ_e at r_e is rotated counterclockwise through an angle $\Delta\theta$ to give the proper entry position θ_e so that the equation of the re-entry orbit becomes

$$r = \frac{r_{a_1}(1 - \epsilon_1)}{1 + \epsilon_1 \cos(\theta - \Delta\theta)} \quad (c)$$

The points of intersection of the vehicle's orbit (equation (b)) and the re-entry orbit (equation (c)) where the transfer may be made are found by equating the equations for the two orbit equations.

Thus,

$$\frac{r_{a_1}(1 - \epsilon_1)}{1 + \epsilon_1 \cos(\theta - \Delta\theta)} = \frac{r_{a_0}(1 - \epsilon_0)}{1 + \epsilon_0 \cos \theta} \quad (d)$$

Solving for the θ 's of the intersections.

Inverting equation (d)

$$\frac{1 + \epsilon_1 \cos(\theta - \Delta\theta)}{r_{a_1}(1 - \epsilon_1)} = \frac{1 + \epsilon_0 \cos \theta}{r_{a_0}(1 - \epsilon_0)} \quad (e)$$

Expanding equation (e)

$$\frac{1}{r_{a_1}(1 - \epsilon_1)} + \frac{\epsilon_1}{r_{a_1}(1 - \epsilon_1)} \cos(\theta - \Delta\theta) = \frac{1}{r_{a_0}(1 - \epsilon_0)} + \frac{\epsilon_0}{r_{a_0}(1 - \epsilon_0)} \cos \theta \quad (f)$$

Let

$$\frac{1}{r_{a_1}(1 - \epsilon_1)} - \frac{1}{r_{a_0}(1 - \epsilon_0)} = A \quad (g)$$

Substituting a trigonometric identity for $\cos(\theta - \Delta\theta)$ and collecting in equation (f)

$$A + \frac{\epsilon_1}{r_{a_1}(1-\epsilon_1)} (\cos \theta \cos \Delta \theta + \sin \theta \sin \Delta \theta) = \frac{\epsilon_0}{r_{a_0}(1-\epsilon_0)} \cos \theta \quad (h)$$

Collecting in equation (i)

$$A + \left[\frac{\epsilon_1 \cos \Delta \theta}{r_{a_1}(1-\epsilon_1)} - \frac{\epsilon_0}{r_{a_0}(1-\epsilon_0)} \right] \cos \theta = \left[-\frac{\epsilon_1 \sin \Delta \theta}{r_{a_1}(1-\epsilon_1)} \right] \sin \theta \quad (i)$$

Let:

And also let

$$B = \left[\frac{\epsilon_1 \cos \Delta \theta}{r_{a_1}(1-\epsilon_1)} - \frac{\epsilon_0}{r_{a_0}(1-\epsilon_0)} \right] \quad C = \left[-\frac{\epsilon_1 \sin \Delta \theta}{r_{a_1}(1-\epsilon_1)} \right] \quad (j)$$

Substituting equation (j) into equation (i) yields

$$A + B \cos \theta = C \sin \theta \quad (k)$$

And squaring

$$A^2 + 2AB \cos \theta + B^2 \cos^2 \theta = C^2 (1 - \cos^2 \theta) \quad (l)$$

Collecting in equation (l) yields:

$$(A^2 - C^2) + 2AB \cos \theta + (B^2 + C^2) \cos^2 \theta = 0$$

$$\text{Let: } K_1 = (A^2 - C^2) \quad K_2 = 2AB \quad K_3 = (B^2 + C^2) \quad (m)$$

where A B and C are defined in equations (g) and (j).

Then:

$$K_1 + K_2 \cos \theta + K_3 \cos^2 \theta = 0 \quad (n)$$

The solution for the θ_i of the intersections is thus:

$$\theta_i = \cos^{-1} \left(\frac{-K_2 \pm \sqrt{K_2^2 - 4K_1K_3}}{2K_3} \right) \quad (o)$$

where $K_1, K_2,$ and K_3 are defined in equation (m).

The radii at the intersections are

$$r_i = \frac{r_a(1 - \epsilon_o)}{1 + \epsilon_o \cos \theta_i} \quad (p)$$

The velocities of the two paths at the intersection points are given by

$$(V_o)_i = \pm \sqrt{g_o R^2 \left(\frac{2}{r_i} - \frac{1}{a_o} \right)} \quad (q)$$

$$(V_1)_i = \pm \sqrt{g_o R^2 \left(\frac{2}{r_i} - \frac{1}{a_i} \right)} \quad (r)$$

The angle between the velocity vectors is given by

$$\Delta\gamma = \pm \gamma_o \pm \gamma_1 = \pm \tan^{-1} \left(\frac{\epsilon_o \sin \theta_i}{1 + \epsilon_o \cos \theta_i} \right) \pm \tan^{-1} \left(\frac{\epsilon_i \sin(\theta_i - \Delta\theta)}{1 + \epsilon_i \cos(\theta_i - \Delta\theta)} \right) \quad (s)$$

The use of the proper sign (\pm) is left up to consideration of a problem sketch. Thus the velocity vector diagram is established by V_1 , V_o , and $\Delta\gamma$.

The ΔV required to transfer from one ellipse to another may be found from the cosine law

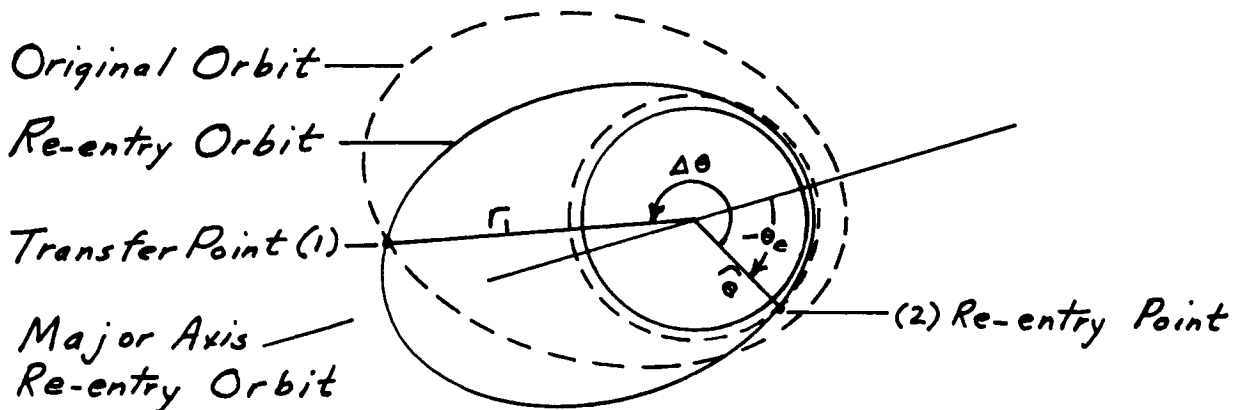
$$\Delta V^2 = (V_1)^2 + (V_o)^2 - 2V_1 V_o \cos(\Delta\gamma) \quad (t)$$

and the angle η between ΔV and V_0 is

$$\eta = \sin^{-1} \left(\frac{\sin \Delta \gamma}{\Delta V} (V_1) \right) \quad (u)$$

Thus the velocity increment required for the transfer and the angle of application is defined. A solution to a problem of this type is given in figure 4-3.

Problem Number IV: As in the above problem it is required to re-enter at a certain θ_e , r_e , and γ_e . The solution to follow is more general than the one given above. Consider the following sketch:



Point (1) is an arbitrarily specified point on the original orbit of a vehicle. It is desired to determine the magnitude and direction of the velocity impulse required at point (1) which would cause the vehicle to go into a re-entry orbit and enter at a specified point (2) with re-entry angle γ_e . Thus r_e , r_1 , $\Delta \theta$, and γ_e are known. The first step is to determine the velocity and direction of velocity required in the re-entry orbit at point (1) to give the desired entry at point (2). Then by simple vector subtraction, the velocity impulse required at (1) in order to cause

the vehicle to leave its normal orbit and go into the re-entry orbit will be determined. The eccentricity and radius at apogee of the re-entry orbit are given by

$$\epsilon = \frac{\tan \gamma_e}{\sin \theta_e - \tan \gamma_e \cos \theta_e} \quad (a)$$

$$r_a = \frac{r_e (1 + \epsilon \cos \theta_e)}{(1 - \epsilon)} \quad (b)$$

$$r_a = \frac{r_1 [1 + \epsilon \cos (\theta_e + \Delta \theta)]}{(1 - \epsilon)} \quad (c)$$

Equating equation (b) to equation (c) and then proceeding to solve for the unknown θ_e

$$r_e [1 + \epsilon \cos \theta_e] = r_1 [1 + \epsilon \cos (\theta_e + \Delta \theta)] \quad (d)$$

thus

$$r_e + \epsilon r_e \cos \theta_e = r_1 + \epsilon r_1 \cos (\theta_e + \Delta \theta) \quad (e)$$

Collecting

$$r_e \cos \theta_e - r_1 \cos (\theta_e + \Delta \theta) = \frac{r_1 - r_e}{\epsilon} \quad (f)$$

Substituting ϵ from equation (a) in equation (f)

$$r_e \cos \theta_e - r_1 \cos (\theta_e + \Delta \theta) = (r_1 - r_e) \frac{\sin \theta_e - \tan \gamma_e \cos \theta_e}{\tan \gamma_e} \quad (g)$$

Trigonometric identity:

$$\cos(\theta_e + \Delta\theta) = \cos\theta_e \cos\Delta\theta - \sin\theta_e \sin\Delta\theta \quad (h)$$

thus substituting equation (h) into equation (g)

$$\begin{aligned} r_e \cos\theta_e - r_i \cos\theta_e \cos\Delta\theta + r_i \sin\theta_e \sin\Delta\theta = \\ \frac{r_i}{\tan\gamma_e} \sin\theta_e - r_i \cos\theta_e - \frac{r_e}{\tan\gamma_e} \sin\theta_e + r_e \cos\theta_e \end{aligned} \quad (i)$$

Collecting in equation (i)

$$\left[r_e - r_i \cos\Delta\theta + r_i - r_e \right] \cos\theta_e + \left[r_i \sin\Delta\theta - \frac{r_i}{\tan\gamma_e} + \frac{r_e}{\tan\gamma_e} \right] \sin\theta_e = 0 \quad (j)$$

and thus

$$\left[r_i (1 - \cos\Delta\theta) \right] \cos\theta_e + \left[r_i \left(\sin\Delta\theta - \frac{1}{\tan\gamma_e} \right) + \frac{r_e}{\tan\gamma_e} \right] \sin\theta_e = 0 \quad (k)$$

let

$$A = r_i (1 - \cos\Delta\theta); \quad B = \left[r_i \left(\sin\Delta\theta - \frac{1}{\tan\gamma_e} \right) + \frac{r_e}{\tan\gamma_e} \right] \quad (l)$$

Thus equation (k) becomes

$$A \cos\theta_e + B \sin\theta_e = 0 \quad (m)$$

From which

$$A + B \tan \theta_e = 0 \quad (n)$$

or

$$\theta_e = \tan^{-1} \left(-\frac{A}{B} \right) \quad (o)$$

where A and B are defined in equation (l).

Equation (o) determines the angle θ_e between the radius r_e and the major axis of the re-entry orbit. Thus the angle θ_e is defined in terms of the knowns.

Using the known θ_e , the eccentricity is found from

$$\epsilon_1 = \frac{\tan \gamma_e}{\sin \theta_e - \tan \gamma_e \cos \theta_e} = \frac{\sin \gamma_e}{\sin(\theta_e - \gamma_e)} \quad (p)$$

Using the known θ_e , r_e , and ϵ the semimajor axis is given by

$$a_1 = \frac{r_e(1 + \epsilon_1 \cos \theta_e)}{(1 - \epsilon^2)} \quad (q)$$

Using the known r_1 and a the velocity required at r_1 to give the specified re-entry conditions is given by

$$V_1 = \pm \sqrt{g_0 R^2 \left[\frac{2}{r_1} - \frac{1}{a_1} \right]} \quad (r)$$

Using the known $\Delta\theta$, θ_e , and ϵ , the angle γ at r_1 is given by

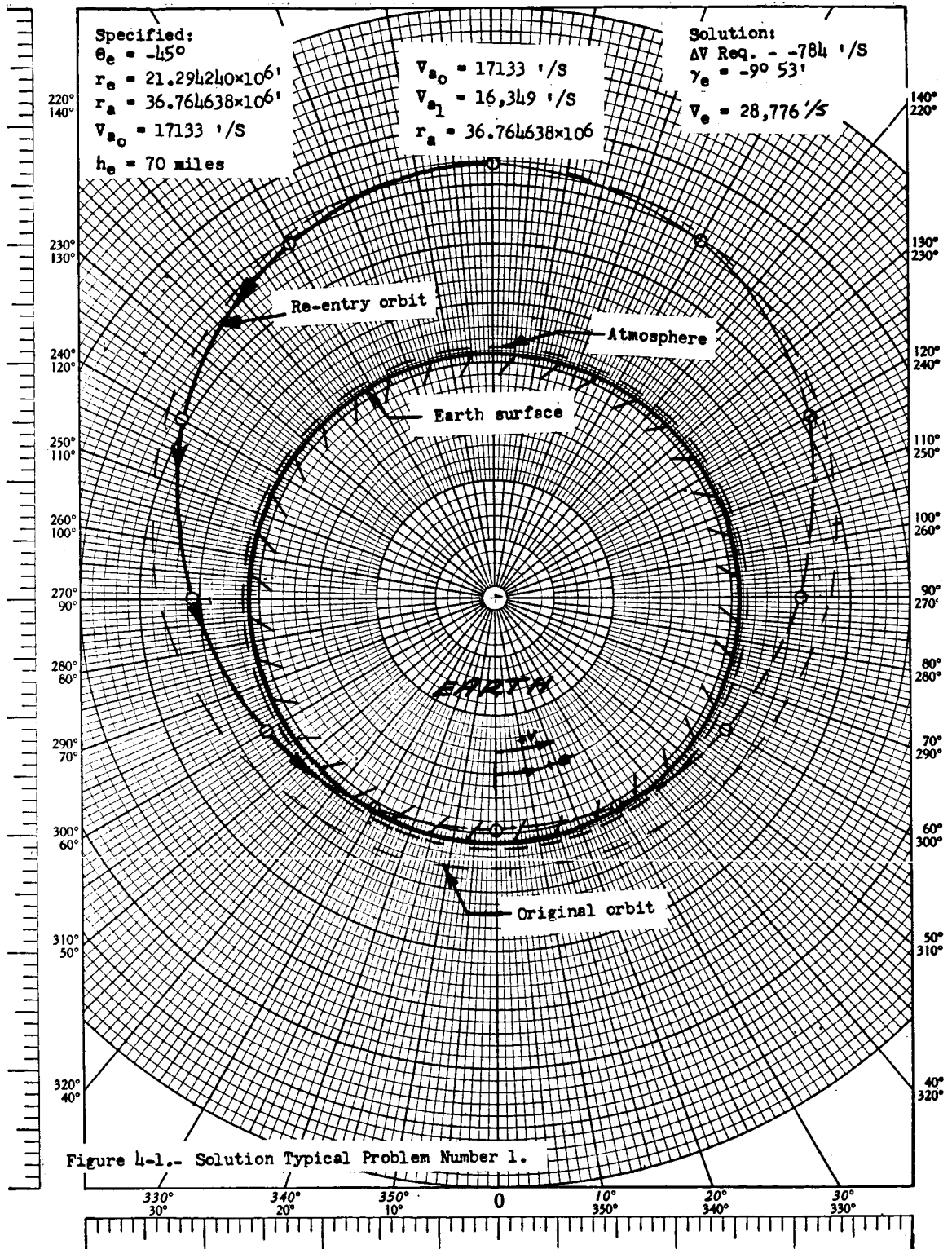
$$\gamma = \tan^{-1} \frac{\epsilon \sin(\theta_e + \Delta\theta)}{1 + \epsilon \cos(\theta_e + \Delta\theta)} \quad (s)$$

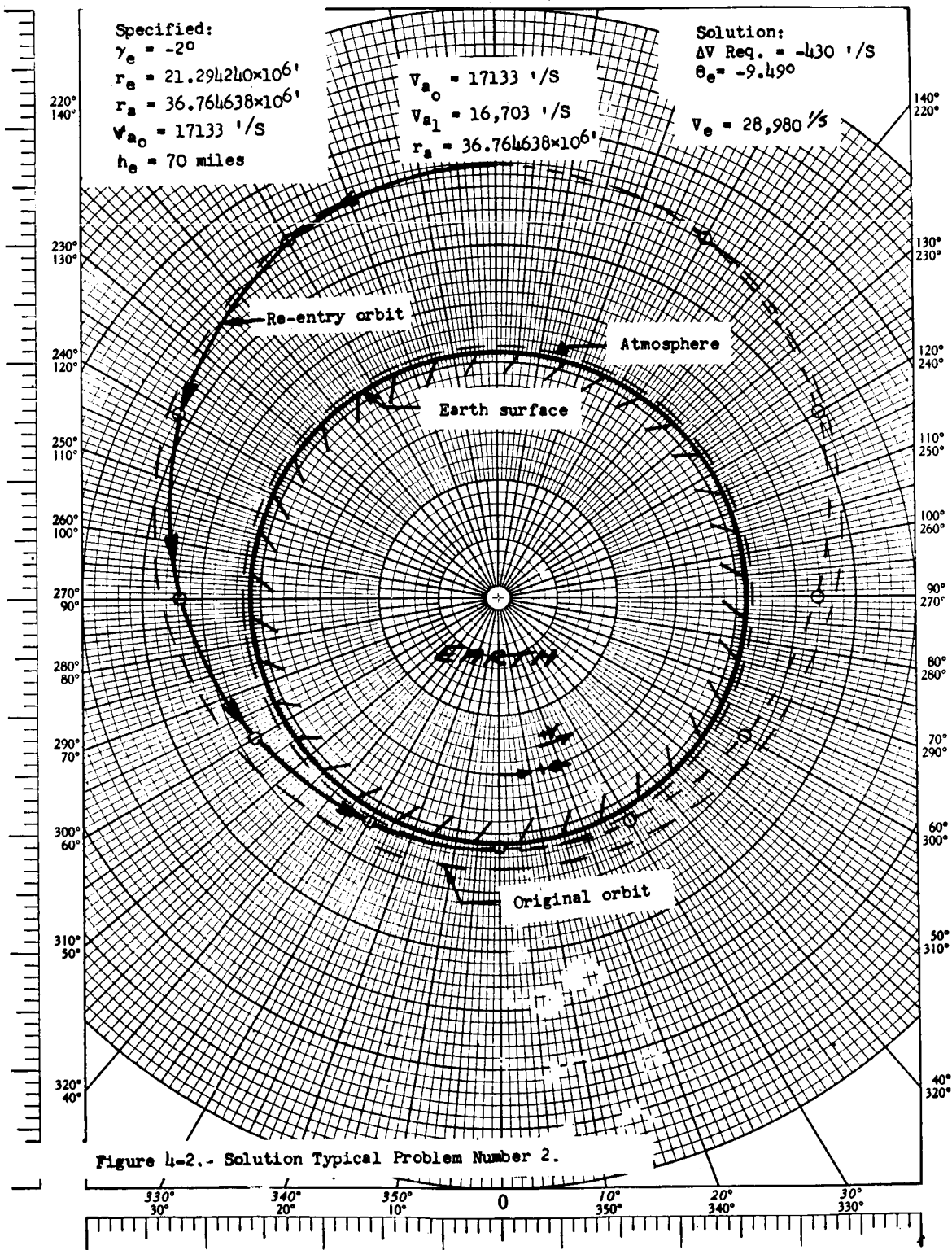
The equation of the re-entry orbit is given by

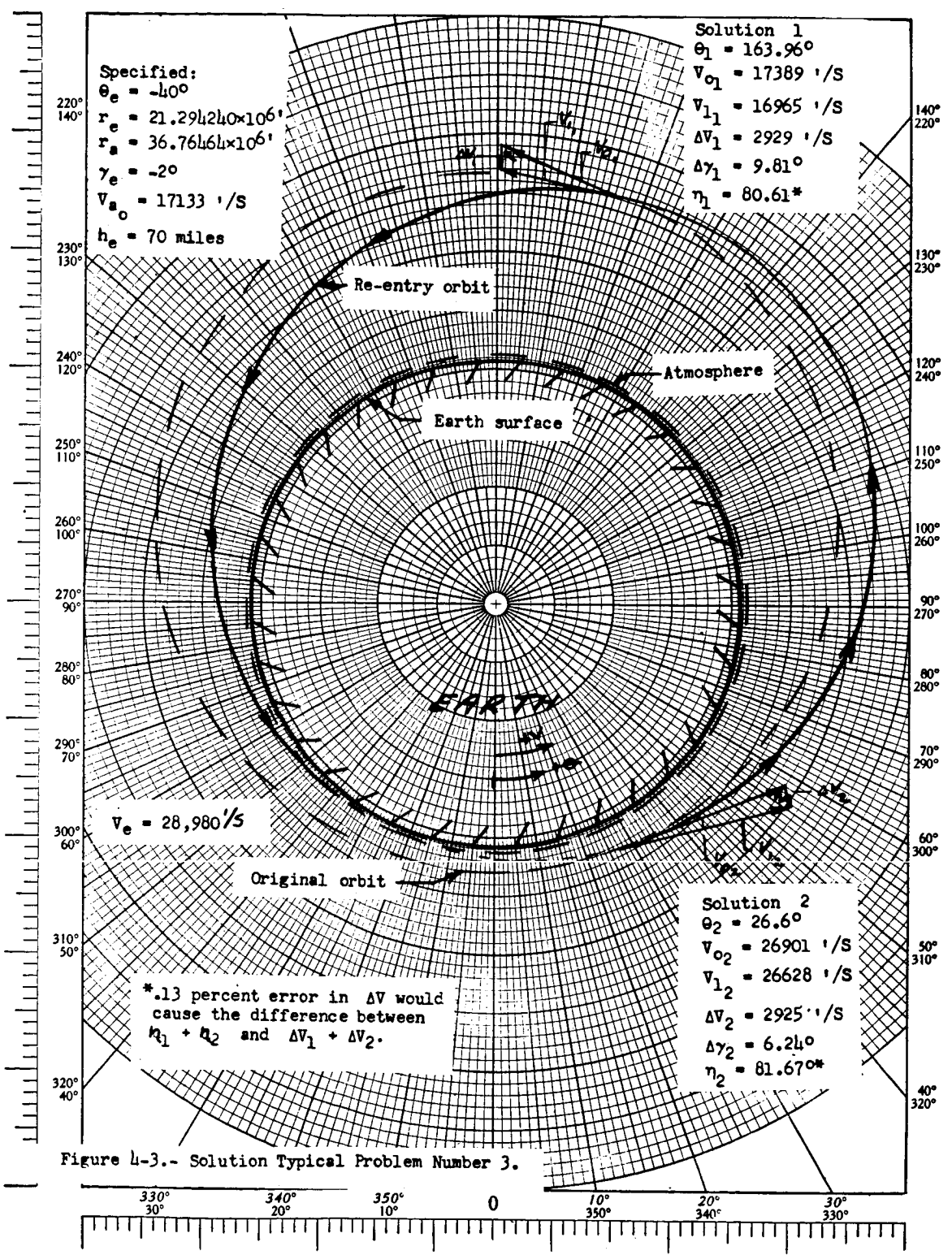
$$r = \frac{a(1 - \epsilon^2)}{1 + \epsilon \cos \theta} \quad (t)$$

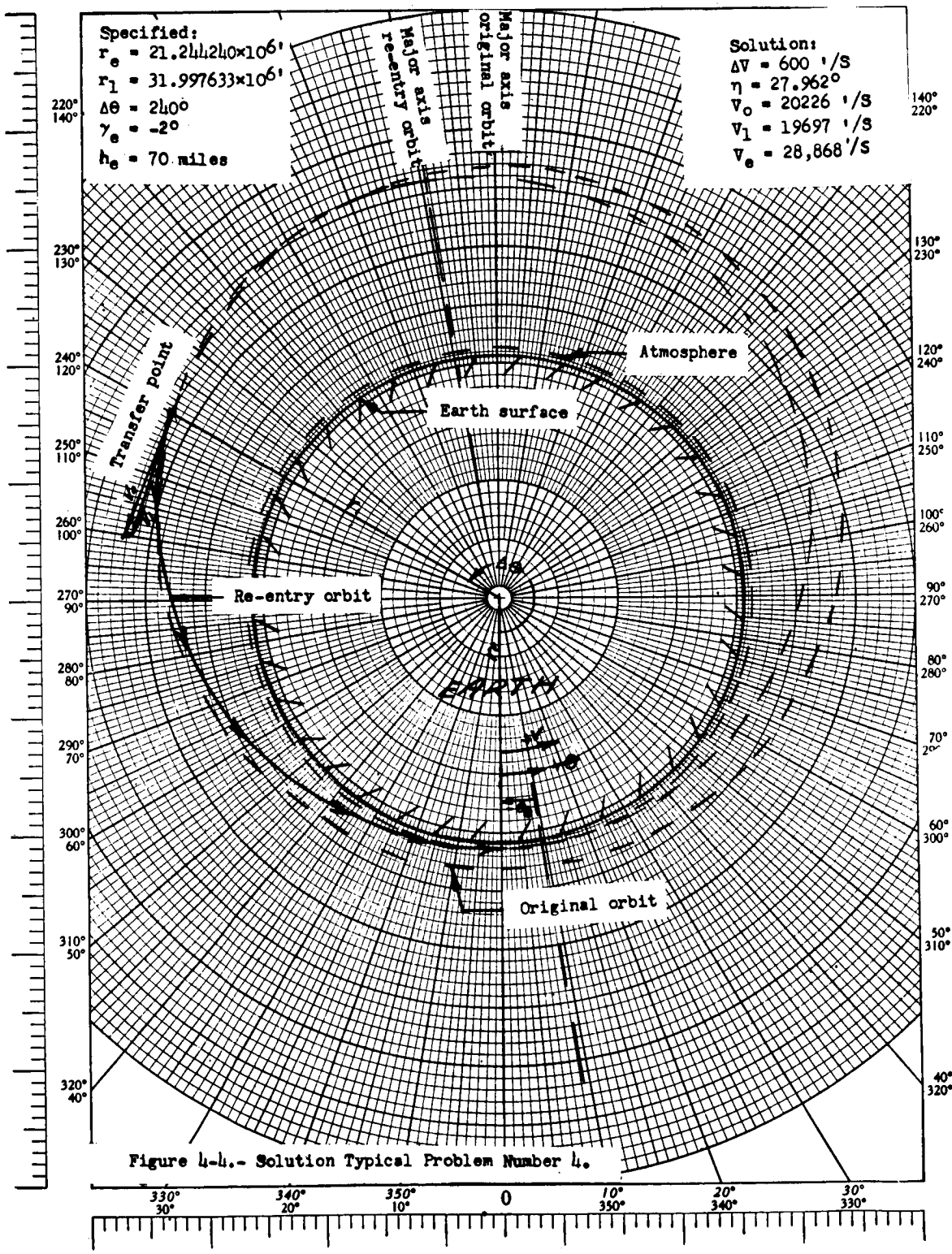
The velocity and direction of the velocity in the re-entry orbit at point (1) are established by equations (r) and (s). The velocity and direction of velocity of the original orbit at point (1) are given by equation (q) of Problem Number III and equation (4.1-19). The procedure for obtaining the required velocity impulse for transfer and its direction may be obtained by use of equations (s) and (t) of the foregoing Problem Number III. The velocity at re-entry may be obtained by means of equation (4.1-21). A solution to a problem of this type is given in figure 4-4.

Consideration up to now has been on the transfer from an existing orbit into a re-entry orbit. The adaptations of the equations to other types of transfers in non-entry considerations and the treatment of minimum energy transfers are left for later considerations.









SECTION V

RE-ENTRY WITH TWO DEGREES OF FREEDOM

5. Introduction.

In the previous SECTION the procedures for determining the position, angle and velocity at re-entry were established. Once these quantities have been established, the complexity of the solution for the paths, velocities, and decelerations in the atmosphere depends on the completeness of the differential equation used. The equations discussed here will be of the simplest nature. The vehicle is to experience lift, drag, gravitational and linear inertia forces only. Even the solution of the simple equations depends on machine integration of the equations. However, there are some further restrictions concerning lift, drag, and air density that can be placed on these simpler equations and some strictly analytical results may be obtained.

There are various paths that may be taken through the atmosphere. It has been proposed from a heating standpoint to use a skip trajectory where a plunge is made, the vehicle heats up, returns to altitude where radiation occurs and cools down for another plunge. The main problem for any path is to slow the vehicle down without excessive heating on decelerations. It has also been shown that another some-

what favorable heat path is a plunge to say 200 -
250,000 feet where pressure drag is of a fair magnitude
and to remain at that altitude until appreciable slow
down occurs. The continuous high drag glide path has
favorable deceleration aspects, but it is fairly un-
favorable from a heating consideration. Only the
skip and glide paths will be discussed and then in a
somewhat limited manner.

SYMBOLS

A	reference area for lift and drag evaluation, sq. ft.
C_D	drag coefficient
C_L	lift coefficient
D	drag, lb.
g	acceleration due to gravity, ft/sec. ²
m	mass slugs
r	distance from center of Earth, ft.
r_c	radius of curvature or flight path, ft.
r_0	radius of Earth, ft.
s	distance along flight path, ft.
S	surface area, sq. ft.
t	time, sec.
V	velocity, ft/sec.
\bar{V}	velocity divided by satellite velocity at Earth's surface
V_s	velocity of satellite at Earth's surface
W	weight, lb.
X	coordinate of fixed axis system
X	range coordinate
y	vertical distance from surface of Earth, ft.
z	coordinate of fixed axes system
β	constant in density altitude relation
γ	angle of flight path to horizon, radians

θ angle between X axis and V radians
 ρ air density slugs/ft.³
 ψ angle between Z axis and r (Section 4.1);
 also remaining range ($\bar{r} - \rho$) (Section 4.3).

Subscripts:

b body axis
 en conditions at entrance to Earth's
 atmosphere
 ex conditions at exit from Earth's
 atmosphere

5.1 Development of Re-entry Equations Involving Lift, Drag, Linear Inertia and Gravitational Forces.

The coordinate system showing the convention of axes and angles is shown in figure (5-1a) and an exploded view of the free body is shown in figure (5-1b). The equations of motion are derived (see reference 5-1) as follows:

Taking a summation of the forces in the X direction:

$$-L \sin \theta - mg \sin \psi - D \cos \theta = m \frac{dV}{dt} \Big|_x$$

but

$$V_x = V \cos \theta$$

and the rate of change of velocity in the X direction is:

$$\frac{dV}{dt} \Big|_x = \dot{V} \cos \theta - \dot{\theta} V \sin \theta$$

and thus:

$$F_x = L \sin \theta - mg \sin \psi - D \cos \theta = m (V \dot{\cos} \theta - V \dot{\theta} \sin \theta) \quad (5.1-1)$$

Similarly summing the forces in the Z direction;

$$F_z = L \cos \theta - mg \cos \psi - D \sin \theta = m \frac{dV}{dt} \Big|_z = m (\dot{V} \sin \theta + V \dot{\theta} \cos \theta) \quad (5.1-2)$$

These two equations are the re-entry equations of motion where only lift, drag, linear inertia, and gravitational forces are involved. The equations are transferred

from the X Z axes to the body $X_b Z_b$ axes, thus providing for easier handling of the aerodynamic forces. The transfer of axes involves a simple rotation of axes by means of the trigometric formulas for axes rotation.

$$F_{X_b} = F_X \cos \theta - F_Z \sin \theta \quad (5.1-3)$$

$$F_{Z_b} = F_X \sin \theta + F_Z \cos \theta \quad (5.1-4)$$

If we substitute F_X and F_Z from equations (5.1-1) and (5.1-2) into equations (5.1-3) and 5.1-4) and cancel like terms and collect,

$$-\frac{D}{W} - \sin \gamma = \frac{\dot{V}}{g} \quad (5.1-5)$$

$$\frac{L}{W} - \cos \gamma = \frac{V\dot{\theta}}{g} \quad (5.1-6)$$

Thus, substituting the expressions for lift and drag weight

$$\dot{V} = -C_D \frac{\rho V^2}{2} S \left(\frac{g}{W}\right) - g \sin \gamma \quad (5.1-7)$$

$$\dot{\theta} = \frac{C_L \alpha \rho V^2 S g}{2 W V} - \frac{g}{V} \cos \gamma \quad (5.1-8)$$

Also from figure (5-1)

$$\dot{X} = V \cos \gamma \quad (5.1-9)$$

$$\dot{\psi} = \frac{V \cos \gamma}{r} \quad (5.1-10)$$

$$\dot{h} = V \sin \gamma = \dot{r} \quad (5.1-11)$$

$$\dot{\gamma} = \dot{\psi} + \dot{\theta} \quad (5.1-12)$$

Equations (5.1-7) through (5.1-12) provide the equations necessary for re-entry calculations where only lift, inertia, gravitational, and drag forces are involved.

The procedure for one means of solution, that is a step by step or digital integration of the equations is somewhat like this. We put the initial conditions $V_0, \gamma_0, \alpha_0, \rho_0, r_0, C_{D0}, C_{L0}$, in the equations and obtain $\dot{\phi}, \dot{V}, \dot{h}, \dot{r}, \dot{\psi}, \dot{X}$, and $\dot{\gamma}$ which when multiplied by the increment of time Δt gives $\phi_1, V_1, h_1, r_1, \psi_1, X_1$, and γ_1 . We put these quantities back into the equation with the appropriate C_D, C_L , and ρ and the process starts all over again to get the various quantities at time 2. It must be remembered that C_L and C_D are functions of Mach number and type of flow which must be known for the body before any computations can be made. Either C_L or α may be programmed into the computations. If there is no lift on the vehicle, the lift term is simply dropped. It might

be mentioned that there are various error reducing procedures that could be used but which would complicate this simple integration technique.

The above equations may be adapted to various problems. Various lift time histories, drag time histories, path angle histories may be programmed into the computations. For the skip and glide path some results may be obtained, with some further restrictions by solely analytical means.

5.2 The Skip Re-entry.

In the skip re-entry the vehicle enters the atmosphere, negotiates a turn and is ejected into a ballistic path.

The equations of motion involving the forces perpendicular and parallel to the flight path are respectively (see reference 5-2).

$$C_L \frac{\rho V^2}{2} A - m g \cos \gamma = \frac{m V^2}{r_c} \quad (5.2-1)$$

$$-C_D \frac{\rho V^2}{2} A + m g \sin \gamma = m \frac{dV}{dt} \quad (5.2-2)$$

We can recognize these as equations (5.1-5) and (5.1-6) previously derived, but using the symbolism of figure (5-3). In the top equation we have the lift term, the weight term, and the centrifugal force due to the path curvature. In the bottom equation we have the drag term, the weight term, and the longitudinal acceleration term.

If in the re-entry turn the effects of gravity are assumed small as compared to other inertia and aerodynamic forces (gravity effects on the downward path are also somewhat cancelled by gravity effects on the upward path), then the two force equations become:

$$\frac{1}{2} C_L \rho V^2 A = -m V^2 \frac{d\gamma}{ds} \quad (5.2-3)$$

$$-\frac{1}{2} C_D \rho V^2 A = m \frac{dV}{dt} \quad (5.2-4)$$

The atmospheric density is assumed to be given by

$$\rho = \rho_0 e^{-\beta y} \quad (5.2-5)$$

Also from figure 5-3 it can be seen that,

$$\frac{dy}{ds} = -\sin \gamma$$

Putting these quantities in equation (5-15) the V^2 and ds go out and

$$C_L \rho_0 A e^{-\beta y} dy = \sin \gamma d\gamma \quad (5.2-6)$$

which can be integrated to give

$$\boxed{\frac{C_L \rho_0 A e^{-\beta y}}{2 \beta m} = \cos \gamma - \cos \gamma_{en}} \quad (5.2-7)$$

where ρ is taken as 0 at the effective outer limits of the atmosphere.

Equation (F) shows that the magnitude of the angle γ in the skip path is a single valued function of y , that is, it has only one magnitude at any particular altitude in all portions of the skip.

Thus if the vehicle returns to the outer atmosphere after each skip $\gamma_{en} = -\gamma_{ex}$ for all skips.

Dividing equation (5.2-3) by equation (5.2-4) we get

$$\frac{L}{D} = \frac{V^2 \frac{d\gamma}{ds}}{\frac{dV}{dt}} \quad (5.2-8)$$

or

$$V^2 \frac{d\gamma}{ds} = \frac{L}{D} \frac{dV}{dt} \quad (5.2-9)$$

But

$$\frac{dV}{dt} = \frac{1}{2} \frac{dV^2}{ds}$$

and thus

$$\frac{1}{2} \frac{dV^2}{ds} = \frac{1}{\frac{L}{D}} V^2 \frac{d\gamma}{ds} \quad (5.2-10)$$

Multiplying by ds and integrating for $L/D = c$

$$\frac{1}{2} \int_V \frac{dV^2}{V^2} = \frac{1}{\frac{L}{D}} \int_{\gamma} d\gamma \quad (5.2-11)$$

$$V = V_{en} e^{-(\gamma_{en} - \gamma) / \frac{L}{D}}$$

This defines the velocity in a skip. The γ at various positions in the skip is defined by equation (5-19). Thus,

the velocity, altitude and γ at various positions in any skip are defined for $L/D = \text{constant}$.

Since

$$\gamma_{en} = -\gamma_{ex}$$

$$\boxed{\frac{V_{ex}}{V_{en}} = e^{-2\gamma_{en} / \frac{L}{D}}} \quad (5.2-12)$$

This defines the velocity loss in every skip in terms of L/D since $\gamma_{en_1} = \gamma_{en_2} = \gamma_{en_n}$.

Now we are interested in the combined effect of a series of skips. It has been shown elsewhere that the range ϕ , of one ballistic phase is given by

$$\boxed{\phi_n = 2 \tan^{-1} \left| \frac{\sin \gamma_{ex} \cos \gamma_{ex}}{\left(\frac{V_s}{V_{ex}}\right)^2 - \cos^2 \gamma_{ex}} \right|} \quad (5.2-13)$$

where V_s is satellite velocity at the Earth's surface.

It is assumed that the skipping process may be approximated by impact problem considerations where the total range is the sum of the ballistic trajectories.

Thus

$$\Phi = \sum_1^n \phi_n \quad (5.2-14)$$

5.3 Glide Re-entry.

The equations of motion (see reference 5-2) are as before:

$$L - m g \cos \gamma = - \frac{m V^2}{r_c} \quad (5.3-1)$$

$$-D + m g \sin \gamma = m \frac{dV}{dt} \quad (5.3-2)$$

The angles are assumed small in the glide so that $\sin \gamma \approx \gamma$; $\cos \gamma \approx 1$ and the atmosphere is comparatively thin so that $\frac{r}{r_0} \approx 1$.

It may be noted that

$$\frac{dV}{dt} = \frac{1}{2} \frac{dV^2}{ds}$$

and from figure 4 it may be seen that

$$-\frac{1}{r_c} = \frac{d(\psi - \gamma)}{ds}$$

$$-\frac{d\psi}{ds} = \frac{\cos \theta}{r} \approx \frac{1}{r_0}$$

Thus equations (5.3-1) and (5.3-2) may be written as

$$L = -m V^2 \frac{d\gamma}{ds} + m g - \frac{m V^2}{r_0} \quad (5.3-3)$$

$$D = -\frac{1}{2} m \frac{dV^2}{ds} + m g \gamma \quad (5.3-4)$$

Dividing equation (5.3-3) by equation (5.3-4) yields:

$$g \left(1 - \frac{L}{D} \gamma\right) + \frac{1}{2} \left(\frac{L}{D}\right) \frac{dV^2}{ds} - V^2 \frac{d\gamma}{ds} - \frac{V^2}{r_0} = 0 \quad (5.3-5)$$

It can be shown that the terms $L/D g \gamma$ and $V^2 \frac{d\gamma}{ds}$

may be neglected. The proof of this will not be considered here. (See reference 5-2)

So

$$\frac{dV^2}{ds} - \frac{2V^2}{r_0 \frac{L}{D}} + \frac{2g}{\frac{L}{D}} = 0 \quad (5.3-6)$$

Since

$$V_s^2 = g r_0$$

equation (5.3-6) can be integrated for constant L/D to give the velocity in non-dimensional form as

$$\boxed{\bar{V}^2 = 1 - (1 - \bar{V}_0^2) e^{2\phi / \frac{L}{D}}} \quad (5.3-7)$$

where \bar{V}_0 is the initial velocity divided by the satellite velocity at Earth's surface. \bar{V} is ratio of velocity to satellite velocity at Earth's surface.

Thus the velocity in the glide path is defined in terms of the lift drag ratio and the range.

From the original normal force equation

$$L - mg \cos \gamma = - \frac{mV^2}{r_c} \quad (5.3-8)$$

$\cos \gamma \approx 1$, $r_c \approx r_0$, and dividing by mg

we get

$$\frac{L}{mg} - 1 = - \bar{V}^2$$

or

$$\bar{V}^2 + \frac{L}{mg} = 1$$

If the quantity for the lift is put in, there results

$$V^2 \left(1 + \frac{C_L A V_s^2 \rho}{2mg} \right) = 1 \quad (5.3-9)$$

$$\bar{V}^2 = \left[\frac{1}{1 + \frac{C_L A V_s^2 \rho}{2mg}} \right] \quad (5.3-10)$$

Thus the velocity is expressed in terms of the density and thus indirectly in terms of the altitude. Using the expression for density vs. altitude, velocity vs. density (5.3-10) and velocity vs. range (5.3-7) the flight path is defined.

The foregoing equations on the skip and glide re-entry were obtained from hypersonic glider re-entry considerations. The velocity of the hypersonic glider may approach orbital

velocity. Recently reference 3 has been written which is also directed toward the re-entry problem under two degrees of freedom. Reference 3 was not available soon enough for consideration when these notes were originally prepared.

REFERENCES

- 5-1. The Use of Lift For Re-entry From Satellite Trajectories. Antonio Ferri, Lewis Feldman, and Walter Daskin, Jet Propulsion, Nov. 1957.
- 5-2. A Comparative Analysis of the Performance of Long-Range Hyper-velocity Vehicles. Alford J. Eggers, H. Julian Allen and Stanford Neice, NACA TN 4046.
- 5-3. An Approximate Analytical Method for Studying Entry Into Planetary Atmospheres. Chapman, Dean R., NACA TN 4276.

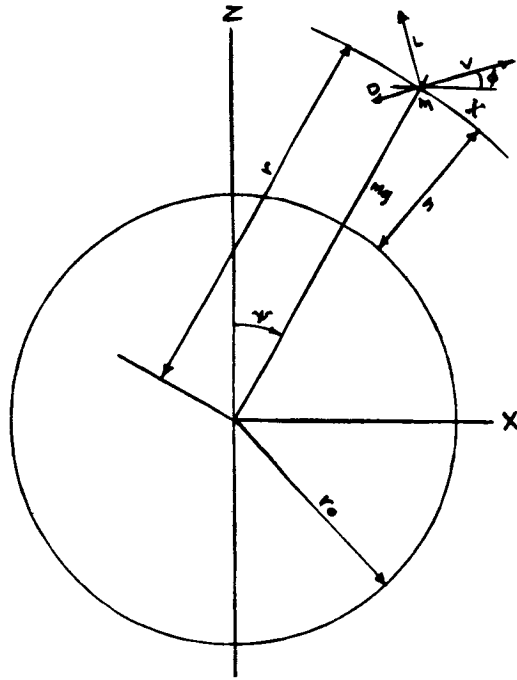


Figure 5-1a. Coordinate system for general equations.

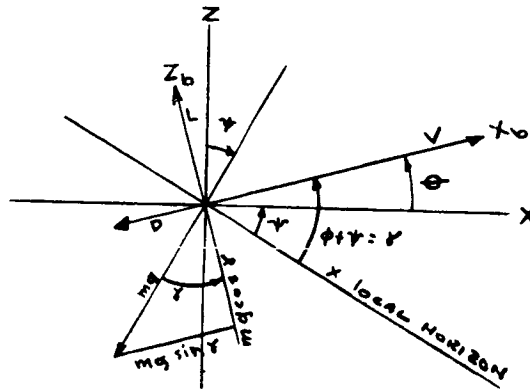


Figure 5-1b. Free body force diagram.

Sketches from reference 5-1.

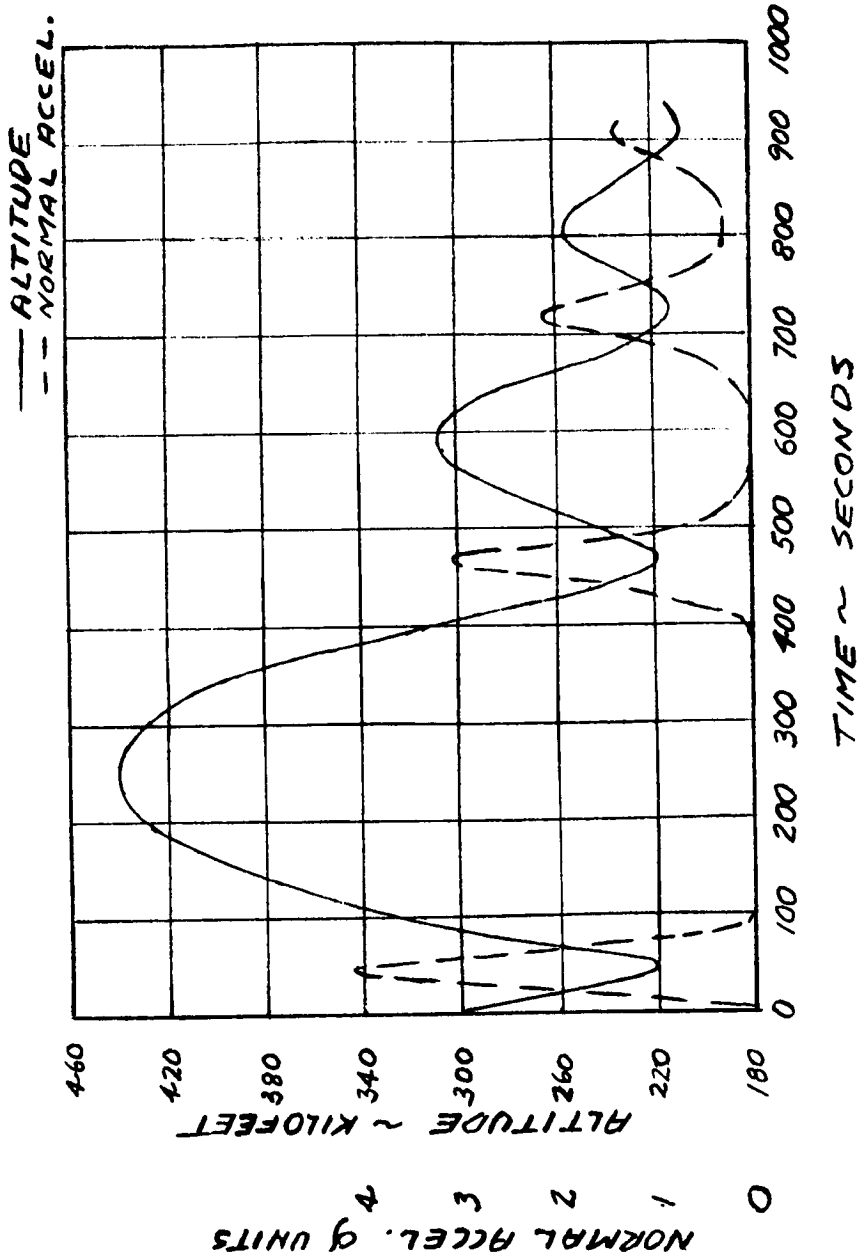


Figure 5-2. Skip trajectory obtained from integration of general equations, $C_D S/W = C_L S/W = .005$, $\gamma_0 = -0.1$ rad, $V_0 = 26,000$ ft/sec, $V_{900 \text{ sec}} \approx 10,000$ ft/sec; range 900 sec $\approx 2,500$ miles.

All data and plot from reference 5-2.

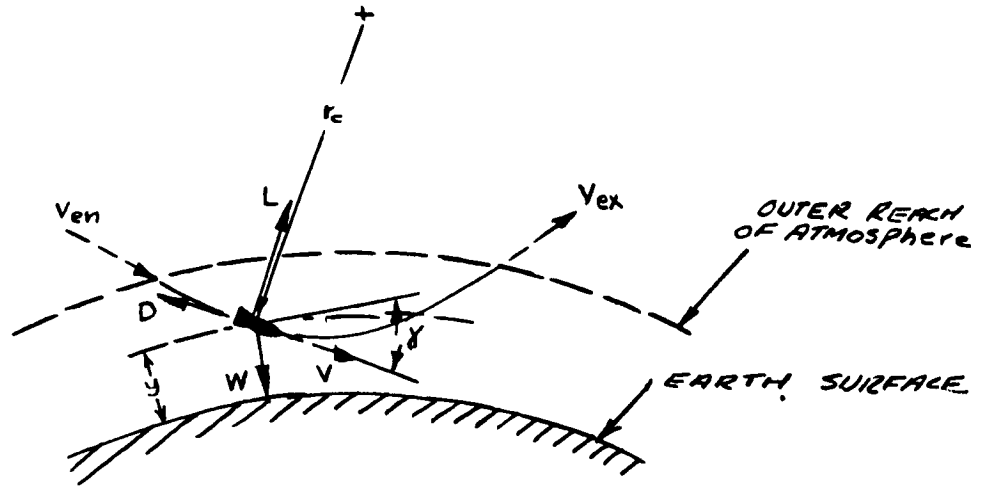


Figure 5-3. Skip re-entry geometry.

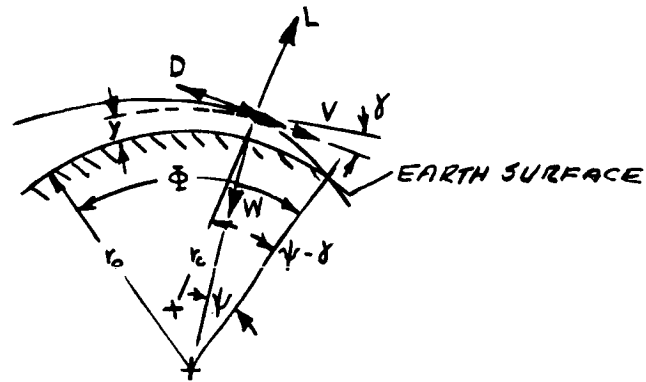


Figure 5-4. Glide re-entry geometry.

Sketch from TN 4046.

SECTION VI

SIX DEGREES OF FREEDOM EQUATIONS OF MOTION AND TRAJECTORY
EQUATIONS OF A RIGID FIN STABILIZED MISSILE WITH VARIABLE MASS

The study of space mechanics thus far has been restricted to a two-dimensional analysis. For many problems however, it is necessary to use a three-dimensional analysis. Some of these problems are; the ballistic missile with guidance whose trajectory is constantly being changed to hit a target; for a space vehicle with guidance devices; for a manned vehicle reentry or orbit which is capable of being steered, for the longitudinal and lateral stability analysis of any space vehicle. Thus it becomes necessary to examine the case of missile motions and trajectories for six degrees of freedom which are general enough to cover all phases of missile motion, including the launch, exit from the atmosphere, space trajectory, reentry to the atmosphere and landing phase.

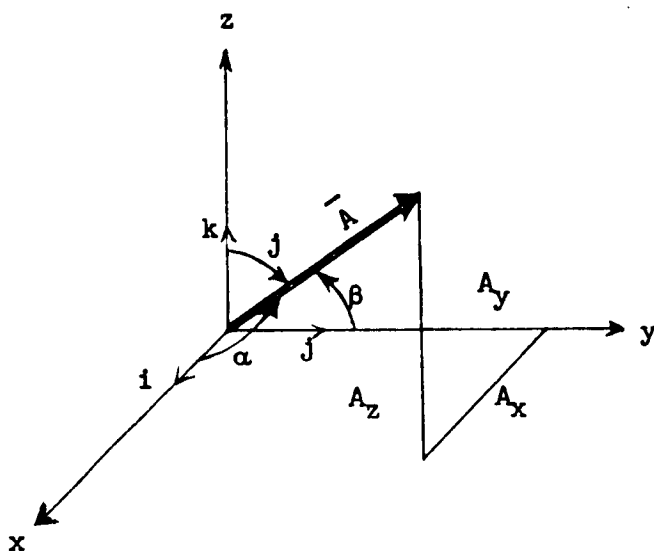
The purpose of this presentation will be to perform the classical derivation of the equations of motion of a missile with variable mass, and then to develop the equations of the missile trajectory referred to special sets of axes. The derivation will be for the general case of all six degrees of freedom.

In order to make the development more meaningful we will briefly review some elements of vector mechanics and the matrix algebra of transformation of coordinates. The presentation will be divided into four sections.

- 6.1. Review of vector mechanics.
- 6.2. Review of matrix algebra of transformations.
- 6.3. Development of the equations of motion of a missile.
- 6.4. Trajectory equations.

6.1. Review of Vector Mechanics

A vector is a quantity which has magnitude and direction. The analytical shorthand of vector analysis has the advantage of permitting treatment of directed quantities such as forces without the need of referring them to an arbitrary set of coordinates. In the final stages of a development, however, we usually define a coordinate system and resolve the vectors into components along the axes.

6.1.1. Resolution of vectors.-

A vector can be written as:

$$\vec{A} = i A_x + j A_y + k A_z \quad 6.1-1$$

where i , j and k are base vectors or unit vectors along the x , y , and z axes respectively and A_x , A_y , and A_z are the components of the vector \vec{A} along the x , y , and z axes.

It is seen that the magnitude of \bar{A} is

$$A = \sqrt{A_x^2 + A_y^2 + A_z^2} \quad 6.1-2$$

and the direction cosines of the vector are

$$l = \cos \alpha = \cos (A, x) = A_x/A \quad 6.1-3$$

$$m = \cos \beta = \cos (A, y) = A_y/A \quad 6.1-4$$

$$n = \cos \gamma = \cos (A, z) = A_z/A \quad 6.1-5$$

further

$$l^2 + m^2 + n^2 = 1 \quad 6.1-6$$

More will be said about direction cosines later.

6.1.2 Addition and Subtraction of vectors.- Addition and subtraction of vectors are performed by the well known force polygon graphical method.

6.1.3 Multiplication of vectors.- There are two types of vector products - scalar or dot products and vector or cross products. The scalar or dot product of two vectors is a scalar quantity and not a vector. It is defined by

$$\bar{A} \cdot \bar{B} = A B \cos (A, B) \quad 6.1-7$$

or in terms of components

$$\bar{A} \cdot \bar{B} = A_x B_x + A_y B_y + A_z B_z \quad 6.1-8$$

By means of relation (6.1-7) it is seen that the scalar products of the unit vectors are

$$\left. \begin{aligned} i \cdot i = j \cdot j = k \cdot k = 1 \\ i \cdot j = i \cdot k = j \cdot k = 0 \end{aligned} \right\} \quad 6.1-9$$

The time honored example of the application of the dot product is:

$$W = \bar{F} \cdot \bar{X} \quad 6.1-10$$

where \bar{F} is a force which moves along a vector distance \bar{X} and W is work done.

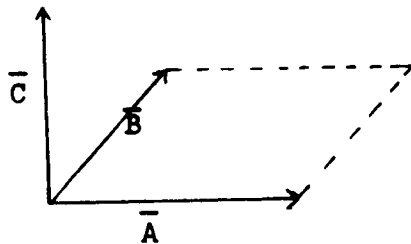
The cross product or vector product of two vectors is a vector and is denoted by

$$\bar{A} \times \bar{B} = \bar{C} \quad 6.1-11$$

where the magnitude of \bar{C} is given by

$$C = A B \sin(A, B) \quad 6.1-12$$

and the direction is given by the right hand rule.



or in terms of components

$$\bar{A} \times \bar{B} = \begin{vmatrix} i & j & k \\ A_x & A_y & A_z \\ B_x & B_y & B_z \end{vmatrix} \quad 6.1-13$$

or

$$\bar{A} \times \bar{B} = (A_y B_z - A_z B_y)i + (A_z B_x - A_x B_z)j + (A_x B_y - A_y B_x)k \quad 6.1-14$$

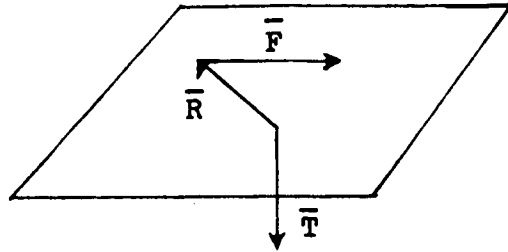
By means of relations (6.1-11) and (6.1-12) it is seen that the vector products of the unit vectors are

$$\left. \begin{aligned} i \times i &= j \times j = k \times k = 0 \\ i \times j &= -j \times i = k \\ j \times k &= -k \times j = i \\ k \times i &= -i \times k = j \end{aligned} \right\} \quad 6.1-15$$

An example of the application of the cross products is

$$\bar{T} = \bar{R} \times \bar{F} \quad 6.1-16$$

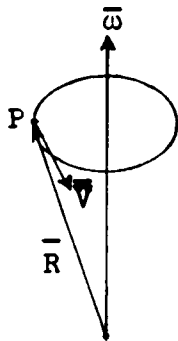
Where \bar{F} is a force acting on a particle whose radius or position vector is \bar{R} and \bar{T} is the torque or moment of \bar{F} about an axis through the origin and perpendicular to the plane of \bar{R} and \bar{F} and directed by the right hand rule.



Another example of the vector cross product is:

$$\bar{V} = \bar{\omega} \times \bar{R} \quad 6.1-17$$

where $\bar{\omega}$ is an angular velocity, \bar{R} is a position vector and \bar{V} is a linear velocity. As indicated previously, \bar{V} is given by



$$\bar{V} = \begin{vmatrix} i & j & k \\ \omega_x & \omega_y & \omega_z \\ R_x & R_y & R_z \end{vmatrix} \quad 6.1-18$$

$$\text{or } \bar{V} = i(R_z \omega_y - R_y \omega_z) + j(R_x \omega_z - R_z \omega_x) + k(R_y \omega_x - R_x \omega_y) \quad 6.1-19$$

$$\text{or } \bar{V} = i V_x + j V_y + k V_z$$

6.1.4 Momentum.- Momentum of a particle of mass m is defined as:

$$\bar{U} = m \bar{V} \quad 6.1-20$$

where \bar{U} is a vector which has the direction of the velocity vector \bar{V} and therefore from (6.1-17) it is seen that

$$\bar{U} = m (\bar{\omega} \times \bar{R}) \quad 6.1-21$$

6.1.5 Moment of momentum or angular momentum.- The moment of momentum or angular momentum \bar{H} is simply the moment of the momentum vector about a given point or axis through that point. From equation (6.1-16) we see that the moment of a vector about a point is simply the radius vector \bar{R} of that vector crossed into the vector \bar{U} .

Therefore:

$$\bar{H} = \bar{R} \times \bar{U} \quad 6.1-22$$

and by (6.1-21)

$$\bar{H} = \bar{R} \times (\bar{\omega} \times \bar{R}) m \quad 6.1-23$$

For later use we note that

$$[\bar{A} \times (\bar{B} \times \bar{C})] = \bar{B} \cdot (\bar{A} \cdot \bar{C}) - \bar{C} (\bar{A} \cdot \bar{B}) \quad 6.1-24$$

and

$$[\bar{R} \times (\bar{\omega} \times \bar{R})] = \bar{\omega} (\bar{R} \cdot \bar{R}) - \bar{R} (\bar{R} \cdot \bar{\omega}) = R^2 \bar{\omega} - \bar{R} (\bar{\omega} \cdot \bar{R}) \quad 6.1-25$$

6.1.6 Vector operators: Gradient operator.- The operator ∇ (the gradient or del) is defined by

$$\nabla \equiv i \frac{\partial}{\partial x} + j \frac{\partial}{\partial y} + k \frac{\partial}{\partial z} \quad 6.1-26$$

If we have a scalar field defined by $\phi = f(x, y, z)$, then

$$\nabla \phi = i \frac{\partial \phi}{\partial x} + j \frac{\partial \phi}{\partial y} + k \frac{\partial \phi}{\partial z} \quad 6.1-27$$

$\nabla \phi$ is the gradient ϕ or del ϕ

An example of an important scalar field is the gravitational field. Consider the potential ϕ due to a concentrated mass, m , in the earth's gravitational field, namely

$$\phi = \frac{km}{r} \quad 6.1-28$$

where r is the distance from the center of the earth to the mass.

Then \bar{F} , the resultant force, is given by

$$\bar{F} = \nabla \phi = i \frac{\partial \phi}{\partial x} + j \frac{\partial \phi}{\partial y} + k \frac{\partial \phi}{\partial z} \quad 6.1-29$$

or the gravitational force is the gradient of the gravitational potential.

To show this we note

$$r = \sqrt{x^2 + y^2 + z^2} \quad 6.1-30$$

and

$$\frac{\partial r}{\partial x} = \frac{x}{\sqrt{x^2 + y^2 + z^2}} = \frac{x}{r} \quad 6.1-31$$

and

$$\frac{\partial \phi}{\partial x} = \frac{\partial \phi}{\partial r} \cdot \frac{\partial r}{\partial x} = -\frac{km}{r^2} \cdot \frac{x}{r} \quad 6.1-32$$

$$\frac{\partial \phi}{\partial y} = \frac{\partial \phi}{\partial r} \cdot \frac{\partial r}{\partial y} = -\frac{km}{r^2} \cdot \frac{y}{r} \quad 6.1-33$$

$$\frac{\partial \phi}{\partial z} = \frac{\partial \phi}{\partial r} \cdot \frac{\partial r}{\partial z} = - \frac{km}{r^2} \cdot \frac{z}{r} \quad 6.1-34$$

and

$$F = \sqrt{\left(\frac{\partial \phi}{\partial x}\right)^2 + \left(\frac{\partial \phi}{\partial y}\right)^2 + \left(\frac{\partial \phi}{\partial z}\right)^2} = - \frac{km}{r^2} \quad 6.1-35$$

Thus, if the mass m is in the gravitational field of many other bodies whose potentials were defined as $\phi_1 = \frac{k_1 m}{r_1}$; $\phi_2 = \frac{k_2 m}{r_2}$; $\phi_3 = \frac{k_3 m}{r_3}$; etc.

then the total potential would be $\phi = \phi_1 + \phi_2 + \phi_3 + \dots$

and the resultant gravitational force would be

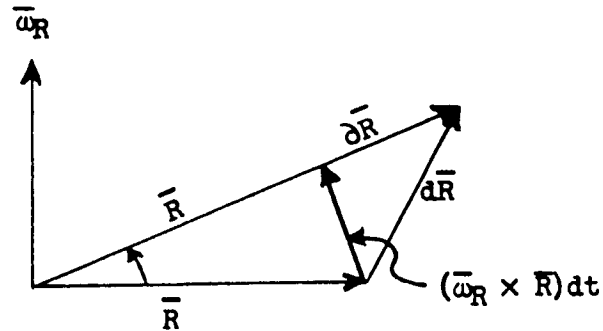
$$\bar{F} = \nabla \phi$$

Other vector operators not used in this development are mentioned here merely for the sake of completeness. The curl of a vector is:

$$\text{curl } \bar{A} = \begin{vmatrix} i & j & k \\ \frac{\partial}{\partial x} & \frac{\partial}{\partial y} & \frac{\partial}{\partial z} \\ A_x & A_y & A_z \end{vmatrix} \quad 6.1-36$$

and the divergence of a vector is:

$$\text{div } \bar{A} = \frac{\partial A_x}{\partial x} + \frac{\partial A_y}{\partial y} + \frac{\partial A_z}{\partial z} \quad 6.1-37$$

6.1.7 Time rate of change of a rotating vector.-

From the diagram it is seen that the vector $d\bar{R}$ is the vector sum of a component $\partial\bar{R}$ along $(\bar{R} + \partial\bar{R})$ and a component \perp to $(\bar{R} + \partial\bar{R})$ equivalent to $(\bar{\omega}_R \times \bar{R})dt$

$$d\bar{R} = \partial\bar{R} + (\bar{\omega}_R \times \bar{R})dt \quad 6.1-38$$

OR

$$\frac{d\bar{R}}{dt} = \frac{\partial\bar{R}}{\partial t} + (\bar{\omega}_R \times \bar{R}) \quad 6.1-39$$

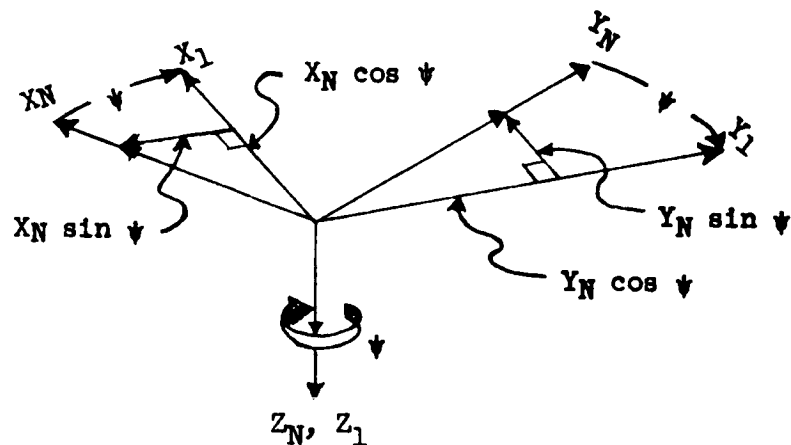
This is the well known transformation for the rate of change of any vector \bar{R} from fixed to moving axes where $\frac{\partial\bar{R}}{\partial t}$ is the rate of change of \bar{R} measured with respect to moving axes, and $\bar{\omega}_R$ is the angular velocity of the moving axes with respect to the fixed axes.

6.2 Matrix Algebra of Transformations

In this section we shall deal only with rotational matrices. A rotation matrix performs an orthogonal transformation on some quantity such as a vector or set of vectors. The coordinate systems considered are Cartesian and are "right-handed" systems.

Orthogonal matrices, which perform only rotations (also called rotation matrices) have special properties. We will discuss some of these properties.

6.2.1 Single rotation.- We start with a set of axes $X_N Y_N Z_N$ as shown below.



By rotating the system about the Z_N axis through an angle ψ we obtain a new coordinate system which we shall designate $(X_1 Y_1 Z_1)$. The transformation or relation between the original and new system is obtained by geometry and is seen to be

$$\begin{Bmatrix} X_1 \\ Y_1 \\ Z_1 \end{Bmatrix} = \begin{bmatrix} \cos \psi & \sin \psi & 0 \\ -\sin \psi & \cos \psi & 0 \\ 0 & 0 & 0 \end{bmatrix} \begin{Bmatrix} X_N \\ Y_N \\ Z_N \end{Bmatrix} \quad 6.2 \cdot 1$$

This transformation is called an orthogonal transformation. The elements are called direction cosines, since each element for instance, $\cos \psi$ is the cosine of the angle between X_N and X_1 . The element $\sin \psi$ is the $\cos (90 - \psi)$ the angle between Y_N and X_1 and the element $-\sin \psi$ is the $\cos (90 + \psi)$ the angle between X_N and Y_1 . Actually each element of the matrix can be considered the scalar product of two unit vectors having the directions of the indicated axes.

If we let

$$[T(\psi)] = \begin{bmatrix} \cos \psi & \sin \psi & 0 \\ -\sin \psi & \cos \psi & 0 \\ 0 & 0 & 1 \end{bmatrix} \quad 6.2-2$$

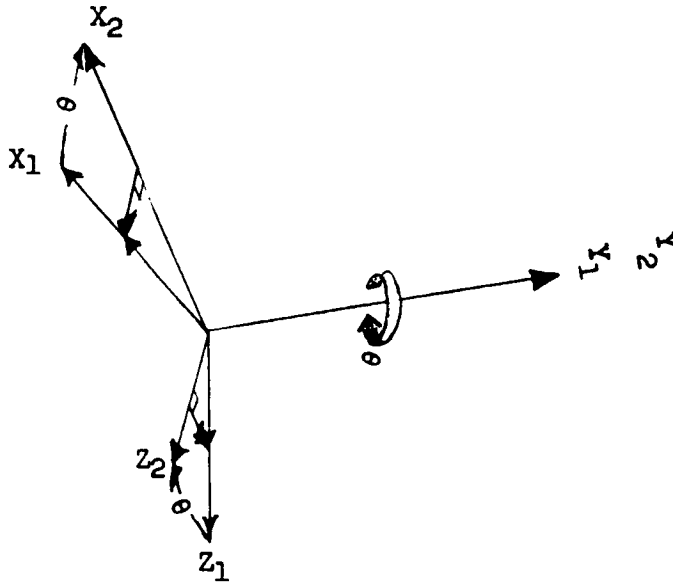
and denote the transpose of $[T(\psi)]$ by $[T(\psi)]'$ and denote the inverse of $[T(\psi)]$ by $[T(\psi)]^{-1}$ and define the matrix $[T(-\psi)]$ as that matrix obtained by replacing (ψ) by $(-\psi)$ in $[T(\psi)]$ then the following property is noted

$$[T(\psi)]' = [T(\psi)]^{-1} = [T(-\psi)] = \begin{bmatrix} \cos \psi & -\sin \psi & 0 \\ \sin \psi & \cos \psi & 0 \\ 0 & 0 & 1 \end{bmatrix} \quad 6.2-3$$

Stated in words the transpose of $[T(\psi)]$ is also its inverse and is also the matrix obtained by replacing (ψ) by $(-\psi)$. Applying this principle to equation (6.2-1) we get

$$\begin{Bmatrix} X_N \\ Y_N \\ Z_N \end{Bmatrix} = \begin{bmatrix} \cos \psi & -\sin \psi & 0 \\ \sin \psi & \cos \psi & 0 \\ 0 & 0 & 1 \end{bmatrix} \begin{Bmatrix} X_1 \\ Y_1 \\ Z_1 \end{Bmatrix} \quad 6.2-4$$

6.2.2 Two rotations.- We originally started with a set of axes $X_N Y_N Z_N$ and rotated about the Z_N axis through an angle ψ to obtain a new set of coordinates $(X_1 Y_1 Z_1)$. Let us now rotate the $X_1 Y_1 Z_1$ system about the Y_1 axis through an angle θ to the new coordinate system $X_2 Y_2 Z_2$ as shown below.



From the geometry of the problem the transformation between the $X_1 Y_1 Z_1$ system and the $X_2 Y_2 Z_2$ is seen to be

$$\begin{Bmatrix} X_2 \\ Y_2 \\ Z_2 \end{Bmatrix} = \begin{bmatrix} \cos \theta & 0 & -\sin \theta \\ 0 & 1 & 0 \\ \sin \theta & 0 & \cos \theta \end{bmatrix} \begin{Bmatrix} X_1 \\ Y_1 \\ Z_1 \end{Bmatrix} \quad 6.2-5$$

or

$$\begin{Bmatrix} X_2 \\ Y_2 \\ Z_2 \end{Bmatrix} = [T(\theta)] \begin{Bmatrix} X_1 \\ Y_1 \\ Z_1 \end{Bmatrix} \quad 6.2-6$$

Combining equations (6.2-6) and (6.2-1) we get

$$\begin{Bmatrix} X_2 \\ Y_2 \\ Z_2 \end{Bmatrix} = [T(\theta)] [T(\psi)] \begin{Bmatrix} X_N \\ Y_N \\ Z_N \end{Bmatrix} \quad 6.2-7$$

This equation implies the rotation ψ is performed first on $X_N Y_N Z_N$ followed by the rotation θ to determine the new coordinates $X_2 Y_2 Z_2$. In order to return to the $X_N Y_N Z_N$ coordinates from the $X_2 Y_2 Z_2$ coordinates, from a consideration of the geometry we would rotate first through a $(-\theta)$ then through a $(-\psi)$ or

$$\begin{Bmatrix} X_N \\ Y_N \\ Z_N \end{Bmatrix} = [T(-\psi)] [T(-\theta)] \begin{Bmatrix} X_2 \\ Y_2 \\ Z_2 \end{Bmatrix} \quad 6.2-8$$

By making use of equation (6.2-3), equation (6.2-8) could be written as

$$\begin{Bmatrix} X_N \\ Y_N \\ Z_N \end{Bmatrix} = [T(\psi)]^{-1} [T(\theta)]^{-1} \begin{Bmatrix} X_2 \\ Y_2 \\ Z_2 \end{Bmatrix} \quad 6.2-9$$

By taking the inverse of the transformation matrix in equation (6.2-7) we can write

$$\begin{Bmatrix} X_N \\ Y_N \\ Z_N \end{Bmatrix} = \left[[T(\theta)] [T(\psi)] \right]^{-1} \begin{Bmatrix} X_2 \\ Y_2 \\ Z_2 \end{Bmatrix} \quad 6.2-10$$

A comparison of equation (6.2-10) and (6.2-9) indicates

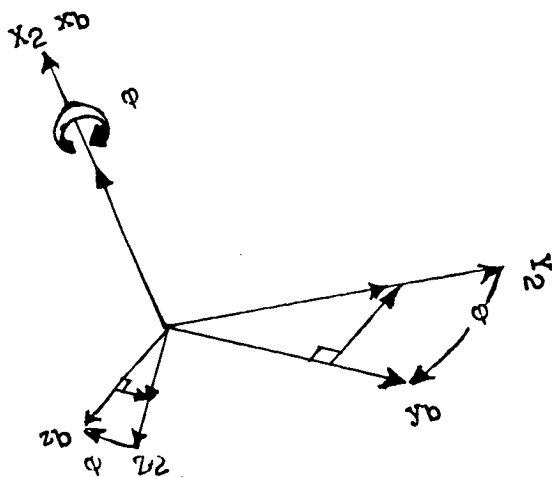
$$\left[[T(\theta)] [T(\psi)] \right]^{-1} = [T(\psi)]^{-1} [T(\theta)]^{-1} \quad 6.2-11$$

Stated in words equation (6.2-11) says the inverse of a product of orthogonal transformation matrices is the product of the inverses of the individual matrices taken in reversed order. This is the reversal property of orthogonal matrices.

For subsequent use we note that equation (6.2-5) may be stated

$$\begin{Bmatrix} X_1 \\ Y_1 \\ Z_1 \end{Bmatrix} = \begin{bmatrix} \cos \theta & 0 & \sin \theta \\ 0 & 1 & 0 \\ -\sin \theta & 0 & \cos \theta \end{bmatrix} \begin{Bmatrix} X_2 \\ Y_2 \\ Z_2 \end{Bmatrix} \quad 6.2-12$$

6.2.3 Three rotations.- We began with a set of axes $X_N Y_N Z_N$ and rotated through an angle ψ to obtain the set of coordinates $X_1 Y_1 Z_1$ which we rotated through an angle θ to obtain the set of coordinates $X_2 Y_2 Z_2$. Let us now rotate the $X_2 Y_2 Z_2$ system about the X_2 axis through an angle ϕ to obtain a new coordinate system which we shall designate $(x_b y_b z_b)$ as shown below



From the geometry we see

$$\begin{Bmatrix} x_b \\ y_b \\ z_b \end{Bmatrix} = \begin{bmatrix} 1 & 0 & 0 \\ 0 & \cos \varphi & \sin \varphi \\ 0 & -\sin \varphi & \cos \varphi \end{bmatrix} \begin{Bmatrix} X_2 \\ Y_2 \\ Z_2 \end{Bmatrix} \quad 6.2-13$$

or

$$\begin{Bmatrix} x_b \\ y_b \\ z_b \end{Bmatrix} = [T(\varphi)] \begin{Bmatrix} X_2 \\ Y_2 \\ Z_2 \end{Bmatrix} \quad 6.2-14$$

Combining equations (6.2-1), (6.2-5), and (6.2-13) we get

$$\begin{Bmatrix} x_b \\ y_b \\ z_b \end{Bmatrix} = [T(\varphi)] [T(\theta)] [T(\psi)] \begin{Bmatrix} X_N \\ Y_N \\ Z_N \end{Bmatrix} \quad 6.2-15$$

and inversely

$$\begin{Bmatrix} X_N \\ Y_N \\ Z_N \end{Bmatrix} = [T(\psi)]^{-1} [T(\theta)]^{-1} [T(\varphi)]^{-1} \begin{Bmatrix} x_b \\ y_b \\ z_b \end{Bmatrix} \quad 6.2-16$$

or

$$\begin{Bmatrix} X_N \\ Y_N \\ Z_N \end{Bmatrix} = \begin{bmatrix} \cos \psi & -\sin \psi & 0 \\ \sin \psi & \cos \psi & 0 \\ 0 & 0 & 1 \end{bmatrix} \begin{bmatrix} \cos \theta & 0 & \sin \theta \\ 0 & 1 & 0 \\ -\sin \theta & \cos \theta & 0 \end{bmatrix} \begin{bmatrix} 1 & 0 & 0 \\ 0 & \cos \varphi & -\sin \varphi \\ 0 & \sin \varphi & \cos \varphi \end{bmatrix} \begin{Bmatrix} x_b \\ y_b \\ z_b \end{Bmatrix} \quad 6.2-17$$

When the matrix multiplication is performed, equation (6.2-17) becomes

$$\begin{Bmatrix} X_N \\ Y_N \\ Z_N \end{Bmatrix} = \begin{bmatrix} (\cos \psi \cos \theta)(\cos \psi \sin \theta \sin \phi - \sin \psi \cos \phi) & (\cos \psi \sin \theta \cos \phi + \sin \psi \sin \phi) \\ (\sin \psi \cos \theta)(\sin \psi \sin \theta \sin \phi + \cos \psi \cos \phi) & (\sin \psi \sin \theta \cos \phi - \cos \psi \sin \phi) \\ (-\sin \theta) & (\cos \theta \cos \phi) \end{bmatrix} \begin{Bmatrix} x_b \\ y_b \\ z_b \end{Bmatrix} \quad 6.2-18$$

For the sake of convenience we can write equation (6.2-18) as

$$\begin{Bmatrix} X_N \\ Y_N \\ Z_N \end{Bmatrix} = [T_1] \begin{Bmatrix} x_b \\ y_b \\ z_b \end{Bmatrix} \quad 6.2-19$$

where

$$[T_1] = \begin{bmatrix} l_{11} & m_{11} & n_{11} \\ l_{12} & m_{12} & n_{12} \\ l_{13} & m_{13} & n_{13} \end{bmatrix} \quad 6.2-20$$

6.2.4 Direction cosines.- The terms l_{1j}, m_{1j}, n_{1j} are called direction cosines and are defined from equation (6.2-18) as

$$\begin{aligned}
 l_{11} &= \cos \psi \cos \theta \\
 l_{12} &= \sin \psi \cos \theta \\
 l_{13} &= -\sin \theta \\
 m_{11} &= \cos \psi \sin \theta \sin \phi - \sin \psi \cos \phi \\
 m_{12} &= \sin \psi \sin \theta \sin \phi + \cos \psi \cos \phi & 6.2-21 \\
 m_{13} &= \cos \theta \sin \phi \\
 n_{11} &= \cos \psi \sin \theta \cos \phi + \sin \psi \sin \phi \\
 n_{12} &= \sin \psi \sin \theta \cos \phi - \cos \psi \sin \phi \\
 n_{13} &= \cos \theta \cos \phi
 \end{aligned}$$

Some interesting relations between these direction cosines or between the directive cosines of any orthogonal transformation are the following

$$\begin{aligned}
 l_{11}^2 + m_{11}^2 + n_{11}^2 &= 1 \\
 l_{12}^2 + m_{12}^2 + n_{12}^2 &= 1 & 6.2-22 \\
 l_{13}^2 + m_{13}^2 + n_{13}^2 &= 1
 \end{aligned}$$

$$\begin{aligned}
 l_{11} l_{12} + m_{11} m_{12} + n_{11} n_{12} &= 0 \\
 l_{12} l_{13} + m_{12} m_{13} + n_{12} n_{13} &= 0 & 6.2-23 \\
 l_{13} l_{11} + m_{13} m_{11} + n_{13} n_{11} &= 0
 \end{aligned}$$

$$\begin{aligned}
 l_{11}^2 + l_{12}^2 + l_{13}^2 &= 1 \\
 m_{11}^2 + m_{12}^2 + m_{13}^2 &= 1 & 6.2-24 \\
 n_{11}^2 + n_{12}^2 + n_{13}^2 &= 1
 \end{aligned}$$

$$\begin{aligned}
 l_{11} m_{11} + l_{12} m_{12} + l_{13} m_{13} &= 0 \\
 m_{11} n_{11} + m_{12} n_{12} + m_{13} n_{13} &= 0 \\
 n_{11} l_{11} + n_{12} l_{12} + n_{13} l_{13} &= 0
 \end{aligned}
 \tag{6.2-25}$$

and

$$\begin{vmatrix}
 l_{11} & l_{12} & l_{13} \\
 m_{11} & m_{12} & m_{13} \\
 n_{11} & n_{12} & n_{13}
 \end{vmatrix} = 1
 \tag{6.2-26}$$

The three rotations from $X_N Y_N Z_N$ through ψ , θ , and ϕ to $x_b y_b z_b$ are indicated on Figure 1. If p , q , and r are defined as the angular velocities about the $x_b y_b z_b$ axes, then from Figure 6-1 it is apparent that

$$\begin{aligned}
 p &= \dot{\phi} - \dot{\psi} \sin \theta \\
 q &= \dot{\theta} \cos \phi + \dot{\psi} \sin \phi \cos \theta \\
 r &= \dot{\psi} \cos \theta \cos \phi - \dot{\theta} \sin \phi
 \end{aligned}
 \tag{6.2-27}$$

In order to get the weight component into the equations of motion (which we will indicate later) the direction cosines must be computed. On an analog type computer, however, the direction cosines are generated by using the derivative forms of the direction cosines which are

$$\begin{aligned}
 \dot{l}_{1j} &= m_{1j} r - n_{1j} q \\
 \dot{m}_{1j} &= n_{1j} q - l_{1j} r \quad \text{where } j = 1, 2, 3 \\
 \dot{n}_{1j} &= l_{1j} q - m_{1j} r
 \end{aligned}
 \tag{6.2-28}$$

These relations are not developed here but may be demonstrated individually in the following manner.

Referring back to equation (6.2-21) it is seen that

$$l_{11} = \cos \psi \cos \theta \quad 6.2-29$$

and differentiating we get

$$\dot{l}_{11} = -\cos \psi \sin \theta \dot{\theta} - \sin \psi \cos \theta \dot{\psi} \quad 6.2-30$$

From equation (6.2-28) it is seen

$$\dot{l}_{11} = m_{11} r - n_{11} q \quad 6.2-31$$

By substituting the values of r and q from equation (6.2-27) and values of m_{11} and n_{11} from equation (6.2-21) into (6.2-31) and performing the indicated multiplication and reduction we get

$$\dot{l}_{11} = -\cos \psi \sin \theta \dot{\theta} - \sin \psi \cos \theta \dot{\psi} \quad 6.2-32$$

which is identical with equation (6.2-30).

List of Symbols

X_N, Y_N, Z_N	right-hand Cartesian coordinate system fixed in non-rotating earth, inertial axes (with Z_N positive down)
ψ, θ, ϕ	angles used in specifying missile attitude referred to as Euler angles (specified order of rotation ψ, θ, ϕ).
x_b, y_b, z_b	body axes - right-handed coordinate system fixed in missile body with the origin at the instantaneous center of gravity. (See Figure 2.)
p, q, r	angular velocities of body-axis system (x_b, y_b, z_b) positive clockwise when looking in positive direction of axes
u, v, w	components of resultant velocity V along body axes x_b, y_b, z_b , respectively
i_b, j_b, k_b	unit vectors along the x_b, y_b , and z_b axes respectively
i_N, j_N, k_N	unit vectors along the X_N, Y_N , and Z_N axes respectively
V	resultant velocity of missile center of gravity
ω	resultant angular velocity of missile or (x_b, y_b, z_b) system $\bar{\omega} = i_b p + j_b q + k_b r$
V_e	jet exit velocity relative to nozzle exit
U	Momentum of missile $\bar{U} = m\bar{V}$
U_T	momentum of missile and jet
m	missile mass (slugs)
H	angular momentum of missile with respect to the center of gravity or moment of momentum
H_T	angular momentum of missile and jet

t	time after missile separated from launcher
F_J	resultant jet thrust
T	resultant jet thrust for the special case when the thrust is along the x_b axis
F_V	resultant jet vane force
F_A	resultant aerodynamic force
F_R	resultant reaction control force
F	resultant external force acting on missile
M_J	resultant jet thrust moment about center of gravity
M_V	resultant jet vane moment about center of gravity
M_A	resultant aerodynamic moment about center of gravity
M_R	resultant reaction control moment
M	resultant external moment acting on missile
Q	lift force on jet vane
ρ	air density
P_e	jet pressure at nozzle exit (gage)
A_e	nozzle exit area
r_e	distance from missile center of gravity to nozzle exit
C_x, C_y, C_z	aerodynamic force coefficients referred to body axes
C_l, C_m, C_n	aerodynamic moment coefficients referred to body axes
S	missile cross-sectional area
l	representative missile length (diameter, chord length, length, etc.)
L_1, L_2, L_3, L_4	distance of jet vane lift forces behind center of gravity

r_1, r_3	distances from x axis to jet vane lift force
W	missile weight, pound
A	azimuth angle of velocity vector measured with respect to the X_g, Y_g, Z_g axes (+ from south to west)
γ	elevation angle of velocity vector with respect to the X_g, Y_g, Z_g axes (+ up)
α	angle of attack
β	angle of sideslip
X, Y, Z	right-hand Cartesian coordinate system fixed in non-rotating earth with Z positive pointing north
X_e, Y_e, Z_e	right-hand Cartesian coordinate system fixed in rotating earth
X_g, Y_g, Z_g	Geographic axes
ω_e	angular velocity of earth (rotational velocity)
λ	longitude
L	latitude
h	distance above earth's surface
R_0	radius of earth
VW	wind velocity with respect to inertial axis
V_e	velocity component of earth's atmosphere
V_a	resultant aerodynamic velocity
V	velocity of missile center of gravity
l, m, n	direction cosines
δ_a	aileron deflection
δ_r	rudder deflection

δ_e elevator deflection
 $\delta_1, \delta_2, \delta_3, \delta_4$ jet vane deflection
 I_x, I_y, I_z missile moments of inertia about $x_b, y_b,$ and z_b axes respectively

$$I_x = \int (y^2 + z^2) dm$$

$$I_y = \int (z^2 + x^2) dm$$

$$I_z = \int (x^2 + y^2) dm$$

I_{yz}, I_{xz}, I_{xy} missile products of inertia about $x_b, y_b,$ and z_b axes

$$I_{yz} = \int yz dm$$

$$I_{xz} = \int xz dm$$

$$I_{xy} = \int xy dm$$

$(\dot{\cdot}) = \frac{d}{dt}$, except that $\dot{m} = -\frac{dm}{dt}$ and $\dot{I} = -\frac{dI}{dt}$

6.3 Derivation of Equations of Motion

The geometry is shown in Figure 6-1. Two sets of Cartesian coordinate axes are used in developing the equations of motion. One set is fixed in the body and is known as body axes and is shown in Figure 6-2. The body axes we designate as x_b , y_b , and z_b . The other set is fixed with respect to the earth and is known as inertial axes which we designate as X_N , Y_N , Z_N .

The orientation of the body axes with respect to the inertial axes is defined by three angular coordinates ψ , θ , and ϕ which are called Euler angles. These angles are shown in Figure 6-1. The rotations must be taken in a certain specified order namely : ψ , θ , and ϕ .

Further definitions of pertinent quantities are given in the list of symbols. In appendix A some of the formulas pertaining to the development are listed. An attempt has been made to use the standard NACA symbols throughout although in certain cases this was not possible.

A schematic diagram of the missile is shown in Figure 6-3. The $\bar{\omega}$ vector represents the resultant angular velocity of the missile or x_b , y_b , z_b , body system.

The equations of motion will be derived by writing the rate of change of momentum and rate of change of angular momentum equations.

6.3.1 Force equations.- From Newton's law we have the equation:

$$\left(\frac{d \bar{U}_T}{dt} \right)_N = \bar{F} \quad 6.3-1$$

The rate of change with respect to inertial space of momentum of the missile and jet can be written

$$\left(\frac{d \bar{U}_T}{dt}\right)_N = \left(\frac{d \bar{U}}{dt}\right)_N + \dot{m}(\bar{V} + \bar{\omega} \times \bar{r}_e - \bar{V}_e) \quad 6.3-2$$

Since \bar{U} is referred to the x_b, y_b, z_b system which is rotating with an angular velocity $\bar{\omega}$ (see Fig. 6-3) with respect to inertial space the rate of change of \bar{U} with respect to inertia space is

$$\left(\frac{d \bar{U}}{dt}\right)_N = \frac{d \bar{U}}{dt} + \bar{\omega} \times \bar{U} \quad 6.3-3$$

as indicated previously in section 6.1.

By differentiating the momentum

$$\bar{U} = m \bar{V} \quad 6.3-4$$

and defining $\frac{dm}{dt} = -\dot{m}$ we get

$$\frac{d \bar{U}}{dt} = m \frac{d \bar{V}}{dt} - \dot{m} \bar{V} \quad 6.3-5$$

If we substitute equations (6.3-5), (6.3-4), and (6.3-3) in (6.3-2) we get

$$\left(\frac{d \bar{U}_T}{dt}\right)_N = m \frac{d \bar{V}}{dt} - \dot{m} \bar{V} + m(\bar{\omega} \times \bar{V}) + \dot{m}(\bar{V} + \bar{\omega} \times \bar{r}_e - \bar{V}_e) \quad 6.3-6$$

which reduces to

$$\left(\frac{d \bar{U}_T}{dt}\right)_N = m \frac{d \bar{V}}{dt} + m(\bar{\omega} \times \bar{V}) + \dot{m}(\bar{\omega} \times \bar{r}_e) - \dot{m} \bar{V}_e \quad 6.3-7$$

Since

$$\frac{d \bar{V}}{dt} = \dot{u} \mathbf{i}_b + \dot{v} \mathbf{j}_b + \dot{w} \mathbf{k}_b \quad 6.3-8$$

and

$$\bar{\omega} = p i_b + q j_b + r k_b \quad 6.3-9$$

and

$$\bar{r}_e = r_{e_x} i_b + r_{e_y} j_b + r_{e_z} k_b \quad 6.3-10$$

and

$$\bar{\omega} \times \bar{V} = \begin{vmatrix} i_b & j_b & k_b \\ p & q & r \\ u & v & w \end{vmatrix} = i_b(wq - vr) + j_b(ur - wp) + k_b(vp - uq) \quad 6.3-11$$

and

$$\bar{\omega} \times \bar{r}_e = i_b(r_{e_z} q - r_{e_y} r) + j_b(r_{e_x} r - r_{e_z} p) + k_b(r_{e_y} p - r_{e_x} q) \quad 6.3-12$$

we have (substituting equations (6.3-12), (6.3-11), and (6.3-8) in (6.3-7))

$$\left(\frac{d \bar{U}_T}{dt} \right)_N = \left\{ m(\dot{u} + wq - vr) + \dot{m}(q r_{e_z} - r r_{e_y}) \right\} i_b + \left\{ m(\dot{v} + ur - wp) + \dot{m}(r r_{e_x} - p r_{e_z}) \right\} j_b + \left\{ m(\dot{w} + vp - uq) + \dot{m}(p r_{e_y} - q r_{e_x}) \right\} k_b - \dot{m} \bar{V}_e = \bar{F}$$

6.3-13

which is the force equation.

6.3.2 Moment equation.- The moment equation about the missile center of gravity is

$$\left(\frac{d \bar{H}_T}{dt} \right)_N = \bar{M} \quad 6.3-14$$

The rate of change with respect to inertia space of angular momentum of the missile with respect to the center of gravity including jet effect is

$$\left(\frac{d\bar{H}_T}{dt}\right)_N = \left(\frac{d\bar{H}}{dt}\right)_N + \dot{m} \bar{r}_e \times (\bar{\omega} \times \bar{r}_e - \bar{V}_e) \quad 6.3-15$$

where

$$\left(\frac{d\bar{H}}{dt}\right)_N = \frac{d\bar{H}}{dt} + \bar{\omega} \times \bar{H} \quad 6.3-16$$

From the definition of angular momentum we can write

$$\bar{H} = \int \bar{R} \times (\bar{\omega} \times \bar{R}) \, dm \quad 6.3-17$$

where

$$\bar{R} = x \, i_b + y \, j_b + z \, k_b \quad 6.3-18$$

The triple vector product as indicated previously (equation (6.1-25)) can be written

$$\bar{R} \times (\bar{\omega} \times \bar{R}) = R^2 \bar{\omega} - \bar{R}(\bar{R} \cdot \bar{\omega}) \quad 6.3-19$$

where

$$R^2 = (x^2 + y^2 + z^2) \quad 6.3-20$$

and

$$\bar{\omega} = p \, i_b + q \, j_b + r \, k_b \quad 6.3-21$$

Substituting equations (6.3-21), (6.3-20), (6.3-19) and (6.3-18) into equation (6.3-17) results in

$$\bar{H} = \int \left\{ (x^2 + y^2 + z^2) (p \, i_b + q \, j_b + r \, k_b) - (x \, i_b + y \, j_b + z \, k_b) (px + qy + rz) \right\} dm \quad 6.3-22$$

By performing the indicated multiplications equation (6.3-22) can be expressed in the following form

$$\bar{H} = \left\{ p \int (y^2 + z^2) dm - q \int x y dm - r \int x z dm \right\} i_b + \left\{ q \int (z^2 + x^2) dm - r \int y z dm - p \int x y dm \right\} j_b + \left\{ r \int (x^2 + y^2) dm - p \int x z dm - q \int y z dm \right\} k_b \quad 6.3-23$$

and by introducing the usual definitions of moment of inertia and product of inertia shown in the list of symbols we finally get

$$\bar{H} = (I_x p - I_{xy} q - I_{xz} r) i_b + (I_y q - I_{yz} r - I_{xy} p) j_b + (I_z r - I_{xz} p - I_{yz} q) k_b$$

6.3-24

It is usually conventional in missile work to choose the body axes as the principal axes so that

$$I_{xy} = I_{yz} = I_{xz} = 0 \quad 6.3-25$$

thus we have the final expression for angular momentum

$$\bar{H} = (I_x p) i_b + (I_y q) j_b + I_z r k_b \quad 6.3-26$$

The rate of change of angular momentum is obtained by differentiating (6.3-26) and becomes

$$\frac{d\bar{H}}{dt} = (I_x \dot{p} - \dot{I}_x p) i_b + (I_y \dot{q} - \dot{I}_y q) j_b + (I_z \dot{r} - \dot{I}_z r) k_b \quad 6.3-27$$

The product $\bar{\omega} \times \bar{H}$ is

$$\bar{\omega} \times \bar{H} = \begin{vmatrix} i_b & j_b & k_b \\ p & q & r \\ I_x p & I_y q & I_z r \end{vmatrix}$$

$$= (I_z - I_y) r q i_b + (I_x - I_z) p r j_b + (I_y - I_x) q p k_b \quad 6.3-28$$

Similarly the thrust term becomes

$$\dot{m} \bar{r}_e \times (\bar{\omega} \times \bar{r}_e - \bar{v}_e) = \dot{m} \left[r_e^2 \bar{\omega} - \bar{r}_e (\bar{r}_e \cdot \bar{\omega}) - \bar{r}_e \times \bar{v}_e \right] \quad 6.3-29$$

$$= \dot{m} \left\{ (r_{e_x}^2 + r_{e_y}^2 + r_{e_z}^2) (p i_b + q j_b + r k_b) - \right.$$

$$\left. (r_{e_x} i_b + r_{e_y} j_b + r_{e_z} k_b) (r_{e_x} p + r_{e_y} q + r_{e_z} r) \right\} -$$

$$\dot{m} \bar{r}_e \times \bar{v}_e$$

By performing the indicated multiplications, equation (6.3-29) can be expressed in the following form

$$\dot{m} \left\{ \bar{r}_e \times (\bar{\omega} \times \bar{r}_e - \bar{v}_e) \right\} = \dot{m} \left\{ p (r_{e_y}^2 + r_{e_z}^2) - r_{e_x} (q r_{e_y} + r r_{e_z}) \right\} i_b +$$

$$\dot{m} \left\{ q (r_{e_z}^2 + r_{e_x}^2) - r_{e_y} (r r_{e_z} + p r_{e_x}) \right\} j_b +$$

$$\dot{m} \left\{ r (r_{e_x}^2 + r_{e_y}^2) - r_{e_z} (p r_{e_x} + q r_{e_y}) \right\} k_b -$$

$$\dot{m} \bar{r}_e \times \bar{v}_e$$

6.3-30

Finally by substituting equations (6.3-30), (6.3-28), (6.3-27), (6.3-16), and (6.3-15) into equation (6.3-4) we get

$$\begin{aligned}
 \left(\frac{d \bar{H}_T}{dt}\right)_N = & \left[I_x \dot{p} - (I_y - I_z) qr - \dot{I}_x p + \right. \\
 & \left. \dot{m} \left\{ p(r_{e_y}^2 + r_{e_z}^2) - r_{e_x} (q r_{e_y} + r r_{e_z}) \right\} \right] i_b + \\
 & \left[I_y \dot{q} - (I_z - I_x) r p - \dot{I}_y q + \right. \\
 & \left. \dot{m} \left\{ q(r_{e_z}^2 + r_{e_x}^2) - r_{e_y} (r r_{e_z} + p r_{e_x}) \right\} \right] j_b + \quad 6.3-31 \\
 & \left[I_z \dot{r} - (I_x - I_y) p q - \dot{I}_z r + \right. \\
 & \left. \dot{m} \left\{ r(r_{e_x}^2 + r_{e_y}^2) - r_{e_z} (p r_{e_x} + q r_{e_y}) \right\} \right] k_b - \\
 & \dot{m} \bar{r}_e \times \bar{V}_e = \bar{M}
 \end{aligned}$$

6.3.3 External force and moment systems.- The resultant external force \bar{F} is the sum of the aerodynamic forces, the gravitational force, the control forces acting on the missile and the force caused by the jet pressure at the nozzle exit or

$$\bar{F} = \bar{F}_A + \bar{F}_G + \bar{F}_C + A_e \bar{P}_e \quad 6.3-32$$

The resultant moment \bar{M} is due to all the forces listed above except the gravitational force which has no moment about the center of gravity.

$$\bar{M} = \bar{M}_A + \bar{M}_C + \bar{r}_e \times A_e \bar{P}_e \quad 6.3-33$$

6.3.3.1 Aerodynamic forces and moments.- The aerodynamic forces and moments along and about the principal axes are defined in the conventional manner as follows:

$$F_x = C_x \frac{\rho}{2} S V_a^2$$

$$F_y = C_y \frac{\rho}{2} S V_a^2$$

6.3-34

$$F_z = C_z \frac{\rho}{2} S V_a^2$$

and

$$M_x = C_l \frac{\rho}{2} S V_a^2 l$$

$$M_y = C_m \frac{\rho}{2} S V_a^2 l$$

6.3-35

$$M_z = C_n \frac{\rho}{2} S V_a^2 l$$

where C_l , C_m , and C_n are the moment coefficients which give the moments about the missile center of gravity.

We can further specify that each aerodynamic coefficient is a function of the variables β , α , $\dot{\beta}$, $\dot{\alpha}$, p , q , and r such that:

$$C_x = -C_{x_0} - C_{x_\alpha} \alpha - C_{x_{\dot{\alpha}}} \left(\frac{\dot{\alpha} l}{2V}\right) - C_{x_q} \left(\frac{q l}{2V}\right)$$

$$C_y = C_{y_\beta} \beta + C_{y_{\dot{\beta}}} \left(\frac{\dot{\beta} l}{2V}\right) + C_{y_p} \left(\frac{p l}{2V}\right) + C_{y_r} \left(\frac{r l}{2V}\right)$$

$$C_z = -C_{z_0} - C_{z_\alpha} \alpha - C_{z_{\dot{\alpha}}} \left(\frac{\dot{\alpha} l}{2V}\right) - C_{z_q} \left(\frac{q l}{2V}\right)$$

6.3-36

$$C_l = C_{l_\beta} \beta + C_{l_{\dot{\beta}}} \left(\frac{\dot{\beta} l}{2V}\right) + C_{l_p} \left(\frac{p l}{2V}\right) + C_{l_r} \left(\frac{r l}{2V}\right)$$

$$C_m = C_{m_0} + C_{m_\alpha} \alpha + C_{m_{\dot{\alpha}}} \left(\frac{\dot{\alpha} l}{2V}\right) + C_{m_q} \left(\frac{q l}{2V}\right)$$

$$C_n = C_{n_\beta} \beta + C_{n_{\dot{\beta}}} \left(\frac{\dot{\beta} l}{2V}\right) + C_{n_p} \left(\frac{p l}{2V}\right) + C_{n_r} \left(\frac{r l}{2V}\right)$$

Definitions of α , β , and V_a will be given later in the development.

6.3.3.2 Gravitational force components.- The components of the weight term which we included in the equations of motion are computed from the transformation equation between inertial and body axes (which was developed in section 2) and are

$$\begin{Bmatrix} W_{x_b} \\ W_{y_b} \\ W_{z_b} \end{Bmatrix} = \begin{bmatrix} l_{11} & l_{12} & l_{13} \\ m_{11} & m_{12} & m_{13} \\ n_{11} & n_{12} & n_{13} \end{bmatrix} \begin{Bmatrix} 0 \\ 0 \\ W \end{Bmatrix} \quad 6.3-37$$

or

$$\begin{aligned} W_{x_b} &= l_{13} W = l_{13} mg = l_{13} mg_0 \left(\frac{R_0}{R_0 + h} \right)^2 \\ W_{y_b} &= m_{13} W = m_{13} mg = m_{13} mg_0 \left(\frac{R_0}{R_0 + h} \right)^2 \\ W_{z_b} &= n_{13} W = n_{13} mg = n_{13} mg_0 \left(\frac{R_0}{R_0 + h} \right)^2 \end{aligned} \quad 6.3-38$$

where $g = g_0 \left(\frac{R_0}{R_0 + h} \right)^2$ and $g_0 = 32.2$.

It should be noted that although these weight components are the ones usually used, they are approximations based on the flat earth concept, since they neglect the nonparallelism of the gravitational attraction at different points of the earth's surface. The true gravitational force or weight components will be specified later in section 6.4.

6.3.3.3 Control forces.- The control forces, of course, depend on the type of controls used on the missile. For purposes of this discussion we shall assume the missile is equipped with three types of controls. (See Figure 6-2.)

1. Conventional aerodynamic controls
2. Reaction controls
3. Jet vane controls

The resultant control force and moment equations can then be indicated as

$$\bar{F}_C = \bar{F}_\delta + \bar{F}_R + \bar{F}_V \quad 6.3-39$$

and

$$\bar{M}_C = \bar{M}_\delta + \bar{M}_R + \bar{M}_V \quad 6.3-40$$

The conventional aerodynamic controls are considered to be aileron δ_a , rudder δ_r , and elevator δ_e . The components of these aerodynamic forces and moments caused by these controls are assumed to be the following:

$$\begin{aligned} F_{\delta_x} &= 0 \\ F_{\delta_y} &= C_{y\delta_r} \frac{\rho}{2} S V_a^2 \delta_r \\ F_{\delta_z} &= C_{z\delta_e} \frac{\rho}{2} S V_a^2 \delta_e \end{aligned} \quad 6.3-41$$

and

$$M_{\delta_x} = C_{l_{\delta_a}} \frac{\rho}{2} S V_a^2 l \delta_a + C_{l_{\delta_r}} \frac{\rho}{2} S V_a^2 l \delta_r$$

$$M_{\delta_y} = C_{m_{\delta_e}} \frac{\rho}{2} S V_a^2 l \delta_e \quad 6.3-42$$

$$M_{\delta_z} = C_{n_{\delta_a}} \frac{\rho}{2} S V_a^2 l \delta_a + C_{n_{\delta_r}} \frac{\rho}{2} S V_a^2 l \delta_r$$

The reaction controls are assumed to be force and moment components along and about the missile principal body axes of magnitudes F_{R_x} , F_{R_y} , F_{R_z} , M_{R_x} , M_{R_y} , and M_{R_z} .

6.3.3.4 Jet vane controls.- The jet vane forces and moments are considered on the basis of the vane arrangement shown in Figures 6-4 and 6-3. The components of the total jet vane force acting on the missile are assumed to be the following:

$$F_{V_x} = - (\text{total drag of all jet vanes}) = 0$$

$$F_{V_y} = (Q_3 + Q_4) = \left(\frac{dQ}{d\delta} \delta_3 + \frac{dQ}{d\delta} \delta_4 \right) = \frac{dQ}{d\delta} (\delta_3 + \delta_4) \quad 6.3-43$$

$$F_{V_z} = (Q_1 + Q_2) = \left(\frac{dQ}{d\delta} \delta_1 + \frac{dQ}{d\delta} \delta_2 \right) = \frac{dQ}{d\delta} (\delta_1 + \delta_2)$$

The components of the total jet vane moment about the missile center of gravity are

$$M_{V_x} = r_1 \frac{dQ}{d\delta} \delta_1 - r_1 \frac{dQ}{d\delta} \delta_2 + r_3 \frac{dQ}{d\delta} \delta_3 - r_3 \frac{dQ}{d\delta} \delta_4$$

$$M_{V_y} = I_1 \frac{dQ}{d\delta} \delta_1 + I_2 \frac{dQ}{d\delta} \delta_2 \quad 6.3-44$$

$$M_{V_z} = -L_3 \frac{dQ}{d\delta} \delta_3 - L_4 \frac{dQ}{d\delta} \delta_4$$

where L_1 , L_2 , L_3 , and L_4 are the distances of the jet vane lift forces behind the missile center of gravity.

Other possible types of missile control not detailed here are control by means of a swiveled or gimballed rocket and control by use of Vernier engines.

6.3.4 Equations of motion. - The equation of motion due to rate of change of momentum

$$\left(\frac{d\bar{U}_T}{dt} \right)_N = \bar{F} \quad 6.3.1$$

becomes (where $\dot{m} \bar{V}_e$ is added to both sides of (6.3-1))

$$\left(\frac{d\bar{U}_T}{dt} \right)_N + \dot{m} \bar{V}_e = \bar{F}_A + \bar{F}_G + \bar{F}_C + \bar{F}_J \quad 6.3-45$$

where

$$\bar{F}_J = A_e \bar{P}_e + \dot{m} \bar{V}_e = \text{jet thrust} \quad 6.3-46$$

The equation of motion due to the rate of change of angular momentum

$$\left(\frac{d\bar{H}_T}{dt} \right)_N = \bar{M} \quad 6.3-14$$

becomes (where $\dot{m} (\bar{r}_e \times \bar{V}_e)$) is added to both sides of equation (6.3-14)

$$\left(\frac{d\bar{H}_T}{dt} \right)_N + \dot{m} (\bar{r}_e \times \bar{V}_e) = \bar{M}_A + \bar{M}_C + \bar{M}_J \quad 6.3-47$$

where

$$\bar{M}_J = \bar{r}_e \times (A_e \bar{P}_e + \dot{m} \bar{V}_e) = \text{jet thrust moment about the c.g.} \quad 6.3-48$$

Equation (6.3-45) resolved into its components thus generates the following three algebraic equations.

$$m (\dot{u} + wq - vr) + \dot{m} (q r e_z - r r e_y) = F_{A_x} + W_x + F_{C_x} + F_{J_x} \quad 6.3-49$$

$$m (\dot{v} + ur - wp) + \dot{m} (r r e_x - p r e_z) = F_{A_y} + W_y + F_{C_y} + F_{J_y} \quad 6.3-50$$

$$m (\dot{w} + vp - uq) + \dot{m} (p r e_y - q r e_x) = F_{A_z} + W_z + F_{C_z} + F_{J_z} \quad 6.3-51$$

Equation (6.3-47) resolved into its components generates the following three algebraic equations

$$\begin{aligned} I_x \dot{p} - (I_y - I_z) qr - \dot{I}_{xp} + \dot{m} \left\{ p(r e_y^2 + r e_z^2) + r e_x (q r e_y + r r e_z) \right\} \\ = M_{A_x} + M_{C_x} + M_{J_x} \end{aligned} \quad 6.3-52$$

$$I_y \dot{q} - (I_z - I_x) r p - \dot{I}_y q + \dot{m} \left\{ q(r e_z^2 + r e_x^2) + r e_y (r r e_z + p r e_x) \right\}$$

$$= M_{A_y} + M_{C_y} + M_{J_y} \quad 6.3-53$$

$$I_z \dot{r} - (I_x - I_y) p q - \dot{I}_z r + \dot{m} \left\{ r(r e_x^2 + r e_y^2) + r e_z (p r e_x + q r e_y) \right\}$$

$$= M_{A_z} + M_{C_z} + M_{J_z} \quad 6.3-54$$

In order to simplify the equations of motion the following assumptions are made. It is assumed the jet exit velocity relative to the nozzle exit is along the x_b axis, that is

$$\bar{V}_e = i_{x_b} V_e$$

or

$$V_{e_x} = V_e, V_{e_y} = V_{e_z} = 0 \quad 6.3-55$$

and

$$\bar{P}_e = i_{x_b} P_e \quad 6.3-56$$

then

$$\bar{r}_e = i_{x_b} r_e \quad 6.3-57$$

or

$$r_{e_y} = r_{e_z} = 0$$

then

$$F_{J_x} = A_e P_e + m V_e = T \quad 6.3-58$$

further

$$F_{J_y} = F_{J_z} = M_J = 0 \quad 6.3-59$$

With these simplifications the six equations of motion become

$$m(\dot{u} + wq - vr) = T + W_x + F_{Ax} + F_{Cx} \quad 6.3-60$$

$$m(\dot{v} + ur - wp) - \dot{m} r_e r = W_y + F_{Ay} + F_{Cy} \quad 6.3-61$$

$$m(\dot{w} + vp - uq) + \dot{m} r_e q = W_z + F_{Az} + F_{Cz} \quad 6.3-62$$

$$I_x \dot{p} - (I_y - I_z) qr - \dot{I}_x p = M_{Ax} + M_{Cx} \quad 6.3-63$$

$$I_y \dot{q} - (I_z - I_x) rp - \dot{I}_y q + \dot{m} q r_e^2 = M_{Ay} + M_{Cy} \quad 6.3-64$$

$$I_z \dot{r} - (I_x - I_y) pq - \dot{I}_z r + \dot{m} r r_e^2 = M_{Az} + M_{Cy} \quad 6.3-65$$

By substituting the components of the aerodynamic force and moments, the weight components and the control force components derived earlier into equations (6.3-60) to 6.3-65) inclusive we arrive at the final set of equations of motion of the missile with variable mass shown on the following page. The equations of motion for coasting flight or the (no thrust) conditions are also indicated on the page following.

6.3.5 Remarks on solution of equations of motion.- The six equations of motion (6.1) and (6.6) contain six unknowns $u, v, w, p, q,$ and r . If the solution is performed on the analog, three more equations are added which generate the direction cosines needed to include the weight term in the equations of motion.

$$\begin{aligned} \dot{l}_{13} &= m_{13} r - n_{13} q \\ \dot{m}_{13} &= n_{13} p - l_{13} r \\ \dot{n}_{13} &= l_{13} q - m_{13} p \end{aligned} \quad 6.3-66$$

Equations of Motion of a Fin Stabilized Missile
with Variable Mass Referred to Principal Body Axes
(Coasting flight, or no thrust condition)

$$m(\ddot{u} + wq - vr) = l_{13} m g_0 \left(\frac{R_0}{R_0 + h} \right)^2 - \frac{\rho}{2} S V_a^2 \left[C_{x_0} + C_{x_\alpha} \alpha + C_{x_z} \left(\frac{\dot{z}}{2V} \right) + C_{x_q} \left(\frac{qL}{2V} \right) \right] + F_{R_x} \quad (1)$$

$$m(\ddot{v} + ur - wp) = m_{13} m g_0 \left(\frac{R_0}{R_0 + h} \right)^2 + \frac{\rho}{2} S V_a^2 \left[C_{y_0} + C_{y_\beta} \beta + C_{y_p} \left(\frac{\dot{p}L}{2V} \right) + C_{y_r} \left(\frac{rL}{2V} \right) + C_{y_s} \delta_s \right] + F_{R_y} \quad (2)$$

$$m(\ddot{w} + vp - uq) = n_{13} m g_0 \left(\frac{R_0}{R_0 + h} \right)^2 - \frac{\rho}{2} S V_a^2 \left[C_{z_0} + C_{z_\alpha} \alpha + C_{z_z} \left(\frac{\dot{z}}{2V} \right) + C_{z_q} \left(\frac{qL}{2V} \right) + C_{z_s} \delta_s \right] + F_{R_z} \quad (3)$$

$$I_y \ddot{p} - (I_y - I_z) q r = -\frac{\rho}{2} S V_a^2 L \left[C_{l_p} \beta + C_{l_p} \left(\frac{\dot{p}L}{2V} \right) + C_{l_r} \left(\frac{rL}{2V} \right) + C_{l_s} \delta_s + C_{l_r} \delta_r \right] + M_{R_x} \quad (4)$$

$$I_y \ddot{q} - (I_x - I_z) r p = -\frac{\rho}{2} S V_a^2 L \left[C_{m_0} + C_{m_\alpha} \alpha + C_{m_z} \left(\frac{\dot{z}}{2V} \right) + C_{m_q} \left(\frac{qL}{2V} \right) + C_{m_s} \delta_s \right] + M_{R_y} \quad (5)$$

$$I_z \ddot{r} - (I_x - I_y) p q = -\frac{\rho}{2} S V_a^2 L \left[C_{n_p} \beta + C_{n_p} \left(\frac{\dot{p}L}{2V} \right) + C_{n_r} \left(\frac{rL}{2V} \right) + C_{n_s} \delta_s + C_{n_r} \delta_r + C_{n_s} \delta_s \right] + M_{R_z} \quad (6)$$

$$l_{ij} = m_{ij} r - n_{ij} q$$

$$m_{ij} = n_{ij} p - l_{ij} r$$

$$n_{ij} = l_{ij} q - m_{ij} p$$

$$j = 1, 2, 3$$

*Equations of Motion of a Fin Stabilized Missile
with Variable Mass Referred to Principal Body Axes
(Powered Flight)*

$$m(\dot{u} + wq - vr) = T + l_{13} m g_0 \left(\frac{R_0}{R_0 + h} \right)^2 - \frac{\rho}{2} S V_0^2 \left[C_{x_0} + C_{x_\alpha} + C_{x_\beta} \left(\frac{\beta}{2V} \right) + C_{x_\gamma} \left(\frac{\gamma}{2V} \right) \right] + F_{R_x} \quad (1)$$

$$m(\dot{v} + ur - wp) + \dot{m} r_e r = m_{13} m g_0 \left(\frac{R_0}{R_0 + h} \right)^2 + \frac{\rho}{2} S V_0^2 \left[C_{y_0} + C_{y_\beta} \left(\frac{\beta}{2V} \right) + C_{y_\gamma} \left(\frac{\gamma}{2V} \right) + C_{y_r} \left(\frac{r}{2V} \right) + C_{y_{\dot{r}}} \delta_1 \right] + F_{R_y} + \frac{dQ}{d\delta} (\delta_3 + \delta_4) \quad (2)$$

$$m(\dot{w} + vp - uq) + \dot{m} r_e q = n_{13} m g_0 \left(\frac{R_0}{R_0 + h} \right)^2 - \frac{\rho}{2} S V_0^2 \left[C_{z_0} + C_{z_\alpha} + C_{z_\beta} \left(\frac{\beta}{2V} \right) + C_{z_\gamma} \left(\frac{\gamma}{2V} \right) + C_{z_\xi} \delta_e \right] + F_{R_z} + \frac{dQ}{d\delta} (\delta_1 + \delta_2) \quad (3)$$

$$I_x \dot{p} - (I_y - I_z) q r - \dot{I}_x p = \frac{\rho}{2} S V_0^2 l \left[C_{L_p} p + C_{L_\beta} \left(\frac{\beta}{2V} \right) + C_{L_r} \left(\frac{r}{2V} \right) + C_{L_{\dot{r}}} \delta_e + C_{L_{\dot{r}}} \delta_e \right] + M_{R_x} + \frac{dQ}{d\delta} [r(\delta_1 - \delta_4) + r_5(\delta_3 - \delta_4)] \quad (4)$$

$$I_y \dot{q} - (I_x - I_z) r p - \dot{I}_y q + \dot{m} q r_e = \frac{\rho}{2} S V_0^2 l \left[C_{m_0} + C_{m_\alpha} + C_{m_\beta} \left(\frac{\beta}{2V} \right) + C_{m_\gamma} \left(\frac{\gamma}{2V} \right) + C_{m_\xi} \delta_e \right] + M_{R_y} + \frac{dQ}{d\delta} [L_1 \delta_1 + L_2 \delta_2] \quad (5)$$

$$I_z \dot{r} - (I_x - I_y) p q - \dot{I}_z r + \dot{m} r r_e = \frac{\rho}{2} S V_0^2 l \left[C_{n_0} p + C_{n_\beta} \left(\frac{\beta}{2V} \right) + C_{n_\gamma} \left(\frac{\gamma}{2V} \right) + C_{n_r} \left(\frac{r}{2V} \right) + C_{n_{\dot{r}}} \delta_e \right] + M_{R_z} - \frac{dQ}{d\delta} [L_3 \delta_3 + L_4 \delta_4] \quad (6)$$

22

$$\begin{aligned} l_{ij} &= m_{ij} r - n_{ij} q \\ m_{ij} &= n_{ij} p - l_{ij} r \\ n_{ij} &= l_{ij} q - m_{ij} p \end{aligned} \quad j = 1, 2, 3$$

(7)

$$\begin{aligned} \alpha &= \tan^{-1} \frac{W_a}{U_a} & l_{11} &= \cos \psi \cos \theta & m_{11} &= \cos \psi \sin \theta \sin \phi - \sin \psi \cos \phi & n_{11} &= \cos \psi \sin \theta \cos \phi + \sin \psi \sin \phi \\ \beta &= \tan^{-1} \frac{v_a}{V_a} & l_{12} &= \sin \psi \cos \theta & m_{12} &= \sin \psi \sin \theta \sin \phi + \cos \psi \cos \phi & n_{12} &= \sin \psi \sin \theta \cos \phi - \cos \psi \sin \phi \\ & & l_{13} &= -\sin \theta & m_{13} &= \cos \theta \sin \phi & n_{13} &= \cos \theta \cos \phi \end{aligned}$$

Note: Gravitational or weight component based on flat earth concept.

The Euler angles ψ , θ , and ϕ which specify the instantaneous missile attitudes can be determined from the equations (6A-2) given in appendix A which are

$$\dot{\psi} = \frac{1}{\cos \theta} (q \sin \phi + r \cos \phi)$$

$$\dot{\theta} = q \cos \phi - r \sin \phi \quad 6.3-67$$

$$\dot{\phi} = p + \tan \theta (q \sin \phi + r \cos \phi)$$

6.3.6 Remarks on choice of axis system.- Principal body axes have been used in this development of the equations of motion; however we could equally as well have chosen stability axes or wind axes. Each set has its inherent advantages and disadvantages.

Choice of body axes offers the advantage that the mechanics of the problem are simplified by the elimination of products of inertia and their rates. The disadvantage of principal body axes is that the aerodynamic coefficients are sometimes difficult to determine in this coordinate system and the true weight or gravitational component is difficult to incorporate in the equations. The weight term is usually approximated.

Stability axes (see x_s in Fig. 6-6c) offer the advantage that the aerodynamic coefficients are easily specified. They have the disadvantage that products of inertia and their rates must be known and the weight component is difficult to incorporate in the equations.

Wind axes are used frequently since the force equations are easily written for this axis system and the weight term is easily incorporated. The moment equations however have moments of inertia and products of inertia which vary not only with the time varying mass, but also with respect to the body attitude in the wind axes.

6.4 Trajectory Equations

The path of the missile center of gravity with respect to a given set of coordinates represents its trajectory in those coordinates. In the development of the missile equations of motion, we defined two sets of axes (x_b, y_b, z_b) body axes and (X_N, Y_N, Z_N) inertial axes.

6.4.1 Inertial axes.- The trajectory of the missile center of gravity in the (X_N, Y_N, Z_N) inertial axes can be computed in several ways, one of which is the following. From a solution of the equations of motion (6.3-60) to (6.3-65) time histories of ($u, v, \text{ and } w$) are obtained. Using the transformation defined in equation (6.2-19) we can obtain the velocity components along the inertial axes from

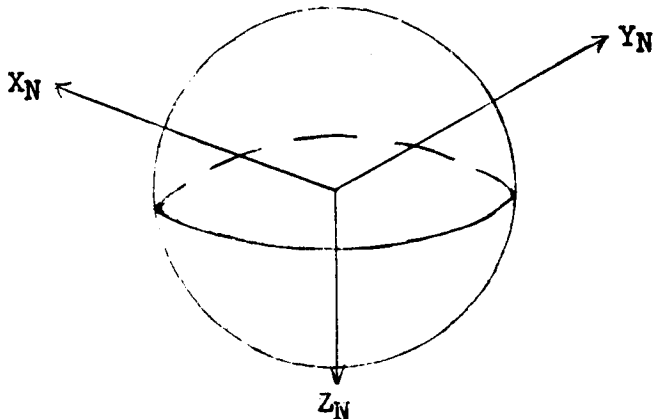
$$\begin{Bmatrix} V_{X_N} \\ V_{Y_N} \\ V_{Z_N} \end{Bmatrix} = [T_1] \begin{Bmatrix} u \\ v \\ w \end{Bmatrix} \quad 6.4-1$$

and an integration of V_{X_N} , V_{Y_N} , and V_{Z_N} , with the proper initial conditions yields the trajectories X_N , Y_N , and Z_N . This operation is indicated by

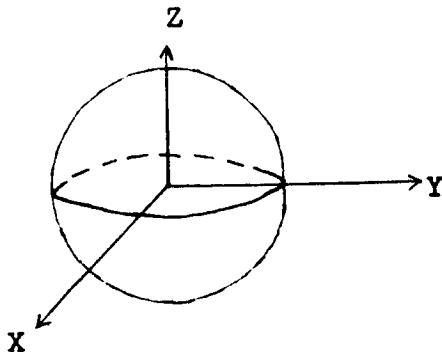
$$\begin{Bmatrix} X_N \\ Y_N \\ Z_N \end{Bmatrix} = \begin{bmatrix} \text{Integrating} \\ \text{Matrix} \end{bmatrix} \begin{Bmatrix} V_{X_N} \\ V_{Y_N} \\ V_{Z_N} \end{Bmatrix} \quad 6.4-2$$

Since further information of a missile trajectory may be desired such as latitude, longitude, and attitude of the missile with respect to a stable table or stabilized platform we define some new sets of axes to yield this information.

If we consider the inertial axes (X_N, Y_N, Z_N) fixed in the non-rotating earth as shown in the following sketch



we note that the earth would rotate about the $(-Z_N)$ axis using the right-hand rule. We would prefer to have the earth rotate about the $(+Z)$ axis; therefore, we define a new axis system (X, Y, Z) such that the $(+Z)$ axis goes through the north pole as shown in the following sketch.



The (X, Y, Z) axis is obtained from the (X_N, Y_N, Z_N) axis system by a rotation of 180° about the Y_N axis. The transformation between the (X_N, Y_N, Z_N) and (X, Y, Z) axes is

$$\begin{Bmatrix} X \\ Y \\ Z \end{Bmatrix} = \begin{bmatrix} -1 & 0 & 0 \\ 0 & 1 & 0 \\ 0 & 0 & -1 \end{bmatrix} \begin{Bmatrix} X_N \\ Y_N \\ Z_N \end{Bmatrix} \quad 6.4-3$$

This may be obtained by letting $\theta = 180^\circ$ in equation (6.2-5). Equation (6.4-3) may be written as

$$\begin{Bmatrix} X \\ Y \\ Z \end{Bmatrix} = [T_4] \begin{Bmatrix} X_N \\ Y_N \\ Z_N \end{Bmatrix} \quad 6.4-4$$

6.4.2 Moving earth axes.- The earth rotates at an angular velocity ω_e . If we let the angle

$$H = \omega_e t \quad 6.4-5$$

and define a set of axes fixed in the rotating earth as (X_e, Y_e, Z_e) , then at a given time the (X_e, Y_e, Z_e) axes would be oriented with respect to the (X, Y, Z) axes as shown in Figure 6-6a.

The transformation between the two sets of coordinate systems becomes

$$\begin{Bmatrix} X_e \\ Y_e \\ Z_e \end{Bmatrix} = \begin{bmatrix} \cos H & \sin H & 0 \\ -\sin H & \cos H & 0 \\ 0 & 0 & 1 \end{bmatrix} \begin{Bmatrix} X \\ Y \\ Z \end{Bmatrix} \quad 6.4-6$$

or

$$\begin{Bmatrix} X_e \\ Y_e \\ Z_e \end{Bmatrix} = [T_2] \begin{Bmatrix} X \\ Y \\ Z \end{Bmatrix} \quad 6.4-7$$

6.4.3 Local geographical axes.- A right-hand set of Cartesian coordinates (X_g, Y_g, Z_g) is defined as shown in Figure 6-6 such that the Z_g axis is always pointing toward the center of the earth and the X_g axis points south. The local geographical axes can be obtained from the (X_e, Y_e, Z_e) moving earth axes by the following three rotations

(1) Rotate (X_e, Y_e, Z_e) about Z_e through the angle λ to obtain the new coordinate system (X_1, Y_1, Z_1) .

(2) Rotate (X_1, Y_1, Z_1) about Y_1 through the angle of \mathcal{L} to obtain the new coordinate system (X_2, Y_2, Z_2) .

(3) Rotate (X_2, Y_2, Z_2) about X_2 through the angle 180° to obtain the new set of geographical axes. (X_g, Y_g, Z_g)

These three rotations are similar to the three performed in section 2 where $\psi = \lambda$, $\theta = \mathcal{L}$, and $\phi = 180^\circ$. The transformation which results from these three rotations on (X_e, Y_e, Z_e) to obtain (X_g, Y_g, Z_g) (which is similar to that of equation (6.2-18)) is

$$\begin{Bmatrix} X_e \\ Y_e \\ Z_e \end{Bmatrix} = \begin{bmatrix} (\cos \lambda \cos \mathcal{L})(\sin \lambda) & (-\cos \lambda \sin \mathcal{L}) \\ (\sin \lambda \cos \mathcal{L})(-\cos \lambda) & (-\sin \lambda \sin \mathcal{L}) \\ (-\sin \mathcal{L}) & 0 & (-\cos \mathcal{L}) \end{bmatrix} \begin{Bmatrix} X_g \\ Y_g \\ Z_g \end{Bmatrix} \quad 6.4-8$$

or

$$\begin{Bmatrix} X_g \\ Y_g \\ Z_g \end{Bmatrix} = \begin{bmatrix} (\cos \lambda \cos \mathcal{L}) & (\sin \lambda \cos \mathcal{L}) & (-\sin \mathcal{L}) \\ (\sin \lambda) & (-\cos \lambda) & 0 \\ (-\cos \lambda \sin \mathcal{L}) & (-\sin \lambda \sin \mathcal{L}) & (-\cos \mathcal{L}) \end{bmatrix} \begin{Bmatrix} X_e \\ Y_e \\ Z_e \end{Bmatrix} \quad 6.4-9$$

we can write equation (6.4-9) as

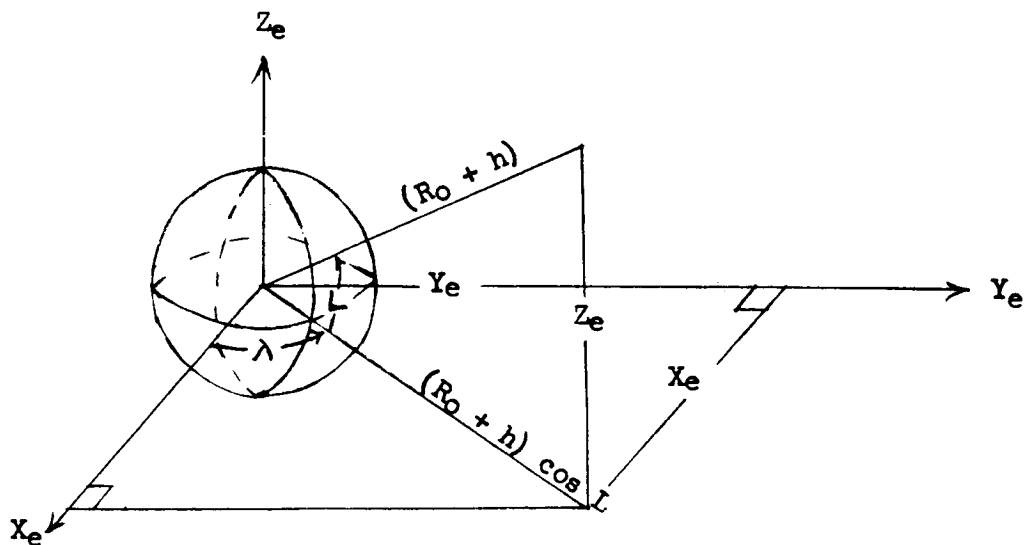
$$\begin{Bmatrix} X_g \\ Y_g \\ Z_g \end{Bmatrix} = [T_3] \begin{Bmatrix} X_e \\ Y_e \\ Z_e \end{Bmatrix} \quad 6.4-10$$

in order to define the transformation matrix $[T_3]$.

6.4.4 Latitude, longitude, and altitude.- Time histories of latitude, longitude, and altitude are derived from time histories of X_e , Y_e , and Z_e . The angles used in specifying the attitude of local geographical axes are λ , the longitude and \mathcal{L} , the colatitude. If the latitude is designated by L , then

$$L = 90 - \mathcal{L} \quad 6.4-11$$

The geometry of the problem is illustrated in the following sketch



From the geometry of the problem the following relations are obtained.

$$(R_0 + h) = \sqrt{X_e^2 + Y_e^2 + Z_e^2}$$

$$\frac{X_e}{(R_0 + h) \cos L} = \sin (90 - \lambda) \quad 6.4-12$$

or

$$X_e = (R_0 + h) \cos L \cos \lambda$$

$$\frac{Y_e}{(R_0 + h) \cos L} = \cos (90 - \lambda) \quad 6.4-13$$

or

$$Y_e = (R_0 + h) \cos L \sin \lambda$$

$$\frac{Z_e}{(R_0 + h)} = \sin L \quad 6.4-14$$

or

$$Z_e = (R_0 + h) \sin L \quad 6.4-15$$

From equations (6.4-15) and (6.4-12) we get the relation for the latitude L which is

$$L = \sin^{-1} \frac{Z_e}{\sqrt{X_e^2 + Y_e^2 + Z_e^2}} \quad 6.4-16$$

Dividing equation (6.4-14) by (6.4-13), we get the relation for longitude which is

$$\lambda = \tan^{-1} \frac{Y_e}{X_e} \quad 6.4-17$$

The velocity vector of the center of gravity is oriented in the geographical axes by the azimuth angle A and the elevation angle γ .

The azimuth angle A is the angle in the X_g, Y_g plane measured in the positive direction from south to west; in a physical sense it is our compass angle plus 180° . The elevation angle γ is measured + up. From the geometry it is seen

$$\begin{aligned}V_{X_g} &= V \cos \gamma \cos A \\V_{Y_g} &= V \cos \gamma \sin A \\V_{Z_g} &= V \sin \gamma\end{aligned}\tag{6.4-18}$$

from these relations we get two expressions for A and γ

$$\tan A = \frac{V_{Y_g}}{V_{X_g}}\tag{6.4-19}$$

and

$$\sin \gamma = \frac{V_{Z_g}}{V}\tag{6.4-20}$$

Time histories of A and γ can be computed from equations (6.4-19) and (6.4-20) if time histories of V_{X_g} , V_{Y_g} , and V_{Z_g} are known. From equations (6.4-1), (6.4-4), (6.4-7), and (6.4-10) we can write

$$\begin{Bmatrix} V_{X_g} \\ V_{Y_g} \\ V_{Z_g} \end{Bmatrix} = \begin{bmatrix} T_3 \\ T_2 \\ T_4 \\ T_1 \end{bmatrix} \begin{Bmatrix} u \\ v \\ w \end{Bmatrix}\tag{6.4-21}$$

which permits the computation of the needed V_{X_g} , V_{Y_g} , and V_{Z_g} . V is computed from

$$V = \sqrt{V_{X_g}^2 + V_{Y_g}^2 + V_{Z_g}^2}\tag{6.4-22}$$

In summary, the geographical set of axes was defined in order to specify the attitude of the missile with respect to a stabilized platform. The attitude is given by time histories of A and γ . The specification of moving earth axes X_e, Y_e, Z_e permits the computation of time histories of altitude, latitude, and longitude. The local geographical axes are the same as the earth axes defined in ASA Y10. 7-1954.

6.4.5 True weight component.- From Figure 6-6c it can be seen that the true weight component W acts along the Z_g axis. The true weight components in body axes may thus be given by

$$\begin{Bmatrix} W_{x_b} \\ W_{y_b} \\ W_{z_b} \end{Bmatrix} = \begin{bmatrix} l_{11} & l_{12} & l_{13} \\ m_{11} & m_{12} & m_{13} \\ n_{11} & n_{12} & n_{13} \end{bmatrix} \begin{Bmatrix} -W \cos L \cos (\lambda + H) \\ W \cos L \sin (\lambda - H) \\ -W \sin L \end{Bmatrix} \quad 6.4-23$$

where the direction cosines $l_{1j}, m_{1j},$ and n_{1j} are defined in section 6.2 equation (6.2-21).

6.4.6 Definition of V_a, α and β .- The velocity vector \bar{V}_a which is used to determine aerodynamic forces and moments is the resultant of three vectors

$$\bar{V}_a = \bar{V} - \bar{V}_e - \bar{V}_w \quad 6.4-24$$

where \bar{V} is the velocity vector of the missile center of gravity referred to inertia axes, \bar{V}_w is any wind velocity vector and \bar{V}_e is the velocity component of a particle of air due to the earth's rotational velocity.

$$\bar{V}_e = \bar{\omega}_e \times \bar{R} = \begin{vmatrix} i & j & k \\ 0 & 0 & \omega_e \\ X_N & Y_N & Z_N \end{vmatrix} \quad 6.4-25$$

or

$$V_e = -i \omega_e Y_N + j \omega_e X_N \quad 6.4-26$$

If the components of \bar{V}_a are \bar{u}_a , \bar{v}_a , and \bar{w}_a as shown in Figure 6-5 then

$$\bar{V}_a = i u_a + j v_a + k w_a \quad 6.4-27$$

We can express \bar{V} as

$$\bar{V} = i u + j v + k w \quad 6.4-28$$

and from equation (6.4-26)

$$\bar{V}_e = -i (\omega_e Y_N) + j (\omega_e X_N) \quad 6.4-26$$

therefore

$$\begin{aligned} u_a &= u + \omega_e Y_N - u_w \\ v_a &= v - \omega_e X_N - v_w \\ w_a &= w - w_w \end{aligned} \quad 6.4-29$$

The angle of attack α and sideslip β are defined by Figure 6-5. It is assumed that the missile sideslips first then performs an angle of attack. From Figure 6-5 it is seen

$$\cos \alpha = \frac{u_a}{V_a \cos \beta} \quad 6.4-30$$

$$\sin \alpha = \frac{w_a}{V_a \cos \beta} \quad 6.4-31$$

$$\sin \beta = \frac{v_a}{V_a} \quad 6.4-32$$

or

$$\alpha = \tan^{-1} \frac{w_a}{u_a} \quad 6.4-33$$

$$\beta = \sin^{-1} \frac{v_a}{V_a} \quad 6.4-34$$

6.4.7 Angular velocity rates.- If we designate p_a , q_a and r_a as the angular velocity terms which cause the aerodynamic moments about the missile center of gravity and note that

$$\bar{\omega}_a = i p_a + j q_a + k r_a \quad 6.4-35$$

and
$$\bar{\omega} = i p + j q + k r$$

then

$$\bar{\omega}_a = \bar{\omega} - \frac{\bar{V} \times \bar{R}}{R^2} \quad 6.4-36$$

where $\frac{\bar{V} \times \bar{R}}{R^2}$ is a correction due to the curvature of the flight path.

This correction is small and therefore usually omitted.

The density ρ is a function of altitude h and would have to be known to perform a computation. The computation of initial conditions to start the problem is a major task and will not be discussed here.

CONCLUDING REMARKS

This has been a brief and rapid introduction of the equations of motion and trajectories of a rigid fin stabilized missile with variable mass for the general case of all six degrees of freedom. If time and space permitted, much more could be said about reducing the general six degrees of freedom to two or three degrees of freedom and simplifying by other techniques such as roll and yaw stabilization. The equations of motion could also be presented referred to wind axes and stability axes, and compared with those usually found in the literature.

It should be noted further that there are also spin stabilized missiles which entail other effects not described here such as magnus effects, gyroscopic effects, aerodynamic effects due to spin and cross-spin, etc. This is another subject in itself, and is not dealt with in these notes.

APPENDIX 6-A

Summary of Formulas Pertaining to the Development

From the geometry of Figure 6-1 we see the angular velocities about the body axes are given by

$$\begin{aligned} p &= \dot{\phi} - \dot{\psi} \sin \theta \\ q &= \dot{\theta} \cos \varphi + \dot{\psi} \sin \varphi \cos \theta \\ r &= \dot{\psi} \cos \theta \cos \varphi - \dot{\theta} \sin \varphi \end{aligned} \quad 6.A-1$$

Equation (6.A-1) can also be written as

$$\begin{aligned} \dot{\psi} &= \frac{1}{\cos \theta} (q \sin \varphi + r \cos \varphi) \\ \dot{\theta} &= q \cos \varphi - r \sin \varphi \\ \dot{\phi} &= p + \tan \theta (q \sin \varphi + r \cos \varphi) \end{aligned} \quad 6.A-2$$

The angular velocities about the inertial axes X_N, Y_N, Z_N , denoted here by $\omega_{X_N}, \omega_{Y_N}$, and ω_{Z_N} are

$$\begin{aligned} \omega_{X_N} &= \dot{\phi} \cos \psi \cos \theta - \dot{\psi} \sin \psi \\ \omega_{Y_N} &= \dot{\phi} \sin \psi \cos \theta + \dot{\theta} \cos \psi \\ \omega_{Z_N} &= \dot{\psi} - \dot{\phi} \sin \theta \end{aligned} \quad 6.A-3$$

The transformation from body axes x_b, y_b, z_b to inertial axes X_N, Y_N, Z_N is given by equation (6.2-1b) which is

$$\begin{aligned}
 X_N &= l_{11} m_{11} n_{11} X_b \\
 Y_N &= l_{12} m_{12} n_{12} Y_b \\
 Z_N &= l_{13} m_{13} n_{13} Z_b
 \end{aligned}
 \tag{6.A-4}$$

The direction cosines l_{1j} , m_{1j} , and n_{1j} are defined in equation (6.2-21)

A vector quantity referred to X_N, Y_N, Z_N axis system denoted by $(=)$ is

$$(=) = ()_{X_N} i_N + ()_{Y_N} j_N + ()_{Z_N} k_N
 \tag{6.A-5}$$

where

$$\begin{aligned}
 ()_{X_N} &= l_{11} ()_{x_b} + m_{11} ()_{y_b} + n_{11} ()_{z_b} \\
 ()_{Y_N} &= l_{12} ()_{x_b} + m_{12} ()_{y_b} + n_{12} ()_{z_b} \\
 ()_{Z_N} &= l_{13} ()_{x_b} + m_{13} ()_{y_b} + n_{13} ()_{z_b}
 \end{aligned}
 \tag{6.A-6}$$

A vector quantity referred to the x_b, y_b, z_b axis system denoted by $(-)$ is

$$(-) = ()_{x_b} i_b + ()_{y_b} j_b + ()_{z_b} k_b
 \tag{6.A-7}$$

where

$$\begin{aligned}
 ()_{x_b} &= l_{11} ()_{X_N} + l_{12} ()_{Y_N} + l_{13} ()_{Z_N} \\
 ()_{y_b} &= m_{11} ()_{X_N} + m_{12} ()_{Y_N} + m_{13} ()_{Z_N} \\
 ()_{z_b} &= n_{11} ()_{X_N} + n_{12} ()_{Y_N} + n_{13} ()_{Z_N}
 \end{aligned}
 \tag{6.A-8}$$

Integration of equation (6.A-2) yields

$$\psi = \int_0^t \dot{\psi} dt + \psi(0)$$

$$\theta = \int_0^t \dot{\theta} dt + \theta(0)$$

6.A-9

$$\varphi = \int_0^t \dot{\varphi} dt + \varphi(0)$$

REFERENCES

1. Sokolnikoff, I. S., and Sokolnikoff, E. S.: Higher Mathematics for Engineers and Physicists, McGraw-Hill Book Co., Inc., 1941.
2. Frazer, R. A., Duncan, W. J., and Collar, A. R.: Elementary Matrices The MacMillan Co., 1946.
3. Doolin, Brian F.: The Application of Matrix Methods to Coordinate Transformations Occurring in Systems Studies Involving Large Motion of Aircraft. NACA TN 3968, 1957.
4. Perkins, Courtland D., and Hage, Robert E.: Aeroplane Performance Stability and Control. John Wiley and Sons, Inc., 1949.
5. Charters, A. C.: The Linearized Equations of Motion Underlying the Dynamic Stability of Aircraft, Spinning Projectiles and Symmetrical Missiles, NACA TN 3350, 1955.
6. Rankin, R. A.: The Mathematical Theory of the Motion of Rotated and Unrotated Rockets, 1949. Library Number N-47545 Phil. Trans. Series A Vol. 241, No. 837.
7. Chang, T.: General Equations of Motion of a Rigid Missile. Cornell Aeronautical Laboratory, Inc., 1952.
8. Rosser, J. B., Newton, R. R., and Gross, G. L.: Mathematical Theory of Rocket Flight, McGraw-Hill Book Co., Inc., 1947.
9. Anonymous: American Standard Letter Symbols for Aeronautical Sciences, The American Society of Mechanical Engineers, 1954. ASA Y10.7-1954.
10. Kooy, J. M. J.: On the Application of the Method of Variation of Elliptic Orbit Elements in Case of a Satellite Vehicle. Astronautica Acta 3(3) p. 179-214, 1951.

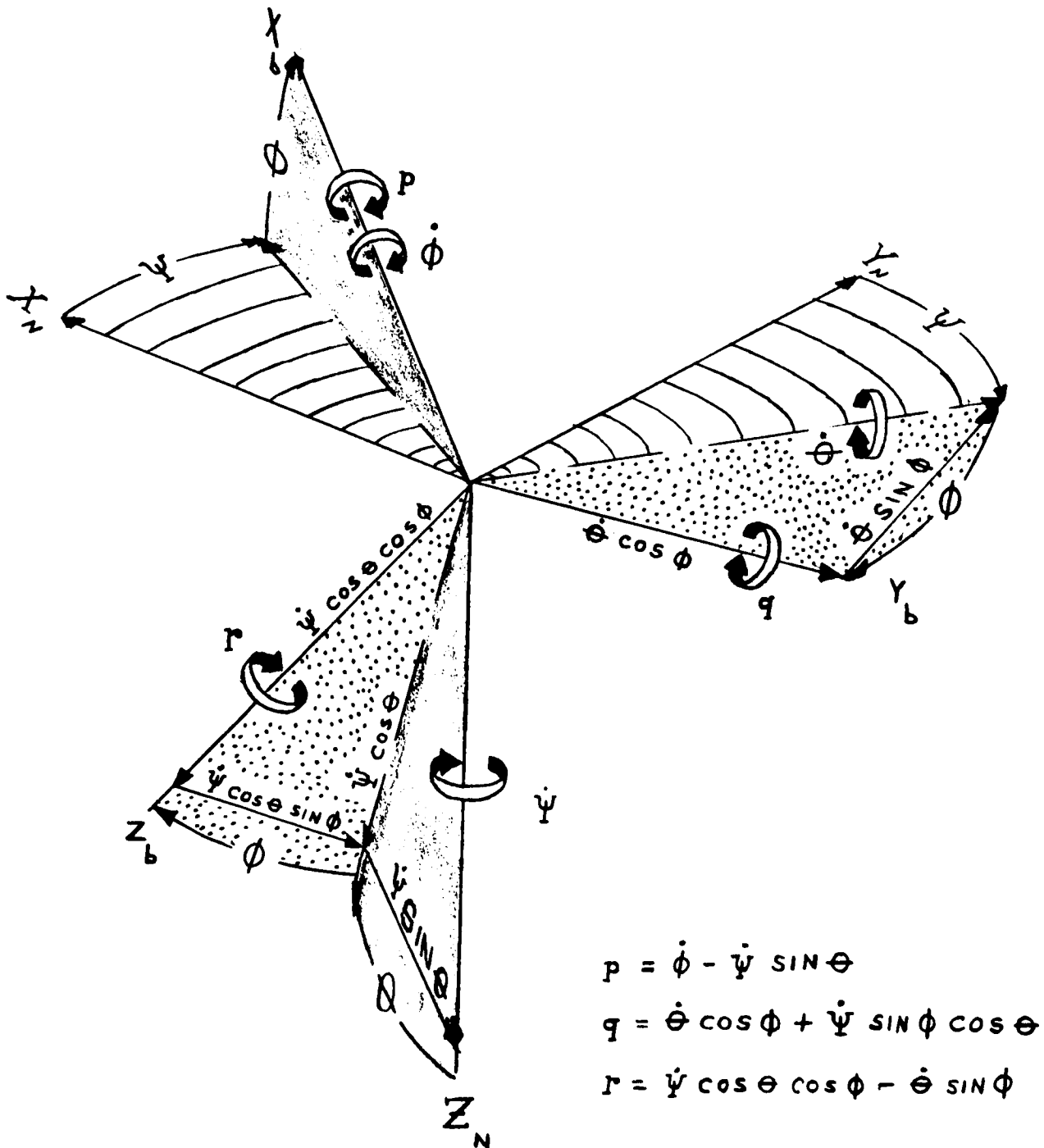


FIGURE 6-1.-ORIENTATION OF BODY AXIS WITH RESPECT TO NEWTONIAN, OR INERTIAL, OR SPACE AXIS. THE ORDER OF ROTATION IS ψ , θ , AND ϕ .

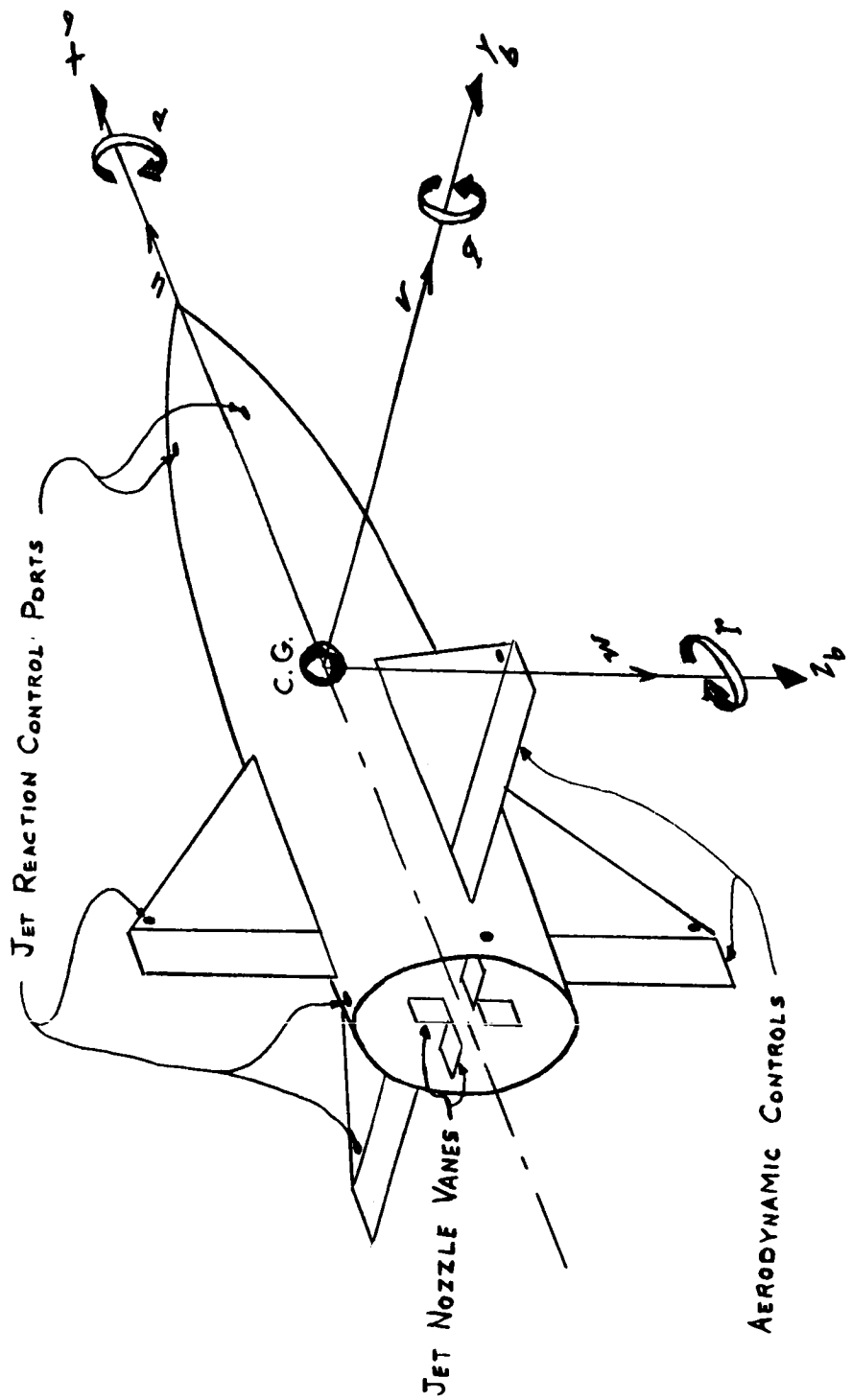
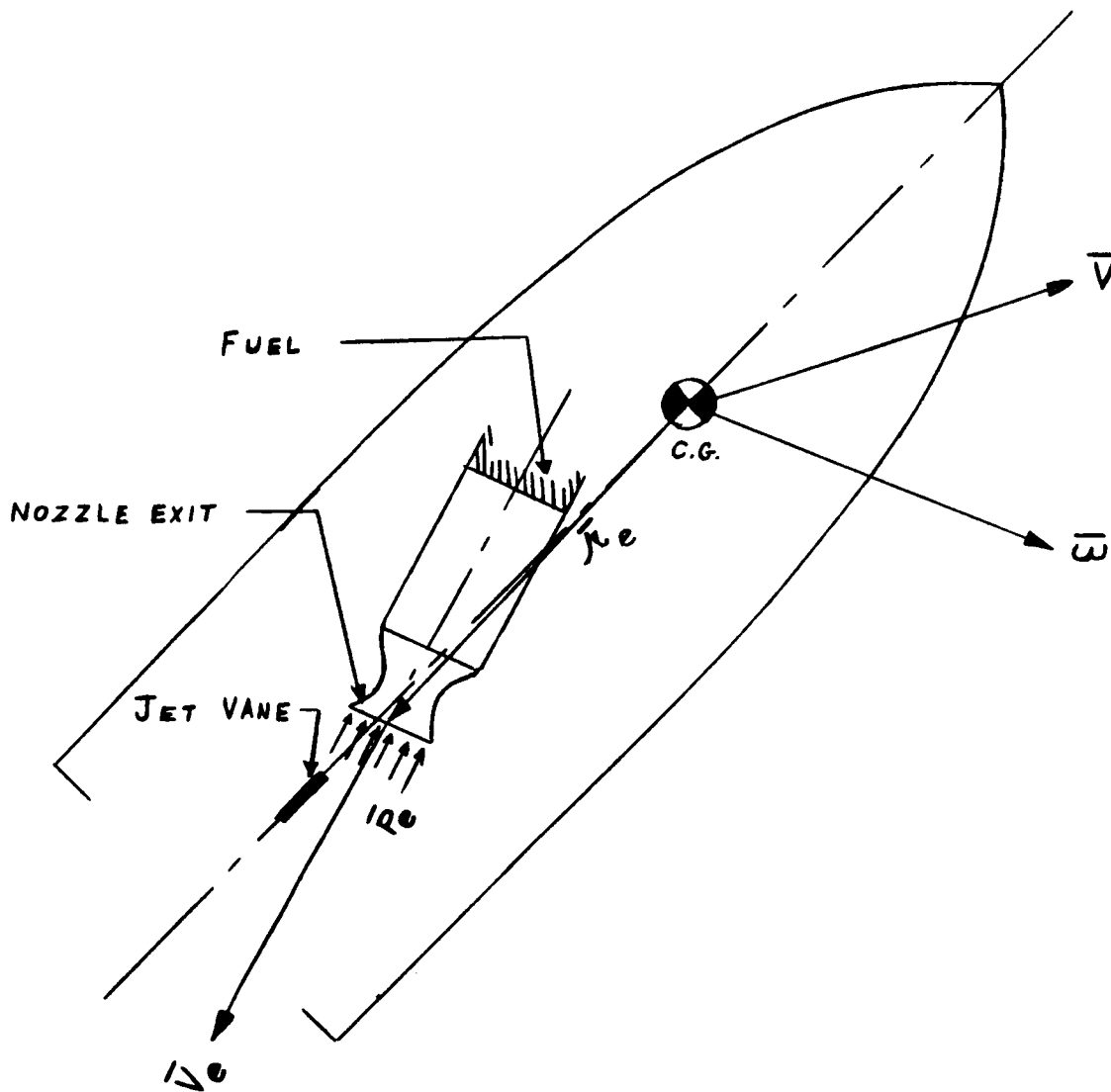


FIG 6-2

FIGURE 6-2. - TYPES OF CONTROLS AND BODY AXIS SYSTEM



\bar{V}_e = JET EXIT VELOCITY RELATIVE TO NOZZLE EXIT

FIGURE 6-3.- SKETCH OF MISSILE (REF. 6-7)

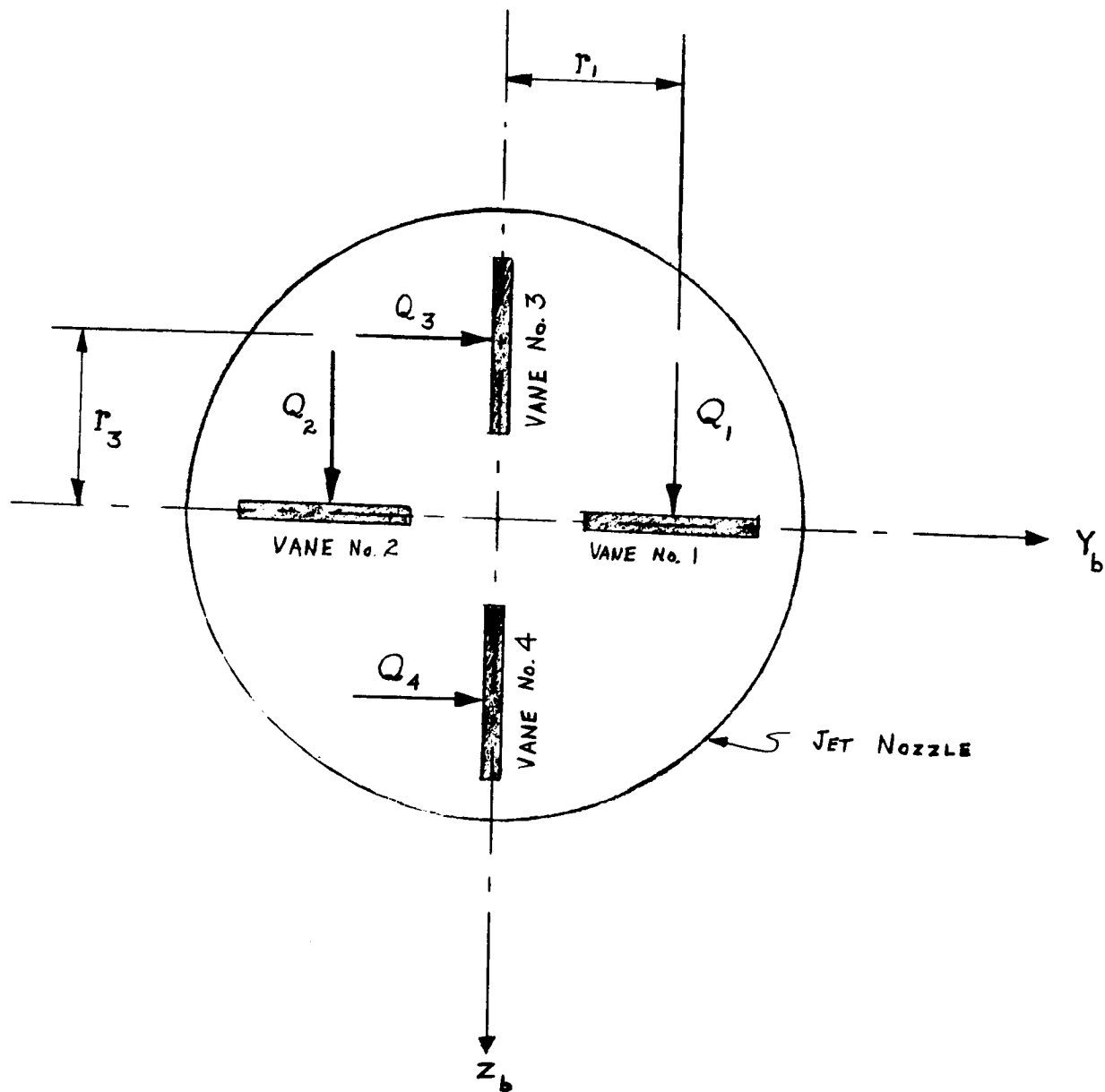
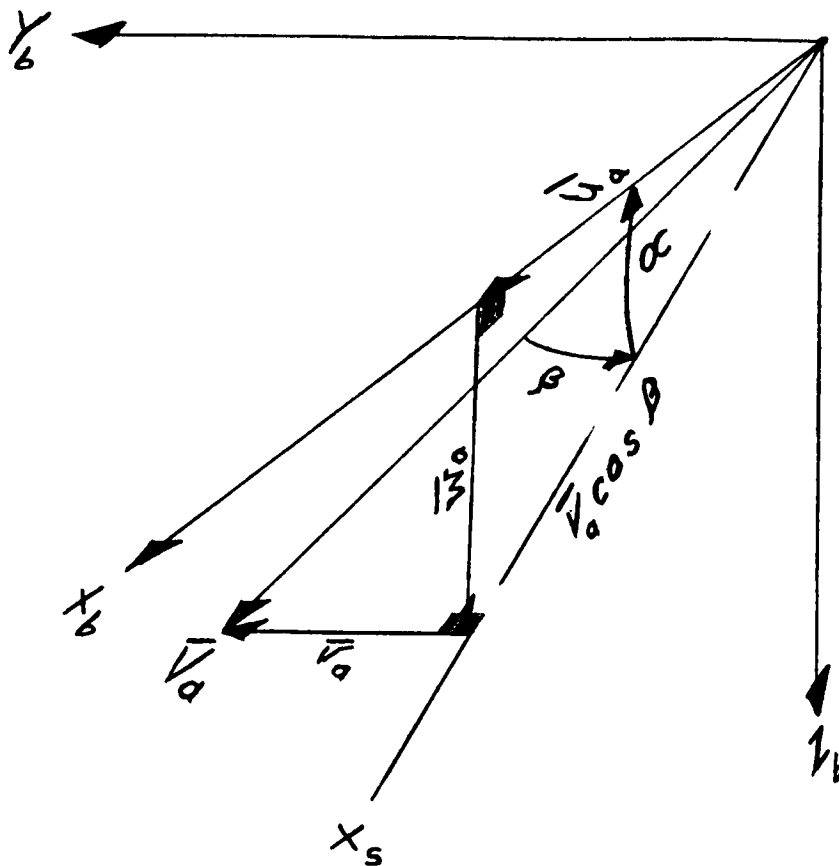


FIGURE 6-4.-TYPICAL JET VANE ARRANGEMENT (LOOKING FORWARD FROM AFT END). (REF. 6-7)



$$\bar{V}_a \cos \beta \cos \alpha = \bar{U}_a$$

$$\bar{V}_a \cos \beta \sin \alpha = \bar{W}_a$$

$$\bar{V}_a \sin \beta = \bar{V}_a$$

\therefore

$$\text{TAN } \alpha = \frac{\bar{W}_a}{\bar{U}_a}$$

$$\text{SIN } \beta = \frac{\bar{V}_a}{\bar{V}_a}$$

FIGURE 6-5. - DEFINITION OF α AND β

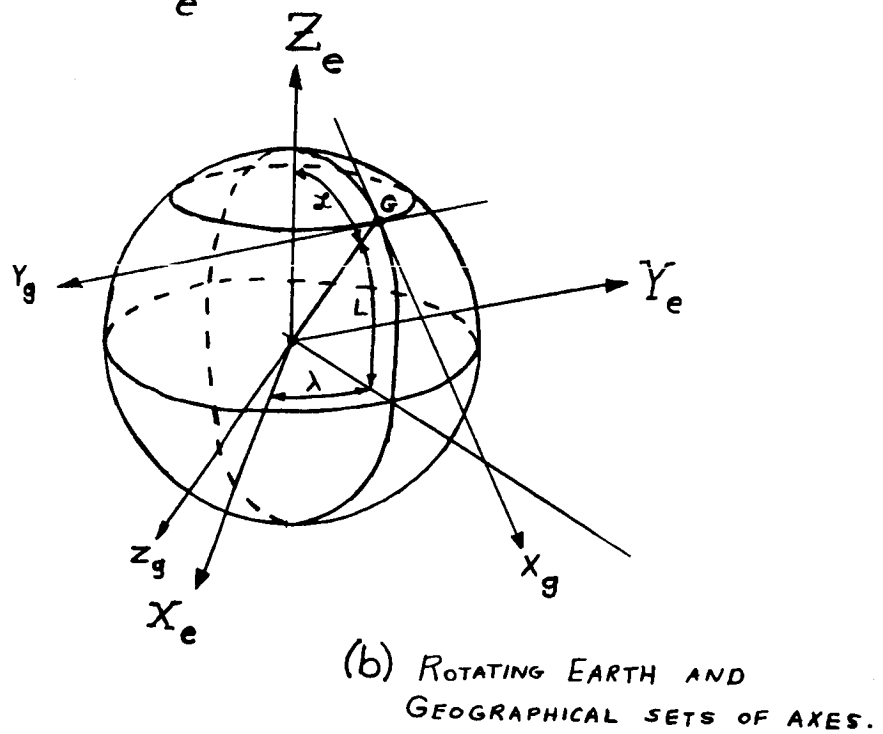
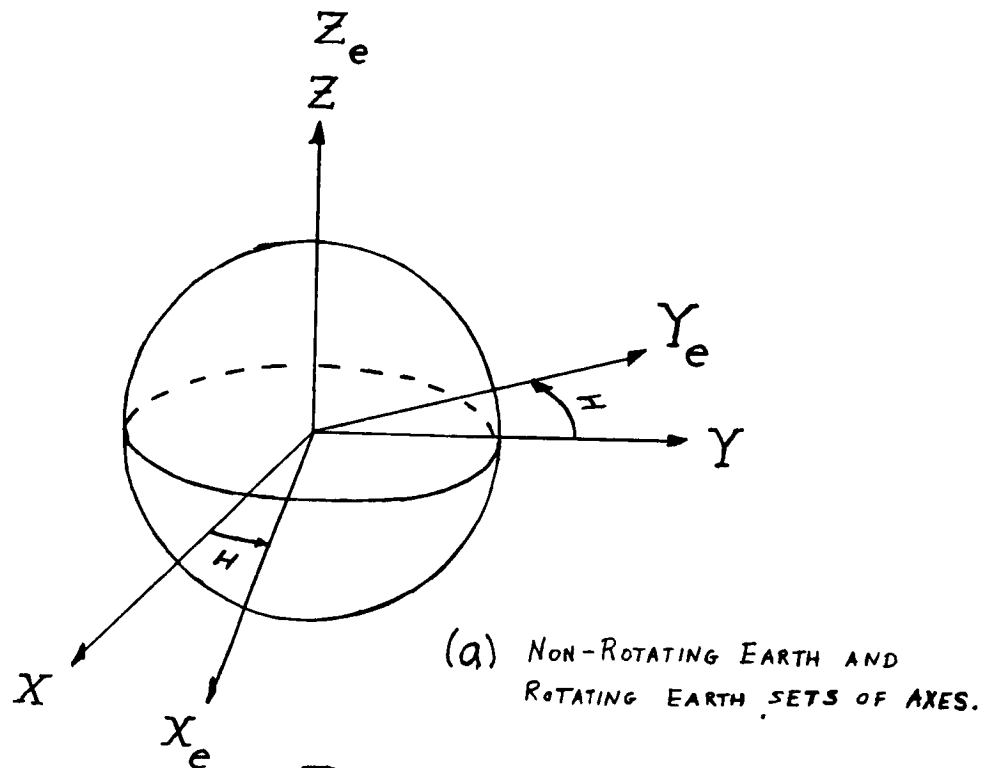
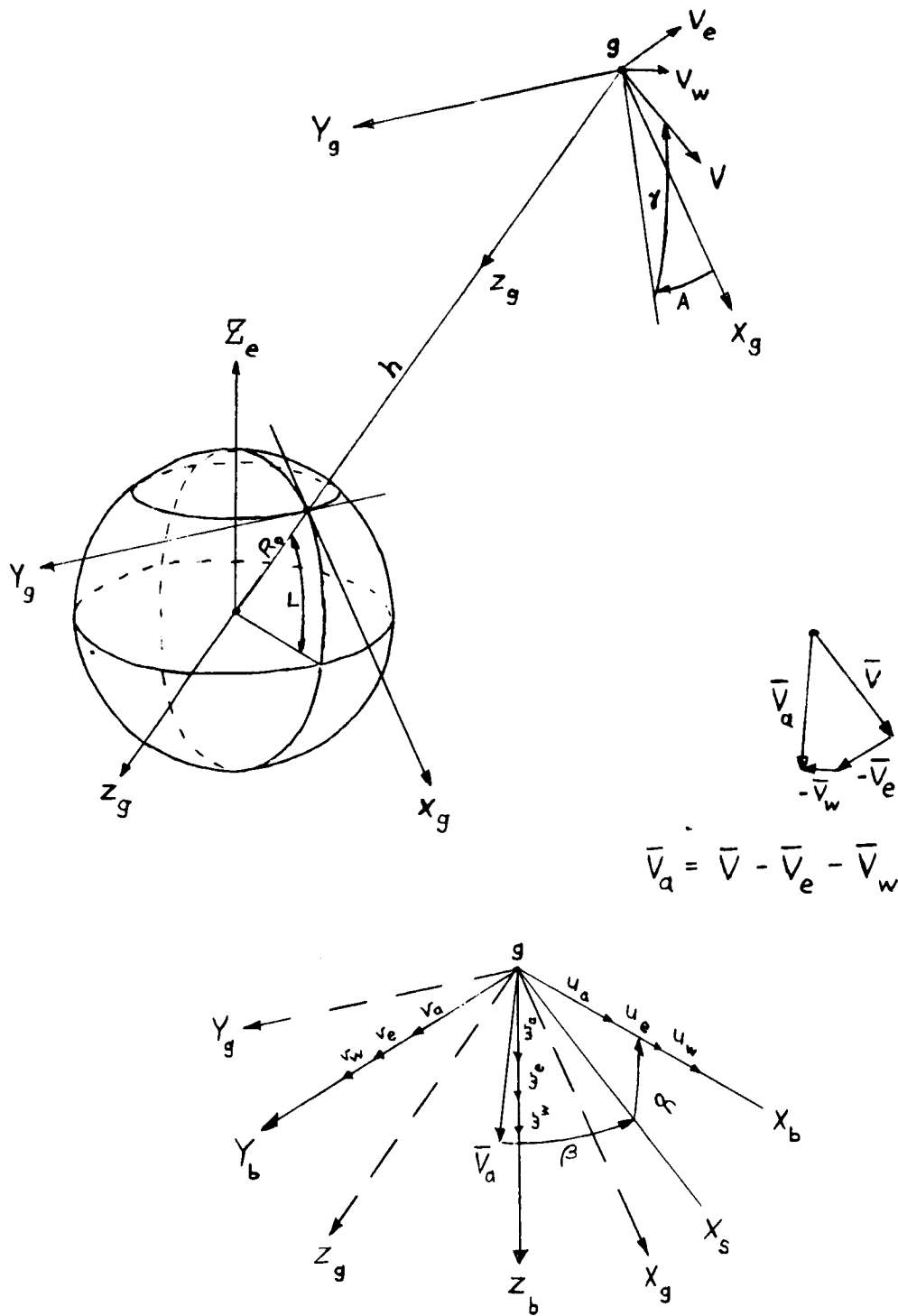


FIGURE 6-6. - GEOMETRY OF VARIOUS SETS OF AXES USED.



(C) GEOGRAPHICAL AND BODY SETS OF AXES

FIGURE 6-6.-CONCLUDED

I

SECTION VII

INERTIAL SPACE NAVIGATION

7.0 Introduction

In the past few years increasing reference has been made to a new type of navigation which has been termed Inertial Navigation. The purpose of this section is to give a brief introduction and discussion of some of the fundamentals of inertial navigation. The material presented is derived from the various references which are listed at the end of the text. In many cases the text and the Figures presented are taken directly from these references.

Although the concepts of Inertial Navigation are relatively new the principles upon which the process is based have been well known for years and essentially it is a simple application of applied mechanics. In order to learn something of the subject it will be approached from the standpoint of trying to answer the questions:

- A. What is it?
- B. Why do we need it?
- C. How does it work?
- D. How well does it work?

7.1 What is Inertial Navigation?

One definition of Inertial Navigation has been given as: Navigation without the use of any radiation, either natural or man made. -- in other words it is self contained. This definition is of a rather negative nature that merely gives one of the attributes of an inertial navigation system. A more descriptive definition would be: A process in which determination of navigational parameters with respect to the fixed stars is made from

measurements of acceleration acting on the body. If the navigation is concerned with position with respect to the Earth (or to another rotating planet) the process would also include a conversion to navigational parameters referenced to the moving earth. An inertial navigation system is then one which is self contained and one that by a process of integration of imposed accelerations determines changes in velocity and position.

7.2 Why do we Need Inertial Navigation?

The present methods of navigation are considered fairly accurate and we have so many means of navigating that it is hard for even the navigators to keep up with them. Airplanes can take off and fly half way around the Earth and land on a particular runway at a particular airport. Bombers can fly over a desired target area with good precision even in conditions of bad weather. The comparatively new developments in Omni DME, Loran, radar navigation systems, etc. are successful to the extent that additional new methods of navigation must be questioned as to their usefulness. Inertial navigation does promise to fill certain needs that are not adequately met by existing systems. The advantages of inertial navigation systems can be placed into two categories: military and civil.

Military advantages:

- (1) Does not depend on ground facilities for reference
- (2) Is not subject to jamming -- Newton's laws of motion and gravitation are difficult to tamper with
- (3) Emits no radiation that can be detected by an enemy
- (4) By virtue of its independence of outside signals there is no limit as to how many systems can be utilized simultaneously.

Civil application advantages:

- (1) Could possibly be used to simplify the existing complex network of navigational facilities
- (2) Would allow continued operation of our commercial transport fleet in times where enemy attack may be threatened and the existing navigational aids would have to be turned off to prevent homing in by enemy

All these reasons are in addition to the obvious advantage in application to outer space flight where most of the present navigation schemes have no meaning.

7.3 How Does Navigation Work?

7.3.1 Basic principle.- Inertial navigation is a rather fundamental application of classical mechanics whereby the position or change in position of a body is determined from measurements of accelerations. It is an application then of Newton's Laws of Motion. In addition there are other principles or facts that have important bearing, such as: (1) Newton's Law of gravitation which states that every mass particle attracts every other mass particle with a force proportional to the product of their masses and inversely proportional to the square of the distance between the particles; (2) the principle of equivalence in the general theory of relativity that says gravitational mass and inertial mass are equivalent; (3) the spatial direction of the Earth's gravitational field at any point serves as a unique identification of that point.

This latter point requires further discussion. As will be pointed out in SECTION XIV the shape of the Earth is not a perfect sphere, but it can

be approximated by Hayford's Spheroid of 1909 which has an ellipticity of $1/297$. Because of this shape the normal to the gravity field does not always head directly to the center of the Earth. For example at 45° latitude there is about 11 minutes of arc between the plumb bob vertical and the true line to the center of the Earth. Shown on Figure 7-1 is the geoid surface which is by definition an equipotential surface of the Earth's gravity field. The direction of the gradient of the gravity potential at the surface of the geoid, the force of gravity, is defined as the vertical. This is defined by a plumb bob with its base fixed with respect to the surface of the Earth. The specific force of gravity is then a vector addition of the gravitation specific force and the centrifugal specific force associated with daily rotation. Because the geoid does not have a smooth surface, the vertical is not in general parallel to the normal to the reference ellipsoid at the same position. The angular deviation, called the station error is generally less than one second of arc.

7.3.2 Coordinate systems.- The uniqueness of the vertical at any point is the basis of astronomical position. The astronomical latitude is the complement between a line parallel to the Earth's polar axis and the local gravity vector. The astronomical longitude is the angle about the Earth's polar axis between a reference vertical (usually that at Greenwich) and the local vertical. The astronomical set of coordinates are very useful in inertial navigation but unfortunately accelerometers measure with respect to inertial space so that other coordinate systems are also necessary. Shown in Figure 7-2 are the Geocentric Inertial coordinate system which is centered in the earth with the axis coincident with the Earth's polar axis. Also

shown in Figure 7-2 are the Geocentric Earth reference coordinates in which the Z axis is again coincident with the polar axis but the X and Y axis are fixed in the Earth and thus rotate around the polar or Z axis at the rate of 15° per hour. Another useful coordinate system is shown in Figure 7-3 and is referred to as the local geographic reference coordinate. In this reference system there is the option of alining one of the axes along a great circle which could include the departure point and destination and thus would simplify the navigation problem. The significant difference between the geographic coordinate of Figure 7-3 and the astronomical coordinate system is that the latter has the Z axis alined with the local vertical rather than normal to the ellipsoid.

Knowing something of the nature of the gravity field about the Earth and the various coordinate systems which are useful it is well to return to the question of how does Inertial Navigation work.

7.3.3 Simplified example.- As a simple example consider a cart on a table top. The cart is initially at rest and a force is applied to move it along the table top. Its position at any time can be determined by measuring and doubly integrating the applied acceleration. Mechanizing this simple problem brings out many of the significant features of inertial navigation.

First of all since acceleration is a vector quantity accelerometers must be mounted on the cart so as to sense the components of the acceleration with respect to the coordinate system within which the measurement of position is to be made. Each accelerometer must be accurate and also must be maintained in a precisely known relationship to the coordinate system — this latter requirement gives rise to the need for a stabilized mount for

the accelerometers that will maintain the desired orientation. Because an accelerometer cannot distinguish between acceleration and gravity either the stable mount must be oriented so that gravity components are not sensed or else corrections must be added to account for this factor.

For such a simple example the components of an inertial navigation system could be split into three groups: (1) accelerometer package to sense accelerations with respect to the axis of the chosen coordinate systems (2) a stable platform (which normally uses integrating rate gyros as its primary instruments) that will maintain the orientation of the accelerometer package and (3) a computer that will doubly integrate the outputs of the accelerometers and put in suitable corrections so that position will be known.

When the range over which the cart on the "table top" travels becomes very large the problem becomes more complicated because the components of gravity which must be accounted for become large. In the sketch of Figure 7-4 which shows the X coordinate tangent to the surface of the Earth it can be seen that as X becomes large with respect to the radius of the Earth the force of gravity (which effectively lies along the line from the center of the Earth to the position of the cart) tend to become alined along the X axis. The acceleration sensed by the X accelerometer is

$$A_x = \ddot{x} + g_x$$

where g_x is the component of gravitational force. This component may be expressed

$$g_x = g_0 \frac{a^2 x}{(a + h)^3}$$

If it is assumed that there is a negligible change in altitude the expression may be simplified to

$$g_x = g_0 \frac{x}{a}$$

and still provide an adequate approximation for g_x for relatively small changes in X .

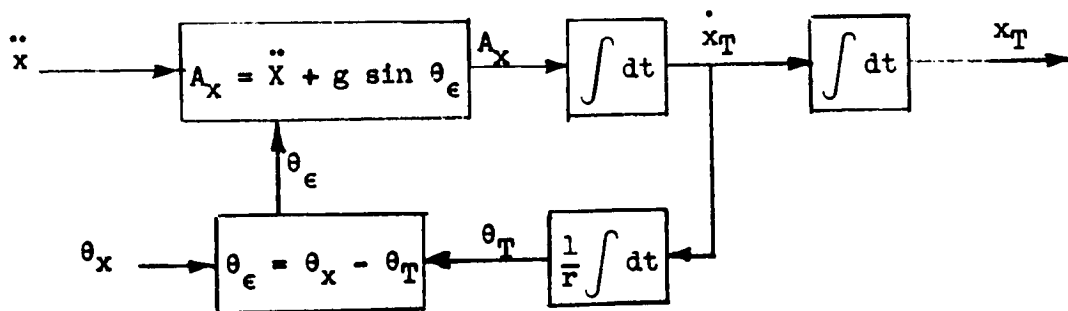
7.3.4 Schuler tuned pendulum.- Even though it is within the capability of a computer to calculate g_x for large changes in X this operation places rather stringent requirements on the computer. Another, perhaps more reasonable, approach is to maintain the orientation of the stable platform upon which the accelerometer is mounted so that it will be normal to the force of gravity and **thus** the accelerometers would not sense the components of gravity. This could be done by mounting a pendulum on the stable table so that as the pendulum aligned itself with the gravity forces the table would be aligned perpendicular to the pendulum. This problem was first approached by Dr. Maximilian Schuler, a German scientist and professor and it was he who first pointed out that what was needed was a pendulum with vertical determination characteristics independent of vehicle movement. A simple pendulum having a reasonably long arm would be subject to disturbances away from the vertical, if its base were accelerated. To be free of such errors the length of the pendulum arm would have to be equal to the radius of the Earth. With such a pendulum the point of suspension or base of the pendulum could be moved about over the surface of the Earth without disturbing the pendulum mass and thus the pendulum would always indicate the vertical. Such a pendulum is, of course, impossible to build and even a distributed mass type of pendulum having the same dynamic characteristics

would be virtually impossible to build because of the extremely small distances required between the centroid of mass and the pivot point.

Because the pendulum is essentially a second order undamped system it is possible to construct a servo system having the same dynamic characteristics. The period of a pendulum is determined from the formula

$$T = 2\pi \sqrt{\frac{L}{g}} \quad \text{where } L \text{ is}$$

the length of the pendulum and g the gravitational acceleration. The Schuler pendulum has a period of 84.4 minutes. A simplified schematic of the operation of a servo system Schuler Pendulum is shown in the following diagram:



θ_T = angular rotation of the table upon which the accelerometer is mounted

θ_x = angular arc over the Earth's surface covered by the x movement of the table

θ_ϵ = error in alinement of table normal to true vertical

The accelerometer is mounted on a tilting platform whose angle of tilt is determined by a motor which is driven by the doubly integrated output of the accelerometer times the constant K . The transfer function relating X to the applied acceleration has a characteristic equation of the form $p^2 + K = 0$ which indicate an undamped second order system having a frequency of oscillation equal to K . If K were adjusted to equal $\frac{g}{L}$ the oscillatory characteristics would be the same as a Schuler pendulum and would be said to be "Schuler tuned". With such a system the tilt angle of the platform becomes equal to the angular arc that the platform has traversed over the Earth's surface. Thus if there were a way to "remember" the orientation of the vertical at the starting point the position of the platform could be obtained by measuring the angle between the instantaneous vertical and the vertical at the start of the problem. This angular position could easily be related to latitude and longitude angles by aligning the X and Y accelerometers along and perpendicular to the meridian lines of the Earth. Thus there are means of determining position both analytically by suitable computer operations on the double integral of acceleration and geometrically (or partly geometrically and partly analytically) by measuring the orientation of the vertical with respect to the reference coordinate system.

7.3.5 Hardware components.- To fully understand the mechanics of inertial navigation it is desirable to understand the operation of some of the basic components -- the accelerometers, rate gyros, stable platforms, computers, etc.

Figure 7-5 is a schematic drawing of the HIG type, single-degree-of freedom gyroscope originally developed by the Instrumentation Laboratory, MIT. Basically, the gyro consists of a spinning wheel driven by an electric motor, mounted on preloaded ball bearings and contained in a hermetically sealed can or float with shaft extensions. The float is completely submerged in a viscous fluid which has the same average density as the float and shaft. This serves to reduce friction about the axis defined by the pivots design. Coaxial with the shaft is a signal generator which gives a voltage proportional to the angular displacement of the float relative to the case, and a torque generator which can be used to apply torque to the float.

The basic principle of operation of the gyro can be explained in terms of the three axes shown in Figure 7-5. The spin reference axis lies along the angular momentum vector (spin axis) of the wheel when the signal generator output is zero. The output axis is normal to the spin reference axis, and is the axis about which the float is free to turn. The input axis is normal to the output axis and spin reference axis. The input quantity to the instrument is an angular motion of the case, relative to inertial space, about the input axis. The resulting output is a movement of the float relative to the case which results in a voltage from the signal generator. The operation is explained by the familiar physical fact that when a torque is applied to a spinning wheel so as to change the direction of its spin axis, the spin axis tends to align itself with the torque vector. Conversely, when the axis of a spinning wheel is forcibly precessed or rotated, the wheel through its bearings exerts a torque about an axis perpendicular to

the axis of forced rotation. In the HIG gyro, movement of the case about the input axis causes a force precession of the gyro wheel about this axis. The gyro wheel thus exerts a torque on the float about the output axis. Initially, this torque accelerates the float, but as the float gains angular velocity, the viscous shear torque reduces the acceleration to zero and the float reaches a steady angular velocity. The gyro torque is then balanced by the viscous shear torque and the output angular rate is proportional to the input angular rate. The fact that the output signal is proportional to the integral of the input angular rate is the source of the term "integrating gyro". The gyro thus serves as an attitude reference.

HIG gyros act as precision angular motion sensors, rather than sources of torques to overcome friction or unbalances. Normally, they have an operating range of only a few degrees and to prevent various cross coupling errors, input angles should be kept small. Therefore, for inertial guidance use, gyros are usually mounted on a platform or base which is servo-driven to maintain the gyro output at or near a null. The platform thus remains fixed in orientation relative to inertial space, or is rotated at a rate determined by torque generator input. A much simplified sketch of the one degree of freedom stabilized platform is shown in Figure 7-6. A typical three degree of freedom stabilized platform configuration is shown in Figure 7-7.

Figure 7-8 is a schematic of a practical type of accelerometer instrument based on the HIG gyro construction. The seismic mass exists in the form of a pendulum and the force generator is the torque generator. The pickoff is the signal generator. Flotation virtually eliminates uncertainty

friction torques at the pivots. Because of the pendulous mass, acceleration of the instrument along the input axis creates a torque about the float pivot axis. This torque causes rotation of the float and a consequent signal generator voltage proportional to θ_0 . This voltage is used to generate a current which is applied to the torque generator to give a torque which "constrains" the pendulum and keeps θ_0 small. The current, I , is thus proportional to acceleration along the input axis. The gain of the feedback system must be kept quite high so that deflection of the pendulum under high input acceleration is small. Otherwise, a "cross talk" torque is developed which is proportional to the product of the acceleration along the pendulous reference axis and the sine of the deflection angle θ_0 . Instruments of this type, called force feedback pendulums or constrained pendulums, are available commercially. They are made with a wide variety of dynamic range and frequency response.

Velocity and position are the quantities of interest in navigation, rather than acceleration. Increased accuracy and reliability may sometimes be obtained by performing integration in the accelerometer. Basically, this is done by making the force acting on the seismic mass proportional to a rate of some kind. For instance, the current fed to the torque generator in Figure 7-8 might be applied in pulses of constant area but variable rate. Pulse rate is then proportional to acceleration and total number of pulses to velocity. Another useful device and one used by the Germans in the V-2 is the pendulous gyro accelerometer (PGA). This instrument is a pendulum in which the force generator is a gyroscopic element. Figure 7-9 is a

schematic of such an instrument based on the HIG gyro construction. The output of the signal generator is fed to the servomotor which rotates the gyro case about the input axis at a rate such that the torque developed by the gyro element just equals the pendulous torque. The angular rate of the gyro case is thus proportional to acceleration and the total angle turned by the gyro case is proportional to velocity. As with the instrument of Figure 7-8, the gain of the feedback loop must be kept high so that θ is very small. The torque generator of the gyro can be used to apply additional torques to the gyro float which add to the pendulous torque. In this way, gravity may be added to the thrust acceleration to give true acceleration and velocity.

7.3.6 Typical configurations.- As is usually the case when engineers are allowed some freedom in development of a system to do a particular job there are a number of configurations of inertial navigation systems in operation or in the design stage. Figures 7-10, 7-11, and 7-12 present three basic configurations of inertial navigation systems. These systems differ quite markedly in the degrees to which the computer must store the reference coordinate system and determine the desired navigational data.

Figure 7-10 presents a three gimbal system in which the accelerometers are mounted on the same platform as the rate gyros which are the heart of the stable table. In this case the table is operated ala the Schuler tuned pendulum so that one axis tracks the local vertical -- the reference coordinate systems being stored analytically in the computer. The stable platform instruments the astronautic reference coordinate system by precessing the gyros. Navigation data is obtained as signals representing

velocity or acceleration measurements relative to the geocentric inertial coordinate system of Figure 7-2 and converted into Earth data by computer operations that convert the signals into the geocentric Earth coordinate of Figure 7-2.

Figure 7-11 shows a five gimbal system in which the platform on which the accelerometer are mounted is Schuler tuned to track the local vertical and instruments the astronomical reference system. The stable platform with the rate gyros is stabilized in inertial space and thus instrument the geocentric inertial coordinate system. This configuration allows direct angular measures to determine positions on the Earth's surface relative to the astronomical coordinate system.

The configuration shown in Figure 7-12 is also a three gimbal system where the accelerometers are mounted on the stable table which is maintained in inertial space. The platform instruments only the geocentric inertial coordinate system and navigation data is obtained from computer operations.

7.4 How Well Does an Inertial Navigation System Work

An inherent disadvantage of an inertial navigation system is that the errors in the increase with the problem time. Determining position by doubly integrating an acceleration measurement causes any error in measurement to show up as a second power function of time. Because of this time dependency of the errors the accuracy requirement of the accelerometers and the rate gyros used to provide stable table operation are much more stringent than has been required of such instruments in previous mechanisms. For

an ICBM type of operation the accuracy requirements of accelerometers and rate gyros for each 1000 foot of tolerable error are given as a function of range in the graph presented in Figure 7-13.

The fact that the operation of inertial navigation systems (which operates independent of outside signals) are based upon nonvariant phenomena (Newton's laws of motions, etc) is an advantage in that any increase in accuracy of the system components results in increased accuracy of the overall system.

Using the principles of the Schuler pendulum enables the system errors to be limited to a somewhat restricted type of oscillatory buildup -- at least on the axes with respect to which the pendulum can be utilized. In this case the amplitude of the error oscillation would be dependent upon a combination of such factors as initial misalignment of the pendulum, accelerometer bias signals and "cross talk" between acceleration components along the other axes caused by misalignment of the stable table. Because the angular drift of the stable table is a function of time the oscillating limits of the computed errors of even a Schuler tuned system increase with time. The principle of a Schuler tuned system has no application to the vertical axis (altitude axis) and thus the errors in altitude measurement would show a parabolic variation with time. These errors in altitude measurement would also affect the measurements along the other axes where the Schuler tuned principle is applied, because the error in altitude would be an error in the effective length of the pendulum and would cause the period of oscillation to be in error as compared to a Schuler tuned system. This difference in dynamics would cause additional errors in the measurement of acceleration due to sensing gravity components.

REFERENCES

1. Wrigley, Walter, Woodbury, Roger B., and Hovorka, John: Inertial Guidance. IAS Preprint 698, presented Jan. 31, 1957.
2. Slater, J. M., and Duncan, D. B.: Inertial Navigation. Aeronautical Engineering Review, Vol 15, No. 1, Jan. 1956.
3. Klass, Phillip J.: Inertial Guidance. Aviation Week Special Report, Vol 64 Nos. 1-4, Copyright 1956.
4. Russell, William T.: Inertial Guidance for Rocket-Propelled Missiles. Jet Propulsion, Vol 28 No. 1, Jan. 1958.
5. Goetz, Ernest A.: ICEM Inertial Guidance. Astronautics, May 1958.
6. Duncan, D. B.: Analysis of an Inertial Guidance System. Jet Propulsion, Vol 28, No. 2, Feb. 1958.

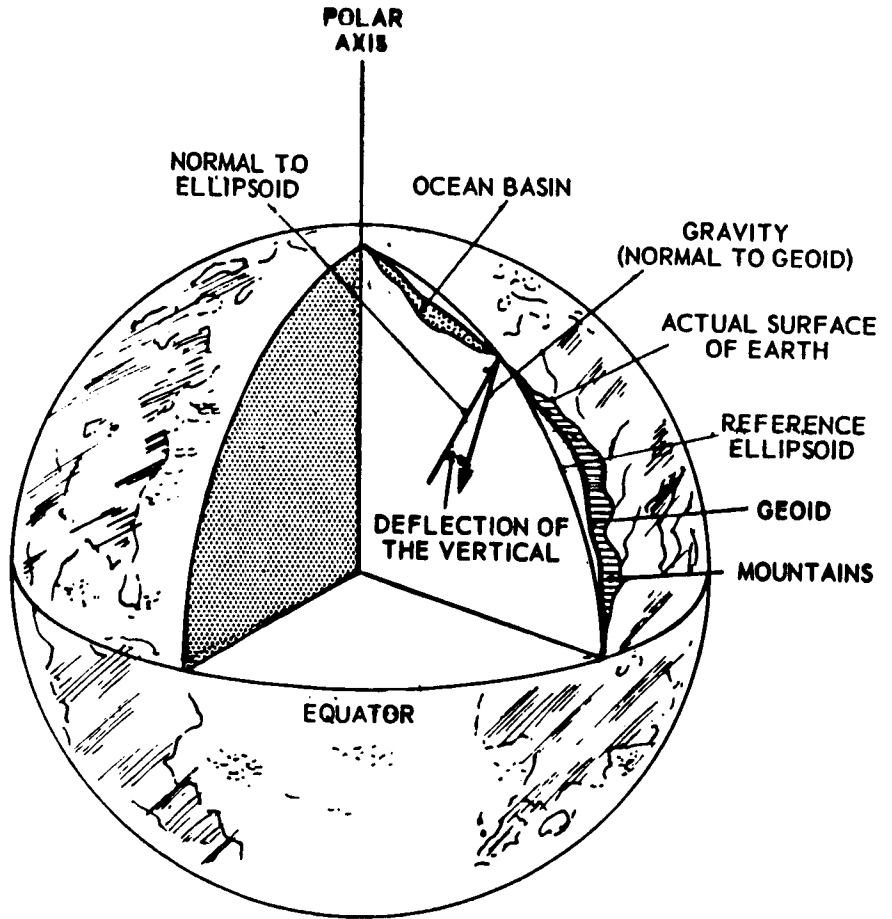


Fig. 7. Relationship of the geoid to a reference ellipsoid.

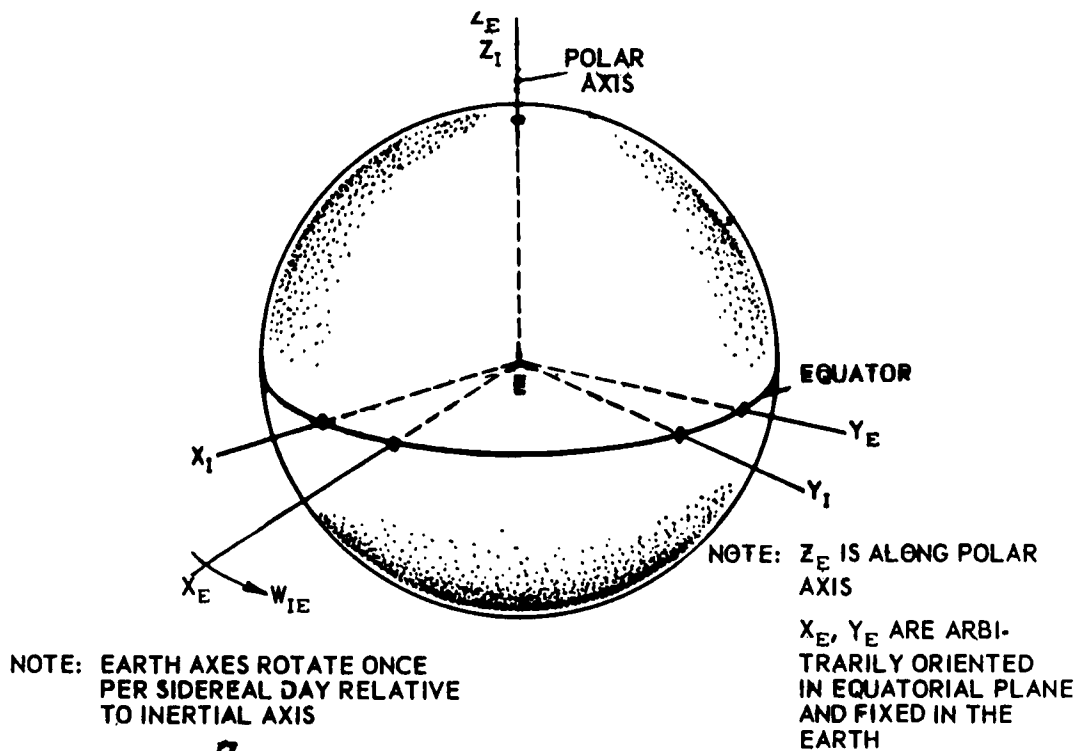


Fig. 2. Geocentric Earth reference coordinate frame.

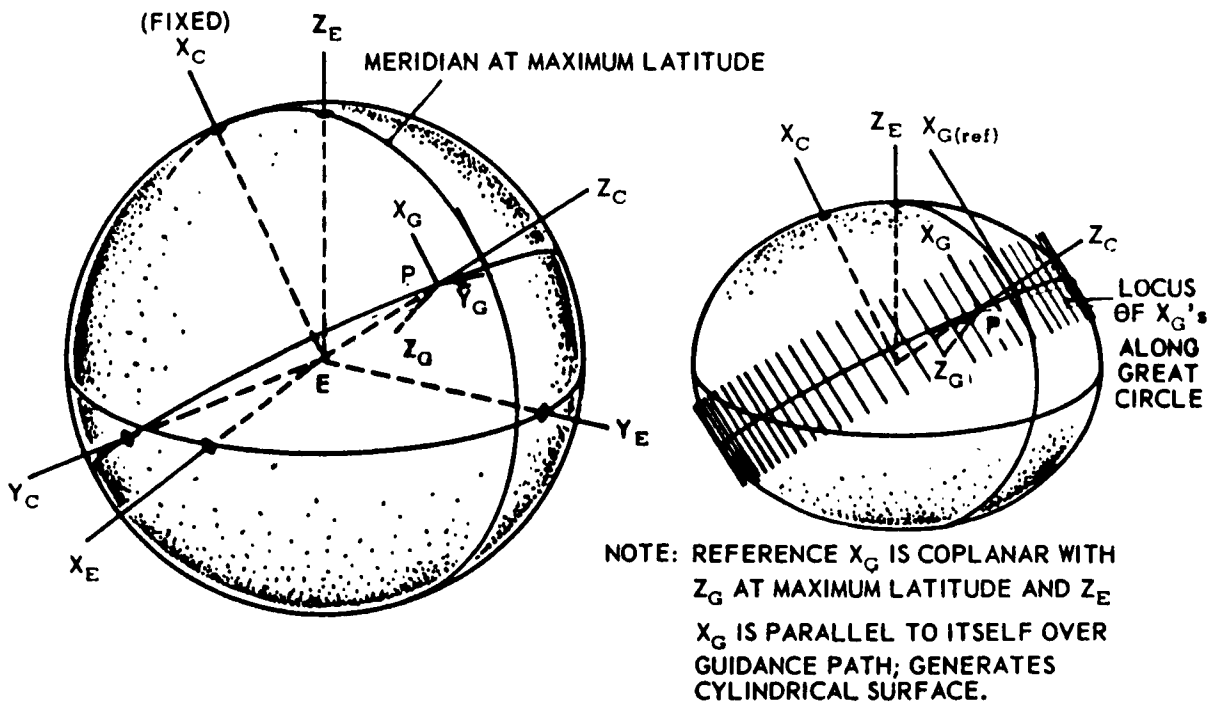


Fig. 3. Local geographic reference frame, great circle grid.

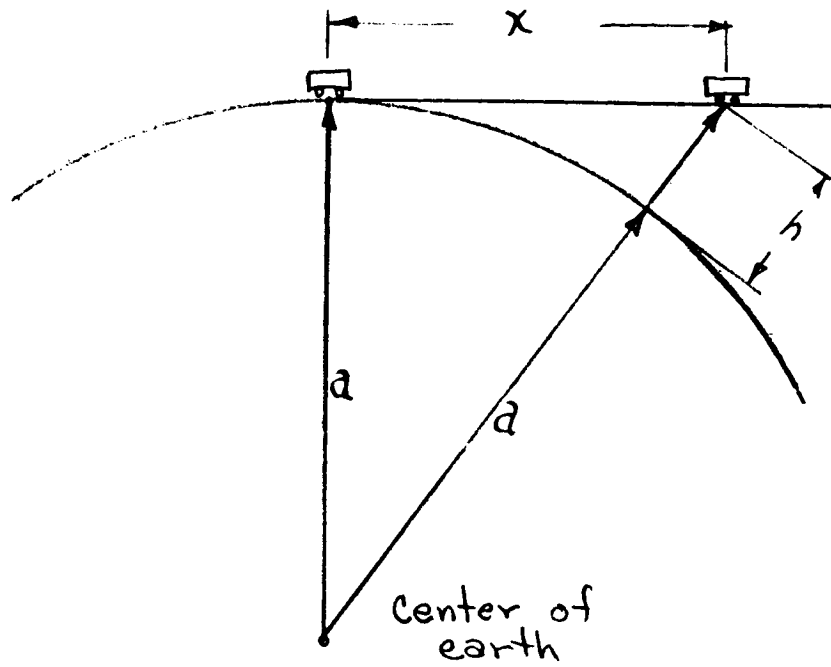


Figure 7.4

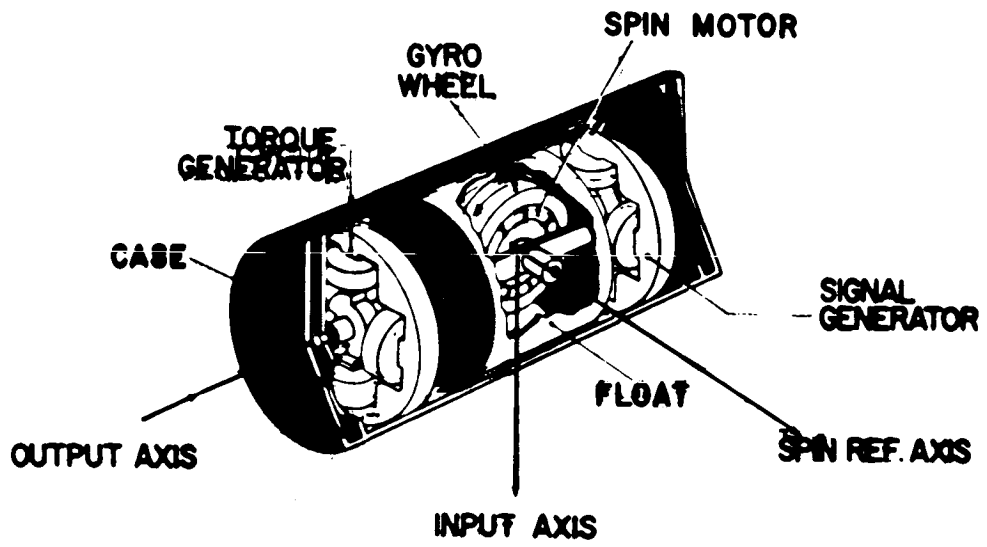
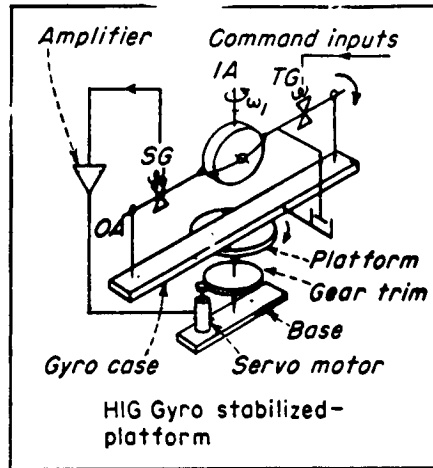


Fig. 7.5 HIG gyroscope



STABILIZED platform (single axis) employing an integrating (HIG) gyro.

7.
FIG. 6

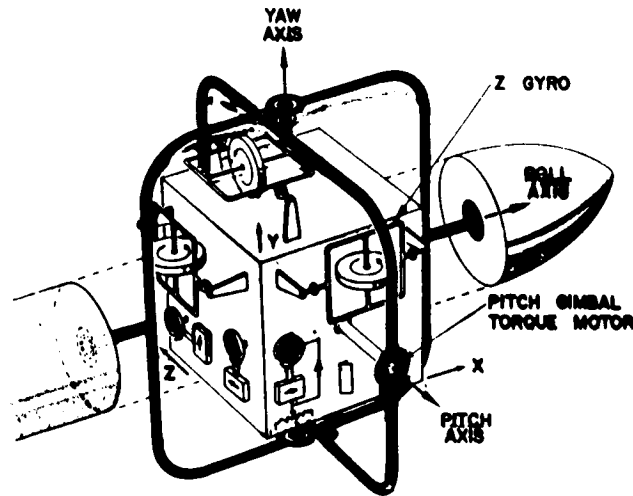


Fig. 7 Stabilized platform

7
FIG 7.7

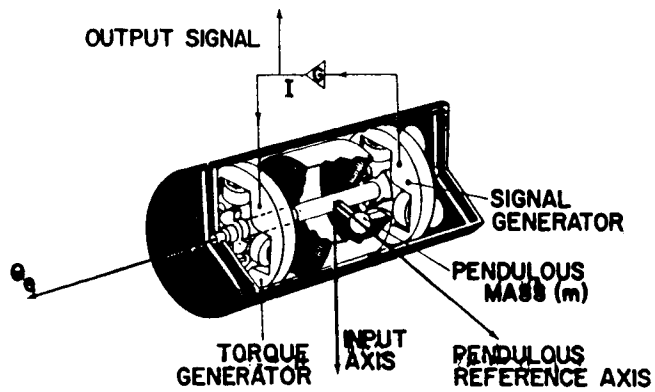


Fig 8 Constrained pendulum accelerometer

JANUARY 1958

7.
FIG 8

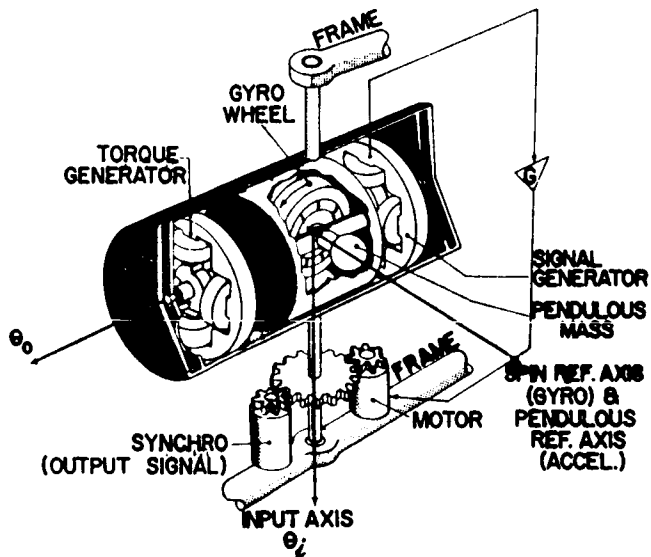


Fig. 7.9 Pendulous gyro accelerometer (PGA)

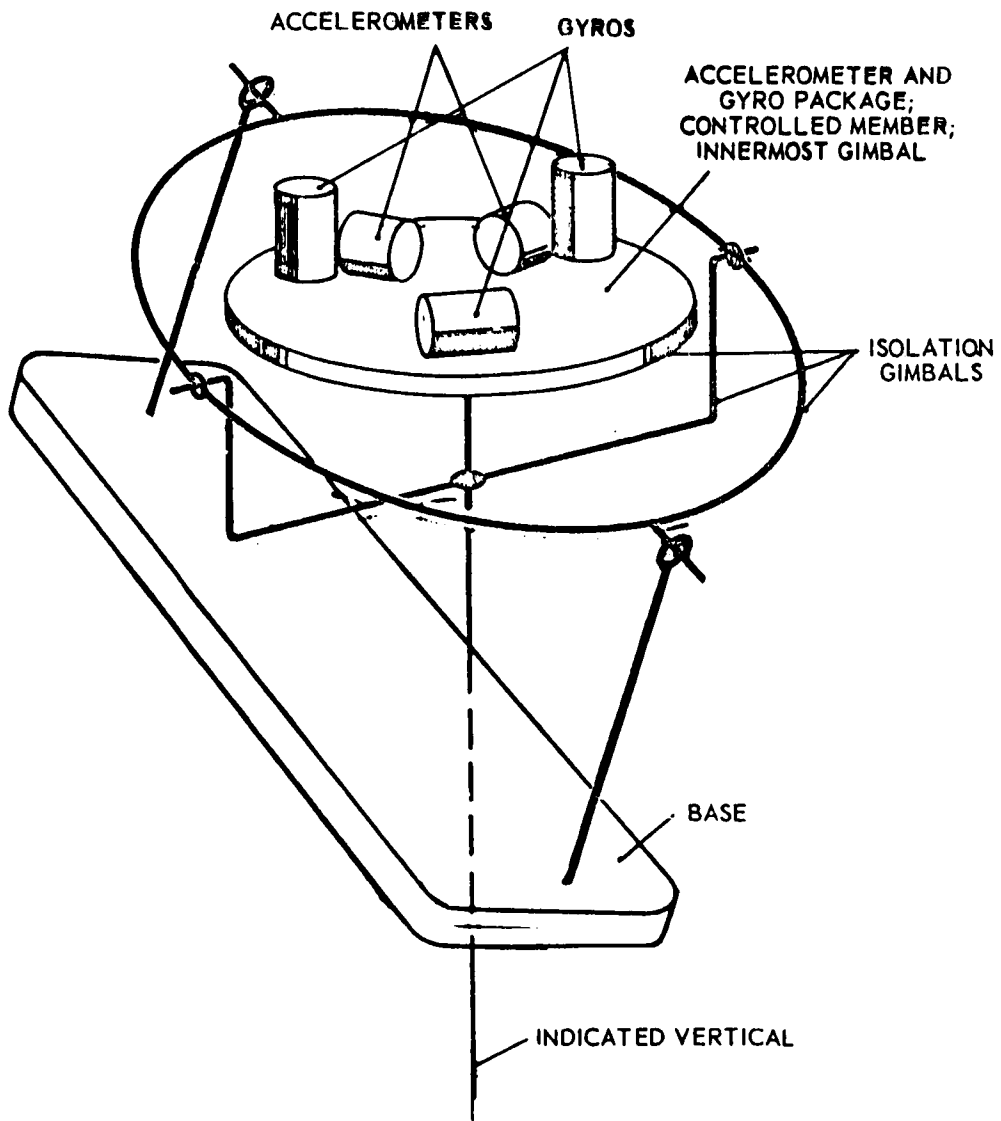


FIG. 7.10 Accelerometer package and gyro package mounted together (3 gimbals).

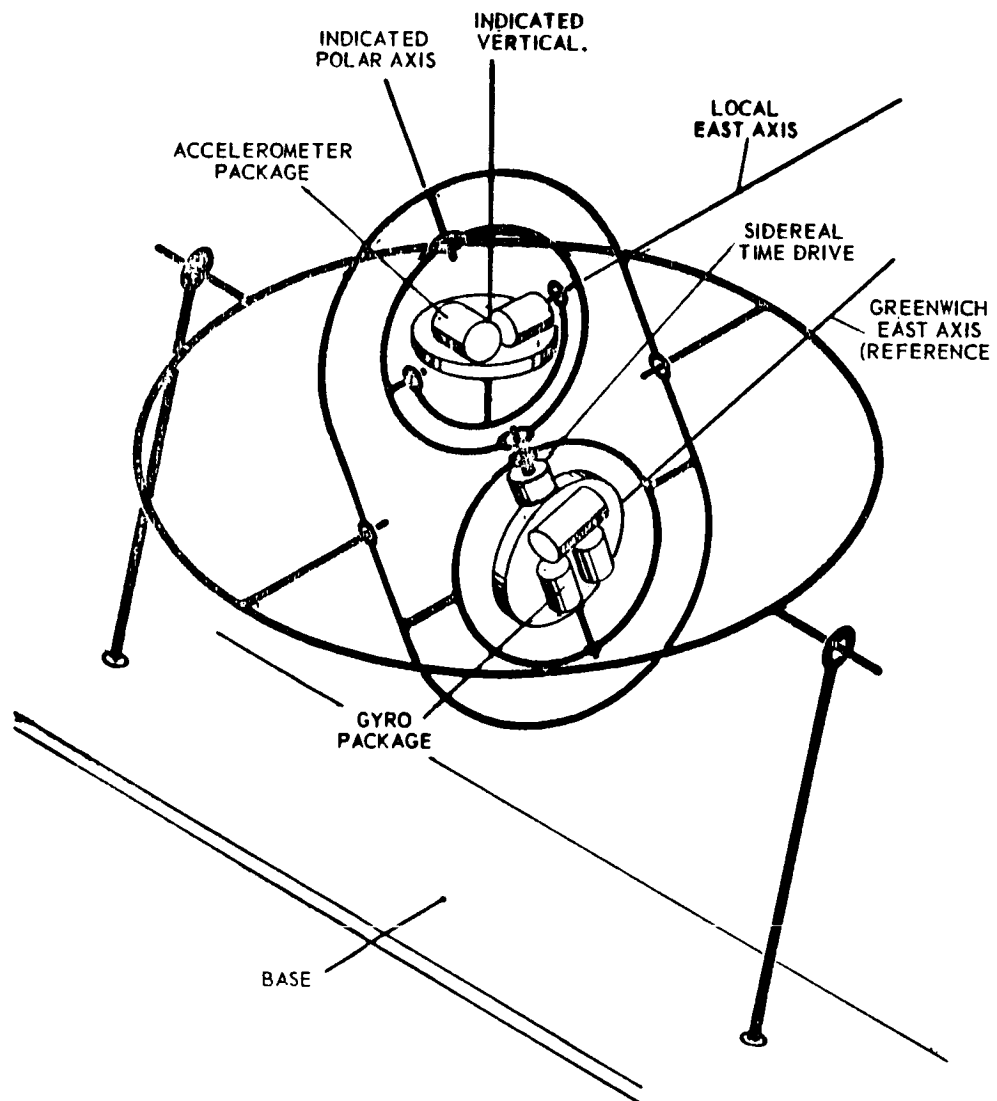


Fig. 7.11 Accelerometer package indicates vertical. Gyro package indicates inertial space (polar axis).

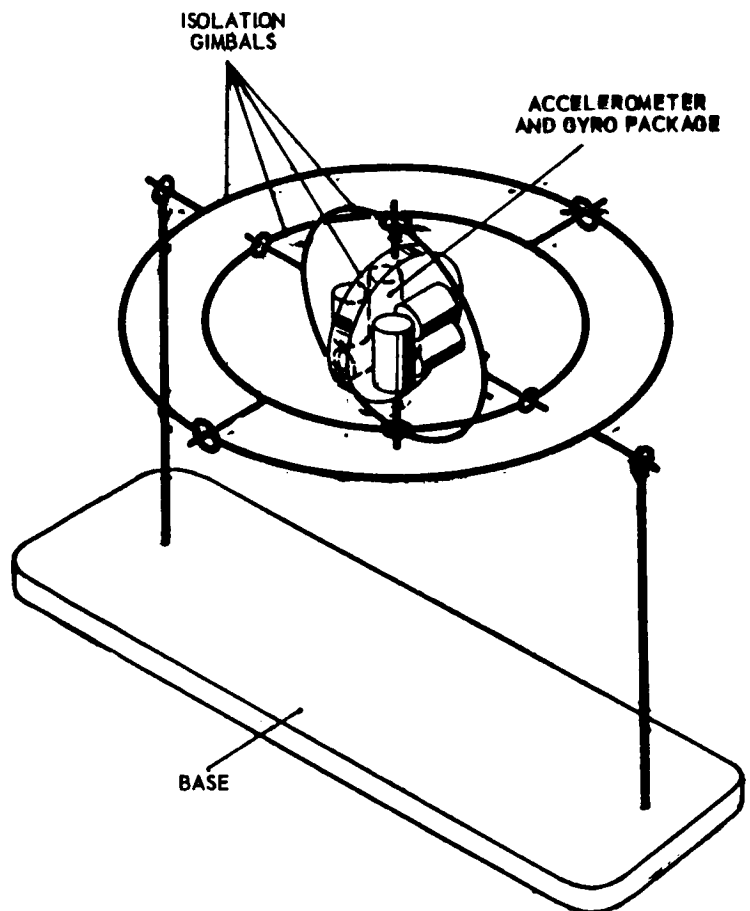


Fig. 7.12 Accelerometer package fixed to gyro package, which is inertial.

ACCURACY REQUIREMENTS FOR GUIDANCE SYSTEM GYROS AND ACCELEROMETERS

FOR 1000' ERROR

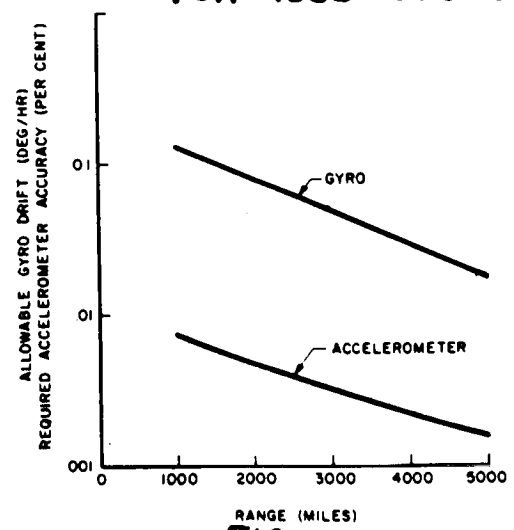


FIG 7.13

SECTION VIII

GUIDANCE AND CONTROL OF SPACE VEHICLES

8.0

Introduction

Guidance as used herein is concerned with the obtaining of input information required to achieve a desired trajectory (as related to space flight), and flight control is concerned with the detailed control of the attitude and velocity (both direction and magnitude) of the space craft for the same purpose. Guidance and flight control systems have reached a state of development where they appear capable from component performance and accuracy standpoints of use in many types of space operations. In spite of this apparent capability, much additional research and development effort will be required in this area before any sort of routine space operations are possible. This situation is chiefly a result of the rather extreme complexity of current high performance systems in relation to the reliability of components and the long operating times required in most space missions. Therefore, in regard to the systems to be described, the problems primarily relate to improvements in reliability and flexibility and reductions in complexity, size, weight, and power requirements. Such improvements may occur in components, system configurations, or in the invention of entirely new guidance and control concepts.

As the basis of discussion of guidance and control systems, we will break down space missions into their various phases such as launching, orbiting, space trajectories, and re-entry. For each mission phase, an attempt will be made to describe the operational concepts; the guidance and control equipment used, contemplated or needed; and the problem areas.

8.1

Launching

As currently envisioned the earth launch phase of most space operations will closely resemble the launch operation of ballistic missiles. A typical launch trajectory is shown in figure 8-1. A multi-staged vehicle will lift off approximately vertically and will be stabilized in the attitude through use of an automatic flight control. After a period of vertical flight the missile will perform an unguided gravity turn by programming the missile to stabilize at tilted attitudes maintaining near zero angle of attack. There also may be periods of unguided coasting following burnout of the various stages. Active guidance will take place in connection with intermediate stages and perhaps in connection with the final stage, although in some current satellite vehicles the final stages are unguided and stabilized through spinning. The main purpose of the guidance is to control accurately the direction of the velocity vector at burnout of the last guided stage. For unguided final stages it is necessary also that the attitude of stage be closely controlled at firing and regulated during burning. Another important guidance function is to accurately control the velocity cutoff of the final stage. A somewhat less critical guidance function is the control of the spacial or geographic position of the vehicle at final stage cutoff.

A number of distinct types of guidance and flight control equipment are currently used in the performance of the functions just discussed. The primary types involve either inertial sensing or electromagnetic tracking. Practically all the attitude systems used for launch control incorporate inertial sensors (gyroscopes and linear accelerometers).

A block diagram of a typical attitude control system is presented in figure 8-2. In an elementary system, the attitude stabilization may be obtained from three single degrees of freedom integrating rate gyros, orthogonally mounted on the body. A high gain control loop is used to accurately slave the missile attitude to the gyro references in order to avoid gyro coupling effects. In fact, less than ten degrees of gyro gimbal freedom is usually provided.

The chief problem associated with these high gain attitude control systems concerns the avoidance of dynamic instabilities resulting from coupling between the control system and the structural or fuel sloshing motions. In most cases the booster configuration is controlled by jet deflection and the control gains must be set high enough to stabilize the system under maximum q conditions (where the configuration's aerodynamic instability is greatest). This requirement results in an excess in stability near lift off and the short period frequency under this condition is fairly high (say 1 cycle per second). Unfortunately, the full fuel configuration results in the lowest frequency condition of the structural modes, and the fundamental fuselage bending mode may have a frequency of just a few cycles a second. An example of the bending modes and their frequency distribution is shown in figure 8-3. The frequency of the fuel motion in the missile may be even lower, and this motion also becomes critical some time after lift off. In most liquid fuel rockets it has been necessary to use some baffling in order to provide damping to the fuel motions. If the open loop frequency response of the control system

is sufficiently high it is possible to add damping to the lowest frequency modes by control action. This approach requires careful choice of sensor location along the body in order to obtain proper phasing and/or requires the use of electronic shaping networks for the same purpose. (See figure 8-2.)

These techniques are not the complete solution to the problem, however, because there are always present higher frequency structural modes which may be excited by control action. In fact, in one case it was necessary to reduce the control response by the order of 100 decibels from its static value in order to avoid trouble with a moderately high frequency mode (only a few octaves above the first-bending mode). This reduction is ordinarily accomplished by electronic filters having a very sharp response cutoff or by the use of notched filters at each critical frequency. One problem here is that the frequency and mode shape of these oscillations vary as the fuel is used. (See figure 8-2.) Deliberate use of certain nonlinearities in the control system is sometimes helpful. For example, small amounts of friction or hysteresis may prevent the control from responding to small-amplitude high-frequency signals generated within the structure. Of course the basic control mode will have a limit cycle oscillation under such a condition, but this oscillation may be small enough to be tolerable.

The use of large solid propellants as first stage boosters would obviate the fuel sloshing problem, and for this and other reasons, they will undoubtedly be used. These solid engines, however, also require

solution of certain problems. These problems include the control of thrust direction without high actuating forces (particularly friction) and the accurate control of thrust cutoff. A related but somewhat more secondary problem is that of thrust modulation of these engines.

The attitude control systems just discussed (using body mounted gyros) can also be used as an inertial guidance system for launching space vehicles. The boosters would be stabilized in roll and yaw and the pitch gyro reference would be programmed so that the missile attitude would follow a trajectory of the type outlined previously. If the thrust also could be accurately controlled to a desired program this attitude system would be all that is needed to achieve a desired launch trajectory; however, because the thrust cannot be programmed with the required accuracy an integrating accelerometer is mounted on the body to measure accelerations along the longitudinal axis (mean thrust direction) and with a gravity correction established from the pitch attitude program the direction or magnitude of the velocity vector can be determined. Guidance systems of this simple type have been used to launch satellites and can be used in other space operations where angle inaccuracies of the order of one-half degree are allowed.

If greater precision is required from an inertial system, the three gyros can be mounted on a gimballed platform which is slaved to the reference nulls of these gyros. Three orthogonally located integrating accelerometers can be mounted on this platform to establish the velocity. The superior accuracy of this system results from the fact that the coordinates of the platform can be maintained with greater accuracy than

those of the missile itself in addition to the fact that all three components of accelerations are measured.

The chief problems with inertial systems relate to initial alignment (setting in the proper initial conditions), drift in the platform orientation, and inaccuracies in the integration of the acceleration. The last two problems have received much attention and components have been developed with extremely good predicted precision. The word "predicted" is used because one of the real problems associated with this equipment is that of testing in the proper environment. The high steady accelerations associated with the launch condition plus the vibration environment obviously introduce structural deflections, unbalance, etc. in excess of those encountered in a laboratory environment. On the other hand, the extreme theoretical precision associated with the zero g environment of space flight cannot be checked in a ground based laboratory.

As has been implied, the errors of an inertial guidance system increase with time of flight. It is possible to get velocity magnitude and direction information from other types of guidance systems wherein errors are predominately a function of distance. Into this category fall a number of ground based equipment using the propagation properties of electromagnetic waves. Perhaps the best known device of this class is the conical scan tracking radar. In this system an indication of the line of sight to the target is obtained as shown in figure 8-4. The center of the lobes of transmitted energy is made to rotate in a conical pattern and the direction to the target is determined by the relative strengths of the

return signal during various portions of the scan. On the basis of this information the tracking head (antenna) is driven to keep pointing at the target. Angle information is taken right off the tracking head gimbals. Range information is obtained by determining the time interval between the transmitted pulses and their reflected return.

The chief problems with radar tracking systems are achievement of the desired range capability and noise in the angle tracking system. This noise problem is aggravated in the launching problem because it is desired to obtain accurate velocity information and this involves differentiation of the basic positional information. To the radar the appearance of the target somewhat resembles the appearance of a crystal chandelier to eye. Slight motions cause the bright areas to shift around. In the case of the radar there is a tendency to track at random various parts of the missile. This condition is aggravated in the case of the conical scan radar by the fact that it depends for angle information on the comparison of the return signal strengths at slightly different times (scan positions). The radar, therefore, cannot distinguish between a general fading of the return from a difference due to the angle error. Fading at the scan frequency can cause the radar to move entirely off the target.

The fading effect on angle tracking can be eliminated by using a monopulse radar in which the return signal strength comparison is made between a single pulse simultaneously lobed in slightly different directions. The noise due to glint is still present in this system, however. Another

way to improve radar position information is to use two (or more) radars in conjunction with long and accurately measured base lines. In this case the positional information can be obtained from the range measurements through use of triangulation techniques. For extremely large ranges the base lines must be proportionately larger to be effective. For flights deep in solar space base lines between two or three 22,000 mile satellites have been suggested.

The problem of range extension of radars and other electromagnetic signaling devices is large one of increasing the peak transmitted power and increasing the signal gathering capabilities of the receiver. The last requirement may dictate the use of extremely large antennas (the size of a football field or even larger). Range extension can also be improved through use of a beacon (transponder) in the target. Use of a beacon may also improve the angle tracking accuracy.

Another factor which may affect the propagation of electromagnetic radiation between the earth and vehicles in space is the presence of the ionosphere. It is well known that this ionized layer reflects electromagnetic waves; however, it is the writer's understanding that the ionosphere will not have much effect on high frequency waves. Refraction of the waves which result from this source will produce small angle tracking errors.

Because during the launch phase the guidance accuracy is most critical to velocity errors, it is desirable to obtain the velocity information in a more direct manner than by the differentiation of position information. Doppler radar can accomplish this objective. As its name implies its

operation depends on a measurement of the doppler frequency shift between transmitted and reflected waves which results from the targets velocity. The frequency shift as a fraction of the transmitted frequency is directly proportioned to the target velocity radial to the transmitter and inversely proportional to the velocity of propagation of the radiation. Because the velocity of propagation of electromagnetic radiation is extremely high (186,000 miles per second) the frequency shift must be measured with extreme accuracy. If the velocity of a vehicle is desired to one hundred feet per second the frequency must be measured to roughly one part in ten million. Thus one of the chief problems associated with the use of doppler systems for space flight is the achievement of ultra stable oscillators. Another problem connected with the use of doppler techniques is that only the radial component of velocity is measured. This problem can be circumvented through use of multiple installations on accurate base lines. The total velocity can be determined from such an arrangement.

Some of the more sophisticated methods of launch guidance do not depend on the use of a single type of equipment but endeavor to make use of the best features of two or more types. For example, a tracking radar might be used for long period information because it is not subject to the drift problems of the inertial system; however, an inertial system might be used at the same time to provide short period guidance. This arrangement would allow very heavy smoothing (filtering) to be applied to the radar data in order to eliminate noise. Similarly a doppler system can be used for velocity information in conjunction with use of

a tracking radar system for position information. This arrangement avoids the noise problems associated with data differentiation and also avoids the drift problems associated with data integration.

8.2 Orbiting the Earth

Once a vehicle has been established in orbit the complexion of the guidance problem changes. Motions about the body axis are essentially neutrally stable (no inherent modes of motion exist), and in most cases, there are no significant external disturbances. It is necessary to apply only small control moments to reduce any initial angular velocities and to keep the vehicle pointed in a particular manner (if desired). Unless the vehicle is launched into an orbit close to the earth where the effect of aerodynamic drag may be significant the trajectory is stable and predictable and desired minor modification to the orbit can be made by relatively small thrust kicks in the appropriate direction and at the appropriate point.

On the other hand the orbital phase of the operation may extend over very long periods of time and cover large distances over the surface of the earth. The first factor mentioned dictates extreme emphasis on simplicity, reliability, drift and low power consumption of the guidance and control systems to be used. The second factor implies that on-board guidance and control systems would be desirable. The ground based systems described in connection with the launch operation (and other types of ground systems) can and are being used in connection with orbital operations but their use is limited by the extreme size of the network required for complete surface coverage.

Most advanced satellite missions require some sort of attitude control. Examples of such missions are earth reconnaissance missions and stellar observation missions. Some of the most elementary attitude control systems include the sensing of gravitation or centrifugal force gradients by control of the vehicle geometry (for earth observation) and the use of solar photon sails (for solar observation). The use of a drag device for stabilization is possible in near earth short-term orbits. These schemes are characterized by extremely small restoring moments and their use is dependent upon the response times achievable as compared to those required in a particular operation. Their practicality is also dependent on the magnitude of disturbances encountered both externally and internally. Another type of simple attitude system which have been used is simply spinning the entire vehicle. The attitude stabilization in this case is with respect to fixed space.

Optical systems appear well suited for orbit attitude control and other guidance functions in space. These systems are capable of very high resolution and are well adapted to use by the human. This combination is felt by many to add up to highly reliable system. Attitude stabilization with respect to the earth can be accomplished by a 360° scan of the horizon. Stabilization with respect to the sun, planets, or stars can be obtained through use of an astro tracker. Systems of this type require a means for conversion of the sensed quantities into control moments. This conversion involves a human pilot or autopilot and suitable moment producing devices. Such devices are now envisioned as inertia wheels or small reaction

jets. Problems associated with such systems are largely in the areas of design information or development. More information is needed on disturbances (particularly internal), on power requirements (novel power sources need to be developed), on the design of small controllable rockets or high reliability, and on the reliability of components and subsystems in general.

In order to perform such functions as orbit transfer or to re-enter from an orbit, information on such parameters as geocentric radius (altitude), velocity, and position. These measurements could be made using inertial platforms of the type already described. The inertial system has an advantage in this and other space flight applications in that it is a self-contained on-board system. It does appear, however, that some backup system may be required in all but short-term operations because of the long-period drifts associated with the inertial systems. The ground-based systems previously described could also be used in orbit determination. In addition, another type of ground-based system is used for such measurements. This system involves the determination of the direction of arrival of a wave front transmitted from the target. The direction to the target is along a line normal to this front. A phase comparison between the signal received at stations along known base lines is used to establish the direction of arrival of the wave front. This type of equipment has the advantage of being basically passive in nature. It is capable of obtaining position information on any target for which a transmitted signal can be detected. It does, however, require a fairly elaborate ground range communication and

computing system. Attitude of a satellite with respect to a ground station can also be obtained using such equipment provided the device for measuring angle of arrival is aboard the satellite.

Optical systems might also be used to advantage in obtaining velocity and position information as illustrated in figure 8-5. For a satellite maintaining a fixed orientation with respect to the earth (as, for example, by means of a horizon scanner) the spacial velocity parallel to the earth's surface can be obtained from rate gyros providing the geometric radius is known ($\vec{V} = R\vec{\omega}$). This radius measurement might be obtained by stadiametric methods using the horizon scanner or by a radar altimeter. Similarly, instantaneous velocity and position with respect to a point on the earth could be obtained optically for an attitude stabilized satellite by topographic identification and drift measurement.

It should be mentioned that the close in phases of merging of orbital position of two vehicles might very possibly be accomplished by homing techniques. The type of guidance system might be much the same as those developed for air-to-air or surface-to-air missiles and could employ optical, radar or infra red tracking.

8.3 Space Travel

The guidance and control devices already described for the orbiting vehicle can also be applied to a vehicle traveling in cislunar space or at even greater distances. There is likely to be one difference, however. Although guidance of vehicles in initial orbiting near the earth may often be accomplished with a fairly elementary computation routine, the trajectories

in space will dictate the use of fairly complex computers in connection with the guidance function. Coupled with long travel time, this computer presents a serious reliability problem. An example is given in a paper by Xenakis in which a circumnavigating lunar trip ending in a re-entry to the earth's atmosphere was considered. The trip time was roughly ten days. The system consisted of an astro tracking system, rate gyro control, inertia wheels, and a computer. The computer was the dominating influence in lowering the probability of success. Using failure rate data for a modern airborne fire control computer but only considering one-tenth the computer capacity, the probability of success of this mission was 0.22. Replacing the computer by a human pilot raised the probability of success to 0.70; however, the probability of success of the computer equipped system could be raised to 0.64 through use of intermittent operation. Even with this intermittent system, the probability of success of a one way trip to Mars would be low (less than one in twenty) because of the long travel time assumed (2400 hours).

Guidance accuracy requirements for such missions as lunar impact, lunar circumnavigation, or large radius lunar orbits are not great. Angle accuracies of the order of one-half degree would be required, however, if return to the surface of the earth is desired much higher precision is required. If a braking ellipse re-entry is used, a first pass perigee altitude precision of about 20,000 feet appears to be required. At 20,000 miles from perigee the angle accuracy would have to be about 0.02 degrees and the velocity accuracy would have to be about 10 fps to

meet this requirement. Thus a need is indicated for some means of limited corrective control (thrust control) as the perigee point is approached.

8.4 Atmosphere Re-entry

The re-entry into the atmosphere of a space vehicle will be made at a shallow angle in order to limit aerodynamic heating rates to acceptable values. In general regulation of re-entry angle and position will be accomplished by small amounts of retro-thrust. The configurations considered for re-entry vehicle vary widely and include balloons, parachutes, ballistic re-entry capsules, and several varieties of winged vehicles. The winged vehicles will probably be operated at high angles of attack (thirty to ninety degrees) in order to limit the heating rates and/or the total heat input. Ballistic re-entry bodies will be high drag configurations, but ultimately might utilize small amounts of lift for maneuvering.

The significant addition to the guidance and control problem here as compared to other phases of the mission is the importance of aerodynamic lift, drag, stability, and control. Blunt (approximately flat faced) bodies such as ballistic capsules or winged vehicles at extreme angles of attack (approaching ninety degrees) are characterized by high drag, negative lift-curve slopes, and very small amounts of static stability. Actually at angles of attack approaching ninety degrees the resultant force coefficient shows little variation with angle of attack both as to its magnitude and as to its direction with respect to the body. The acceleration time history during re-entry, therefore is controlled

by controlling the trajectory through the atmosphere. Because no immediate effect on the accelerations results from control action piloting problems are likely to occur. Adding to this difficulty is the effect of the negative lift-curve slope. The vehicle must be pitched down in order to apply lift in an upward direction (pull out).

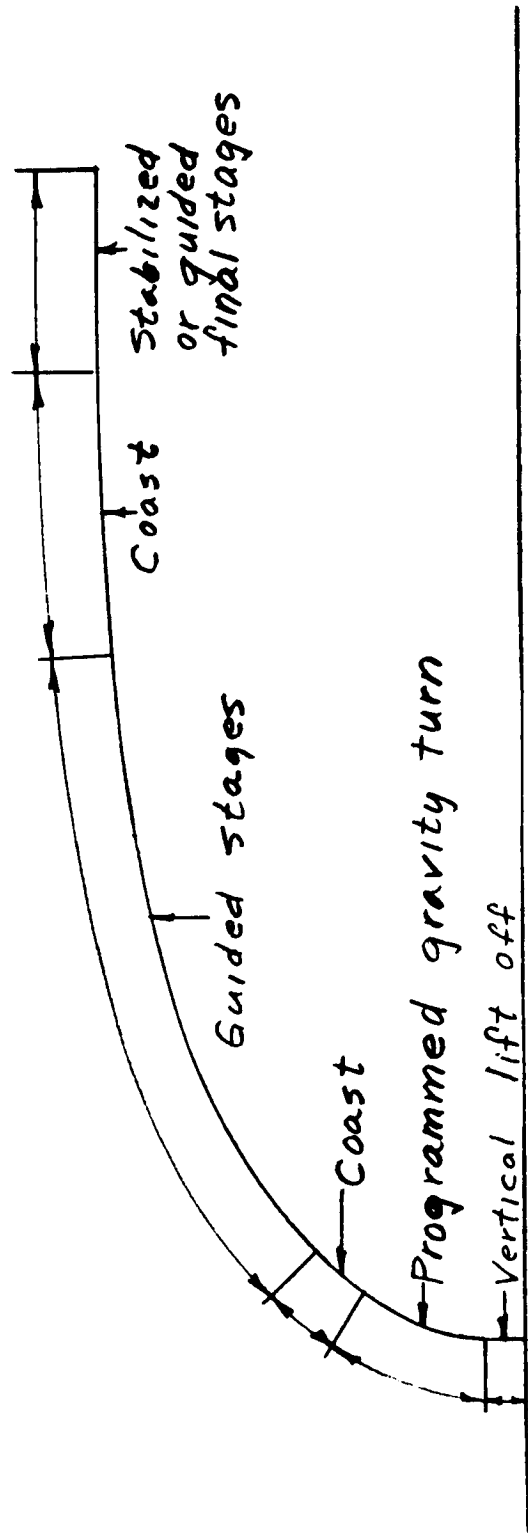
Another problem common to all re-entry configurations is low damping of the short-period modes. In fact, the negative lift-curve slope associated with the blunt configurations may make the damping slightly negative in this case. In general, however, the amplitude of this oscillatory motion tends to decrease during the re-entry because of the increasing density. The decrease in amplitude is approximately proportional to the decrease in period because in the absence of continued disturbances the energy in the oscillation will remain about constant. These conditions result in the maximum angular accelerations increasing in proportion to the increase in period. In the case of the blunt body, these motions should not produce significant transverse accelerations nor oscillations in the total accelerations for the reasons given previously. This result would not exist for wing vehicles re-entry at angles of attack of 35 or 45 degrees.

The winged vehicles operating in the range of 45 degrees angle of attack may also encounter problems associated with strong aerodynamic and inertial coupling of the moments about one axis due to motions about another. This problem is particularly difficult if the angle of attack must be varied. Although the effects might be compensated in the design (or by automatic means for one angle of attack, such compensation would

not be possible over a range of angles of attack. Control deflection coupling has been found particularly bothersome. In certain instances the moments produced about the control axis has been smaller than the moments produced about another axis.

Added to the perhaps more subtle problems previously mentioned, there are the problems relating to the rapid changes in control effectiveness, static stability, trim, and response associated with the rapid variations in Mach number and dynamic pressure during these re-entry maneuvers. These characteristics will require considerable adaptive capabilities on the part of the human pilot or the autopilot.

341<



342 <

Figure 8-1. - Schematic of phases of launch.

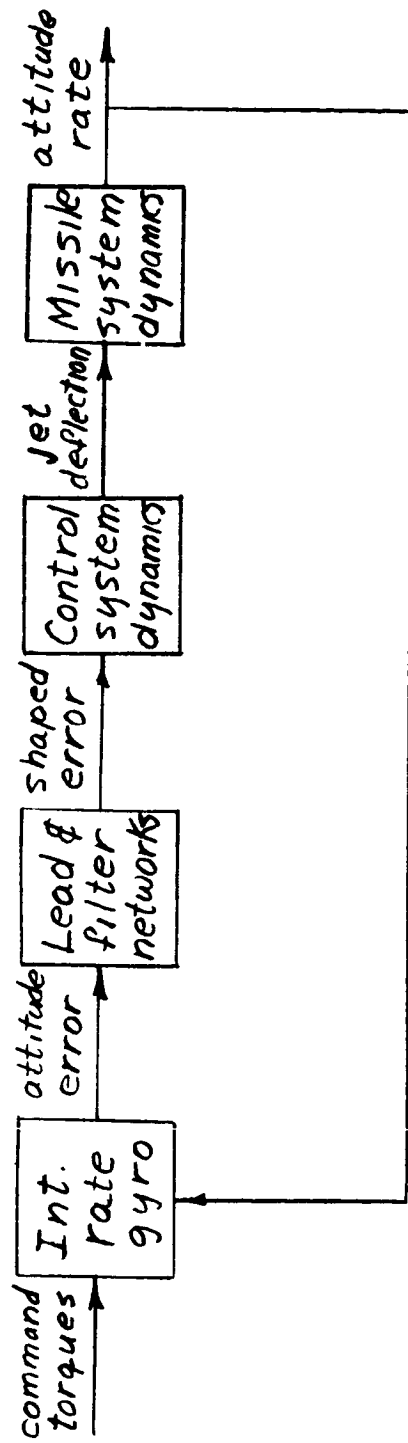


Figure 8-2:- Missile attitude control system.

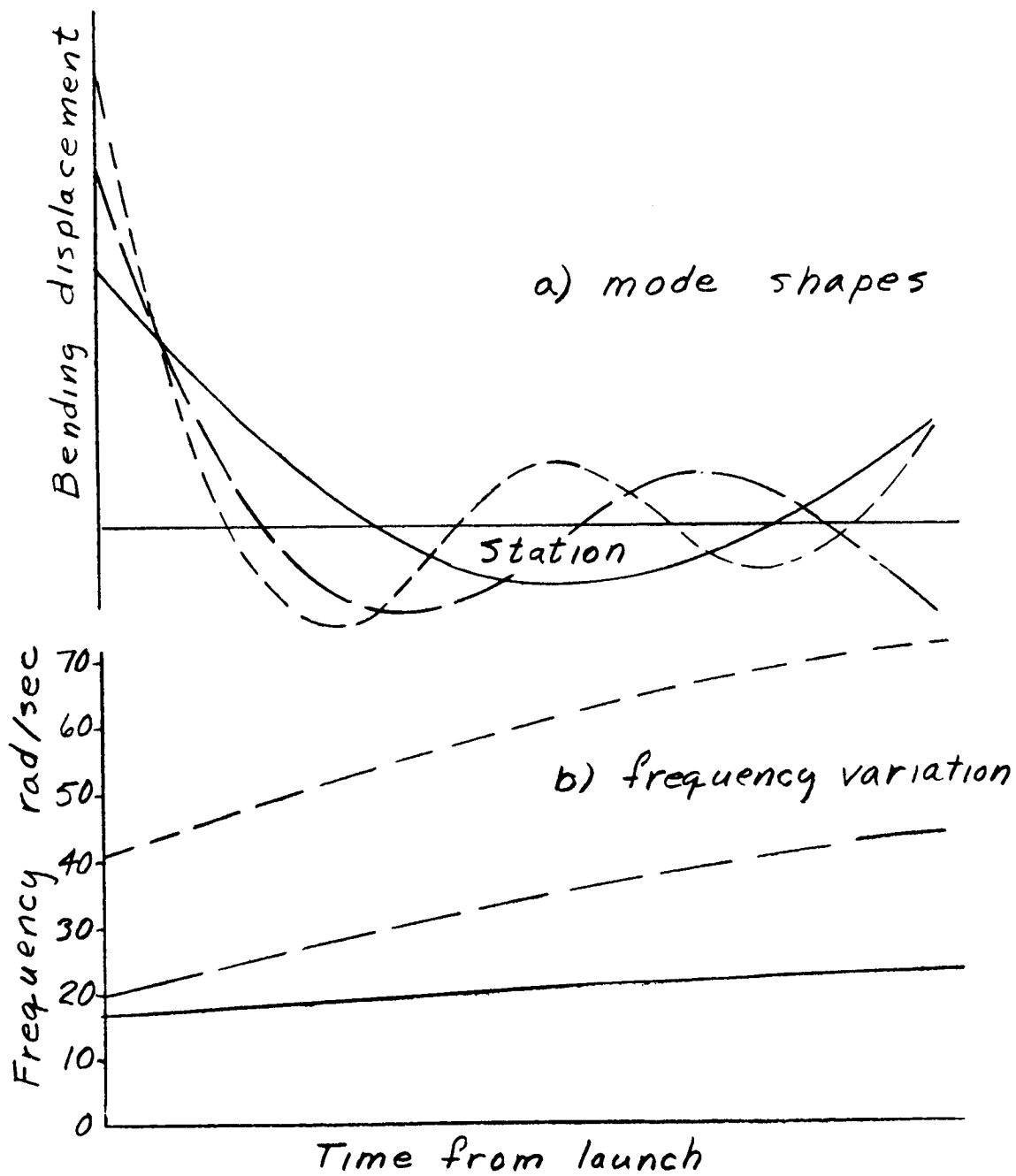


Figure 8-3.-Typical missile bending modes.

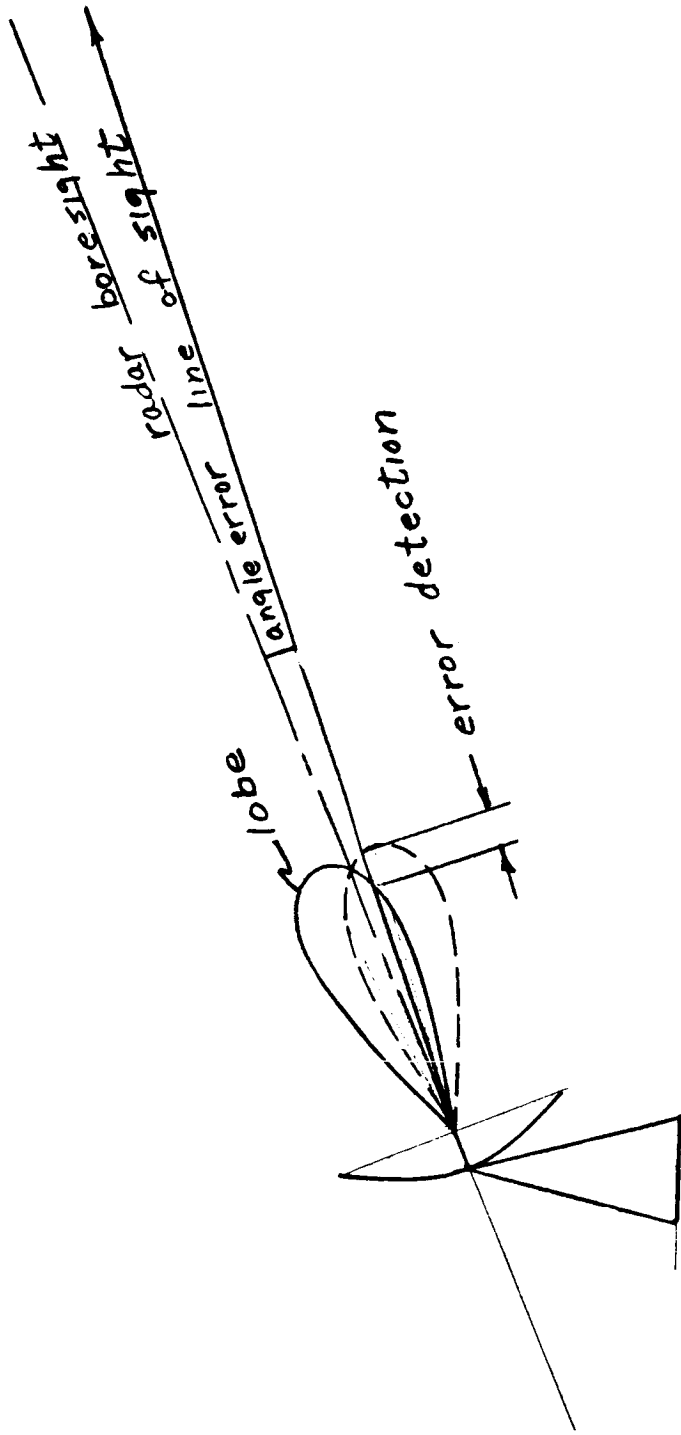


Figure 8-4.- Angle error detection by conical scan radar.

Note: vehicle is also stabilized to vertical by horizon scan

$$h = R_0 \left(\frac{1}{\sin \delta} - 1 \right)$$

$$\vec{V} = \frac{R_0}{\sin \delta} \vec{\omega}$$

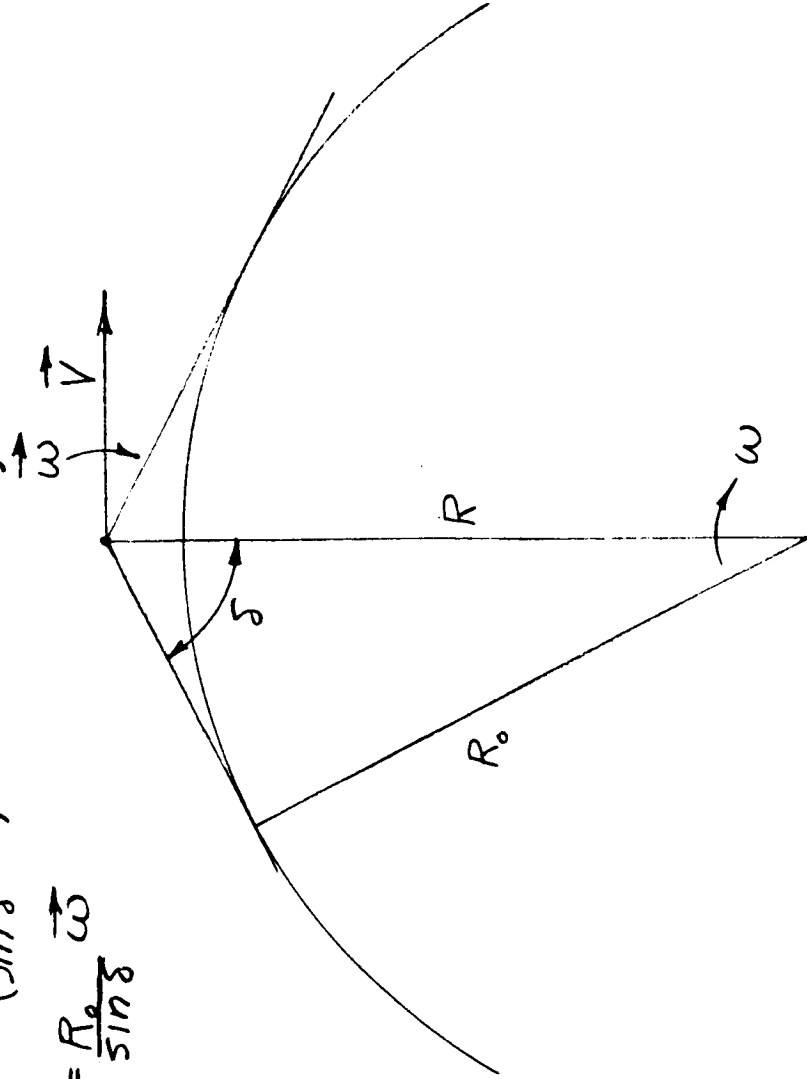


Figure 8-5.-Velocity and altitude sensing by horizon scan.

SECTION IX

ELEMENTS OF ROCKET PROPULSION

9.1 History of Rockets

The history of rockets will be briefly discussed. Only those few names and dates which are considered sufficient for a brief outline of the subject will be mentioned.

The first recorded use of the rocket occurred in 1232 A.D. when the Mongol, Ogadai, the third son of Genghis Khan, began his attack on Kaifeng, capital of Honan Province in China. Rockets were used by the defenders of Kaifeng and were described as fire arrows. They were nothing more than rockets attached to arrows to increase their range.

It is probable that the rocket principle was known to the Greeks several centuries earlier, possibly as far back as the 8th century. Going back still farther the Chinese have been credited by some with the use of gunpowder rockets as early as several centuries B.C. Of course, all propellants used in those times were solid. In fact, gunpowder or its variations was the only known type of rocket propellant until early in the 20th century.

Assuming the 13th century as the starting point in rocket history, the most rapid advances were made in the Orient during the next 500 years. The Indian soldiers used large numbers of rockets with telling effect against British troops during the Indian campaigns. Their success aroused the interest of many in England, one in particular being Sir William Congreve. He began earnest study in 1804. His rockets were used against Napoleon

and also against American troops in the War of 1812....whose red glare is mentioned in the Star-Spangled Banner.

The long, trailing stick on the rocket which was used for stability was eliminated around the middle of the 19th century. It was replaced by small curved vanes built into the path of the jet which were able to spin-stabilize the rocket. This idea of spin stability was also applied to artillery shells by rifling the bores. By the end of the 19th century the rocket was replaced by artillery because of this increased accuracy due to rifling and because of rapid developments made whereby the range of the artillery was greatly increased.

In 1903 Ziolkovsky of Russia made a definite proposal for a liquid-propellant rocket unit in an article dealing with the possibility of rocket space travel. Nevertheless, credit for rebirth of rockets in the 20th century is generally given to Dr. Robert Goddard of Massachusetts. Although the basic idea of utilizing the rocket principle to attain extreme altitudes had been conceived in the middle of the 18th century, Dr. Goddard conducted the first scientific experiments along these lines. He became interested in the subject in 1909 and began experiments as early as 1915 with solid propellants. Financial backing for his experiments was provided by the Smithsonian Institution who published his report, "A Method of Reaching Extreme Altitudes" in 1919, the first publication on this subject. In it, Dr. Goddard claimed it was theoretically possible to send a rocket to the moon. In 1920, Goddard saw the need for liquid-propelled rockets in order to obtain the required speeds, altitudes, and endurance. In 1926 he succeeded

in making the first flight with a liquid-propelled rocket, and in 1932, the first flight of a rocket stabilized by a small gyroscope.

In the meantime, shortly after Goddard had renewed the interest in rockets others from all over the world followed with work on the subject, notable among these being Hermann Oberth in Germany. Except for Goddard, the bulk of rocket research in the first half of the 20th century was centered in Germany.

The rocket was used in World War I, but not as an offensive weapon. In World War II many different uses of the rocket as a major weapon were made by each of the powers. Since World War II, the application of rocket power has been rapidly accelerated as exemplified by the development of intercontinental ballistic missiles and the launching of the artificial satellites of the earth.

9.2 Rocket Principles

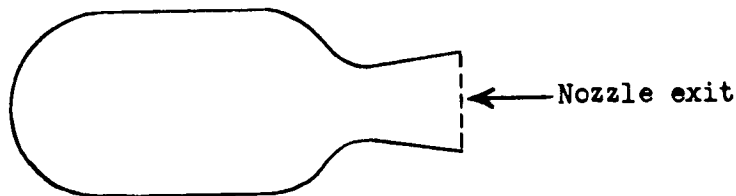
An attempt will be made to derive and explain a few of the more common quantities associated with rocket motors.

9.2.1 Equation for the Acceleration of a Rocket.

The propelling action of a rocket motor is derived from the generation of large quantities of gases by the chemical reaction of suitable propellants within the rocket motor. The force which is produced by the generation of the gases is called thrust and is the basic performance parameter of a rocket since it determines the speed and distance which can be obtained.

The equation for the acceleration of a rocket can be derived from a special principle of the momentum theorem which takes into account the fact that a burning rocket is continuously losing part of its mass. This principle states that for a system of S particles, the vector sum of all the exterior forces acting on S is equal to the time rate of change of the total momentum of S plus the rate at which momentum is being transferred out of S by the particles that are leaving S .

In deriving the equation for the rocket acceleration consider the rocket shown below



where the rocket system consists of the metal parts of the rocket, the unburnt fuel, and the gas inside the geometric surface. The momentum of the system is equal to the mass of the system times its velocity, that is, $M\mathbf{v}$. The rate at which the departing particles remove momentum from the system is just the rate at which momentum crosses the exit surface. If the velocity of the gas relative to the rocket at the exit of the nozzle is \mathbf{v}_e , then the gas crossing the exit surface has a velocity of $\mathbf{v} - \mathbf{v}_e$. If \dot{m} is the rate at which gas is streaming through the exit surface, then the jet is taking momentum from the system at the rate of $\dot{m}(\mathbf{v} - \mathbf{v}_e)$, and, by the above principle

$$\begin{aligned}\sum F_{\text{external}}(t) &= \frac{d}{dt}(Mv) + \dot{m}(v - v_e) \\ &= M\dot{v} + \dot{M}v + \dot{m}(v - v_e)\end{aligned}$$

The rate of gas streaming through the exit \dot{m} which is the rate at which the fuel is being burnt must equal the rate of change in mass of the system.

$$\frac{d}{dt} M = -\dot{m}$$

Therefore

$$\begin{aligned}\sum F_{\text{external}}(t) &= M\dot{v} - \dot{m}v + \dot{m}(v - v_e) \\ &= M\dot{v} - \dot{m}v_e\end{aligned}$$

or

$$M\dot{v} = \dot{m}v_e + \sum F_{\text{external}}(t) \tag{9-1}$$

9.2.2 Derivation of the Thrust of a Rocket.

Among the external forces acting on the system, as shown in equation (9-1), are the gas pressures over the surface of the system. The gas pressures consist of atmospheric pressure over the outside of the rocket and the jet pressure over the exit surface.

The force due to the jet pressure is $p_e A_e$ where p_e is the jet pressure at the exit surface and A_e is the area of the exit plane. The atmospheric pressure is composed of the static atmospheric pressure plus the aerodynamic forces due to motion through the air. The force due to the static atmospheric pressure over the outside of the rocket is just the

negative of the force that would be produced by static atmospheric pressure over the exit surface. (This is obtained by summing up all the forces due to atmospheric pressure acting on the rocket exterior excluding the nozzle exit surface.) Therefore, in terms of the jet, the force due to static atmospheric pressure over the outside of the rocket is $-p_a A_e$ where p_a is the static atmospheric pressure.

As previously stated the remaining forces due to atmospheric pressure are due to motion through the air and are considered as aerodynamic forces F_a .

Collecting the above and other external forces the total external force is

$$\sum F_{\text{external}}(t) = p_e A_e - p_a A_e - F_a - Mg_x - F \quad (9-2)$$

The term Mg_x is the force due to gravity and the term F includes all other exterior forces, for instance, if the rocket is towing out a line, etc.

From equation (9-1) then

$$M\dot{v} = \dot{m}v_e + (p_e - p_a)A_e - F_a - Mg_x - F \quad (9-3)$$

Now consider a rocket held motionless by a test stand. The term $M\dot{v}$ becomes zero since $\dot{v} = 0$. Also, there are no aerodynamic forces on the stationary rocket, so that $F_a = 0$. If the rocket is held in a horizontal position, then $Mg_x = 0$. Thus, the term F in equation (9-3) becomes the thrust, as measured by the thrust gage.

$$F = \dot{m}v_e + (p_e - p_a)A_e \quad (9-4)$$

or

$$F = (\dot{w}/g)v_e + (p_e - p_a)A_e \quad (9-5)$$

where \dot{w} is the weight rate of propellant flow. The thrust is composed of two terms. The first term is known as the momentum thrust. The second term is known as the pressure thrust and consists of the product of the cross-sectional area of the exhaust jet and the difference between the exhaust pressure and the atmospheric pressure. From equation (9-4) it is evident that a rocket exhaust nozzle is usually designed so that the exhaust pressure is equal to or slightly higher than the atmospheric pressure.

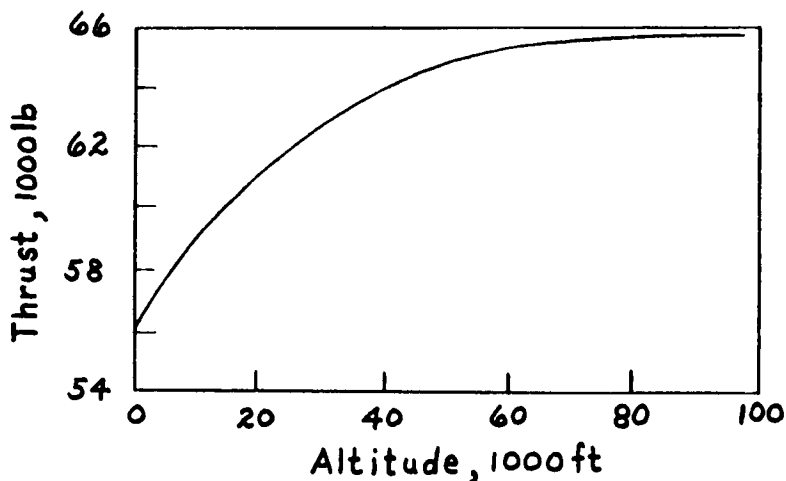
If the atmospheric pressure is equal to the exhaust pressure, the thrust is

$$F = (\dot{w}/g)v_e$$

and gives a maximum thrust for a given chamber pressure. The rocket nozzle design which permits the expansion of the propellant products to the same pressure of the surrounding fluid is referred to as the rocket nozzle with optimum expansion ratio.

For underexpansion (that is, when the exhaust gas pressure is higher than atmospheric pressure) a portion of the energy of the gases is not converted into kinetic energy and is lost as far as thrust development is concerned.

If a motor is to operate at different altitudes, the area ratio ($A_{\text{exit}}/A_{\text{throat}}$) must be selected so that it is the best compromise for the operating conditions. Usually, the nozzle is designed so that it will operate with a slight underexpansion at the most significant operating altitude. In this case the thrust at sea level would be reduced. The German V-2 is a typical example and its thrust variation with altitude is shown below.



9.2.3 Effective Exhaust Velocity.

In order to explain the meaning of effective exhaust velocity reference can be made to equation (9-5) which is

$$F = (\dot{w}/g)v_e + (p_e - p_a)A_e$$

The term effective exhaust velocity is introduced as a convenient way of defining the thrust in the above equation only in terms of the propellant weight rate of flow and an exhaust velocity which is called the effective exhaust velocity. The effective exhaust velocity c is defined as

$$c = \frac{F}{\dot{w}/g} = v_e + \frac{(p_e - p_a)A_e g}{\dot{w}} \quad (9-6)$$

(When $p_e = p_a$, the effective exhaust velocity c is equal to the exhaust velocity of the propellant gases v_e .) With this definition of exhaust velocity, then

$$F = c(\dot{w}/g) \quad (9-7)$$

Typical values for a rocket might be

$$v_e = 6,200 \text{ ft/sec}$$

$$c = 7,300 \text{ ft/sec}$$

Effective exhaust velocity depends on the atmospheric pressure (see equation (9-6)); therefore, when values of effective exhaust velocity are stated the corresponding atmospheric pressure is also stated. Thus the use of effective exhaust velocity relates the performance or thrust of a rocket on a standard basis and one rocket can be easily compared with another rocket.

In the actual testing of a rocket motor to determine its performance the value of the effective exhaust velocity can be easily determined from measurements of the thrust and propellant flow, as is shown below.

The total weight of the propellants consumed is

$$W_p = \dot{w} \Delta t$$

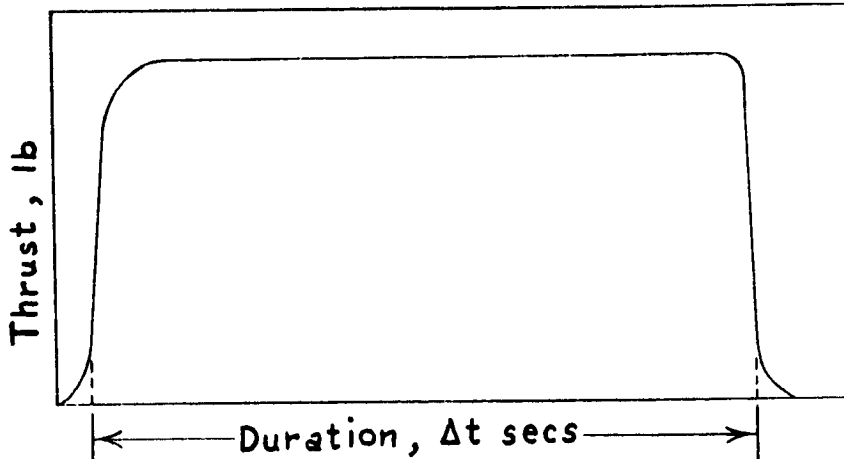
Then from equation (9-7)

$$c = F \Delta t \frac{g}{W_p} \quad (9-8)$$

or

$$c = I \frac{g}{W_p} \quad (9-9)$$

where I is called the impulse in pound-seconds and is the integral of the thrust vs. time duration curve. (See below.)



The use of impulse is handy, especially for solid propellant rockets where it is often difficult to measure the propellant flow rate accurately.

The effective exhaust velocity is one of the most important criteria of rocket-motor performance and a continual effort is being made to increase its value.

If the thermodynamic properties of the propellant gases are known, the effective exhaust velocity can be calculated from the following equation.

$$c = \sqrt{2g \frac{k}{k-1} RT_c \left[1 - \left(\frac{p_e}{p_c} \right)^{\frac{k-1}{k}} \right]} \quad (9-10)$$

where p_c is the combustion chamber pressure

k is the specific heat ratio

R is the gas constant per unit weight and is equal to the universal gas constant (1,544 ft-lb/mole $^{\circ}R$) divided by the molecular weight (lb/mole)

T_c is the chamber temperature, $^{\circ}R$

$\frac{p_e}{p_c}$ is the expansion ratio

Actually, equation (9-10) gives the effective exhaust velocity for the optimum expansion ratio, that is, $p_e = p_a$. In the above equation the specific-heat ratio and expansion ratio can exert only a minor influence on the magnitude of the effective exhaust velocity. Therefore,

$$c \sim \sqrt{T_c R} \sim \sqrt{\frac{T_c}{\text{molecular wt.}}} \quad (9-11)$$

For gases generated by the liquid propellants currently being used, the values of R vary from 60 to 80. Combustion chamber temperatures range from 3500 $^{\circ}R$ to 6000 $^{\circ}R$. A typical chamber pressure is 300 psia, while some are as high as 500 psia. Rockets are generally designed for a constant chamber pressure.

9.2.4 Specific Impulse.

Rocket motor performance is frequently expressed in terms of specific impulse of the propellants. This is the impulse delivered per unit weight of propellant consumption.

$$I_s = \frac{I}{W_p}$$

or

$$I_s = \frac{F}{\dot{w}} \quad (9-12)$$

In terms of the effective exhaust velocity (equation (9-6)) which is

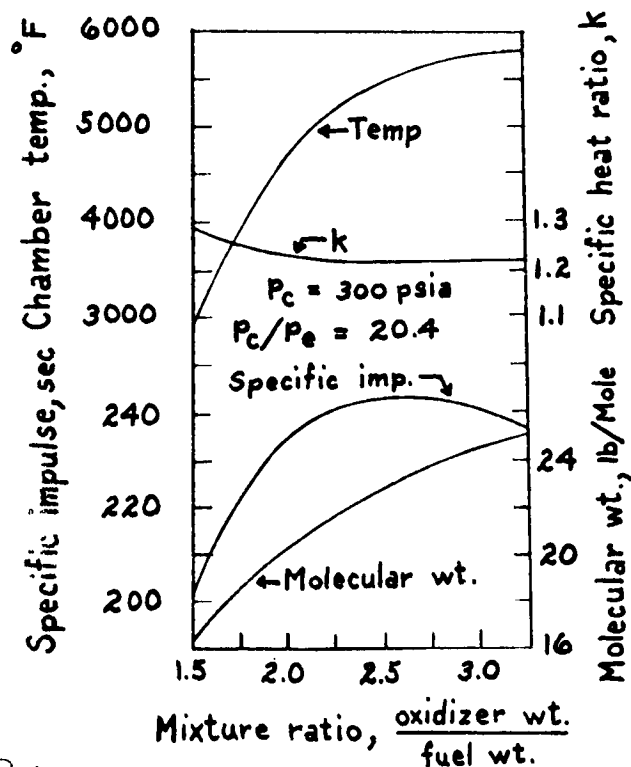
$$c = \frac{F}{\dot{w}/g}$$

the specific impulse is

$$I_s = \frac{c}{g} \quad (9-13)$$

Therefore, it is seen that specific impulse is merely another way of expressing rocket performance and is convenient to use when it is possible to measure the propellant flow rate and thrust (usually in liquid-propellant rockets).

In the figure below is a typical calculated performance of a liquid oxygen-gasoline propellant system.



It is seen that one definite mixture ratio (oxidizer weight to fuel weight) gives an optimum rocket performance. This optimum mixture ratio occurs usually at a value which is richer in fuel than the stoichiometric mixture ratio, at which all the fuel is theoretically completely oxidized and the flame temperature is a maximum. In general, the mixture ratio of the rocket is so selected as to be very close to the optimum value. In liquid propellant rockets this ratio determines the proportions of the propellant tank volumes and in solid propellant rockets it determines the proportions of oxidizer and fuel to be used during propellant preparation.

9.2.5 Propulsive Efficiency.

There are various efficiencies defined in connection with rockets. These are not commonly used in designing rockets; however, they permit an understanding of the energy balance of a rocket. One efficiency, known as the propulsive efficiency, will now be briefly discussed.

The propulsive efficiency determines how much of the kinetic energy of the exhaust jet is useful for propelling a vehicle. It is defined as

$$\eta_p = \frac{\text{vehicle energy}}{\text{vehicle energy} + \text{residual kinetic jet energy}}$$

$$= \frac{Fv}{Fv + \frac{1}{2} \left(\frac{\dot{w}}{g} \right) (c-v)^2}$$

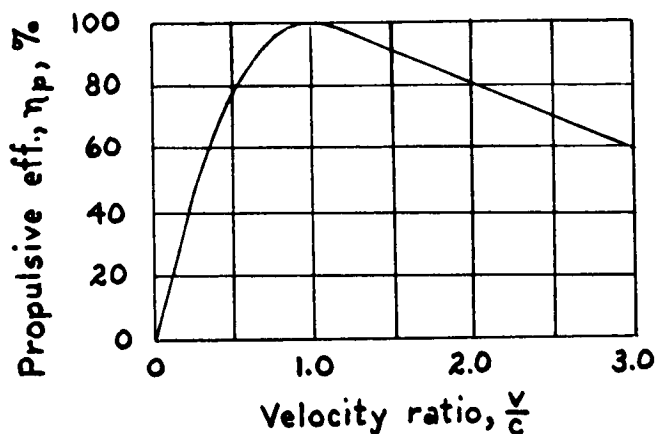
and since $F = c \frac{\dot{w}}{g}$

$$\eta_p = \frac{2 \frac{v}{c}}{1 + \left(\frac{v}{c} \right)^2} \quad (9-14)$$

where v is the vehicle velocity and c is the effective exhaust velocity.

The term $(c-v)$ is the absolute exit velocity of the propellant gases.

The following figure shows the instantaneous propulsive efficiency of the rocket jet as a function of the velocity ratio $\frac{v}{c}$.



The propulsive efficiency is a maximum when the forward vehicle velocity is equal to the exhaust velocity, that is, when the absolute velocity of the jet is zero. This means that the total available kinetic energy is being used to propel the vehicle. Since the object of a rocket is usually to attain as high a flight speed as possible the speed is constantly increasing, thus the propulsive efficiency varies during the flight of a rocket. It is apparent from the figure shown above that the rocket is an inefficient propulsion system at speeds comparable to those of our present-day airplanes.

9.2.6 Ideal Velocity of a Rocket.

If the external forces $\sum F_{\text{external}}(t)$ in equation (9-1) are neglected, then

$$M\dot{v} = \dot{m}c \quad (9-15)$$

From this very useful expression the ideal velocity of the rocket can be obtained; that is, the speed the rocket would attain neglecting the effect of drag or gravity. The effective exhaust velocity c is assumed to be constant. The ideal velocity is determined from equation (9-15) by first remembering that

$$\dot{m} = -\frac{d}{dt}M$$

so that

$$M\dot{v} = -\frac{d}{dt}Mc$$

Multiplying through by dt , then

$$Mdv = -c dM$$

or

$$dv = -c \frac{dM}{M}$$

Both sides of the equation can be integrated over the period of burning as shown below

$$\begin{aligned} \int_0^f dv &= \int_0^f -c \frac{dM}{M} \\ v_f &= -c (\ln M_f - \ln M_0) \\ &= c (\ln M_0 - \ln M_f) \\ &= c \ln \frac{M_0}{M_f} \quad \text{or} \quad \frac{M_0}{M_f} = e^{\frac{v_f}{c}} \end{aligned} \quad (9-16)$$

where v_f is the final velocity and M_0 and M_f are the masses of the rocket (plus fuel) at the beginning and end of burning, respectively. It should be noted that for equation (9-16) the velocity is given in terms of the final velocity reached for a rocket started initially from rest. If the rocket is at some speed at the beginning of firing, then the v_f term becomes incremental velocity Δv .

Equation (9-16) can be expressed in terms of the propellant mass ratio \mathfrak{S} .

$$v_f \text{ or } \Delta v = -c \ln(1 - \mathfrak{S}) \quad (9-17)$$

where \mathfrak{S} is the ratio of the mass of the propellant to the gross mass of the rocket $\frac{M_p}{M_0}$.

Since the end result of a rocket is that of delivering a useful load or pay load it is convenient to express equation (9-17) in terms of a parameter known as the pay-load ratio $\frac{M_l}{M_0}$ where M_l is the mass of the pay load. By introducing an additional parameter ϵ , called the structural factor, and by substituting this term along with the pay-load ratio into equation (9-17) the expression for the velocity becomes

$$v_f \text{ or } \Delta v = -c \ln [\epsilon(1 - \lambda) + \lambda] \quad (9-18)$$

where λ is the pay-load ratio $\frac{M_l}{M_0}$

and

$$\epsilon = \frac{M_f}{M_f + M_p} = \frac{M_f}{M_0 - M_l}$$

such that

$$\xi = (1 - \lambda)(1 - \epsilon)$$

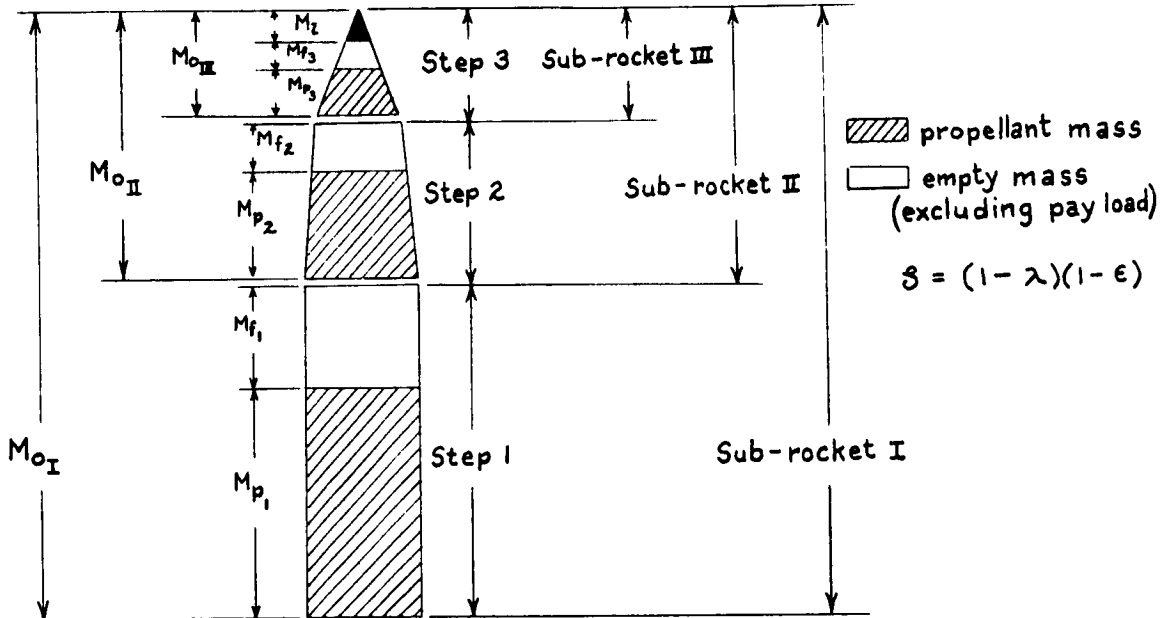
It should be noted that M_f does not include the mass of the payload.

Although these results for ideal conditions cannot be applied directly, they give an approximation of the maximum speed which can be expected for a given rocket. The difference between the "ideal" and actual performance varies for every rocket. A small fireworks rocket may actually only attain 2 or 3 percent of this "ideal" performance. The German V-2 attained some 70 percent of its ideal performance. The larger the rocket the smaller the difference between the two values; a rocket capable of overcoming the whole gravitational field of the earth would probably attain better than 95 percent of "ideal" performance.

9.2.7 Multiple-Step Rockets.

It is obvious from equation (9-17) that very high final velocities cannot be obtained with a single rocket because the propellant mass ratio $\frac{M_p}{M_c}$ that would be required becomes physically impossible using present-day propellents. The disadvantage of a single rocket in regard to attaining high velocities lies in the fact that the entire empty mass of the rocket must be continually accelerated even after the major portion of that empty mass is no longer useful. For this reason the step principle was conceived in that a rocket consists of several steps, each of which operates independently. As the propellant is exhausted in each step, the step is separated from the rocket and propulsion for the remaining unit is provided by the next step.

This principle is briefly discussed below by taking a three-step rocket as an example. In order to avoid confusion, the individual rockets are defined herein as the steps and the combinations of the steps are referred to as sub-rockets.



pay-load ratio

$$\lambda_I = \frac{M_{oII}}{M_{oI}}$$

$$\lambda_{II} = \frac{M_{oIII}}{M_{oII}}$$

$$\lambda_{III} = \frac{M_z}{M_{oIII}}$$

structural factor

$$\epsilon_I = \frac{M_{f1}}{M_{f1} + M_{p1}}$$

$$\epsilon_{II} = \frac{M_{f2}}{M_{f2} + M_{p2}}$$

$$\epsilon_{III} = \frac{M_{f3}}{M_{f3} + M_{p3}}$$

propellant mass ratio

$$\delta_I = \frac{M_{p1}}{M_{oI}}$$

$$\delta_{II} = \frac{M_{p2}}{M_{oII}}$$

$$\delta_{III} = \frac{M_{p3}}{M_{oIII}}$$

In the case of a step rocket the ideal velocities of the sub-rockets may be added, so that the total ideal velocity of the three-step rocket shown above is

$$V_3 = \sum \Delta v = -c_I \ln[\epsilon_I(1-\lambda_I) + \lambda_I] - c_{II} \ln[\epsilon_{II}(1-\lambda_{II}) + \lambda_{II}] - c_{III} \ln[\epsilon_{III}(1-\lambda_{III}) + \lambda_{III}] \quad (9-19)$$

It is assumed that each step starts to fire immediately after the preceding step has ceased firing, and is discarded immediately after it has stopped firing.

If it is assumed that all the steps are designed with the same structural factor ϵ and that the pay-load ratios for all the sub-rockets are equal (it is believed that these assumptions are not far from the truth for an actual multiple-step rocket) then the velocity of the rocket at the end of burning of the third step is

$$V_3 = -3c_a \ln[\epsilon(1-\lambda) + \lambda] \quad (9-20)$$

where c_a is the average value of effective exhaust velocity over the entire firing period.

In case the mass of the pay load of the final step M_2 and the mass of the entire rocket M_{oI} are given then the pay-load ratio λ in equation (9-20) for each of the sub-rockets is

$$\lambda^3 = \frac{M_2}{M_{oI}} \quad (9-21)$$

In practice, each step multiplies the total weight by a factor up to 10, so that for reasons of shear bulk, rockets of more than 5 steps are not often contemplated.

In equations (9-16) through (9-20) the effects of drag and gravity have been neglected. Actually, even under conditions where flight is made in the atmosphere at low altitude the effect of drag on the final velocity is practically negligible (about 5 percent) for large, slender rockets. The deceleration due to gravity can be included in these equations by simply adding the term $-gt_p$, where t_p is the duration of powered flight in seconds. The acceleration due to gravity at sea level is used here for the value of g since the error introduced by assuming a constant g will be very small if the burning stops at a distance above the earth which is small compared with the radius of the earth. It is apparent that the shorter the burning time, the less the effect of gravity is on the final velocity of a rocket.

REFERENCES

1. Sutton, George P.: Rocket Propulsion Elements, 1956.
2. Zucrow, M. J.: Jet Propulsion and Gas Turbines, 1948.
3. Rosser, J. B., Newton, R. R., and Gross, G. L.: Mathematical Theory of Rocket Flight, 1947.
4. Ley, Willy: Rockets, Missiles, and Space Travel. Revised Edition, 1957.
5. Seifert, H. S., Mills, M. M., and Summerfield, M.: The Physics of Rockets. American Jour. of Physics, Jan.-Feb., Mar.-Apr., May-June, 1947.
6. Malina, F. J., and Summerfield, M.: The Problem of Escape from the Earth by Rocket. Journal of the Aeronautical Sciences. V. 14, no. 8, August 1947.

SECTION X

CHARACTERISTICS OF MODERN ROCKETS AND PROPELLANTS

10.1 General Comments

A few brief remarks will be made about rockets in general so as to provide an overall picture of the varied details involved in rocket engineering.

There are vast differences between liquid- and solid-propellant rockets in regard to their design and operation. It has been apparent that liquid-propellant rockets have been much more complicated in relation to solid-propellant rockets. Since the solid-propellant rockets are more convenient and easier to maintain - and thus cheaper - they have been used exclusively where short duration and relatively small thrusts are required. The magnitude of the thrust of solid rockets has been limited because the size of the propellant is limited by the manufacturing process.

Nowadays, there are those who are convinced that solids will completely replace all liquid-propellant systems in the near future. Others give the small missile field to solids, equal billing in the medium thrust range, but probably less importance to solids in large motors since solids increase in complexity and handling difficulty to a point where they lose any advantage they once had over the liquids. No matter which is better, there will undoubtedly be much to see and hear about both until higher energy systems are developed. One fact worth mentioning about these advanced systems is that some may still be in the form of liquid-propellant systems. For instance, it will be possible to use the heat generated by

an atomic pile to vaporize a liquid (which can be called the fuel) and heat the vapor to any desired temperature at a high pressure. Thus a fuel such as water could be used. If hydrogen were heated to 4,000° C at a pressure of 300 psi and allowed to expand down to atmospheric pressure a jet exhaust velocity of nearly 30,000 ft/sec could theoretically be obtained. This is about three or four times more than is being achieved at present.

A simple definition of a rocket is a jet reaction motor that carries its own working fluid. The propulsion unit is called a motor since it has no moving parts. In a rocket, thermal energy is converted into kinetic energy producing an impulse which is a thrust for a period of time. Fuels available for present or future use are chemical, nuclear, solar, and ion or magnetic (sometimes called plasma). A comparison of the energy of various fuels can be made with the use of the term jet horsepower which is obtained by

$$\text{jet horsepower} = \frac{\text{thrust} \times \text{exhaust velocity}}{550}$$

Typical values of jet horsepower for several rockets as well as for a jet engine are shown in the following table. Each of the jet-horsepower values given correspond to a 30 pound thrust.

For 30 pound thrust			
	Exhaust velocity ft/sec	Mass flow lb/sec	Jet horsepower
Turbojet	2,700	0.3	150
Chemical rocket (present)	7,500	.12	400
Chemical rocket (advanced)	15,000	.07	800
Nuclear rocket	45,000	.023	2,500
Ion rocket Photon rocket } }	3,000,000 up to the velocity of light	.00032	160,000 and up

In SECTION IX it was shown that the energy of a chemical rocket is limited by temperature and molecular weight (and to a lesser extent, by specific heat).

$$\text{exhaust velocity} \sim \sqrt{\frac{\gamma T_c}{M}}$$

where γ is the specific heat ratio

T_c is the temperature in the combustion chamber

M is the molecular weight

A high performance can be obtained by high temperature or low molecular weight. The higher temperatures for better performance are in turn limited due to cooling difficulties. Thus, high performance depends on high efficiency in that as little thermal energy as possible must be lost from the working fluid to the chamber and nozzle walls. Nuclear systems must have high efficiencies or else the very high temperatures will damage the rocket unit. The energy in an ion rocket is proportional to

$$\sqrt{\frac{QV}{M}} \quad \text{where } Q \text{ is the charge, } V \text{ is the voltage, and } M \text{ is the molecular}$$

weight. Here, for high performance the fuel must have a high charge, a high voltage, or a low molecular weight.

In regard to chemical propellants, they can be classified into three groups: (1) liquid, (2) solid, and (3) hybrid, which can be a combination of a liquid fuel and solid oxidizer or a combination of a solid fuel and liquid oxidizer. Further discussion of hybrid fuels will not be made since they have not been used with much success. The word propellant refers to both the fuel and oxidizer which are combined to produce burning. Fuel can be referred to as the reducing agent and the oxidizing agent is that compound that increases the proportion of oxygen or acid forming elements or radicals when combined with another compound. Liquid propellants require a mixing apparatus (injector) and in most cases must have pumps. Solid propellants are mixed during the manufacturing process and, of course, need no pumping.

10.2 Liquid Rockets and Propellants

In contrast to the solid rocket there seem to be many more items to be covered when discussing the more complicated liquid-propellant rocket. It should be noted that the statements made herein are general in nature. Actually, all the various rocket units now in existence will differ from each other in many respects since each is designed for a specific task.

In regard to the size of the combustion chamber, it must be large enough to allow for complete combustion of the propellants. A spherical

shape is desired since for a given volume this shape provides the minimum wall-surface area, therefore, the least weight. Also, manufacturing considerations indicate a preference for a spherical or cylindrical shape. In addition, the cooling jackets are more difficult to design and build for the more complicated shapes.

As for feeding the propellants into the combustion chamber, it is important to realize that they have to be forced into the chamber under considerable pressure since the high temperature gases in the chamber are already at high pressure. Of the many ways of feeding the propellants to the chamber two are most widely used. The first employs a gas pressure feed system and is used on low-thrust, short-duration units. In this system the propellants are forced out of the tanks by replacing them with high pressure gas. This system is not used on large rocket units because large tanks would be required. Since these have to be made to withstand pressures greater than the combustion chamber pressure, their weight would become excessive. For the high-thrust, long-duration rocket use is made of the turbopump system. Here the propellants are pressurized by pumps which, in turn, are usually driven by turbines. Ordinarily a series of centrifugal pumps would be used to generate the high pressures, but due to the weight limitations in a rocket, only a single pump is likely to be used. This will result in the pump being run at an abnormal speed. The power to drive the turbines can be obtained in many ways, but normally is obtained from a gas generator either having its own propellant supply or using the same propellants as the rocket combustion chamber. Other means by which turbines are powered are by bleeding gas directly from

the combustion chamber or by using gas given off from solid-propellant charges burning at a slow rate.

Two important features of the combustion chamber are the injector and the igniter. The injector has a dual job in that it must spray both the fuel and oxidizer into the chamber as finely divided mists and at the same time properly mix them in the correct proportion. There are many kinds of injectors in use; some spray in jets, some in thin sheets, while others use a conical spray. Different propellants require different types of injectors, with the best injector usually being found by testing. An igniter is not always necessary, as some propellants ignite spontaneously on contact. Where it is needed, the igniter itself may be a very small liquid-propellant rocket, which can be ignited by a spark plug. This produces a pencil of flame which can be used to light off the main stream of propellants. This arrangement allows the rocket motor to be switched on and off.

It is often claimed that the starting is the most difficult operation in running a combustion chamber. The start must be accurately controlled to produce a smooth and even combustion. Care must be taken to avoid forming an unignited explosive mixture of propellants. The initial propellant flow is usually regulated to be less than full flow and the starting mixture ratio of the propellants is different from that used during normal operation. Frequently, a more reliable ignition is assured when one of the propellants is intentionally made to reach the combustion chamber first. Ordinarily, for a fuel-rich mixture the fuel is admitted first and vice versa for an oxidizer-rich mixture.

It seems almost unnecessary to mention the fact that the problem of cooling a liquid-propellant rocket motor is a large one. As for solid-propellant rockets, they are almost exclusively uncooled; however, liquid rockets are usually cooled, especially when used for a long duration. In these rockets some or all of the metal parts in contact with the hot gases must be cooled - such as the chamber walls, nozzle walls, injector faces, etc. The cooling jacket, which provides for the circulation of the coolant, is designed so that the coolant velocity is the highest at the critical regions and the fresh, cold coolant enters the jacket at or near these regions. Helical cooling passages are frequently used, especially at the critical regions where high velocities are needed. Regenerative cooling is used by the majority of flying liquid-propelled rockets. This method involves circulating one of the propellants through the cooling jacket on its way to the combustion chamber. It is of interest to note that the initial energy content of the propellant is thus augmented prior to injection increasing the exhaust velocity up to 1-1/2 percent. Water is often circulated in cooling jackets and is used extensively in static test stand firings. Another method of cooling is known as film cooling. Here, a thin fluid film covers and protects the exposed wall surfaces from excessive heat transfer. The film is introduced by injecting small quantities of fuel, oxidizer, or inert fluid at very low velocity in a large number of places along the exposed surfaces. This method is effective in that it forms a relatively cool boundary layer and the coolant is able to absorb a considerable amount of heat by evaporation. A special type of film cooling which has been tried is

called sweat or transpiration cooling. This method uses a porous wall material which admits coolant through pores over the surface. However, difficulty has been encountered in making the coolant distributions uniform due to variations in the pressure drop across the combustion chamber, particularly in the nozzle. Also, difficulty arises in the manufacturing for this process. The German V-2 used a combination of film and regenerative cooling with the fuel being the coolant.

Considerable research effort has been expended to find materials to meet rocket requirements. In brief, the wall materials have to withstand relatively high temperatures, high local gas velocities, the chemical action of corrosion and oxidation, high stresses, and initial heat shock. In addition, the walls have to permit high heat transfer rates and thermal expansion. These severe conditions are somewhat alleviated by the comparatively short operational duration of the rocket. High thermal conductivity and high strength at elevated temperatures, two important properties required in the inner walls of a cooled rocket combustion chamber, are not usually found in the same material. For instance, stainless steel withstands high stress at high temperature, but its walls have to be made thin for good heat transfer. Thus, material of this type would not be strong enough to be used in a large combustion chamber. On the other hand, high conductivity materials such as copper and aluminum have low strength at the higher temperatures and, therefore, require heavy and thick chambers. Some materials that have been used successfully are aluminum alloys, low carbon steel, alloy steels, and stainless steels.

There are many chemical compounds that are used for the fuel and oxidizer in liquid propellants. Some of the more common oxidizing agents and liquid fuels are listed below along with a few pertinent remarks about each.

Oxidizing Agents :

- (1) Hydrogen peroxide (H_2O_2).- This compound, which is liquid at room temperature, does not have a very high energy content. It is difficult to handle in that it is quite unstable, decomposing readily into H_2O and O_2 . This reaction, which is often spontaneous, occurs with most organic material such as grease and oil (explosive) or skin (burns). In addition, it is poisonous and very corrosive.
- (2) Nitric acid + nitrogen tetroxide ($HNO_3 + N_2O_4$).- This is liquid at room temperature, easy to handle, but very corrosive.
- (3) Liquid oxygen (O_2).- This abundantly available element is liquid only at very low temperatures. It is difficult to handle because of the severe cold and must be kept away from oil because of the fire hazard.
- (4) Liquid fluorine (Fl_2).- Fluorine is liquid at very low temperatures, only, and is very toxic and spontaneously reactable with many materials and metals.

Liquid Fuels (Reducing Agents) :

- (1) Gasoline (C_8H_{18}).- This was one of the first fuels used and is still in wide use today.

- (2) Alcohol (C_2H_5OH).- Alcohol is readily available and, therefore, used in many of the liquid-propellant rockets.
- (3) Aniline ($C_6H_5NH_2$).- Aniline is a hydrocarbon that ignites spontaneously with nitric acid; therefore, this propellant combination does not require an ignition system. Spontaneously ignitable propellants are often termed hypergolic.
- (4) Ammonia (NH_3).- This is a very stable compound; it can be mixed with other compounds without danger of explosion. Ammonia can be made hypergolic with nitric acid by addition of lithium.
- (5) Methane (CH_4).- Methane is non-corrosive and stable, but presents a high fire hazard. In addition, it is an asphyxiating agent.
- (6) Hydrazine (N_2H_4).- This has a loosely bonded chemical structure, therefore, high energy. It is a fire hazard and only slightly corrosive.
- (7) Unsymmetrical dimethyl hydrazine [$N_2H_2(CH_3)_2$].- This has good storability; that is, the liquid can be stored in ordinary tanks over long periods and at many temperatures without decomposition or change of state.
- (8) Liquid hydrogen (H_2).- Liquid hydrogen is very cold and, therefore, its contact with metals causes severe brittleness. Because of its low specific gravity large tanks are required resulting in a heavier tank weight.

Performance of a rocket is expressed in terms of the effective exhaust velocity c or the specific impulse c/g . Specific impulse is the thrust delivered per unit weight of propellant consumption, its units being

lb/lb/sec or just sec. Calculated values of specific impulse for a few propellant combinations are given below:

<u>Oxidizer and Fuel</u>	<u>Specific Impulse (sec)</u>
Hydrogen peroxide - gasoline	250
Hydrogen peroxide - hydrazine	260
Nitric acid - ammonia	240
Nitric acid - aniline	240
Liquid oxygen - gasoline	260
Liquid oxygen - alcohol	260
Liquid oxygen - hydrazine	280
Liquid oxygen - liquid hydrogen	360

The above values are for a chamber pressure of 500 psi and expanded at sea level pressure; the chamber temperatures are from 4500 to 5500° F.

In combination with most fuels, liquid fluorine affords higher values of performance than most other oxidizers. Several examples are shown below for a chamber pressure of 500 psi expanded to sea level pressure:

<u>Oxidizer and Fuel</u>	<u>Specific Impulse (sec)</u>	<u>Chamber Temperature (°F)</u>
Liquid fluorine - ammonia	300	7200
Liquid fluorine - hydrazine	320	7900
Liquid fluorine - liquid hydrogen	380	5100

Expansion at higher altitudes with a larger nozzle may increase the specific impulse by as much as 70 to 80 percent. In actual practice, three to ten percent less than the above values is obtained.

Combustion temperatures above 6500° F are usually not feasible since the molecules will become unstable and dissociate, consuming some of the energy of the gases. Fluorine rockets can be run at higher temperatures than most other chemical systems since fluorine is much more stable at these temperatures. For a fluorine-hydrogen rocket half as much hydrogen would have to be carried than for an oxygen-hydrogen rocket since only one H₂ molecule is required for each F₂ molecule whereas two are required for each O₂ molecule. This is a big advantage since the low density of hydrogen requires bulky fuel tanks. In regard to the highest energy content which can be expected there are no known chemical propellants which have an energy content twice that of those now in common use.

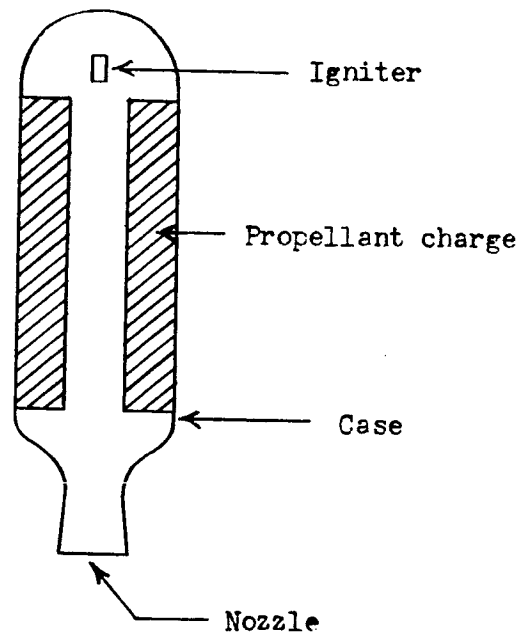
Fuel utilization is an important problem with a liquid fuel system. The optimum case would be that all fuel and oxidizer are used up at burnout. This means very close control must be maintained over the amounts of fuel and oxidizer carried and over the combining of these two compounds in the proper ratio for the desired thrust. Any oxidizer or fuel left over at burnout means a reduction in the performance of the rocket..... as can be seen by referring to equation (9-16) in SECTION IX.

$$v_f = c \ln \frac{M_0}{M_f}$$

where v_f is the drag and gravity free velocity at burnout, c is the effective exhaust velocity, M_0 is the mass of the rocket (plus fuel) at the beginning, and M_f is the mass at burnout.

10.3 Solid Rockets and Propellants

Solid-propellant rockets are storable and thus do not require long delays after a decision is made for firing. Since solid fuel is more dense than liquid fuel, a solid-propellant rocket will be smaller than a liquid rocket for a given impulse. Due to the high temperatures at which a solid fuel burns and since solid-propellant rockets are not cooled, they can be operated for only a short time; otherwise, the case would be melted or weakened. The solid rocket has no moving parts such as valves or pumps; it consists of the four parts shown in the simple sketch below:



Essentially, the entire solid-propellant rocket is pressurized, as the solid fuel comprises most of the rocket. The igniter emits a hot gas over the entire exposed surface of the propellant. Solid propellants can be ignited almost instantly, the shortest time being 10 or 12 milliseconds.

The design and manufacture of the propellant or grain, which is the name given to describing the physical body of the propellant, allows the thrust to be predetermined and programmed. Recent developments have been made where the solid rocket can be turned off and reignited.

There are two principal types of solid propellants. The first is referred to as double base propellant type because the propellant is mainly a combination of two chemical compounds, nitrocellulose $[C_6H_7O_2(ONO_2)_3]$ and nitroglycerin $[C_3H_5(ONO_2)_3]$. These are unstable compounds which are capable of combustion without the addition of an oxidizing material. These double-base compositions are either extruded or cast. The specific impulse of extruded Ballistite (JPN), which is 51.5 percent nitrocellulose and 43.0 percent nitroglycerin is 246 seconds at a chamber pressure of 1000 psi and 239 seconds at a chamber pressure of 500 psi. In the future, the specific impulse of solid propellants will probably reach a value as high as 300 seconds.

The other type of solid propellant is called composite propellant type and contains two principal ingredients, a fuel and an oxidizer, neither of which will burn satisfactorily without the presence of the other. The propellant usually consists of a finely ground oxidizer mixed with a fuel (while the fuel is in the liquid state and often at an elevated temperature) and is usually cast. Typical chemicals used as oxidizers are ammonium perchlorate (NH_4ClO_4) and ammonium nitrate (NH_4NO_3) and are used with such fuels as Thiokol, polyurethanes, polyesters, and butyl rubbers. Usually, 60 to 80 percent of these mixtures is the oxidizing

agent. The ammonium perchlorate produces an exhaust gas which is toxic and highly corrosive to many materials.

In both types of solid propellants, other chemicals are included, in addition to the principal ingredients, to control the physical and chemical properties of the propellant.....such as serving as a catalyst to accelerate or decelerate the burning rate.

For a solid propellant rocket the highest efficiency is obtained when the rocket is operated at a constant pressure. When this happens then the mass of the fuel burned equals the mass discharged.

$$\dot{m}_b = \dot{m}_d$$

Now

$$\dot{m}_b = R S \rho_p$$

where R is the burning rate or the velocity at which a solid propellant is consumed

S is the propellant burning area

ρ_p is the propellant density

and

$$\dot{m}_d = C_d P_c A_t$$

where C_d is the discharge coefficient

P_c is the chamber pressure

A_t is the nozzle throat area

Then

$$R S \rho_p = C_d P_c A_t$$

The burning rate is a function of the chamber pressure,

$$R = a p_c^n$$

where a and n are constants. (The constant a depends upon the temperature of the propellant grain prior to combustion.)

Thus

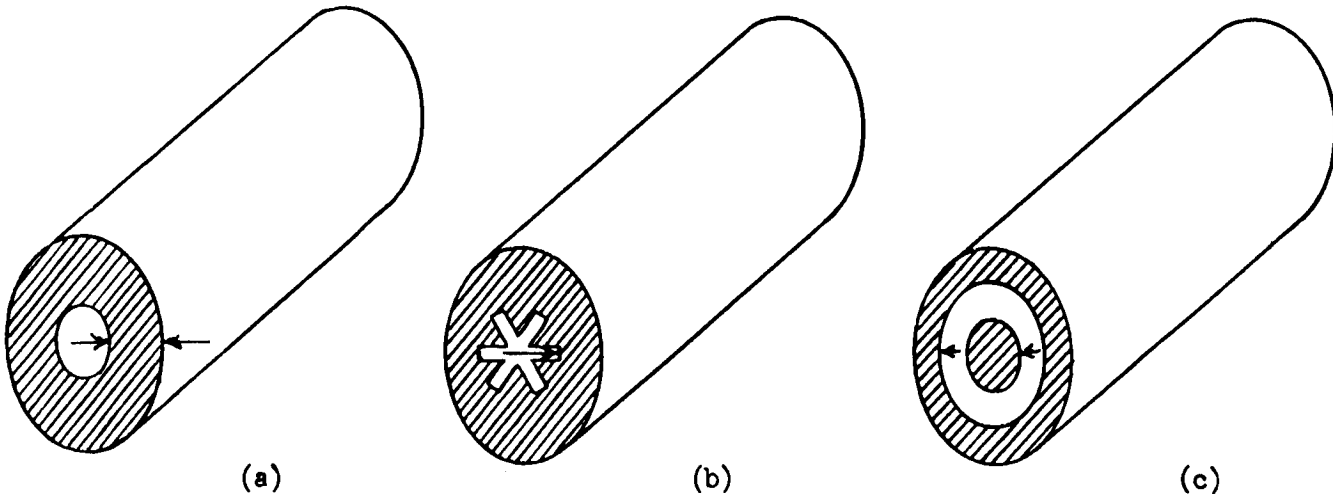
$$a p_c^n S_p = C_d P_c A_t$$

or

$$p_c = \left(\frac{a S_p}{A_t C_d} \right)^{\frac{1}{1-n}} = K \left(\frac{S}{A_t} \right)^{\frac{1}{1-n}}$$

where the constant K is determined by the choice of the propellant. The ratio of the burning area to the nozzle throat area is an important quantity in the design of solid propellant rockets. For example, the relation permits an evaluation of the variation necessary in the throat area if the chamber pressure (and therefore the thrust) is to be changed.

From the foregoing development it appears that the problem in grain design is to make the shape of the grain such that its burning will maintain a constant pressure. This is done by trying to design the grain so that the burning surface will always be a constant area during burning. Some examples of grain design where it is possible to obtain a constant burning area are shown below: (Arrows indicate burning surface.)



(a)

(b)

(c)

In the case of an internal burning design, as illustrated by (b) or (c), none of the heat of combustion gets to the case; therefore, the case can be made lighter giving a rocket of better performance.

SECTION XI

AERODYNAMIC HEATING AND HEAT TRANSMISSION

11.1 General Physical Principles, Temperature, Heat and Energy

We are all familiar with the kinetic energy of a body, due to its mass in motion, or its potential energy, due to its position in a gravitational field. Many engineers do not frequently work quantitatively with heat energy; the purpose of these notes is, therefore, to review some of the physical principles, the concepts, and the quantities which are used in this field.

We all have an instinctive idea of what we mean by temperature and heat. We say that heat is that which causes a body to rise in temperature, and temperature is a quantitative measure of the degree of hotness or coldness of a body. It is rather like a potential, and we ordinarily adopt some arbitrary scale, and arbitrary reference. The ice point and boiling point of water are two standard points, given values of 0 to 100 degrees on the Centigrade scale, 32 degrees and 212 degrees on the Fahrenheit scale. These values are old standards, new physics has associated with heat the vibrational energy of the molecules that make up the substances. This energy becomes zero at a temperature of zero on the absolute scale of temperature, 0 degrees Kelvin for the cgs system,

0 degrees Rankine in the Fahrenheit scale. The generally adopted relations are

$$T, (^{\circ}\text{K}) = T (^{\circ}\text{C}) + 273.18 \quad (11.1-1)$$

$$T (^{\circ}\text{R}) = T (^{\circ}\text{F}) + 459.72 \quad (11.1-2)$$

Now it was one of the great illuminating principles of science that energy in its various forms can be measured, and compared on a common basis, by reducing each to the amount of mechanical work it can do. This point has not always been as obvious as it seems now, in fact it was not believed generally true, especially in the biological sciences until Helmholtz, as recently as 1847 published his famous paper, "On the Conservation of Energy".

Since the kinetic energy of a mass m is $1/2 mV^2$, the work done in lifting a one pound weight one foot against the force of gravity will give that same weight a velocity $V = \sqrt{\frac{2}{m}} = \sqrt{2 \times 32.2} \sim 8$ ft/sec. Conversely, a weight of one pound moving at 8 ft/sec, would, in coming to rest, do one ft-lb of work. Some sharp fellow, probably a blacksmith, noticed that if the weight was a hammer that he was swinging with all his might against an anvil, so that it stopped dead, then the hammer, and also the anvil got warm. This was a great mystery at first; it's not so long ago that it was finally demonstrated that the same amount of work always produced the same amount of heat, and we were led to the idea of the mechanical equivalent of heat, J for the British physicist Joule who measured it in 1843. The modern value

is that J is 778.26 ft-lb per BTU; that is 778.26 ft-lb of work done will generate sufficient heat to raise the temperature of one pound of water by one degree Fahrenheit. The BTU, British Thermal Unit, is the quantitative measure of heat, the amount of heat required to raise the temperature of one pound of water one degree Fahrenheit.

In an earlier SECTION on the Orbits of Satellites we discussed the concept of the total energy of a satellite, $U = \frac{1}{2} mV^2 - \frac{R^2 g_0 m}{r}$. It is instructive to consider this energy, not only from the standpoint of the usual measure, ft-lb, but also as U/J, or the heat capacity.

For a circular orbit of radius r the speed of the satellite is $V_c = \sqrt{\frac{R^2 g_0}{r}}$ and its total energy is

$$U = \frac{1}{2} m V_c^2 - \frac{R^2 g_0 m}{r}$$

Since the value of total energy uniquely fixes the semi-major axis a and thus the size of any elliptical orbit, we can regard this value of total energy as U_a the total energy of any elliptical orbit of semi-major axis a, regardless of eccentricity and write

$$\begin{aligned} U_a &= \frac{1}{2} m \frac{R^2 g_0}{a} - \frac{m R^2 g_0}{a} \\ &= - \frac{1}{2} \frac{m R g_0}{a/R} \end{aligned}$$

or

$$\frac{U_a}{mRg_0} = \frac{-0.5}{(a/R)}$$

For the same satellite at rest on the earth ($V = 0$, $a = R$)

$$\frac{U}{mRg_0} = -1$$

These relations are illustrated in figure 1, where the total energy is plotted as a function of a/R . The abscissa is discontinuous to cover a wide range. The ordinate on the left is an orbital energy scale, where the zero applies to a body at rest at infinity. The scale on the right is the total energy of a mass of 1 pound in an orbit at a/R , expressed in BTU/lb. The zero for this scale is taken as at rest on the ground. 14,000 BTU/lb are required to establish an orbit of radius R , very little more would move the orbit out to 400 miles ($a/R = 1.1$), twice would put it at infinity.

14,000 BTU/lb is a lot of heat, when it is recalled that 180 BTU will raise a pound of water from the ice point to the boiling point. An additional 970 BTU will vaporize a pound of water into steam, 143 BTU will melt a one pound block of ice at 32°F. Thus a one pound satellite has enough energy to turn an 11 pound block of ice into steam. Conversely, this much energy must be dissipated if a satellite in orbit is to be returned to earth. Much of this energy can be dissipated as drag, some will appear as heat, which must in turn either be disposed of by radiation or be conducted to the interior and absorbed. The following sections will review

the principles of radiation, conduction and convection. Symbols and definitions of quantities generally used in this discussion are defined in the table.

11.2 Modes of Heat Transmission

Heat is moved from place to place in three ways, by radiation, by conduction and by convection. The laws governing these modes of transmission are of great engineering importance, and have been studied for a long time, by many of the great names of science. Fourier (1822) invented Fourier series to deal with the problem of the flow of heat in solids, Newton stated the law of heat transfer from a solid to a fluid in 1701.

11.3 Radiation

Every body emits radiant energy in all directions. When this energy strikes another body some may be absorbed, some reflected, and some transmitted through the body. The part absorbed is transformed into heat. The law of thermal radiation was discovered empirically (1879) then derived theoretically (1884). The quantity of heat radiated per second from a surface of area A at a temperature T is

$$\frac{dQ}{dt} = A \sigma T^4 \quad (11.3-1)$$

This law as written applies to a so-called "black body", an ideal radiator, or what is the same thing, a perfect absorber, at all wavelengths. Most substances reflect some part of the illumination that falls on them and are thus not

black bodies. They are characterized by a quantity ϵ called the emissivity, which is defined as the ratio of the total energy radiated by a body at temperature T to the energy radiated by a black body at the same temperature, i.e.

$$\epsilon = \frac{(dQ/dt)_{\text{surface}}}{(dQ/dt)_{\text{black body}}} \quad (11.3-2)$$

Polished metallic surfaces at room temperatures have low values of emissivity, the lowest being gold with a value of 0.018. Most polished surfaces darken as the temperature increases, due to oxidation of the surface; under these conditions the emissivity may range up to values between 0.8 to 0.98. Extensive tables of emissivities have been published.

The constant σ in equation (11.3-1) is the Stephan-Boltzmann radiation constant, the value of which has been determined as 0.47594×10^{-12} BTU/(Sq ft)(Sec)($^{\circ}$ R)⁴. Thus for practical surfaces the total energy per second emitted as radiation may be written as

$$\frac{dQ}{dt} = 0.47594 \epsilon A \left(\frac{T}{1000} \right)^4 \quad (11.3-3)$$

This radiant flux is distributed continuously over a range of wavelengths in the spectrum of electromagnetic radiation which includes radio waves, and light, on down to the very short such as X-rays. Some representative points and bands in this spectrum are tabulated below, where the wave lengths

are expressed in Angstrom Units; one AU is 10^{-8} centimeter.

Spectrum of Electromagnetic Radiation

<u>Radiation</u>	<u>Wave Length AU</u>
X-rays	10 - 150
Ultra Violet, less than	4,000
Visible spectrum	4,000 - 7,000
Infra red, greater than	7,000
Hertzian waves, greater than	2.2×10^6
Radar	10^9
WVEC - TV	6.26×10^9
WVEC	2.012×10^{12}

The energy per unit area per unit time emitted by a black body in the wave length range λ to $\lambda + d\lambda$ is expressed by Planck's Spectral Distribution Law as

$$\frac{1}{A} \frac{dQ}{dt} \Big|_{\lambda} = \frac{2\pi hc^2 \lambda^{-5}}{e^{ch/k\lambda T} - 1}$$

$$\sim \frac{\lambda^{-5}}{e^{c_2/\lambda T} - 1} \quad (11.3-4)$$

Where

c = velocity of light

h = Planck's constant

k = Boltzmann's constant

$c_2 = 1.4387 \text{ cm}^\circ\text{K} = 2.5897 \text{ cm}^\circ\text{R}$

The total area under this function, i.e., integration between $0 < \lambda < \infty$ leads to equation (11.3-3). The shape of the spectral distribution was first determined experimentally but classical physics was unable to explain it, or provide a formula for it. It remained a puzzle until Planck proposed the quantum theory and in 1901 derived his distribution function which agreed with the hitherto inexplicable curve.

The spectral distribution has a single peak at a wavelength λ_p which varies inversely with the absolute temperature in a relation known as Wien's Displacement Law,

$$\lambda_p T = 0.28836 \text{ (cm) (deg K)} \quad (11.3-5)$$

or

$$\left(\frac{\lambda_p}{10,000} \right) \left(\frac{T}{1000} \right) = 5.1905 \text{ (AU) (deg R)} \quad (11.3-6)$$

The movement of this peak from the red end of the spectrum to the blue with increasing temperature is reflected in the increasing whiteness of luminous sources such as light bulb filaments with increasing temperature. Practical use is made of this property in use of the color scale of temperature.

For many practical purposes, radiant energy has its source on hot walls of a solid, and the temperature of a body can be estimated visually from its color by use of the following table.

Color Scale of Temperature

<u>Color</u>	<u>Temp. °R</u>
Incipient Red	1390 - 1480
Dark Red	1660 - 1840
Bright Red	2020 - 2200
Yellowish Red	2380 - 2560
Incipient White	2740 - 2920
White	3100 - 3280

Gases like nitrogen and oxygen do not radiate to any extent, nor do they absorb. Carbon dioxide and water vapor on the other hand, like many other gaseous compounds have complicated absorption bands especially in the infra-red and thus can emit a certain amount of heat. The net effect of all atmospheric components has been correlated on the basis of an empirical relation which treats the atmosphere as a radiator at the ambient atmospheric temperature T_A with an emissivity δ which varies linearly with the square root of the atmospheric pressure. The relation for this sky radiation factor may be written as

$$\delta = 0.54 + 0.14 \sqrt{\frac{P}{P_0}} \quad (11.3-7)$$

and thus an expression for the radiant energy from space and the outer atmosphere absorbed on a surface is

$$\frac{dQ}{dt} = A \epsilon \sigma \delta T_A^4 \quad (11.3-8)$$

This relation, based principally on ground observations, should be applicable at moderate altitudes, its suitability for use in the upper fringes of the atmosphere is not known, since here some atmospheric components are ionized or atomic rather than molecular. The energy exchanges associated with ionization and dissociation of gases are frequently good sources of radiant energy, the sun for example. As a source of radiation the sun is not a black body, but the radiant flux from the sun has a value known as the solar constant C and taken as 0.1192 BTU/(sq ft)(sec). This value is taken as applying at the top of the atmosphere, at the mean distance between the sun and the earth. Thus the heat absorbed from the sun can be written

$$\frac{dQ}{dt} = \epsilon AC \quad (11.3-9)$$

where ϵ is used instead of the absorptivity for solar radiation, a quantity which for some materials differs to some degree from the absorptivity for black body radiation.

11.4 Convection

Newton, in 1701, defined the relation for the heat transfer between fluid at a temperature T and a surface at a temperature T_s . The relation may be written as

$$\frac{dQ}{dt} = hA(T - T_s) \quad (11.4-1)$$

Equation (11.4-1) is not a physical law but an expression of experimental observations which is applicable to many surfaces and fluids; the latter may be liquids or gases. The

convective heat transfer coefficient h is not a calculable quantity but theoretical considerations indicate that it should be a function of both the flow conditions and the thermal properties of the fluid. Flow conditions can be correlated by means of the dimensionless ratio, the Reynold's Number Re , fluid properties in terms of the Prandtl Number Pr ; the convective heat transfer coefficient is expressed in dimensionless terms by the Nusselt Number, Nu . Theory does not provide an indication of the functional nature of the relationship between these three dimensionless ratios, but experimental evidence tends to confirm the general indications of theory. A number of experimental correlations have been published, one frequently used is of the form

$$Nu = A(Re)^n (Pr)^m \quad (11.4-2)$$

$$\text{or} \quad \frac{hL}{k} = A \left(\frac{\rho VL}{\mu} \right)^n \left(\frac{c_p \mu g}{k} \right)^m \quad (11.4-3)$$

where A is some constant and L is some characteristic dimension and the exponent m appears to have a value about 0.31. For spheres in air equation (11.4-3) takes the form

$$\frac{hD}{k} = 0.37 \left(\frac{\rho VD}{\mu} \right)^{0.6} \quad (11.4-4)$$

For use of equation (11.4-4) temperature T for the fluid is required. In aeronautical applications T will

not ordinarily be the ambient temperature of the atmosphere because of the phenomenon of aerodynamic heating. To discuss this subject several special temperatures must be defined. Stagnation temperature T_T , adiabatic wall temperature T_{aw} , and surface temperature T_S .

Stagnation temperature: Consider a body moving with a velocity V through air at rest at a temperature T_A . At a stagnation point on the body the air is at rest relative to the body and has thus also acquired a speed V relative to the ambient air. Work has thus been done on this air, increasing both temperature and pressure, increasing its total energy. For a perfect gas theory expresses the stagnation temperature in terms of T_A , the Mach number, and the adiabatic exponent γ which is the ratio of the specific heat of the gas at constant pressure to the specific heat at constant volume. This relation

is

$$T_T = T_A \left(1 + \frac{\gamma-1}{2} M^2 \right) \quad (11.4-5)$$

Although useful for values of Mach number up to 2 or 3, equation (11.4-5) is strictly applicable only for the limited range of temperatures and pressures over which the specific heat of air is substantially constant. More accurate values of stagnation temperature are obtained from enthalpy tables. Enthalpy is a measure of the total energy of a gas. Air at rest and an ambient temperature T_A has

a value of enthalpy per unit mass h_{T_A} given in Table 2. An increase in speed to a value V provides an enthalpy increase $\Delta h = V^2/2gJ$. The stagnation temperature is then that temperature corresponding to the enthalpy h_{T_T} where

$$h_{T_T} = h_{T_A} + \frac{V^2}{2gJ} \quad (11.4-6)$$

A comparison of values of stagnation temperature computed by equations (11.4-5) and (11.4-6) is given below for $T_A = 518.4$ or sea level in the standard atmosphere.

M	T_T $\gamma = 1.4$	T_T enthalpy basis
1	622	622
2	933	929
3	1451	1418
4	2177	2060
5	3110	2844
6	4251	3770
7	5599	4830
8	7154	6040

Adiabatic Wall Temperature: At any point on a moving object which is not a stagnation point, the air is also at rest, but through the boundary layer there is a transition to free stream conditions. The nature of this transition is such that the surface may assume an elevated temperature near but less than the stagnation temperature. If the heating process is an adiabatic one, free from the

effects of conduction and radiation, the temperature reached is termed the adiabatic wall temperature T_{aw} . Data on T_{aw} are correlated by a temperature recovery factor K which is indicative of the proportion of the total temperature rise $T_T - T_A$ achieved, that is

$$\frac{T_{aw} - T_A}{T_T - T_A} = K \quad (11.4-7)$$

The actual value of K varies with the boundary layer, being smaller for laminar than for turbulent boundary layers. Theoretical studies by Polhausen indicate that for flat plates parallel to the stream K is a function of the Prandtl number, based on a Prandtl number for air at ordinary temperatures of 0.72, these studies indicate

$$\text{Laminar boundary layer, } K = (Pr)^{\frac{1}{2}} = 0.85$$

$$\text{Turbulent boundary layer, } K = (Pr)^{\frac{1}{3}} = .895$$

values which are in general confirmed by experiment. For blunt bodies, the recovery factor will, in general, vary with the shape ranging upward from the flat plate values toward unity.

Surface Temperature: The temperature actually assumed by a surface under the action of convective heating depends not only on the adiabatic wall temperature and convective heat transfer coefficient, but also on any exchange of energy

by radiation, and by conduction of heat to some other parts. Under steady conditions a surface initially at a temperature T_S would reach a temperature T_{aw} under the action of aerodynamic heating alone, but radiation to other bodies, the earth and outer space can reduce this value considerable.

Equilibrium Temperature: Under the combined actions of aerodynamic heating, and radiative processes, with or without solar heating a body will ultimately reach an equilibrium temperature T_e which is ordinarily less than the value of T_{aw} appropriate to the operating conditions. At T_e the net rate of heat transfer is zero. The time taken to reach this equilibrium temperature depends to a large extent upon the magnitude of the heat transfer coefficient. Consider a conducting flat plate initially at a temperature T_S , one face of which with area $A/2$ is receiving solar radiation, the other earth radiation. The total aerodynamic heating input would be, by equation (11.4-1) $hA(T_{aw} - T_S)$, the solar input would be $\epsilon \frac{A}{2} C$. The radiation exchange with the earth and space would be expressed by $\epsilon \sigma A (\delta T_A^4 - T_S^4)$. At equilibrium where $T_S \rightarrow T_e$, the sum of these terms is zero and

$$hA(T_{aw} - T_e) + \epsilon \frac{A}{2} C + \epsilon A \sigma (\delta T_A^4 - T_e^4) = 0 \quad (11.4-8)$$

With due attention to the areas involved, and the presence or absence of solar heating, similar expressions can be written for other shapes. These expressions are all of the

form $aT_e^4 + T_e - b = 0$, the positive real root is the equilibrium temperature.

When speeds are of the order of satellite speeds, T_{aw} is of a different order of magnitude than T_A , for such speeds more is known at present about the product hT_{aw} appearing in equation (11.4-8) than about either h or T_{aw} alone. Under such conditions, a frequently used correlation is that by Romig, which gives the heat transfer rate at the stagnation point of a hemispherical nose of radius R_n in terms of the Mach number M and free stream pressure p as

$$\frac{1}{A} \frac{dQ}{dt} = 0.0145 M^{3.1} \sqrt{\frac{p}{R_n}} \quad (11.4-9)$$

11.5 Conduction

In an opaque solid, conduction is the only mechanism of heat flow. Under the influence of a temperature gradient, kinetic energy is transferred from a molecule to adjacent molecules. The flow of heat through a medium is thus in many ways analogous to the flow of electricity. Heat flows from a region of high potential (temperature) to a region of low potential; a substance is characterized by its conductivity k , a sort of reciprocal resistivity. Just as electricity can be stored by increasing the charge in a condenser, heat is stored in a substance by increasing the temperature. These two properties of flow and storage, are characterized by two equations which are fundamental to any

consideration at the conduction of heat.

The flow equation:

$$\frac{dQ}{dt} = -kA \frac{dT}{dx} \quad (11.5-1)$$

expresses the quantity of heat passing a boundary in the medium in terms of the temperature gradient dT/dx at that boundary. The storage equation:

$$\frac{dQ}{dt} = cw(A\Delta x) \frac{dT}{dt} \quad (11.5-2)$$

relates the quantity of heat stored in a volume of area A and thickness Δx , to the rate of temperature increase and the heat capacity of the medium. The heat capacity, the quantity of heat required to raise one cubic foot of the substance one degree fahrenheit, is the product cw , of the specific heat c (BTU per pound) and the specific weight w (pounds per cubic foot). Values of c and w for some representative materials are given in Table 2.

The application of these two equations to heat conduction problems is illustrated by the classical Fourier Heat Conduction equation for one-dimensional heat in steady heat flow. Consider a homogeneous medium, either a rod of area A and length L insulated so that heat can flow only in the x direction, or a small section of a large slab of thickness L uniformly heated so that heat flow in the y and z directions can be ignored. If at some point x in the medium we consider a boundary across which heat is flowing, the quantity of heat which flows per unit time by

equation (11.5-1) is

$$\left(\frac{dQ}{dt}\right)_x = -k A \left(\frac{dT}{dx}\right)_x$$

Between the boundaries at x and $x + \Delta x$ there lies a slab of thickness Δx , and heat capacity cw . The difference between the heat which flows into the slab at x , and that which flows out at $x + \Delta x$, is

$$\left(\frac{dQ}{dt}\right)_x - \left(\frac{dQ}{dt}\right)_{x+\Delta x} = k A \left[\left(\frac{dT}{dx}\right)_{x+\Delta x} - \left(\frac{dT}{dx}\right)_x \right] \quad (11.5-3)$$

This is the heat which remains in the slab and which by the storage equation produces a rate of temperature increase dT/dt specified by the relation

$$cw(A\Delta x) \frac{dT}{dt} = k A \left[\left(\frac{dT}{dx}\right)_{x+\Delta x} - \left(\frac{dT}{dx}\right)_x \right] \quad (11.5-4)$$

The temperature gradient at $x + \Delta x$ is related to that at x by the relation

$$\left(\frac{dT}{dx}\right)_{x+\Delta x} = \left(\frac{dT}{dx}\right)_x + \left(\frac{d^2T}{dx^2}\right) \Delta x \quad (11.5-5)$$

where the second derivative is evaluated at some point between x and $x + \Delta x$. For vanishingly small values of Δx , then the bracketed term in equation (11.5-4) becomes

$$\left(\frac{dT}{dx}\right)_x + \left(\frac{d^2T}{dx^2}\right) \Delta x - \left(\frac{dT}{dx}\right)_x = \left(\frac{d^2T}{dx^2}\right) \Delta x \quad (11.5-6)$$

hence, the equation for one dimensional unsteady heat flow,

$$cw(A\Delta x) \frac{dT}{dt} = kA \frac{d^2T}{dx^2} \Delta x \quad (11.5-7)$$

or

$$cw \frac{\partial T}{\partial t} = k \frac{\partial^2 T}{\partial x^2} \quad (11.5-8)$$

where the partial derivative is used since T is a function of both time t and the coordinate x .

In heat transmission problems, equation (11.5-8) is generally written as

$$\frac{\partial T}{\partial t} = \alpha \frac{\partial^2 T}{\partial x^2} \quad (11.5-9)$$

where the quantity $\alpha = k/cw$ termed the diffusivity, and which has the dimension (length squared) is a useful measure of the heat conducting properties of a material, the meaning of which can perhaps be best illustrated by a solution of equation (11.5-9).

As a partial differential equation, there are no simple direct methods for the solution of equation (11.5-9). Solutions to a number of special problems are known, however, (see for example reference 1). The nature of each solution is determined by the boundary conditions, that is the temperatures at particular times at particular points in the medium. As an example of some practical interest, consider a plate of thickness L , initially at a uniform temperature T_0 ,

one edge of which, (that at $x = 0$) is instantaneously changed to a temperature T_1 . Such a problem represents an idealization of a thick skin, one face of which is suddenly subjected to a high temperature as in a jet, i.e., where the heat transfer rate is taken as infinite. For this problem the initial, or boundary conditions, are, for all values of t

$$(1) \quad T = T_1 \quad \text{at} \quad x = 0$$

$$(2) \quad \frac{dT}{dx} = 0 \quad \text{at} \quad x = L$$

This second boundary condition follows from the assumed idealization that no heat can flow across the unheated face at $x = L$. The solution to equation (11.5-9) is then found by the method of separation of variables, in which it is assumed that the functional dependence of temperature on both x and t can be expressed by the product of two functions, here denoted Θ and X where Θ is a function of t alone, and X is a function of x alone, that is

$$T(x, t) = \Theta(t) \cdot X(x)$$

Often it is easier to solve for the unachieved temperature rise

$$T = \frac{T(x, t) - T_0}{T_1 - T_0} \quad (11.5-10)$$

Thus if $T = \Theta(t) \cdot X(x)$

$$\frac{\partial T}{\partial t} = X \frac{d\theta}{dt} \quad (11.5-11)$$

and
$$\frac{\partial^2 T}{\partial x^2} = \theta \frac{d^2 X}{dx^2} \quad (11.5-12)$$

substitution of these relations in equation (11.5-9) gives

$$X \frac{d\theta}{dt} = \alpha \theta \frac{d^2 X}{dx^2} \quad (11.5-13)$$

or dividing both sides by $T = \theta \cdot X$

$$\frac{1}{\alpha \theta} \frac{d\theta}{dt} = \frac{1}{X} \frac{d^2 X}{dx^2} \quad (11.5-14)$$

This relationship can apply only if both sides of equation (11.5-14) are equal to a constant, which can be written as $-b^2$. Then

$$\frac{d\theta}{dt} + b^2 \alpha \theta = 0 \quad (11.5-15)$$

$$\frac{d^2 X}{dx^2} + b^2 X = 0 \quad (11.5-16)$$

It can be verified that

$$\theta = C e^{-b^2 \alpha t}$$

is a solution to equation (11.5-15), also that

$$X = A \cos bx + B \sin bx \quad (11.5-17)$$

is a solution to equation (11.5-16) and thus that T is given by the product of these two relations, or

$$T = e^{-b^2 \alpha t} [D \cos bx + F \sin bx] + G$$

where the constant G is added as a constant of integration. The boundary conditions are now used to determine the values of d , F , G and b .

From the first condition $T = T_1$ at $x = 0$, therefore, $T = 1$. Thus $D = 0$, since $e^{-b^2 \alpha t}$ is not zero, and $G = 1$. Hence $T = 1 + Fe^{-b^2 \alpha t} \sin bx$

$$\frac{dT}{dx} = Fbe^{-b^2 \alpha t} \cos bx$$

From the condition that $\frac{dT}{dx} = 0$ at $x = L$, it follows that $F \neq 0$, and $b = \frac{n\pi}{2L}$, $n = 1, 3, 5, \dots$ and thus

$$T = 1 + Fe^{-(n\pi/2L)^2} \sin \frac{n\pi x}{2L}$$

$$n = 1, 3, 5, \dots$$

There are a number of terms $F \sin \frac{n\pi x}{2L}$ each of which represents a solution of the equation, hence their sum represents a solution, and thus

$$T = 1 + \sum F_n e^{-n^2 t/t_c} \sin \frac{n\pi x}{2L} \quad (11.5-18)$$

where $t_c = \frac{(2L/\pi)^2}{\alpha} \quad (11.5-19)$

At $t = 0$, $T = T_0$ and $T = 0$ for $0 < x \leq L$, hence the F_n can be established from the Fourier series relation for a unit step,

$$\frac{4}{\pi} \left[\sin \frac{\pi x}{2L} + \frac{1}{3} \sin \frac{3\pi x}{2L} + \frac{1}{5} \sin \frac{5\pi x}{2L} + \dots \right] = 1 \quad [0 < x < 2L]$$

$$= 0 \quad [x = 0]$$

Hence,

$$\frac{T(x,t) - T_0}{T_1 - T_0} = 1 - \frac{4}{\pi} \left[e^{-t/t_c} \sin \frac{\pi x}{2L} + \frac{1}{3} e^{-9t/t_c} \sin \frac{3\pi x}{2L} + \frac{1}{5} e^{-25t/t_c} \sin \frac{5\pi x}{2L} + \dots \right] \quad (11.5-20)$$

is the solution to the problem. The temperature distribution expressed by equation (11.5-20) is plotted in figure 11-2 for various values of the ratio t/t_c . The initial temperature step to T_1 at the face $x = 0$ penetrates farther and farther into the slab with the passage of time. There is essentially no warming of the inner face at $x = L$ until a time t slightly in excess of $0.1t_c$ has passed after which the temperature increase is rapid. The time interval t_c which appears in each of the exponential terms of equation (11.5-20) is a characteristic time fixed by the thickness L and the diffusivity α which is thus seen to be the square of a characteristic dimension of the substance. This dimension is a measure of the distance into the material which an initial surface temperature increase will penetrate in a given time. The two values of diffusivity used for illustration in figure 11-2 are representative of iron and carbon, the solutions are for the unheated surface of one inch slabs of these two materials.

Carbon, with its higher diffusivity, experiences a much more rapid temperature increase than does iron.

Equation (11.5-18) converges rapidly, and is, therefore, easy to use for calculations. In order to obtain it, however, simplifying assumptions were necessary, infinite heat transfer at the heated surface, and no radiation. These assumptions would generally be too unrealistic for any practical aeronautical applications. The assumption of infinite heat transfer is not a necessary one, the solution is known (reference 1) for a finite value of heat transfer coefficient from a constant temperature medium, but it does not converge rapidly, and is awkward to use. If radiation must be accounted for, exact solutions of the differential equation of heat conduction have not been found, and recourse must be had to approximate or to numerical methods, some of which will be discussed under Heat Protection, SECTION XII.

Reference

1. Carslaw, H. S., and Jaeger, J. C.: Conduction of Heat in Solids. The Clarendon Press (Oxford), 1947.
2. McAdams, William H.: Heat Transmission. McGraw-Hill Book Company, Inc., Third Edition, 1954.

SYMBOLS

C	solar constant, 0.1192 (BTU)/(Sq ft)(sec)
c	specific heat of material (BTU)/(lb)(°F)
c_p	specific heat at constant pressure (BTU)/(lb)(°F)
c_v	specific heat at constant volume (BTU)/(lb)(°F)
g	acceleration due to gravity, 32.1740 ft/sec ²
h	convective heat transfer coefficient (BTU)/(sec)(sq ft)(°F)
h _T	enthalpy per unit mass of air corresponding to temperature T, (BTU)/(lb)
J	mechanical equivalent of heat (778.26 ft-lb/BTU)
K	temperature recover factor
k	thermal conductivity $\frac{\text{BTU}/(\text{sec})(\text{sq ft})}{\text{deg F}/\text{ft}}$
ℓ	characteristic length
p	atmospheric pressure (lb)/(ft) ²
Q	quantity of heat, BTU
q	rate of heat flow per unit area BTU/(ft) ² sec
Re	Reynolds number, (V ℓ ρ/μ)
T	temperature °F and °R
t	time, seconds
V	velocity, (ft/sec)
w	specific weight of material, (lb)/(cubic ft)
Nu	Nusselt number, (h ℓ/k)
Pr	Prandtl number, ($c_p \mu g/k$)
α	diffusivity, k/cw
ε	emissivity
γ	Adiabatic exponent, c_p/c_v
ρ	density (slugs)/(cubic ft)
σ	Stefan-Boltzmann radiation constant 0.47594 x 10 ⁻¹² BTU/(sq ft)(sec)(°R) ⁴
μ	coefficient of viscosity (lb)(sec)/(sq ft)

TABLE XI-1
ENTHALPY OF AIR h_T , BTU/lb

T, °R	0	10	20	30	40	50	60	70	80	90	A
300	-23.95	-21.56	-19.16	-16.77	-14.37	-11.98	-9.58	-7.19	-4.79	-2.40	2.39
400	0.00	2.40	4.79	7.19	9.59	11.98	14.38	16.78	19.18	21.57	2.40
500	23.97	26.37	28.77	31.17	33.57	35.98	38.38	40.78	43.19	45.59	2.40
600	48.00	50.41	52.81	55.22	57.63	60.04	62.46	64.87	67.28	69.70	2.40
700	72.11	74.53	76.95	79.38	81.80	84.23	86.65	89.08	91.51	93.95	2.40
800	96.38	98.82	101.26	103.70	106.14	108.59	111.04	113.49	115.94	118.40	2.45
900	120.86	123.32	125.78	128.25	130.72	133.19	135.67	138.14	140.63	143.11	2.47
1000	145.59	148.09	150.58	153.07	155.57	158.07	160.58	163.09	165.60	168.11	2.50
T, °R	0	100	200	300	400	500	600	700	800	900	--
1000	145.59	170.62	195.96	221.62	247.60	273.89	300.48	327.36	354.50	381.90	26.40
2000	409.55	437.42	465.48	493.73	522.16	550.74	579.48	608.36	637.37	666.51	28.62
3000	695.77	725.14	754.62	784.19	813.85	843.61	873.45	903.38	933.38	963.46	29.78
4000	993.61	1023.82	1054.11	1084.46	1114.87	1145.34	1175.86	1206.44	1237.07	1267.75	30.49
5000	1298.48	1329.25	1360.07	1390.94	1421.85	1452.80	1483.80	1514.83	1545.91	1577.02	30.97
6000	1608.16	1639.35	1670.57	1701.83	1733.12	1764.45	-----	-----	-----	-----	31.26

$$h_{TT} = h_{TA} + \frac{V^2}{2gJ}$$

Reference: Keenan and Kaye,
"Thermodynamic Properties of Air"

444

Table 2

THERMAL PROPERTIES OF MATERIALS^(a)

Substance	MP	BP	w	c _p ^(b)	cpw	kx10 ⁴	x10 ⁴	μx10 ⁷	Heat of Fusion	Heat of Vap'n
Platinum	3651	7782	1334.1	0.324 0.400	43.3	117	2.70		49	
Gold	2405	5172	1204.6	0.312 0.327	37.6	472	12.5		28.4	
Nickel	3105	5712	537-555	.105 .145	57.6	94.5	1.64		133	
Iron	3255	5892	487-493	.115-.190 ^(c)	56.5-88	89-64 ^(c)	1.57-0.73		9.9-14	
Gallium	545	4100	369.1	.080(11q.)	29.5	--	--		34.5	
Titanium	3730	5900	280.9	.1125	31.7	25.6	.81		--	
Aluminum	1677	3732	168.5	.211 .282	35.6	331	9.3		138.2	
Carbon	6790	Subl.	140.5	.17 .57	24	242	10.1		--	
Beryllium	2922	3246	115.5	.397	45.9	230	5.02		621.9	
Lithium	826	3388	33.2	.790 1.371 ^(c)	26.2	.472	.018		59.02	
Water	491.7	671.7	62.43	1.00	62.43	1.09	.0175		143	970
Air ^(d)			.076475	.238	.0182	.0407	224	3.745	--	--

(a) Units in ft-lb-sec²R-BTU system.

(b) Where two values are given, first is at 80°F, second near melting or sublimation point of material unless otherwise noted.

(c) Varies markedly with temperature and change of state.

(d) Properties at sea level in Standard Atmosphere.

(e) Molten.

THERMAL PROPERTIES
 OF INSULATORS
 (from reference 2)

Insulator	Temp. °R	w lb/ft ³	k $\frac{\text{BTU/sec ft}^2}{\text{°F/ft}}$
Magnesite	858	158	6.1×10^{-4}
	1661		4.45
	2651		3.05
Diatomaceous earth (moulded and fixed)	858	42.3	0.390
	2059		.528
Kaolin	852	19	.139
	1860		.314
Aluminum foil sandwich	560	.2	.069
	811		.106

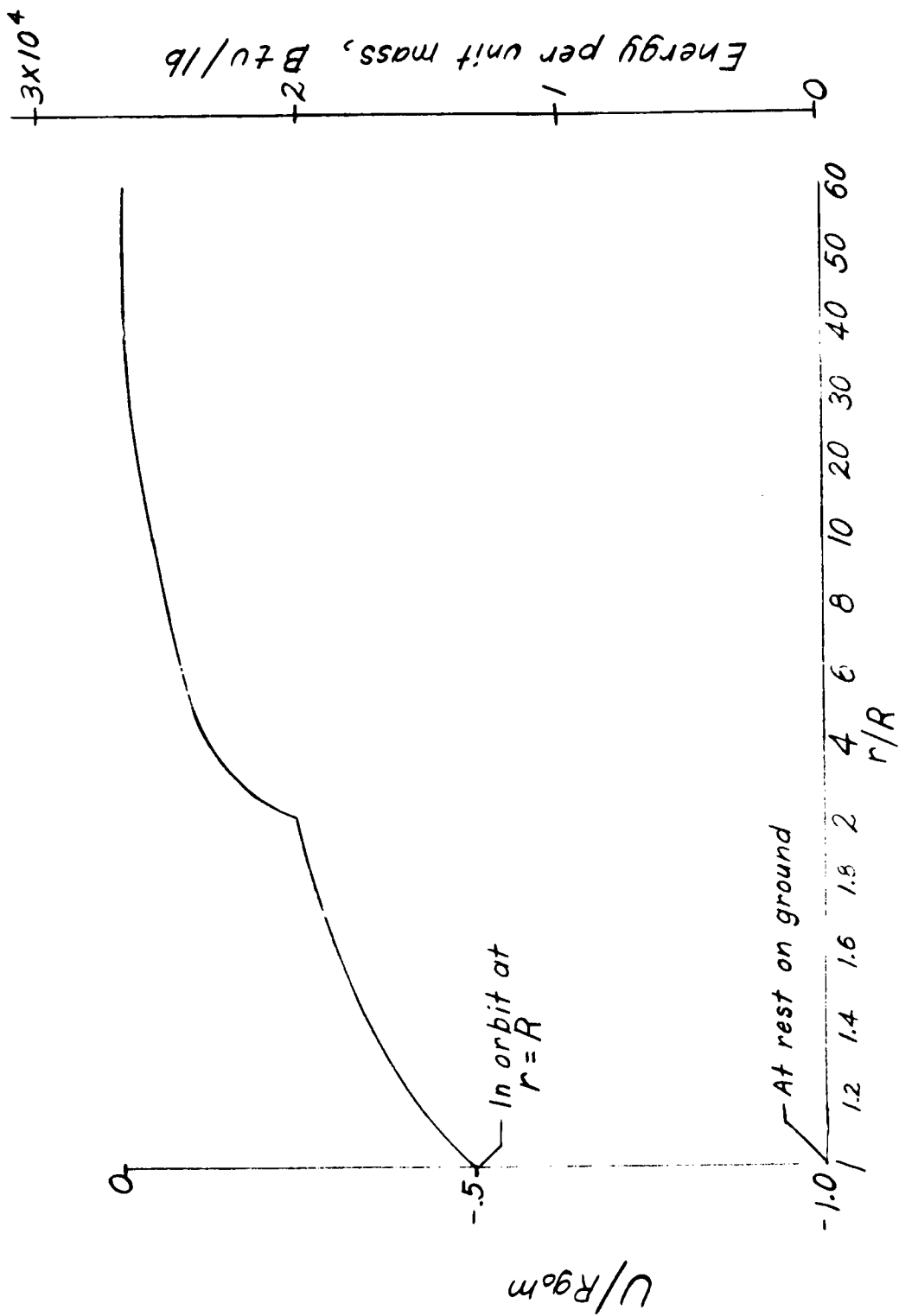


Figure 11-1. Total energy U of a satellite of mass m in a circular orbit of radius r , and its thermal equivalent for a mass equivalent to one pound, i.e. $\frac{1}{g_0}$ slugs.

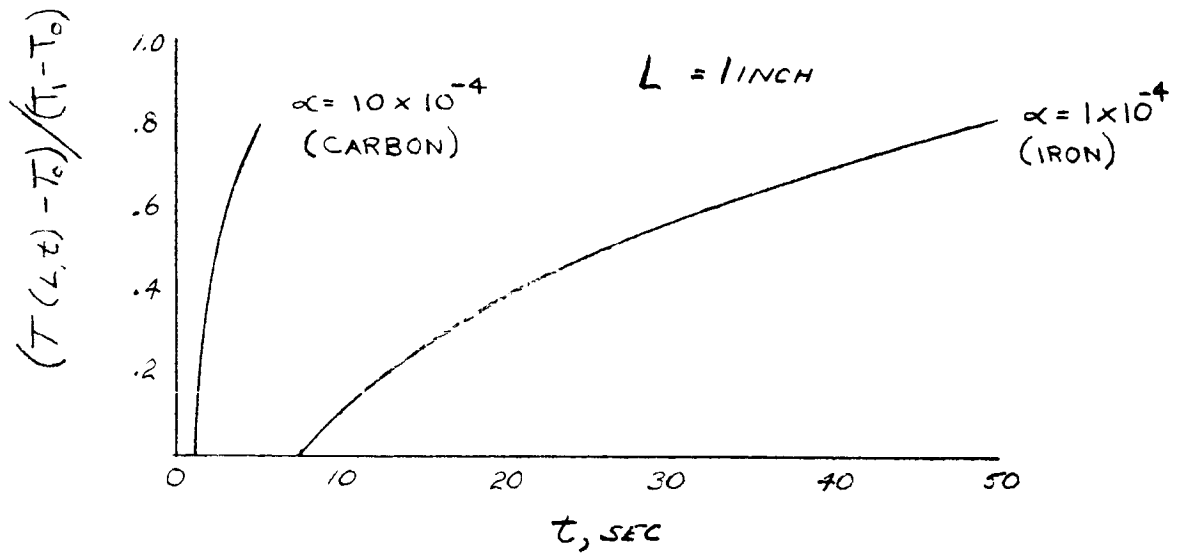
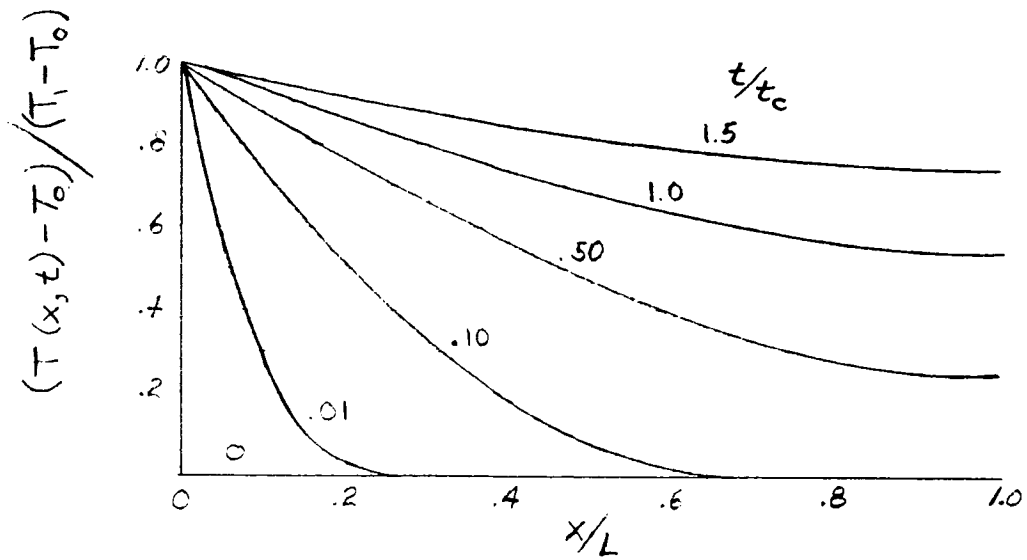


Figure 11-2

Temperature variation with position and time for semi-infinite slab subjected to step temperature input at face $x = 0$.

SECTION XII

HEAT PROTECTION

12.1 Introduction

In the discussion of basic heat concepts in SECTION XI it was pointed out that energy equivalent to 14,000 BTU/lb must be expended to return objects to earth from satellite speeds. Some of this energy is dissipated in the form of drag, that is, velocity changes, while the remainder must be absorbed as heat or reradiated. The energy values which enter into the heat protection problems to be considered here are only a small fraction of the 14,000 BTU/lb figure. For example, to return a winged vehicle similar to that proposed by the Flight Research Division from orbit requires the disposal of only 150 BTU/lb. This amount of heat, for example, for a 4,000 pound airplane could be absorbed by 600 pounds of beryllium with a temperature rise of 2,000°F. This, of course, may not be the most efficient way to handle the heating as will be demonstrated later.

There are available structural materials which retain sufficient strength to be used at temperatures as high as 2000°F. There is considerable question at the present time, however, whether practical structures can be operated at

2000°F. One important feature sometimes glossed over is the effect of temperature gradients which would be associated with hot structures under transient heating conditions. For example, a Rene 41 (nickel alloy) structure could support temperature gradients of only about 350°F before approaching failure from buckling considerations.

Several means are available to limit structural temperature to 2000°F or any desired lower value (practical limits arise, of course, in the size and weight of the insulating or shielding material). The various heat protection schemes may be classified as

- a. Radiators
- b. Insulators
- c. Heat sinks
- d. Surface evaporators
- e. Internal coolers

Every heat disposal scheme contains elements of most of the others. First let us consider the methods just listed to see what physical processes are involved in each.

a. Radiators.- The ideal radiator is a black body and most materials radiate heat from the surface only but it is still impossible to raise the surface temperature of a radiator to a point for efficient radiation without conduction of some heat to the interior of the material.

b. Insulators.- The ideal insulator has, of course, a low conductivity but large bulk even with low density is usually associated with insulating materials.

c. Heat sinks.- The process here is to attempt to retain in some non-structural item the heat input associated with high-speed flight. Materials with high specific heat are desired and if high specific heat can be associated with low density so much the better.

d. Surface evaporators.- Under this classification we can consider the melting, evaporation, sublimation or ablation of various metals and or synthetic compounds such as teflon. In these processes the latent heat of fusion or vaporization is used to lower the surface temperature. In an ablation process a change of state brought about by a chemical reaction and relatively high temperatures may be required for efficient heat absorption.

e. Internal cooling.- With this system of heat protection complications arise from the plumbing requirements and the difficulties involved in forced convection heat transfer calculations.

The major portion of these notes will be directed toward presentation of equations useful in the evaluation of heat transfer problems for Radiators, Insulators, Heat Sinks and I hope combinations of these three schemes.

The basic laws of heat transfer have been covered in SECTION XI but the actual solution of most heat transfer problems is difficult compared to the apparent simplicity

of the basic principles. For the remainder of this discussion simplifying assumptions will be made so that some answers and some physical pictures of the processes involved along with numerical answers may be obtained.

The first simplifying assumption will be that the heat input to our structure is independent of the structural temperature and has been specified by some independent calculation. Thus we will be discussing time histories of heat inputs such as are shown in figure 12-1. Figure 12-1a is the heat input in BTU/ft²sec. as calculated for the re-entry of a large flat object at 90° angle of attack from orbit at an altitude of about 70 miles. Figure 12-1b has about the same total heat input over a shorter period of time similar to a pulse which would correspond more nearly to the heating rate time history of a capsule vehicle during re-entry.

12.2 Radiation

If all the heat input could be radiated back, the temperature time history of the skin of the structure could be computed from the equation for radiant heat interchange

$$q_{1 \rightleftharpoons 2} = A_1 \sigma (T_1^4 - T_2^4) \frac{1}{\frac{1}{\epsilon_1} + \frac{1}{\epsilon_2} - 1}$$

if body 2 (the atmosphere) be considered a black body with $T_2^4 \approx 0$ then

$$\begin{aligned}
 q_{1 \rightarrow 2} &= A_1 \sigma T_1^4 \frac{1}{\frac{1}{\epsilon_1} + \frac{1}{1} - 1} \\
 &= A_1 \epsilon_1 \sigma T_1^4
 \end{aligned}
 \tag{12.2-1}$$

Where q is the rate of heat radiated

A the area

σ the Stefan Boltzman constant

ϵ the emissivity

and T the absolute surface temperature

Note: ϵ can range from 0.018 for gold to .98 for flat black lacquer; for metals ϵ increases with temperature until they become molten. For most nonmetallic substances ϵ decreases with increase in temperature. Quartz has a large negative gradient of ϵ with T and is one of the few substances whose thickness effects the radiation properties.

A generally used value for emissivity is 0.8. Thus equation (12.2-1) becomes

$$\frac{q}{A} = .3807 \left(\frac{T_1}{1000} \right)^4
 \tag{12.2-2}$$

where q is in BTU/sec

A in ft^2

T_1 in degrees Rankine

The surface temperature time histories using equation (12.2-2) for the time histories of heating rates in figure 12-1 are shown in figure 12-2.

12.3 Heat Shield Case

The forgoing example is, of course, entirely hypothetical since all the heat has been re-radiated and none conducted or absorbed by the structure. A heat shield or sink may be used to reduce the surface temperature to a level at which structural elements retain some strength. A heat shield is most efficiently constructed of materials which have a high specific heat. Two substances in liquid form, water and lithium have high specific heats 1 and 1.4, however, aside from the difficulty of containing these fluids as liquids the operating temperatures of concern here are such that both would become vaporized. For both, of course, vaporization would absorb large amounts of heat but then they would not strictly speaking, be heat sinks.

The material which seems most suited for a heated shield is the metal beryllium which has a specific heat ranging from 0.4 at 0°F to about 0.75 at 1600°F, the variation is not linear. Another metal whose specific heat is of interest is nickel with a specific heat of 0.1 at 0°F and 0.15 at 1600°F.

The following material will cover the calculation of the temperature rise due to the absorption of heat for the heat in-

puts of figures 12-1a and 12-1b for beryllium and nickel. The appropriate formula for use in heat absorption calculations is

$$dQ = V w c dT \quad (12.3-1)$$

In this equation Q is the quantity of heat in BTU, V the volume in ft^3 , w the density in lbs/ft^3 , c the specific heat, and T the absolute temperature in degrees R. (As used herein) In the derivation of equation (12.3-1) (see reference 1) the assumption was made that the material was thin with a high conductivity and thus no temperature gradient existed from the front to back face. Equation (12.3-1) may also be written as

$$Q = V w \int_{T_0}^T c dT \quad (12.3-2)$$

when the specific heat varies with temperature.

Since W the weight = wV equation (12.3-2) is

$$\frac{Q}{A} = \frac{W}{A} \int_{T_0}^T c dT \quad (12.3-3)$$

where

$$\frac{Q}{A} = \int \frac{q}{A} dt \quad \text{and } T_0 \text{ is the temperature at time } 0.$$

In figure 12-3 the specific heat curves for beryllium and nickel as a function of temperature are shown while in figure 12-4 the variation of $\int_{T_0}^T c dt$ as a function of T are given for an initial $T_0 = 500^\circ\text{R}$. Equation (12.3-3) is then used to calculate the temperatures which nickel and beryllium will reach when subjected to the

heating rate curves of figure 12-1a and 12-1b. The results are shown in figure 12-5 for unit weights (W/A) of nickel = 12 lbs/ft² and beryllium equal to 3 lb/ft². Different weights were necessarily used otherwise the nickel would melt before absorbing the total heat input.

The results shown in figure 12-5 were quantitatively obvious from figure 12-5 where it could be seen that roughly 5 times as much nickel as beryllium would be required to absorb the heat input equivalent to about 2300°R.

The efficiency of beryllium as a heat shield is demonstrated by these examples, however, in the actual physical case where radiation enters the picture there will occur instances where the heat shield only adds useless weight.

12.4 Radiation Plus Heat Shielding

Equation 12.2-2) applies for the case of single surface radiation. The thin materials we are speaking of here may radiate from both surfaces at the same temperature, thus equation (12.2-2) may be written as

$$\frac{q}{A} = .3807 \left(\frac{T_1}{1000} \right)^4 S \quad (12.4-1)$$

where S is either 1 or 2.

Integration of equation (12.4-1) gives

$$\frac{Q}{A} = .3807 S \int_{t=0}^{t=nat} \left(\frac{T_1}{1000} \right)^4 dt + C \quad (12.4-2)$$

If heat is both radiated and absorbed combination of equations (12.3-3) and (12.4-2) gives

$$\frac{Q}{A} = .3807 S \int_{t=0}^{t=n\Delta t} \left(\frac{T_1}{1000}\right)^4 dt + \frac{W}{A} \int_{T_0}^{T_1} c dT + C \quad (12.4-3)$$

The solution of equation (12.4-3) for T_1 can probably be handled by some very high grade mathematics but the approach detailed in the following produces answers in a reasonably short period of time by trial and error. The value of C is very small for the examples to be used and will be discarded. The time interval chosen is Δt and trapezoidal integration will be employed.

$$\begin{aligned} \frac{1}{.3807 S} \left(\frac{Q}{A}\right) &= \int_0^{t=\Delta t(n-1)} \left(\frac{T_1}{1000}\right)^4 + \frac{\Delta t}{2} \left(\frac{T_1}{1000}\right)_n^4 + \frac{\Delta t}{2} \left(\frac{T_1}{1000}\right)_n^4 + \frac{1}{.3807 S} \frac{W}{A} \int_{T_0}^{T_1} c dT \\ \frac{\Delta t}{2} \left(\frac{T_1}{1000}\right)_n^4 + \frac{1}{.3807 S} \frac{W}{A} \int_{T_0}^{T_1} c dT &= \frac{1}{.3807 S} \left(\frac{Q}{A}\right) - \int_0^{t=\Delta t(n-1)} \left(\frac{T_1}{1000}\right)^4 dt - \frac{\Delta t}{2} \left(\frac{T_1}{1000}\right)_{n-1}^4 \end{aligned} \quad (12.4-4)$$

Equation (12.4-4) may be solved by trial and error or by guess until the left hand side equals the right hand side.

As an example let us use 2 lb/ft² of beryllium with double surface radiation, $\frac{\Delta t}{2} = 5$ and the heat input curve of figure 12-1b. Equation (12.4-4) becomes

$$\frac{5}{2.627} \left(\frac{T_1}{1000}\right)_n^4 + \int_{T_0}^{T_1} c dT = .5 \left(\frac{Q}{A}\right) - \frac{1}{2.627} \int_0^{\Delta t(n-1)} \left(\frac{T_1}{1000}\right)^4 dt - \frac{5}{2.627} \left(\frac{T_1}{1000}\right)_{n-1}^4$$

The time chosen for evaluation is 10 sec., thus $n = 1$

and

$$1.903 \left(\frac{T_1}{1000} \right)_1^4 + \int_{T_0}^{T_1} c dT = .5 \left(\frac{Q}{A} \right) - \frac{1}{2.627} \int_0^{10} \left(\frac{T_1}{1000} \right)^4 dt - 1.903 \left(\frac{T_1}{1000} \right)_0^4$$

$$= .5(60) - 0 - 1.90 (.5)^4$$

$$= 30.00 - 0 - .12$$

$$= 29.88$$

try $T_1 = 800$ then $\int_{T_0}^{T_1} c dt$ from figure 12-4

$$= 145$$

and the lefthand side becomes

$$1.903 (.8)^4 + 145 = .78 + 145 \neq 29.88$$

From this it is seen that the temperature in this temperature range is primarily determined by the heat capacity, so from figure 12-4, (T_1) est $\approx 560^\circ R$

$$1.903 (.56)^4 + 29.5 = .19 + 29.5 = 29.69 \approx 29.88$$

This is about as accurately as the temperature (560°) can be obtained from the scales used in figure 12-4.

The temperature time histories for various unit weights of beryllium when both radiation and absorption effects are considered are shown in figure 12-6 for the heat input of figure 12-1b. Increasing the unit weight from 1 lb/ft² to 4 lb/ft² lowers the heat shield temperature 1020°F or in other words, an additional heat shield of 3 lb/ft² of beryllium lowers the temperature 1020°F.

12.5 Comparison of Radiation and Absorption Effects for Pulse Type Input

A rehash of some of the previously presented data for the pulse type of heat input of figure 12-1b demonstrates the effectiveness of the heat shield as indicated in figure 12-1. For the case where all the heat is assumed to be radiated the surface temperature follows the heat rate input curve and a maximum temperature of about 3500°R is reached. When the temperature is calculated using the absorption formula (and $W/A = 4.0 \text{ lb/ft}^2$) the surface temperature time history has the shape of the integral of the heat rate input curve with a maximum temperature of about 1700 degrees. The combination of both effects which is quite close to the actual physical case reaches a maximum temperature of about 1600 deg. after which heat is lost by radiation. For this type of heat input with the relatively large amount of beryllium used, radiation has a relatively small effect on the maximum temperature. As the unit weight of the heat absorbing material is reduced the time history will tend to approach the shape of the radiation case curve as indicated in figure 12-6.

12.6 Low Heating Rate Re-entry

In this section the effects of single and double surface radiation in combination with the heat absorption capabilities of beryllium and nickel for the low heat rate data of figure 12-1a are presented.

Equation (12.4-3) is used for the following cases although the actual calculations were made by means of equation (12.4-4) or minor modifications of (12.4-4). The cases calculated for illustration are shown in figure 12-8 and listed in the following table:

Material	W/A	Type Radiation	Curve No.
Beryllium	2.0	single	a
Beryllium	2.0	double	b
Beryllium	1.0	double	c
Nickel	1.0	double	d
Nickel and Beryllium	1.0 for each	double	e

Several conclusions may immediately be drawn.

- a. The maximum temperature reached for single surface radiation as compared to double surface radiation (curves 12-8a and 12-8b) is only about 200° higher for beryllium.
- b. A $W/A = 1$ for beryllium, curve 12-8c reaches a temperature only 150° higher than the $W/A = 2$ for beryllium, curve (b), suggesting that an efficient way of handling the heat input is by radiation.
- c. The observation of (b) above is born out by consideration of curves (d) and (e) where curve (d) can be considered a nickel structure with skin weight of 1 lb/ft² the temperature of which is not

materially effected by the addition of a 1.0 lb/ft² beryllium heat shield as shown in curve (e).

A rapid temperature rise for the nickel skin occurs early in the time history allowing the structure to radiate a large portion of the heat input.

12.7 Heat Shield vs Radiator

The decision as to the most efficient type of heat dissipation to use to keep the all up aircraft or capsule weight within reasonable bounds depends, of course, on the type of heat input as previously demonstrated. One more figure will be presented to belabor this point for the last time. In figure 12-9 the effectiveness of heat shielding for the two types of heat input used is shown. The solid curves correspond to an unprotected nickel structure while the dashed curves have a 1 lb/ft² heat shield of beryllium added. For relatively high heating rates such as illustrated for figure 12-1b data the heat shield reduces the maximum temperature about 350°F, but for the slow heating rate data of figure 12-1a the temperature drop is only about 70°F and the structural weight has been unnecessarily penalized. Of course, the maximum allowable structural temperature must also be considered in deciding upon the most efficient form of heat protection including the use of insulating or ablating materials.

12.8 Insulators and Conductors

The solution of heat protection problems involving insulators is a considerably more complex problem than anything discussed so far. The general differential equation which must be solved is

$$\frac{1}{wc} \left[\frac{\partial}{\partial x} \left(k_x \frac{\partial T}{\partial x} \right) + \frac{\partial}{\partial y} \left(k_y \frac{\partial T}{\partial y} \right) + \frac{\partial}{\partial z} \left(k_z \frac{\partial T}{\partial z} \right) \right] = \frac{\partial T}{\partial t} \quad (12.8-1)$$

If the conductivity k is assumed to be constant, and the substance is homogeneous and isotropic, the equation for an infinite slab i.e., one directional heat flow becomes

$$\frac{k}{wc} \frac{\partial^2 T}{\partial x^2} = \frac{\partial T}{\partial t} \quad (12.8-2)$$

Numerical methods have been developed which make the application of equation (12.8-2) to practical cases somewhat easier. The following is from reference 1 and is based on the "General Numerical Method of Dusenberre". Figure 12-10 shows the cross section of a large slab of thickness x divided into 4 equal slices of Δx each. The heat balance for the cross hatched zone a b c d is written as

$$\frac{k(T_0 - T_1)}{\Delta x} - \frac{k(T_1 - T_2)}{\Delta x} = \Delta x \frac{wc(T_1' - T_1)}{\Delta t} \quad (12.8-3)$$

by using $\left(\frac{T_0 - T_1}{\Delta x} \right) = - \left(\frac{dT}{dx} \right)_{\text{at plane } a_d}$

and $\left(\frac{T_1 - T_2}{\Delta x} \right) = - \left(\frac{dT}{dx} \right)_{\text{at plane } b_c}$

and T_1^1 is the new temperature at plane 1 after a lapse of time Δt .

Equation (12.8-3) may be solved for T_1^1 as

$$T_1^1 = \frac{T_0 + (M-2)(T_1) + T_2}{M} \quad (12.8-4)$$

$$\text{where } M = \frac{\Delta x^2 w c}{k \Delta t} = \Delta x \frac{W}{A} \left(\frac{c}{k \Delta t} \right)$$

I believe that quite accurate solutions may be obtained using equations of the type of (12.8-4) if M is kept large by using small values of Δt .

12.9 Constant Heating Rate

If the conductor or insulator in this case is assumed to have a specific heat of zero, zero emissivity, and a constant heating rate input the heat balance for the conductor may be written as

$$q = \frac{kA(T_0 - T_1)}{x}$$

or

$$\frac{q}{A} = \frac{k(T_0 - T_1)}{x} \quad (12.9-1)$$

For a specified thickness of insulation x the temperature gradient $(T_0 - T_1)$ which can be maintained is only a function of the heating rate factor q/A .

Equation (12.8-4) is most useful for home insulation purposes.

12.10 Cases with Heat Transfer at a Surface

The steady conduction case occurs only infrequently in aerodynamic problems and the Dusinger numerical method of solution previously given has to be modified to account for a variable heat input and changes in the heat balance equation due to radiation.

To handle this case figure 12-10 may again be referred to and a heat balance on the half slice *oaddo* is written

as

$$\frac{q}{A} = \frac{\Delta x w c (T_p' - T_p)}{2 \Delta t} + k \frac{(T_o - T_i)}{\Delta x} + \epsilon \sigma (T_o')^4 \quad (12.10-1)$$

where q/A is the variable heat input, the first term on the right is the heat absorbed, the second term the heat transmitted and the third term the heat radiated.

As an approximation the term

$$T_p' - T_p = T_o' - T_o$$

Thus equation (12.10-1) becomes

$$\frac{q}{A} = \frac{W c}{A 2 \Delta t} (T_o' - T_o) + k \frac{(T_o - T_i)}{\Delta x} + \epsilon \sigma (T_o')^4 \quad (12.10-2)$$

Equation (12.10-2) is solved for T_o' by the equation

$$\frac{q}{A} = P(T_o' - T_o) + Q(T_o - T_i) + \epsilon \sigma (T_o')^4$$

$$\frac{q}{A} + T_o(P - Q) + T_i Q = P T_o' + \epsilon \sigma (T_o')^4 \quad (12.10-3)$$

As an illustrative example use an insulator 3 inches thick with 3 slices

$$k = .13 \frac{\text{BTU}}{\text{hr ft}^2 \text{ } ^\circ\text{F/ft}}$$

$$\frac{W}{A} \text{ perslice} = 3 \text{ lbs/ft}^2$$

$$c = .12 \frac{\text{BTU}}{\text{lb deg F}}$$

$$\Delta t = 10 \text{ sec}$$

then

$$P = \frac{W}{A} \frac{c}{2\Delta t} = \frac{3 \times .12}{20} = .018$$

$$Q = \frac{.13 \times 12}{1 \text{ in} \times 3600} = .000433$$

equation (12.10-3) becomes

$$\frac{q}{A} + (.018 - .000433) T_0 + .000433 T_1 = .018 T_0' + .3807 \left(\frac{T_0'}{1000} \right)^4$$

or

$$55.555 \frac{q}{A} + .976 T_0 + .024 T_1 = T_0' + 21.150 \left(\frac{T_0'}{1000} \right)^4 \quad (12.10-4)$$

Equation (12.10-4) serves for the determination of the surface temperature T_0' using the heating rate q/A at the time of interest and T_0 and T_1 which were determined for the previous time.

To determine the temperature T_1 direct use may be made of the Dusinger equation (12.7-4). For the example chosen

$$M = 1 \text{ in} \times \frac{3 \text{ lb}}{\text{ft}^2} \times .12 \frac{\text{BTU}}{\text{lb}^\circ\text{F}} \times \frac{1}{.13 \frac{\text{BTU}}{\text{hr ft}^2 \text{ }^\circ\text{F}/\text{ft}}} \times \frac{1}{10 \text{ sec}}$$

$$= .2769 \frac{\text{in-hr}}{\text{ft-sec}} = .2769 \times \frac{3600}{12} = 83.07$$

and equation (12.7-3) becomes

$$T_1' = \frac{T_0 + 81.07 T_1 + T_2}{83.07} \quad (12.10-5)$$

similarly T_2^1 becomes

$$T_2^1 = \frac{T_1 + 81.07 T_2 + T_3}{83.07} \quad (12.10-6)$$

The temperature T_3 must be established on the basis of a heat balance equation similar to equation (12.10-2). If the rear surface is assumed to radiate heat at its temperature T_3 the heat balance for the last slice may be written

$$\text{as}$$

$$0 = \frac{W}{A} \frac{c}{2\Delta t} (T_3' - T_3) + \frac{k(T_2 - T_3)}{\Delta x} + \epsilon \sigma (T_3')^4 \quad (12.10-7)$$

Using the same properties of the insulator as were used previously

$$.976 T_3 + .024 T_2 = T_3' + 21.150 \left(\frac{T_3'}{1000} \right)^4 \quad (12.10-8)$$

now all necessary equations have been written and the temperatures T_0^1 , T_1^1 , T_2^1 , and T_3^1 may be solved for in a

step by step process using equations (12.10-4), (12.10-5), (12.10-6) and (12.10-8). An illustrative example of results of the numerical procedure is shown in figure 12-11 where the initial heat input is that of figure 12-1b and the time interval chosen is 10 sec.

Changing the number of temperature calculating stations has an effect on the calculations which should be investigated before the procedure is adopted. The surface temperature gradually approaches the equilibrium radiation temperature and the rear face temperature decreases as the number of stations increases.

The insulator is a very effective way to handle heat inputs but there is a weight penalty involved. The insulator used in the present example which keeps the rear surface temperature to less than 600°R weighs 9 lbs/ft^2 .

Equations have been presented which may be used to obtain temperature time histories for any combination of heat shields and insulators which include the effects of transient conduction, radiation and variable heat inputs. The only restrictions to the equations are that they are one-dimensional and numerical procedures must be used thus producing some variation in results dependent upon the size of the time intervals used and the number of intermediate temperatures determined.

A recent report, reference 2, presents a method of calculating the temperature distribution of thick walls which uses time series and the response to a unit triangle

variation of surface temperature. Details of use of the method for cases involving surface radiation are not given for the case where the surface temperature is unknown.

References

1. McAdams, William H.: Heat Transmission. McGraw-Hill Book Company, Inc., Third Edition, 1954.
2. Hill, P. R.: A Method of Computing the Transient Temperature of Thick Walls From Arbitrary Variation of Adiabatic-Wall-Temperature and Heat-Transfer Coefficient.

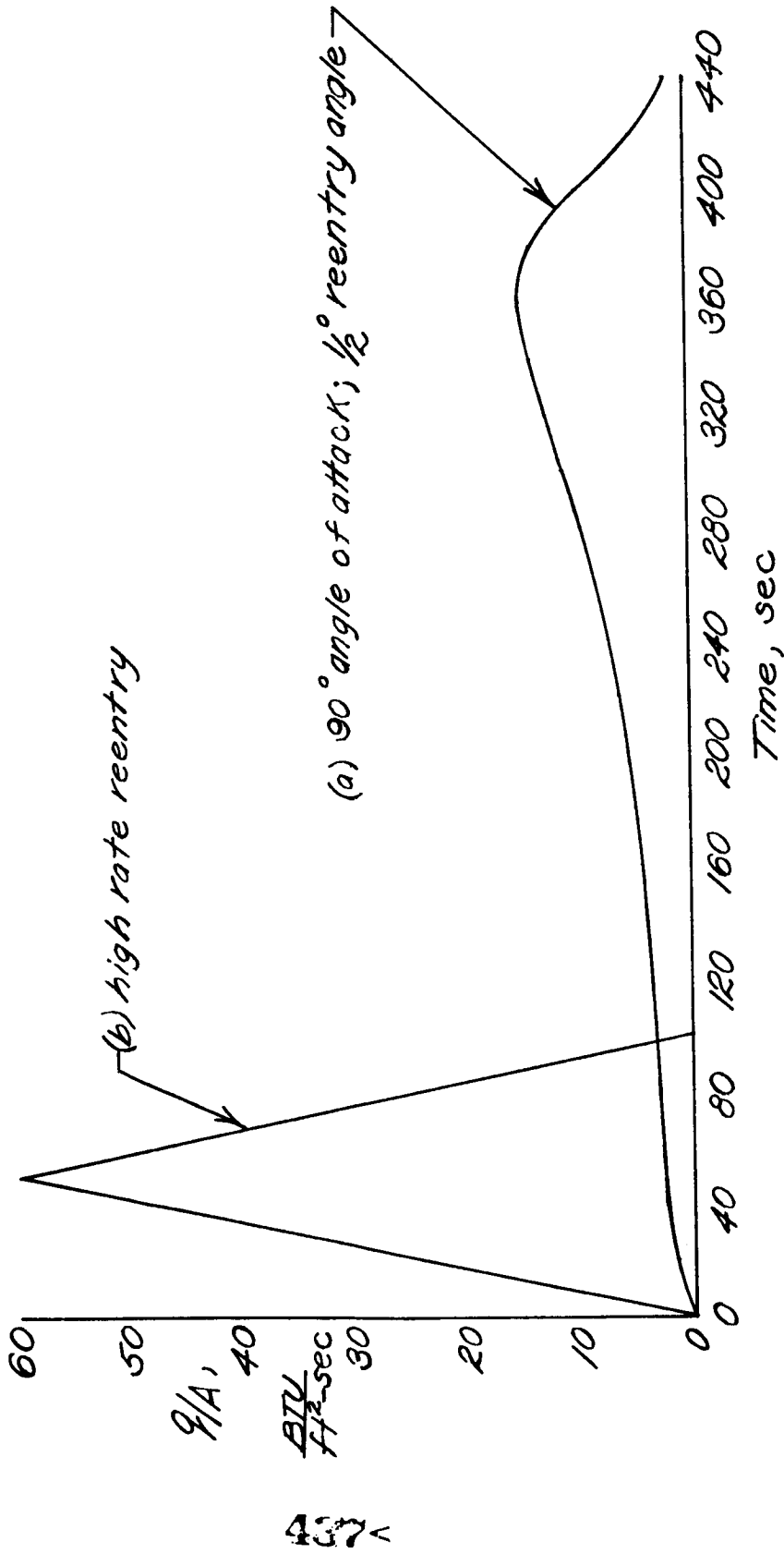


Figure 12-1.—Typical heating rate time histories.

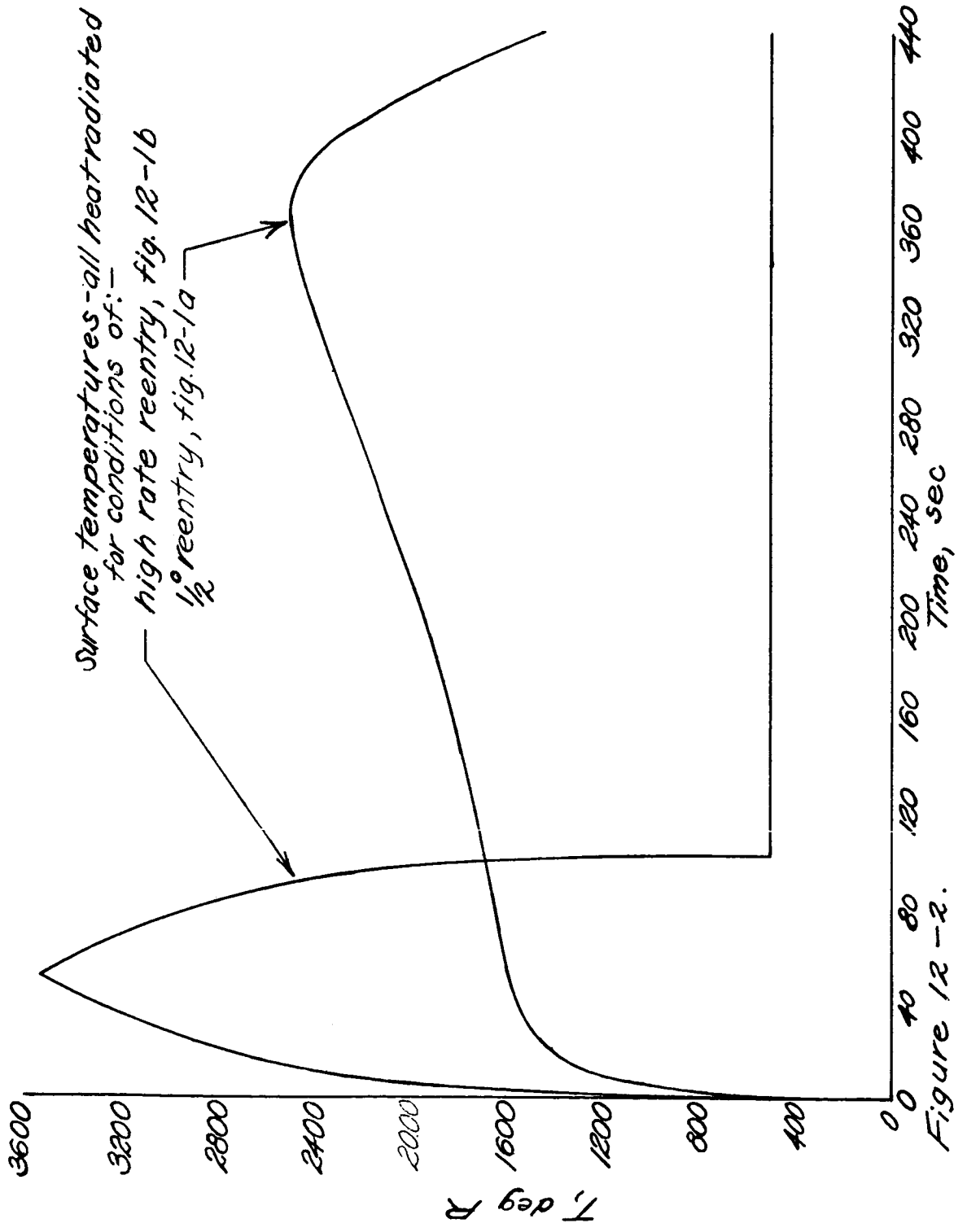


Figure 12-2.

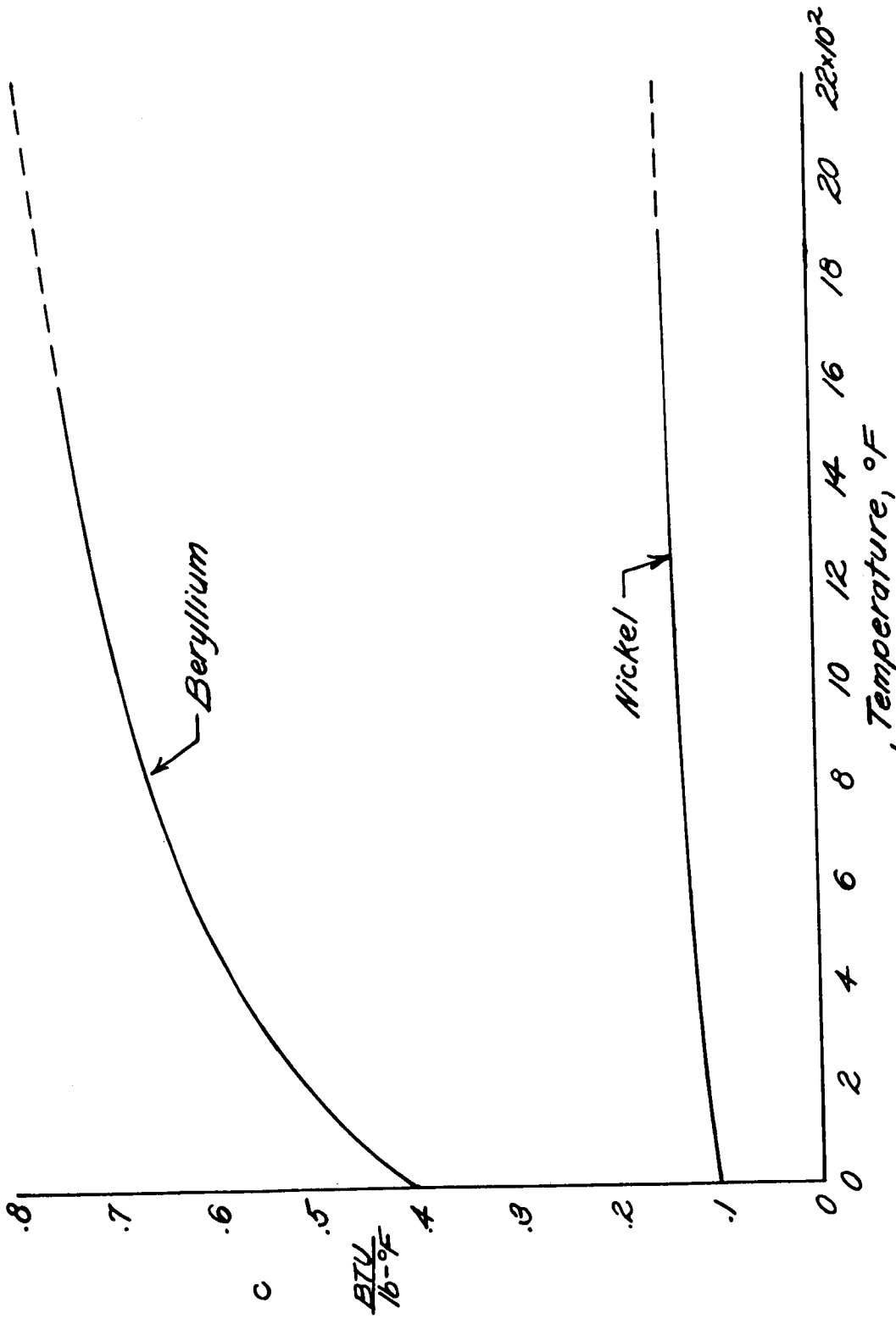


Figure 12-3.- Specific heat.

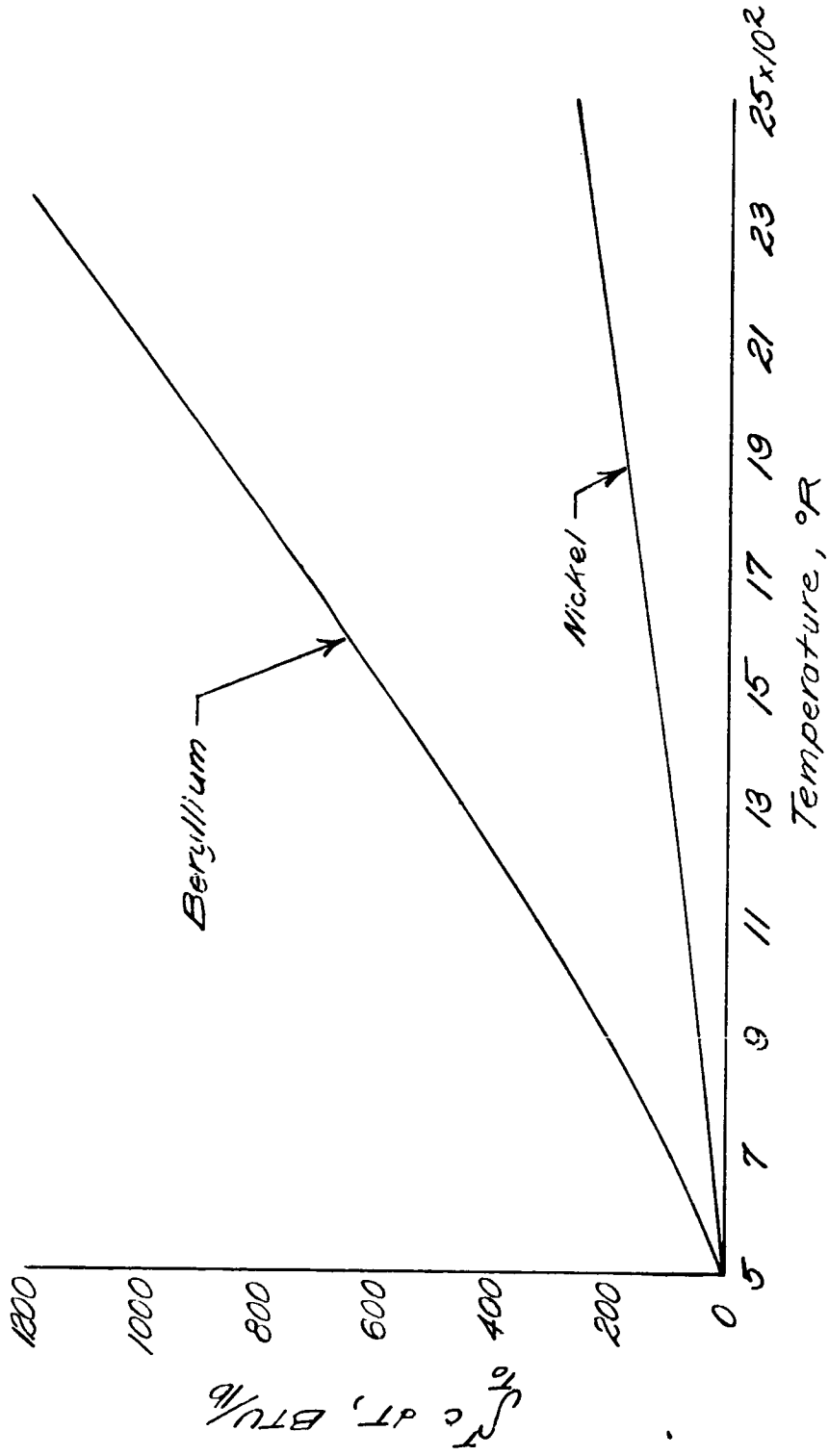


Figure 12-4 Heat absorption per lb.

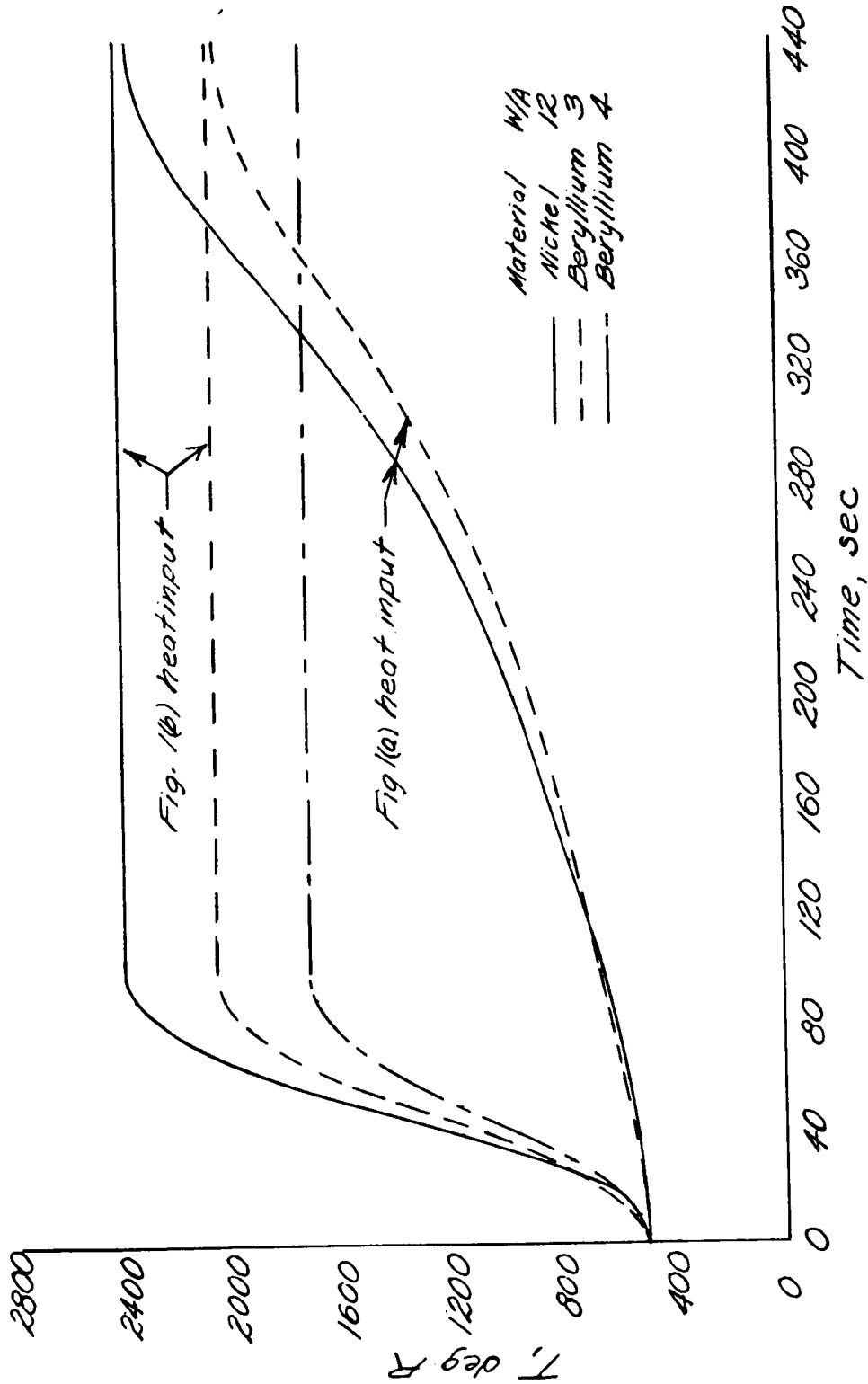


Figure 12-5.-Heat shield temperatures-all heat absorbed.

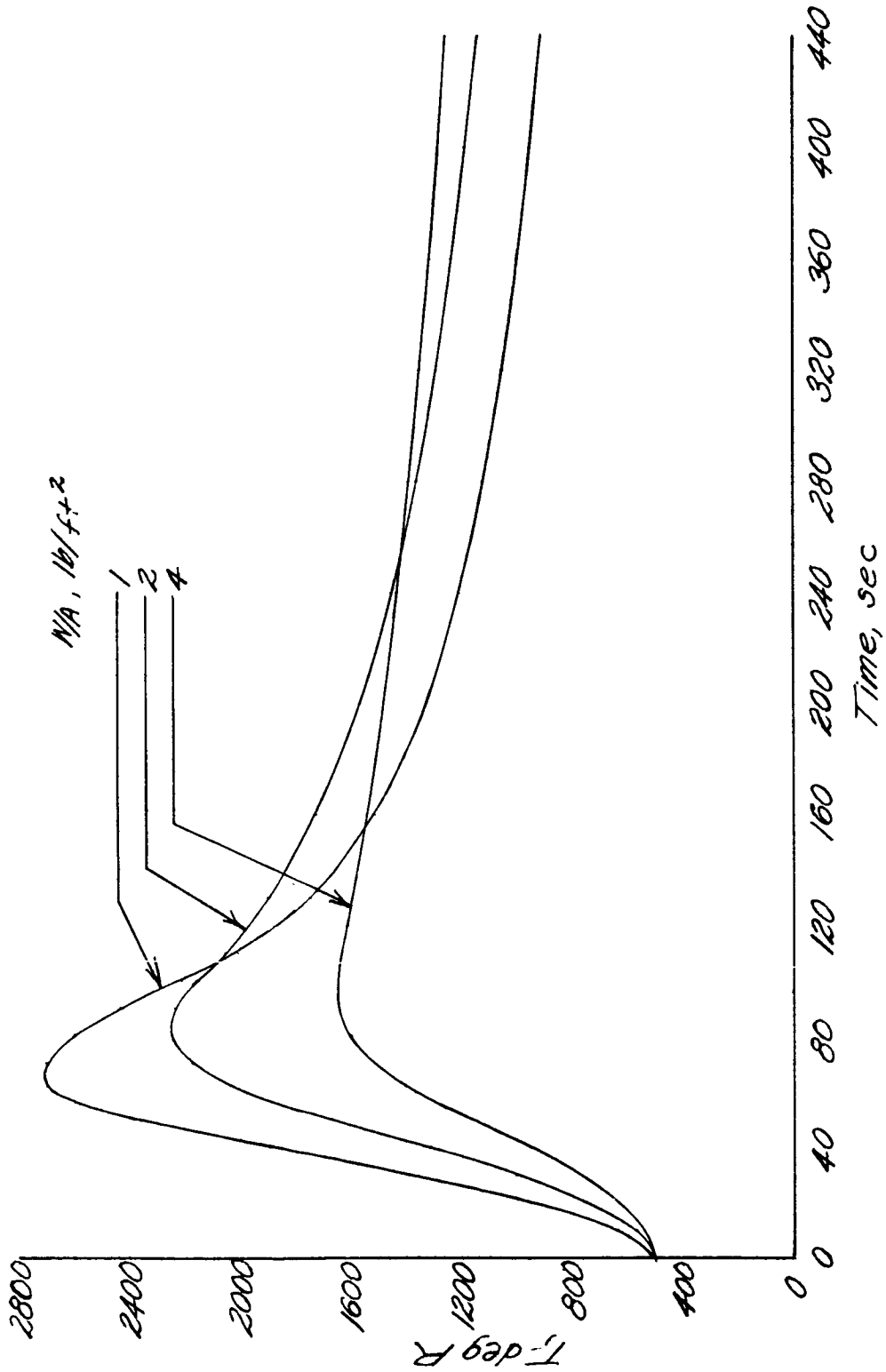


Figure 12-6. Temperatures of beryllium heat shields for heat input of Fig. 12-1b.

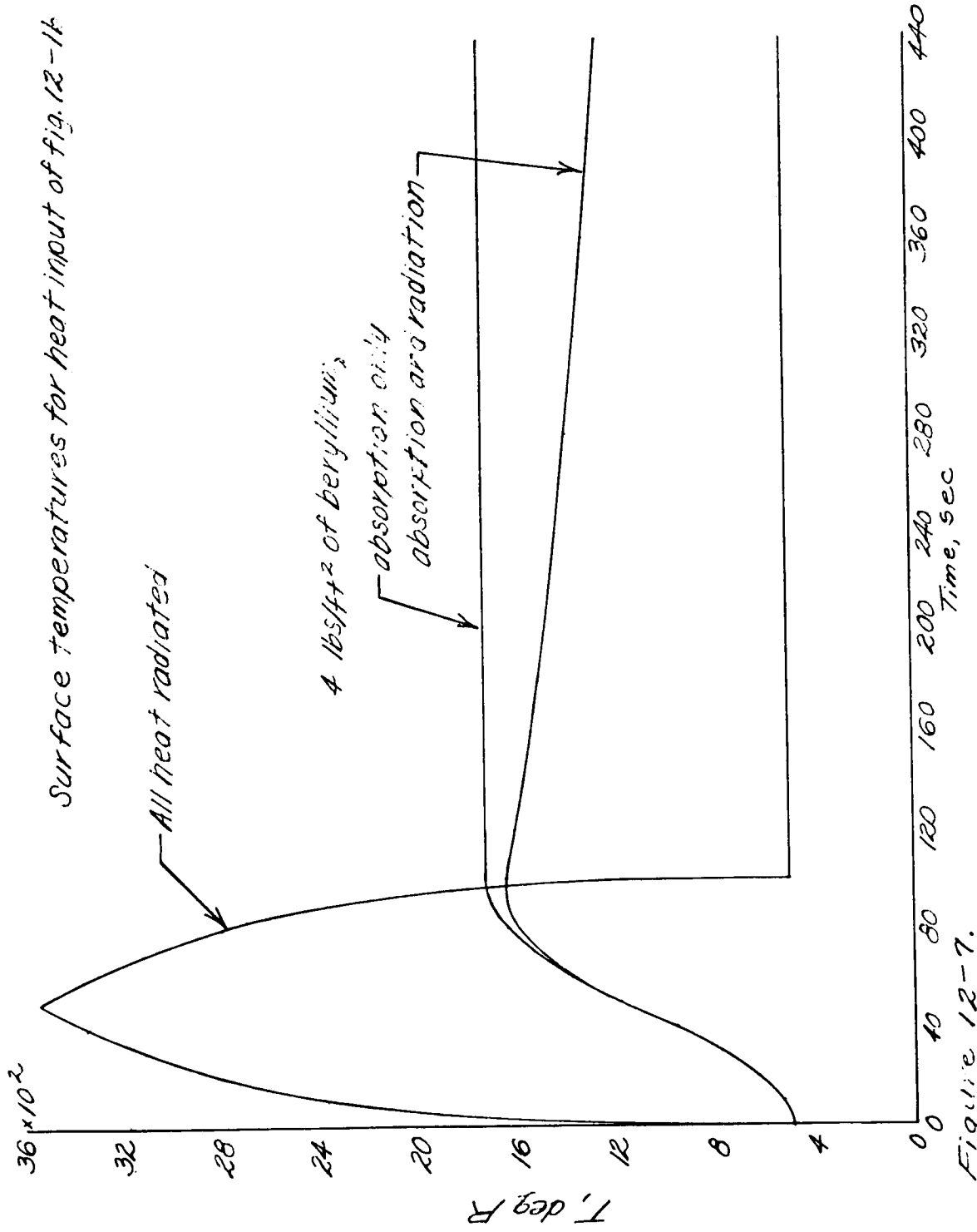


Figure 12-7.

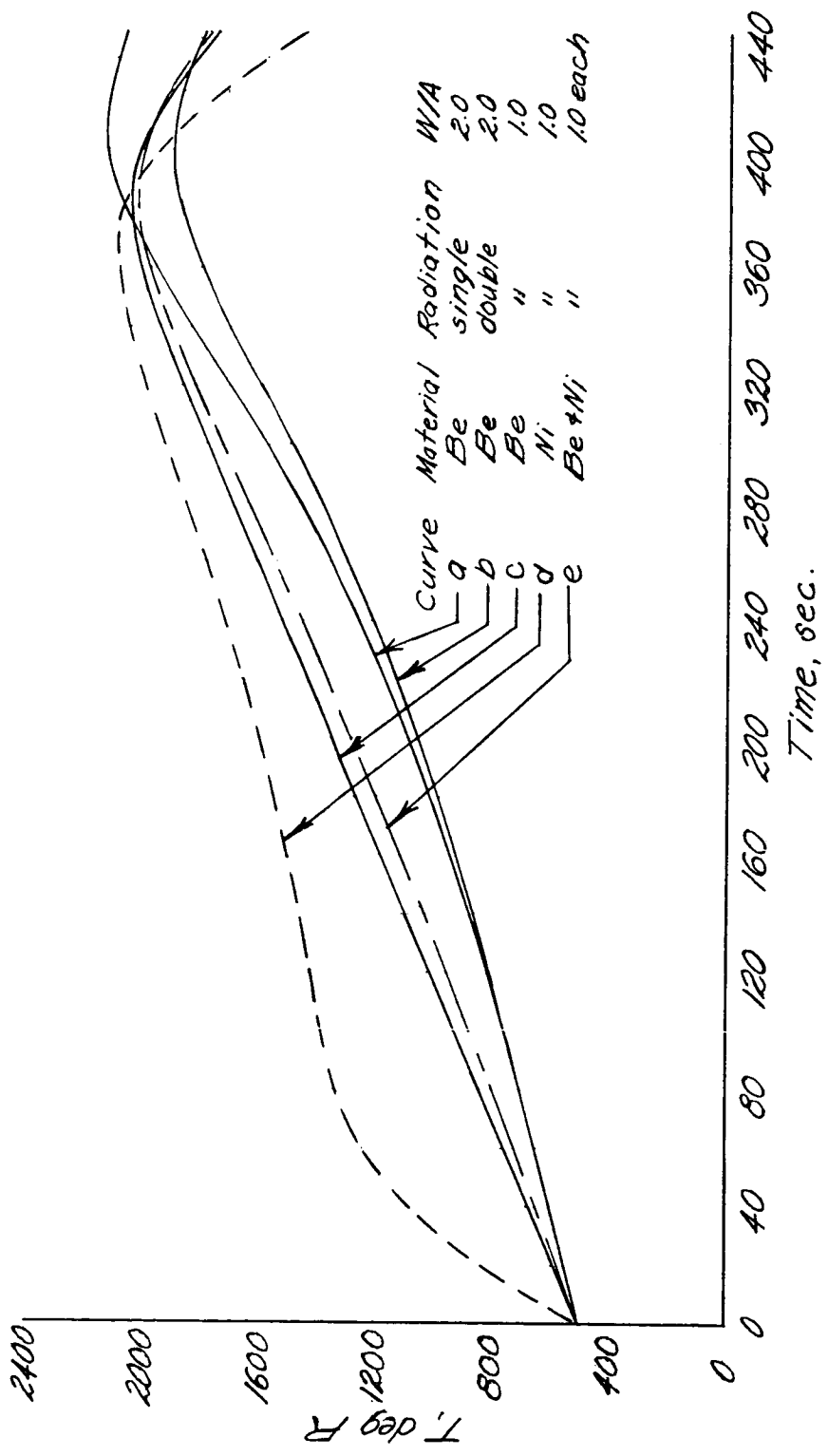


Figure 12-8. Temperatures considering radiation and absorption for heating rate of figure 12-1a.

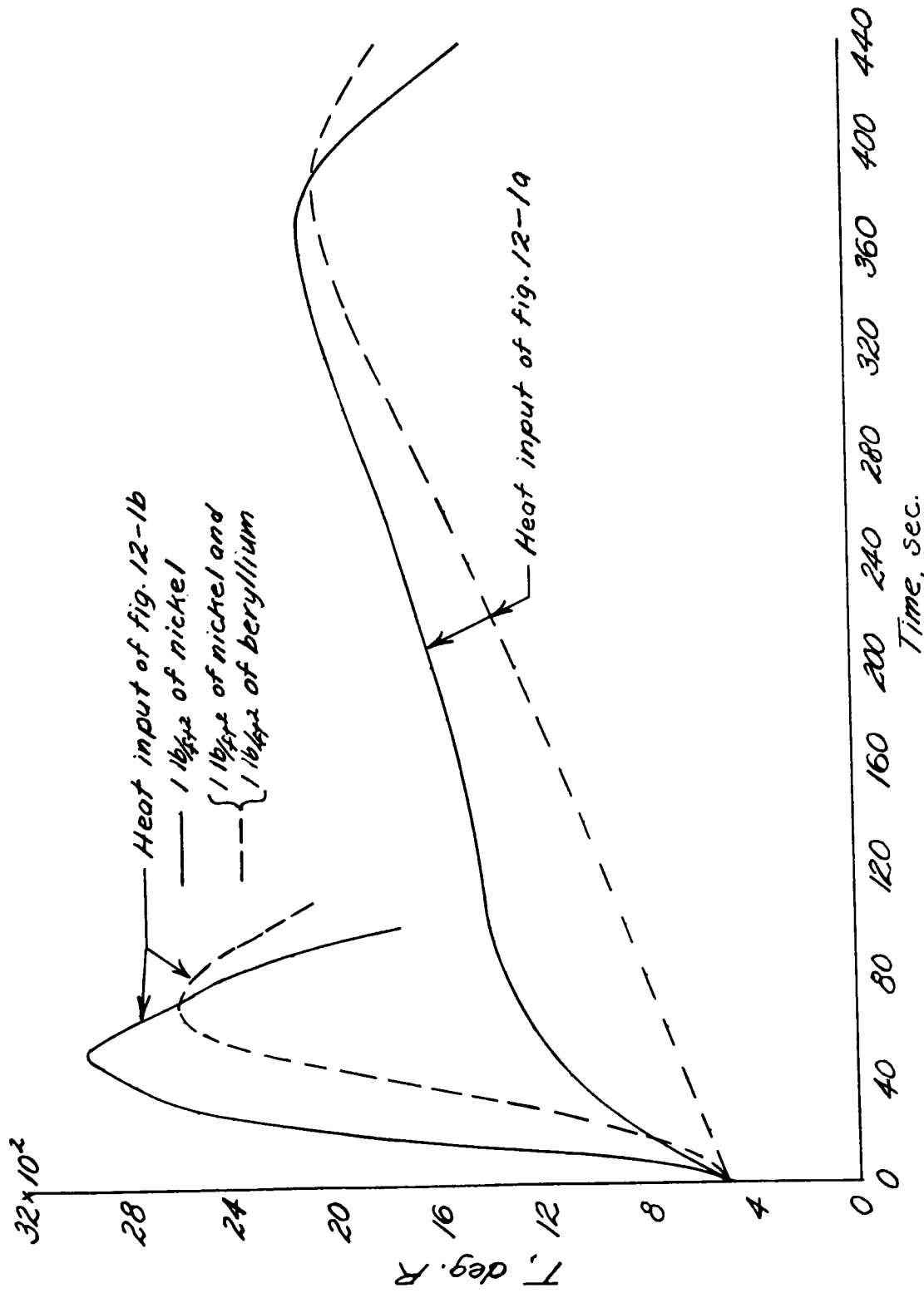


Figure 12-9. Effectiveness of heat shielding.

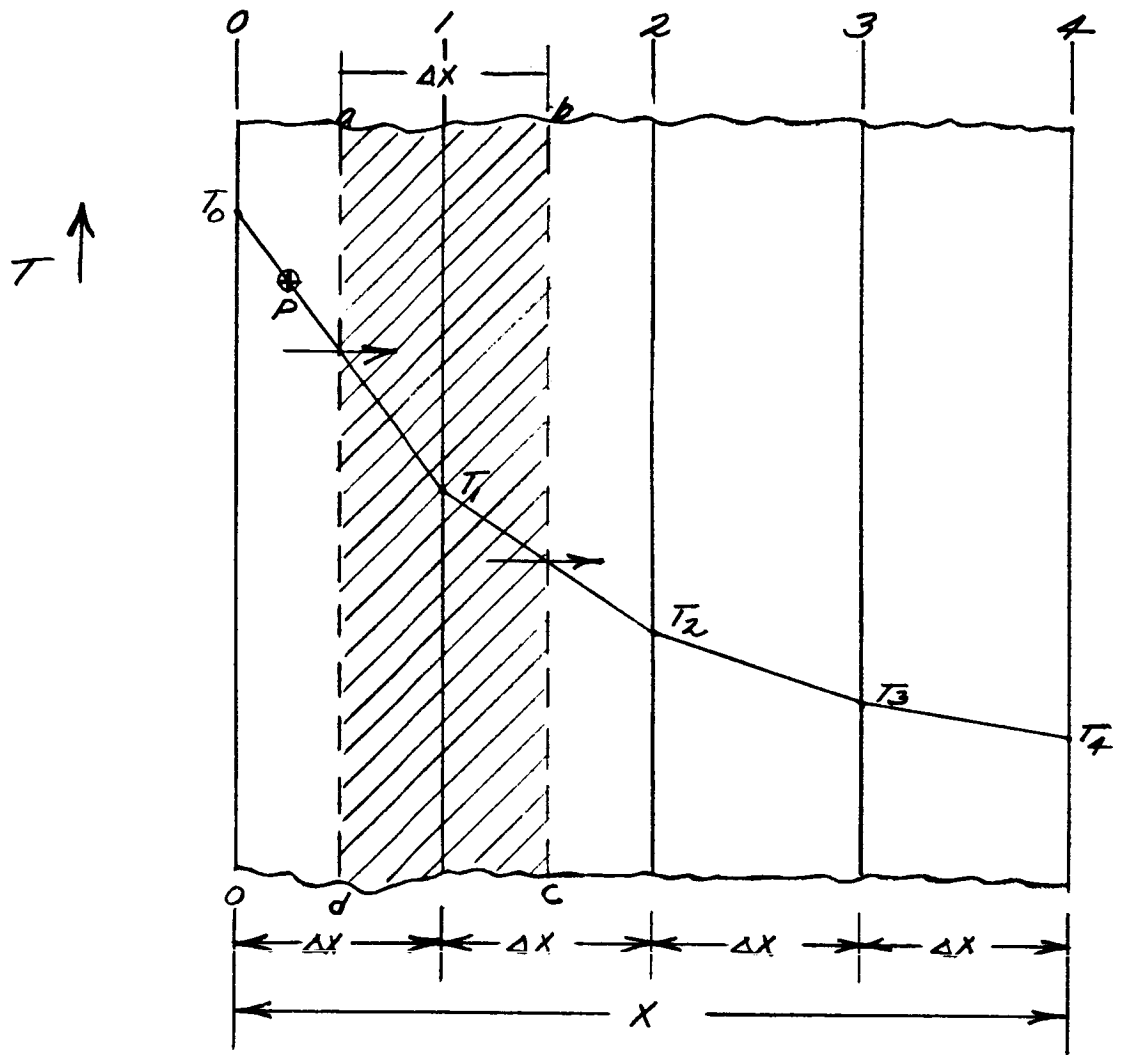


Figure 12-10. - Dusinberre diagram

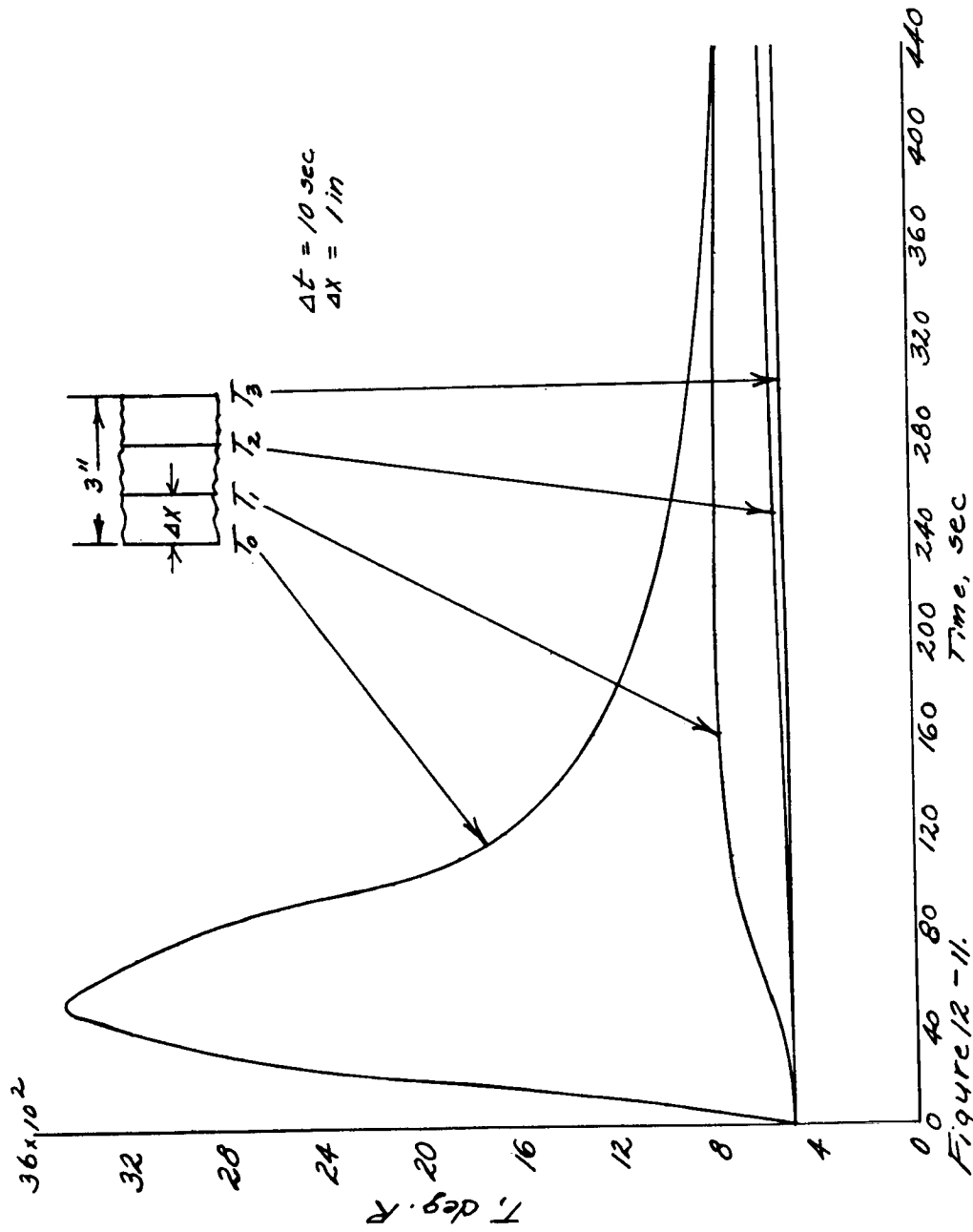


Figure 12-11.

447<

SECTION XIII

PROPERTIES OF HIGH-TEMPERATURE MATERIALS

13. General.

In flight through the atmosphere, compression of the air layer around the body heats the air and the body. The temperature of the heated air increases roughly as the square of the increase in speed, and the heat transferred from the hot air to the body becomes a problem above $M \approx 2$. For a perfect gas, the temperature of the hot-air layer around the body (boundary layer) is given approximately by $T_{B.L.} \approx T_{atmosphere} (1 + 1/5 M^2)$ and even at high altitudes $T_{atmosphere} \geq 400^\circ F$ so that at $M = 5$ the boundary layer temperature is $> 2,000^\circ R$ and at $M = 10$ the boundary layer temperature is $> 7,000 - 8,000^\circ R$. The actual boundary layer temperatures are somewhat less, due to a number of factors, but flight at $M \approx 6$ will melt iron and flight at $M \approx 12$ will melt all known substances, neglecting body radiation. This does not mean that it is impossible to fly at $M = 6$ or 12 , since other factors such as duration of flight, shape of noses and wings, artificial cooling, and beneficial body radiation enter the picture. It does mean, however, that disaster lurks continually for the unwary and that prodigious effort and ingenuity are required for hypersonic ($M > 5$) flight in the atmosphere. Everyone is familiar with the fiery trails of meteors and with the fact that many of the meteors are

metallic. The meteors are fiery because they are burned up by air friction. Meteor velocities on entering the atmosphere range from $M \approx 25 - 30$ upward and these speeds are only about twice the $M \approx 12 - 15$ speeds that can be achieved by pilotless vehicles at present.

The foregoing serves to point out that vehicle speeds which can be achieved at present are great enough to cause rapid destruction of the vehicle and occupants due to heating from air friction. Since sustained flight at $M \approx 4$ will melt magnesium and aluminum and at $M \approx 6$ will melt steel it is clear that speeds of $M \approx 10 - 15$ will require more exotic materials having a high melting point, plus probably artificial cooling, plus in some cases possibly controlled destruction of parts of the vehicle to take advantage of the beneficial cooling resulting from material destruction. The rest of the discussion will deal only with some of the high-temperature materials, some effects of temperature on materials properties, and some uses of materials in high-speed vehicles.

13.1 Materials.

The existence of high temperature materials has been known for many years. The discovery of carbon occurred in pre-historic times. Tungsten, platinum, and molybdenum were discovered in the 1700's. Tantalum, Niobium, Beryllium, and Rhodium were discovered in the 1800's. Rhenium was discovered in 1925. Unfortunately, most of the high temperature

materials are quite hard and brittle and are thus unworkable. In addition, most of them are expensive to produce and the lack of a commercial demand has prevented the lengthy research and development that will be necessary to produce more usable forms of these materials. As a result, most of these materials have remained laboratory curiosities. However, within the past 3 or 4 years extensive and intensive research and development efforts have been applied to the field of high temperature materials and alloys, and it is hoped that this continuing effort will pay off with new materials or more-workable forms of the known materials.

13.1.1 Melting Temperatures.

The majority of the elements are shown in figure 1, with melting temperature plotted against molecular weight. The elements are divided into the periodic groups and the melting temperature has been plotted against increasing molecular weight within each group. It is immediately apparent that the melting temperature varies at random with molecular weight and with periodic group. Figure 13-1 serves to illustrate that there doesn't seem to be a reasonable relation between the melting temperature and the properties of the elements. However, figure 13-1(a) does show that the high-melting elements appear to be grouped roughly around the molecular weights of 12, 48, 96, and 192; the significance of this grouping is not apparent. As far as can be determined, there does not seem to be any correlation

between melting temperature and physical or chemical properties of the elements.

13.1.2 Compounds.

Few of the elements are used in their pure form, and it is of some interest to list the elements and their corresponding refractory compounds that may have high-temperatures uses. The majority of the elements are listed in Table 13-1 in order of decreasing melting temperatures, and the melting temperature of a number of their known compounds that melt above 2,500°F are listed. There are three main items of interest in Table 13-1.

(1) Two of the carbides are the highest-melting two-element compounds known and their melting-temperatures are several hundred degrees higher than either of the constituent elements.

(2) Over half of the compounds have higher melting temperatures than either of the constituent elements.

(3) The carbides and nitrides tend to have the highest melting points, averaging about 4,700°F.

13.1.3 Some Oxides.

Some of the oxides that melt above 4,000°F are listed in Table 13-2 (a) in decreasing order of melting temperature, and qualitative information on their oxidation and thermal

shock resistance are included. It should be stressed that the oxidation resistance in particular is qualitative, since the oxides as a class are generally considered to have indifferent or poor resistance to oxidation because most of the oxides tend to be somewhat porous. A body made entirely of an oxide would, of course, be completely oxidation resistant with the exception of the few oxides that change to higher forms under heat and a generous supply of oxygen. Most refractories are too weak and brittle for load-carrying applications, so that their main use is as a protective coating over a strong, but oxidation-prone strength member. For coating applications, then, the porosity of the protective coating is of paramount importance since a porous coat allows the free oxygen of the air to attack the load-carrying "protected" member.

The thermal shock resistance is roughly tied to the thermal conductivity and expansion characteristics of a material. Thermal shock is a descriptive phrase used to indicate the break-up of a material from uneven temperature distributions, and broadly speaking comes about because of the material's inability to conduct heat away from a hot spot coupled with a tendency to expand when hot. Thus, a material with bad thermal shock properties, when heated on one face while the other face remains unheated except for conduction from the hot face, expands at the hot face and breaks up the cooler portions because the relatively poor

conductivity keeps the heat from equalizing throughout the material.

It can be seen from Table 13-2 that the oxides tend to break up under transient heating. The oxides, then, as a class for general application are not too highly regarded for high temperature protective coatings or as homogeneous bodies for transient-heating applications.

13.1.4 Some Carbides.

Listed in Table 13-2 (b) are some carbides that melt above 4,000°F, and some information on their qualitative resistance to oxidation and thermal shock is included. The oxidation and thermal shock properties are not well known for the carbides. As noted in Table 13-1, the highest-melting compound known, hafnium carbide, is found among the carbides. From melting considerations only, a missile made entirely of H_fC could fly indefinitely at $M = 12$.

The carbides are characterized by extreme hardness, and they have been used for years as abrasive grits on grinding wheels and as cutting tool tips and masonry drill tips. Tungsten carbide is perhaps the best known of the carbides for these applications.

The use of carbides for bodies and protective coating has not met with unqualified success. The carbides are very hard and almost impossible to shape or work, and generally are quite brittle; these qualities tend to discourage their

use as refractory bodies. Their brittleness makes them less desirable as protective coatings, but it is felt that there is room for considerable progress in developing carbides with good high-temperature characteristics. The PARD Vapor-Desposition Laboratory plans to spend some time in basic research into the carbides to be used as protective coatings.

There is a tendency to think of a carbide as a coating on carbon, but carbides may be formed on many materials such as tantalum, zirconium, titanium, tungsten, etc.

13.1.5 Some Borides.

Several borides are listed in Table 13-2 (c), and the most outstanding characteristic of the borides is the lack of knowledge concerning their properties. All of the borides contain boron, and the literature indicates that there is little commercial use for the pure boron; most boron uses are as compounds in mild antiseptics, washing powers, and enamels and glasses for covering refrigerators and the like.

Several of the borides have attractive melting temperatures (ranging up to 5,500°F) and more intensive research may reveal other useful high-temperature properties. As of the present, however, the borides are more a laboratory curiosity than useful products.

The borides are generally quite hard and brittle, and one investigator postulates that some of the borides may become superconductive (electrically) at high temperature

and may thus be useful as a temperature-sensing element.

13.1.6 Some Nitrides.

Several nitrides that melt above 4,000°F are listed in Table 13-2 (d). The general information available indicates that several of the nitrides have good thermal shock properties, but their oxidation resistance is either generally unknown or thought to be poor.

The higher-melting nitrides are metallic in appearance and range in color from gold (ZrN) to gray (TaN). The nitrides tend to be quite brittle and hard, although one source reports that TaN at high temperature is about as soft as copper is at room temperature.

There is a scarcity of data in the literature concerning the use of nitrides as refractory bodies or coatings. This lack of interest may be due to the inherent hardness and brittleness of the nitrides.

13.1.7 Some Other Refractories.

Table 13-2 (e) lists several other refractories thought to have good oxidation resistance. The lowest-melting refractory, MoSi₂, has been included because the author has some knowledge of the behavior of MoSi₂ from personal experience. MoSi₂ at about 3,000°F has good oxidation resistance. A molybdenum model coated with MoSi₂ was tested in the PARD hot air jet and lasted for nearly 10 minutes while

the uncoated model lasted about 6 seconds.

13.2 Temperature Effects.

In general, it may be stated that things get worse as the temperature increases. There are certain exceptions to this rule, such as the increasing e.m.f. with increasing temperature for thermocouples and the increasing emissivity with increasing temperature characteristic of many materials.

13.2.1 Effect of Temperature on Strength.

The strength of a material usually goes to pot when the material gets hot. The effects of temperature on the strength of a few "high-temperature" materials are shown in figure 13-2. These "high-temperature" materials are basically Ni-Cr-Fe alloys except for the 0.5% Ti-Mo which is almost pure molybdenum. It can be seen in figure 13-2 (a) that most of the materials have lost about half their ultimate strength at 1,600°F or below, and in general this is the story of material commonly used for load-carrying members in aircraft and missiles; airframes have to be "beefed up" and far over-strength at ordinary temperatures so they will be strong enough when heated up by high flight speeds. One of the significant things to be seen in figure 13-2 (a) is the strength of the molybdenum alloyed with 0.5% titanium, even at high temperatures. Molybdenum unfortunately oxidizes badly above 1,300 - 1,400°F and catastrophically at 1,800 - 2,000°F and this one characteristic has been (and still is) a major reason for not being

able to utilize the high-temperature strength of molybdenum. A high-temperature protective coating that is tightly bonded, oxidation resistant, self-healing, and ductile for molybdenum would permit the utilization of its great high-temperature strength.

Figure 13-2 (b) shows the effects of temperature on the 100-hour-rupture strength of stainless steel, several super-strength alloys, and molybdenum. It is obvious that high temperatures drastically reduce the allowable loading. Again, the alloyed molybdenum shows a considerable advantage, assuming of course that some means of protecting the molybdenum from oxidation can be found.

If the highest temperature that a structure will reach is not more than 1,100 - 1,200°F, figure 13-3 shows that beryllium is an attractive material. The upper part of figure 13-3 shows the relative weight of a thin-wall structure plotted against atomic number of the material of construction for room temperature. The weight of the structure when made of aluminum is the base for comparison. The lower part of figure 13-3 is the same type of plot, except that the temperature is 1,200°F and a steel structure is the base for comparison.

It can be seen that at room temperature several materials are better than aluminum purely on a strength basis. At 1,200°F many of the materials are no longer usable. It is interesting to note that beryllium appears to be an excellent material at both temperatures. These comparisons are on a

strength basis alone and do not consider cost, workability, availability, and oxidation effects.

13.2.2 Effect of Temperature on Thermal Conductivity

Figure 13-4 (a) shows that in general the thermal conductivity generally tends to decrease with increasing temperature. There are enough exceptions to this to generate plenty of argument. A decreasing conductivity with increasing temperature is advantageous from an insulation viewpoint but disadvantageous from a thermal shock viewpoint unless the expansion rate also decreases.

It may be noted from figure 13-4 (a) that copper and silver are 5,000 - 6,000 times more conductive (thermally) than some of the better insulators. This might indicate that of course copper and silver would be worthless as insulators and indeed they are if the generally-accepted definition of insulation is used. However, there are some special cases where copper is used as an "insulator" and this will be discussed in the Heat Sink section of this discussion.

It is seen in figure 13-4 (a) that most of the usual airframe materials and the refractories have about the same order of magnitude of conductivity as indicated by the cross-hatched areas at the bottom of the figure, although there are exceptions to this.

Figure 13-4 (b) shows the effect of temperature on the thermal conductivity of several refractories. ZrO_2 (zirconia) has a rather low conductivity and BeO (beryllia) has a high

conductivity which decreases rapidly with increasing temperature. These refractories show an almost consistent decrease of conductivity with increasing temperature.* Some of these refractories such as ZrO_2 and Al_2O_3 have low enough conductivity to make them attractive as insulators in certain flight applications. In general, however, the refractories are fairly dense and are not thought of as efficient insulators because of their weight; it is usually more efficient to use the so-called insulators which are lightweight and have relatively low conductivity.

Figure 13-4 (c) shows the effect of temperature on the thermal conductivity of several insulators that are suitable for high temperature application, and the conductivity curve for air is included for comparison. In contrast to the refractories shown in figure 13-4 (b), the insulators show an increasing conductivity with increasing temperature. All of the insulators shown (except air) are made of fibrous materials surrounded by air spaces, and this construction is typical of the light-weight insulators. As an item of interest, the thermoflex is actually a refractory ($Al_2O_3 \cdot SiO_2$) in fibrous form.

* Some sketchy information indicates that porous refractories may tend to show an upward trend of thermal conductivity with temperature beginning at about $2,000^\circ F$, due to radiation across the internal air spaces.

At low temperatures, air is a good insulator and a vacuum is considered to be almost a perfect insulator. However, at temperatures above 1,500 - 2,000°F, neither air nor a vacuum are good insulators because of the radiation. At 2,000°F, for example, the heat conducted across a 1 foot thick airspace would be about 0.04 Btu/ft²-sec but the heat radiated from the hot surface to the cool surface could be as much as 15 or 16 Btu/ft²-sec. If the space were a vacuum the conduction would be absent but the radiation would still be 15 or 16 Btu/ft²-sec. On the other hand, a fibrous type insulation such as quartz fibers would have a total conductivity of .05 or .06 Btu/ft²-sec since the solid materials effectively block radiation.

The selection of a certain type of insulation for a particular application is not a straight forward cut-and-dried process. Assuming that the insulation will take the temperature, there must be a consideration of such things as conductivity, difficulty of holding the insulation in place, tendency of the insulation to vitrefy and compact, and the weight of the entire insulation assembly. In some cases, such as for missile noses and wing leading edges, it may be better to use one of the relatively heavy refractory semi-insulators such as ZrO₂.

The difficulty of insulating a high speed flight vehicle is compounded to a staggering degree by the weight restrictions

imposed. At the present time no one can be positive about the allowable weight of insulation, but there seems to be a sort of tacit agreement that about 2 - 3 lb/ft² is near the upper limit. At 3 lb/ft², a 3-foot-diameter vehicle 25 feet long would require 500 - 600 lbs of insulation on the body alone.

13.2.3 Effect of Temperature on Specific Heat.

The specific heat is the ability of a material to store heat, and generally a high value is desirable because a high specific heat means a relatively low temperature rise for a given heat input.

Figure 13-5 shows that most materials have a higher specific heat at high temperatures than at low temperatures and that the curves tend to keep rising with temperature. Graphite has a different trend, with a highest value at about 2,000°F.

As can be seen by comparing figure 13-5 with figure 13-4 (a), there is not such a wide variation of specific heat between materials as was shown for thermal conductivity.

13.2.4 Effect of Temperature on Emissivity.

The emissivity of a material is a measure of its ability to radiate heat. A perfect radiator is called a "black body" and has an emissivity of 1.0 and a body that does not radiate any energy has an emissivity of zero; thus, all materials

have emissivities between 1.0 and 0.0. The desirability of having a high or low emissivity depends on the function of the material. In general, materials considered for high speed missile skins should have a high emissivity so that when the skin heats up it will radiate to space and tend to "cool" the skin. For example, a skin having a heat input of 8 Btu/ft²-sec will come to equilibrium at 1,600°F for $\epsilon = 1$ and at 2,600°F for $\epsilon = 0.2$. There is no known perfect radiator ($\epsilon = 1$) but graphite comes close ($\epsilon \approx .95 - .96$ according to some investigators; $\approx .75 - .78$ according to others).

Figure 13-6 (a) shows the effect of temperature on the emissivity of a few selected materials. It can be seen that in general the emissivity tends to increase with temperature increases.

Figure 13-6 (b) shows the effect of temperature on the emissivity of Inconel which has had various previous heat treatments. Since emissivity is essentially a surface phenomenon, changing the surface conditions (roughness) of a material will generally change the emissivity. In general, surfaces that appear dark to the eye under ordinary light have a high value of ϵ because absorbtivity and emissivity are the same thing. Conversely, surfaces that appear bright to the eye under ordinary lighting are poor radiators (but good reflectors).

13.2.5 Effect of Temperature on Oxidation.

There appears to be a considerable store of knowledge concerning the oxidation of many materials in various atmospheres near room temperature. However, oxidation behavior at high temperatures particularly in the presence of a high speed airstream is little understood and sparsely documented. The oxidation problem is a serious one for high speed vehicles and is attracting considerable interest. The reason that oxidation is important is that practically all materials (except the oxides) are prone to oxidation and heat is almost always given off in the oxidation process. This heat liberated tends to heat the material to higher temperature where the oxidation reaction is accelerated. In some cases a high speed oxidation reaction may set in that is self-regenerative and violent enough to destroy the material in a matter of seconds. A familiar example of oxidation is the operation of the oxy-acetylene cutting torch which works on the principle of heating the material to be cut to 1500°F and then impinging on the hot metal a jet of oxygen. Steel plate 12" to 48" thick can be cut at 2" to 6" per minute by this method. Flame machining is also done, using the principle of material removal by surface oxidation; metals may be oxidized in this process at the rate of 10 lb - 15 lb per minute.

The oxidation of materials in high speed flight in air is not well understood or predictable. It is a serious problem, as evidenced by the fact that molybdenum (M.P. 4700°F) will break into flaming destruction at 2800°F in a supersonic air jet and steel (M.P. 2800°F) has been made to flame like a torch in a 600°F supersonic air jet when the steel was preheated with a torch to red heat.

Figure 13-7 (a) shows some effects of temperature on the oxidation of SiC powder and some effects of adding water vapor to the air when the temperature is held at about 2000°F. It is seen that higher temperatures aggravate the oxidation problem for SiC powder, and this is generally true for other materials. The magnitude of carbon lost in the upper part of figure 13-7 (a) is not of paramount importance from a flight-vehicle standpoint since missile skins will not be made of powder. The size of the powder particles has a large influence on the oxidation rate; everyone is familiar with the explosions of dust-laden air.

Figure 13-7 (b) shows the effects of temperature on the oxidation rate of molybdenum which has a melting temperature of about 4700°F. It is interesting to note the large jump in oxidation rate in going from 1350°F to 1500°F. This is due to the behavior of MoO_3 which is formed as a solid oxide below 1350°F but which melts at about 1350°F and increases the oxidation rate manyfold of the remaining molybdenum.

There are many forms of oxides formed on materials such as titanium, steel, aluminum, molybdenum, tungsten, etc. Some of the oxides are relatively hard and impervious and tend to retard further oxidation once a thin oxide layer has formed, aluminum being an example of such protective oxidation. Other oxides are too fragile to provide any protection, such as the iron oxides.

13.3 Uses and Arrangements.

No attempt will be made to cover all of the uses and arrangements of materials for high temperature use in high speed vehicles. The protection of missiles from high temperatures by use of insulation and "heat sinks" will be discussed briefly as illustrations.

13.3.1 Insulation.

In insulating an object, a layer of low-conductivity material is placed between the hot gases and the object. Any object can be kept at near room temperature for hours even when surrounded by gases at 5000°F if there are no restrictions concerning the cost or weight of the insulation; for example, an aluminum plate 1/10 inch thick protected from 5000°F gases by 150 feet of firebrick will rise from 32°F to room temperature in about 4 hours.

The effect of insulation is to delay the temperature rise of such vehicle components as the load-carrying members, electronic instruments, and the inhabitants. Insulation

keeps the inside cool only in a relative sense, in that regardless of how much insulation is used the entire vehicle will finally come to an equilibrium temperature unless some sort of cooling scheme is used. This equilibrium temperature may be 2000°F or higher, and it is obvious that insulation is used only to delay the temperature rise of the interior of the vehicle for a reasonable time so that the vehicle can perform its intended function.

Figure 13-8 shows the qualitative effect of insulation on the flight time of a hypothetical missile in the atmosphere. It can be seen that a thicker insulation extends the flight time, a fact that would be intuitively clear. The obvious conclusion to draw from this figure is that the flight time could be extended at will by using thicker and thicker insulation, and this is true to a very limited extent. However, the one factor that makes the insulation problem so difficult is that the weight of the insulation and insulation-supporting structure quickly mount to several pounds per square foot and such added weights are intolerable. It seems generally agreed that the weight of the insulating structure for high speed flight vehicles will have to be less than about 2 to 3 lb/ft² and this weight immediately translates into insulation thicknesses of the order of a few inches and flight times of a few minutes. The problem of insulation is a back-breaker and a number of people are at this minute racking their brains trying to solve it.

13.3.2 Heat Sink.

Another method of using materials to protect against high temperatures is the so-called "heat sink" approach which might also be generally thought of as insulation. In the heat-sink arrangement, the material's ability to store heat is of primary importance. The theory of the heat sink is as follows: the high-heat input areas of a high speed vehicle are covered on the outside with a material which has a high heat capacity per degree temperature rise and a conductivity high enough to carry the heat to the interior of the heat sink material. The heat input to the skin is absorbed in raising the temperature of the heat-sink material instead of being conducted to the interior of the vehicle. It is desirable that the heat-sink material have a conductivity just high enough to prevent surface melting, and this necessary conductivity of course varies with the heat input rate.

Figure 13-9 (a) shows a comparison of several conventional materials on the basis of time to start melting at various heat input rates for an infinitely-thick slab. For a given heat input, the time to start melting is a function of the material heat capacity, conductivity, and melting temperature. It is interesting to note that copper ranks quite high although its melting temperature is relatively low (about 1900°F); the reason it ranks high is because of its

heat capacity and conductivity. Molybdenum is one of the highest-ranking materials but is less attractive than copper because of brittleness and oxidation characteristics.

In using a material as a heat sink, it would seem that the thicker the material the longer it would take to start melting. This is true only up to a certain point, as will be shown by figure 13-9 (b). In this figure thin plates of Inconel are considered, and it is surprising to note that there is little reason for using thicknesses greater than $1/4$ " to $1/2$ " except for very low heating rates. The reason for this is that Inconel conductivity is relatively low and at moderate to high heating rates the surface heat cannot be conducted away fast enough to keep the surface from melting.

Figure 13-9 (c) shows the same type of plot for copper. The main point from this figure is that the greater conductivity of copper allows more surface heat to be conducted away and the maximum thickness of copper would be of the order of 2" to 3".

13.4 Ablation.

The process of removal of surface material from a vehicle in flight, through heating and the scrubbing action of the boundary layer, is called ablation. The process of ablation thus includes melting, boiling, sublimation, and the removal of material in the form of discrete particles. Ablation is the controlled destruction of a vehicle surface

so as to use up heat supplied by the boundary layer and thus cool the vehicle.

A good ablating material must have a low thermal conductivity so that the surface will remain much hotter than the interior and thus the ablation process will be confined to the surface. A further requirement is that this material have good thermal shock properties; i.e., the material will resist breakup due to large thermal gradients. It goes without saying, of course, that such a material will not oxidize exothermically and supply additional heat to the unablated portion.

Surprisingly enough, a number of materials meet the above requirements to some degree. Even more surprising, some good ablation materials have a low melting temperature. Nylon, for example, with a softening temperature of 400-500°F is attractive from an ablation viewpoint.

The cooling achieved by the ablation process comes mainly from the following:

- (1) Raising the material surface temperature to the melting or subliming point. This is generally a very small part of the total heat carried away by the ablation process.
- (2) Changing the material state, from a solid to a gas or a solid to a liquid and to a gas, without a change in temperature. In most cases, this is not a

large part of the total heat carried away by the ablation process.

(3) Mixing of the relatively cool gases from the ablating material with the hot boundary layer. This results in a cooler boundary layer next to the ablating surface, and the heat transferred to the surface is lowered. This process in many cases accounts for a large part of the total heat carried away by the ablation process.

The desired effect of the ablation process is to keep the underlying structure from getting too hot. The underlying structure receives heat by conduction through the ablating material and the heat conducted is a linear function of the outside surface temperature of the ablation material. A good ablation material will have an essentially-constant surface temperature for a wide range of boundary layer temperatures and heat transfer rates, since an increase in heat transfer rate to the outside of the ablating surface will result in more lbs/sec of ablating material being boiled away rather than an increase in surface temperature.

Suggested reading: (1) "Sublimation," Aircraft and Missile Engineering, Feb., 1958; (2) Aviation Week, pp 52 et. seq., May 12, 1958

Figure 13-10 shows the calculated effectiveness of beryllium oxide and plexiglass used as ablating materials.

TABLE 13-1

< Melts Below 2500 °F
 xx Not Given

xxxx This compound melts
 at higher temp. than
 either constituent

NAME	SYMBOL	MELT TEMP. °F	OXIDE	BORIDE	CARBIDE	NITRIDE	SILICIDE	SULFIDE
Carbon	C	6700						
Tungsten	W	6170	2683	5288	5184	--	3956	--
Rhenium	Re	5740	<	--	--	--	>3092	--
Tantalum	Ta	5425	3434	3632	7011	5396	3992	--
Osmium	Os	4900	--	--	--	--	--	--
Molybdenum	Mo	4760	<	3956	4874	--	3686	<
Ruthenium	Ru	4500	--	--	--	--	--	--
Iridium	Ir	4450	--	--	--	--	--	--
Columbium	Cb	4380	3222	>3632	6332	3686	3587	--
Boron	B	4200	<	--	4442	4946	--	--
Rhodium	Rh	3570	--	--	--	--	--	--
Chromium	Cr	3430	4109	3632	3434	--	2795	2822
Thulium	Tm	3400	xx					
Titanium	Ti	3300	3344	4712	5684	5342	2804	3722
Zirconium	Zr	3200	4851	5423	6386	5396	2768	3812
Platinum	Pt	3230	--	--	--	--	--	--
Lutecium	Lu	3100	xx					
Hafnium	Hf	3100	5031	5544	7029	5990	--	3902
Vanadium	V	3150	3591	--	5126	3686	--	3452
Iron	Fe	2800	2849	2822	3002	--	--	<
Palladium	Pd	2830	--	--	--	--	2552	--
Yttrium	Y	2700	4370	--	--	--	--	3497
Ytterbium	Yb	2700	xx					
Cobalt	Co	2720	3281	--	--	--	<	<
Erbium	Er	2650	xx					
Dysprosium	Dy	2600	xx					
Holmium	Ho	2650	xx					
Nickel	Ni	2650	3542	<	--	--	<	--
Silicon	Si	2600	3142	--	3812	--	3452	--
Gadolinium	Gd	2500	xx					
Beryllium	Be	2340	4622	--	3902	3992	--	--
Samarium	Sm	2370	--	--	--	--	--	3452
Scandium	Sc	2190	--	--	--	4802	--	--
Manganese	Mn	2270	3236	--	2768	--	--	2948
Europium	Eu	2100	xx					
Copper	Cu	1980	xx					
Gold	Au	1945	xx					
Silver	Ag	1760	xx					
Germanium	Ge	1760	xx					
Praseodymium	Pr	1700	xx					

TABLE 13-1 CONTINUED

< Melts Below 2500 °F
 xx Not Given

xxxx This compound melts
 at higher temp. than
 either constituent

NAME	SYMBOL	MELT TEMP. °F	OXIDE	BORIDE	CARBIDE	NITRIDE	SILICIDE	SULFIDE
Calcium	Ca	1560	4712	>3812	4172	--	--	--
Neodymium	Nd	1540	xx					
Cerium	Ce	1500	3542	>3812	--	--	--	3434
Arsenic	As	1490	xx					
Strontium	Sr	1420	4379	>3812	>3501	--	--	> 3632
Barium	Ba	1300	3483	>3812	>3236	--	--	> 3632
Magnesium	Mg	1202	5072	--	--	--	--	> 3632
Aluminum	Al	1220	3659	<	5072	4046	--	<
Antimony	Sb	1170	xx					
Lanthanum	La	1519	4181	>3812	--	--	--	--
Zinc	Zn	787	xx					
Tellurium	Te	840	xx					
Cadmium	Cd	609	xx					
Terbium	Tb	621	xx					
Lead	Pb	621	xx					
Thallium	Tl	572	xx					
Tin	Sn	449	xx					
Bismuth	Bi	520	xx					
Selenium	Se	428	xx					
Lithium	Li	367	xx					
Indium	In	313	>3600	--	--	--	--	--
Sodium	Na	207	xx					
Sulfur	S	246	xx					
Iodine	I	237	xx					
Potassium	K	145	xx					
Rubidium	Rb	102	xx					
Gallium	Ga	85	3164	--	--	--	--	<
Phosphorus	P	111	xx					
Cesium	Cs	82	xx					
Bromine	Br	19	xx					

173<

TABLE 13-2 (a)

SOME OXIDES

<u>NAME</u>	<u>COMPOSITION</u>	<u>APPROX. MELTING TEMPERATURE °F</u>	<u>OXIDATION RESISTANCE</u>	<u>THERMAL SHOCK RESISTANCE</u>
Thoria	ThO ₂	5500	Good	Poor
Hafnia	HfO ₂	5100	Good	Poor
Magnesia	MgO	5000	Good	Poor
Zirconia	ZrO ₂	4800	Good	Poor
Cerium Oxide	CeO ₂	4700	Good	Poor
Calcium Oxide	CaO	4600	Good	Poor
Beryllia	BeO	4500	Good	Poor
Strontium Oxide	SrO	4400	Good	Poor
Chromium Oxide	Cr ₂ O ₃	4400	Good	Poor
Yttria	Y ₂ O ₃	4300	Good	Poor
Lanthia	La ₂ O ₃	4200	Good	Poor

TABLE 13-2 (b)

SOME CARBIDES

<u>NAME</u>	<u>COMPOSITION</u>	<u>MELTING TEMPERATURE °F</u>	<u>OXIDATION RESISTANCE</u>	<u>THERMAL SHOCK RESISTANCE</u>
Hafnium Carbide	HfC	7500	?	?
Tantalum Carbide	TaC	7000	?	?
Zirconium Carbide	ZrC	6400	Poor	Good
Columbus Carbide	CbC	6300	?	?
Titanium Carbide	TiC	5700	Poor	Good
Vanadium Carbide	VC	5100	?	?
Tungsten Carbide	WC	5000	Fair	?
Thorium Carbide	ThC ₂	5000	?	?
Silicon Carbide	SiC	4900	?	Good
Molybdenum Carbide	Mo ₂ C	4300	?	?
Boron Carbide	B ₄ C	4200	?	Poor
Calcium Carbide	CaC ₂	4100	?	?

13-14

TABLE 13-2 (c)

SOME BORIDES

<u>NAME</u>	<u>COMPOSITION</u>	<u>MELTING TEMPERATURE °F</u>	<u>OXIDATION RESISTANCE</u>	<u>THERMAL SHOCK RESISTANCE</u>
Hafnium Boride	HfB	5500	?	?
Tantalum Boride	TaB ₂	5400	?	?
Zirconium Boride	ZrB ₃	5400	?	?
Titanium Boride	TiB ₂	5400	?	?
Tungsten Boride	WB, WB ₆	5300	?	?
Thorium Boride	ThB	4500	?	?

TABLE 13-2 (d)

SOME NITRIDES

<u>NAME</u>	<u>COMPOSITION</u>	<u>MELTING TEMPERATURE °F</u>	<u>OXIDATION RESISTANCE</u>	<u>THERMAL SHOCK RESISTANCE</u>
Tantalum Nitride	TaN	6100	?	Good
Hafnium Nitride	HfN	6000	?	Good
Zirconium Nitride	ZrN	5300	Poor	Good
Titanium Nitride	TiN	5200	Poor	Good
Boron Nitride	BN	4900	?	Good
Scandium Nitride	ScN	4800	?	Good
Aluminum Nitride	AlN	4000	?	?
Barium Nitride	Ba ₃ N ₂	4000	?	?
Beryllium Nitride	Be ₃ N ₂	4000	Poor	Good

TABLE 13-2 (e)

SOME OTHERS

<u>NAME</u>	<u>COMPOSITION</u>	<u>MELTING TEMPERATURE °F</u>	<u>OXIDATION RESISTANCE</u>	<u>THERMAL SHOCK RESISTANCE</u>
Chromite	FeO·Cr ₂ O ₃	4000	Good	Poor
Stabilized Zirconia	ZrO ₂ ·CaO·SiO ₂ ·TiO ₃ ·HfO ₂	4600	Good	Poor
Cesium Sulphide	CeS	4400	?	?
Thorium Sulphide	ThS	4000	?	?
Molybdenum Disilicide	MoSi ₂	3400	Good	?
Tantalum Disilicide	TaSi ₂	4300	Good	?

412

MELTING TEMPERATURES OF THE ELEMENTS
 PLOTTED AGAINST MOLECULAR WEIGHT, AND
 ALSO COMPARED WITHIN PERIODIC GROUPS

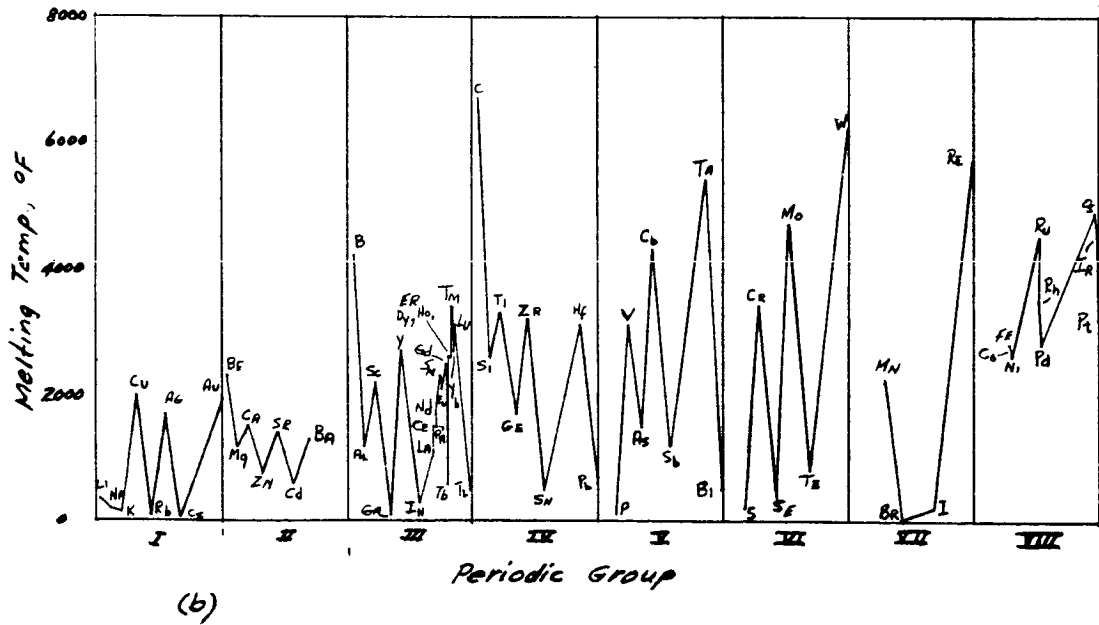
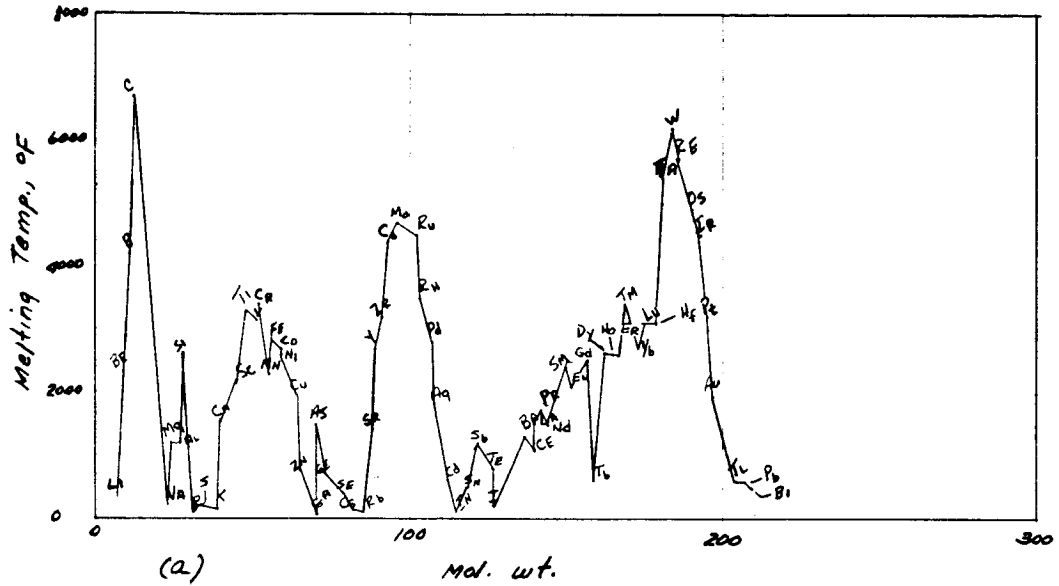


Figure 13-1 Melting temperature of the elements, by molecular weight and periodic group.

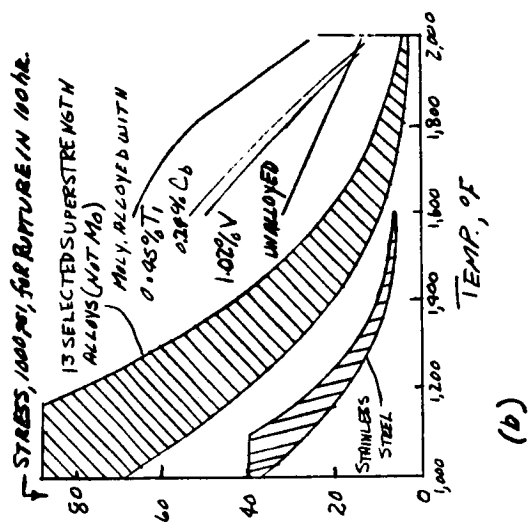
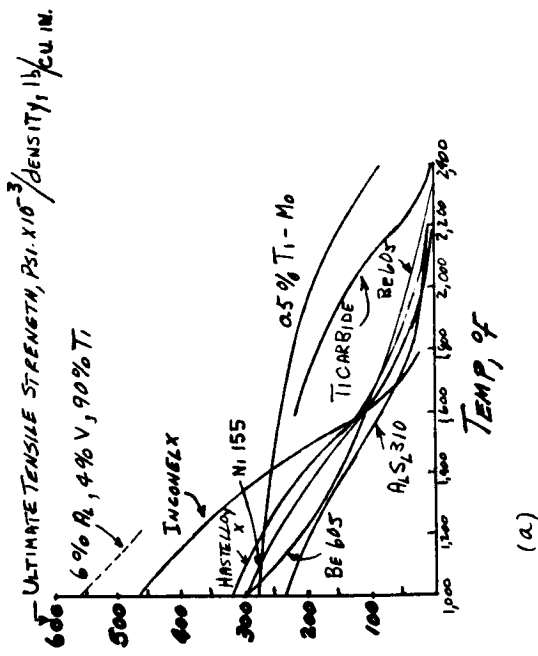


Figure 13-2- Effect of temperature on strength of a few high-temperature materials.

FROM: CHEMICAL ENGINEERING, MARCH, 1957

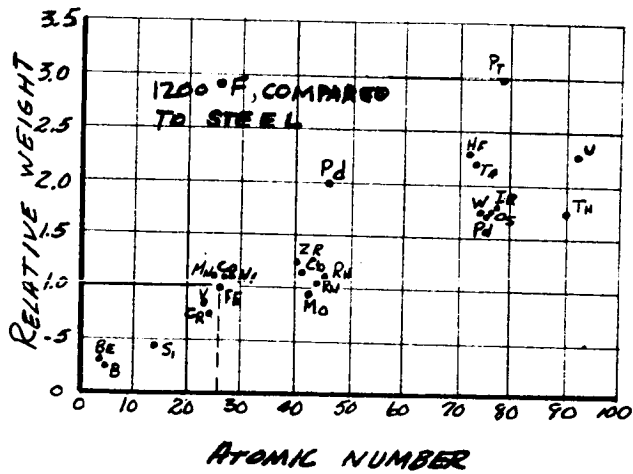
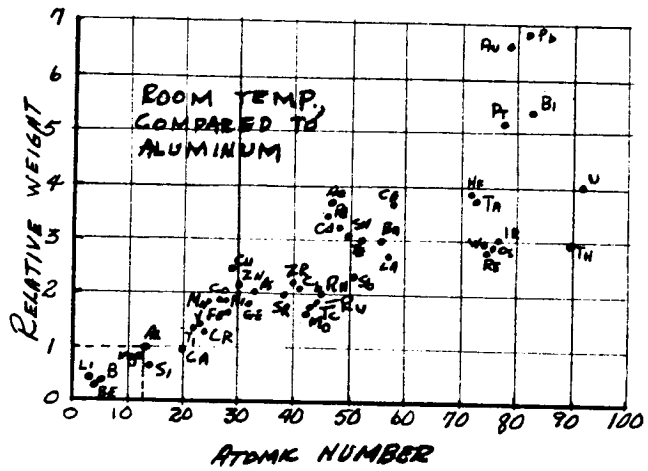


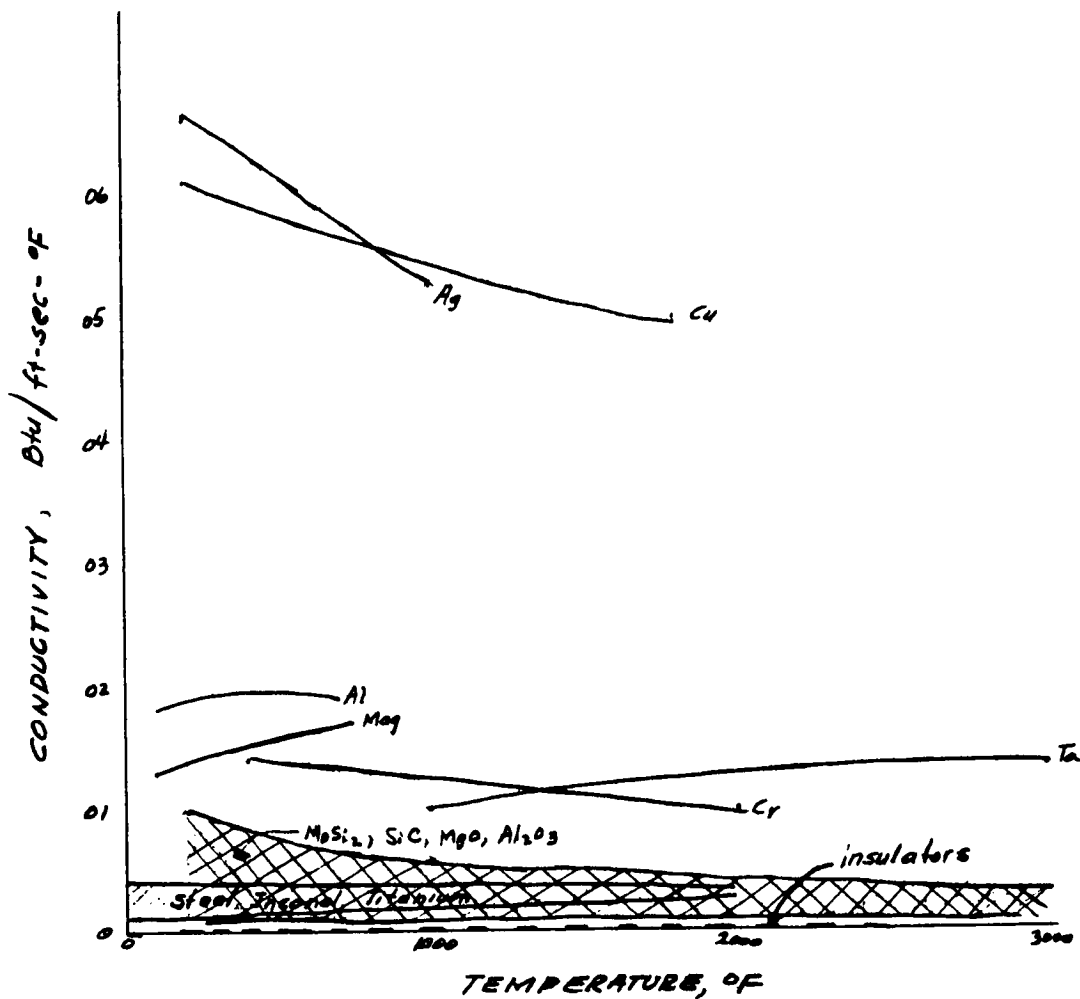
Fig. 13-3

RELATIVE WEIGHTS OF THIN-WALL STRUCTURES, BASED ON BUCKLING CRITERIA, PLOTTED AGAINST ATOMIC NUMBER FOR 70°F & 1200°F

FROM: AERONAUTICAL ENGINEERING REVIEW, FEB, 1957

CONDUCTIVITIES OF SOME SELECTED MATERIALS

This figure is illustrative only



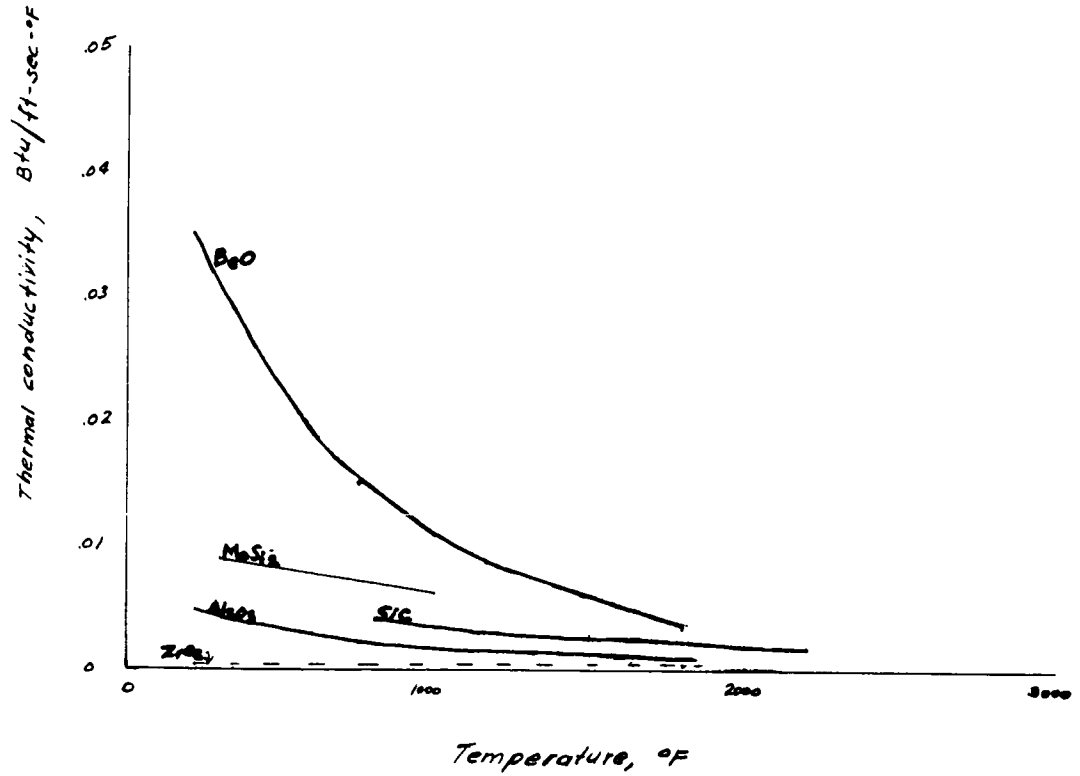
(a) Overall comparison

Figure 13-9 Effect of temperature on thermal conductivity

CONDUCTIVITY OF SOME
SELECTED REFRACTORIES

*This figure for illustrative
purposes only*

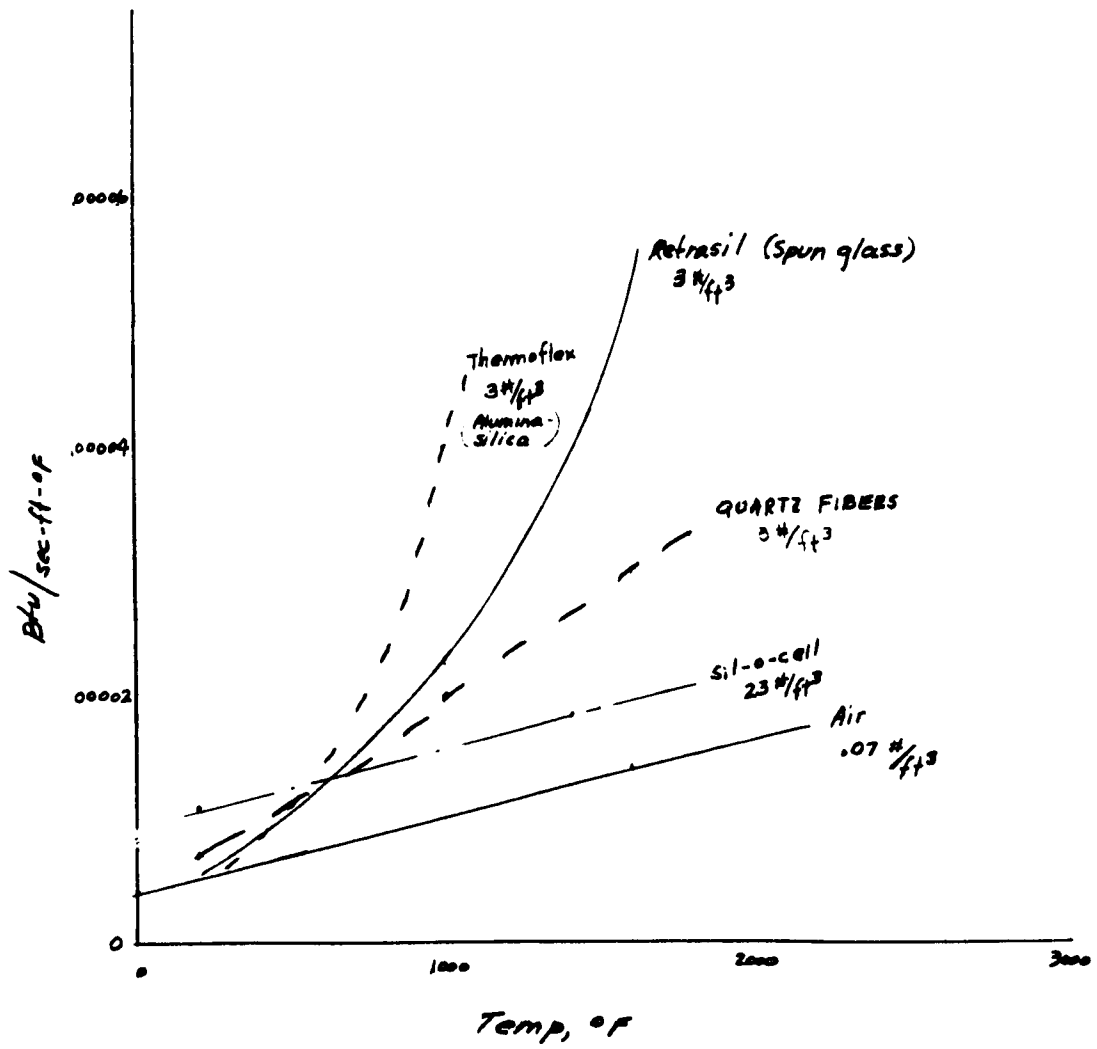
SOURCE: JOUR OF AMER. CERAMIC SOC., JAN, 1955



(b) several refractories

Figure 13-9 continued

CONDUCTIVITIES OF SOME
SELECTED INSULATIONS



(c) several insulators

Figure 3.4 concluded

SPECIFIC HEAT VS TEMP FOR SEVERAL MATERIALS

This figure is illustrative only

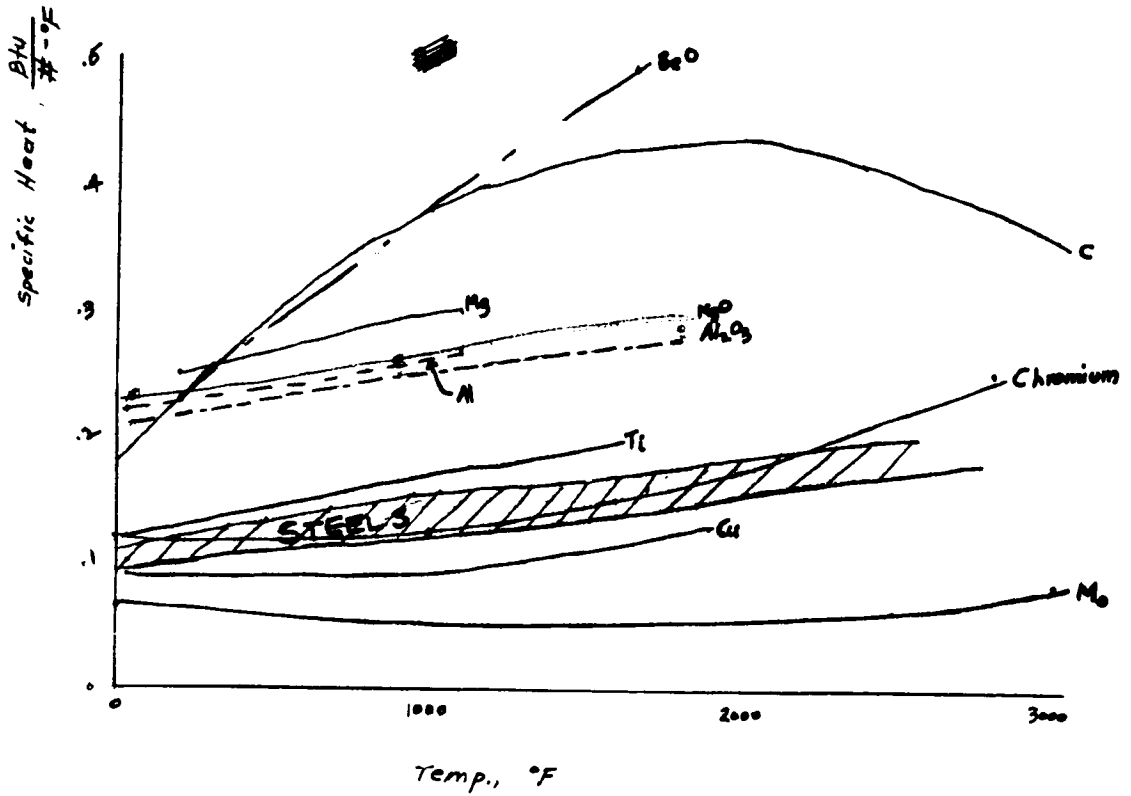
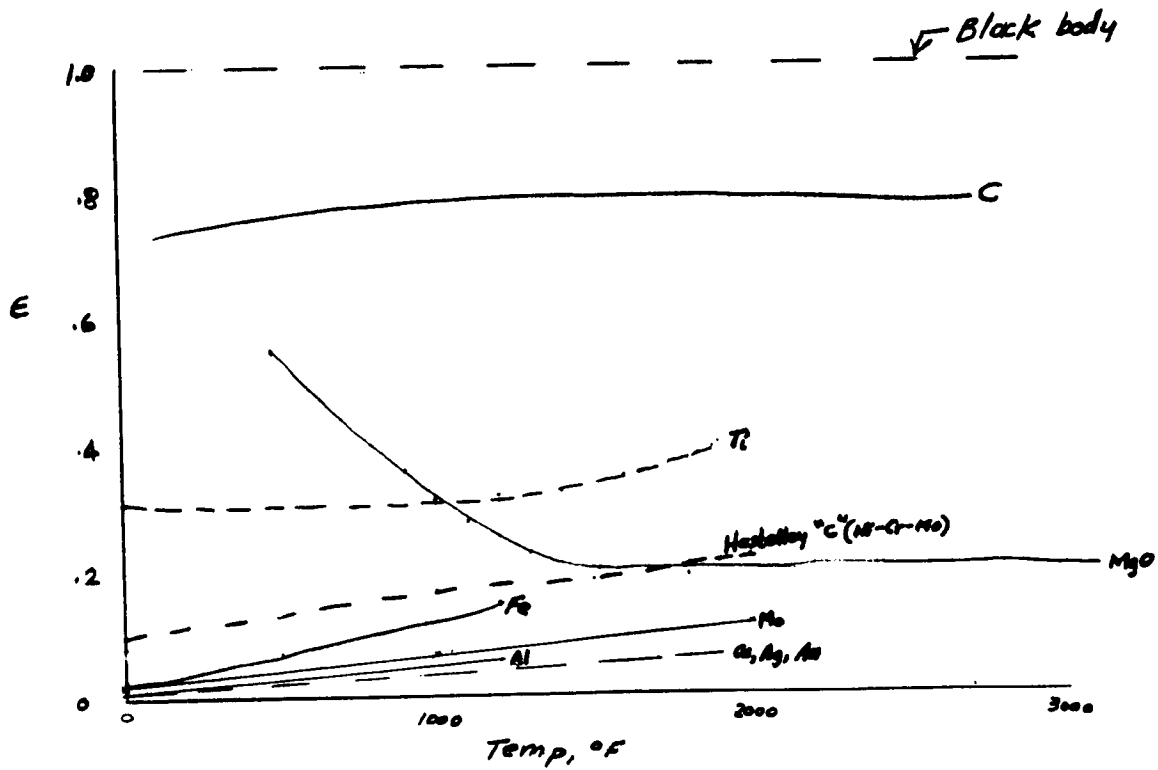


Figure 13-5- Effect of temperature on specific heat.

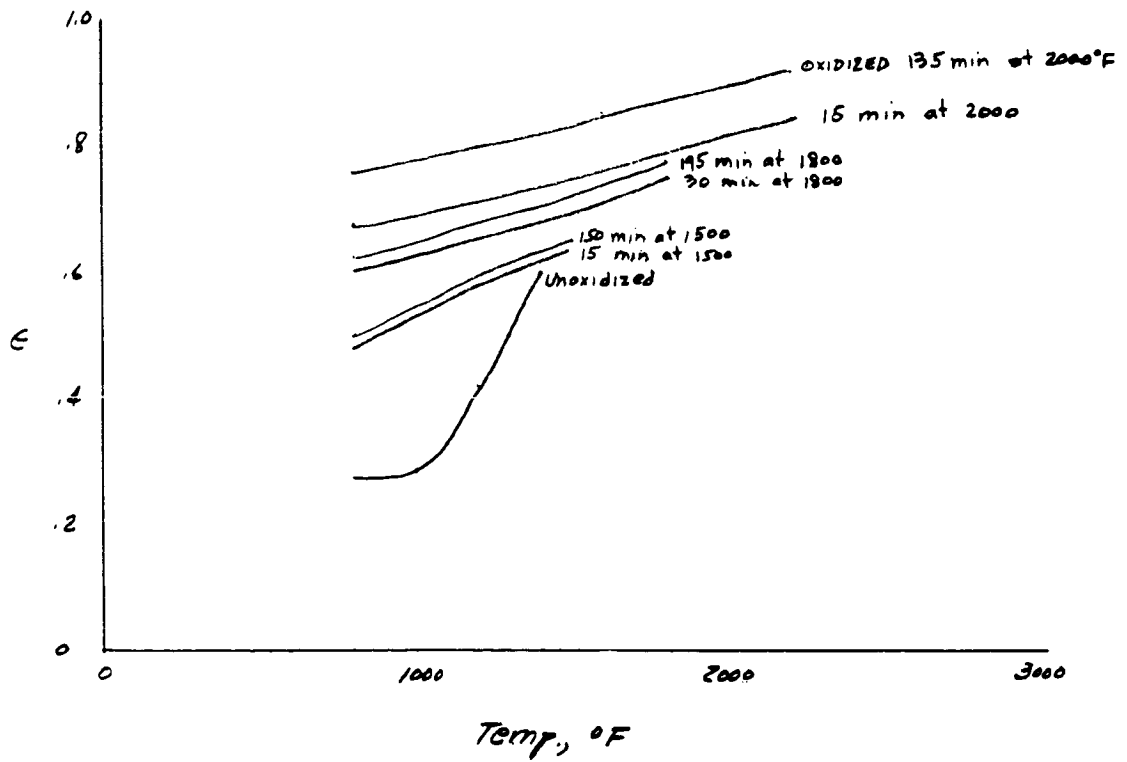
EMISSIVITY OF SOME MATERIALS



(a) Stably-oxidized surface

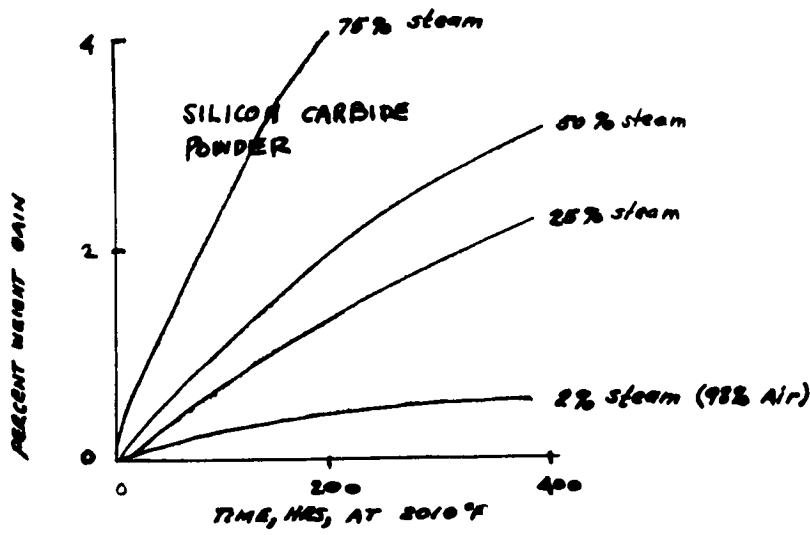
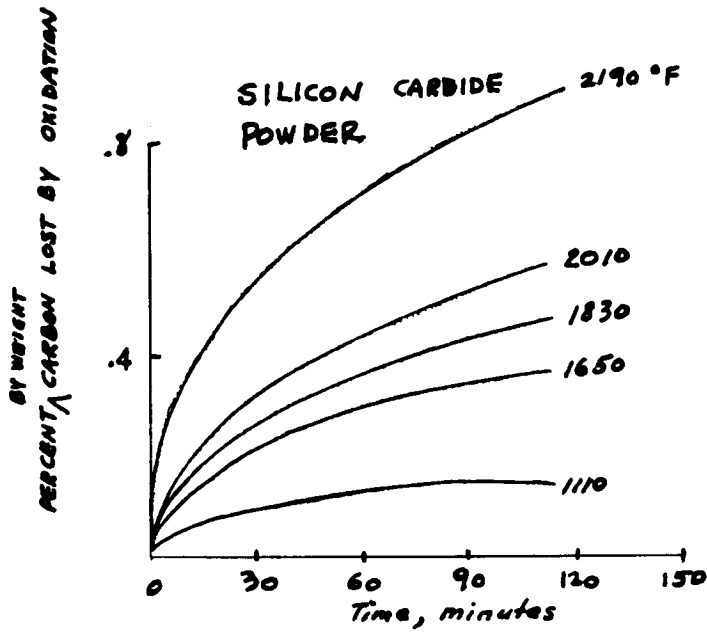
Figure 13-6 Effect of temperature on emissivity.

EMISSIVITY OF INCONEL



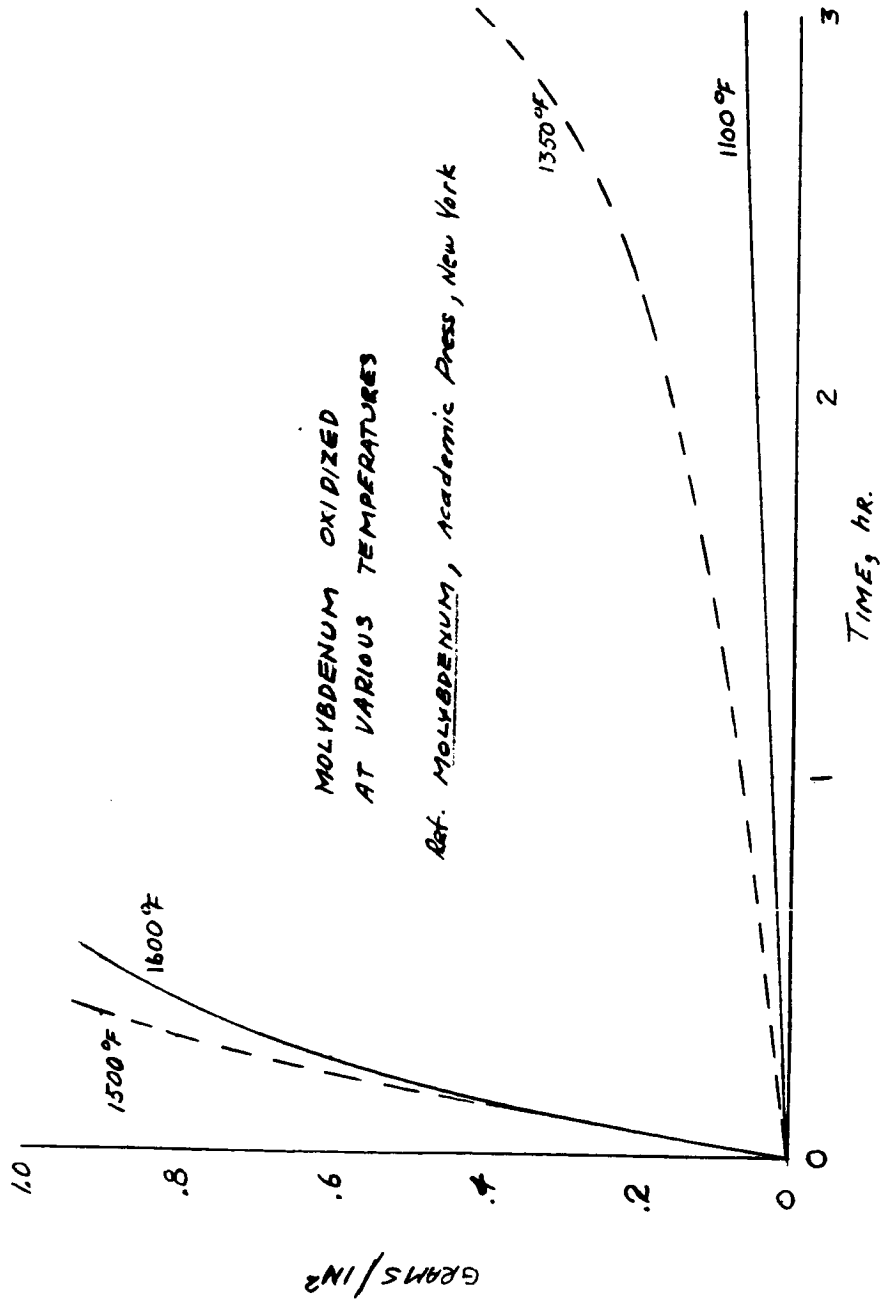
(b) Inconel with various oxidation histories

Figure 13-6 concluded



(a) Silicon carbide powder

Figure 13-7 Effect of temperature on oxidation.



MOLYBDENUM OXIDIZED
AT VARIOUS TEMPERATURES

Ref. MOLYBDENUM, Academic Press, New York

(b) Molybdenum

Fig. 13-7 concluded

1000

EFFECT OF INSULATION

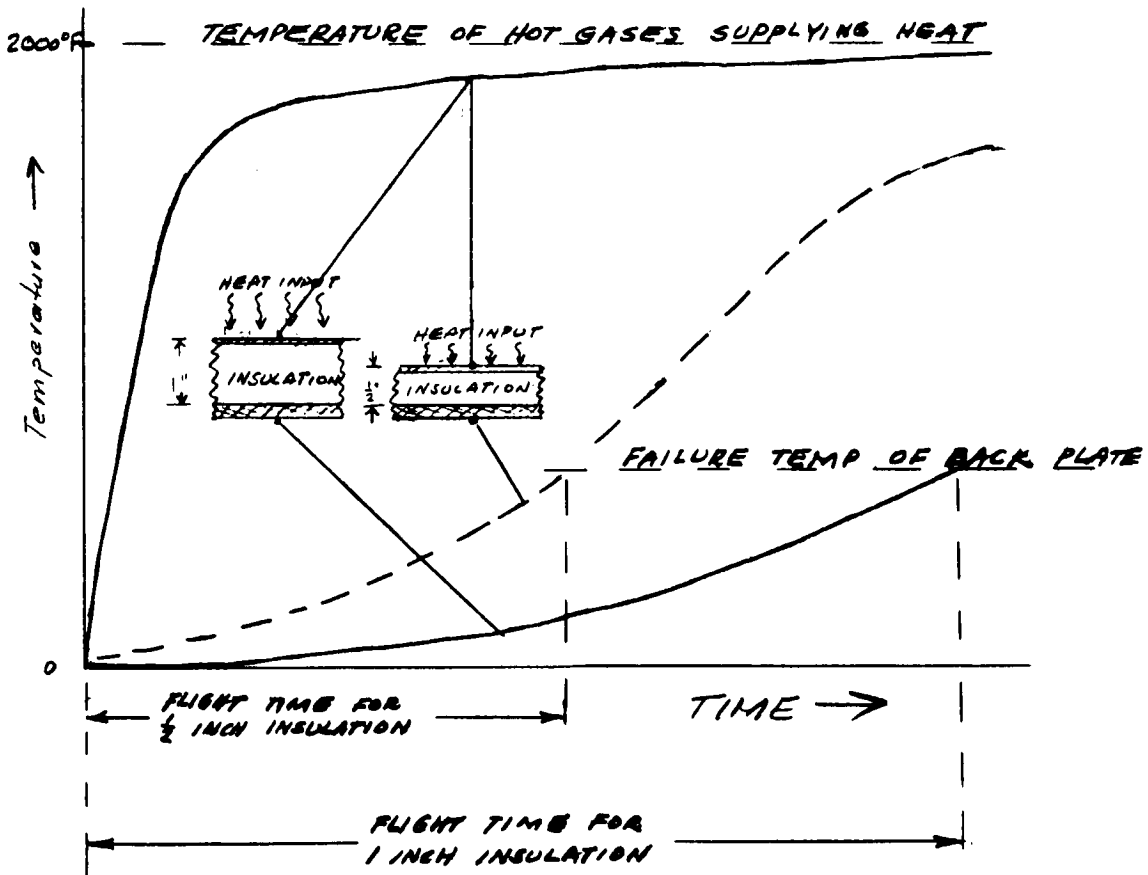
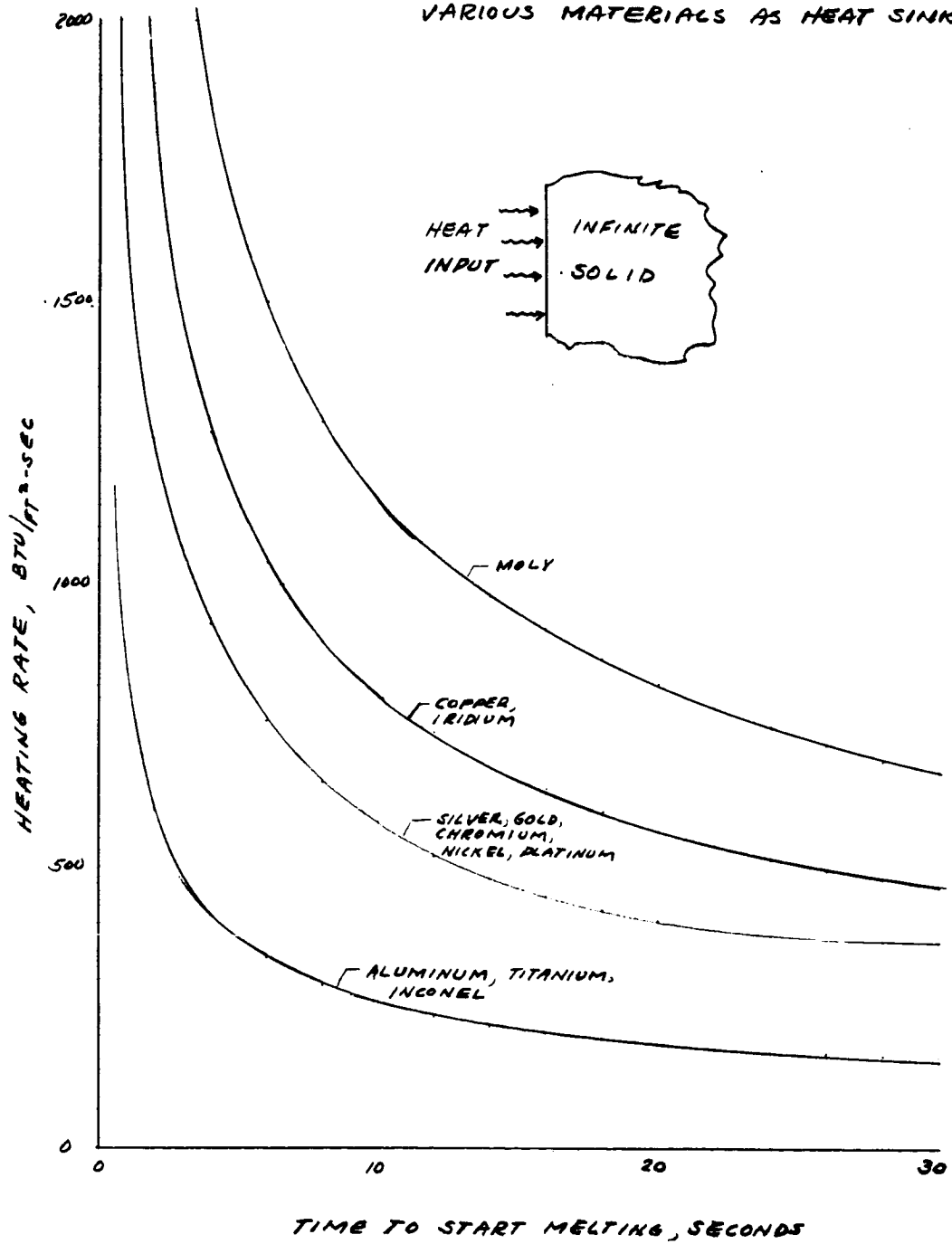


Figure 13-8 Effect of insulation on flight time.

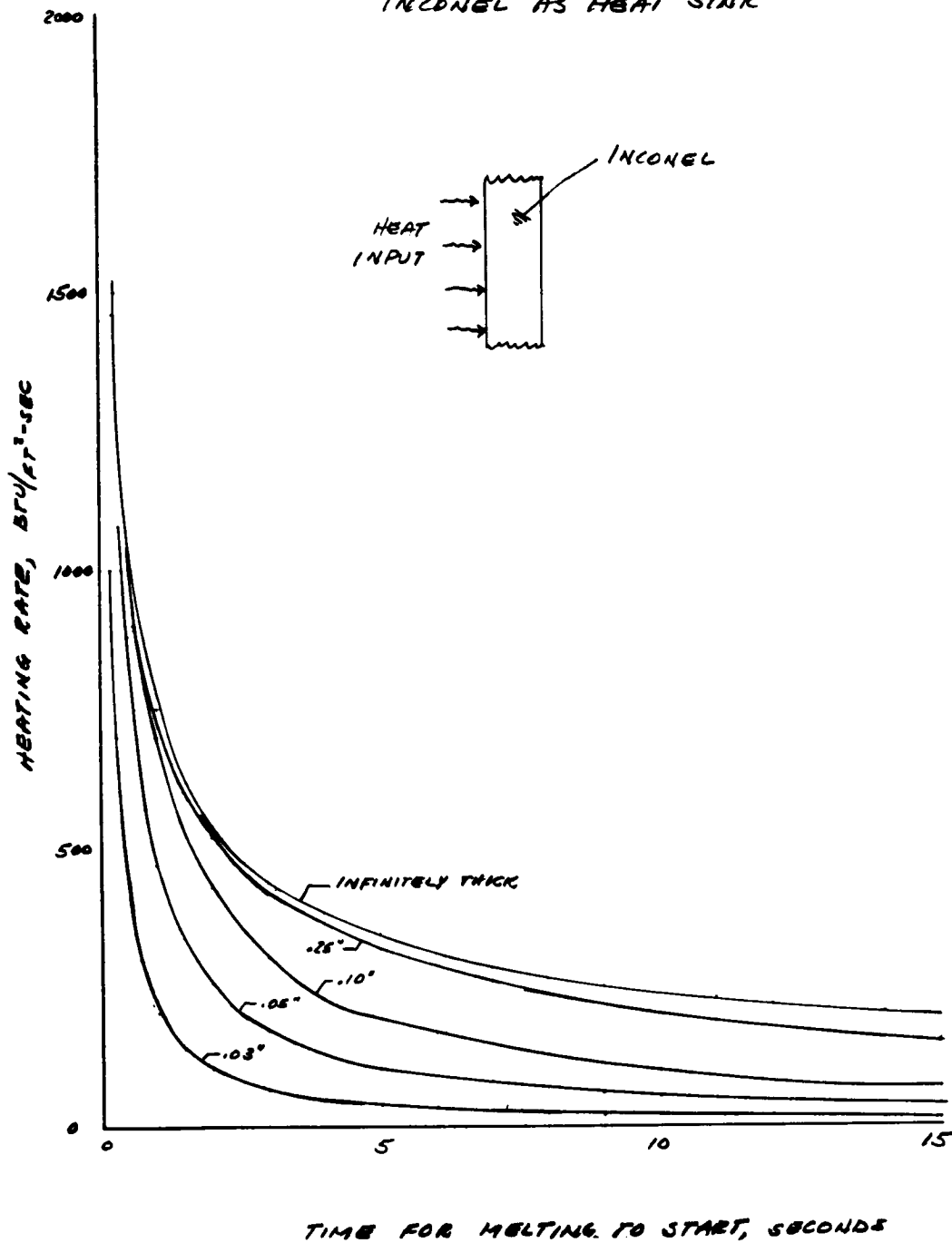
VARIOUS MATERIALS AS HEAT SINKS



(9) Infinitely - thick slab.

Figure 13-9 effect of heat input rate on time to start melting.

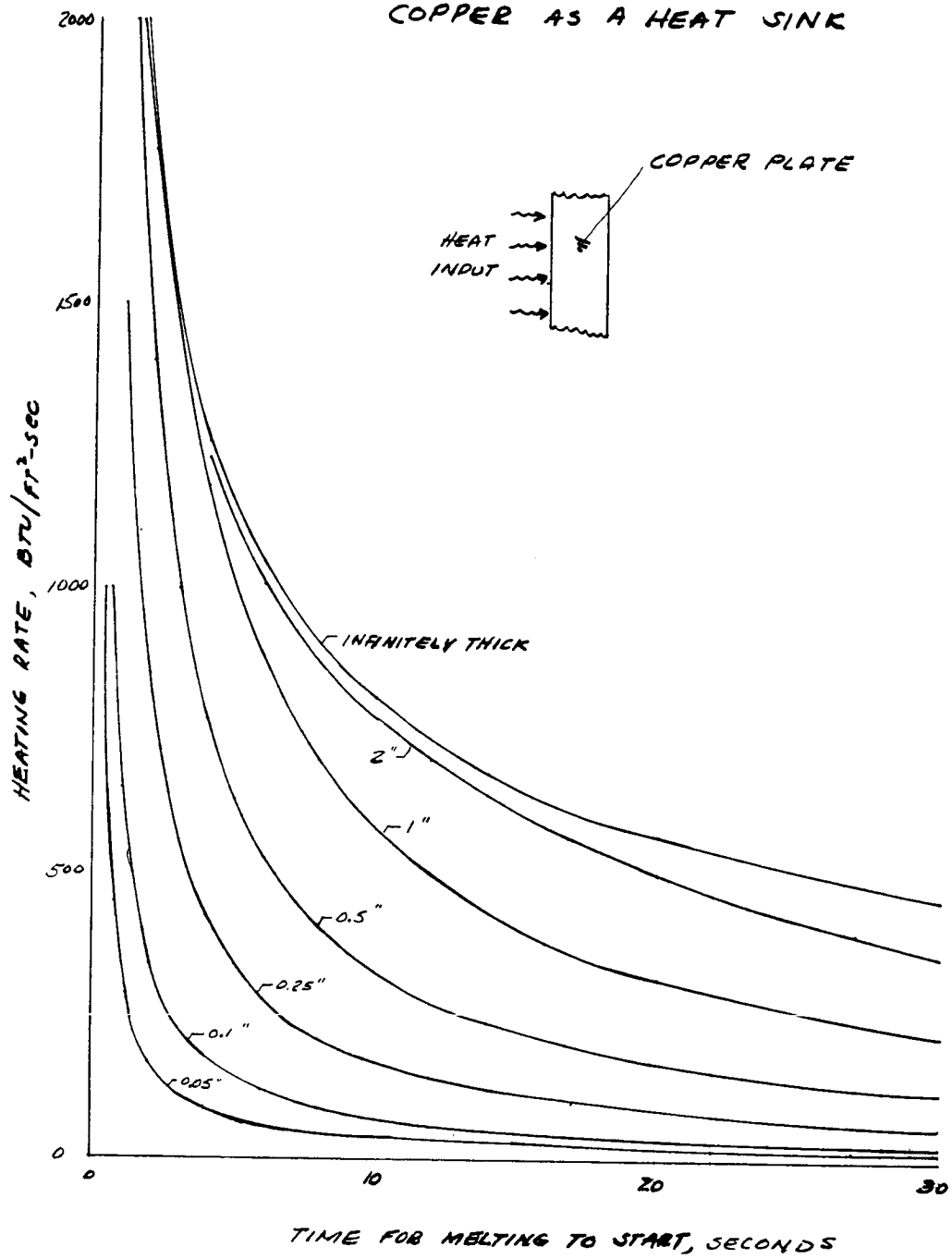
INCONEL AS HEAT SINK



(b) Thin slab of Inconel.

Figure 13-9 continued

COPPER AS A HEAT SINK



(c) Thin slab of copper

Figure 13-9 concluded.

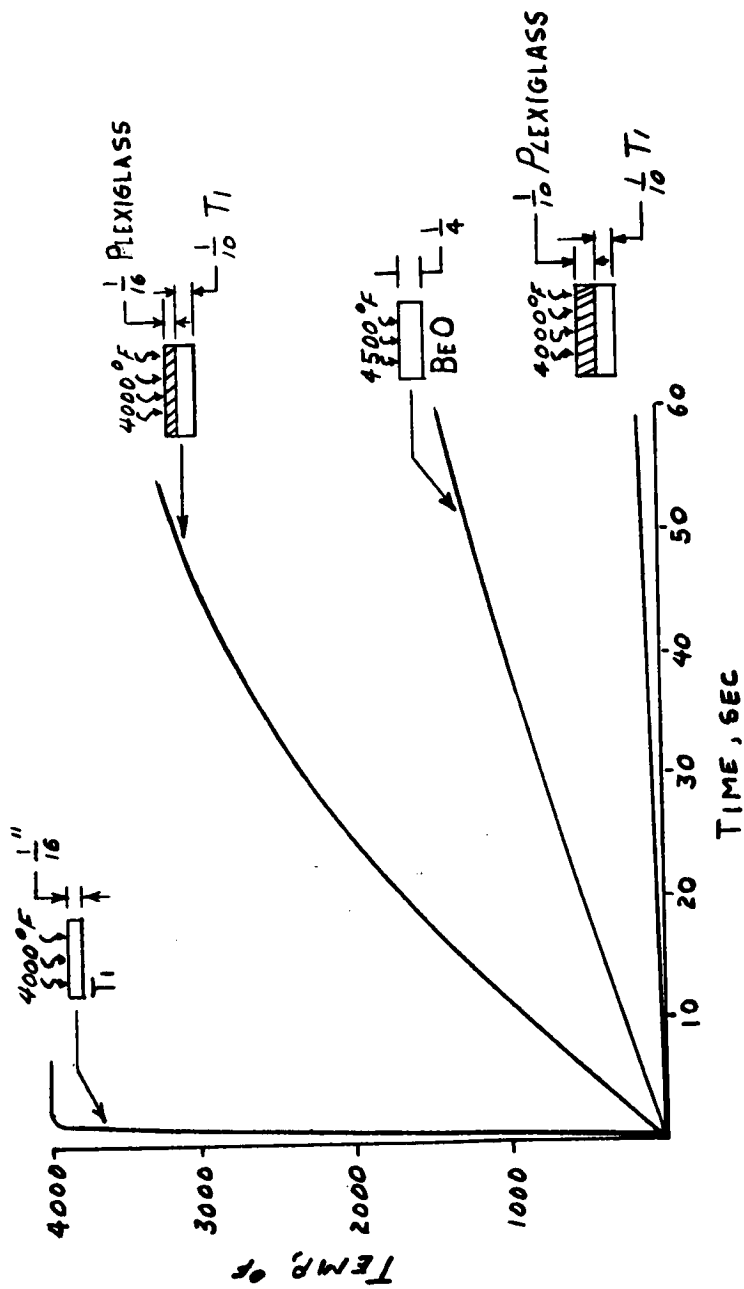


FIG 13-10-CALCULATED TRANSIENT TEMPERATURE RISE IN TITANIUM (UNPROTECTED, AND COVERED WITH PLEXIGLASS) AND BERYLLIUM OXIDE. FROM "SUBLIMATION," AIRCRAFT AND MISSILE ENGINEERING. FEB. 1958

SECTION 14

THE SOLAR SYSTEM

A study of space technology would not be complete without some reference being made to the members of our own solar system. Since there are complete books dealing with the various aspects of this subject the following notes are more in the category of a summary of the available information covering the physical make-up of our solar system. For details and/or a more complete understanding of a particular point one of the references listed at the end of these notes may be consulted.

The notes essentially consist of two parts; the first part being more in the nature of a general discussion of the members of the solar system; while the second part contains tabulations of numerical data as well as a brief discussion of terms and coordinate systems used in Astronomy.

The origin of the solar system is still a matter of conjecture. However, it has been fairly well established that our solar system is merely a small part of a tremendous galaxy made up of countless other bodies and matter. The galaxy of which our solar system is a part is believed to be of the spiral type and our system is located about two thirds of the way out in one of the arms.

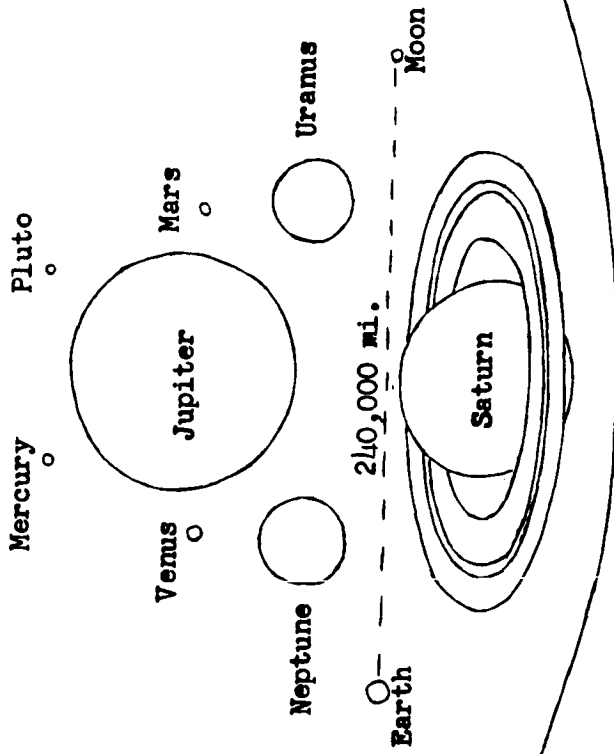
It is estimated that the galaxy is 6×10^{17} or 600,000,000,000,000 miles in diameter or 98,000 light years. The galactic system rotates in a clockwise direction as viewed from its north pole (located at the hour angle $\alpha = 12^h 44^m$, and declination $\delta = 24^\circ$). The galactic rotational velocity in the vicinity of our Sun is 178.3 mi/sec. This was determined in 1934.

Now the Sun which is the center of our solar system is 33,000 light years from the galactic center and has a period of revolution about the galactic center of 224,000,000 years.

Our solar system is moving with a velocity of 12.5 mi/sec toward an apex near $\alpha = 18^h$, $\delta = 30^\circ$ which is not far from the direction of the star μ Hercules (the end point of the constellation Hercules). The diameter of our solar system is about 7,340,000,000 miles or $0.0000000734 \times 10^{17}$ miles as compared to 6×10^{17} for the galaxy.

The members of the solar system are generally considered to be the Sun and the nine planets with their satellites plus many other smaller bodies called asteroids or planetoids. Also contained in the solar system are such things as comets, meteor showers and other so called cosmic matter. These notes will only be concerned with the Sun, planets with their satellites and the asteroids. The sketch on the next page gives some idea of the relative sizes of the principal members of the solar system. It is apparent that the Sun is by far the largest object of our solar system. The planets are usually grouped as the terrestrial planets (Mercury, Venus, Earth, and Mars) and the major planets (Jupiter, Saturn, Uranus, and Neptune). The planet Pluto is so remote that not much is known about it and of such a size that it is sometimes classed as a planetoid.

The general discussion of the solar system to follow will first take the Sun and then each of the planets in order according to their distance from the Sun.



Approx. Relative Size of Planets

Sun

The Sun is the ruler of our solar system. It controls the motions of the planets, comets, meteoric bodies, and other satellites. The Sun is a star. It is not the largest or brightest star but it is the nearest one to us. The next nearest star is 275,000 times as far away. Radiation of the Sun is sole source of power, warmth, activity, and life on Earth, with the exception of tides and volcanic action.

The diameter of the Sun is approximately 864,000 miles. It's volume is 1,300,000 that of Earth and its mass is 333,000 that of Earth. Its density is 1.4 times that of water, and gravity at its surface is 27.6 times that at the Earth's surface. Its surface temperature is about $6,000^{\circ}$ C. and its internal temperature is estimated to be $20,000,000^{\circ}$ C.

The Sun rotates in the same direction as the Earth on an axis inclined 83° to the plane of the ecliptic (equator inclined 7° to ecliptic plane). The poles of the Sun are directed toward a point about halfway between the stars Polaris and Vega. The points coordinates are $\alpha = 18^{\text{h}} 44^{\text{m}}$, $\delta = + 64^{\circ}$.

The Sun is of a gaseous nature and its equator turns faster than the poles. The sidereal rotational period is about 25 days at the equator, 27.5 days at lat. $\pm 45^{\circ}$ and about 33 days at $\pm 80^{\circ}$ lat.

The rate of the Sun's outpour of energy is expressed as a solar constant of radiation. The solar constant of radiation is defined as the number of calories which would be received from the Sun each minute upon a surface one centimeter square, if the surface were exposed perpendicularly to the Sun's rays outside the Earth's atmosphere, at the Earth's mean distance from the Sun. The value is 1.94 ± 5 percent. One calorie is the amount of energy

required to raise the temperature of one gram of pure water at 15° C. to 16° C. It is equal to 4.18×10^7 ergs. The solar constant of radiation is therefore equal to 1.35×10^6 ergs per square centimeter per second.

The Sun's mass is 2×10^{33} grams. This is equivalent to 1.8×10^{54} ergs of energy. The Sun gives off energy at the rate of 1.2×10^{41} ergs per year and its mass is diminishing at the rate of 1.3×10^{20} grams or 1.7×10^{14} tons per year (4,200,000 tons a second). If we assume that all the energy of the Sun is due to destruction of matter, it will continue to give off energy at this same level and rate for 1.5×10^{13} years (15 million million).

Taking the intensity of the Sun's light and heat at the Earth's distance as unity, we have the following values of the intensity at the mean distances of the various planets.

Mercury	6.7	Saturn	0.01
Venus	1.9	Uranus	0.003
Earth	1.0	Neptune	0.001
Mars	0.43	Pluto	0.0006
Jupiter	0.04		

Light from the Sun takes 498.6 seconds or 8.31 minutes to reach the Earth.

Mercury

Mercury is the planet nearest the Sun. With the exception of Pluto and some of the asteroids it has the most highly inclined and most eccentric orbit and the least diameter and mass of any object in our solar system.

Mercury seems to have some sort of atmosphere (at least according to some observers). Following are comments by Antoniadi, one of the most able visual observers, compiled in 1934 using a 33 inch refractor telescope.

(a) The haze on Mercury is whitish; it occurs more frequently and is denser than that on Mars.

(b) It is rare that a dark surface marking on Mercury retains its normal intensity for as long as several weeks.

(c) The haze on Mercury presents all degrees of concentration, from very tenuous to a density sufficient to obliterate the darkest surface markings.

(d) The haze is usually invisible in the central portions of the disc but appears chiefly toward the limb (a result of perspective) and less often near the terminator; near the limb it may extend over an arc of 5000 km (3000 miles).

(e) The changes observed in the haze may be very rapid; in a single day dark surface markings, 3500 km in size, may disappear completely, while the opposite may also occur.

(f) The invisibility of surface markings may last many days.

(g) Light haze may cover a region for weeks, with improved and diminished visibility alternating.

(h) The north pole region, usually clear, once showed a bright haze for six days.

(1) One particular dark region, on the equator and at 60° longitude from the sub-polar point (to the right in the image, with South on top), is much more often covered by haze than any other surface marking; two regions at the same longitude but at $\pm 40^\circ$ latitude respectively are covered less often than the equatorial region mentioned, while the whole left half of the visible hemisphere is covered still less frequently.

It has been suggested that the haze described by Antoniodi might be carbon monoxide plus other inert gases and cosmic dust due to impacts (possibly replenished by these impacts). The dust particles being the reflectors that make the haze visible. At any rate the atmosphere of Mercury must not have much depth since other means of detection have not yielded positive results.

As far as we know the planet rotates on its own axis with the same period as it revolves about the Sun and, therefore, the side of Mercury facing the Sun has a temperature of 685° K. at perihelion and 550° K. at aphelion. The dark hemisphere is intensely cold (10° to -20° K.) and tends to freeze out all but the most volatile compounds of the atmosphere.

A transit of a planet occurs when one planet passes between the Sun and another planet. As far as the Earth is concerned the only planets that can have transits are Mercury and Venus. Transits are important astronomically for observational reasons. The transits of Mercury occur as follows

Date	Time GMT	Date	Time GMT
1957 May 5	13	1986 Nov. 12	16
1960 Nov. 7	5	1993 Nov. 5	16
1970 May 8	20	1999 Nov. 15	9
1973 Nov. 9	23	2003 Nov. 6	19

Venus

Venus has the most circular orbit of the planets and has about the same diameter as the Earth. It has high reflectivity and is easily visible however, not a great deal is known about its surface. This lack of knowledge about its surface is due to the dense layers of clouds and dust in the atmosphere of Venus.

Visual observations and spectrographic analysis of the atmosphere of Venus have resulted in the conclusion that carbon dioxide makes up about 90 percent of the atmosphere. There is undoubtedly some nitrogen, argon, and possibly free oxygen. No trace of water has been found.

The atmosphere is estimated to be 6000 mile deep with a CO₂ cloud layer at least 15 miles deep near the surface. There is a haze layer about 4000 feet thick near the bottom of the atmosphere with either the planets surface or an opaque layer beneath. It is believed that the atmosphere is very dusty (both from cosmic dust and from wind erosion of the surface).

The period of rotation of Venus on its own axis is open to question. It was originally thought that its period was the same as its period of revolution around the Sun, however, the latest opinion is that its period of rotation is about 20-30 days. This is partly based on the fact that the temperature on the bright side (50°-60° C.) is not too much different than that on the dark side (-32° C.).

The fact that the temperature on the dark side does not approach -273° C. can be partly attributed to atmospheric circulation. However, this cannot account for all the difference, thus the planet must rotate slowly on its own axis.

Transits of Venus occur at intervals of 8, 121-1/2, 8, 105-1/2, 8, 121-1/2, 8, years etc. Some dates of transits of interest to us are

Date

1874 Dec. 9

1882 Dec. 6

2004 June 8

2012 June 6

Earth

The Earth is a mean distance of 92.9×10^6 miles from the Sun. It is an oblate spheroid having a diameter of 7,927 miles at the equator and 7,900 miles at the poles. The Earth is 29 percent land and 71 percent water. It travels around the Sun at a velocity of 18.5 miles per second. The mass of the Earth is 6×10^{21} metric tons or 6.593×10^{21} short tons. The mean density is 5.52 times that of water and it rotates once in 24 sidereal hours. The magnetic pole is about 20° from the geographic pole.

The attraction of gravity of the Earth is about $1/190$ of itself less at the equator than at the poles. One hundred ninety pounds at the pole would only weigh 189 pounds at the equator on a spring balance. One pound out of 289 of this difference is due to centrifugal force, and one pound out of 555 is due to the Earth's shape.

From Hayford "Spheroid of 1909" we get the following dimension for Earth:

Equatorial radius	3,963.34 miles
Polar radius	3,949.99 miles
Oblateness	$\frac{3963.34 - 3949.99}{3963.34} = \frac{1}{297} = 0.0034$

Latitude	Length of one degree of arc miles
0	
0	68.708
15	68.757
30	68.882
45	69.056
60	69.231
90	69.407

533<

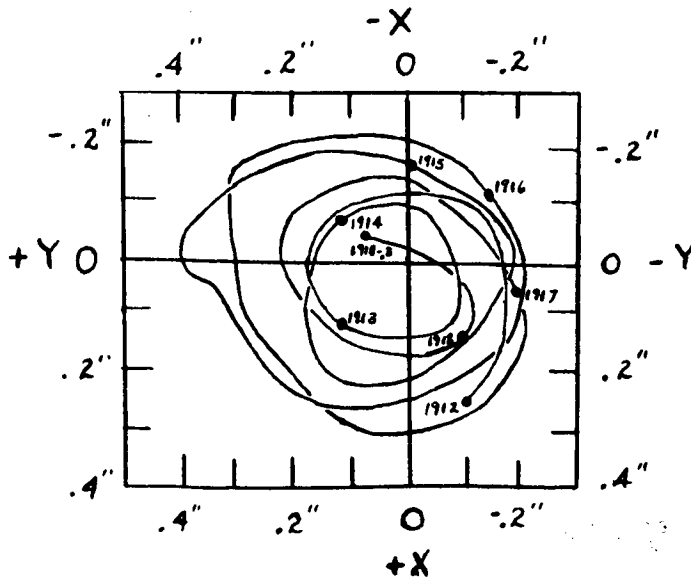
Note: One statute mile equals 1.1516 times a nautical mile.

Perturbations of the Earth.- The Earth experiences three detectable perturbations; precession, nutation, and variation of latitude.

Precession.- Pole moves in a circle. One revolution takes about 25,800 years. Discovered in 120 B.C. by Hipparchus. The rate of rotation of poles is $50''26$ per year. This precession displaces equinox by about 30° in 2,150 years. That is why the first point of Aries is now in the constellation Pisces. Star nearest pole 4,000 years ago was α Draconis. It is now α Ursae Minoris. In 12,000 years it will be Vega.

Nutations.- Nutations are departures of the poles from perfect circular motion. They are caused mainly by Sun and Moon. The largest effect is the Moon. This lunar effect has a period of 18.6 years and an amplitude of $9''2$ in latitude.

Latitude variation.- Two small effects - one with a 14-month period and the other with a 1-year period with amplitudes of about $0''2$ - are called latitude variations. The 14-month effect is due to the elasticity of the Earth. The annual effect is due to seasonal displacement of matter over the Earth. Both discovered by Chandler in 1891 and explained by Newcomb. Cause period of Earth's rotation to slow down by 2 to 5 milliseconds.



This sketch shows the variation of latitude from 1912 to 1918.

Perturbation of the Earth's orbit:

1. The line of apsides is revolving eastward at a rate that, if continued, would carry it entirely around in about 108,000 years; it will not continue always at the same rate.
2. The eccentricity of the orbit which is now 0.016 is diminishing and will continue to do so for about 24,000 years at which time it will be about 0.003. It will then increase for some 40,000 years but will never exceed 0.07.
3. The plane of the orbit is slowly changing position. The value of obliquity is now $23^{\circ}27'$ and is diminishing at the rate of $0''5$ a year. This decrease will continue for about 15,000 years, after which the obliquity will increase. It oscillates in this manner about 195 on either side of the mean.

Earth is at perihelion about January 3 and at aphelion about July 5. The Earth and the Moon rotate about a common apparent center of mass. This center is about 2,880 miles from the center of the Earth or about 1,000 miles within the surface of the Earth.

The Earth has one known satellite.

The Moon

The Moon is about an average of 60 Earth radii from the Earth. Its nearest distance is 222,000 miles and its furthest distance is about 253,000 miles from the Earth. The Moon's diameter which lies in a line with the Earth is about 2,163 miles. The equatorial diameter (at right angles to above) is about $1/3$ mile shorter and the polar diameter is about 1 mile shorter. The Moon's mass is $1/81.5$ that of Earth and its mean density

is 3.39 that of water. The surface gravity is $1/6$ that of the surface gravity of Earth. It reflects about 7 percent of the light that it receives.

Its sidereal period around the Earth is $27^{\text{d}} 7^{\text{h}} 43^{\text{m}}$ and its period of rotation about its axis is the same as its rotation around the Earth. The Moon axis is tilted 6.5° to its orbit and its orbit is tilted 5° to the plane of the ecliptic. It rotates and revolves West to East. The eccentricity of its orbit is 0.056.

The temperature is greater than 100° C. on sunlight side and less than -150° C. on unlight side. The temperature drops rapidly as Earth shadow falls on it. Material of Moon, therefore, is a low conductor of heat and has a low specific heat. The only substance that we know of having such properties are loosely packed dust, ash, coarse powder, etc.

The Moon has no atmosphere as we think of an atmosphere and no water. There is some chance that the heavier gases may be found in some of the craters and possibly enough moisture to sustain some low types of moss.

Polarization studies indicate that the chemical composition of the Moon's surface is similar to that of the Earth's crust.

The surface of the Moon is made up of maria, mountains, craters, rills and rays. Some of these can be seen in the following pictures.

The maria were originally thought to be seas but actually they are comparatively flat areas marked by small craters, hills, and cracks.

Some of the mountains are very high, above 25,000 feet and are mostly in chains or groups.

Rills are narrow crevices - ten to 300 miles long and less than two miles wide.

Rays are narrow streaks, lighter in color than their surroundings, radiating out from prominent craters. They extend hundreds of miles across the face of the moon.

Craters are by far the most numerous lunar formations. They vary in size from 150 miles in diameter to 1/10 mile in diameter.

Slopes on the Moon in excess of 45° are quite rare. There are no great clefts or faults which are tremendously deep. The faults of the Moon have slopes of about 45° .

The Moon's surface has not changed noticeably since observations of it were first recorded. There is some speculation that this is not exactly true. Some observers claim to have detected some changes but these have not been verified.

Mars

Mars has a diameter of 4,200 miles. It's day is 24 hours, 37 minutes - about 37 minutes longer than ours. Mars is a mean distance of 142.5 million miles from the Sun and revolves about the Sun once in 687 days. The closest Mars comes to Earth is 35 million miles and its greatest distance at opposition is 61 million miles. The seasons on Mars are about twice as long as ours.

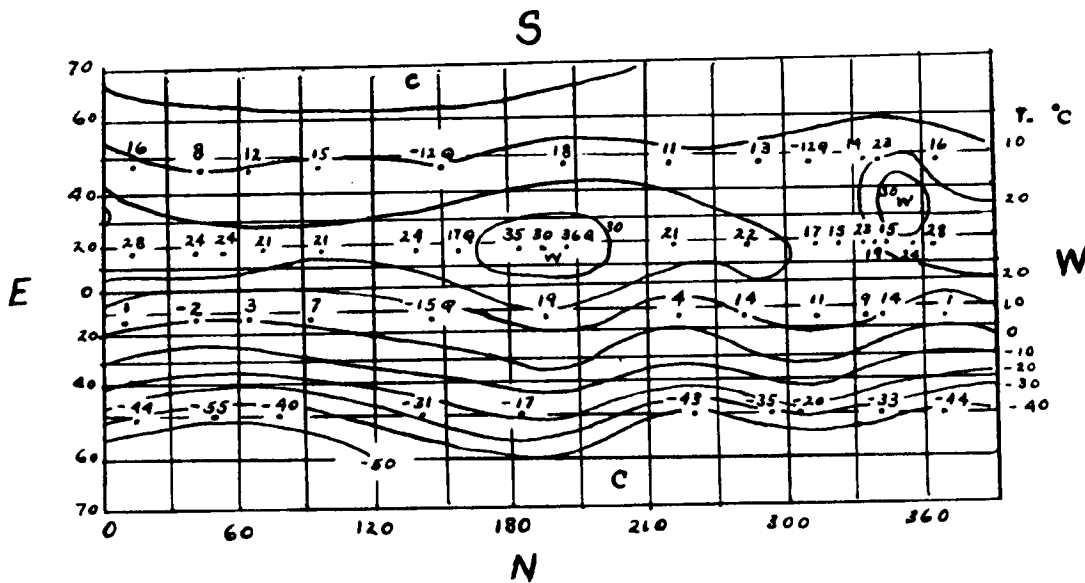
Mars and Earth are in opposition about every 2-1/8 Earth years. Opposition is when Earth, Mars, and Sun are in straight line. The closest oppositions occur every 15 to 17 years. The last one was on September 10, 1956. The next opposition then will be on October 25, 1958, (approx.).

Indications are that Mars is a living planet. Faint atmospheric belts have been detected across the face of the planet - and clouds have been detected around the northern ice cap in fall and winter. Sometimes atmosphere is clear and at other times opaque (called blue haze). It changes rapidly for unknown reasons. Whatever atmosphere there is contains very little oxygen. Only heavier gases remain (nitrogen, CO₂, argon, and H₂O). This is probably due to small mass of planet (small gravitation attraction). The atmospheric pressure is not known but it is estimated to be about 1/10 that of Earth at the surface of Mars. Other estimates place the pressure at 1.16 lb/in.². Atmospheric circulation on Mars is similar to that on Earth. However, weather is more regular due to geography of its surface.

The temperature at the equator during the day is about 70° to 80° F. and at night about -95° F. At poles it is far below zero both day and night.

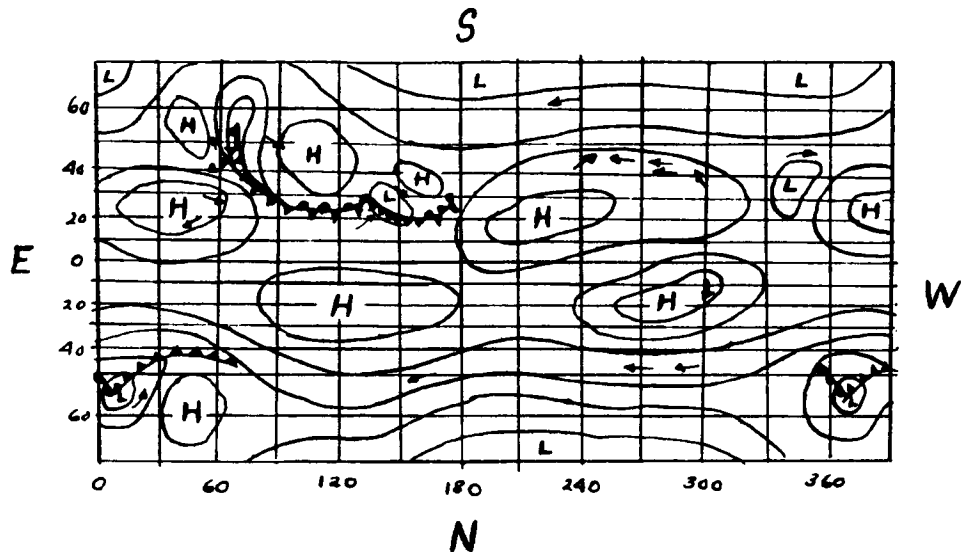
These temperatures were measured with a vacuum thermocouple which can measure the heat of a candle 40 miles or more away.

Radiometric measurements permit estimation of surface temperatures over areas as small as 200 miles in radius. This allows delineation of the general temperature field. Such a description is presented in the following sketch.



The distribution of temperature ($^{\circ}$ C.) on Mars in Northern Hemisphere winter. Values marked Q are questionable. Measurements made in 1926.

Streamline maps can be drawn consistent with the temperature distributions. Such a chart is shown below.



A schematic streamline map for Mars in Northern Hemisphere winter. The arrows represent observed cloud drift directions. Cloud drift observations made in 1894.

The most striking aspect of these two sketches is their resemblance to terrestrial weather maps. This indicates as was mentioned earlier that Mars has an atmospheric circulation very similar to Earth's.

The poles of Mars are covered by ice caps but these caps are probably only a few inches to a couple of feet thick.

The famous "canals" on Mars are real. They seem to be the lines that the water from the melting polar ice caps follow. Vegetation grows along these canals in summer. Some people believe they are artificial since they are so straight and intersect - one runs 1500 miles. Some believe they may be fault lines. These fault lines have been caused by collision with meteorites or asteroids. Others seem to think that they may be wind rows of volcanic dust blown into patterns that we see and that they are clearer in spring because the winds increase. The only sure thing

is that there is some sort of network of so-called canals that appear to lead the water from the melting polar caps to the equator.

Mars has two tiny satellites. They are probably less than 20 miles in diameter. They revolve in circular orbits in the plane of the planet's equator. The nearer, Phobos, is only 5,800 miles from the center of the planet. It revolves in the direction of the planet's rotation and its period is 7^h 40^m.

The other satellite, Deimos, revolves at a distance of 14,600 miles from the center of the planet and its period is 30^h 18^m.

The Asteroids

First discovered by Piazzi in 1801 (based on Bode's law). Between Mars and Jupiter there are many asteroids or minor planets; 1300 have been cataloged and it has been estimated that there are as many as 30,000.

Of the first 900 cataloged, the main body begins at a distance of 2.1 astronomical units and continues to 3.5; then there is a gap and a group of 6 at 3.9 units (Hilda group); then an isolated one, Thule, at 4.3 units; and finally, the Trojan group (6) at 5.2 units.

The eccentricities vary: 209 have eccentricity of 0 to 0.087; 375 from 0.087 to 0.174; 248 from 0.174 to 0.259; 49 from 0.259 to 0.342; 7 from 0.342 to 0.423 and 4 stragglers, Albert, Alinda, Ganymede, and Hidalgo that have eccentricity greater than 0.50.

The inclination of their orbits to the ecliptic also varies - 222 being inclined 0° to 5° ; 297 from 5° to 10° ; 222 from 10° to 15° ; 98 from 15° to 20° ; 35 from 20° to 25° ; 14 from 25° to 30° and 3 above 30° .

There is a tendency for high eccentricity and inclination to go together. The diameters also vary - there are 195 that have diameters greater than 61 miles; 502 between 61 miles and 25 miles; 193 between 25 miles and 10 miles and 22 less than 10 miles.

Some of the bigger ones are

Name	Dia. (miles)	Albedo	Inclination of orbit to ecliptic
Ceres	488	.06	$10^{\circ} 37'$
Pallas	304	.07	$34^{\circ} 43'$
Vesta	248	.26	
Juno	118	.12	

Eros is another important minor planetoid. It is only 17 miles in diameter. It has a period of revolution of 643 days, an eccentricity of 0.222. It is important because it comes to within 14,000,000 miles of Earth and 1.13 astronomical units from the Sun. Its orbit is greatly affected by the mass of the Earth and Sun. Observation of these perturbations will aid in determining the mass of the Earth and Sun. However, it only comes nearest to the Earth about every 40 years. Its orbit is greatly inclined to the Earth's orbit.

A recently discovered asteroid called Geographos is one of few asteroids whose orbit is inside that of our Earth's. Its plane of revolution is inclined 13° to ours. Its period of revolution about the Sun is 17 months. The Earth and Geographos will be 4 million miles apart during August 1969, the closest for this century.

Jupiter

Jupiter is the largest planet and the second brightest. Its equatorial diameter is 88,800 miles; its polar diameter 82,000 miles. One Jupiter year equals 11.86 Earth years. One Jupiter day is about 9 hours and 55 minutes. Its rotational speed at equator is about 28,800 miles per hour. The temperature at the top of the atmosphere is between -130° C. to -180° C. Its bulk is equal to 1,300 Earths.

Rotational speed of Jupiter plus its gaseous atmosphere causes the planet's "atmosphere" to appear to have an alternately dark and light band like structure. This rapid rotation causes rapid heating and cooling of the atmosphere which in turn probably causes wind and electrical storms far surpassing any on Earth. The dark bands are called belts and the light bands are zones. The bands are blue and yellow in color.

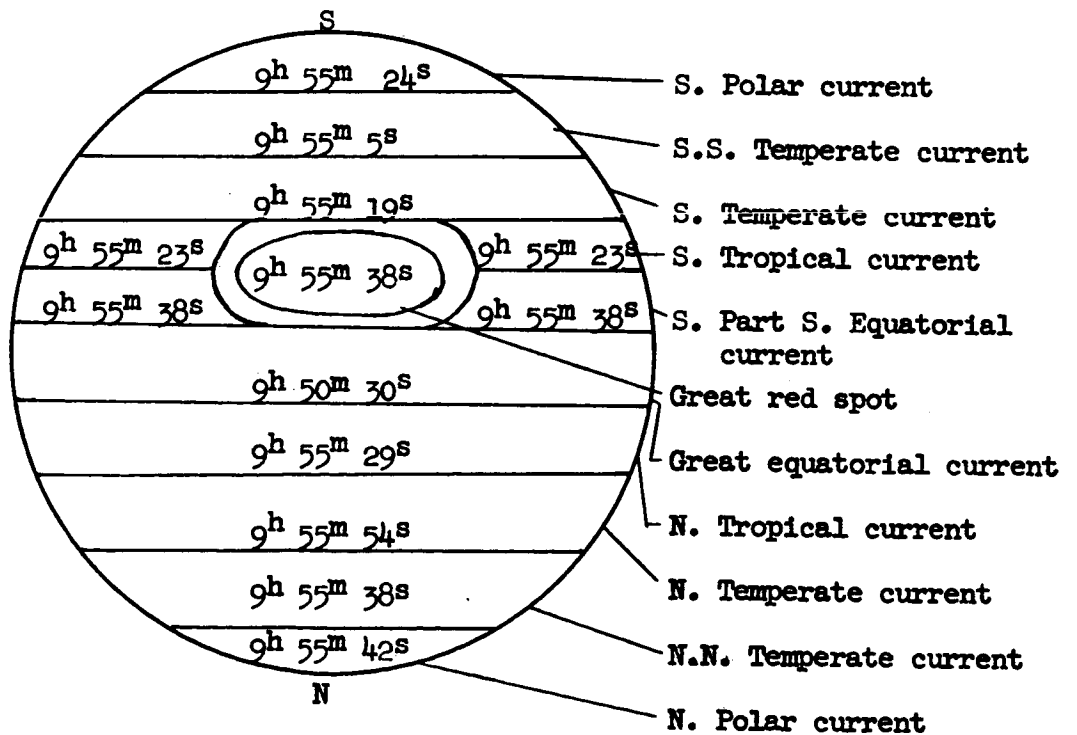
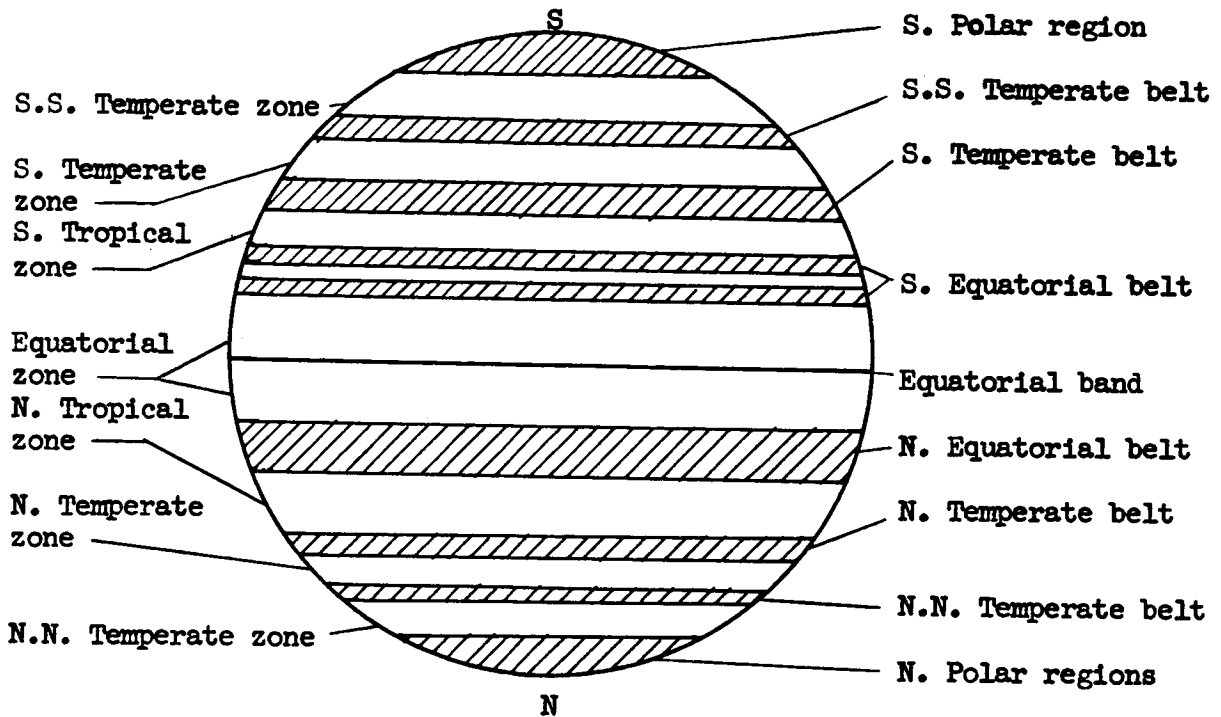
Atmosphere probably consists of clouds of frozen ammonia floating in a sea of methane, also probably some hydrogen and helium. The atmosphere is estimated to be 1000's of miles deep. Colors and spectra can be reproduced by frozen-free radicals of ammonia and methane in the Laboratory. Free radicals are made by exposing molecules to proper wave length of light and proper temperature. They are stable at low temperatures (order of -200° C.). When heated they combine to form molecules and heat. Could be a possible source of fuel. The circulation of Jupiter's atmosphere is similar to that of Earth.

The years of greatest sun spot activity are the years of maximum spottedness of Jupiter.

The great red spot of Jupiter is of unknown composition. The opinion is that it floats in the atmosphere and there is no doubt but that it affects the atmospheric flow near it.

Jupiter has 12 satellites. The seven outer ones are subject to enormous perturbations by the Sun. Their plane of orbit is highly inclined to the plane of the equator. The inner five about coincides with Jupiter's equatorial plane. Jupiter VIII, IX, XI, and XII revolve in the retrograde direction. Jupiter V is sometimes called Amalthea.

Name	Distance from center of Jupiter in miles	Sidereal period of rotation	Diameter in miles	Inclination of orbit to Jupiter orbit	Eccentricity	Density water = 1	Albedo
Jupiter V	112,500	11 ^h 57 ^m	100 ?	3° 6'9"	0.0028	---	---
Io	261,000	1 ^d 18 ^h	2200	3° 6'7"	0	2.7	.69
Europa	415,000	3 ^d 13 ^h	1925	3° 5'8"	.0003	2.6	.76
Ganymede	664,000	7 ^d 4 ^h	3490	3° 2'3"	.0015	1.5	.45
Callisto	1,167,000	16 ^d 17 ^h	3350	2° 4'7"	.0075	1.0	.16
Jupiter X	7,200,000	260 ^d 12 ^h	20	---	.08	---	---
Jupiter VI	7,300,000 ±	266 ^d ±	80 ?	29°	.1550	---	---
Jupiter VII	7,500,000 ±	277 ^d ±	25 ?	48°	.2070	---	---
Jupiter XII	13,000,000	625 ^d 0 ^h	14	---	---	---	---
Jupiter XI	14,000,000	692 ^d 12 ^h	18	---	.210	---	---
Jupiter VIII	14,600,000 ±	740 ^d ±	17 ?	148°	.3800	---	---
Jupiter IX	14,900,000 ±	758 ^d ±	15 ?	156°	.2500	---	---



Zones, belts, currents, and rotational times of Jupiter

Saturn

Only known planet with rings around it. The planet is probably coated with ice surrounded by a gaseous mantle of methane.

Its mean distance from Sun is 886,000,000 miles. One year equals 29.46 Earth years. It rotates in 10 hours 14 minutes. Its equatorial diameter is 75,000 miles. Its rotational speed differs at different latitudes as in the case of Jupiter and the Sun. Its temperature is about -150° C. Saturn is more flattened at the poles than Jupiter. Its polar diameter is 67,000 miles compared to 75,000 miles for the equator. Its surface (like Jupiter) is marked by dusky belts with light intermediate zones.

The outstanding feature of Saturn is its rings. These rings are translucent and are composed of tiny, highly reflective solid particles or moonlets. The rings are in the plane of the equator of Saturn and are inclined about 27° to the ecliptic.

Rings of Saturn

	Miles
Radius of outer limit of ring system	86,300
Width of outer ring (called A)	11,100
Width of Cassini's division (1675)	2,200
Width of ring (B)	18,000
Width of Crepe ring (C)	11,000
Distance of inner edge of ring C to surface of Saturn	6,000
Thickness of rings	less than 100 probably 20 to 40

Another feature of Saturn has been the periodic observation of a white spot on its disk. This spot was observed in 1876, 1903, and 1933. The spot has varied in size from about $1/5$ the planet diameter to $2/3$ the planet diameter. The 1933 spot started with an East-West diameter equal to $1/5$ of the planets equatorial diameter. It grew to $2/3$ of the planets equatorial diameter and finally dissolved into a white band $1/2$ the planets equatorial diameter in size. A second spot emerged from the center of the first one and merged into the previously existing bright zone changing it in appearance. The rotational period of $10^h 16^m$ decreased to $10^h 13^m$. There also has been observed a semiregular fluctuation in the reflectivity of Saturn. This fluctuation has a period of 10 years for Saturn.

Saturn has nine satellites. The orbits of the five inner ones are circular and lie in the plane of the planet's equator and rings. Titan and Hyperion also revolve nearly in the plane of the rings but Japetus is inclined about 10° . Phoebe revolves in the retrograde direction in the plane of the orbit of Saturn. Hyperion has an orbital retrograde motion of $18^\circ 40'$ annually.

Satellites of Saturn

Name	Distance from center of Saturn in miles	Sidereal period of revolution	Inclination of orbit to ecliptic	Eccentricity	Diameter miles	Date of discovery
		d h	o ' "			
Mimas	117,000	0 22.6	26 44.7	0.0190	600 ±	1789
Enceladus	157,000	1 8.9	26 44.7	.0001	800 ±	1789
Tethys	186,000	1 21.3	26 44.7	.0000	1200 ±	1684
Dione	238,000	2 17.7	26 44.7	.0020	1100 ±	1684
Rhea	332,000	4 12.4	26 44.9	.0009	1500 ±	1672
Titan	771,000	15 22.7	26 7.1	.0289	3080 ±	1655
Hyperion	934,000	21 6.6	26 0	.1043	500 ±	1848
Japetus	2,225,000	79 7.9	16 18.1	.0284	2000 ±	1671
Phoebe	8,000,000	550 10.6	174.7	.1659	200 ±	1898

Uranus

Uranus was accidentally discovered by Herschel in 1781. Uranus appears as a pale green oblate spheroid. It seems to have bands or belts and streaks across its surface. It has a rotational period of about $10\frac{2}{3}$ hours. The equator is inclined 82° to plane of orbit. Its rotation is retrograde. Its temperature is about -170° C.

Whereas the outer atmospheres of Jupiter and Saturn consist mainly of hydrogen and helium, with methane the next most common element; neon and other inert gases with lower boiling points may be more abundant on Uranus and Neptune.

A semi-regular long period fluctuation in the reflectivity of Uranus of 0.4 years has been observed.

Uranus has five satellites which revolve in same plane as planet's equator. Their motion is retrograde.

Satellites of Uranus

Name	Distance from center of Uranus, miles	Period sidereal	Diameter (approx.) miles
Ariel	120,000	2 ^d 12.5 ^h	500
Umbriel	167,000	4 ^d 3.5 ^h	400
Titania	273,000	8 ^d 17.0 ^h	1000
Oberon	365,000	13 ^d 11.0 ^h	800
Miranda	75,000	1 ^d 10.0 ^h	200

Neptune

Diameter of Neptune (discovered in 1846) is about 28,000 miles. Its period of rotation is about 16 hours. It has a dense atmosphere. A semi-regular fluctuation in the reflectivity of 8.4 yrs. has been observed. Predicted by Adams and Leverrier. Neptune has two satellites which are called Triton and Nereid. Tritons motion is retrograde.

Other characteristics of Triton are:

Diameter - 2,000 miles

Distance from center of Neptune - 222,000 miles

Sidereal period - 5 days, 21 hours

Inclination of orbit to ecliptic - 35°

Discovered in 1846

The characteristics of Nereid are:

Diameter - 200 miles

Distance from center of Neptune - 3,500,000 miles

Sidereal period - $359^{\text{d}} 0^{\text{h}} 0^{\text{m}}$

Pluto

There is nothing much known about Pluto. Its diameter and mass are smaller than that of earth. It has a yellowish appearance. Predicted by Prof. Lowell in 1915. He worked from 1905 to 1915. His prediction was not very accurate, placing the planet in one of two opposite regions of the Zodiac. After Lowell's death in 1916, the planet was finally discovered in 1930 by Tombaugh.

Some claim that the discrepancies of the orbits of Uranus and Neptune cannot be caused by Pluto because of its small mass. Pluto, because of its size, probably belongs in the class of smaller planets or even asteroids.

Having disposed of the general discussion of the solar system and the major elements therein, the remaining part of the notes is devoted to the presentation of numerical data and definitions of terms.

The tables present the numerical data for the Sun, the planets, the satellites of the planets and for some of the asteroids. A particular value presented in the tables is a compilation of values obtained from many sources and therefore may not be exactly consistent with other values in the tables, however, it is believed that the values presented are the best that are available, at least to the knowledge of the author. Values not included or marked with question marks are subject to question, either because they cannot be measured accurately or because the various sources presented widely different values.

Symbols

a	semi-major axis
b	semi-minor axis
c	distance between center of ellipse and foci
d	time in days (sometimes used as superscript)
e	eccentricity
h	time in hours (sometimes used as superscript)
i	inclination of orbit to the ecliptic
L	mean heliocentric longitude
M	mean anomaly of a planet at a specific epoch. (The same angle as θ used in previous lectures.)
m	time in minutes (sometimes used as superscript)
P	sidereal period
s	time in seconds (sometimes used as superscript)
T	time of perihelion passage
yr.	time in years
α	right ascension
δ	declination
π	longitude of perihelion
μ	mean daily motion
ω	argument of the latitude of perihelion
Ω	longitude of ascending node

Definition of Terms Used in Astronomical Literature

1. Sidereal day - The period of one rotation of the Earth relative to the stars.
2. Sidereal month - The interval between two successive arrivals of the moon at a given apparent place among the stars.
3. Sidereal year - The interval between two successive arrivals of the Sun at a given apparent place among the stars.
4. Solar day - The interval between two successive meridian passages of Sun.
5. Synodic month - The time of a revolution of the Moon with respect to the apparent place of the Sun - that is from conjunction to conjunction.
6. Nodical month - The time of the Moon's revolution with respect to either node.
7. Tropical year - The interval between successive arrivals of the Sun at the Vernal equinox.
8. Anomalistic year - The interval between two successive arrivals of the Sun and Earth at the same true anomaly.
9. Sidereal time - The hour angle of the Vernal equinox or the right ascension of the meridian.
10. Solar time - The hour angle of the Sun. It differs from sidereal time by the right ascension of the Sun.
11. Astronomic latitude - The angle between the plane of the equator and the direction of gravity at the location in question.
12. Geocentric latitude - The angle between the plane of the equator and a straight line passing from the location in question to the center

of the earth. It differs from astronomic latitude due to the oblateness of the Earth.

13. Geographic latitude - The angle between the plane of the equator and a normal to the standard spheroid. It differs from astronomic latitude only by the effects of local deviations of the direction of gravity.
14. Geocentric longitude - The arc of the ecliptic, measured Eastward from the Vernal equinox to the apparent position of the Sun as seen from the Earth.
15. Heliocentric longitude - Same definition as Geocentric longitude except that it is as seen from the Sun. It is 180° opposite Geocentric longitude.
16. Geocentric - As seen from or referred to the Earth.
17. Heliocentric - As seen from or referred to the Sun.
18. Conjunction - A time at which either the body is between the Sun and the Earth (inferior conjunction) or when the Sun is between the body and the Earth (superior conjunction).
19. Opposition - A time when the Earth is between the Sun and the body.
20. Synodic period - The time between two successive oppositions or successive superior conjunctions.
21. Transits - An occurrence in which one planet passes directly between another planet and the Sun, thus appearing as a black dot upon the photosphere of the Sun.
22. Equinox - points of intersection of the apparent path of the Sun (the ecliptic) and the Earth's equator.

23. Vernal equinox - The equinox where the Sun crosses from South to North of the equator. (Occurs in the spring.)
24. Line of apsides - A line of infinite length passing through the apes (perihelion and aphelion) and through the foci of the elliptic orbit. The major axis of the ellipse is a segment.
25. Solar parralax - The apparent semi-diameter of the Earth as Sun from the Sun.
26. Nutation - A small oscillation of the Earth's poles of rotation due to the regression of the Moon's nodes.
27. Aberration - The effect of the orbital motion of the Earth upon the apparent direction of the light that comes to us from a star.
28. Albedo - A measure of reflective power. The ratio of light reflected to light received.
29. Diornal motion - The apparent revolution of all the heavenly bodies a around the Earth.
30. Mean Anomaly - The angle the radius vector sweeps through as the planet revolves around the Sun measured from perihelion.
31. Hour angle - The arc of the celestial equator included between the meridian and the star's hour circle. The meridian and hour circle are defined later under Coordinate Systems Used in Astronomy.

Plane ECLI represents the plane of the Earth's orbit (or the ecliptic) and ORBI the plane of the orbit of another planet. The line of intersection, NN' which passes through the sun is the line of nodes. The planet passes from the South to the North side of the ecliptic at the point n, which is the beginning of the ascending node.

The line $S\gamma$ is drawn from the center of the Sun toward the position of the vernal equinox on the celestial sphere. The angle between S and NN' measured toward the ascending node (Eastward) is the longitude of the ascending node Ω . The angle between the two planes is i , the inclination. These two elements (Ω and i) define the position of the orbit plane.

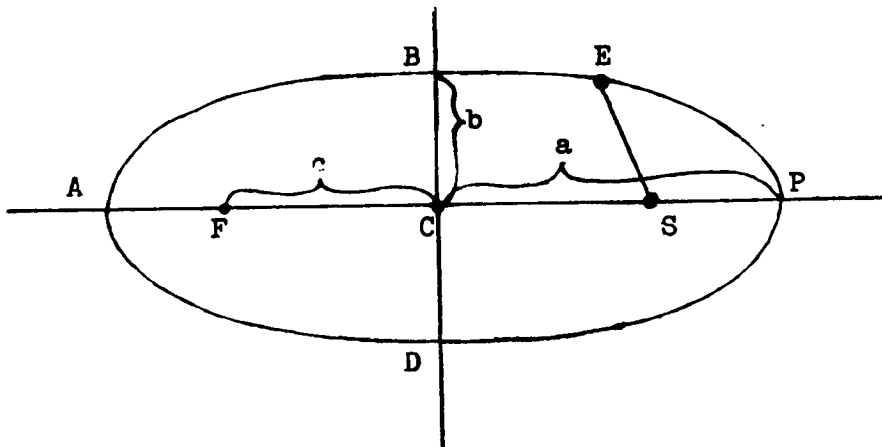
The orientation of the orbit within its plane may be described by the angle ω , measured in the plane of the orbit and in the direction of the body's motion (eastward for planets but westward for many comets) between SN and SP, P being the perihelion. For the principal planets, however, it is customary to substitute for ω , the longitude of perihelion π which is the sum of ω and Ω .

The semi-major axis, a , or mean distance of the planet from the Sun, defines the size of the orbit. It is usually expressed in astronomical units, which is based on the semi-major axis of the Earth's orbit, (92,900,000 miles or 149,500,000 kilometers).

The eccentricity, e , defines the shape of the orbit. It is the ratio of c over a , c being the distance of the foci or Sun from the center of the orbit and a being the semi-major axis.

To determine the position of the planet at any time we must know the position at a specific time (at Epoch) and the time of revolution P , or the mean daily motion, μ , which is simply 360° divided by the number of days in P .

Elements of an Elliptic Orbit



F and S are Foci.

AP is the longest diameter and is called the major axis.

BD is the shortest diameter and is called the minor axis.

a denotes the semi-major axis.

b denotes the semi-minor axis.

c denotes the distance from the center C to the foci F or S.

The eccentricity is ϵ and equals $\frac{c}{a}$ and is never greater than 1.

The smaller the eccentricity the more nearly circular the ellipse.

If S is the foci about which the planet is revolving then P is called the perihelion and A is called the aphelion. The line SE is called the radius vector and the angle PSE is called the true anomaly.

Table 14-1

	Symbol	Equatorial diameter miles	Equatorial dia. compared to Earth	Mass $\odot = 1.0$	Mass $\oplus = 1.0$	Volume $\oplus = 1$	Density water = 1	Density $\oplus = 1$	Density gm/cm ³
Sun	\odot	864,000	109.3	1.000	333,434	1,306,000	1.4	.255	1.41
Moon	\circlearrowleft	2,160	.273	1/27,100,000	1/61.27	.0203	---	.607	3.34
Mercury	☿	3,100	.39	1/7,500,000	.037	.055	3.73	.76 ?	4.1 ?
Venus	♀	7,575	.973	1/408,000	.826	.910	5.21	.90	4.9
Earth	\oplus	7,927	1.000	1/333,420	1.000	1.000	5.53	1.00	5.52
Mars	♂	4,215	.532	1/3,093,500	.108	.150	3.95	.70	3.85
Ceres	♁	478	.060	4×10^{-10} ?	1/8,000 ?	.0002	---	.6 ?	3.3 ?
Eros	♁	12.5 ?	1.6×10^{-3} ?	10^{-4} ?	2×10^{-9} ?	4×10^{-9} ?	---	.5 ?	2.8 ?
Jupiter	♃	88,700	10.97	1/1047.4	318.40	1312	1.34	.241	1.33
Saturn	♄	75,060	9.03	1/3499	95.20	763	.69	.13	.71
Uranus	♅	32,900	4.00	1/22,870	14.60	64	1.22	.24	1.26
Neptune	♆	30,900	3.90	1/19,310	16.90	60	1.30	.29	1.61
Pluto	♇	7,890 ?	1.0 ?	1/360,000	.93	1.0 ?	---	1.0 ?	5.5 ?

550

Table 14-1 Continued

	Distance from sun (mean) astro units	Distance from sun (mean) 10^6 mi	Distance from sun (max) 10^6 mi	Distance from sun (min) 10^6 mi	Distance from earth (max) 10^6 mi	Distance from earth (min) 10^6 mi	Surface gravity earth = 1	Escape velocity mi/sec	Escape velocity km/sec
Sun	---	---	---	---	94.452	91.342	27.91	384.3	618
Moon	---	---	---	---	.253	.222	.165	1.49	2.4
Mercury	.387099	36.0	43.355	28.566	136.0	50.0	.29 ?	1.99	3.8
Venus	.723331	67.2	67.653	66.738	161.0	25.0	.86	6.51	10.2
Earth	1.00000	92.9	94.452	91.342	---	---	1.00	6.95	11.2
Mars	1.523688	141.5	154.760	128.330	248.0	35.0	.37	3.22	5.0
Ceres	---	---	---	---	---	---	.04 ?	.31 ?	.5 ?
Eros	---	---	---	1.13 A.U.	---	14.0	.001 ?	.006 ?	.01 ?
Jupiter	5.20	483.3	506.710	459.940	600	367	2.64	38.04	60
Saturn	9.536843	886.1	935.570	836.700	1028	744	1.17	23.53	36
Uranus	19.190978	1782.8	1866.800	1698.800	1960	1606	.91	14.40	21
Neptune	30.070672	2793.5	2817.400	2769.600	2910	2677	1.12	12.95	23
Pluto	39.600	3680.0	4600.00	2760.00	4700	2670	1.0 ?	6.82 ?	11 ?

14-37b

Table 14-1 Continued

	Oblateness	Intensity of solar radiation received Earth = 1	Reflective power (albedo) percent	Ave. probable temp. at top of atmosphere ° C.	Inclination of equator to orbit	Semi-major axis of orbit $\oplus = 1$	Eccentricity of orbit (e)	Inclination of orbit to ecliptic (i)	Annual sidereal motion of perihelion $\Delta\lambda$
Sun	0	---	---	6,000	7° 10' 15"	---	---	0 0 "	"
Moon	.0004	---	7.0	---	6° 40' 17"	---	.0549	5-8-33	---
Mercury	0	6.7	7.0	---	Near zero	.387099	.2056261	7-0-14.2	5.7
Venus	0	1.9	59.0	-44	0° 0'	.723331	.0067930	3-23-39.2	00.3
Earth	.0034	1.0	44.0	-27	23° 26' 59"	1.0000	.0167268	---	11.6
Mars	1/192	.43	15.0	-56	25° 12'	1.523688	.0933663	1-50-59.8	15.9
Ceres	---	---	6.0	---	---	2.767303	.07653	10-36-56	---
Eros	---	---	---	---	34°	1.458296	.22297	10-49-40	---
Jupiter	.06	.04	50	-171	3° 6' 19"	5.202803	.04837	1-18-19.7	7.7
Saturn	.11	.01	63	-197	26° 44' 17"	9.538843	.05582	2-29-24	20.2
Uranus	.09	.003	63	-224	98°	19.190978	.04710	0-46-22.9	8.0
Neptune	1/45	.001	73	-231	29°	30.070672	.00855	1-46-26.1	-18.9
Pluto	---	.0006	3	---	---	39.51774	.24684	17-8-38.4	0.0

14-37c

522 ^

Table 14-1 Continued Epoch of Jan. 0, 1920 GMT

	Annual sidereal motion of ascending node $\Delta\Omega$	Sidereal period in days	Mean daily motion μ	Synodal period days	Orbital velocity (average) mi/sec	Axial rotational period	Longitude of		
							ascending node Ω	perihelion π	planet at epoch
	"	days	o' " "	days	mi/sec	d h m s	o' " "	o' " "	o' " "
Sun	---	---	---	---	12.5	25-9-7-12	---	---	---
Moon	---	27.3	---	29.53	---	27-7-43-11.5	---	---	---
Mercury	-7.6	87.96925	4-5-32.42	116	29.73	87-23-15-48	47-22-59	76-12-39	192-59-36
Venus	-17.8	224.70080	1-36-7.67	584	21.75	20-30 or 224-16-49-9	75-57-35	130-26-44	166-36-34
Earth	---	365.25636	0-59-8.2	---	18.50	h m s 23-56-4	---	101-33-53	99-51-02
Mars	-22.6	686.9797	0-31-16.5	760	14.98	24-37-23	48-56-25	334-35-12	162-05-15
Ceres	---	1681.449	---	---	11.12	---	80-45-29	149-26-12	223-19-21
Eros	---	643.230	---	---	15.33	---	303-35-09	121-25-32	28-36-33
Jupiter	-13.9	4332.588	0-4-59.1	399	8.11	9-55-41	99-38-24	13-02-01	125-18-37
Saturn	-18.9	10759.20	0-2-0.5	378	5.99	10-14-24	112-57-24	91-28-50	151-16-01
Uranus	-31.9	30685.93	0-0-42.2	370	4.22	10-8----	73-35-27	169-22-07	329-20-35
Neptune	-10.7	60191.71	0-0-21.5	367	3.40	15-40----	130-53-56	43-55-50	128-59-54
Pluto	0.0	90740.0	0-0-14.3	367	3.00	---	108-57-16	222-28-34	121-24-14

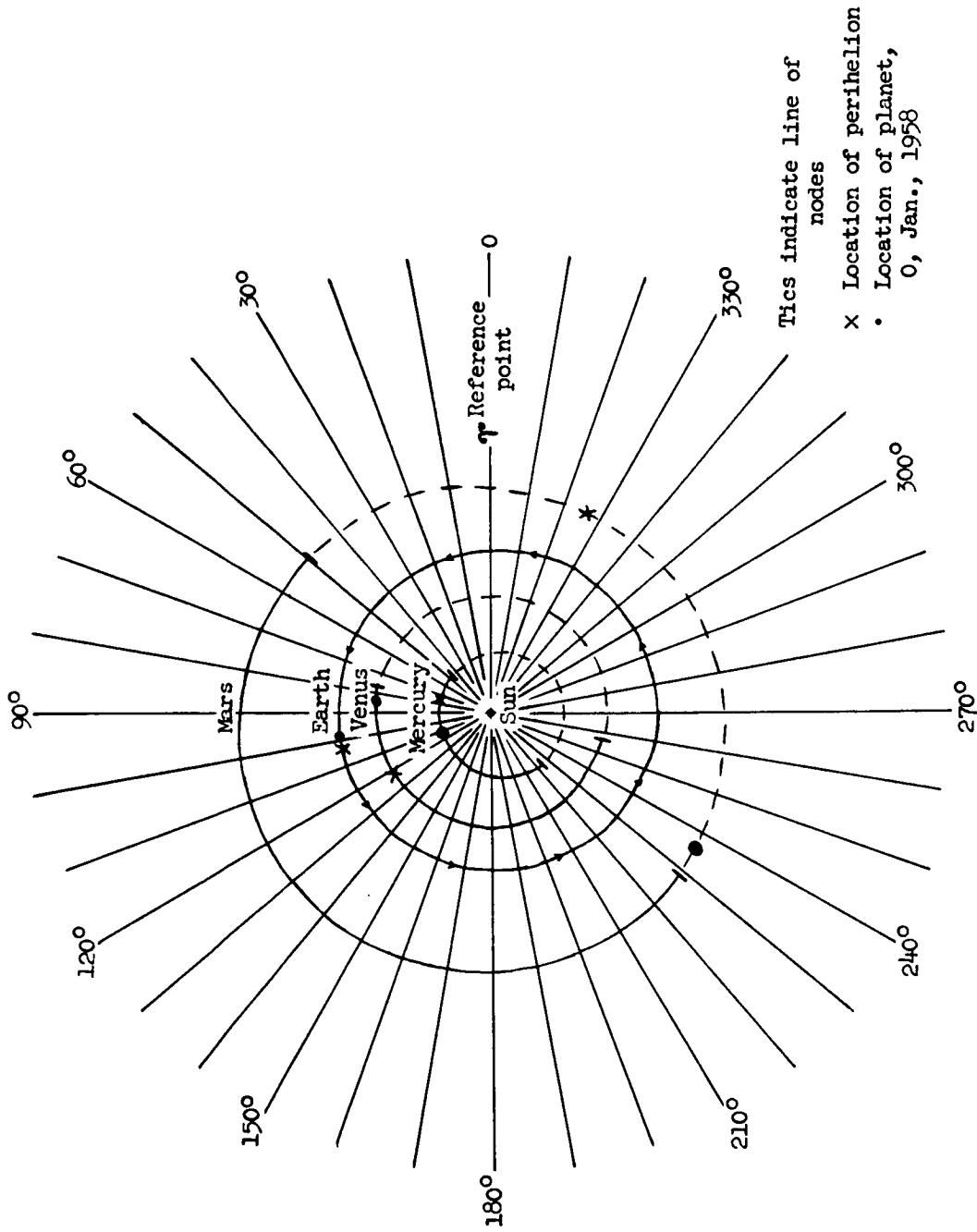
14-37a

57
(2)
62
A

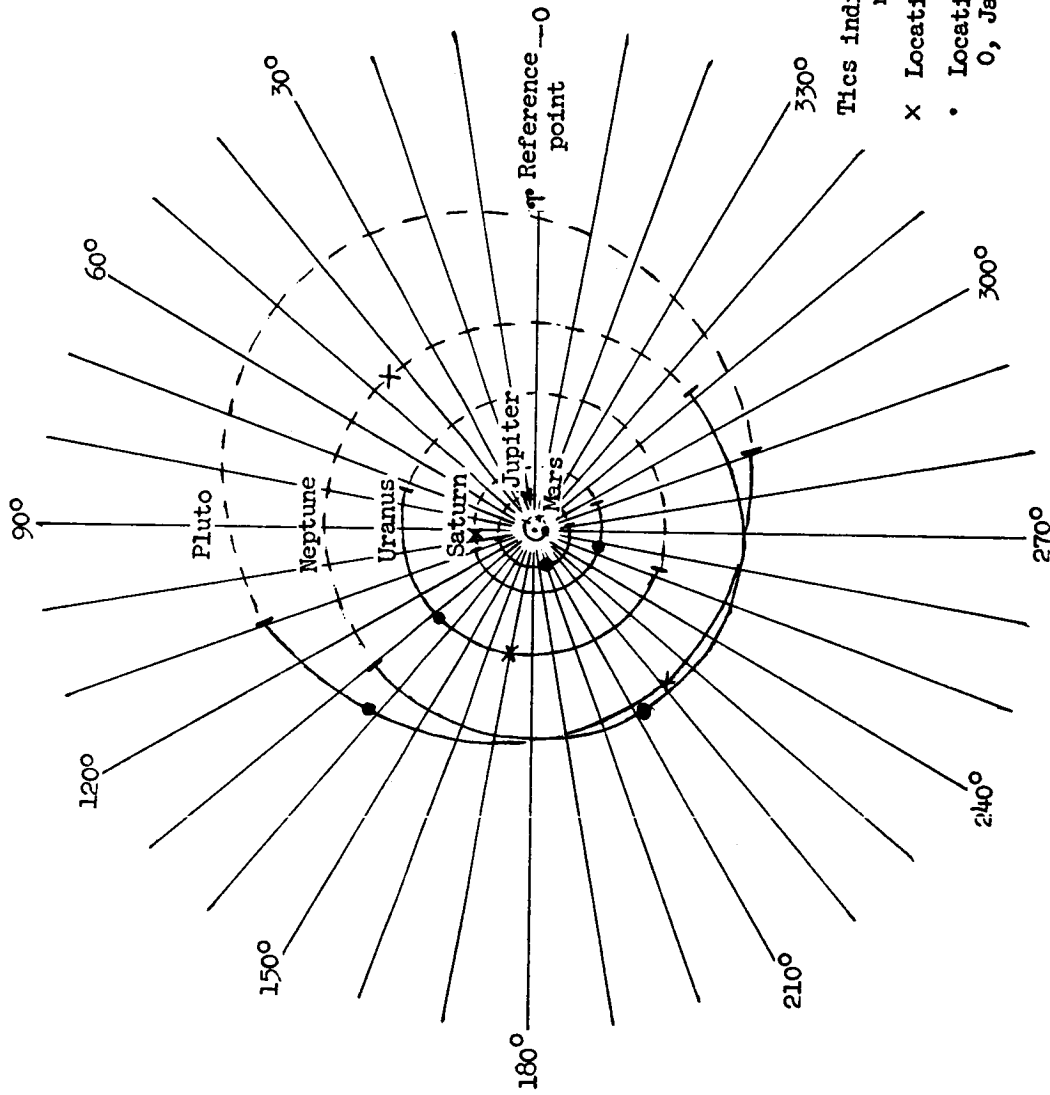
Table 14-1 Concluded

	Epoch of Jan. 0, 1925 GMT			Epoch of Jan. 0, 1935 GMT			Epoch of Jan. 0, 1958 GMT		
	Longitude of ascending node Ω	Longitude of perihelion π	Longitude of planet at epoch	Longitude of ascending node Ω	Longitude of perihelion π	Longitude of planet at epoch	Longitude of ascending node Ω	Longitude of perihelion π	Longitude of planet at epoch
Sun	---	---	---	---	---	---	---	---	---
Moon	---	---	---	---	---	---	---	---	---
Mercury	47-26-32.1	76-17-18.9	105-40-25.3	47-42----	76-24----	291-----	47-50-.3	76-48-7.1	111-5-38.6
Venus	76-0-16.7	130-30-56.8	212-10-10.23	76-06----	130-42----	303-18----	76-18-6.1	130-58-48.5	83-6-32.3
Earth	---	101-39-2.3	99-38-33.1	---	101-48----	99-12----	---	102-13-5.1	99-38-59.8
Mars	48-58-45	334-40-42.2	39-2-29.19	49-06----	334-54----	152-54----	49-14-1.0	335-17-9.1	235-40-16.6
Ceres	---	---	---	---	---	---	---	---	---
Eros	---	---	---	---	---	---	---	---	---
Jupiter	99-41-26.3	13-6-51.4	277-6-16.69	99-48----	13-18----	220-42----	100-1-27.1	13-38-45.5	199-3-48.7
Saturn	113-0-5.7	91-34-42	212-26-2.9	113-06----	91-48----	334-48----	113-17-24	92-13-30.9	256-11-3.84
Uranus	73-36-57.7	169-26-56.8	350-50-7.04	73-42----	169-36----	33-48----	73-47-9.8	169-58-42.3	132-42-3.2
Neptune	130-57-13.3	43-58-27.9	139-59-22.7	131-06----	44-06----	162-0----	131-19-3.8	44-15-23.3	212-32-26.3
Pluto	---	---	---	109-24----	223-18----	143-36----	109-38-.2	223-10-30.2	137-38-8.0

534



Orbits and planet positions as of
Jan. 0, 1958 GMT



Tics indicate line of nodes
 x Location of perihelion
 • Location of planet, 0, Jan., 1958

14-38b

Orbits and planet positions as of Jan. 0, 1958 GMT

Table 14-2
PHYSICAL DATA OF THE NATURAL SATELLITES

Name	Discovery	Mean dist. in equatorial radii of planet	Mean distance		Sidereal period	Inclination of orbit to plane of nodal regression	Mean inclination of proper plane (or orbit) to planets orbit	Eccentricity	Dia. (Km)	Mass	
			Km	Mile						Primary = 1	Moon = 1
Satellites of EARTH											
Moon	---	60.267	384,403	238,857	27 ^d 7 ^h 43 ^m 11.5 ^s	28°35' to 18°19' †	5°0'33"	.05490	3476	.01227	1.000
Satellites of MARS											
Phobos	Hall 1877	2.79	9,350	5,815	0 ^d 7 ^h 39 ^m 13.9 ^s	1° 48'	25° 11'	.021	15 †	---	---
Deimos	Hall 1877	6.93	23,500	14,600	1 ^d 0 ^h 17 ^m 55 ^s	1° 46'	24° 16'	.003	8 †	---	---
Satellites of JUPITER											
No name	Barnard 1892	2.540	181,500	112,800	0 ^d 11 ^h 57 ^m 22.7 ^s	0° 27.3'	3° 6.9'	.0028	150 †	3.8 x 10 ⁻⁵	.99
Io	Gallileo 1610	5.905	422,000	262,200	1 18 27 33.5	0 1.6	3 6.7	.0000	3750	2.48 x 10 ⁻⁵	.64
Europa	Gallileo 1610	9.401	671,400	417,200	3 13 13 42.1	0 28.1	3 5.8	.0003	3150	8.17 x 10 ⁻⁵	2.11
Ganymede	Gallileo 1610	14.995	1,071,000	665,500	7 3 42 33.4	0 11.0	3 2.3	.0015	5150	5.09 x 10 ⁻⁵	1.32
Callisto	Gallileo 1610	26.379	1,884,000	1,170,600	16 16 32 11.2	0 15.2	2 42.7	.0075	5180	---	---
No name	Perrine 1904	161.000	11,500,000	7,120,000	250 ^d 7	181 †	(28° 45')	.155	120 †	---	---
No name	Perrine 1905	165.000	11,750,000	7,300,000	260.0	243 †	(27° 58')	.207	50 †	---	---
No name	Micholson 1938	165.000	11,750,000	7,300,000	260.0	82 †	(28°)	.08	20 †	---	---
No name	Malotte 1908	330.000	23,500,000	14,600,000	759	208 †	(148°1)	.378	50 †	---	---
No name	Micholson 1914	332.000	23,700,000	14,700,000	758	61 †	(157°)	.270	22 †	---	---
No name	Micholson 1938	315.000	22,500,000	14,000,000	692	232 †	(163°)	.210	25 †	---	---
No name	† †	---	---	13,000,000	625	---	---	---	14 †	---	---

502A

Table 14-2 Concluded

PHYSICAL DATA OF THE NATURAL SATELLITES

Name	Discovery	Mean dist. in equatorial radii of planet	Mean distance		Sidereal period	Inclination of orbit to plane of nodal regression	Mean inclination of proper plane (or orbit) to planets orbit	Eccentricity	Dia. (km)	Mass	
			Km	Mile						Primary = 1	Moon = 1
Satellites of SATURN											
Mimas	Herschel 1789	3.11	185,700	115,400	0 ^d 22 ^h 37 ^m 5.25 ^s	1° 31'	26° 44.7'	.0201	450 †	6.68 × 10 ⁻⁸	5.16 × 10 ⁻⁴
Enceladus	Herschel 1789	3.99	238,200	148,000	1 8 53 6.82	0 1.4	26 44.7	.0044	500 †	1.5 × 10 ⁻⁷	1.17 × 10 ⁻³
Tethys	Cassini 1684	4.94	294,800	183,200	1 21 18 26.1	1 5.6	26 44.7	.0000	1100 †	1.14 × 10 ⁻⁶	8.8 × 10 ⁻³
Dione	Cassini 1684	6.33	377,700	234,700	2 17 41 9.5	0 0	26 44.7	.0022	1100 †	1.85 × 10 ⁻⁶	.014
Rhea	Cassini 1672	8.84	527,500	327,800	4 12 25 12	0 20.5	26 41.9	.0010	1600 †	4 × 10 ⁻⁶ †	.05 †
Titan	Huygens 1655	20.48	1,223,000	759,900	15 22 41 24	0 18.3	26 7.1	.0289	4200 †	2.48 × 10 ⁻⁴	1.92
Hyperion	Bond 1848	24.82	1,484,000	922,000	21 6 38 24	17° to 56'	26° 0'0	.1043	400 †	< 8 × 10 ⁻⁸	< 6 × 10 ⁻⁴
Iapetus	Cassini 1671	59.68	3,563,000	2,213,000	79 7 55 32	13° 51:8	16° 18'1	.0283	1300 †	2.5 × 10 ⁻⁶	.019
Phoebe	Pickering 1899	216.8	12,950,000	8,044,000	550 ^d 44	14899 †	(174.97)	.1660	300 †	---	---
Satellites of URANUS											
Ariel	Lassell 1851	7.35	191,800	119,200	2 ^d 12 ^h 29 ^m 21 ^s	0°	97° 59'	.007	500 †	---	---
Umbriel	Lassell 1851	10.20	287,300	166,100	4 3 27 37	0	97 59	.008	400 †	---	---
Titania	Herschell 1787	16.80	438,700	272,600	8 16 56 27	0 0'	97 59	.023	1000 †	---	---
Oberon	Herschell 1787	22.40	586,600	364,500	13 11 7 04	0 0	97 59	.010	900 †	---	---
Miranda	---	---	---	75,000	1 10 0 0	---	---	---	333 †	---	---
Satellites of NEPTUNE											
Triton	Lassell 1846	14.2	354,000	220,000	5 ^d 21 ^h 23 ^m 59 ^s	160° †	140° (1900)	.000	4500 †	1.3 × 10 ⁻⁵	1.8
Nereid	---	---	---	3,900,000	359 ^d 0 ^h 0 ^m	---	---	---	333 †	---	---

† - To planets equator

‡ - Longitude of ascending node

For most of the satellites the orbit plane is inclined at substantially a fixed angle to a "proper plane" on which the nodes regress. In these cases the inclinations of the orbit plane to this plane, and of this plane to that of the planet's orbit, are given in the 7th and 8th columns. For the moon, the six outer satellites of Jupiter, Phoebe and the satellite of Neptune the 8th column gives the inclination of the orbit plane to the planet's orbit, at the given date, while the 7th column is used to give other data as indicated by the footnotes.

57
63
88
A

Table 14-3
 AN INDEX TO THE ABILITY OF SOME OF THE SATELLITES AND PLANETS TO
 RETAIN AN ATMOSPHERE

Order	Name	Mass $\oplus = 1$	Radius $\oplus = 1$	Mean density $\oplus = 1$	Mean distance from sun $\oplus = 1$	Albedo	Escape velocity (Km/sec)	Order of ability to retain atmosphere
1	Jupiter	316.35	10.97	.241	5.203	.44	61.0	92.0
2	Saturn	95.30	9.03	.130	9.539	.42	36.7	64.0
3.	Neptune	17.26	3.50	.400	30.070	.49	25.1	59.0
4.	Uranus	14.58	4.00	.230	19.19	.45	21.6	45.0
5	Earth	1.00	1.00	1.000	1.00	.29	11.3	11.3
6	Venus	.814	.967	.900	.723	.73	10.4	9.6
7	Pluto	< .10	.460	< 1.000	39.52	.17	< 5.3	< 13.0
8	Triton*	.022	.350 ?	.51 ?	30.07	.28 ?	2.8 ?	6.6 ?
9	Mars	.108	.532	.70	1.524	.15	5.1	5.7
10	Titan*	.0235	.373	.45	9.539	.28	2.8	5.0
11	J III*	.0260	.391	.44	5.203	.35	2.9	4.4
12	J I*	.0121	.264	.66	5.203	.53	2.4	3.7
13	J IV*	.0160	.360	.34	5.203	.14	2.4	3.6
14	Mercury	.0543	.390	.92	.387	.063	4.2	3.3
	J II*	.0079	.236	.60	5.203	.55	2.1	3.1

Table 14-3 Concluded

Order	Name	Mass $\oplus = 1$	Radius $\oplus = 1$	Mean density $\oplus = 1$	Mean distance from sun $\oplus = 1$	Albedo	Escape velocity (Km/sec)	Order of ability to retain atmosphere
16	Moon*	.0123	.273	.607	1.000	.07	2.4	2.4

* Satellite

This table based on size, escape velocity, and mean molecular velocity of various elements. Represents only a rough index.

Table 14-4

SOME DETAILS OF THE ATMOSPHERES
OF THE PLANETS

	Most important probable atmospheric constituents in order of abundance	Probable value of adiabatic lapse rate ($^{\circ}$ C. Km $^{-1}$)	Approximate pressure at "visible" surface (mb)	Approximate Temperature at visible surface in sunlight ($^{\circ}$ C.)
Venus	N ₂ ?, CO ₂	10.0*	> 160	50-100
Earth	N ₂ , O ₂ , H ₂ O, A, CO ₂	9.6	1000	10
Mars	N ₂ , ? A ?, CO ₂ , H ₂ O	3.7 †	50-100	0
Jupiter	H ₂ , He, CH ₄ , NH ₃	4.4 †	> 50 †	- 120
Saturn	H ₂ , He, CH ₄ , NH ₃	2.0 †	> 50 †	- 150
Uranus	H ₂ , He, CH ₄	1.5 †	>170 †	----
Neptune	H ₂ , He, CH ₄	1.9 †	>350 †	----

* For a pure CO₂ atmosphere; in a predominately N₂ atmosphere the value is 8.0.

† For a predominately N₂ atmosphere.

‡ Assuming a mixture of six molecules of H₂ to one of CH₄. In such a mixture the amount of He affects neither the adiabatic lapse rate nor the molecular weight.

Dimensions of the Terrestrial Spheroid

(From Hayford's Spheroid of 1909)

Equatorial radius $a = 6378.388 \text{ Km} = 3963.34 \text{ mi}$ Polar radius $b = 6356.909 \text{ Km} = 3949.99 \text{ mi}$ Mean semidiameter, $1/3 (2a + b) = 6.37123 \times 10^8 \text{ cm} = 6371.23 \text{ km}$
 $= 3958.89 \text{ mi}$ Oblateness $a-b/a = 1/297$ 1° latitude, φ . (in statute miles) $= 69.0569 - .3494 \cos 2\varphi + .0007 \cos 4\varphi$ 1° longitude (in statute miles) $= 69.2316 \cos \varphi - .0584 \cos 3\varphi + .0001 \cos 5\varphi$ The distance of the sea horizon in miles is equal to the square root of $3/2$ of the observer's height in feet.

The dip of the horizon in minutes of arc is equal to the square root of the observer's height in feet.

Astronomical Constants

Length of day:

Sidereal = $23^{\text{h}} 56^{\text{m}} 4^{\text{s}}.091$ of mean solar time.Mean solar = $24^{\text{h}} 3^{\text{m}} 56^{\text{s}}.555$ of sidereal time.

Length of year (in mean solar units), 1900 - Newcomb

Tropical = $365^{\text{d}} 24219879 = 365^{\text{d}} 5^{\text{h}} 48^{\text{m}} 45^{\text{s}}.98$ Sidereal = $365^{\text{d}} 25636042 = 365^{\text{d}} 6^{\text{h}} 9^{\text{m}} 9^{\text{s}}.54 = 3.1558 \times 10^7 \text{ sec}$ Anomalistic = $365^{\text{d}} 2564134 = 365^{\text{d}} 6^{\text{h}} 13^{\text{m}} 53^{\text{s}}.01$

Length of month (in mean solar units) (according to Brown)

Synodical = $29^{\text{d}} 530588 = 29^{\text{d}} 12^{\text{h}} 44^{\text{m}} 2^{\text{s}}.8$ Sidereal = $27^{\text{d}} 321661 = 27^{\text{d}} 7^{\text{h}} 43^{\text{m}} 11^{\text{s}}.5$ Nodical = $27^{\text{d}} 212220 = 27^{\text{d}} 5^{\text{h}} 5^{\text{m}} 35^{\text{s}}.8$

Obliquity of the ecliptic = $23^{\circ} 27' 8''.26 - 0''.4684 (t - 1900)$ } Newcomb
 General precession = $50''.2564 + ''000222 (t - 1900)$

Constant of nutation = $9''.21$ }
 Constant of aberration = $20''.47$ } Adopted for Ephemeris purposes
 Solar parallax = $8''.80$ } Paris conference, 1911

Velocity of light = $299,776 \text{ km/sec} = 186,273 \text{ mi/sec}$ (Birge 1941)

Constant of gravitation, $G = (6.670 \pm .005) \times 10^{-8}$ C.G.S. units (Birge 1941)

Acceleration of gravity, g , (in meters) = $9.8060 - .0260 \cos 2\phi - 2h/R g$
 (from Helment), in which h is the elevation above sea level in meters
 and $\log R = 6.80416$.

Earth's weight = $(5.975 \pm .004) \times 10^{27}$ grams = 6.59×10^{21} short tons

Sun's weight = 1.992×10^{33} grams

Sun's mean radius = 6.965×10^{10} cm

One astronomical unit (A.U.) = 1.4968×10^8 km = 9.3×10^7 mi

One light year = 6.322×10^4 A.U. = 9.460×10^{12} km = 5.88×10^{12} mi

One parsec = 3.263 light years = 2.06265×10^5 A.U. = 3.087×10^{13} km
 = 1.92×10^{13} mi

Kepler's Laws of Planetary Motion

1. Each planet moves in an ellipse which has the Sun at one of its foci.
2. The radius vector of each planet passes over equal areas in equal intervals of time (law of areas).
3. The cubes of the mean distance of any two planets from the Sun are to each other as the squares of their periodic times or $a_1^3:a_2^3::P_1^2:P_2^2$.

Bode's Law

The approximate mean distance of the planets from the Sun may be conveniently remembered by a relation first pointed out by Titus but now commonly known as Bode's law. If we write a series of 4's and add to them the number 0; $3 \times 1 = 3$; $3 \times 2 = 6$; $6 \times 2 = 12$; $12 \times 2 = 24$; etc. thus

4	4	4	4	4	4	4	4	4
<u>0</u>	<u>3</u>	<u>6</u>	<u>12</u>	<u>24</u>	<u>48</u>	<u>96</u>	<u>192</u>	<u>384</u>
4	7	10	16	28	52	100	196	388
Mercury	Venus	Earth	Mars	Asteroids	Jupiter	Saturn	Uranus	Neptune

we get a series of numbers that are approximately ten times the mean distances of the planets in astronomical units. There is no known reason why this maneuver works.

Units

Astronomical units are usually used in talking about distances in the solar system. For distances greater than those of our solar system the astronomical unit is too small since it is based on the semidiameter of the earth's orbit.

The English have invented a new unit called a parsec. The parsec is based on the distance a star is from the Earth that has a parallax of 1". The distance of a star whose parallax is P seconds is then simply $1/P$ parsecs.

Approximate Equivalents

	Light yrs.	Parsecs	Ast. units	Millions of mi.	Centi- meters
One light yr.	1.00	0.32	63,000	6	10^{18}
One parsec	3.26	1.00	206,265	20	3.10^{18}
Distance of proxima	4.20	1.28	264,400	25	4.10^{18}

Proxima is the nearest star to us.

Coordinates System Used in Astronomy

In astronomy the sky is considered a celestial sphere with the earth at the center. The apparent position of the stars is described by locating its projection upon the celestial sphere. There are four coordinate systems used to locate the objects on the celestial sphere and they all have common elements.

1. Fundamental circle - great circle of the sphere. Poles are located 90° to this circle.
2. Secondary great circle - these circles pass through poles (correspond to circles of longitude on Earth).
3. Parallels - smaller circles parallel to fundamental circles.

The four systems are as follows:

Horizon System

1. Fundamental circle - it is the horizon. The poles are called the zenith (overhead) and Nadir. Their position is defined by the direction of gravity.
2. Secondary circles - they are called Vertical circles. The vertical circle going through north and south is called the meridian and the one going through east and west is called the prime vertical.
3. Parallels - Almucanters. Coordinates of a star are azimuth and altitude. Azimuth is the arc of the horizon measured in the clockwise direction from the south point to point of the star's vertical circle. It is expressed in degrees (0° to 360°). Altitude of a star is the arc of a vertical circle included between the star and the horizon in degrees. The complementary angle of the altitude is the zenith distance.

Equator System

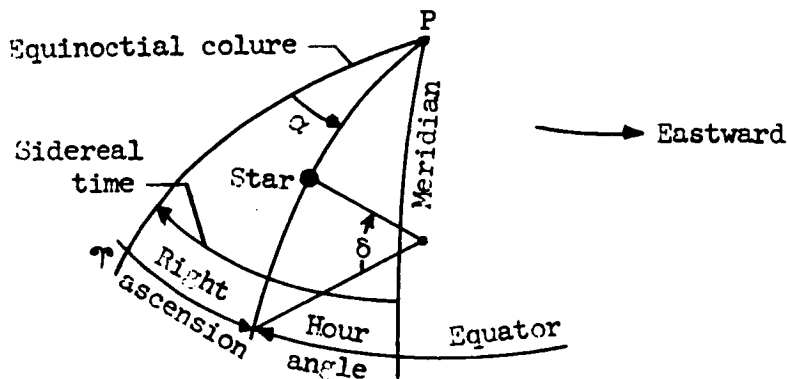
1. Fundamental circle - it is called the celestial equator. Poles are points in the sky which have no diurnal motion. These are points where the earth's axis intersect the celestial sphere.
2. Secondary circle - hour circle.
3. Parallels - Parallels of declination.

The declination of a star is the arc of an hour circle included between the star and the celestial equator. Reckoned in degrees, + if above equator. Symbol is δ .

The hour angle is the arc of the celestial equator included between the meridian and the star's hour circle. It is usually measured westward and is expressed in hours. It is measured from the observer's meridian.

Right ascension of a star is the arc of the celestial equator included between the vernal equinox and the star's hour circle. It is reckoned eastward from vernal equinox and is expressed in hours. Its symbol is α .

One complete revolution of the celestial sphere is called a sidereal day. It is about 4 minutes shorter than solar day. Sidereal noon occurs when the vernal equinox is on the meridian. Sidereal time at any moment is the hour angle of the vernal equinox or right ascension of the meridian.



$$\text{Star hour angle} = \text{sidereal time} - \text{right ascension}$$

Ecliptic System

1. Fundamental circle - path of sun among the stars is called the ecliptic. Angle at which it intersects equator ($23\frac{1}{2}^{\circ}$) is the obliquity and the points of intersection of the equinox. 90° to the equinox is the solstice. Hour circle that passes through the equinoxes and solstices are known as the equinoctical and solstitial colures.
2. Secondary circles - they are called secondaries to the ecliptic. They are great circles passing through the north and south poles.
3. Parallels - they are called parallels to latitude. They are smaller circles parallel to the ecliptic.

Celestial longitude of a star is the arc of the ecliptic measured eastward from the vernal equinox to the secondary circle that passes through the star. Celestial latitude is the arc of the secondary between the star and the ecliptic. It is + if the star lies north of the ecliptic.

Galactic System

1. Fundamental circle - Galactic circle. It is the centerline of the milky way. It is inclined 62° to celestial equator. North pole is at right ascension $12^{\text{h}} 44^{\text{m}}$ and declination $+ 27^{\circ}$.
2. Secondary circles - secondaries to galactic circle. Same as secondaries to the ecliptic.
3. Parallels - parallels of galactic latitude. Same as parallels of latitude in the ecliptic system.

Galactic longitude is reckoned from the intersection of the galactic circle with the celestial equator at $\alpha = 18^{\text{h}} 44^{\text{m}}$. Galactic latitude and longitude are related to the galactic circle exactly as celestial latitude and longitude are related to the ecliptic.

General Remarks on Coordinate Systems

The horizon system moves with the observer. The equator system is based on the earth's rotation about its axis. It is the same for everybody on earth. The ecliptic system is based on earth's revolution around the sun (earth's orbit). This system is also the same for everybody on earth. The galactic system is based on structure of visible universe of stars. It would hold for all planets of our solar system and nearby neighboring stars.

Comparison of Systems of Coordinates

System	Geographic	Horizon	Equator	Ecliptic	Galactic
Basis	Rotation of earth	Direction of gravity	Diurnal motion of celestial sphere	Orbital motion of earth	Structure of visible universe
Fundamental circle	Terrestrial equator	True horizon	Celestial equator	Ecliptic	Center line of milky way
Poles	Terrestrial poles	Zenith and Nadir	Axis of rotation	Poles of ecliptic	Poles of galaxy
Secondary great circles	Meridians	Vertical circles	Hour circles	Secondaries to ecliptic	Secondaries to galactic circle
Parallels	Parallels of latitude	Almucantors	Parallels of declination	Parallels of latitude	Parallels of galactic latitude
Coordinates	Latitude, ϕ Longitude, λ	Altitude Azimuth	Declination, δ Right ascension, α or hour angle	Latitude, β Longitude, λ	Galactic latitude Galactic longitude
Origin of second coordinate	Meridian of Greenwich	South point of horizon	Vernal equinox, meridian	Vernal equinox	Intersection of galactic circle and equator
Circles fixed with respect to	Surface of Earth	The observer	The stars	The stars	The stars

REFERENCES

1. Rice, F. O.: The Chemistry of Jupiter. Scientific American. V. 194, no. 6, pp 119-120, 122, 124, 126. June 1956.
2. Slipher, E. C., Hess, Seymour L., Blackodar, Alfred K., Gidos, H. L., Shapiro, R., Lorenz, E. N., Gifford, F. A., Mintz, Y., and Johnson, H. L. The Study of Planetary Atmospheres. (Final Rept.) (Sponsored by Air Force Cambridge Research Center). Lowell Observatory. September 30, 1952.
3. Menzel, D. H.: Harvard College Observatory. Exploring Our Neighbor World, The Moon. The National Geographic Magazine. Page 277-296. February 1958.
4. Slipher, E. C.: New Light on the Changing Face of Mars. The National Geographic Magazine. Pp 427-436. September 1955.
5. Bowen, I. S.: Sky Survey Charts the Universe. The National Geographic Magazine. Pp. 780-790. December 1956.
6. Duncan, J. C.: Astronomy. Harper and Brothers Publishers.
7. Astronomy - I - The Solar System. Russell, Dugan, and Stewart. Ginn and Co.
8. Some Aspects of the Meteorology of Mars. Journal of Meteorology. 7: 1-13 (1950)
9. Compendium of Meteorology, American Meteorology Society, 1951. p 391-397.
10. Reports on Progress in Physics. Vol XIII. 1950. Planetary and Satellite Atmospheres. p. 249. G. P. Kuiper.
11. The Atmosphere of Venus. S. H. Dole. The Rand Corporation. October 12, 1956.
12. Encyclopedia Britannica.
13. Interim Report on Search for Small Earth Satellites for Period 1953-1956. C. W. Tombaugh, Physical Science Laboratory, State College, New Mexico.
14. The Atmospheres of the Earth and Planets. Revised Edition, KT The University of Chicago Press, Chicago Ill. Edited by G. P. Kuiper.
15. The American Ephemeris and Nautical Almanac, 1958.

APPENDIX

THE EARTH'S ATMOSPHERE

By

W. J. O'Sullivan, Jr. and J. L. Mitchell

Up until about 1946 the atmosphere had been explored in detail - pressure, temperature, density, and composition - at altitude up to a maximum of about 150,000 feet by means of sounding balloon, i.e., radiosonde techniques. On the basis of an average of these measurements the International Civil Aviation Organization, ICAO, agreed to the adoption of a standard atmosphere for altitudes to 65,800 feet. This ICAO standard atmosphere is published as NACA TR 1235, reference 1.

After about 1946, the sounding rocket came into use as a powerful research tool for upper atmospheric research. The initial sounding rocket research was conducted under the guidance of a panel of upper atmospheric scientists officially designated as the V-2 panel. The V-2 panel later changed its name to Upper Atmosphere Rocket Research Panel and is now called the Rocket and Satellite Panel. Under this panel (whatever its name) was coordinated the upper atmospheric research done prior to the International Geophysical Year, using the V-2 and later the Aerobee, Viking and Nike-Deacon or Cajun sounding rockets. These sounding rockets have extended the direct measurements of the atmosphere up to a maximum height of about 700,000 feet. As a result, up to about 400,000 feet we now know a great deal about the detailed pressure, temperature, density, and composition of the air.

The results of these direct sounding rocket data available up to about 1955, along with indirect meteor and aurora data and deductions from theory, were used to compile a model atmosphere up to 1,850,870 feet. This atmosphere was published by the Air Force Cambridge Research Center as "The ARDC Model Atmosphere 1956", reference 2.

At the present time, May 1958, first results from Sputnik I and Explorer I satellites have given values of atmospheric density considerably higher than the "ARDC Atmosphere" at altitudes of about 720,000 feet and 1,200,000 feet, respectively. On the basis of these measurements, Sterne, Folkert, and Schilling of the Smithsonian Institution Astrophysical Observatory, reference 3, have suggested a revision of the "ARDC Atmosphere". Figure 1 shows the two satellite points, the "ARDC Atmosphere" and the proposed revision. Explanations for some of the changes in the various curves are given on the figure.

Since the concept of geopotential altitude is of interest, an explanation regarding the relationship of geopotential and geometric altitude is in order. A detailed discussion will be found in the ARDC Model Atmosphere Report. The basic definition of geopotential is as follows: The geopotential of a point is defined as the increase in potential energy per unit mass lifted from mean sea level to that point against the force of gravity.

Now the increase in potential energy per unit mass of a body lifted against the force of gravity, from sea level, through a vertical distance to a given point is:

$$\frac{\Delta E}{m} = \int_0^z g dz \equiv \text{G.P.}$$

(1)

ΔE = increase in potential energy, ft-lb

m = mass of body in slugs

g = acceleration of gravity at point z f/sec²

z = geometric altitude above mean sea level, ft

G.P. = geopotential in ft-lb/slugs

Now if we define a geopotential altitude H to be that value of altitude through which the mass must be raised at a constant standard value of acceleration of gravity, i.e., G to get the same change in potential energy:

$$\text{G.P.} = GH \quad (2)$$

then

$$H = - \int_0^z g dz \quad (3)$$

further using the inverse square law for the variation of g with z , i.e.,

$$g = g_\varphi \left[\frac{r_\varphi}{r_\varphi + z} \right]^2 \quad (4)$$

g_φ = sea level value of g at latitude of φ of the point, f/s²

r_φ = radius of the Earth at latitude φ ft

$$H = \frac{g_\varphi}{G} \int_0^z \left[\frac{r_\varphi}{r_\varphi + z} \right]^2 dz \quad (5)$$

integrating gives

$$H = \frac{g_{\phi}}{G} \frac{r_{\phi} z}{r_{\phi} + z} \quad (6)$$

or

$$Z = \frac{r_{\phi} H}{\frac{g_{\phi}}{G} r_{\phi} - H} \quad (7)$$

The definition of G is such that at latitude $45^{\circ} 32' 40''$, $g_{\phi}/G = 1$.

At this latitude $r = 20,855,531$ feet, so

$$H = \frac{z}{1 + \frac{z}{20,855,531}} \quad (8)$$

The significance and usefulness of the geopotential altitude is that the average atmospheric properties on a nonspheroidal Earth are invariant with geopotential altitude rather than geometric altitude.

The equation of hydrostatic equilibrium for instance is

$$dp = - \rho g dz \quad (9)$$

where g depends on latitude and altitude by equation (4).

Differentiating equation (3) we get

$$G dH = g dz \quad (10)$$

so that independent of latitude

$$dp = - G \rho dH \quad (11)$$

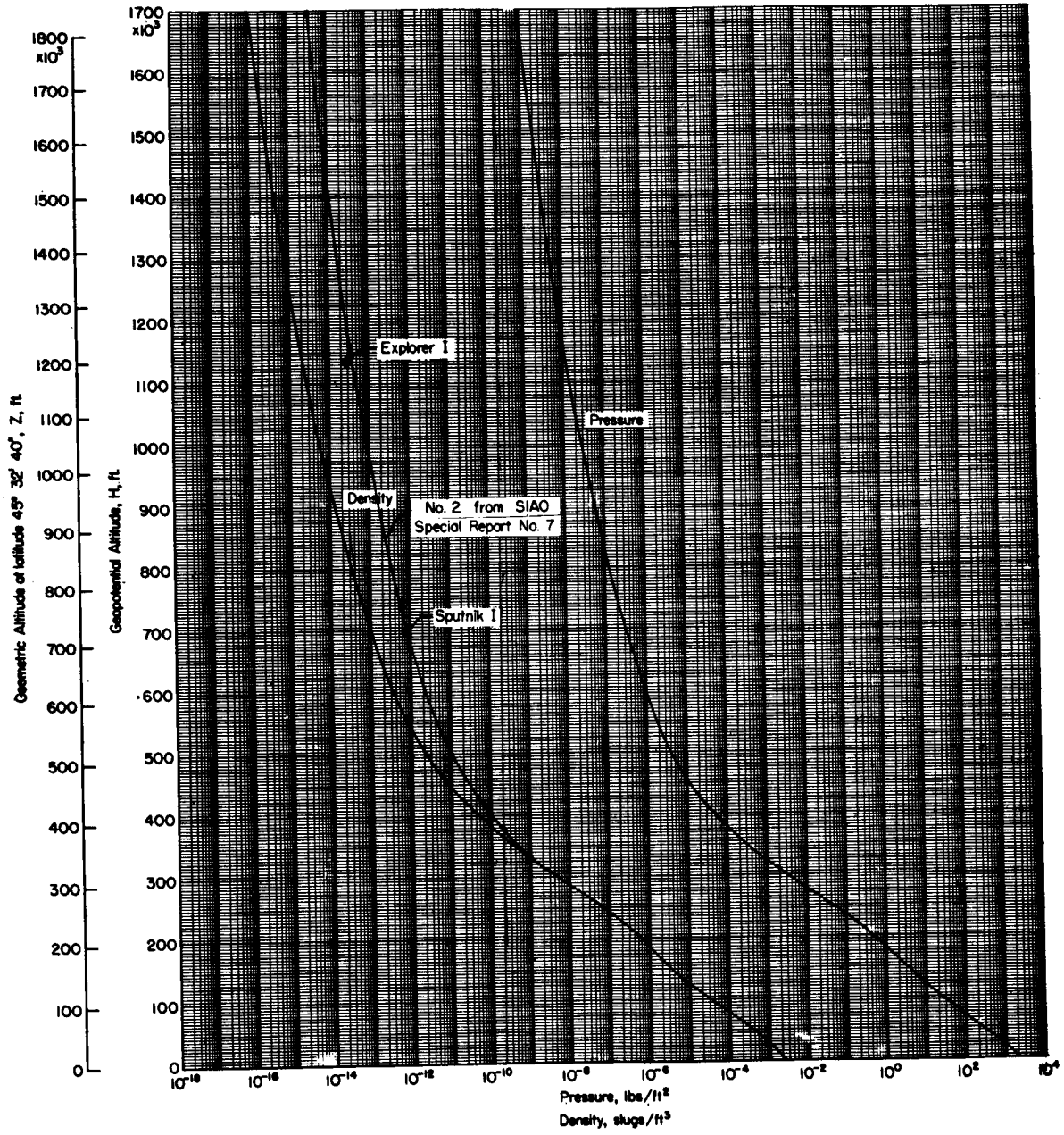
Equation (11) along with the perfect gas law, the molecular weight of the air, a specified variation of temperature with height (usually

geopotential height), and a sea level value of pressure have been used to calculate the standard atmospheres in the reports referred to previously.

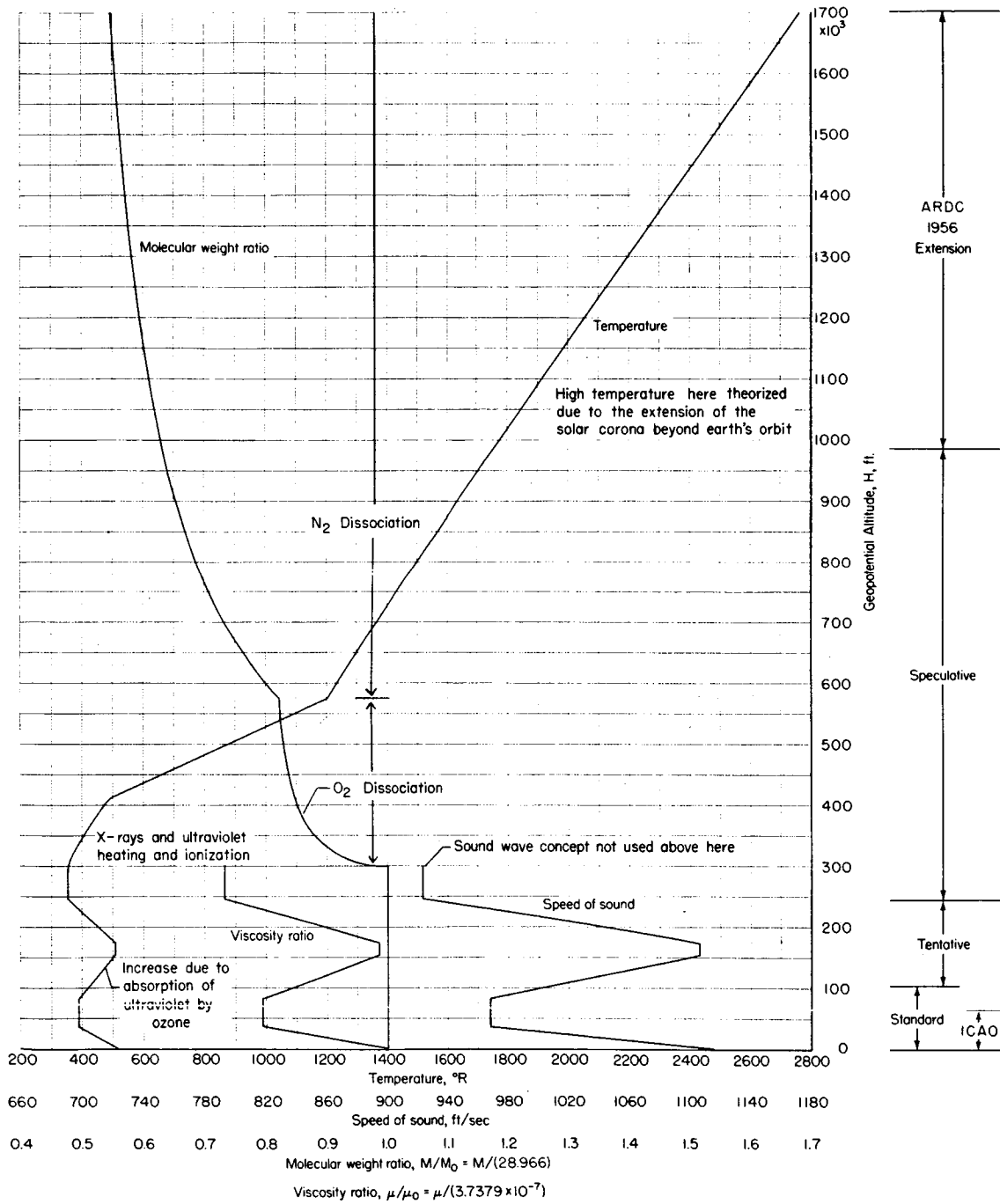
A brief history of standard atmospheres and detailed analysis of the theory and calculation procedures are given in reference 2. A summary of radiosonde temperature measurements is given in reference 4. Reference 5 presents a summary of sounding rocket measurements to January 1952. Sounding rocket techniques are discussed in reference 6. Reference 7 is an extensive study of the atmosphere and contains a wealth of basic references for further study.

REFERENCES

1. TR 1235 (NACA), Standard Atmosphere-Tables and Data for Altitudes to 65,800 Feet (1955).
2. Minzner, R. A., and Ripley, W. S.: The ARDC Model Atmosphere, 1956. Air Force Surveys in Geophysics, No. 86, December 1956.
3. Smithsonian Institution Astrophysical Observatory. Special Report No. 7, IGY Project No. 30.10, An Interim Model Atmosphere Fitted to Preliminary Densities Inferred From USSR Satellites.
4. Tolefson, Harold B.: A Summary of Radiosonde Temperature Observations for Altitudes up to 100,000 Feet Over Several Geographical Areas. NACA TN4169.
5. Physical Review, volume 88, no. 5, pages 1027-1032, December 1, 1952.
6. Boyd, R. L. F., and Seaton, M. J.: Rocket Exploration of the Upper Atmosphere.
7. Kuiper, Gerard P.: The Earth as a Planet.



ATMOSPHERE



SECTION XV

Communications and Tracking

For many years to come, the major purpose of each vehicle sent into space will be to gather information both for application to the design of future vehicles and for the furtherance of general scientific knowledge. A system of communicating this information to earth, as soon as possible after it is collected, is an essential part of any foreseeable space vehicle.

The ability to track a space vehicle is essential also, for the position and velocity of the vehicle are required for guidance and for observing possible disturbances in flight path.

Since electromagnetic waves form the only known practical medium for communication through space, it will be well to consider some of the factors which influence the transmission and reception of these waves and the relative merits of some methods of impressing information signals upon them. For the present, visible wavelengths will not be considered.

The first consideration in designing a transmitter will be choosing the frequency of the carrier wave. Several factors enter here. The earth's atmosphere, particularly the layer called the ionosphere, attenuates, refracts or reflects radio waves depending on the frequency of the radio waves and the angle of incidence. Commercial, military and amateur radio transmissions pretty well cover the practical wavelengths, to say nothing of interference from radio stars. As a kind of optimum, U. S. satellite designers have chosen 108 megacycles per second. This frequency occurs at the upper edge of the commercial F.M. band,

and most home F.M. sets can be modified easily to receive the stronger U.S. satellite signals.

Another matter for consideration is the manner in which the radio carrier wave is to be modulated by the information to be transmitted. The two most common methods are frequency modulation, where the carrier frequency is changed in proportion to the information signal, and amplitude modulation, whereby the strength of the carrier wave is made proportional to the information signal while its frequency is held constant. Of these two methods, the A.M. has the advantage that a very selective receiver may be used, since the major frequency content of the transmitted signal is at the carrier frequency. High receiver selectivity is very desirable for eliminating noise interference. It is not difficult to see that the fewer the noise frequencies allowed in to be amplified along with the useful signal, the more the signal will stand out. Everyone has had experience with the interference of one commercial radio broadcast with another at some near frequency. A complete lack of selectivity would allow all the stations up and down the dial to be received at the same time.

A.M. is not suited for data transmission if it is used in the usual manner, that is, where the amplitude of the carrier varies directly with the information signal. Too many things, besides the information signal, can influence the received amplitude, as you well know. The solution is to modulate the carrier amplitude with another carrier frequency, which may be

in the audible range (up to about 15 Kcps.). The frequency of this subcarrier is then varied according to the magnitude of the measured quantity to be transmitted. The actual amplitude of the received signal now has no significance whatever with regard to the information content. In this manner the best characteristics of both F.M. and A.M. are combined.

The power required of the space vehicle's transmitter will depend on the sensitivity of available earth-based receiving equipment, distance, atmospheric attenuation and noise levels. Receivers have been designed which are sensitive to 10^{-18} watts power input. With this sensitivity, however, information could only be sent at the slow rate of one "bit" per second. The major stumbling block to increasing sensitivity appears to be the noise generated in the receiver circuitry. If you turn up the volume on a high gain radio receiver, you may hear the effects of random motions of electrons in the vacuum tubes and even in the wires and other components of the set. These noises are in large part due to thermal agitation of molecules and atoms. Some reduction in receiver noise level can be gained by cooling parts of the receiver to very low temperatures.

Noise which originates outside the receiver can be reduced by the same methods used by owners of TV sets, though much refined. Maximum receiver selectivity restricts the noise to a narrow range of frequencies, while highly directional antennas will pick up only the noise which comes from the same direction

as the signal. The TV set owner increases selectivity by installing high pass, low pass or band-pass filters in the antenna system, whereas high selectivity (usually variable) is built into communications receivers. Directional TV antennas with remote controlled rotators are not uncommon. Many steerable parabolic reflectors of large diameter, 80 to 250 ft., have been built for use in radio astronomy and have been brought into play for tracking and receiving telemetered data from the U.S. and Russian satellites.

The reason for all the concern over receiver sensitivity, antenna gain and so on is that transmitter power is expensive when it must be carried on a satellite or other space vehicle. At the present state of the craft, batteries "cost" about 2.5 pounds per watt-hr. The extra rocket fuel required to get one more watt-hr. into space is tremendous. For this reason, U.S. satellite transmitters have all been less than .1 watt. (The Russians used a 1 watt transmitter.) WVEC-AM pours out 250 watts, WGH-AM uses 5,000, just for comparison.

In order to guide a vehicle properly during the launching phase, some accurate system of tracking is required. This system will later be used to observe the trajectory of the vehicle. Any deviation (or for that matter, lack of deviation) from the predicted path is of great interest.

Tracking systems are of two main types, the radar system which uses power transmitted from the ground and reflected back from the vehicle, and the directional receiver system which uses

the power transmitted from the vehicle. Most of us are familiar with the principles of radar. The most accurate of the other systems is known as the radio interferometer. Basically, it consists of two antennas located some distance apart and feeding into a common receiver. A signal source moving across the field of this antenna system will produce signals in the two antennas which alternately cancel and reinforce. As usual, between the basic system and something workable, there is a wide discrepancy. With the aid of a few blocks, I will try to explain some of the details of an actual system built by a group of radio amateurs out in California. This system is a simplified version of the Microlock tracking and communications system developed by the Jet Propulsion Laboratory of the California Institute of Technology. Most of the quite complicated circuitry shown in figure 1 is used to correct for frequency shifts in the incoming signal due to Doppler effect. For this purpose, a single reference is used. This reference antenna is also used for receiving the telemetered information. Beginning with the reference antenna, the signal from the satellite is picked up and sent to a pre-amplifier, (1). The output of the preamp., still at the satellite frequency of 108 mc., is fed into a mixer, (2), where it is mixed with (added to) a 127 mc. signal from a voltage controlled oscillator, block 6 . The output from the mixer consists of the sum and difference of the 108 and 127 mc. signals. Block 3 is an ordinary communications type receiver tuned to receive only the difference frequency, 19 mc. This receiver has its own local

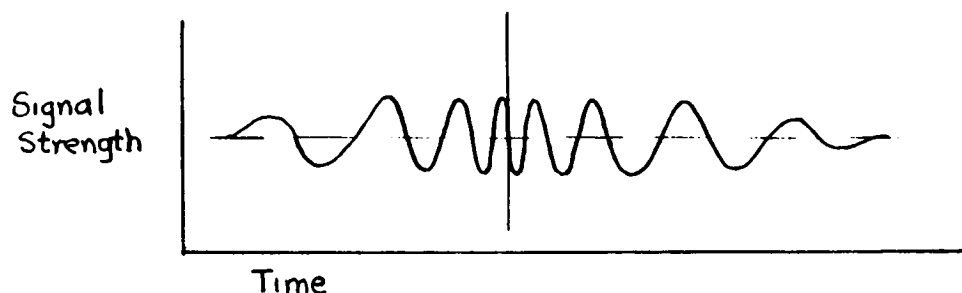
oscillator which is tuned to 19.455 mc., producing an output of 455 KC. (19.455-19) when mixed with the 19 mc. input. Now, if there is a shift in input frequency due to motion of the satellite, the input to receiver (3) will no longer be 19 mc., but some other frequency. The output will also no longer be 455 KC. One method of keeping the output of receiver (3) at a constant 455 KC is to vary the frequency of the oscillator, (6), the required amount to keep a constant 19 mc. difference from the satellite signal. This can be done automatically as follows. The output of receiver (3) is compared with the output of a crystal controlled 455 KC. reference oscillator, (7), by the phase detector in block (4). This phase detector is a device which produces a voltage proportional to either the sine of the phase angle or the frequency difference between two inputs. The instant the output of receiver (3) begins to differ from the 455 KC. reference oscillator, either in frequency or phase, a correcting voltage from the phase detector is sent through the filter (5) to the voltage controlled oscillator (6) which changes frequency in such a manner as to bring the output of receiver(3) back to exactly 455 KC. The filter (5) limits the response of the correcting system so that no change in frequency faster than 10 cycles per second will be corrected. Thus any telemetered data in the form of frequency modulation faster than 10 cps will not be destroyed. Without filter (5), the system could not distinguish between the relatively slow changes in frequency due to

Doppler affect and the rapid changes in frequency due to F.M., and would cancel out both types of frequency change.

The output of receiver (3) is also fed to a telemeter detector and recorder.

Thus far, the only accomplishment has been the establishment of a constant 455 KC. output frequency and the recording of the telemeter data. The interferometer channel is also controlled by oscillator (6). A separate receiver is used, block 11, and the local oscillator (19.455 mc.) of this receiver must be synchronized with that of receiver (3) to avoid undoing the work of the frequency correction network. (The local oscillator in receiver (3) may drift, but such changes in frequency would be corrected as if they were changes in satellite frequency. Receiver (11) is not in the feedback loop of the correction system, and drifting of its oscillator would not be corrected. Therefore, receivers (11) and (3) must, effectively, use the same local oscillator. This is indicated by the dashed line joining (3) and (11).) Signals from the satellite reach the receiver (11) through mixers (9) and (10). Since the antennas E and W (East and West) are separated by some distance, the two signals fed into (9) will differ in phase according to the relative positions of the satellite and the two antennas. The output of (9) can thus be considered a phase modulated signal of 108 mc. frequency. This is reduced to 19 mc. in mixer 10 and again to 455 KC. in receiver (11), retaining the phase modulation. Phase detector (12) detects the difference in phase between the satellite signal and the

455 KC. reference oscillator, converts it into signal strength variations which are recorded on an ink-recorder, (13). The resultant record looks like this, as a satellite crosses the antenna field.



By proper interpretation of the recorded time history, the angular position of the satellite with respect to the antenna base line at any time can be determined very accurately.

Time correlation of all satellite signals is very important, so that records from several interferometer stations can be used to predict the path of the vehicle. Radio station WWV, operated by the Bureau of Standards on several frequencies, broadcasts extremely accurate time signals which can easily be used for the necessary correlation.

The frequency shift due to Doppler effect, which was so carefully avoided in measuring angular position and receiving telemetered data, is used in other apparatus to measure the range rate (radial velocity) of the space vehicle. The stability of the satellite transmitter is sufficient to allow accurate measurements of this sort. For a satellite coming toward or going away from an observer at 18,000 mph., the Doppler shift is about ± 2 KC. from 108 mc. The most sophisticated circuitry may detect a shift

of a fraction of a cycle per second. The actual range of the vehicle may be obtained from one station by radar or from two or more correlated stations by triangulation using interferometer data. As the range increases to interplanetary distances, neither of these methods will be sufficient. A solution might be to establish a base on the Moon for triangulation purposes, with the other base on earth.

A recent discovery by Dr. John D. Kraus of Ohio State U., resulting from some efforts to receive the radio signals from Sputnik I, may be of aid in detecting ICBM's approximately one minute earlier than can be accomplished by ordinary radar methods. The discovery came about in this manner: it was noticed at a receiving station in central Ohio, that the 20 mc. signal from Sputnik I was not received clearly until the satellite had passed over. Furthermore, the 20 mc. signal from station WWV, which is not normally heard at night in central Ohio, was received in this area each time the satellite passed over, and reception began before the satellite itself came up over the radio horizon. The indications were that a cloud of ionized particles was being pushed ahead of the satellite. This cloud reflected the satellite transmitter's signal away from the receiving station while it reflected the WWV signal toward the receiver. The short wavelength signals from radar equipment pass through such a cloud, and thus cannot detect it.

Since an ICBM would be travelling through the ionosphere at approximately satellite speeds, it is expected that a low frequency radar-type installation could be used to detect the concentration of ionized particles ahead of the missile. This cloud, according to calculations, can be as much as 300 to 400 miles in length, giving an extra minute of warning. When it is considered that radar would only give at most nine minutes warning, the extra minute can be seen to be very important.

This phenomenon had been observed earlier as meteors entered the ionosphere, but at that time it was attributed to the meteor trail.

Now, let us examine the data telemetering system of a U.S. satellite. The quantity to be measured acts on a transducing element to vary one of its electrical properties. For instance, changes in temperature might act on a device called a thermistor to vary its electrical resistance. Micrometeorites might erode away parts of a thin metal film, increasing the edge-to-edge resistance of the film. These are techniques with which most of us are familiar. In the Vanguard satellite which didn't quite make it on April 28, 12 quantities were to have been measured. To transmit all this data at once would require a large bandwidth of transmitted frequencies. Since most of the quantities are only slowly changing, a pulse type of transmission was to have been used. In this system, each pulse consists of a sine wave superposed on the 108 mc. carrier frequency by carrier amplitude modulation. The frequency of the impressed sine wave is proportional to one of the measured quantities, the duration of the pulse

(up to about 30 milliseconds) is proportional to a second quantity, and the interval between the first pulse and the second represents a third quantity. The frequency of the second pulse can represent a fourth quantity, and so on until each of the measured quantities has been transmitted as a frequency, pulse duration or interval together with any desired calibration pulses (similar in principle to the calibrate deflections and galvanometer zeros used on oscillograph records). At the end of each sequence of pulses, or frame, as it is called, a pulse or interval of recognizable duration will appear as a marker, and another cycle of pulses begins. At the earth station, these pulses can be recorded on magnetic tape together with a time signal from WWV. The transmission rate is about 3 to 4 frames per second.

Probably the most complicated piece of equipment in the satellite is the encoder, which determines whether each quantity is to be represented by a pulse frequency, pulse duration or interval between pulses, and the sequence in which the data is to be transmitted. It also must determine the frequency and duration of each pulse, and the duration of each interval between pulses in accordance with pre-set calibrations. This remarkable gadget is contained in a disc $3/4$ " thick, $5-1/2$ " in diam. weighing $3-1/2$ oz. and consuming 8 to 10 milliwatts of power. There are no moving parts.

Transistor amplifiers are used in place of vacuum tubes in the U.S. satellites.

Signals can only be received from the satellite when it is in the line of sight. In view of this fact, some advantage is to be gained by storing the recorded data for readout only once each orbit as the satellite passes near one of the receiving stations. A tape recorder has been incorporated for ^{this} purpose in one of the "Explorers" which is now in orbit. The data are recorded at a rather slow tape speed. On receiving a code signal from one of the earth stations, the tape is played back at high speed and the data transmitted to earth. At the same time, the tape is erased for use on the next orbit.

The power requirements for satellite transmitters are very small. 100 milliwatts can give a very good signal from a distance of several thousand miles. The power required varies directly with the square of the distance to be covered. If 10 mw., for instance, are the minimum requirement for a distance of 2500 miles, then 100 watts would give the same signal at the distance of the moon, 250,000 miles. However, present satellites are radiating power in all directions. If some method can be found for orienting an antenna in the direction of the earth at all times, the radio power can be concentrated into a small cone. A cone of about 2° apex angle would permit the 10 milliwatt transmitter to cover the distance between the Earth and Moon. However, even with the reflecting antenna, the power required still increases with the square of the distance. When the vehicle reaches

25,000,000 miles (not quite out to the nearest point on the orbit of Mars) the power required is again 100 watts with the 2° beam. The extent to which the beam may be narrowed depends upon the wave length of the radio waves and the diameter of the reflector. Out in interplanetary space, a very large reflector could be carried because its strength requirements would be small. For instance, one of the large plastic balloons could be used as a reflector by aluminizing only half of it. Such antennas have actually been used on earth in radar installations, where they could be shielded from wind forces.

If trips to the outer edges of the solar system are to be successful, it will probably be necessary to establish some method of relaying messages between the earth and space vehicles. It may be possible to establish automatic repeater stations on each planet visited, gradually working outward. These stations might be atomic powered, or they might be powered by natural movements of the planet's atmosphere or ground fluids. In addition to furnishing a relay station for messages, each would furnish a beacon, identified by some code, for navigational purposes.

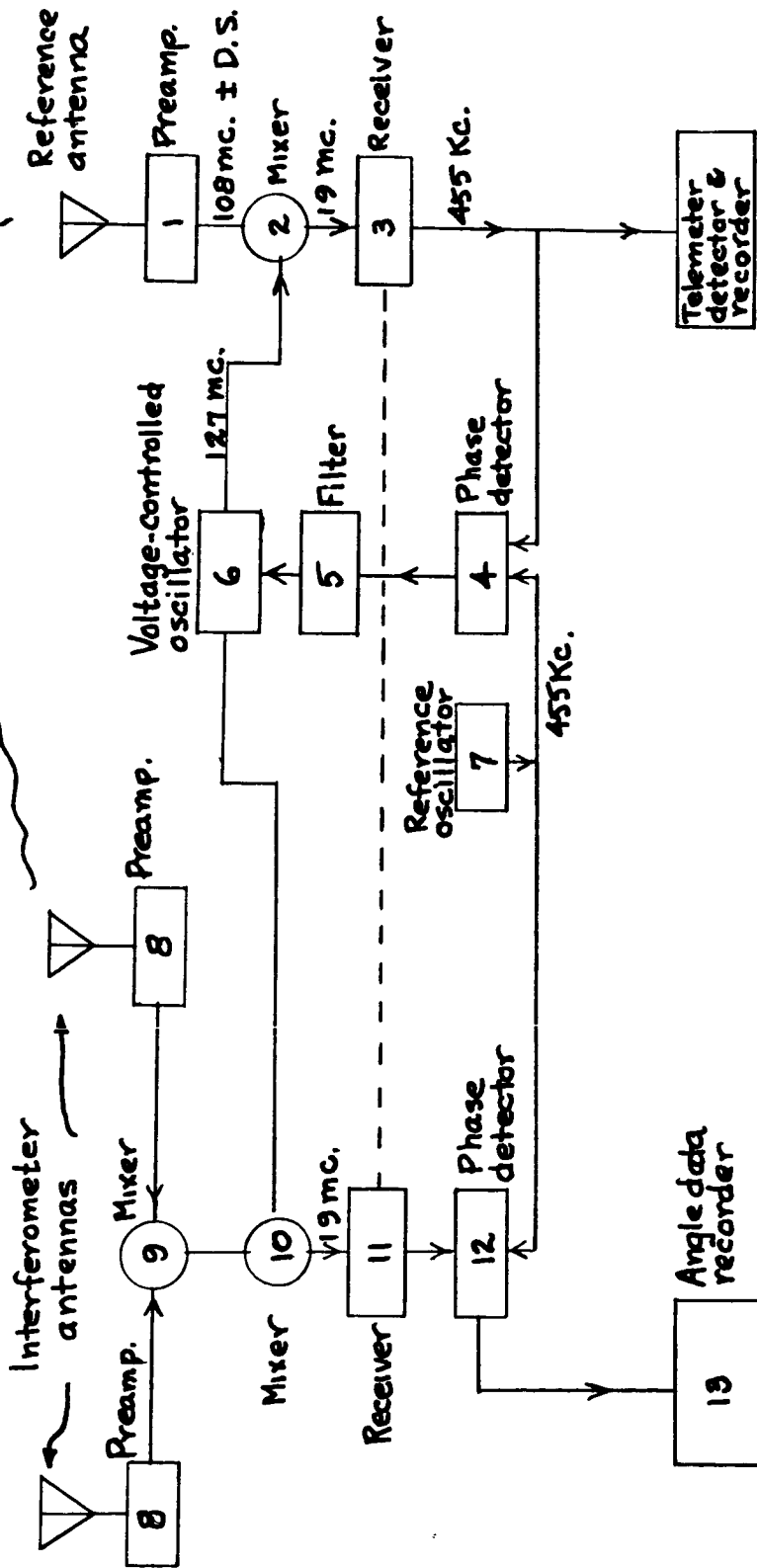
Another fact which may have to be taken into account is that there will be no "urgent" messages as we know them. The radio operator in the neighborhood of Pluto who says, "Rush this message through to Earth" must reconcile himself to the fact that he will have to wait at least 10 hours for a reply. The velocity of propagation of electromagnetic waves is one thing we haven't been able to speed up yet.

Many phases of communications theory and practice could not be touched upon in this presentation. It is hoped that these objectives have been obtained: to show how, in a general way, it is possible to get back enough information to justify a space vehicle; to show how the path of this vehicle may be followed from the ground, and to state some of the obstacles to communications over very long distances.

References:

- QST (magazine) Dec. 1957
- Radio and TV News March 1958 and May 1958
- Science and Mechanics May 1958
- Missiles and Rockets February 1958
- Westinghouse Engineer May 1958

Satellite signal
@ 108 mc. \pm Doppler shift



15 - 15

573 <

Block diagram illustrating Microlock receiving station.

SECTION XVI

SOME DYNAMICAL ASPECTS OF THE SPECIAL
AND GENERAL THEORIES OF RELATIVITY

- 16.1 Special Theory of Relativity
- 16.11 Evolution of Special Theory of Relativity

Towards the close of the last century Michelson and Morley performed an experiment. At the outset it appeared just another routine experiment. No one expected it to turn out, as indeed it did, to be one of the most significant experiments in the whole of scientific history. The experiment had as its objective the determination of the velocity of the earth's drift through the all prevailing ether. At that time it was generally supposed that light and electromagnetic phenomena in general were propagated through the ether with constant velocity. If a light wave were to meet the earth head on as the earth drifted through the ether, the velocity of the light relative to the earth would be somewhat augmented. On the other hand, if the light signal were to overtake the earth the velocity would be correspondingly reduced. The apparatus (figure 16-1) consisted in principle of a light source S located at the intersection of two mutually perpendicular arms SP and SQ, both of equal length, at the extremities of which were mounted two mirrors.

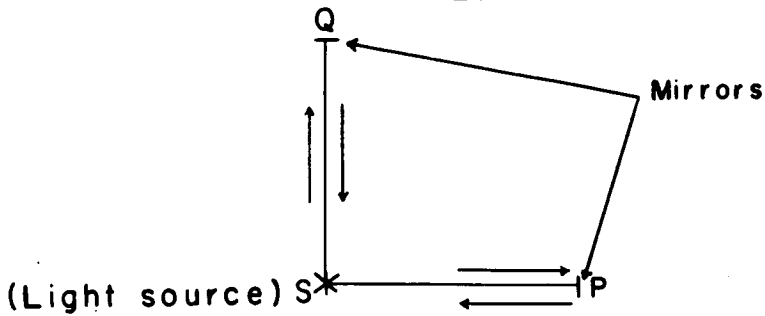


Figure 16-1

By comparing the times taken for a light pulse initiated at S to traverse the respective arms and back again the velocity of the earth's drift could be calculated. The apparatus was sufficiently sensitive to detect a velocity of drift of 1 mile per sec. As is so frequently the case, it was the unexpected that happened; they got a null result. Of course, there was a possibility that the earth was drifting in a direction bisecting the angle PSQ. This was eliminated by rotating their apparatus through 45° and repeating the experiment and again getting a null result. There remained a further possibility, an unlikely one albeit, that the velocity of the earth relative to the ether was zero, (or at any rate less than 1 mile per sec). This possibility was eliminated when they repeated their experiment after an elapse of six months (the earth's velocity having in the meantime changed by about 38 miles per sec.) and again obtained a null result.

Something was clearly wrong with the current concept of propagation of light through space. Nor would it have helped to revert to the corpuscular theory for this demanded that the velocity of light be dependant on the velocity of the

emitting source - a result known to be at variance with experimental results. Einstein was the first to overcome this impasse, only, however, by abandoning the intuitive concept of space and time.

16.12 Kinematics of Special Theory of Relativity

Einstein took the experimental result at its face value viz the velocity of light is constant relative to all observers. Consider two observers 0 and 0' figure 16-2

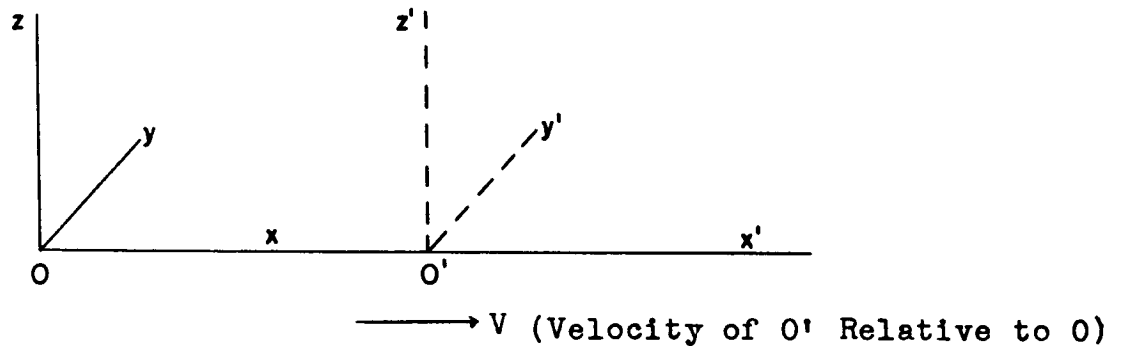


Figure 16-2

and let us suppose a light pulse is initiated at A (event I) and let it be subsequently received at B (event II).

Let observer 0 assign

coordinates:	x	y	z	t	(event I)
	x+dx	y+dy	z+dz	t+dt	(event II)

Similarly let observer 0'

assign coordinates:

	x'	y'	z'	t'	(event I)
	x'+dx'	y'+dy'	z'+dz'	t'+dt'	(event II)

Since by hypothesis the velocity of light is the same for both observers (say equal to c)

$$\begin{aligned} \text{then } 0 &= dx^2 + dy^2 + dz^2 - c^2 dt^2 \\ \text{and } 0 &= dx'^2 + dy'^2 + dz'^2 - c^2 dt'^2 \end{aligned}$$

i.e.,

$$dx^2 + dy^2 + dz^2 - c^2 dt^2 = dx'^2 + dy'^2 + dz'^2 - c^2 dt'^2 \quad (16.12-1)$$

This differential relationship is assumed to hold for all contiguous pairs of events. Clearly it implies some form of functional relationship between x' y' z' t' on the one hand and x y z t on the other. Let us seek the integrated form of equation (16.12-1). To simplify the discussion let us disregard the y and z coordinates.

$$dx^2 + (icdt)^2 = dx'^2 + (icdt')^2 \quad (16.12-2)$$

Compare this with

$$dx^2 + dy^2 = dx'^2 + dy'^2$$

This latter defines simply a rotation of xy axes through some angle θ as depicted in figure 16-3.

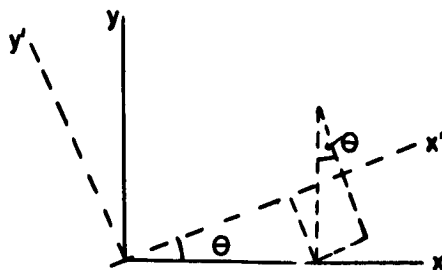


Figure 16-3

$$x' = x \cos \theta + y \sin \theta$$

$$y' = -x \sin \theta + y \cos \theta$$

Clearly then the integration of (16.12-2) leads to

$$x' = x \cos \theta + ict \sin \theta$$

$$ict' = -x \sin \theta + ict \cos \theta \quad (16.12-3)$$

or
$$ct' = ix \sin \theta + ct \cos \theta$$

(where θ is the constant of integration)

Since x, t and x', t' are all real this implies θ is purely imaginary, say $i\alpha$.

$$\cos(i\alpha) = \cosh \alpha$$

$$i \sin(i\alpha) = \sinh \alpha$$

Thus the equations (16.12-3) take the form

$$x' = x \cosh \alpha - ct \sinh \alpha$$

$$ct' = -x \sinh \alpha + ct \cosh \alpha \quad (16.12-4)$$

α can be expressed in terms of V . Thus since velocity of O' ($x' = 0$) relative to O is V .

$$0 = x \cosh \alpha - ct \sinh \alpha; \quad \frac{x}{ct} = \frac{V}{c} = \tanh \alpha.$$

Hence

$$\cosh \alpha = \frac{1}{\sqrt{1 - \frac{V^2}{c^2}}} \quad \text{and} \quad \sinh \alpha = \frac{\frac{V}{c}}{\sqrt{1 - \frac{V^2}{c^2}}}$$

Substituting in (16.12-4) we obtain finally

$$x' = \frac{x - Vt}{\sqrt{1 - \frac{V^2}{c^2}}}$$

$$t' = \frac{t - \frac{xV}{c^2}}{\sqrt{1 - \frac{V^2}{c^2}}}$$

(16.12-5)

These are the Lorentz Transformations.

16.121 Dilatation of Time

This is most readily obtained from the differential expression

$$-c^2 ds^2 = dx^2 + dy^2 + dz^2 - c^2 dt^2$$

(ds defines the absolute interval between two events: - The spacial and temporal separations of the events are simply components which vary from observer to observer).

Let us suppose O observes a particle P in motion and let us further suppose a clock is carried on P.

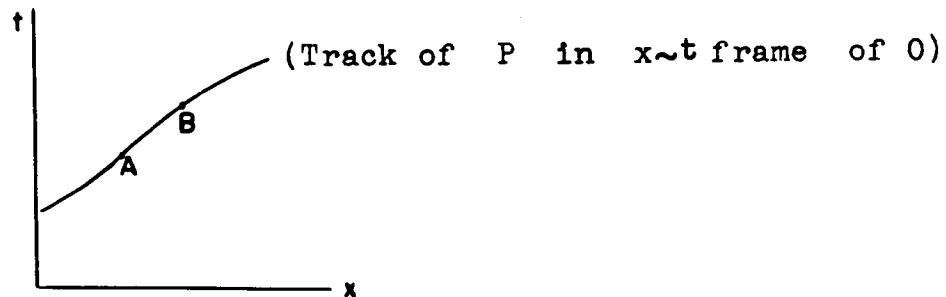


Figure 16-4

Assume light blips are initiated at A and B. (These

events are designated I and II respectively.)

O assigns coordinate differences dx dy dz dt to the interval separating these two events. However, the clock carried by P will actually mark off the true interval of separation ds .

Now
$$-c^2 ds^2 = dx^2 + dy^2 + dz^2 - c^2 dt^2$$

$$\frac{\text{Time between blips as registered by moving clock}}{\text{Time between blips as registered by observers clock}} = \frac{ds}{dt} = \sqrt{1 - \frac{v^2}{c^2}} = \sqrt{1 - \beta^2} \quad (16.12-6)$$

i.e., clock in motion appears to be running slow by a factor $\sqrt{1 - \beta^2}$

16.122 Lorentz-Fitzgerald Contraction.

To obtain this we must appeal to the integrated forms of the equations: -

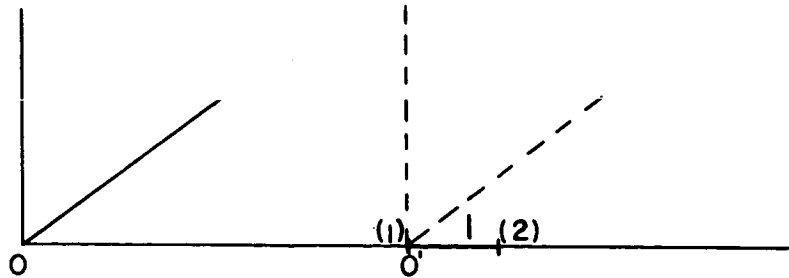


Figure 16-5

Assume O' is carrying a measuring scale which extends from his origin $x_1' = 0$ to $x_2' = 1$. O measures the length of 1 by determining the coordinates of its extremities at the same instant t_1 (according to his own clock).

$$x_1' = 0 = \frac{x_1 - Vt_1}{\sqrt{1 - \frac{V^2}{c^2}}}$$

$$x_2' = l = \frac{x_2 - Vt_1}{\sqrt{1 - \frac{V^2}{c^2}}}$$

$$l = \frac{x_2 - x_1}{\sqrt{1 - \frac{V^2}{c^2}}}$$

(16.122-1)

Thus the measuring rule in motion appears to be reduced in length by a factor $\sqrt{1 - \frac{V^2}{c^2}}$ (This is the so called Lorentz-Fitzgerald Contraction).

Thus in effect what Einstein has accomplished in his special theory of relativity is the welding together of space and time. We are not saying that time is of the same intrinsic nature as space. Quite the contrary. The mathematician recognizes the difference by attaching the identifying label t to the time coordinate. The physicist recognizes the distinction by using clocks to measure time like separations and measuring rules to measure space like separations. We ourselves intuitively recognize a difference between them. Of the two time is a more mysterious entity than space. It is rather interesting to speculate on the reason for this. We as individuals are somewhat of the nature of four dimensional worms - relatively extended in the time dimension. Thus we are much more intimately associated with time than

with space and this may conceivably explain why we regard it as so mysterious.*

16.13 Dynamics of the Special Theory of Relativity

It is clearly impossible to detect uniform motion. This implies that the laws of motion must have the same form relative to all inertial observers,** i.e., the equations of motion if correctly formulated must be invariant with respect to the Lorentz transformation. To put it another way, the terms appearing in the equation must transform according to the same rules. (They must be vectors or tensors in the revised 4 dimensional sense.) Clearly we will be assisted in this reformulation by the fact that our modified equations must tend to the Newtonian form as $V \longrightarrow 0$.

Look at the equations of motion as formulated by Newton.

$$\frac{d}{dt} (mv_i) = X_i$$

where

$$(i = 1, 2, 3)$$

$$v_i = \frac{dx_i}{dt}$$

(16.13-1)

* By the same token we find material things much less mysterious than our own psyche.

** Newton concurred in this and his equations of motion are indeed invariant with respect to Galilean transformation. His error lay in assuming that the Galilean transformation accurately described the transformation from one inertial frame to another.

Consider the velocity vector $v_1 \ v_2 \ v_3$. This is not a vector in the extended 4 dimensional sense. Let us for a moment look at the situation of a particle moving with relatively low velocity relative to our own $x-t$ reference frame.

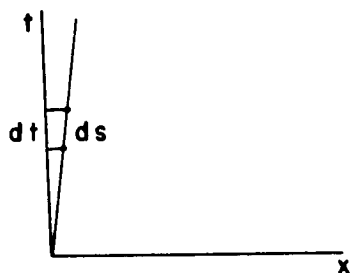


Figure 16-6

Its world track will depart only slightly from the time axis. Consider a segment of its track ds . At low velocities it would hardly be surprising if ds were confused with dt since the two are so nearly equal.

In place of $v_1 = \frac{dx_1}{dt}$ introduce $u_1 = \frac{dx_1}{ds} = \frac{dx_1}{dt} \frac{dt}{ds} = \frac{v_1}{\sqrt{1 - \beta^2}}$

$v_2 = \frac{dx_2}{dt}$ $u_2 = \frac{dx_2}{ds} = \frac{dx_2}{dt} \frac{dt}{ds} = \frac{v_2}{\sqrt{1 - \beta^2}}$

$v_3 = \frac{dx_3}{dt}$ $u_3 = \frac{dx_3}{ds} = \frac{dx_3}{dt} \frac{dt}{ds} = \frac{v_3}{\sqrt{1 - \beta^2}}$

$u_4 = \frac{dx_4}{ds} = \frac{dx_4}{dt} \frac{dt}{ds} = \frac{ic}{\sqrt{1 - \beta^2}}$

(N.B. $u_1 \ u_2 \ u_3 \ u_4$ is a proper vector in our 4 space. Moreover its spatial components $u_1 \ u_2 \ u_3$ tend respectively $v_1 \ v_2 \ v_3$ as velocity tends to zero thus it satisfies all the requirements imposed in this reformulation).

By the same token in the left hand side of (16.13-1) we replace differentiation with respect to t by differentiation with respect to s . On making these substitutions we find the left hand side is now truly invariant with respect to Lorentz transformations. We must similarly doctor the right hand side. Here we need to replace the force vector $X_1 \ X_2 \ X_3$ by an appropriate 4 vector. Electromagnetic theory tells us how to make this generalization.

$X_1 \ X_2 \ X_3$ are replaced by $K_1 \ K_2 \ K_3 \ K_4$

$$\text{where } K_1 = \frac{X_1}{\sqrt{1 - \beta^2}}; \quad K_2 = \frac{X_2}{\sqrt{1 - \beta^2}}; \quad K_3 = \frac{X_3}{\sqrt{1 - \beta^2}}; \quad K_4 = \frac{i}{c} \frac{\vec{F} \cdot \vec{V}}{\sqrt{1 - \beta^2}}$$

($K_1 \ K_2 \ K_3 \ K_4$ is a proper vector and moreover its three spatial components tend to $X_1 \ X_2 \ X_3$ at low velocities.)

Thus in place of Newton's equations we have

$$\frac{d}{ds} (m u_i) = K_i \quad (i = 1, 2, 3, 4)$$

(16.13-2)

Writing this out in terms of xyz coordinates

$$\frac{d}{dt} \left(m \frac{u}{\sqrt{1-\beta^2}} \right) \frac{dt}{ds} = \frac{X}{\sqrt{1-\beta^2}} \quad \text{or} \quad \frac{d}{dt} \left(m \frac{u}{\sqrt{1-\beta^2}} \right) = X$$

$$\frac{d}{dt} \left(m \frac{v}{\sqrt{1-\beta^2}} \right) \frac{dt}{ds} = \frac{Y}{\sqrt{1-\beta^2}} \quad \text{or} \quad \frac{d}{dt} \left(m \frac{v}{\sqrt{1-\beta^2}} \right) = Y$$

$$\frac{d}{dt} \left(m \frac{w}{\sqrt{1-\beta^2}} \right) \frac{dt}{ds} = \frac{Z}{\sqrt{1-\beta^2}} \quad \text{or} \quad \frac{d}{dt} \left(m \frac{w}{\sqrt{1-\beta^2}} \right) = Z$$

$$\frac{d}{dt} \left(m \frac{ic}{\sqrt{1-\beta^2}} \right) \frac{dt}{ds} = \frac{i}{c} \frac{\vec{F} \cdot \vec{V}}{\sqrt{1-\beta^2}} \quad \text{or} \quad \frac{d}{dt} \left(\frac{mc^2}{\sqrt{1-\beta^2}} \right) = \vec{F} \cdot \vec{V}$$

(16.13-3)

The fourth equation deserves special note.

$$\frac{d}{dt} \left(\frac{mc^2}{\sqrt{1-\beta^2}} \right) = \vec{F} \cdot \vec{V}$$

However,

$$\frac{mc^2}{\sqrt{1-\beta^2}} = mc^2 + \frac{1}{2} mv^2 + \dots$$

At all but the highest velocities it suffices to retain only two terms of the above expansion:

$$\frac{d}{dt} \left(mc^2 + \frac{1}{2} mv^2 \right) = \vec{F} \cdot \vec{V}$$

Note the similarity with the classical equation

$$\frac{d}{dt} (\text{K.E.}) = \vec{F} \cdot \vec{V}$$

Consider the collision between two lead masses (assuming no rebound).

$$\sum \frac{d}{dt} \left(mc^2 + \frac{1}{2} v^2 \right) = \sum \vec{F} \cdot \vec{V} = 0$$

$$\frac{d}{dt} \left\{ c^2 \sum m + \sum \frac{1}{2} mv^2 \right\} = 0$$

$$c^2 \sum m + \sum \frac{1}{2} mv^2 = \text{constant}$$

At impact the K.E. is entirely destroyed since there is assumed to be no rebound. Since c itself is constant the disappearance of a certain amount of energy is associated with an increase in mass.

$$\Delta M = \frac{\Delta E}{c^2} \quad (16.13-4)$$

In place of the two classical laws

I Conservation of Mass

II Conservation of Energy

we now have only single law of conservation of mass + energy. The laws of motion (16.13-3) between them express the conservation of momentum and conservation of mass and energy.

We shall find how these results are further generalized in terms of general theory of relativity.

16.2 General Theory of Relativity

16.21 Evolution of General Theory of Relativity.

Newton had recognized the impossibility of devising an experiment to detect uniform motion (which in itself implies the invariance of form of the equations of motion relative to all sets of inertial axes see footnote page 16-9) On the other hand, however, he believed it possible to detect absolute rotation (his criterion: simply hold a bucket full of water in your hand - if the surface of the water is curved you are rotating, if it is flat you are at rest).* Bishop Berkeley held a contrary viewpoint on philosophic grounds. A hundred years later Ernest Mach discerned an illogicality in the concept of absolute rest in a rotating sense. Mach argued thusly; consider a pail rotating uniformly in a universe otherwise at rest. Clearly there is nothing to distinguish this situation from one in which the pail is at rest and the remaining masses of the universe rotating about it. Thus if by some means the masses of the universe could be set into a rotation about a pail of water at rest in this instance also the surface of the water would be curved. Thus the curvature of the surface i.e., centrifugal and centripetal forces etc.,

* The possibility of detecting a condition of absolute rest implies that in a rotating frame indeed in accelerated frames in general the laws of motion are not invariant in form - this is reflected by the presence of additional terms i.e., Centrifugal Force Terms, etc.

are in the last resort attributable to the influence of the remaining masses of the universe. They are gravitational in origin. Mach's hypothesis, if accepted, explains the proportionality of inertial mass and gravitational mass, a circumstance which Newton and other scientists who followed him had been at a loss to explain. Inertial mass entered the scheme of Classical Mechanics via Newton's law of motion, gravitational mass on the other hand entered via Newton's law of gravitation. Now in view of there being no discernable tie up between these two laws the strict proportionality between the two kinds of masses was somewhat perplexing. Bessel and Eotvos had carried out delicate experiments with the aim of detecting slight differences between them if they existed. Their experiments consisted of measuring the direction of pull on masses of various sizes suspended at the earth's surface. Two forces in this instance are operative, a centrifugal force due to earth's rotation (proportional to inertial mass) and gravitation (proportional to gravitational mass). If the inertial and gravitational masses were not strictly proportional this would show up in a change of direction of the resultant pull as the mass changed. No such effect was observed. Following Mach, Friedman attempted to detect "centrifugal" force on a particle at rest near the center of a rotating spherical mass. This experiment too yielded a null result. We know now that the effect for which he was looking was much too small to be

detected. Einstein being a student of Machs was exposed to and accepted his radical viewpoint. It is to Einstein that we owe the rather convincing example of the "man in the lift", an example which further supported the essential equivalence of inertial and gravitational mass. Einstein argued thusly - imagine a lift being acclerated upwards at 32 ft/sec.^2 in a gravity free field. All experiments performed in this lift will yield the same result as would be obtained if the experiment were performed in a laboratory on the surface of the earth. Thus projected particles will in both cases describe parabolic paths. Note, however, that the man in the lift interprets mass as inertial mass whereas the man in the earth bound laboratory interprets mass as gravitational mass.

Having convinced himself of the equivalence of inertial and gravitational mass it remained for him to explain the latter.

The following story is attributed to Eddington. The gist of it is this: Up to the time of the middle ages it was popularly believed that the earth was flat. Let us suppose this belief had persisted down to the present day. A mercators chart would thus have been regarded as giving an accurate description of the disposition of places on the earth's surface. If our mercators chart were centered on the USA, the chart would serve adequately so long as our journeys were

limited to the confines of the USA. Consider, however, the case of travelers to Greenland. They would find that they apparently covered immense distances with relatively little expenditure of effort. Scientists would doubtless explain the phenomenon by inventing a demon who helped travellers to Greenland on their journeys. Being scientists they wouldn't choose to use the word "Demon" but would probably use a word of Greco-Latin derivation such as "gravity". Consider now our scientific colleagues in Greenland. They would use a mercators chart centered in their own country and they would see the demon operative in the USA. The demon is never where we are always where the other fellow is. If you'll reflect a moment you'll see the situation is quite analogous to the situation with respect to gravity. Just as the demon owes his existence to the circumstance that we are trying to force a spherical surface into a flat surface so gravitational forces result from our regarding what is in reality a twisted space time continuum as being flat. (Particles instead of describing curved paths in flat space actually follow straight or geodesic paths in curved space). Einstein having come this far the rest was relatively straight forward.

In reformulating his law of gravitation Einstein instead of saying something about a force had now to say something about curvature. Fortunately there are relatively few things we can say about curvature. Thus in the case of a twisted two dimensional surface in 3-space there is only a single

intrinsic measure of curvature- the so called Gaussian or spherical curvature.* Passing from two dimensions to four dimensions we find the latter by comparison relatively ingenious in devising new contortions - this is exemplified by the fact that it takes a Euclidian space of 10 dimensions to accommodate a twisted four dimensional domain. In place of a single intrinsic measure of curvature a 4-dimensional domain has twenty - ten of which are principal and ten of which are secondary.** What was Einstein to say about these curvatures? If he'd set them all zero he'd have been back where he started with flat space time. If he'd left them all entirely arbitrary this would have implied absence of any constraint or law. He chose a middle of the road course and set the ten principal measures of curvature equal to zero.

$$G_{\mu\nu} = \begin{bmatrix} x & x & x & x \\ & x & x & x \\ & & x & x \\ & & & x \end{bmatrix} = 0$$

($G_{\mu\nu}$ is a symmetric tensor and has ten components as indicated)

This still left him with ten degrees of freedom which was sufficiently flexible to enable him to adopt his law to any

* There are, of course, other measures of curvature, however, these are only meaningful to beings external to the surface. We must clearly limit ourselves to measures of intrinsic curvature.

** To understand the rather subtle distinction between principal and secondary curvatures one has to delve rather deeply into Riemannian Geometry - See Eisenhart: Riemannian Geometry.

particular physical situation.

16.22 Kinematics of General Theory of Relativity

What is meant by the curvature of space time. Clearly there is no point to be served by attempting to look at the thing from a conceptual standpoint. The best we can do is to formulate the mathematical equations and draw our implications from them. It is a relatively easy matter to evaluate the gravitational field associated with a single mass particle. This is tantamount to solving the gravitational equation $G_{\mu\nu} = 0$ imposing the condition of spherical symmetry.

In figure 16-7 M is an isolated mass the presence of which results in a deformation of space time. "A" is an observer at a distance r_0' (as measured by its own measuring rods).

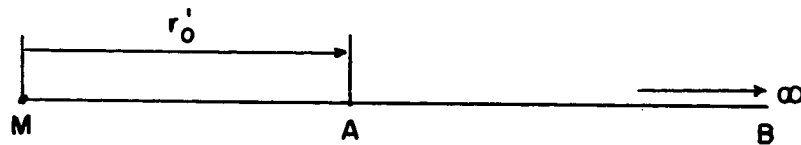


Figure 16-7

Relative to the observer A the interval separating two contiguous events is given by the expression*:-

* The units have been selected to make the velocity of light in free space unity.

$$ds^2 = - \left(\frac{1 + \frac{2m'}{r_o'}}{1 + \frac{2m'}{r_o'} - \frac{2m'}{r'}} \right) dr'^2 - r'^2 d\theta'^2 - r'^2 \sin^2 \theta' d\phi'^2 + \left(1 + \frac{2m'}{r_o'} - \frac{2m'}{r'} \right) dt'^2 \quad (16.22-1)$$

m' is a measure of mass m as determined at "A".

r' is the distance to the two adjacent events.

dr' $d\theta'$ $d\phi'$ dt' are the coordinate differences relative to A, separating the two events.

In the special case of an observer at infinity (designated B in figure 16-7) the expression for interval becomes

$$ds^2 = - \frac{dr^2}{\left(1 - \frac{2m}{r}\right)} - r^2 d\theta^2 - r^2 \sin^2 \theta d\phi^2 + \left(1 - \frac{2m}{r}\right) dt^2 \quad (16.22-2)$$

Let us suppose the observers A and B both observe the same pair of events. The interval ds separating is the same for all observers.** Hence

* Note mass m appearing in (16.22-2) is to be distinguished from the mass m' appearing in (16.22-1) since it is to be expected that different observers will assign different measures to the mass of the gravitating body.

** ds provides an absolute measure of separation (See Special Theory).

$$\begin{aligned}
 ds^2 &= - \left(\frac{1 + \frac{2m'}{r_0}}{1 + \frac{2m'}{r_0} - \frac{2m'}{r'}} \right) dr'^2 - r'^2 d\theta'^2 - r'^2 \sin^2 \theta' d\phi'^2 + \left(1 + \frac{2m'}{r_0} - \frac{2m'}{r'} \right) dt'^2 \\
 &= - \frac{1}{\left(1 - \frac{2m}{r} \right)} dr^2 - r^2 d\theta^2 - r^2 \sin^2 \theta d\phi^2 + \left(1 - \frac{2m}{r} \right) dt^2
 \end{aligned}$$

(16.22-3)

This differential relationship is strictly analogous to the relationship

$$c^2 ds^2 = - dx^2 - dy^2 - dz^2 + c^2 dt^2 = - dx'^2 - dy'^2 - dz'^2 + c^2 dt'^2$$

which appeared in the Special Theory of Relativity. In the Special Theory we were able to integrate the expression quite simply. With regard to (16.22-3) no one to my knowledge has been clever enough to express the relationship in integrated form. We do not therefore have in the case of the gravitational field the equivalent of the Lorenz equations of Special Theory. Fortunately we are able to deduce quite a lot from the relationship in its differential form.

16.221 Variation of the Velocity of Light

The velocity of light is obtained by setting $ds = 0$.

Thus in Special Theory

$$0 = 1 - \frac{dx^2 + dy^2 + dz^2}{c^2 dt^2} \quad \text{or } v^2 = c^2 .$$

i.e., the velocity of light is uniformly equal to c .

We derive an expression for the velocity of light in the gravitational case by again setting $ds = 0$.

Thus for observer A

$$\left(\frac{1 + \frac{2m'}{r_0'}}{1 + \frac{2m'}{r_0'} - \frac{2m'}{r'}} \right) \dot{r}'^2 + r'^2 \dot{\theta}'^2 + r'^2 \sin^2 \theta' \dot{\phi}'^2 = 1 + \frac{2m'}{r_0'} - \frac{2m'}{r'}$$

N.B. The velocity of light varies with direction. Thus in the case of transverse propagation (θ' varying r' and ϕ' constant)

$$c = \left(1 + \frac{2m'}{r_0'} - \frac{2m'}{r'} \right)^{1/2}$$

whereas in the radial direction

$$c = \frac{\left(1 + \frac{2m'}{r_0'} - \frac{2m'}{r'} \right)}{\left(1 + \frac{2m'}{r'} \right)^{1/2}}$$

Restricting our attention to radial propagation as r' becomes smaller i.e., the more closely we approach the gravitating mass the more sluggish does light become. On the other hand as $r' \rightarrow \infty$

$$c \rightarrow \left(1 + \frac{2m'}{r'} \right)^{1/2} > 1$$

Bearing in mind that in terms of present units the velocity of light in free space is unity. Thus for the observer A the velocity of light can be either less than or greater than its velocity in gravity free space.

For the observer at infinity

$$c = 1 - \frac{2m}{r}$$

(16.221-1)

This equation at first sight has rather startling implications. i.e., if we make m large enough and r

small enough c can be made zero or indeed negative. This clearly demands further scrutiny. Let us to begin by seeking the radius of a mass (having uniform density equal to that water) such that at its boundary $\frac{2m}{r} = 1$ and hence $c = 0$.

Let the radius of the mass be $R \times 10^6$ Kms

$$\text{Mass of sphere} = \frac{4}{3} \pi (R \times 10^6)^3 \times (10^5)^3 \text{ gms.}$$

$$\text{Mass of the sun} = \frac{4}{3} \pi (0.695 \times 10^6)^3 \times (10^5)^3 \times 1.41 \text{ gms.}$$

$$m^* = \frac{\frac{4}{3} \pi R^3 \times 10^{18} \times 10^{15} \times 1.5}{\frac{4}{3} \pi 0.695^3 \times 10^{08} \times 10^{15} \times 1.41} \text{ kms.}$$

Therefore

$$\frac{2m}{R} = \frac{3R^3}{R \times 10^6 \times 0.695^3 \times 1.41} = 1$$

$$R^2 = \frac{0.695 \times 1.41}{3} \times 10^6$$

$$R = 395.$$

i.e., the radius of the mass in question = 395,000,000 kms.

If we delve more deeply into the general theory we find that this mass results in a closing in of space upon itself. Thus the presence of mass induces a curvature of space time. Adding more and more mass produces ever greater distortion and if we add enough it will cause space to curve back on itself and become closed. If we direct a light signal to-

* The m appearing in our equations for interval though proportional to mass is not measured in gms. As a result of our choice of units it has dimensions of length. Expressed in appropriate units the sun's mass is 1.5 kms.

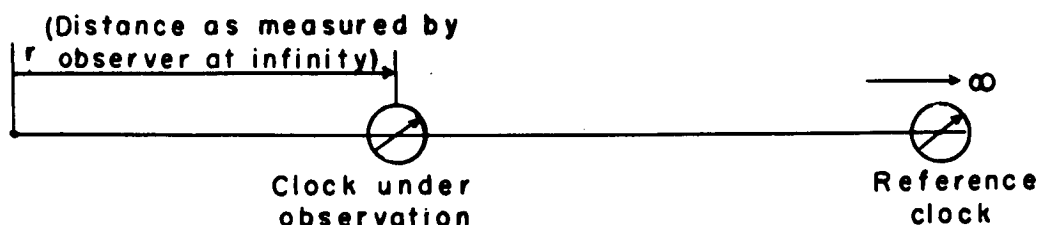
wards such a mass as it approaches its boundary the light signal will slow down to zero and will never actually attain it. A material particle if projected towards it can therefore never reach it. Thus there is no possibility of our adding more water from the outside. Can water be added from the inside? If we look at the relevant equations we find the velocity of light is zero at all interior points and that clocks stand still. There can be no activity whatever, therefore, on the inside. It is impossible to send a signal from an interior point to an exterior point and vice versa. If such masses exist there can be no means of our knowing it.

Let us return to rather more mundane matters.

16.222 Time Dilatation in Gravitational Field.

In the Special Theory we were able to evaluate time dilatation effects on the basis of the differential expression and we can do likewise here. Consider in the first place a clock at rest and let us compare its timekeeping with our reference clock at infinity.

Since the clock is assumed to be at rest $dr = d\theta = d\phi = 0$
 $ds^2 = (1 - \frac{2m}{r}) dt^2$



The clock under observation marks off true interval ds .

$$\frac{ds}{dt} \frac{(\text{clock under observation})}{(\text{clock at infinity})} = 1 - \frac{2m}{r}$$

(16.222-1)

To our observer at infinity the clock under observation appears to be running slow by a factor $1 - \frac{2m}{r}$. i.e., the more closely the clock approaches the gravitating mass the more sluggish it appears to become. Table I tabulates the degree to which clocks located at the surface of various gravitating bodies are slowed down relative to clock at infinity. (Effects of rotation of bodies are ignored.)

TABLE I

	m(kms)	Radius (kms)	Extent to which clocks run slow referenced to clock at infinity
Sun	1.5	695,000	2 parts in 10^6
Typical red giant (α Scorpii A).	45.0	480 x 695,000	1/8 parts in 10^6
Typical white dwarf (α Can.Maj. B).	1.44	0.034 x 695,000	5.6 parts in 10^5 (1/2 hr. in a year approximate)

We note from this table that the most dense agglomerations of matter we know of i.e., the white dwarfs, result in only a slight wrinkling of space time. Turn next to the slowing down of clocks carried by bodies moving in gravitational fields.

$$ds^2 = - \frac{dr^2}{1 - \frac{2m}{r}} - r^2 d\theta^2 - r^2 \sin^2\theta d\phi^2 + \left(1 - \frac{2m}{r}\right) dt^2$$

$$\left(\frac{ds}{dt}\right)^2 = \left(1 - \frac{2m}{r}\right) - \left(\frac{\dot{r}^2}{1 - \frac{2m}{r}} + r^2\dot{\theta}^2 + r^2 \sin^2\theta \dot{\phi}^2\right)$$

Now P.E. = $-\frac{m}{r}$ (P.E. is referenced to infinity) (16.222-2)

$$\text{K.E.} = \dot{r}^2 + r^2 \dot{\theta}^2 + r^2 \sin^2\theta \dot{\phi}^2 \quad (16.222-3)$$

In the unit system we have adopted the expressions of P.E. and K.E. are their values in customary units divided by c^2 . Both are therefore small quantities and can be treated as such. To a first order therefore:

$$\left(\frac{ds}{dt}\right)^2 = 1 + 2(\text{P.E.}) - 2(\text{K.E.})$$

$$\frac{ds}{dt} \frac{(\text{clock in motion})}{(\text{reference clock at infinity})} = 1 + (\text{P.E.}) - (\text{K.E.}) \quad (16.222-4)$$

Thus because of their smallness the effects of gravitating field and the motion of the body in question can be superimposed.

Apply (16.222-4) to a clock carried by the earth (effects of earth's rotation about its axis are quite negligible). The influence of the gravitational field results in a slowing down of 1 part in 10^8 . In addition since the earth is following to all intents and purposes a circular path the K.E. of its motion is equal to about 1/2 (P.E.) and hence, the motion results in a further slowing down of about

$1/2$ part in 10^8 . Hence aggregate slowing down amounts to about $1-1/2$ parts in 10^8 . In the case of Neptune the aggregate slowing down amounts to about $1/3$ part in 10^9 .

Consider next the case of spaceship following the elliptic orbits designated I and II in figure 16-8.

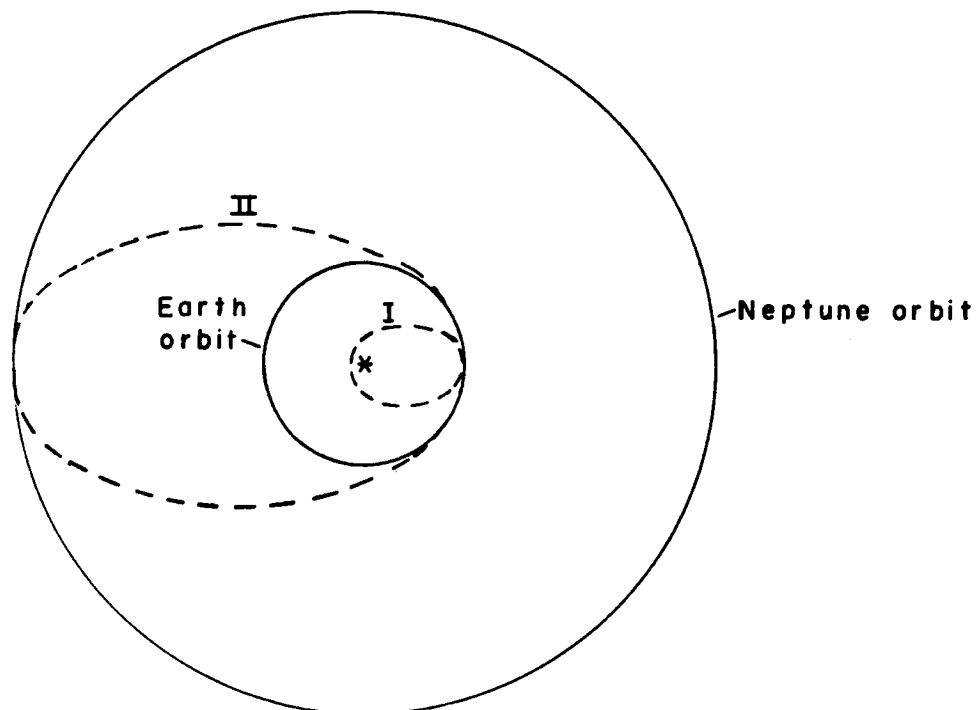


Figure 16-8

Orbit I. The spaceship approaches close to the Sun and by comparison with earth's clocks the clocks carried by the spaceship will be running slow. In this instance the space traveller will age somewhat less than his earthbound counterpart.

Orbit II. A significant portion of the time is spent in relative close proximity to Neptune orbit where clocks run fast relative to the earth. On such a voyage this space

traveller will be somewhat older on return than his earth-bound counterpart.

Bear in mind, however, that the extent of relative aging is so slight in all interplanetary flights as to be utterly insignificant from the point of view of changing man's lifespan. The only way in which his lifespan could be materially extended is by providing him with a means of attaining velocities comparative in magnitude with speed of light.

A further example of somewhat current interest is the possibility of verifying the general theory by comparing the timekeeping of a clock carried by a satellite with an identical clock at the earth's surface.

For a consideration of this problem it suffices to disregard all masses save that of the earth. Let our observer at infinity make the comparison for us.

The clock on the earth's surface is slowed down as the result of it being in the earth's gravitational field (the additional slowing resulting from the earth's rotation is quite negligible).

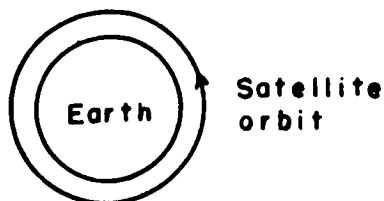


Figure 16-9

The clock of the satellite is slowed down:

- (a) As a result of the earth's gravitational field.
- (b) As a result of its motion in its orbit.

If we suppose the satellite to be in a relatively tight orbit around the earth the gravitational affects are about the same on both clocks. And the difference in their respective rates is attributable almost wholly to the motion of the satellite in its orbit. Thus experimental comparison of their rates of timekeeping would provide us with a test of the Special Theory of Relativity rather than the General Theory. A test of General Theory could be made by placing the second clock on the moon's surface for then gravitational effects are significantly different. Even here, however, if a quantitative check on General Theory were to be made an accuracy in time measurement of the order of 1 part in 10^{10} would be demanded. So much for the kinematics of General Theory. Let us proceed now to the discussion of Relativistic Dynamics.

16.23 Dynamics of General Theory of Relativity

As we have had occasion to mention previously there is no means of our detecting absolute rotation or indeed acceleration in any shape or form. Clearly then this implies that our equations of motion must assume identically the same form in all frames of reference. For otherwise if the form of the equation changed as we passed from one accelerated frame to another this fact could in itself be utilized to

distinguish one accelerated frame from another and hence, define zero rotation etc.*

All frames of reference are then equivalent and the equations of motion if correctly formulated must therefore be invariant with respect to quite arbitrary transformations of space time. This invariance will be achieved if we can express our equations in tensorial form (i.e., all terms having the same tensorial characteristics and hence, subject to the same transformation rules).

In Galilean frame of reference the classical equations of motion assume the form:-

$$\frac{\partial \rho}{\partial t} + \frac{\partial(\rho v_i)}{\partial x_i} = 0 \quad \begin{array}{l} \text{(equation of} \\ \text{continuity)} \end{array} \quad (16.23-1)$$

$$\rho \frac{Dv}{Dt} = \quad F_e \quad + \quad F_i \quad \begin{array}{l} \text{(equation of} \\ \text{momentum)} \end{array} \quad (16.23-2)$$

(external forces) (internal forces)

With reference to external forces (i.e., gravity and inertial forces) these have been shown to be fictitious (they result from our mistakenly regarding what is in reality a twisted space time continuum as being flat) and can therefore, be dis-

* In the classical set-up the equations of motion did assume characteristic form when referred to rotating axes, i.e., Centrifugal and Centripetal forces appeared. By ensuring that these inertial force terms vanished we were able to define a condition of absolute rest in a rotational sense.

regarded. We cannot so easily dismiss the forces F_i since these are atomic in origin.

We can rewrite (16.23-2) in the form

$$\rho \frac{\partial v_j}{\partial t} + \rho v_i \frac{\partial v_j}{\partial t} = \frac{\partial X_{ij}}{\partial x_i} \quad (j = 1, 2, 3) \quad (16.23-3)$$

or making use of (16.23-1)

$$\frac{\partial(\rho v_j)}{\partial t} + \frac{\partial}{\partial x_i} (\rho v_i v_j - X_{ij}) = 0 \quad (16.23-4)$$

Following the example of Special Theory, we replace it by x_4 . If we then define

$$\begin{aligned} T_{ij} &= T_{ji} = \rho v_i v_j - X_{ij} & (i, j = 1, 2, 3) \\ T_{i4} &= T_{4i} = i \rho v_i \\ T_{44} &= -\rho \end{aligned} \quad (16.23-5)$$

Then the classical equations of motion (16.23-1) and (16.23-4) can be expressed in the symmetric form: -

$$\frac{\partial T_{ij}}{\partial x_i} = 0 \quad (j = 1, 2, 3, 4) .$$

Thus setting $j = 1, 2, 3$.

$$\frac{\partial T_{1j}}{\partial x_1} + \frac{\partial T_{2j}}{\partial x_2} + \frac{\partial T_{3j}}{\partial x_3} + \frac{\partial T_{4j}}{\partial x_4} = 0$$

$$\frac{\partial}{\partial x_i} (\rho v_i v_j - X_{ij}) + \frac{\partial(i \rho v_j)}{\partial t} \cdot \frac{dt}{dx_4} = 0 .$$

$$\frac{\partial}{\partial t} (\rho v_j) + \frac{\partial}{\partial x_i} (\rho v_i v_j - X_{ij}) = 0$$

Setting $j = 4$

$$\frac{\partial T_{14}}{\partial x_1} + \frac{\partial T_{24}}{\partial x_2} + \frac{\partial T_{34}}{\partial x_3} + \frac{\partial T_{44}}{\partial x_4} = 0$$

$$i \frac{\partial (\rho v_1)}{\partial x_1} + i \frac{\partial (\rho v_2)}{\partial x_2} + i \frac{\partial (\rho v_3)}{\partial x_3} - \frac{\partial \rho}{\partial t} \frac{dt}{dx_4} = 0$$

$$\frac{\partial \rho}{\partial t} + \frac{\partial}{\partial x_i} (\rho v_i) = 0.$$

However, T_{ij} is not a tensor since $v_i v_j$ are not even vectors in the 4 dimensional sense nor is stress component X_{ij} a tensor in a 4 dimensional sense. We proceed to doctor the equations in much the same way as we did in Special Theory.

Thus in place of the velocity components:

$$v_1 = \frac{dx_1}{dt} \quad \text{we introduce} \quad u_1 = \frac{dx_1}{ds} = v_1 \frac{dt}{ds}$$

$$v_2 = \frac{dx_2}{dt} \quad u_2 = \frac{dx_2}{ds} = v_2 \frac{dt}{ds}$$

$$v_3 = \frac{dx_3}{dt} \quad u_3 = \frac{dx_3}{ds} = v_3 \frac{dt}{ds}$$

$$u_4 = \frac{dx_4}{ds} = i \frac{dt}{ds}$$

N.B. $\frac{dt}{ds} \approx 1$ at low speed and the spatial components

of our 4 vector \vec{u} will tend to equality with our classical velocity vector \vec{v} .

In addition we seek a new stress tensor X_{ij} ($i, j = 1, 2, 3, 4$) such that at low speeds the spatial components of

$$X_{ij} \longrightarrow X_{ij} \quad (i, j = 1, 2, 3).$$

and at the same time X_{i4}, X_{4i} and $X_{44} \rightarrow 0$

Having proceeded thus far redefine T_{ij} by replacing

$v_1 v_2 v_3$ by $u_1 u_2 u_3 u_4$ and X_{ij} by X_{ij}

Yielding

$$T_{ij} = T_{ji} = \rho u_i u_j - X_{ij} \quad (i, j = 1, 2, 3, 4) \quad (16.23-6)$$

T_{ij} as defined by (16.23-6) is a tensor which approximates closely to (16.23-5) at low speeds. In our Galilean frame of reference it seems reasonable therefore, to replace the classical equations by the equation

$$\frac{\partial T_{ij}}{\partial x_i} = 0$$

or $\text{Div } T_{ij} = 0$

This equation being in tensoral form it is immediately applicable to all frames of reference (in which divergence is appropriately interpreted)

$\text{Div } T_{ij} = 0$ or after we can write it alternatively as

$$(T_{\mu}^{\nu})_{;\nu} = 0 \quad (16.23-7)$$

Let us look at the equation of motion a little more closely

$$\text{Div } (T_{\mu}^{\nu}) = 0 \quad (16.23-8)$$

Whenever the divergence of an entity vanishes this implies permanence of the entity in question, i.e., the entity in this instance, the stress-energy tensor, is conserved.

Thus by making our transition from classical mechanics to special relativity we replaced the two laws of conservation of mass and conservation of energy by the single law of conservation of mass + energy. We have now generalized even further and shown that what is in reality conserved is the stress energy tensor which in addition to embracing mass and energy, has momentum and internal stress as additional facets.

It is rather interesting to apply the equation of motion (16.23-8) to the case of the single mass particle. In this instance the equation of motion assumes the form

$$\frac{d^2 x_\mu}{ds^2} + \{a\beta, \mu\} \frac{dx_\alpha}{ds} \frac{dx_\beta}{ds} = 0 \quad (16.23-9)$$

This is the equation of a geodesic i.e., particles describe geodesic (or straight) paths in curved space time rather than curved paths in flat space time; this latter representing the classical viewpoint.

We can rewrite (16.23-9) in the form

$$\frac{d}{ds} \left(m \frac{dx_\mu}{ds} \right) = - m \{a\beta, \mu\} \frac{dx_\alpha}{ds} \frac{dx_\beta}{ds}$$

Compare this with the equation of motion as derived on the basis of Special Theory of Relativity

$$\frac{d}{ds} \left(m \frac{dx_\mu}{ds} \right) = K_\mu$$

Bearing in mind that the only forces we have taken into consideration are the gravitational forces (and, of course,

inertial forces) we note that in the formulation of general relativity in place of force we have the expression

$- m \{ \alpha_{\beta, \mu} \} \frac{dx_{\alpha}}{ds} \frac{dx_{\beta}}{ds}$ which defines a twisting of our reference frame.* Since $\{ \alpha_{\beta, \mu} \}$ is intimately tied up with our choice of reference frame which can be changed quite arbitrarily it is for this reason we regard forces and the associated concept of potential energy as quite fictitious. Thus we can deliberately choose a twisted reference frame (i.e., accelerated frame) in flat space time. In this instance the forces (as manifested in the term $- m \{ \alpha_{\beta, \mu} \} \frac{dx_{\alpha}}{ds} \frac{dx_{\beta}}{ds}$) which appear in our equations of motion are of reducible nature and can be removed at will. (i.e., centrifugal and centripetal forces are examples.) On the other hand if space time is itself twisted there does not exist a transformation which makes the Christoffel three symbols $\{ \alpha_{\beta, \mu} \}$ vanish and in this case the force field is irreducible (i.e., non-uniform field of a gravitating mass).

It may be shown that $\text{Div} (G_{\mu}^{\nu} + \frac{1}{2} g_{\mu}^{\nu} G) = 0$.

It would be natural therefore to make the identification

$$G_{\mu}^{\nu} + \frac{1}{2} g_{\mu}^{\nu} G = T_{\mu}^{\nu} \quad (16.23-10)$$

This relationship is of significance in the following

* Not to be it noted a twisting in space time - for the symbol $\{ \alpha_{\beta, \mu} \}$ is not a tensor and hence, does not define anything intrinsic in space time.

respect. The left hand side involves G_{μ}^{ν} in terms of which the law of gravitation is formulated ($G_{\mu\nu} = 0$). The right hand side involves T_{μ}^{ν} in terms of which the law of motion is formulated ($(T_{\mu}^{\nu})_{,\nu} = 0$). By virtue of (16.23-2) which ties G_{μ}^{ν} and T_{μ}^{ν} together we would deduce that the law of motion is deducible from the law of gravitation and vice versa.

It is to Eddington we owe the following rather graphic explanation of the nature of this tie up.

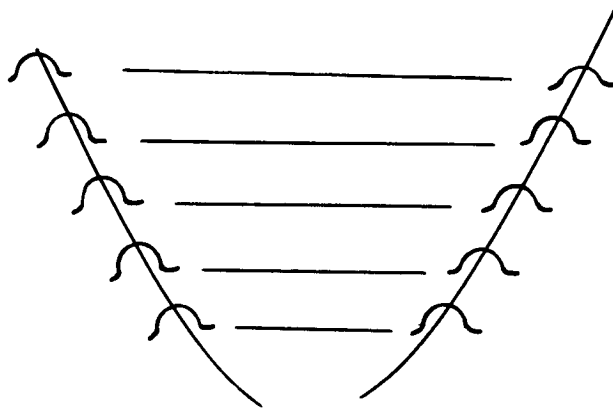


Figure 16-10

Consider two material particles in space time. Along their world lines space time is creased (figure 16-10). The law of gravitation states $G_{\mu\nu} = 0$ in the intervening space, in other words, nature is a rather fastidious tailor who will not tolerate ripples in free space. Such being the case the creases must run in prescribed directions if ripples are to be avoided. Thus the relative motion of the particles is the direct outcome of the law of gravitation.

SECTION XVII

ENVIRONMENTAL REQUIREMENTS

17. Introduction

Prior to a study of the problems confronting man in space travel it perhaps would be proper to list some of the reasons given as to why it would be desirable to have manned space vehicles.

The most sublime reason given is that man's expansion into new lands is necessary for his survival and therefore, because of the limitations of earth, the survival of the human race depends upon space travel; there being an estimated 100,000 planets in the known universe capable of sustaining life as we know it.

The reason most often given for manned vehicles is that generally, man has a much greater tolerance to vibration, shock, and temperature changes and is lighter in weight and more versatile than the most elaborate electrical brain or man-made man.

Finally, the proposed "National Aeronautics and Space Act of 1958" in part declares that "adequate provisions ... be made for the development ... of ... satellites and other space vehicles, manned and unmanned ...".

Initial steps taken to obtain recruits for the space vehicles would be to screen applicants to assure that they

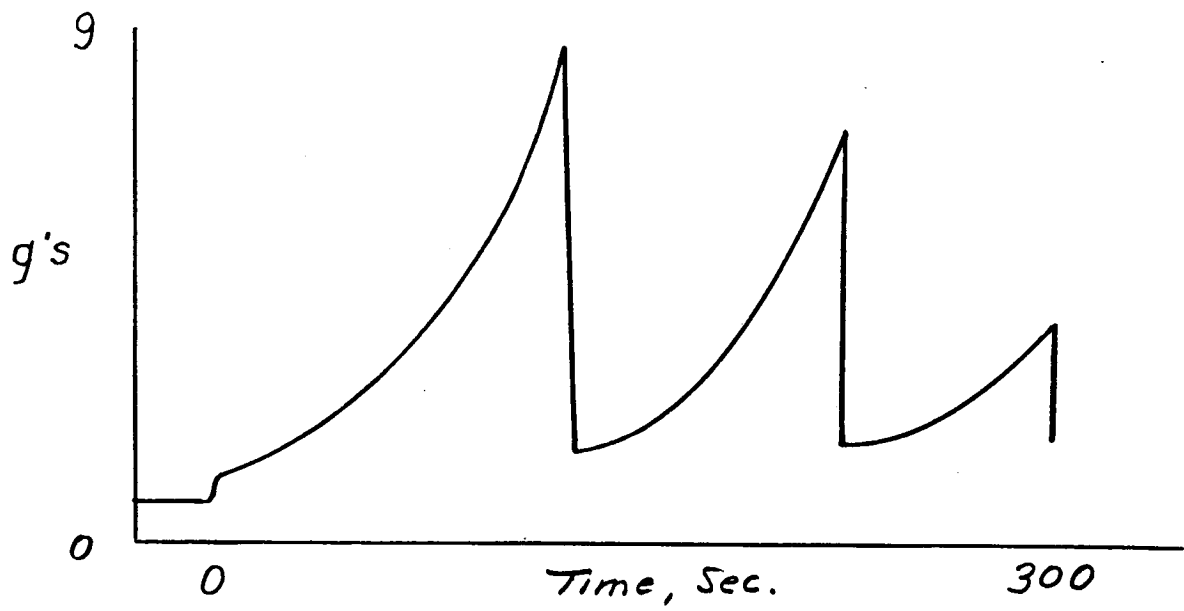
stand up under the physical and mental stresses commonly experienced by flying personnel such as those induced by hazards, combat, authority relations, space living conditions, and separation from family. A recruit of mature judgement and emotional stability is desired.

The manned vehicle will be subjected to high linear accelerations and possibly some stabilizing rotation during launch. While in orbit or while traveling within the solar system the vehicle, equipment, and occupants will experience weightlessness, cold, heat, darkness, brilliant sunlight, vacuum, relatively unknown and unnatural atmospheres of other planets, cosmic radiation and meteorites. The final stages of travel, re-entry into earth's atmosphere or entry into any planets atmosphere, will probably mean the space vehicle will experience high aerodynamic heating and the occupants will feel the effects of rapid deceleration.

Man has, rather definite, but most certainly, limitations, as to what he can withstand physically and still be able to perform prescribed tasks. Man's physical makeup has remained effectively constant over the years and is expected to remain so in the foreseeable future. These limitations will necessarily be considered then in the design of any manned vehicle.

17.1 Launching of Vehicle

Presently reasonable linear accelerations and time-durations needed to place a three stage rocket in an orbit about the earth have been calculated to be of the following order:



Also the time-duration of continuous accelerations required for a vehicle to reach the escape velocity of the earth have been calculated to be:

Acceleration (g)	Time endured
3	9 min 31 sec
4	6 21
5	4 45
6	3 48
7	3 10
8	2 40
9	2 20
10	2 6

Humans have withstood these accelerations in a centrifuge for the listed times without blacking out. In fact the subjects riding the three-stage rocket-launch cycle felt good enough to have the test repeated several times in succession. One man withstood 17 g's for a minute with the acceleration acting in a direction nearly at right angles to the spine.

The subjects, withstanding 10 g's, during a period of 2 minutes and 6 seconds were able to converse in mono-syllables. Their vision was clear, and they were mentally alert and able to respond to visual and auditory signals. They also retained relatively unimpaired control of their hands, wrists, and ankles.

Generally speaking the individuals tolerance of linear

acceleration acting from head to foot is a function of the column of arterial blood, between the heart and brain, that is approximately 12 inches in height. The heart normally pumps blood up this column at a pressure of 120 mm Hg. At an acceleration of about 5 g's the downward force acting on the blood in the artery about equals the upward force. The blood cannot then flow to the brain and eyes and also the blood in the lower body and extremities can not return to the heart. The result is that the eye, the first to notice an oxygen-carrying-blood lack, greys out between 3.5 and 5 g's and blacks out between 4 to 5.5 g's. When the g force is increased to 4.5 to 6 g's and maintained for three to five seconds unconsciousness will result.

We have mentioned previously, however, that human subjects have withstood as high as 17 g's without losing consciousness. It was found that if the acceleration occurs from the front to the back of the body, the subject being in the supine position, or from the back to the front of the body, the prone position, human tolerance to acceleration is increased considerably. Tolerances of the average man to various linear accelerations for a given length of time are shown in figure 17-1.

In figure 17-2 the tolerances of five human subjects to linear accelerations at various degrees of supination are given. In an upright position the subjects blacked out at about 4 g's, however, when supinated 85° the blood was not subjected to pooling and they all withstood 15 g's without

blackout.

When subjected to minus g, acceleration acting from feet to head, the blood rushes to the head causing an increase of pressure in the brain. The practical limit of tolerance is about a minus 3 g's for 10 to 15 seconds. The so-called red out, occurring at minus g accelerations, is apparently due to the lower eye lid acting as a red curtain over the eye.

If the space vehicle is rotated or tumbles during flight and if the occupants rotate or tumble with the vehicle another physical problem is encountered of which the human body has but a certain endurance. When the body is rotated the blood tends to accumulate at the extremities. In figure 17-3 are presented the results of tests of humans being rotated about axes through the heart and pelvis region. The tests were run at different revolutions per minute and the duration of time spent at each rpm was limited by the occurrence of pain and ocular hemorrhage. The greatest endurance occurred when the body was rotated about an axis through the heart.

A g-suit will increase tolerance of plus acceleration about 2 g's. What is probably an ultimate in a "g-suit" is obtained by immersing the body in a capsule of water. As the capsule is subjected to increasing g's the increasing water pressure on all parts of the body prevents pooling of the blood and g-tolerance is greatly extended. An additional

advantage of this type "g-suit" would be relative freedom to move the limbs.

Adequate provisions should be made to protect the orbiting vehicle and contents from the heat and noise generated by the propulsion units.

Somewhat of a guide to noise level restrictions may be derived by knowing that the ear usually feels uncomfortable at a noise level of 120 decibels and feels a strong tickling sensation at 130 decibels and deep pain at 140 decibels and above. Men have withstood 115 decibels for a 56 hour period. This noise level, however, caused a temporary hearing loss of approximately 50 decibels which cleared up in 4 days. A hearing loss of 50 decibels is considered a serious hearing impairment and makes it difficult to understand even loud speech.

17.2 Orbiting and Travel in Space.

While in space the temperatures to be encountered have the aweinspiring range of from near absolute zero (-273°C) in the shade of some planets to near 6000°C near the surface of the sun.

Although it may be difficult, temperature can be regulated within a space vehicle by establishing a balance between reflectors and absorbers on the vehicle surface to reflect and absorb radiant heat, primarily from the sun.

A few measurements made in the nose section of the satellite, Explorer I, while in orbit, are presented in figure 17-4 along with the calculated temperatures that were expected to be measured.

Human tolerance to heat and cold depends upon the body environment, health, activity, and type and amount of clothing worn. Safe heat and cold exposure times to air over a range of temperatures for normal healthy men at rest, clothed and partly or wholly exposed, in a black-walled room free of forced draft and radiation are presented in figure 17-5.

Some pain may be experienced by the human skin if it is heated to 44°C and at 45°C the pain becomes unbearable. If the skin is held at a temperature of 55°C for more than 10 seconds burns will occur.

Time-tolerance to cold exposure for humans, sitting and doing no more than light manual work, for several types of clothing are given in figure 17-6.

Additional experience gained by the personnel wintering at the South Pole indicates that man, properly clothed, can withstand -100°F for several hours. They also found out that the pain felt at plus 40°F , if improperly dressed, is as much as can be felt at -40°F . The reason given is that the nerves are limited to the amount of pain that they can feel due to cold.

Combinations of vehicle interior air temperature, interior surface temperature, and relative humidity can cause interior frosting. Frosted instruments, control knobs and observation ports may be uncomfortable and a hazard to the safety of the vehicle. Curves similar to those shown in figure 17-7 may be of convenience to the designer.

The effect that the strange and mysterious weightlessness or zero g state may have on man over prolonged periods will probably not be resolved until man is put into orbit. Weightlessness can be felt for a few seconds during a dive into a swimming pool or when jumping down to the ground from above until the resistance of the air becomes appreciable. In experimental work with a F-94c airplane weightlessness has been experienced for periods of 43 seconds by flying in a prescribed parabolic arc. (figure 17-8)

Subjects experiencing zero g in these tests had varied reactions. Most, however, enjoyed the weightless state. A sobering thought on weightlessness is provided, however, by an experienced test pilot Major Chuck Yeager, who, after 8 - 10 seconds at zero g, felt his head grow thick and he got the impression that he was spinning around slowly in no particularly defined direction.

Here on earth, many persons have chewed, swallowed and begun to digest food while upside down, or effectively at minus one g and hence, could probably eat with little or no

difficulty at zero g. Drinking, though, while in a weightless state may cause drowning; for liquids would float freely and could flow into the nose. However, squeeze tubes could be used to force fluid into the mouth where muscular action would move the fluid down the throat.

Man orientates himself in an environment by using three different body systems: the eye; the semicircular canals and otolith organs of the inner ear; and by the kinesthetic system. At zero g the eye will be a reliable system for orientation. However, it has been determined that two of the three systems are required for positive orientation.

The three semicircular canals, aligned in the three planes of space, and the otolith organs of the inner ear are responsive to the rate of rotation of the head and linear accelerations along one particular direction respectively. These organs evolved in a state of one g and adjustment to the zero state will have to be made.

The kinesthetic system gives us a sense of orientation through the nerves in the skin, muscles, and connecting tissues of the body. Here on earth the body can be subjected to a one g gravity field at any one time in one of six directions (to the right, left, back, front, and up and down) without undo discomfort. Therefore it is expected that the kinesthetic system will adjust readily to the zero gravity state.

17.3 Air Equivalent

The oxygen partial pressure at sea level is 3 psi.; at this oxygen pressure the blood is normally saturated to 95% and the body works fine. At 15,000 feet the oxygen pressure is but 1.5 psi. and oxygen saturation of the blood drops to 70%. The person used to breathing air at sea level if suddenly placed in an atmosphere with but 1.5 psi. oxygen pressure for about two hours would experience fatigue, drowsiness, headache, and poor judgment. Due to a practically total lack of oxygen in space the air equivalent needed by the occupants of any space vehicle will have to be taken along.

It has been determined that one cubic ft/hr/man of oxygen (probably carried in liquid state) is required when light exercise or work is performed and 2.26 cubic ft/hr/man under moderate exercise conditions.

Experiments have been carried out during the past several years to develop an economical system to furnish oxygen and food in a space vehicle from crops of algae. The system can be described briefly. The algae takes light from the sun or other source, carbon dioxide from the air, and nitrogen, water, and other foods from the soil. These are synthesized into carbohydrates, proteins and fats. Man could then eat a percentage of the plants and breathe the excess oxygen produced by the plants during photosynthesis. Human wastes, (including the carbon dioxide exhaled from the lungs) containing almost exactly the necessary foods to promote

vigorous algae growth, would be returned to the soil to serve as food for the algae and to start the cycle anew.

An internal cabin pressure as low as practical would be desirable from the vehicle structural designers standpoint. The differential between internal and external vehicle pressures would then be at its lowest while orbiting in the near vacuum of space. However, the vehicle would probably be pressurized while on the ground just prior to launch. The most practical differential pressure value then from a structural consideration would be the value half way between the sea level pressure (if launched at sea level) and the vacuum or zero pressure level. Under these assumptions the internal cabin pressure would be 7.35 lbs/in^2 , equivalent to an altitude of about 18,000 feet.

One disadvantage of flying around in space enjoying a cabin pressure of 7.35 lbs/in^2 is that it might slowly or suddenly vanish. Machine failure or puncture of the space vehicles skin could cause loss of pressure.

Suddenly losing the atmosphere or even a partial loss of pressure will subject the traveler to decompression. At the time of decompression, if the breath is held, or swallowing is taking place, the rapid exit of air from the lungs will be prohibited or slowed down. The trapped

gases in the lungs will then expand causing chest pains, blurred vision, nausea, and headaches. Other body organs that are sensitive to pressure changes are the ears and sinuses. In figure 17-9 are pressure differentials causing middle ear pain.

In addition to the effects of rapid decompression even a slow reduction of pressure on the body may produce ill effects. Man breathes nitrogen in normal air and some of it is dissolved in the tissues of the body. If the pressures on the body are reduced to 615 lb/ft^2 the nitrogen will be released from the tissues to form bubbles in the joints, called "bends", and in the pulmonary mechanisms of the body, called "chokes". Still further reduction in air pressure to about 130 lb/ft^2 will cause "boiling" of the body fluids. This is called ebullism and is undoubtedly the lowest pressure limit a man could stand.

It was mentioned before that carbon dioxide is exhaled in the breath. If the carbon dioxide content of the air is allowed to build up to where it's more than 0.3% by volume (ten times the normal content of air) it will cause labored breathing, headaches, and if greatly exceeded even death. Figure 17 - 10 shows the tolerance of man to a sudden exposure to varying amounts of carbon dioxide.

The standard technique of absorbing carbon dioxide in a closed compartment is by using an oxide of an alkalin

earth metal. An example being Lithium which requires 325 grams/man/day to remove the carbon dioxide that is exhaled from the lungs at the rate of 1 kg/man/day.

17.4 Radiation

When man removes himself from the protective covering of the earth's atmosphere he will be subjected to intense solar radiation and primary cosmic rays.

Serious sunburn hazards will exist and the viewing of objects will be anything but comfortable at high altitudes. Inside a cabin, with sunlit patches adjacent to deep shadows, viewing will be made even more uncomfortable, and it is recommended that sun glasses be worn.

The earth's atmosphere is equivalent to a lead shield about three feet thick and when this is left behind the space vehicle will be bombarded by the primary cosmic rays.

When a primary cosmic-ray particle enters matter, such as a space vehicle, it has two main processes by which it may give up its great kinetic energy: it may gradually give up its energy by ionizing the atoms of the material it enters, or, it may collide with an atomic nucleus, producing a violent nuclear reaction, called a "star". The energy of the ray is distributed among the fragments of the colliding nuclei.

It's common to specify the radiation dosage received in terms of intensity, or numbers of roentgens per hour and the time of duration. A roentgen is the amount of

irradiation which will produce 2.1×10^9 pairs of ions in a cubic centimeter of air at 0°C and 760 mm Hg pressure.

According to the Bureau of Standards, the maximum permissible dose of ionization based on year-round exposure for male humans is 300 milliroentgens per week for X-, γ -, and β -rays and 15 mr per week for α -rays.

Up to 10,000 mr can be accumulated below the age of 30 and up to 50,000 mr below the age of 40 years without damage to offspring or shortening of life.

17.5 Meteorites

The meteorite is the particle which causes the atmospheric effect we see and call a meteor.

In navigating in space it would probably be best to avoid the fundamental plane of the solar system, especially between the planets Mars and Jupiter, where there are high concentrations of meteorites.

Calculations have been made on the probability of a space vehicle being hit and penetrated by a meteorite. The calculations were based on the number of observations made of meteors over a certain period. However, meteors are only visible from a maximum of about 80 miles from the earth and meteorites may be more abundant in space.

Chances of a space vehicle being penetrated by a meteorite, according to these calculations, are about 1 in 2000 over a

24 hour period. Data collected from orbiting unmanned vehicles will undoubtedly be of great help in this respect.

17.6 Re-entry

The foremost problems to solve, or design for, during re-entry are deacceleration and aerodynamic heating.

Human tolerance to various magnitudes of vehicle deacceleration can be considered the same as to acceleration if the occupants face aft during the re-entry.

Aerodynamic heating during re-entry was considered in previous papers.

Glossary

- Aeroembolism - decompression sickness
- Astrobiognosis - the study of the support of life in space
- Astronautics - design, production, and operation of space craft
- Bends - pain in and about the joints due to the formation of nitrogen bubbles
- Blackout - loss of sight due to lack of blood in the eyes
- Bioastronautics - human factors involved in astronautics
- Chokes - symptoms of aeroembolism referable to the thorax - blockage of pulmonary vessels by bubbles.
- Clo - amount of clothing a seated man needs to be comfortable in 70°F air with a relative humidity of 50% and air movement of 20 feet per minute
- Dysbarism - the effects of reduced barometric pressure on the body
- Ebullism - "boiling" of body fluids
- Ecosphere of the sun - limited area or belt in the planetary system within which life (as we know it) is conceivable
- Greyout - vision becomes cloudy due to lack of blood in the eyes
- Hyperventilation - breathing three a four times the normal rate, thereby upsetting nature's balance of oxygen and carbon dioxide, causing dizziness and loss of coordination
- Hypoxia - lack of oxygen in the blood
- Iliac crest - in the region of the dorsal and upper end of the three bones composing either lateral half of the pelvis
- Kinesthetic apparatus - special receptors situated in muscles, tendons, connective tissues, skin, etc. and their nervous connections with the brain

Milieu - environment

Otolith organ - cavity of ear responsive to linear acceleration

Roentgen - an amount of radiation as would have produced 2.1×10^9 pairs of ions in a cubic centimeter of air at 0°C, 760 mm Hg pressure

Squeeze - fluid and blood being squeezed into the lungs

Supine - lying on the back - opposed to prone

Trauma - an injury, wound, shock

Vestibular system - paired small balance organs and their nervous connections with the cerebral cortex as the center of perception

Test Facilities doing Work on Human Tolerances

1. Naval Research Laboratory, Washington, D. C.
2. U. S. Naval School of Aviation Medicine, NAS, Pensacola, Fla.
3. Naval Medical Research Institute, Bethesda, Maryland
4. U. S. Navy Aeronautical Medical Equipment Laboratory, Philadelphia, Pa.
5. Naval Medical Research Laboratory, New London, Conn.
6. Aviation Medical Acceleration Laboratory, Johnsville, Pennsylvania.
7. USAF School of Aviation Medicine, Randolph Field, Texas.
8. Aero Medical Laboratory WADC, Wright-Patterson A. F. B., Dayton, Ohio.
9. Holloman A. F. B., New Mexico
10. Gunter A. F. B., Montgomery, Alabama.
11. Army Medical Research Laboratory, Fort Knox, Kentucky.
12. The Lovelace Foundation for Medical Education and Research, Albuquerque, New Mexico.

References

1. Realities of Space Travel, Edited by L. J. Carter.
2. Your Body in Flight, Department of the Air Force manual 51-7.
3. Rockets, Missiles, and Space Travel, Willy Ley.
4. Physics and Medicine of the Upper Atmosphere. *C.S. White, O.O. Benson Jr.*
5. Missiles and Rockets, Dec. '56, Jan '57, Feb. '58 and Apr. '58.
6. The Journal of Aviation Medicine, Aug. '54, Dec. '54 and Feb. '58.
7. Scientific American, Feb. '56 and Jan. '57.
8. Aeronautical Engineering Review, Mar. 1958 and Apr. '58.
9. Air Force Magazine, Mar. 1958.
10. Aviation Age, March 1958.
11. Aviation Week, Aug. '57, March '58 and Jan. '58.
12. The National Geographic Magazine, Aug. 55 and Apr. '58.
13. Spaceflight, Apr. '57.
14. Journal British Interplanetary Society, 1954.
15. Summary Session Astronautics Symposium, Feb. 18-20, 1957, under sponsorship of USAF Office of Scientific Research.

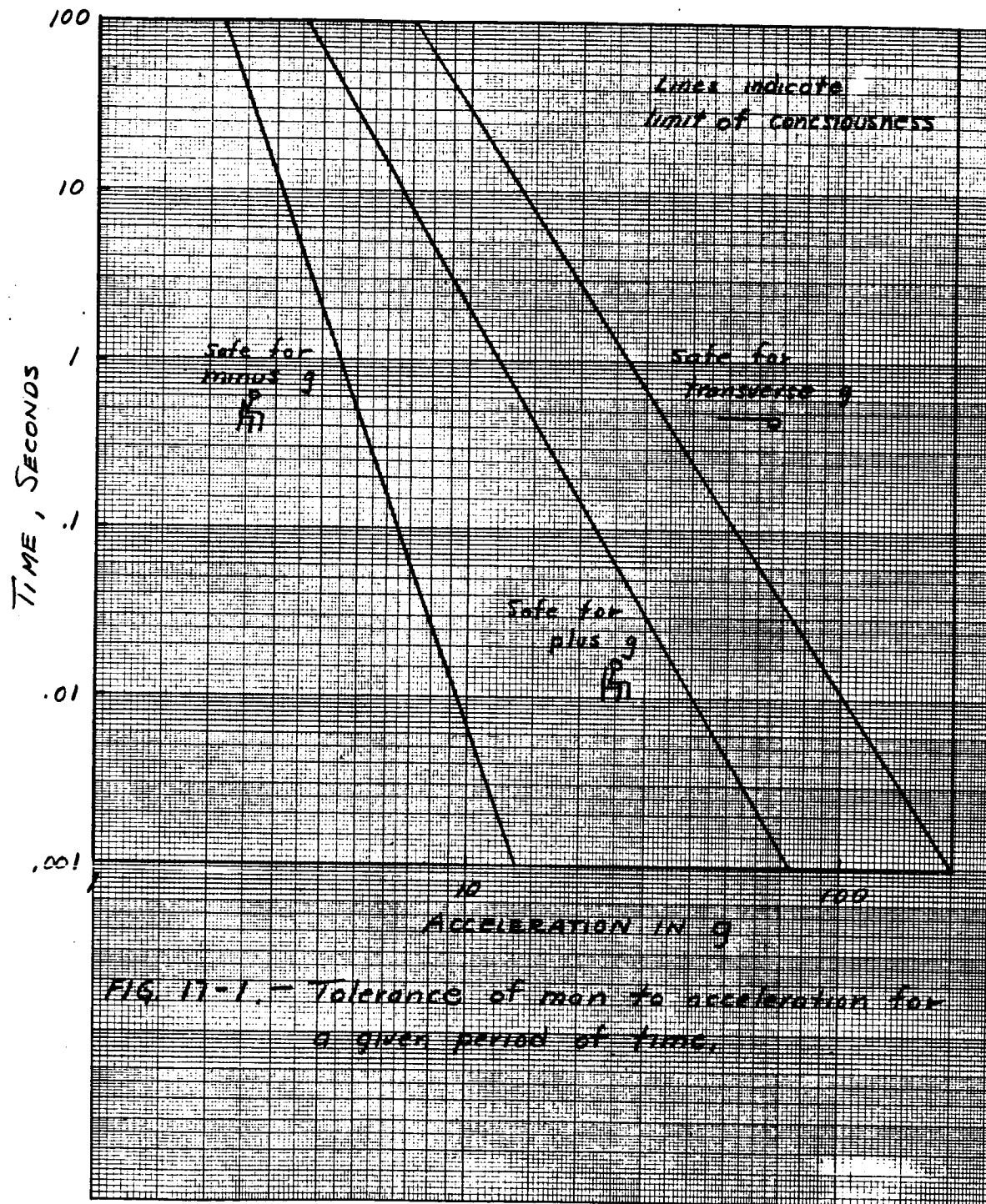


FIG. 11-1. — Tolerance of man to acceleration for a given period of time.

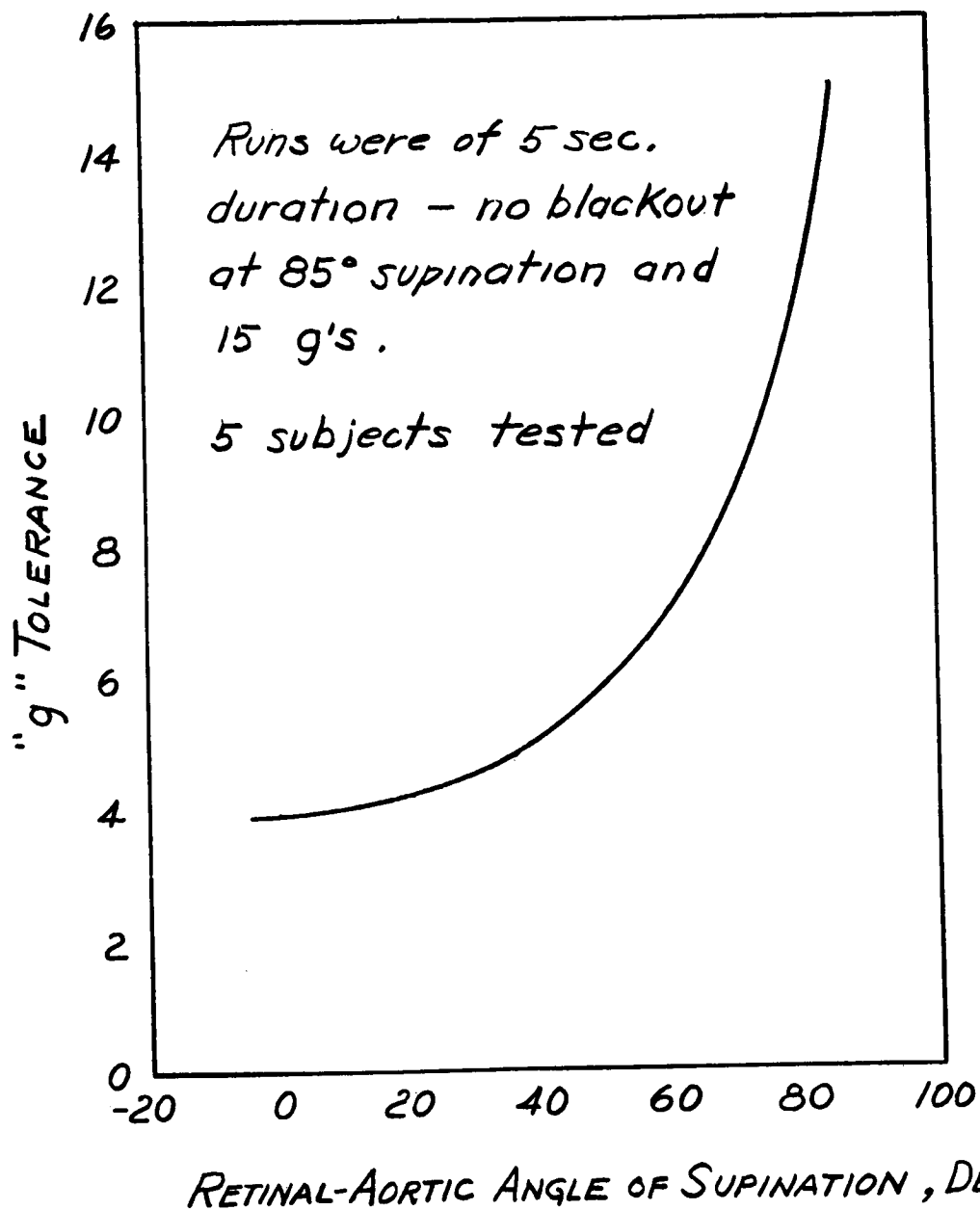


Fig. 17-2. - Tolerances to linear acceleration at various degrees of supination.

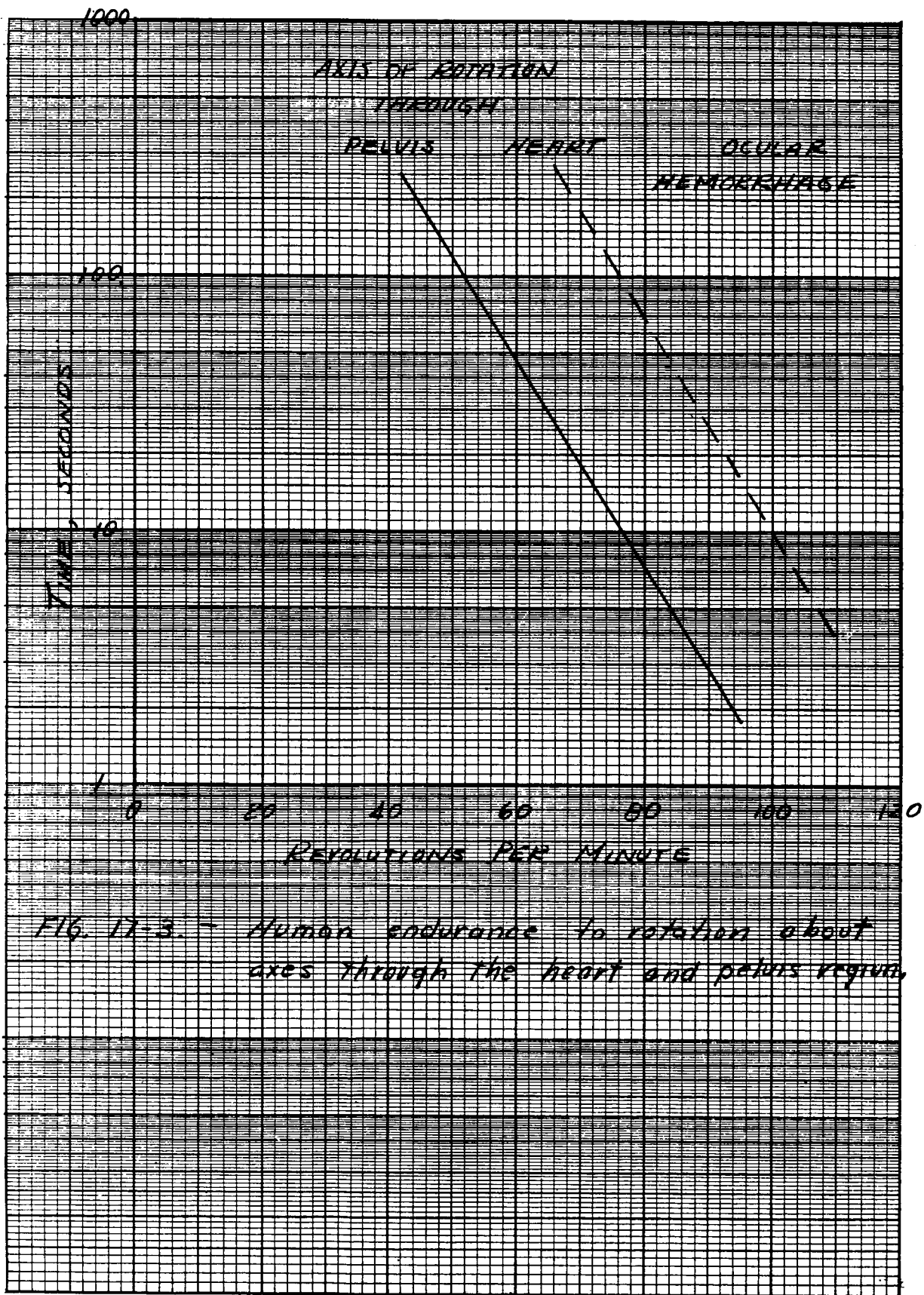
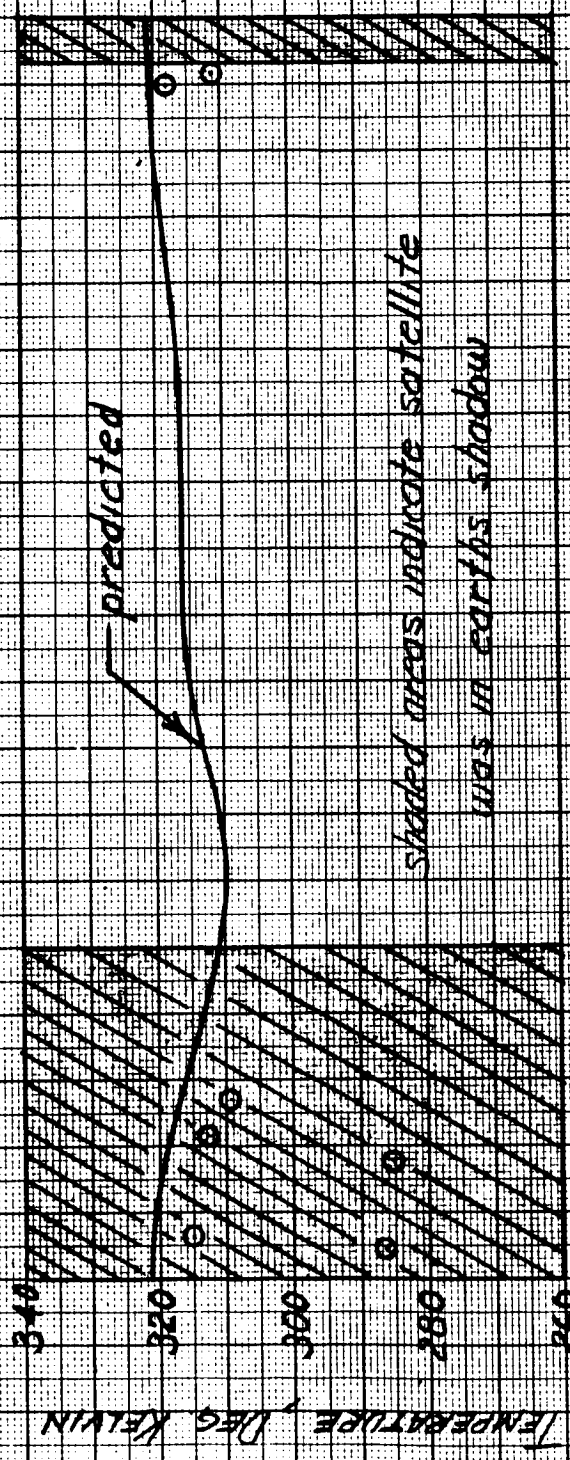
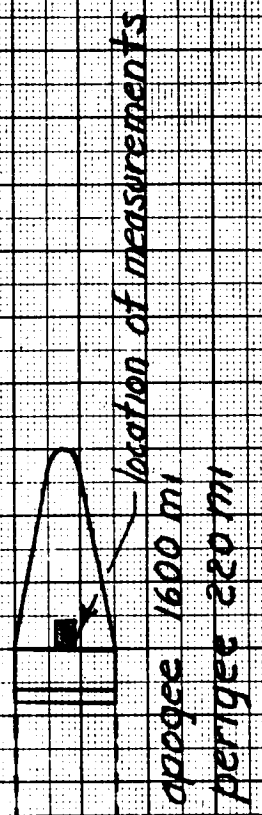


FIG. 17-3. - Human endurance to rotation about axes through the heart and pelvis region.

EXPLORER I

Instrument temperature received from satellite



PATH OF ORBIT

Fig 17-4

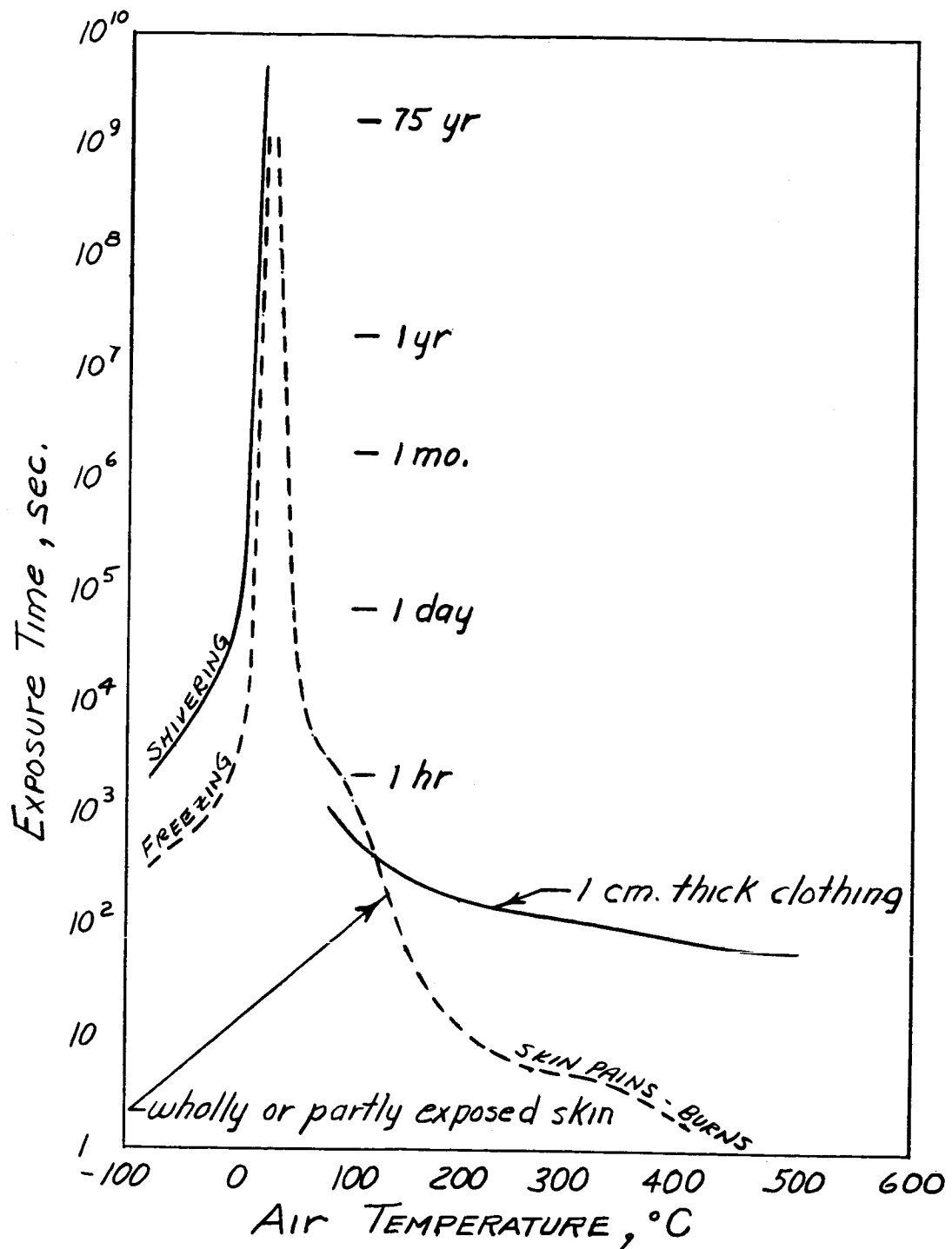


Fig. 17-5. - Exposure times to environmental air for healthy men at rest.

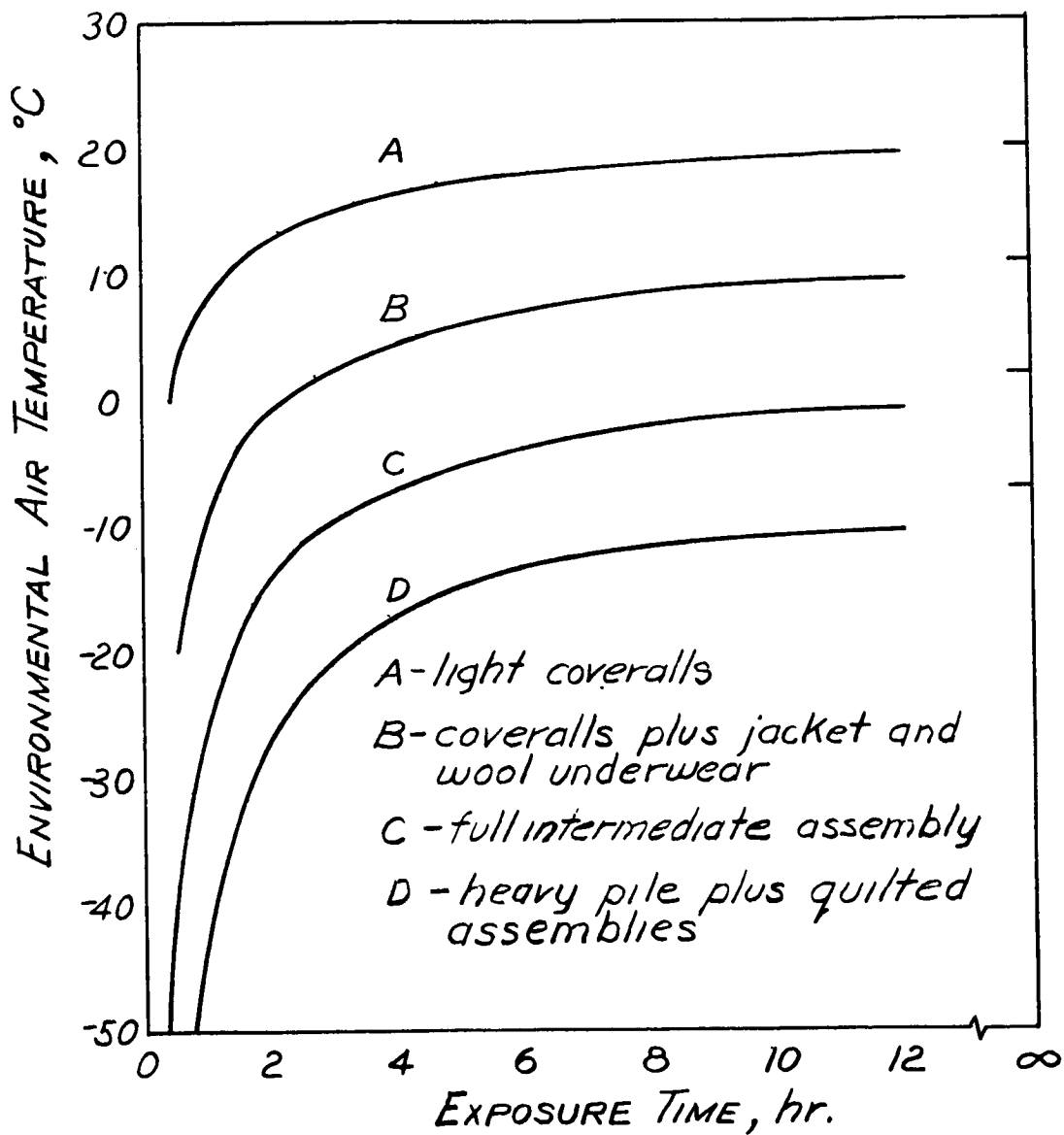


Fig. 17-6. - Time-tolerance in cold exposure. Subjects sitting, air motion 200 feet per minute.

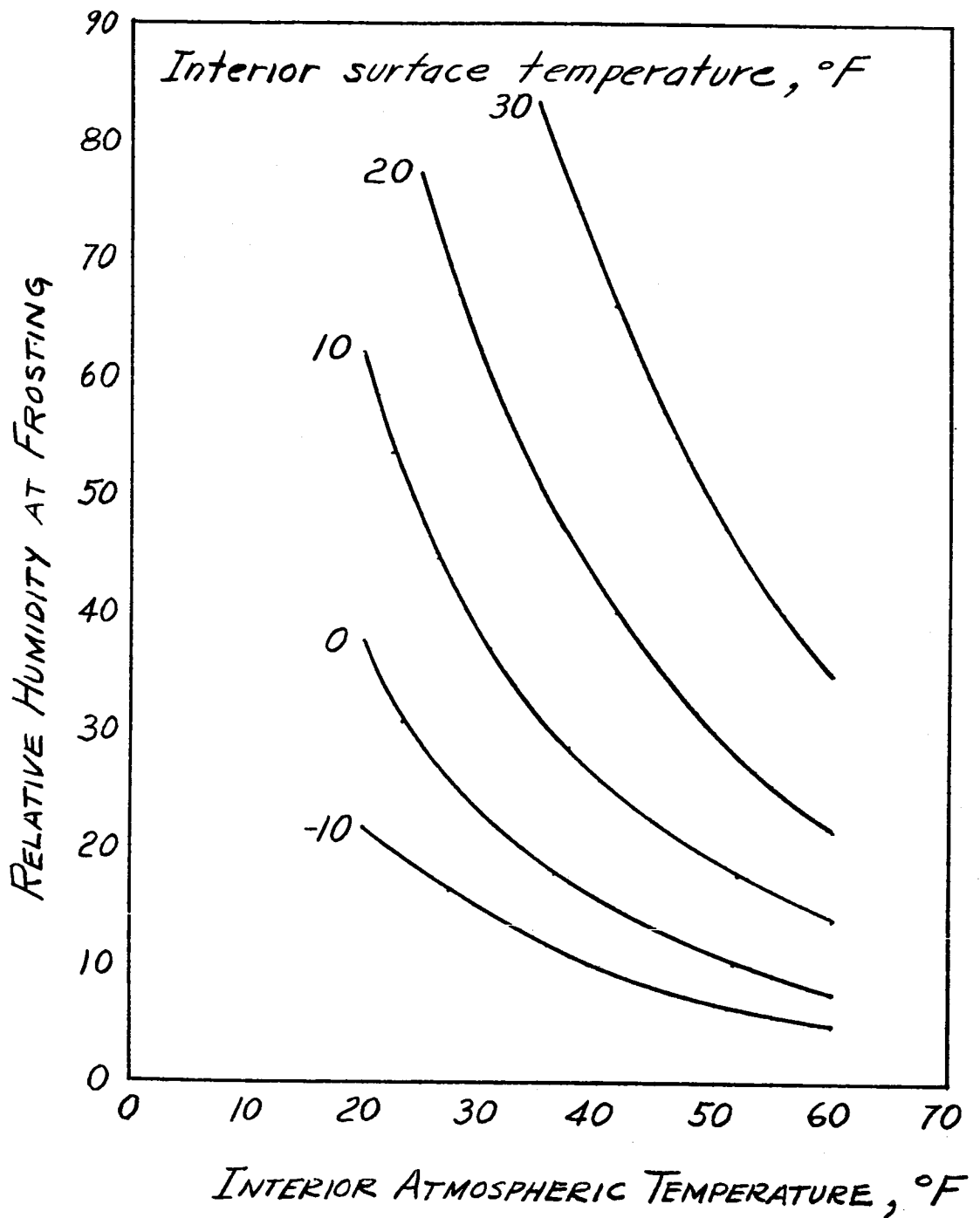


Fig. 17-7. - Temperature and humidity factors for interior hull frosting conditions.

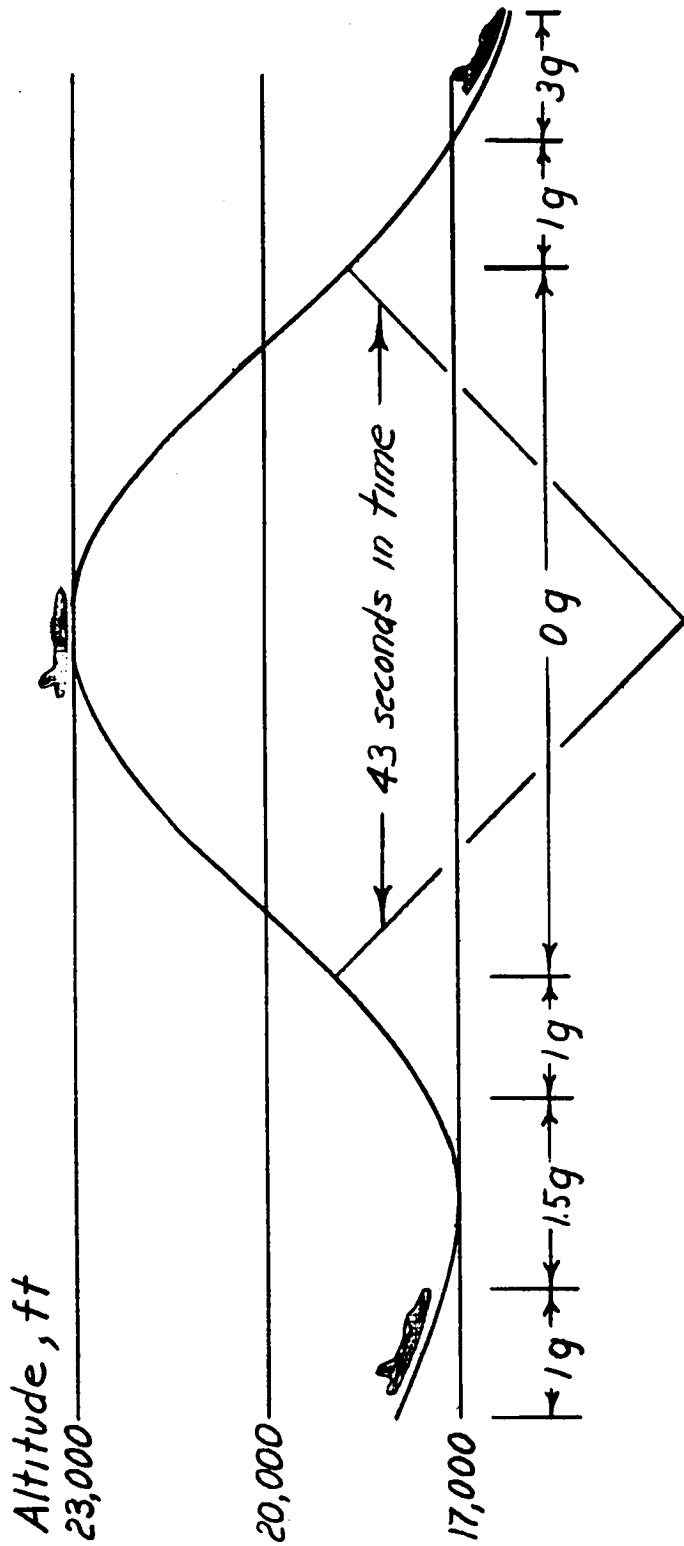


Fig 17-8.- Flight path of F-94C to reach 0 g and remain at 0 g for up to 43 seconds.

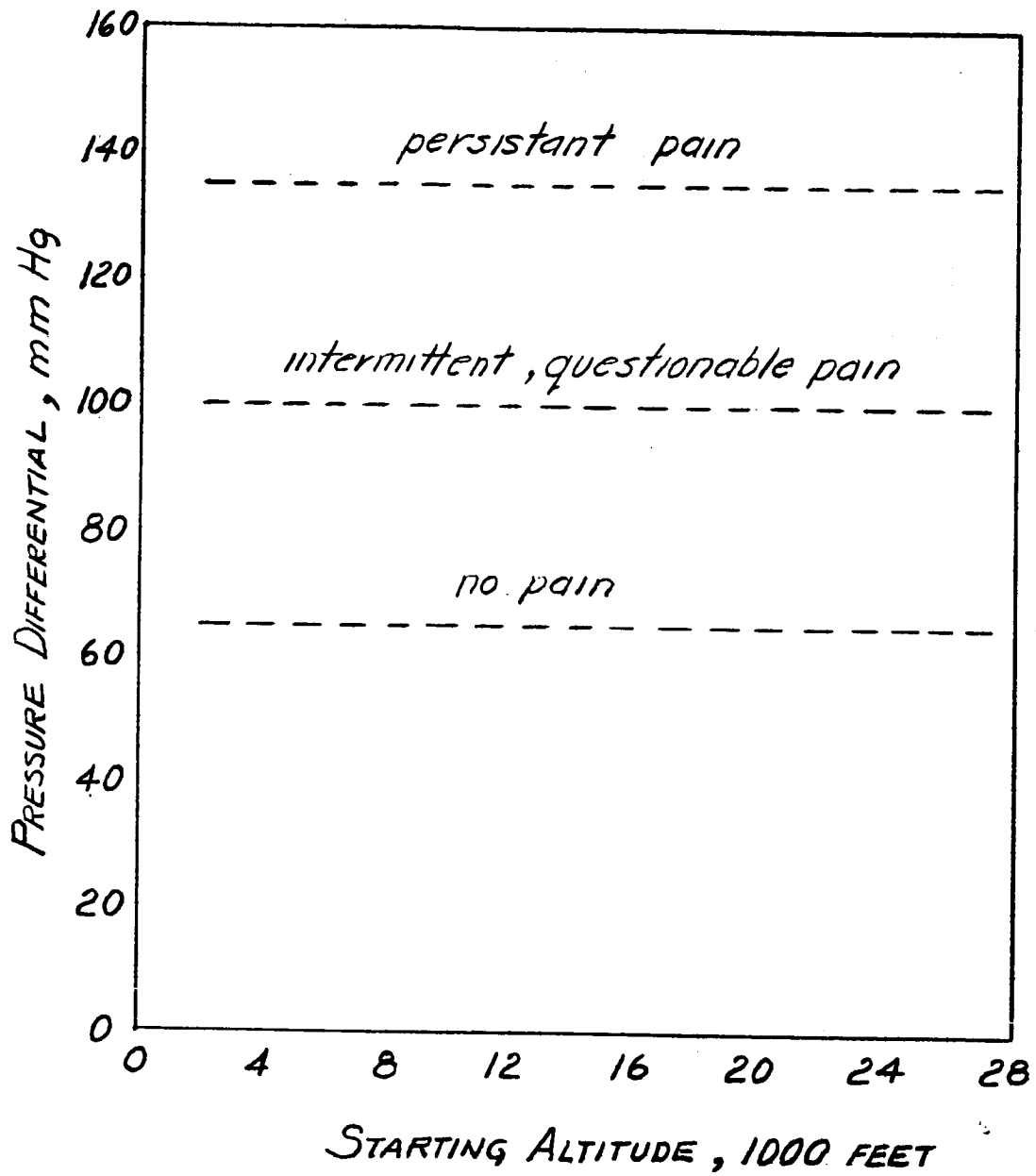


Fig 17-9. - Pressure differentials causing middle ear pain in relation to the altitude at which descent was started.

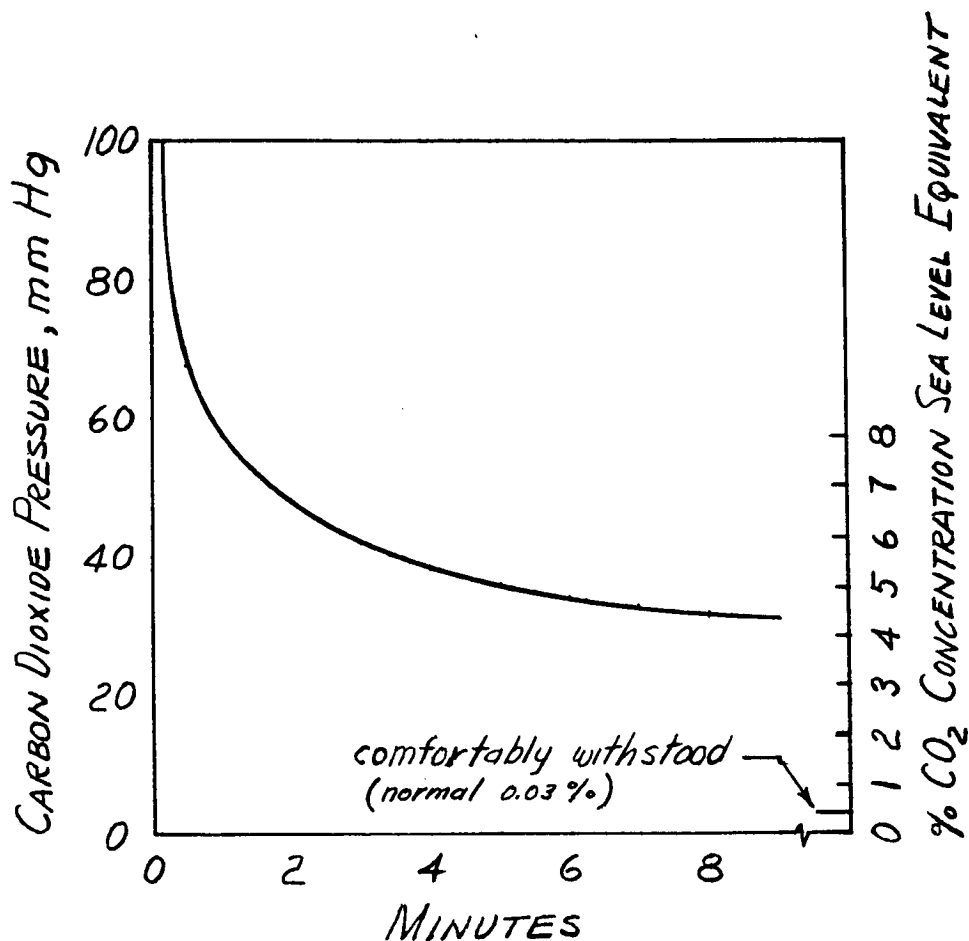


Fig 17-10. - Estimation of human tolerance in sudden exposure to CO₂ in inspired gas expressed in partial pressure against time.